

TNO Built Environment and Geosciences

COMPANY CONFIDENTIAL

Business Unit Geo-Energy &
Geo-Information
Princetonlaan 6
P.O. Box 80015
3508 TA Utrecht
The Netherlands

TNO report

NITG 05-155-C

Hydrocarbon potential of the Pre-Westphalian in
the Netherlands on- and offshore - report of the
PETROPLAY project

www.tno.nl

T +31 30 256 4640
F +31 30 256 4605

Date	February 24, 2006
Author(s)	B.M. Schroot, F.v.Bergen, O.A. Abbink, P.David, R.v.Eijs, H. Veld
Assignor	EBN, Gaz de France, NAM, Petro-Canada, Total, TNO, Wintershall
Project number	005.73037
Classification report	confidential
Title	
Abstract	
Report text	
Appendices	
Number of pages	436 (incl. appendices)
Number of appendices	

All rights reserved. No part of this report may be reproduced and/or published in any form by print, photoprint, microfilm or any other means without the previous written permission from TNO.

All information which is classified according to Dutch regulations shall be treated by the recipient in the same way as classified information of corresponding value in his own country. No part of this information will be disclosed to any third party.

In case this report was drafted on instructions, the rights and obligations of contracting parties are subject to either the Standard Conditions for Research Instructions given to TNO, or the relevant agreement concluded between the contracting parties. Submitting the report for inspection to parties who have a direct interest is permitted.

© 2006 TNO

COMPANY CONFIDENTIAL

Summary

The Petroplay project was a Joint Industry study conducted by TNO in 2004 and 2005 for a consortium consisting of six sponsors active in oil & gas exploration in the Netherlands: Energie Beheer Nederland (EBN), Gaz de France Production Nederland B.V., Nederlandse Aardolie Maatschappij B.V., Petro-Canada, Total E&P Nederland B.V., Wintershall Noordzee B.V. as well as for TNO itself. The main objective of the Petroplay project was to assess the petroleum geological potential of pre-Westphalian sediments in the Netherlands on- and offshore. Particular attention was paid to source rock potential, maturity and timing of hydrocarbon generation. The study used organic geochemical, biostratigraphic and general geological tools. The project aimed at a better assessment of risks related to pre-Westphalian hydrocarbon play concepts in the otherwise rather mature Southern North Sea hydrocarbon basin (including the Netherlands onshore) and the identification of prospective areas in this basin.

All available information from released Dutch on- and offshore wells that were known to have penetrated pre-Westphalian sedimentary successions was used, supplemented by a selection of data from nearby Belgian, German and UK wells. Although many of these wells were quite old, a comprehensive inventory and interpretation of all of this data had not been made or brought to the public domain previously.

The project followed an "area by area" approach, i.e. four selected areas of interest in the Netherlands on- and offshore were selected for detailed studies. The scope for finding pre-Westphalian sediments at the right burial depth (in view of the required maturity of source rock and preserved reservoir quality) was expected to be higher in these selected areas than elsewhere. For each of these potentially prospective areas independent assessments of hydrocarbon potential were made by data gathering, geochemical analyses, well log interpretations and seismic interpretation.

The result of the project was a first nation-wide inventory and overview of geological and geochemical data of the pre-Westphalian sedimentary sequences, covering both the Netherlands onshore territory and the Dutch North Sea Sector, as well as an interpretation of that data in terms of hydrocarbon play potential. A comprehensive digital database of all relevant geochemical data and analytic results from the used wells was made and is attached to this report (in MS-Excel format). Another product of the project was an updated stratigraphic framework based on biostratigraphic interpretations, which links the various regions in the Netherlands on- and offshore that each have their own stratigraphic units in the current lithostratigraphic nomenclature of the Netherlands.

The study confirmed that there is hydrocarbon potential for pre-Westphalian sediments. In particular, the widespread occurrence of potential source rocks was established. Based on geochemical analyses and interpretation it was concluded that the pre-Westphalian sequences contain source rocks with good initial potential in all areas. This conclusion is supported by the observation of TOC rich zones at different levels. The most promising source rocks occur in deposits at the near-base Namurian stratigraphic level. These rocks include TOC rich shales equivalent to the Geverik Member and the Bowland Shale Formation in the UK. In addition, other potential source rocks were found within the Dinantian and Namurian sequences. It was concluded that within the pre-Westphalian sequences levels with initially good source rock potential are almost

omni-present throughout the areas studied. However, the present-day hydrocarbon potential varies from area to area. Timing of hydrocarbon generation is a very critical factor with respect to the hydrocarbon potential of a particular area. In addition, the presence and preservation of reservoir quality and the presence of adequate seals were identified as critical factors which can be highly variable throughout the research area.

In Area 1 (the northern margin of the London-Brabant Massif) there is fair present-day remaining source rock potential in the Namurian and near-base Namurian sequences. Hydrocarbon generation and expulsion has however occurred pre-dominantly during the Carboniferous, but it has continued at a lower level throughout geological history until recently. Depending on the local circumstances this leaves scope for exploration in parts of Area 1. The prospectivity for hydrocarbons generated from pre-Westphalian sediments can be narrowed down to a rather limited elongated area parallel to the trend of the London-Brabant Massif.

In Area 2 (the Northern offshore, including the A, the western B and northern E blocks) there is fair present-day remaining source rock potential in the Namurian and Dinantian units, and even good potential in the sequences near the Dinantian to Namurian transition. In this Area hydrocarbon generation and expulsion took place much later than in Area 2, a substantial part of the generation has been recent. The most prospective parts of Area 2 are the eastern and southern margins of the Elbow Spit High, because there the pre-Westphalian source rocks have been buried deep enough to become mature. In addition, in those margins adequate seals for trapped hydrocarbons are most likely to be present. The main risks in Area 2 are reservoir quality, migration path and quality of the seal.

In Area 3&4 (the central to eastern and north-eastern Netherlands onshore) there must have been good initial source rock potential in the Namurian and near-base Namurian sequences, but the present-day potential is low. The geochemical analyses and 3D basin modelling demonstrated that in Area 3&4 source rocks are generally over-mature. This is partly due to a higher than average heat flow, which needs to be assumed in order to fit all data in the 1D and 3D basin modelling. Only under specific and probably very local circumstances could there still be some hydrocarbon potential in Area 3&4. One of those conditions could e.g. be the occurrence of a lower heat flow in areas not penetrated by wells to date. Another one may be the very early trapping of hydrocarbons into a structure which has not been disturbed since the Carboniferous. Based on seismic interpretation the presence of an intra-Namurian unconformity was interpreted at approximately Late Arnsbergian level. Also from seismic data the presence of at least one Dinantian carbonate build-up was interpreted in the Noordoostpolder.

	Area 1 (Northern Margin LB Massif)	Area 2 (Northern- most offshore)	Area 3 & 4 (Eastern onshore)
Namurian	Fair	Fair	
Base Nam. – Top Din.	Fair	Good	
Dinantian		Fair	
Devonian			

Table 0.1 Summary of pre-Westphalian present-day source rock potential per area

Contents

	Summary	3
1	Introduction	7
1.1	General	7
1.2	Petroleum geological background	7
1.3	Objectives	8
1.4	Scope of the work	8
1.5	Overview of well data used for this study	11
1.6	Confidentiality of this report	12
2	Pre-Westphalian geological setting of the Netherlands	13
2.1	Stratigraphic standards	13
2.2	Geological history with notes on source rock and reservoir rock development	15
2.3	Stratigraphic units	30
2.4	Lithology distribution maps	36
3	Pre-Westphalian source rocks and their maturity	47
3.1	Devonian	50
3.2	Dinantian	55
3.3	Top Dinantian – base Namurian	62
3.4	Namurian	67
3.5	Evaluation of potential source rocks	72
4	Hydrocarbon potential of Area 1	75
4.1	Geological and seismic interpretation	75
4.2	Source rocks	80
4.3	Reservoirs	80
4.4	Seals	84
4.5	Hydrocarbon generation and its timing	85
4.6	Possible play concepts	92
5	Hydrocarbon potential of Area 2	95
5.1	Geological and seismic interpretation	95
5.2	Source rocks	101
5.3	Reservoirs	104
5.4	Seals	105
5.5	Hydrocarbon generation and its timing	105
5.6	Possible play concepts	109
6	Hydrocarbon potential of Areas 3 & 4	111
6.1	Geological and seismic interpretation	111
6.2	Source rocks	116
6.3	Reservoirs	116
6.4	Seals	120
6.5	Hydrocarbon generation and its timing	120
6.6	Possible play types	125
7	Conclusions	127

8	Acknowledgements	129
9	Literature	131
10	Signature	145

Appendices

- A Description of analytical methods
- B Geochemical Database
 - B1 - MS Excel spreadsheet RE_CS_VR (digital file only)
 - B2 - MS Excel spreadsheet GCMS_GCIRMS (digital file only)
 - B3 - Maturity Curves
- C Stratigraphic database
 - C1 - Explanation
 - C2 - Biostratigraphic interpretations (MS Excel spreadsheet)
 - C3 - Stratabugs charts (3 PDF files)
 - C4 - Well lithology plots
- D Construction of well correlation panels
- E Seismic sections (A3-size)
- F Hydrocarbon - source rock correlation
- G Input and parameters for the basin modelling
- H Results and discussion of the 1-D maturity modelling
- I Results of the 3-D basin modelling
- J Maturity maps
- K Gravity modelling of the Netherlands on- and offshore

Enclosure 1 – Well correlation panel Devonian (A0-size)

Enclosure 2 – Well correlation panel Dinantian (A0-size)

Enclosure 3 – Well correlation panel Namurian (A0-size)

1 Introduction

1.1 General

This document reports the result of the Petroplay project. The Petroplay project was a two-year oil & gas exploration research study conducted by TNO in 2004 in 2005 for a Joint Industry consortium consisting of Energie Beheer Nederland (EBN), Gaz de France Production Nederland B.V., Nederlandse Aardolie Maatschappij B.V., Petro-Canada, Total E&P Nederland B.V., Wintershall Noordzee B.V. and TNO itself (in the context of the tasks commissioned to TNO by the Netherlands Ministry of Economic Affairs related to building and maintaining the DINO database of the Dutch subsurface). The objective of the project was to investigate the potential for pre-Westphalian petroleum systems in the Southern North Sea Basin and the Netherlands onshore.

The costs of the project were equally shared between the seven participants. The terms of reference for the project are given in TNO's quotation GE 03-10.078 of April 16th 2003, which includes a detailed project plan ("Development of new pre-Westphalian play concepts in the Southern North Sea Basin"). In addition, a Consortium Agreement was made between all seven parties, dealing with (amongst others) the relationships between the parties in the project and confidentiality matters. The project started on October 23rd 2003. At the start of the project a Steering Committee was established with representatives from each sponsor. The main task of the Steering Committee was to monitor progress of the project. To this end (after a kick-off meeting in The Hague on October 23rd 2003) progress meetings were held in Utrecht on April 22nd 2004, November 18th 2004, May 17th 2005 and October 4th 2005. During these meetings intermediate results were presented to the Consortium and discussions were held on how to proceed. In accordance to the contract a 'go/no-go' decision was asked from all sponsors after the end of the first year. All parties provided their approval to proceed in January 2005. On January 31st 2006 a concluding workshop was held during which the draft report was discussed with the sponsors.

1.2 Petroleum geological background

The Southern North Sea Basin is a mature petroleum province where most petroleum reservoirs are known to be sourced from source rocks of Mesozoic or Late Carboniferous age (predominantly the Lower Jurassic Posidonia Shale Formation for oil and the Upper Carboniferous Westphalian Coal Measures for gas). There are however some indications that pre-Westphalian source rocks may also have contributed to the charging of Carboniferous, Permian and Mesozoic reservoirs (Gerling *et al.*, 1999). Therefore, pre-Westphalian plays may also exist if pre-Westphalian reservoirs are present and other conditions for plays are fulfilled. Only few pre-Permian reservoirs have been drilled to date. In fact, the lower limit of the petroleum fairways is not well established (Cameron and Ziegler, 1997). At this moment this lower limit in the area is defined by gas fields in the Upper Carboniferous (e.g. in UK Quadrants 43/44 region and Netherlands quadrants D and E, Leckie *et al.*, 1995; Cameron and Ziegler, 1997). In addition, there are scarce examples of pre-Westphalian fields. The gas discoveries in block E12 are reported to be in reservoirs of Namurian age and in the United Kingdom

there is the example of the Namurian Welton oil field. In literature, the potential of pre-Westphalian plays in the Southern North Sea Basin has been postulated several times. Within this study the lower limit of the petroleum fairway of the Southern North Sea Basin is taken at the top of the (low-grade metamorphic or igneous) Caledonian basement.

The possible occurrence of pre-Westphalian source rocks in the Southern North Sea Basin implies that hydrocarbon accumulations can be expected in areas where the traditional source rocks are absent. These areas have not been extensively explored. The development of new pre-Westphalian play concepts therefore opens further exploration opportunities in the Southern North Sea Basin.

The Petroplay project used all available released wells from the Netherlands on- and offshore which penetrated sediments of pre-Westphalian age. According to the databases available at the start of the project 7 Dutch wells were supposed to have penetrated rocks of Devonian age (revised interpretations made by the project changed one of these to be of Tournaisian age) and the Dinantian was reached by slightly more wells, but these included a concentration of non-E&P related wells in Limburg. The well data set was supplemented with German, Belgian and UK wells.

1.3 Objectives

The main objective of the Petroplay project was to assess to petroleum geological potential of the pre-Westphalian in the Netherlands on- and offshore. Particular attention was paid to source rocks potential, maturity and timing of hydrocarbon generation. The study used organic geochemical, biostratigraphic and general geological tools. The project aimed at a better assessment of risks related to pre-Westphalian hydrocarbon play concepts in the Southern North Sea Basin and the identification of prospective areas in this basin.

Specific objectives were to:

1. Build a geochemical database of source rock and hydrocarbon samples.
2. Make a stratigraphic framework using available literature, well correlations and biostratigraphic data and reports.
3. Make vitrinite reflectance equivalent maturity-depth plots of the wells.
4. Make maturity maps at a regional scale of the main source rocks.
5. Make tentative depth maps of the top Dinantian and, if possible of other pre-Permian markers, using seismic interpretation and available literature or geological concepts.
6. Develop more insight into play concepts by the interpretation of the available data.
7. Consolidation and dissemination of the results of the project.

1.4 Scope of the work

From the specific objectives a plan of activities was developed which consisted of six work packages. The content of these work packages is described in detail in the Project Plan of 16 April 2003.

In summary these work packages and their main activities consisted of:

Work Package A: Database and geochemical analyses

- Collection of general well, lithological and stratigraphic data from Belgian and German and UK wells that drilled potential source rocks
- Sampling of source rocks from selected wells
- Geochemical analyses of the samples
- RockEval-VI analyses (TOC, Tmax, HI, OI, etc.)
- Vitrinite reflectance on selection of samples
- GC-MS analysis on selection of samples
- GC-IRMS analysis on selection of samples
- Biostratigraphic analyses of samples

Work Package B: Maturity analyses

- Vitrinite reflectance equivalent maturity-depth plots of the selected wells based on new data and review of existing public data on a regional scale, using the geochemical database

Work Package C: Relationships (between samples from source rocks and hydrocarbons).

- Evaluation of existing and new GC-MS and GC-IRMS data

Work Package D: Structural interpretation

- Seismic interpretation with an emphasis on the top Dinantian event
- Specific goals were:
 - Establishing the feasibility of interpreting Lower Carboniferous events
 - Defining areas where top Dinantian is interpretable
 - To make indicative grids or maps of top Dinantian and other Pre-Permian surfaces
 - Backstripping of gravimetric data for both the onshore and the offshore of the Netherlands

Work Package E: Geological interpretation

- Construction of a pre-Westphalian stratigraphic framework which takes into account age determinations, existing lithostratigraphic information and well log correlations
- Investigation of Dinantian and Namurian geology
- 1D maturity modelling of selected wells
- 3D basin modelling (using the PetroMod software) of Areas 1, 2 and 3/4

Work Package F: Evaluation and reporting

- Integration all results in order to evaluate play concepts
- Dissemination of results (final report, including the databases and concluding workshop)

It should be noted that there are minor deviations in this list of activities actually performed, compared to the initial list of foreseen activities in the Project Plan. For example, in the course of the project it became clear that given the available data seismic mapping resulting in grids was not feasible in the onshore Areas 3&4, where both density and quality of seismic data is generally lower. For the onshore areas the project limited itself to a brief seismic screening, correlating the wells. On the other hand, regarding the basin modelling a more ambitious full 3D hydrocarbon generation basin modelling could be performed instead of the anticipated 2D modelling. Such

deviations were discussed with the Steering Committee at the project progress meetings.

The project was executed in two phases. The first phase, which more or less coincided with the first half year of the project, included a lot of data gathering, the first seismic screening (interpretation of a few key lines) and the evaluation of 1-2 key wells per area. It was then decided to execute the second phase according to an "area by area" approach. The four selected areas of interest represent different structural basins, together with their adjacent highs, where the potential to find pre-Westphalian sediments at the right burial depth (in view of required maturity of source rock and preserved reservoir quality) is thought higher than elsewhere.

Figure 1.1 shows the location of these 4 selected study areas. For practical reasons it was decided in the course of the project to merge the work (such as basin modelling) and the reporting of Area 3&4.

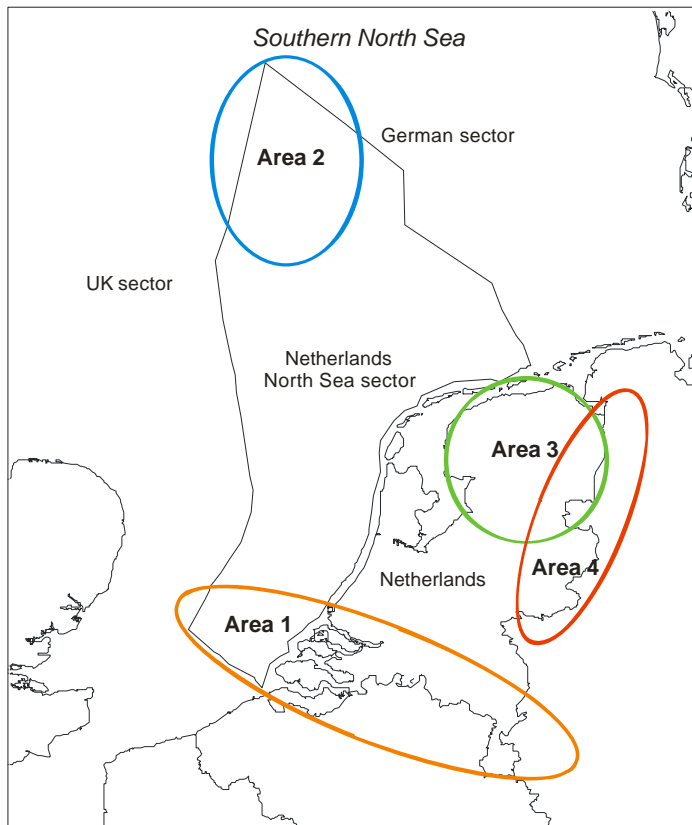


Figure 1.1 The four study areas defined at the start of the Petroplay project

- Area 1** The area north of the London-Brabant Massif (Zeeland Platform) and adjacent area, on- and offshore, including relevant Belgian, German and UK wells
- Area 2** The A, B and northern D and E blocks, offshore
- Areas 3& 4** The north-eastern and east-central part of the Netherlands onshore

"Hydrocarbon potential of the Pre-Westphalian in the Netherlands on- and offshore"

1.5 Overview of well data used for this study

Area	Well Shortname	Well Name	Country	X-Coord (UTM-3)	Y-Coord (UTM-3)	Used for				Total Depth [m]	Stratigraphy at TD
						Geological	Geochemical	Seismic Int.	Basin Mod.		
1	BHG-01	Brouwershavensgat-01	NL	553151	5738103	x	x	x		3024	Devonian
1	EVD-01	Everdingen-1	NL	646059	5758822				x	2196	Westphalian
1	GAG-01	Gaag-1	NL	584982	5756811				x	3659	Westphalian
1	GVK-01	Geverik-01	NL	695318	5645499	x	x			1687	Dinantian
1	HVS-01	Hellevoetsluis-1	NL	580663	5746015				x	3841	Westphalian
1	HEU-01	Heugem-1/1a	NL	691097	5634270	x				503	Dinantian
1	KSL-02	Kastanjelaan-02	NL	688638	5637468	x	x			501	Devonian
1	KTG-01	Kortgene-01	NL	558052	5714032	x		x		1900	Silurian
1	OTL-01	Ottoland-1	NL	629914	5749760				x	3096	Westphalian
1	OVE-01	Overflakkee-1	NL	571490	5736486				x	1800	Westphalian
1	PRW-01	Pernis-West-1	NL	594236	5750010				x	3460	Westphalian
1	RSB-01	Rijsbergen-01	NL	617191	5710124	x	x	x	x	4645	Namurian
1	SPL-01	Schiphol-1	NL	617294	5792987				x	2232	Westphalian
1	WAS-23-S2	Wassenaar-23-S2	NL	593360	5774300				x	3915	Westphalian
1	WDR-01	Woensdrecht-01	NL	677972	5869331			x		1205	Dinantian
1	WOB-01	Woubrugge-1	NL	606604	5780544				x	2751	Westphalian
1	O18-01		NL	494812	5775856	x	x	x	x	3051	Silurian
1	P10-01		NL	510112	5812715		x		x	2696	Westphalian
1	P16-01		NL	511941	5775630	x	x	x	x	2587	Dinantian
1	Q13-03		NL	571721	5796810		x		x	3247	Westphalian
1	S02-01		NL	538347	5756022			x		1800	Westphalian
1	S02-02		NL	541942	5745321	x	x	x	x	2878	Devonian
1	S05-01		NL	538850	5738236	x	x	x	x	2230	Devonian
1	53/12-02		UK	452591	5827161		x			2332	Dinantian
1	124E KB-455	Tournai	B	527646	5605030		x			1271	Silurian
1	125E KB-298	Leuze	B	543651	5604084		x			1536	Silurian
1	16E KB-176	Rijkevorsel	B	620819	5690953		x			1408	Dinantian
1	DZH-01	Heibaart	B	618331	5694359		x				Namurian or older
1	7E KB-205	Meer (Hoogstraten)	B	622400	5700930		x			2515	Namurian
1	95W KB 152	Nieuwkerke	B	486851	5619112		x				Devonian or older
1	KB-120	Turnhout	B	635841	5687707		x			2673	Dinantian
1	KB-131	Halen	B	648245	5645995		x			1339	Dinantian
1	KB-132	Booischoot	B	623494	5656958		x			695	Dinantian
1		Rollegem-Tombroek	B	520293	5622493		x				Dinantian or older
1		's Gravenvoeren	B	694897	5626944		x				Dinantian or older
1		Wervik - Laag-Vlaandere	B	505844	5625256		x				Dinantian or older
1	17W KB-265	Beerse-Merksplas	B				x				Dinantian or older
2	A11-01		NL	535448	6147143		x	x	x	3900	Namurian
2	A14-01		NL	538869	6117385	x	x	x	x	3014	Dinantian (Farne Grp)
2	A15-01		NL	544754	6117561			x		3912	Namurian
2	A16-01		NL	516154	6108805	x	x	x	x	2708	Dinantian (Farne Grp)
2	A17-01		NL	542083	6097329	x	x	x		3044	Caledonian basement
2	B10-02		NL	566940	6133198			x		3972	Dinantian (Farne Grp)
2	D12-03		NL	495885	6021142		x		x	3999	Westphalian
2	D15-02		NL	497858	6014700		x		x	3905	Westphalian
2	E02-01		NL	537296	6091503	x	x	x	x	2595	Dinantian (Tayport)
2	E02-02		NL	523747	6088759		x	x	x	2647	Dinantian (Farne Grp)
2	E06-01		NL	545213	6069481	x	x	x	x	3200	Devonian (Tayport)
2	E12-02		NL	544025	6028262	x	x	x	x	4428	Dinantian (Farne Grp)
2	E12-03		NL	545198	6036716	x	x	x	x	3788	Namurian
2	B10-01		G	574439	6142306		x			3188	Dinantian (Farne Grp)
1	Q/1	Q/1 (renamed G03-01)	NL	583732	5863831	x				3353	Devonian
2	30/16-5		UK	449300	6249563		x				
2	38/16-01		UK	441180	6138184			x			Dinantian (Farne Grp)
2	38/25-01		UK	491312	6127338				x	2216	Devonian (Old Red Grp)
2	38/3-1		UK	471209	6202507	x	x				Devonian (Kyle Group)
2	39/07-01		UK	522243	6178525	x	x	x		3614	Dinantian (Farne Grp)
2	41/20-01		UK	299303	6028229		x				Dinantian
2	41/24a-02		UK	304772	6020802		x				Dinantian
2	42/10-01		UK	368717	6074760		x				Dinantian (Farne Grp)
2	43/02-01		UK	393383	6087443		x			3855	Dinantian (Farne Grp)
2	43/03-01		UK	405182	6094166		x			3614	Dinantian (Farne Grp)
2	43/10a-01		UK	431177	6060838		x				Dinantian
2	43/17b-02		UK	392181	6027202		x				Dinantian
2	43/20b-02		UK	433348	6029837		x			4639	Dinantian
2	44/02-01		UK	460956	6081415		x				Dinantian (Tayport)
2	44/07-01		UK	454969	6073635		x			3047	Dinantian (Farne Grp)
2	44/16-01		UK	442702	6024240		x			4670	Namurian
2	44/16-01Z		UK	442702	6024240		x			4851	Namurian
2	44/16-02		UK	442148	6025817		x			4538	Namurian
2	48/03-03		UK	402793	5975096		x			4591	Namurian

Area	Well Shortname	Well Name	Country	X-Coord (UTM-3)	Y-Coord (UTM-3)	Used for				Total Depth [m]	Stratigraphy at TD
						Geological	Geochemical	Seismic Int.	Basin Mod.		
3&4	AKM-02	Oudega-Akkrum-02	NL	689086	5884779				x	2487	Westphalian
3&4	APN-01	Apeldoorn-1	NL	706533	5790902				x	1553	Westphalian
3&4	BHM-01	Blijham-1	NL	772972	5890743				x	3502	Westphalian
3&4	CLD-01	Collendoorn-01	NL	744846	5832665				x	3135	Westphalian
3&4	COR-01	Corle-1	NL	751222	5764839				x	1284	Westphalian
3&4	COV-10	Coevorden-10	NL	744002	5838358				x	3241	Westphalian
3&4	DAL-07	Dalen-7	NL	756320	5844832				x	4020	Westphalian
3&4	DEW-05	Deurninge-Weerselo-5	NL	761550	5804467				x	2190	Westphalian
3&4	DRO-01	Dronten-1	NL	690631	5819702				x	3504	Westphalian
3&4	DWL-02	Dwingelo-2	NL	726287	5858931				x	3797	Westphalian
3&4	EMM-07	Emmen-7	NL	759168	5855149				x	4364	Westphalian
3&4	EMO-01	Emmeloord-01	NL	689532	5844252	x	x	x	x	2548	Namurian
3&4	GEL-01	Gelria-1 (Lichtenvoorde)	NL	750052	5768004				x	1017	Westphalian
3&4	GLH-01	Goldhorn-1	NL	772154	5902026				x	4498	Westphalian
3&4	GRL-01	Grolloo-1	NL	748538	5872052				x	4652	Westphalian
3&4	HAR-01	Haren-1	NL	742702	5897720				x	3489	Westphalian
3&4	HAW-01	Harlingen West-1	NL	653205	5892526				x	3348	Westphalian
3&4	HGL-01	Heiligerlee-1	NL	766446	5897369				x	2900	Westphalian
3&4	HGV-01	Hengeveide-1	NL	749644	5789259				x	1500	Westphalian
3&4	HKS-01	Haaksbergen-1	NL	752591	5786814				x	1008	Westphalian
3&4	HLD-01	Hellendoorn-1	NL	731613	5809431				x	1493	Westphalian
3&4	HRL-01	Harlingen-1	NL	663732	5890699				x	3103	Permian (Rotl. Grp)
3&4	JPE-01	Joppe-1	NL	721134	5788380				x	1495	Westphalian
3&4	KLH-01	Kloosterhaar-1	NL	748835	5824453				x	2670	Westphalian
3&4	LUT-06	De Lutte-6	NL	773454	5805532				x	3206	Westphalian
3&4	NAG-01	Nagele-01	NL	685417	5833615	x	x	x	x	4303	Namurian
3&4	NOR-01	Norg-1	NL	731132	5886143				x	3330	Westphalian
3&4	NSL-01	Nijensleek-01	NL	711822	5859079				x	2327	Westphalian
3&4	PLG-01	Plantengaarde-1	NL	758889	5763058				x	1134	Westphalian
3&4	RAT-01	Ratum-1	NL	761471	5765065				x	1380	Westphalian
3&4	RAW-01	Radewijk-1	NL	751024	5831239				x	3046	Westphalian
3&4	RLO-01	Ruurlo-1	NL	738805	5776870				x	1503	Westphalian
3&4	ROT-01-S1	Roode Til-1 St1	NL	762457	5901209				x	2805	Westphalian
3&4	SLO-01	Slochteren-1	NL	751722	5898016			x		2709	Permian (Rotl. Grp)
3&4	TBR-01	Ten Boer-1	NL	743127	5907672				x	2890	Permian
3&4	TJM-02	Tjuchem-2	NL	759174	5909576	x	x	x		6011	Namurian
3&4	TJM-02-S1	Tjuchem-2 St1	NL	759174	5909576				x	5815	Namurian
3&4	TUB-08	Tubbergen-8	NL	764491	5817114				x	3206	Westphalian
3&4	VLV-01	Veelerveen-1	NL	779097	5887227				x	4191	Westphalian
3&4	WDV-01	Annerveen-Wildervank-1	NL	755549	5889425				x	3186	Westphalian
3&4	WSK-01	Winterswijk-1	NL	753924	5759441	x	x	x	x	5010	Devonian
3&4	ZBR-01	Zuidbroek-1	NL	759624	5897550				x	3780	Westphalian
3&4	ZED-01	Zeddam-1	NL	725514	5755938				x	1965	Westphalian
3&4	ZEW-01	Zeewolde-1	NL	672990	5825466				x	2000	Westphalian
3&4	ISSB-03	Isselburg-3	G	743631	5734641			x		4367	Devonian
3&4	MSTL-01	Munsterland-01	G	789785	5770339	x	x			5956	Devonian
3&4	SWLT-1001	Schwalmtal-1001	G	731572	5681080			x			Dinantian

1.6 Confidentiality of this report

The contract for the Petroplay study states that the results of the study will remain confidential for a period of 5 years from the start of the project. This means that after October 23rd 2008 the contents of this report will no longer be considered as "company confidential".

2 Pre-Westphalian geological setting of the Netherlands

The first part of this chapter gives a broad overview of the general geological history from Cambrian to Namurian times, including the plate tectonic context and the depositional aspects, with a specific focus on features relevant to the distribution of potential source rocks and reservoir rocks. In the second part of this chapter a stratigraphic subdivision of the Dinantian and Namurian is introduced, consisting of six stratigraphic units. Based on these units a set of conceptual lithological distribution maps was made for two separate scenarios. These distribution maps were input to the 3D basin modelling described in Appendix I.

2.1 Stratigraphic standards

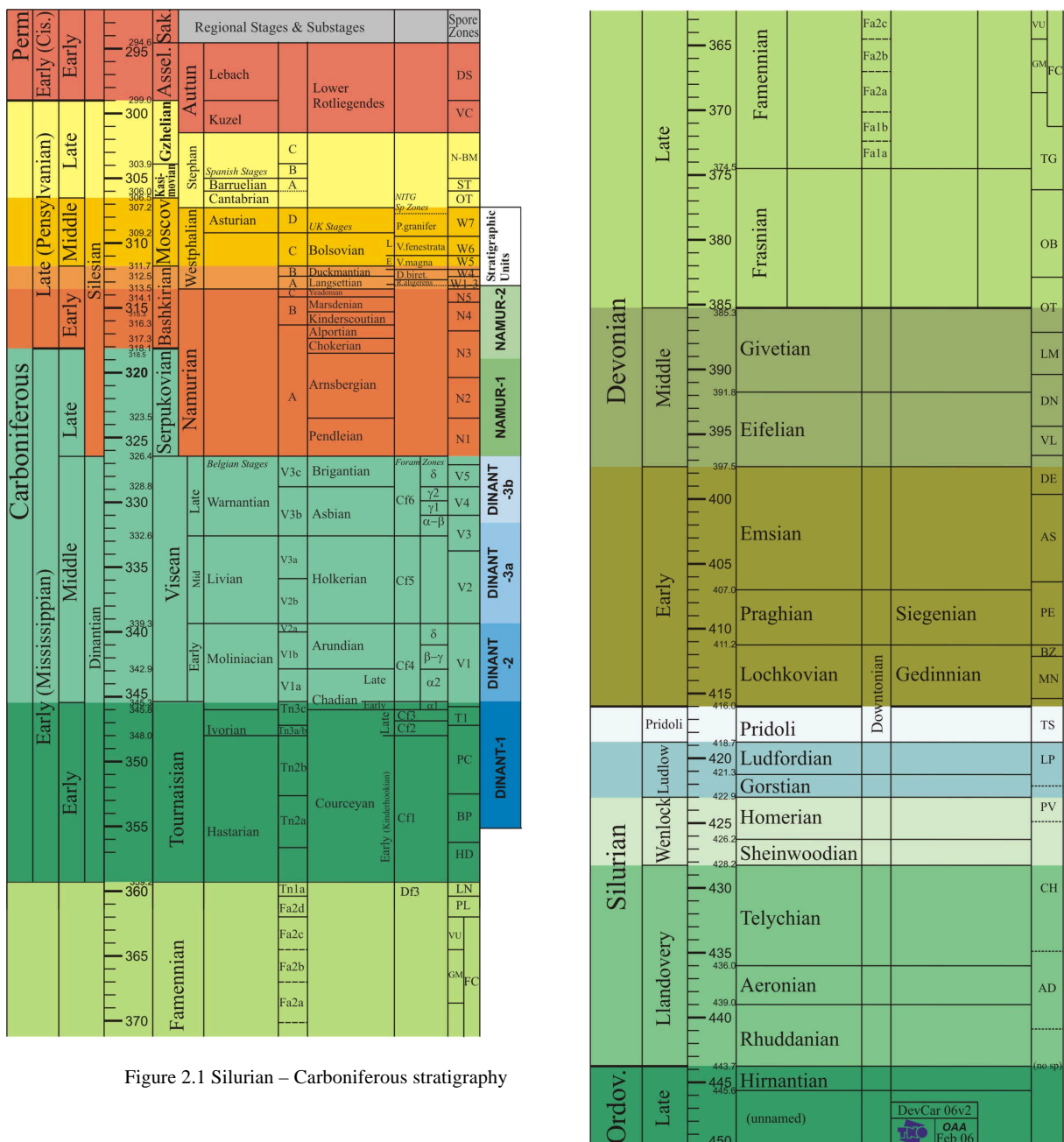


Figure 2.1 Silurian – Carboniferous stratigraphy

Figure 2.1 shows the general stratigraphic chart for the Silurian, Devonian and Carboniferous with regional stages and substages. The chronostratigraphy of the wells used for the age interpretation has been updated in this project. The underlying information for Figure 2.1 is given in Appendix C1. The stratigraphic framework commonly used in the Netherlands is the Stratigraphic Nomenclator (Van Adrichem Boogaert and Kouwe, 1993-1997). The Devonian and Carboniferous part is shown in Figure 2.2. Since this is a lithostratigraphic framework it has the disadvantage that the diachronous units cannot easily be correlated from one part of the basin to the other.

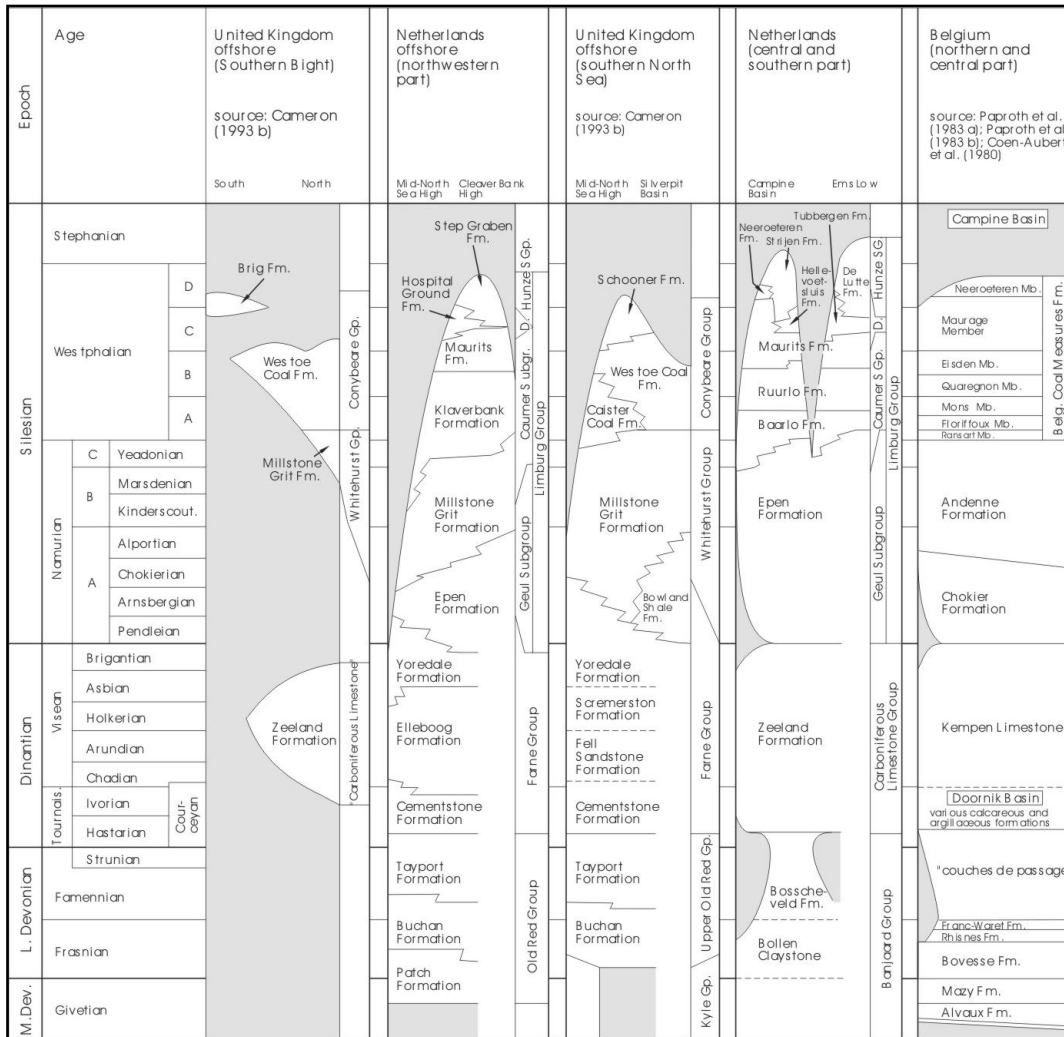


Figure 2.2 Regional lithostratigraphic correlation chart of the Devonian and Carboniferous (from Van Adrichem Boogaert and Kouwe, 1993-1997)

Because the Petroplay project had to cover the entire Netherlands on- and offshore and also used well information from three neighbouring countries, it was decided to work with a stratigraphic framework which was largely driven by chronostratigraphic data, but also supported by well log correlations. This framework used the age interpretations of the selected wells (for details: Appendix C).

2.2 Geological history with notes on source rock and reservoir rock development

There is little data on the Early Paleozoic (and Late Precambrian) history of area of interest, consisting of The Netherlands onshore and the adjacent Dutch part of the Southern North Sea (SNS). There are no Lower Paleozoic outcrops and the oldest sedimentary rocks drilled by wells are not older than Silurian. Based on data from other areas (e.g. UK, Baltic Shield) and on literature compilations (Ziegler 1978, 1990, 1991; Glennie, 1998, 2005; Cameron and Ziegler, 1997; Cocks & Torsvik, 2005) a general picture can be obtained. Most authors (Ziegler 1978; Besly 1998; Coward 1993) agree that the dominant events during the Paleozoic, responsible for the overall tectonic framework, are the Caledonian (550-400 Ma) and Variscan (400-300 Ma) orogenies. Coward (1993) also suggests that already Middle and Late Proterozoic tectonic events, namely the Laxfordian and Svecofennian (1800-1600 Ma), and the Grenville (1100-900 Ma) episodes respectively, influenced the later tectonic framework, leaving structural features in the basement rocks. The description given here is based on an amalgamation of the sparse field data together with these literature datasets.

2.2.1 Precambrian - Ordovician

The area of interest (including the present day Netherlands) probably came into existence as terrain accretion on the Iapetus Ocean margin of the supercontinent Rodinia. The process of closure of the Iapetus Ocean and the resulting structural framework were very important in defining the structural configuration of basins and highs and the subsequent depositional patterns during the Devonian and Carboniferous (Glennie, 2005).

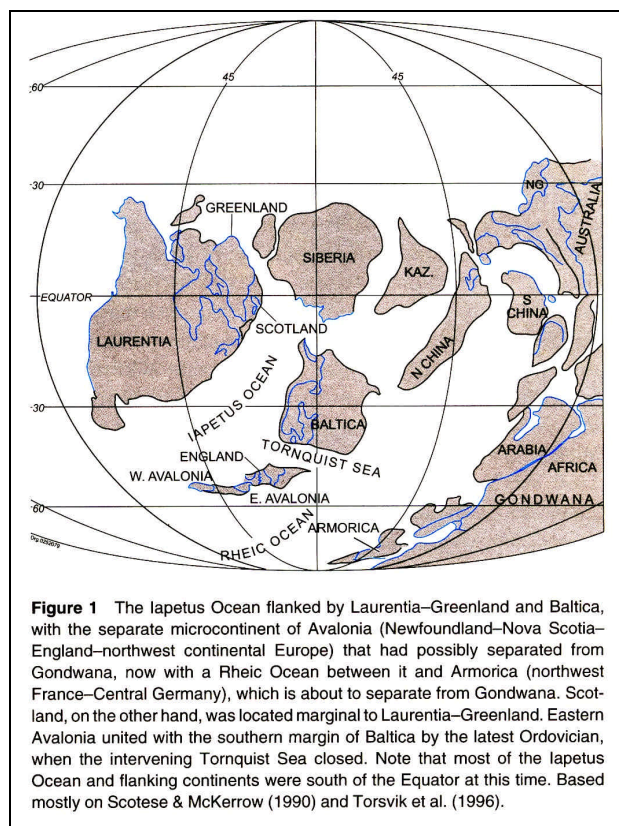


Figure 2.3 Plate tectonic configuration before the Caledonian orogeny (from Glennie, 2005)

At the end of the Precambrian, Rodinia fragmented into separate plates (Pannotia, Angara (Siberia), and North China). During the latest Precambrian Pannotia fragmented in turn into the continents of Laurentia, Gondwana, and Baltica (Figure 2.3). The area of interest remained, as part of the “northern” margin of Gondwana, submerged and probably accumulated sediment (Figure 2.4). This would imply that most of the deep basement consists of Late Precambrian - Ordovician (metamorphic) rocks.

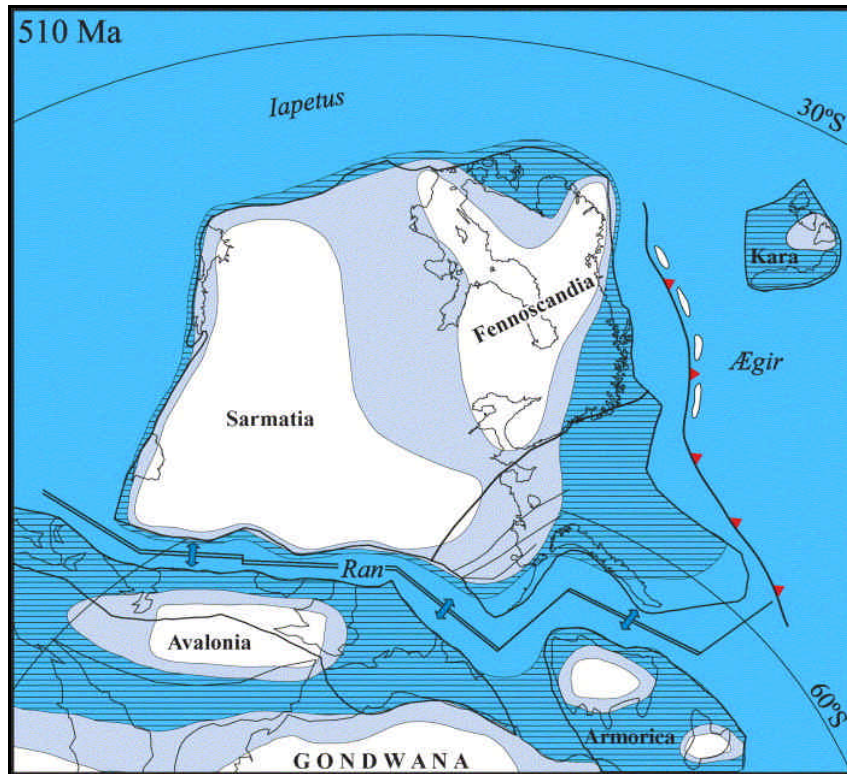


Figure 2.4 Late Cambrian palaeogeography (after Cocks & Torsvik, 2005). The Baltic plate consisted of Sarmatia (European Russia) and Fennoscandia. The area of the later Central and Southern North Sea and the Netherlands onshore belonged to the northern margin of Gondwana and can be seen as the (north)eastern margin of Avalonia. Note that the Baltic plate must have made a rotation of almost 180 degrees after the Late Cambrium

The Cambrian Alum Shale represents an important pre-Permian source rock in Northern Europe and the Baltic States (Gérard *et al.*, 1993). Based on the paleogeography, it is unlikely that this shale has been deposited in The Netherlands. The Alum Shale area was located on the North side of Fennoscandia (Figure 2.4), while the area of interest was located on its south side (Figures 2.3 and 2.4). In any case, if there would be any Cambrian source rocks present in the southern part of The Netherlands or the adjacent North Sea, they are expected to be over mature as a result of later deformation phases and the thick overburden.

The next phase in tectonic evolution of the area was the detachment of Avalonia from Gondwana in the Early Ordovician. Our area of interest formed the eastern part of Avalonia which ranged from the Appalachians of the USA and Maritime Canada (West Avalonia) via the southern UK and Ireland to northwest Germany and south Denmark (East Avalonia). This microcontinent gradually moved northwards until it collided with the Baltic plate.

2.2.2 Silurian

During the Late Ordovician - Early Silurian the collision of East Avalonia with the SW part of Baltica resulted in a suture which passes through the middle of present day Denmark. This collision implied the closure of the Tornquist Sea (Figure 2.3). It is suggested that the trends of basins and faults parallel the Tornquist suture line (Figure 2.5). Possibly, the metamorphic basement underlying the Devonian Old Red deposits in the northern offshore was formed during the Silurian. During the Early and Middle Silurian the area was situated on a continental shelf with a landmass to the west and the Rheic Ocean to the southeast (Figure 2.5). Clastic sediments were deposited in a general west-east trend. Silurian rocks comprise the oldest sedimentary rocks in the Netherlands. In wells O18-01 and Kortgene-1 dark, turbiditic claystones and sandy claystones of possibly Middle Silurian age are found near the final depths. The dark colour of the Silurian rocks and the common lack of bioturbation indicate initially high TOC values. The Silurian deposits are probably overmature throughout the southern part of The Netherlands. However, they may not be overmature in the northern part of study area. On the stable Midland Massif in the UK part of the London-Brabant Massif Silurian rocks are not over- mature (Cameron and Ziegler, 1997).

During the Middle - Late Silurian the Iapetus Ocean closed and Baltica/Avalonia collided with Laurentia (the Late Caledonian orogeny). This probably ended all sedimentation in the Netherlands until Middle Devonian times. The Iapetus suture and the Tornquist suture remained as important lineaments for later tectonic development. The NW-SE trending wedge between Laurentia and Baltica may be seen as a predecessor of the Dutch Central Graben. Also part of the Caledonian orogeny is the simultaneous collision of Armorica with Avalonia in the south, causing the formation of the London Brabant Massif (LBM). From the Late Silurian onwards, the LBM would form a relatively rigid structural high, with very little sediment accumulation.

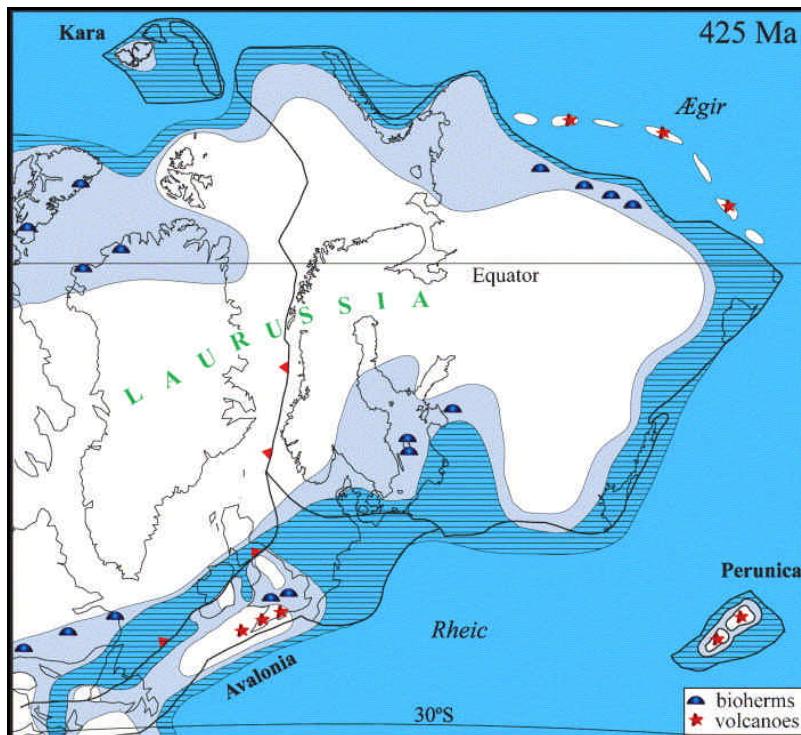


Figure 2.5 Middle Silurian paleogeography. Note the direction of the Tornquist and Iapetus suture lines (after Cocks & Torsvik, 2005)

In summary, the whole Caledonian orogeny from the Cambrium to the Early Devonian can be seen as a process of closure of the Iapetus Ocean by the accretion of magmatic island arcs and old continental fragments onto the North American (Laurentian) continental craton, in a dominantly NW direction. In addition to the main orogenic belt, a branch running from southern Norway through the central Southern North Sea (SNS) connects to the Caledonides of north Germany and Poland (Figure 2.6) and a third branch further south, called the Mid-European Caledonides, links the German Caledonides and the Ardennes to the British Isles (Ziegler, 1978). From such a plate-tectonic model it would thus appear that two Caledonian structural grains (NE-SW and N-S to NW-SE respectively) are relevant to the later SNS Carboniferous Basin. This seems to be confirmed by the pre-Carboniferous modelling of gravity and magnetic data of the southern North Sea by Horscroft *et al.* (1992), which revealed the same trends. When considering the Carboniferous basin-bounding faults and their underlying basement grain, Corfield *et al.* (1996) distinguished three different structural domains in and around the British Isles, each of them having their own local dominant basement lineament. The Southern North Sea would be within the Tornquist Domain, with a dominant NW-SE structural grain inherited from the Lower Paleozoic thrust and fold belt. The low-grade metamorphic basement to the later Carboniferous deposits was intruded by numerous post-orogenic late-Caledonian plutons (Ziegler, 1978). One of these granites has been drilled in Dutch well A17-01. This pluton was recently dated again (pers. comm. BGS), yielding a new age of 410 ± 8 Ma (Earliest Devonian).

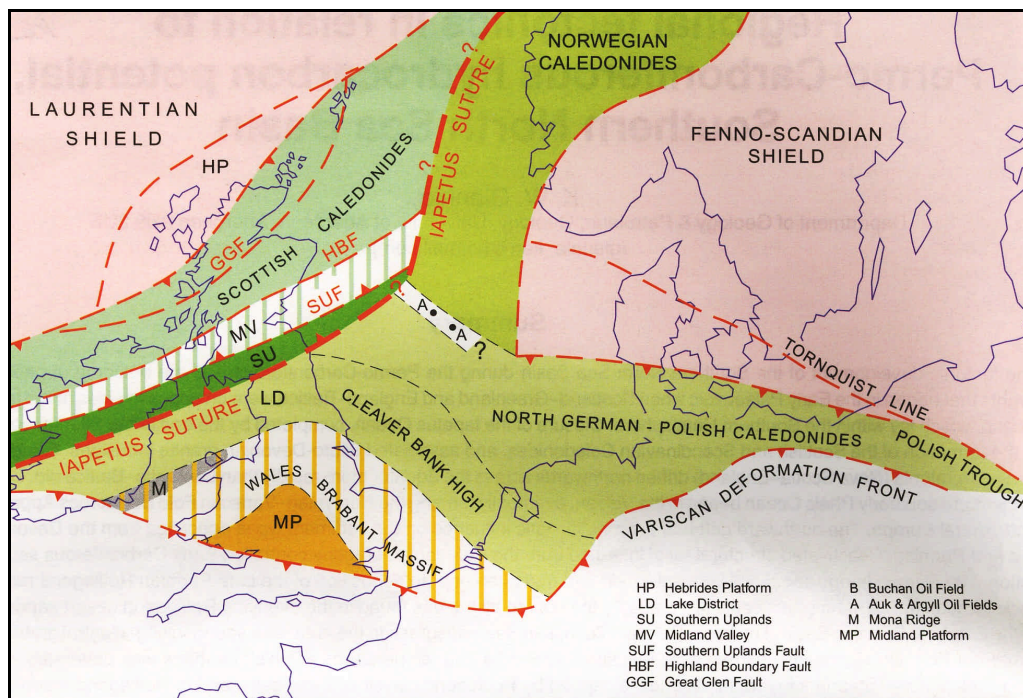


Figure 2.6 Plate tectonic setting after the end of the Caledonian orogeny (from Glennie, 2005)

2.2.3 Devonian

By the start of the Devonian the area including the present day Netherlands was more or less established as an intra-plate area. It was affected by the Early Devonian uplift, the last episode of the Caledonian orogeny. During the Middle Devonian first predominantly terrestrial and later marine sediments were deposited. The areas of deposition probably followed the old oceanic sutures to the northeast and northwest. In

the course of the Devonian the sea transgressed from the southeast to the north across the easternmost part of the London-Brabant massif, but also into the central part of the Southern North Sea through a branch of the Rheic Ocean coinciding with the old Tornquist suture (Figure 2.7). In the northernmost part of the Petroplay project study area (the Dutch A and northern E blocks) the presence of shelf carbonates of the Kyle Group, as found in the UK Auk and Argyll fields (e.g. well 30/16-5) and in nearby well 38/3-1 (Marshall & Hewett, 2003; Glennie, 2005) is interpreted from seismic data (see also Appendices E6, E7, E8 and E10). Of the wells available to the Petroplay project the German well Munsterland-01 to the southeast shows a limestone section of Givetian age (Enclosure 1).

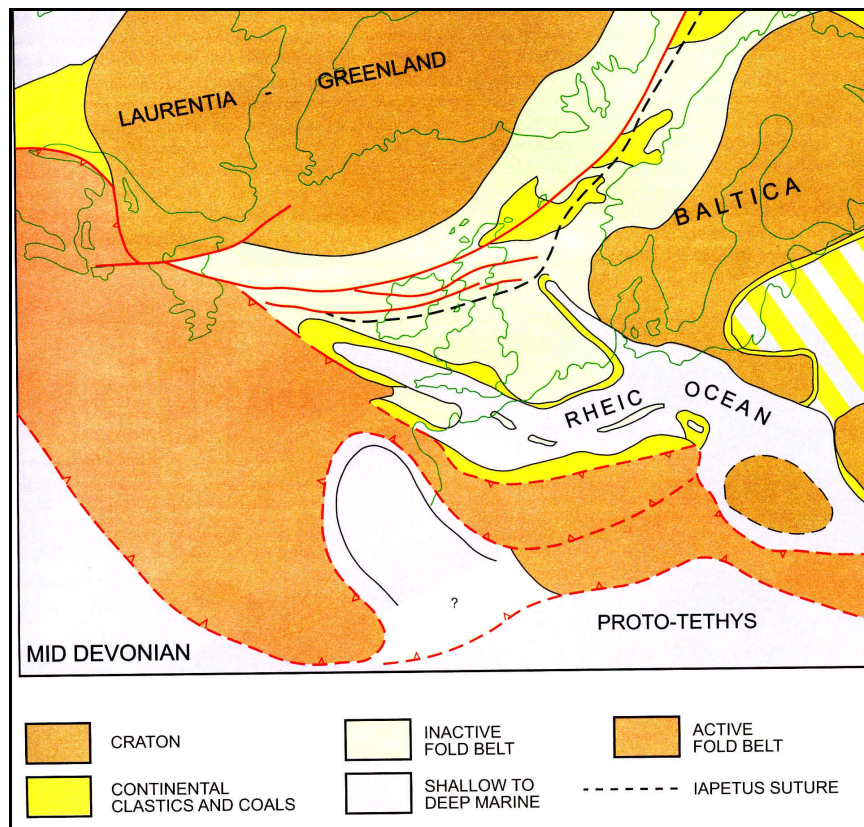


Figure 2.7 Mid-Devonian paleogeographic map. The Devonian Old Red continent covered eastern Laurentia-Greenland, present day England, Scotland and Scandinavia. A NW-SE trending branch of the Rheic Ocean coincided with the old Tornquist suture. In it Mid-Devonian limestones were deposited. (from Glennie, 2005)

Mid Devonian sediments were deposited under relatively quiet conditions, which suggest that they may have source rock potential (Figures 2.7 and 2.8). The Mid-Devonian Kyle Group consists of a sequence of limestones, carbonates, evaporites and mudstones. Cameron (1993) distinguishes in the Kyle Group a limestone dominated unit K1 unit, overlain by a mudstone dominated unit K2. Seismic data indicate that the Kyle group may be present over a wider area of the (proto-)Central Graben (Marshall & Hewett, 2003). The Devonian has been drilled in the northern Netherlands offshore in wells A17-01 and the E06-01. In the German offshore territory, east of the F-blocks, the Devonian was penetrated by well Q/1 (also known as G03-01). In this well, located on the eastern North Sea High, 738m of Devonian (Old Red facies), overlies the crystalline basement. It consists of siltstones alternating with fine- to coarse grained sandstones and some conglomerate beds, all predominantly red. Between 3616 and 3777m

numerous marine fossils were encountered indicative for Early to Middle Devonian age. This shows that during this period marine influences extended far northward into the Old Red facies realm (Best *et al.*, 1983). The Rotliegendes directly overlies the Devonian in well Q/1 (Best *et al.*, 1983).

In the south of the Netherlands on- and offshore it was thought that the Devonian was reached in several wells (O18-01, S02-02, S05-01, Brouwershavense Gat-1 and Kortgene-1). In O18-01, Brouwershavense Gat-1 and Kortgene-1 it is our interpretation that rocks of Middle Silurian age are probably present. The overlying shales are still interpreted as (Late) Devonian, although very little (bio)stratigraphic evidence is present. Devonian was reached in the onshore of Zuid-Limburg (Kastanjelaan-2, Van Adrichem-Boogaert and Kouwe, 1993-1997). It is uncertain when and where sedimentation resumed following the final Late Caledonian deformation phase in this area. Since the lower Dinantian is also missing in some wells (e.g. O18-01 and S05-01) there can be two possibilities. First, it is possible that there is no Devonian present in the SW part of the Dutch on- and offshore. Alternatively, it is also possible that there is an additional hiatus between the Upper Devonian and the Dinantian, which may be related to the latest phase of the collision between Iberia and the Armorica terrain in Middle and Southern Europe.

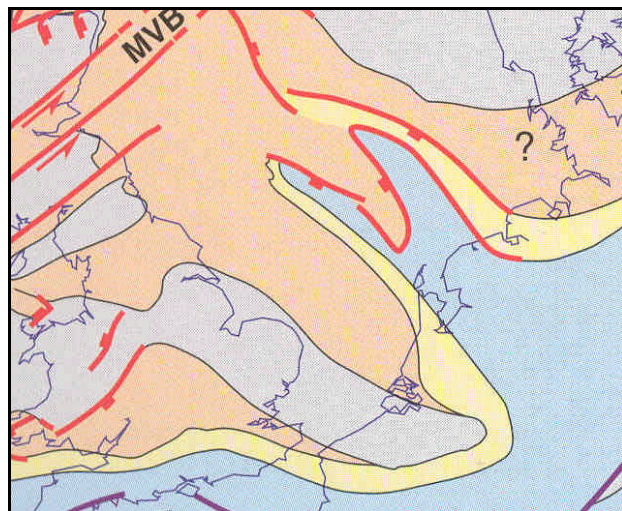


Diagram a

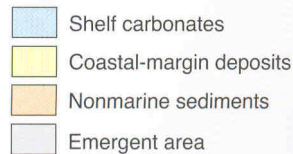


Figure 2.8 Palinspastic map of active structures and sediment facies during the Mid-Devonian (from Marshall & Hewett, 2003)

During the Late Devonian, the sea retreated from the present-day North Sea area, resulting in the continued deposition of continental red-bed facies, the Old Red Group. Locally, in the area of the Elbow Spit high, acid volcanism occurred. The rhyolite found in the Buchan Formation in well A17-01 (from 2157 – 2296m) was dated at 341 ± 30 Ma (Sissingh, 2004). Marine conditions persisted in the eastern part of the London-Brabant Massif area. The latest Devonian experienced a period of falling sea level. Locally, regressive clastics and carbonates (e.g. the Bosscheveld Formation, if indeed Late Devonian) were deposited and preserved (Van Adrichem Boogaert and Kouwe,

1993-1997). Further to the south and east sandstones (such as the Condruz Sandstone) were deposited by long-shore currents during the late Famennian in the sea that bordered the Old Red continent and the (partially) emergent London-Brabant Massif (Paproth *et al.*, 1986).

By the end of the Devonian the area north of the future Variscan deformation front (including the SNS and the onshore Netherlands) showed the characteristics of a relatively stable plate, until during the last part of the Devonian a purely extensional rifting phase started. It has been observed (Leeder & Hardman, 1990) that some of the structural highs of this rifting phase seem to have one of the Late Caledonian plutons as a core.

2.2.4 *Dinantian*

The dominant structural grain associated with the Late Devonian – Early Carboniferous tectonic extension became east-west in the British onshore, bending to SE-NW in the SNS and the Netherlands (Besly, 1998). Fraser & Gawthorpe (1990) noted that during the late Devonian rifting phase the north-south extensional stress regime reactivated both the NW-SE and the NE-SW trending zones of weakness, which had been inherited from the Caledonian orogeny. Strongly asymmetric grabens were formed. East-west trending basins have been well described on the British onshore (e.g. Soper *et al.*, 1987; Fraser & Gawthorpe, 1990; Hollywood & Whorlow, 1993). The extension is put into the context of a back-arc basin (Leeder, 1982), which related to the northwards directed subduction, closing the Rheic Ocean. Hundreds of kilometres to the south the Variscan orogenic belt had become the dominant expression of a new collision system. The African portion of Gondwanaland started to collide with the European portion of Laurussia, but this only started to affect the area of interest in the Late Carboniferous. It has been argued (e.g. Maynard *et al.*, 1997) that a simple two-phase tectonic model for the Carboniferous basin evolution consisting of a back-arc related north-south extension followed by a thermal sag phase (starting in the Namurian) appears to be oversimplified.

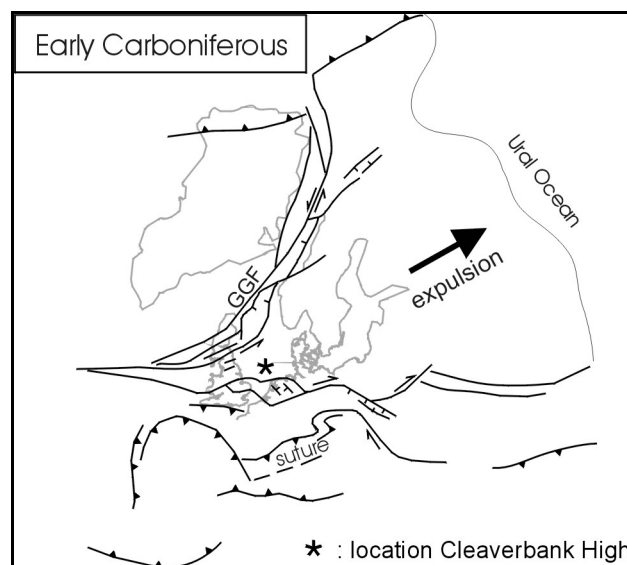


Figure 2.9 Simplified Early Carboniferous tectonic map illustrating the continental expulsion of the North Sea - Baltic block, implying dextral transtension along the shear zones of its southern boundary (after Coward 1993)

Coward (1990 and 1993) proposed a regional model which involves escape tectonics of a triangular plate fragment named the North Sea-Baltic block, comprising the present North Sea area, the Baltic area, and most of Britain and Scandinavia. During the Devonian and Early Carboniferous this block would have been squeezed out in an eastward direction from the colliding plates of Gondwanaland and Laurentia (Figure 2.9). The implications of this model obviously are important strike-slip components in the movements. The prevailing stress regime would have been dextral transtension along the southern boundary of the block (close to the southernmost part of the North Sea area) and sinistral transtension along the northern systems such as the Great Glen fault. The release from the interior also allowed the block to expand in the NW-SE direction. Maynard *et al.* (1997) subscribe to this escape tectonics model to a large extent, but mention N-S extension within the plate (also due to the release of the confining forces as the block moved eastwards). They noted that the configuration in the Early Carboniferous may have been quite similar to what can be observed today in the eastern Mediterranean, where the Turkish and Greek plates are in a process of westward translation. A detailed 3D seismic interpretation of the Cleaver Bank High showed the presence of dominant east-west shearzones that are not always visible at first glance, because they have been frequently reactivated throughout the Paleozoic and Mesozoic (Schroot & de Haan, 2003). These zones and the observation of strike slip movements along them fit the model proposed by Coward.

The Dinantian basin was delineated by the Mid North Sea-Ringkøbing-Fyn high to the north and the London Brabant Massif to the south (Gerling *et al.*, 1999). Whether the majority of the sub-basins were symmetric grabens or half-grabens is a matter of discussion (Gawthorpe, 1987). During the Dinantian much of Europe was characterised by the development of platform carbonates and deep marine shales and chert layers in areas of low clastic input (Bless *et al.*, 1976; Cameron *et al.*, 1992). Areas in the vicinity of clastic sources were dominated by shallow deltaic, deep-water deltaic and turbidite deposition. Many of the major late Palaeozoic basins in other parts of the world are characterised by a similar structural and depositional history.

The structural setting during the Early Carboniferous had important effects on Dinantian deposition. The highs were preferential sites of carbonate-platform deposition. The lineaments of these highs followed the old Iapetus and Tornquist sutures. The flanks of the London-Brabant Massif constituted such highs and possibly a 'proto-Texel-IJsselmeer High' and the Cleaverbank high (Cameron & Ziegler, 1997) did so too (Figure 2.10). The platform carbonates typically show deepening-upward trends. Early Dinantian carbonate deposition occurred in shallow water. Accelerated tectonic subsidence through the course of the Early Carboniferous resulted in progressively deeper water facies (Bless *et al.*, 1976). Consequently the margins of carbonate platforms were becoming steeper through time. The carbonate platform successions are locally characterised by levels of karstification. Certain areas on the London Brabant Massif were repeatedly karstified due to long-term emergence, e.g. in South Limburg (Wells Heugem-1/1a & Kastanjelaan-2; Bless *et al.*, 1981) and in the Namurian Basin of the Ardennes.

We have subdivided the Dinantian into three main chronostratigraphic units, called Dinant-1, -2 and -3, and corresponding approximately to the Tournaisian, the Late Chadian-Arundian and the Holkerin-Asbian-Brigantian respectively. This division can be followed from the calcareous deposits in the south (Zeeland Formation) to the clastic

deposits in the North (the Tayport, Cementstone, Elleboog and Yoredale Formations). The transitions can be followed e.g. in wells E02-01 & E06-01 (in the north) - O18-01 & S02-02 (in the south). The lithology of the two areas differs significantly, with limestones in the south and predominantly clastics in the north. However, log patterns show time equivalent changes in lithological character. The Tournaisian interval is often missing, or only partly developed (e.g. in wells Brouwershavense Gat-1, S02-02 and S05-01). The upper interval is occasionally missing implying an unconformity between the Dinantian and the Namurian sequences (e.g. well Brouwershavense Gat-1).

Carbonates from Dinantian outcrops across Western Europe have been intensely studied. These carbonates developed on structural highs. In general, deposition failed to keep up with the rapid subsidence of basement blocks. This caused the progressive shift from shallow-water ramp deposition to deeper-water steep-margined platform deposition (Gawthorpe, 1987). Locally deeper-water environments were occupied by so-called Waulsortian build-ups; these structures are mud mounts with initial vuggy porosity (Lees & Miller, 1985; Lees *et al.*, 1985; Poty, 2001). In places the carbonate system was drowned near the end of the Visean when carbonates were overlain by shale, organic-rich shale and chert (Bless *et al.*, 1976). In the northern part of the basin, sediments were deposited in a fluvial/deltaic to shallow marine setting (a marginal deltaic facies): the Yoredale deposits (Gerling *et al.*, 1999; Cameron *et al.*, 1992). In the Dutch North Sea sector these sequences are referred to as the Yoredale and Elleboog Formations belonging to the Farne Group. Their age ranges from Chadian to Pendleian (Van Adrichem Boogaert and Kouwe, 1993-1997; this study). These clastic deposits had a northerly source.

Equivalent sediments in northern England comprise stacked sequences of Yoredale cycles (e.g. Maynard & Dunay, 1999), which by Brigantian times were being deposited from the England/Scotland border to at least as far south as the Tees estuary (Leeder, 1982). Yoredale deposition continued through the Pendleian into the early Arnsbergian across most of northeastern England and persisted into the Kinderscoutian (Middle Namurian) over the Alston Block (Ramsbottom *et al.* 1978). Wells have encountered the unit in Quadrants 41, 42 and 43, and on the north-eastern flank of the Mid North Sea High.

In the UK part of the Southern North Sea the Yoredale Formation rests on late Dinantian coal measures (the Scremerston Formation). Its base has not been penetrated elsewhere, but it may rest locally on Asbian platform carbonates, similar to the situation in the onshore Alston Block, or on basinal marine sediments as in the Stainmore Trough. The Yoredale Formation is either conformably overlain by basinal mudstones or deltaic deposits of the Whitehurst Group, or unconformably overlain by Permian strata. In the Dutch sector, the Yoredale Formation of Asbian to Brigantian age characteristically contains numerous thin beds of marine limestone within deltaic deposits (Van Adrichem Boogaert and Kouwe, 1993-1997; Lithostratigraphic Nomenclature of the U.K. North Sea).

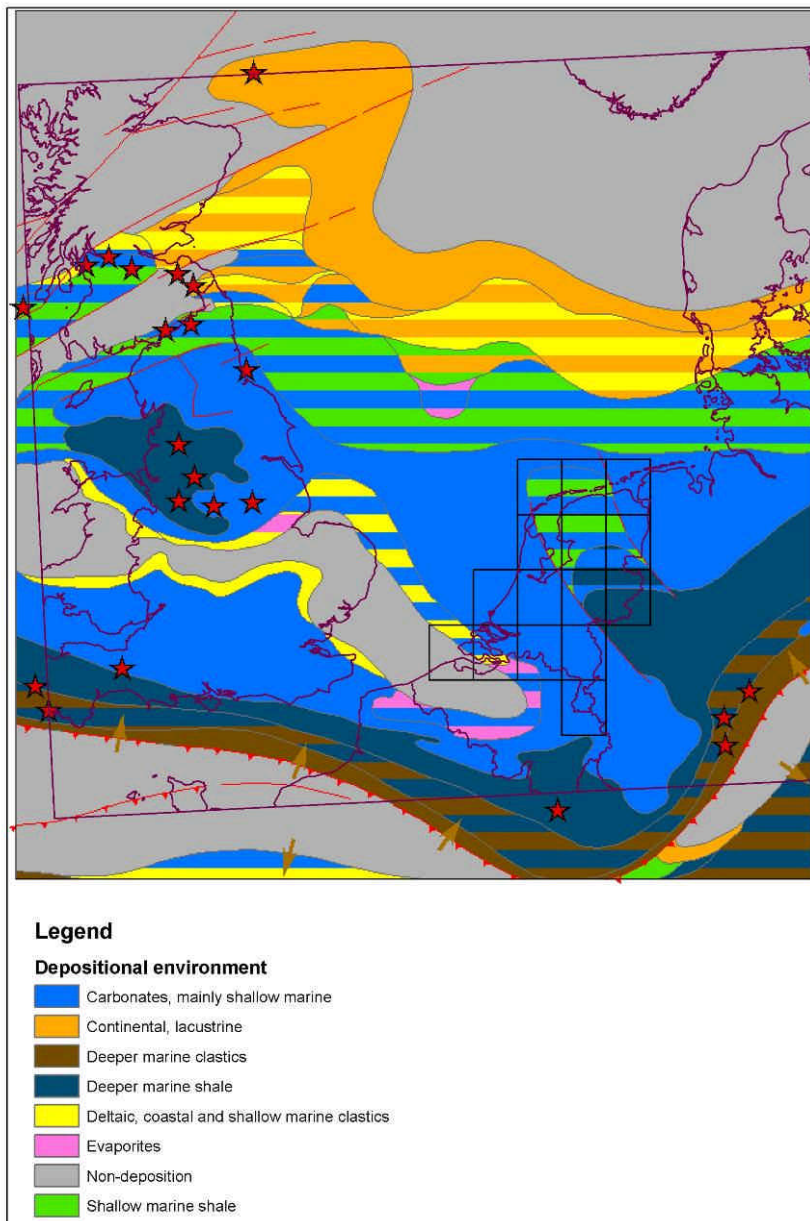


Figure 2.10 Paleogeographical map of the Dinantian depositional environments; after Ziegler (1990)

Within the Yoredale succession thin coal seams occur. Organic matter is of Type III kerogen, with TOC contents generally between 0.89 and 1.87 % (Gerling *et al.*, 1999), but locally almost up to 9% (Graf Pannatier *et al.*, 2000). Although transgressive cyclothems with marine influences at the base could be clearly recognised, there are no marine oil prone source rocks in these deposits.

Little is known about the time-equivalent sediments of the Southern North Sea away from the immediate extensions of the onshore highs and platforms (Cameron & Ziegler, 1997). In the central part of the basin no wells have reached the Dinantian (Gerling *et al.*, 1999). Seismic surveys suggest that a broad, rift-induced basin is present containing a thick sedimentary infill probably of Namurian age (e.g. Dutch wells Nagele-1, Tjuchem-2). Most of the study area is underlain by an extensive carbonate platform,

stretching from the UK to NW Germany (Gerling *et al.*, 1999). Quirk (1997) has interpreted on 2D seismic data basinal carbonates on the Cleaver Bank High in the Netherlands offshore. Intra-platform basins are known from central England (e.g. Northumberland, Stainmore, Cleveland, and Widmerpool basins), but they may well exist in other places in the southern North Sea (Gerling *et al.*, 1999). Maynard and Dunay (1999) interpreted a block and basin structure in the SNS, with some of the blocks being underpinned by granites. This block and basin structure was earlier postulated by Collinson *et al.* (1993) and observed onshore UK (Fraser and Gawthorpe, 1990).

Figure 2.10 shows the anticipated position of the basins in relation to the surrounding carbonate platforms and the southward prograding Yoredale delta (Ziegler, 1991). In the Netherlands offshore, the Yoredale facies is present on the Elbow Spit High, whereas on the Cleaver Bank High most of the Upper Dinantian is expected to consist of Visean limestones, due to minimal terrestrial input (Figure 2.11). Using the regional 2D seismic data of the 1980s it was not possible to confirm this hypothesis in the current project. The major part of the basin between the Elbow Spit and Cleaver Bank Highs and the London Brabant Massif was geographically remote from the Yoredale delta. Anoxic bottom conditions are expected to have existed in this area, at least part of the time (Cameron & Ziegler, 1997). Therefore, these basins probably were the sites of deposition of shales, organic-rich shales and chert layers that have developed on top of drowned platforms. Black shales with oil-generating potential have been observed in several parts of the Variscan foreland, mainly at the base of the Namurian (Cornford, 1998). Similar shales may be present within the Dinantian sequence.

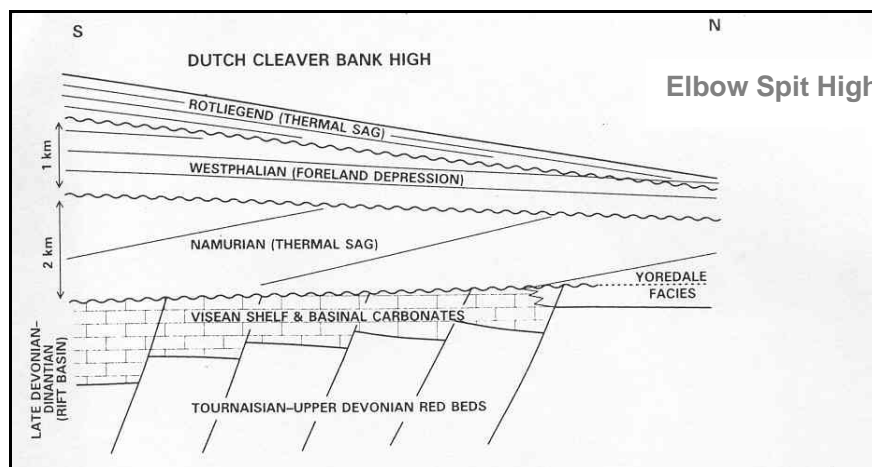


Figure 2.11 Idealised geological cross section showing the main tectonic units of the Upper Palaeozoic on the Cleaver Bank High, flattened at Top Dinantian level (from Quirk, 1997)

2.2.5 *Namurian*

Traditionally, the Namurian to Westphalian C is considered as a long period of relative tectonic quiescence in the basin. This period of roughly 20 Ma was earlier described as a classical sag phase according to the model of McKenzie (1978). Uniform thermal subsidence was supposed to have occurred across the SNS, related to a gradual cooling and strengthening of the lithosphere.

However, tectonic events affected the area. Our study has found evidence for an intra-Naumarian angular unconformity on the seismic lines near wells Nagele-1 and Tjuchem-2 (Appendices E17 & E18). It is our interpretation that the interpreted surface implies both erosional truncation and onlap onto that surface. Correlation to the wells shows that both in Nagele-1 and in Tjuchem-2 the surface can be dated as Late Arnsbergian. Furthermore, there is evidence of Namurian volcanism (e.g. in well Nagele-1, Sissingh, 2004), which may mean local crustal thinning. All things considered, it is evident to a simple sag model is too simple. Active tectonics during the Namurian should be taken into account.

The basin-fill comprises first the basal Namurian marine shales, draping the morphological features remaining of the half-grabens. Subsequently, the later Namurian regression caused continental deposits from the middle Namurian onwards. The regression was related to the onset of glaciations in the southern hemisphere and possibly also to the Variscan orogeny.

During the evolution of the Variscan orogen the deformation front migrated gradually northwards and the back-arc seaway was closed and deformed into major nappe complexes. The loading imparted by these complexes led to the formation of a flexural foreland basin, which also migrated northwards (Besly, 1998). In general, the impact of the Variscan front was smaller and later in the northern part in comparison to the area off the London Brabant Massif. By the Late Westphalian this flexural foreland basin had reached its northernmost position.

The transition from the Dinantian to the Namurian is expressed by a marked drop in carbonate sedimentation in NW Europe and, in particular, in the Southern North Sea. Because the clastic sediment input in the earliest Namurian remained low, the lack of carbonates instigated sedimentation of only clays and organics. This resulted in clay sedimentation throughout NW Europe (Bowland, Pendle and Edale Shales (UK) and the Epen Formation in the Netherlands). It is suggested that these shales have been draped over the pre-existing Dinantian topography. Occasionally, these shales have high TOC values (e.g. Geverik Member). This lithological change is suggested to be caused by a climate change in combination with a change in marine circulation patterns (Figures 2.12 and 2.13).

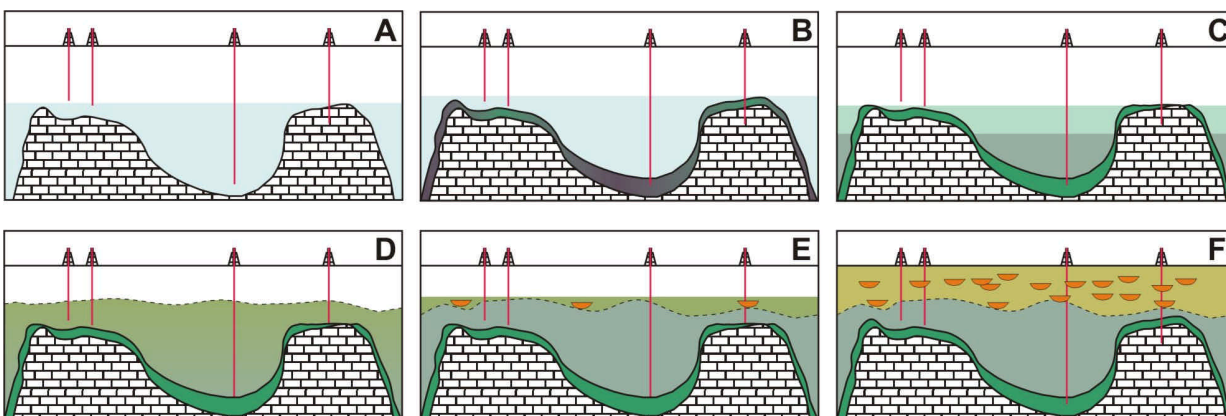


Figure 2.12 Development of the Namurian, including the “Geverik draping” event. A=Late Dinantian; B=Pendleian (Geverik Mb and equivalents); C=Early Arnsbergian (Epen Fm.); D=Late Arnsbergian (unconformity); E=Chokerian; F= Chkerian – Yeadonian (“sandy” Epen Fm. and base Baarlo Fm)

In the northern part of the Southern North Sea, the deposition of the Yoredale Formation also passes into the Epen Formation. However, there is not a marked change or unconformity, at least not in the UK onshore area and in the Elbow Spit High (Quirk, 1997). Also our study has not found any evidence on seismic lines for an unconformity between the Dinantian and the Namurian in the northern offshore. On the London Brabant Massif in the south an unconformity was recognised between the Dinantian carbonates and the Namurian shales (Bless *et al*, 1976). On the London Brabant Massif the contact between Dinantian and Namurian is an erosional unconformity. In Zuid-Limburg, there is a hiatus present rather than an unconformity.

It is unknown if the intra-platform basins, postulated for the Dinantian, existed in the Namurian between the highs in the north on the London Brabant Massif in the south. In the southern part of the basin, the basal Namurian mainly developed as shale. Black shales are known from both the Lower Namurian as well as the Dinantian (Bless *et al*, 1976). These organic rich formations, which developed in the Early Namurian, are referred to in the UK as the Bowland Shale Formation and the time equivalent Edale Shale or Pendle Shale (UK Nomenclature). The occurrence of black shales at the base of the Namurian sequence is proven in certain locations in the UK, the Netherlands and in Germany (Leeder *et al*, 1990). If the intra-platform basins existed in the Namurian, they may have contained these basal Namurian source rocks. There are not enough published wells to define the extent of deepwater Bowland Shale Formation (Cameron *et al*, 1992; Cameron, 1993). However, their existence and regional development can be assumed (Maynard & Dunay, 1999). A major deepwater shale basin existed for much of the Namurian in the southern North Sea, essentially in the same basin as the Dinantian (Cameron, 1993; Gerling *et al.*, 1999; Cameron & Ziegler, 1997; our Figure 2.13). Possibly, the Dinantian carbonate platforms acted as barriers that prevented terrestrial influx into the intra-platform basins.

The Dutch equivalent of these deposits is the Namurian Epen Formation, with its basal organic-rich Geverik Member (Namurian A, Van Adrichem Boogaert and Kouwe, 1993-1997). The Geverik Member constitutes the base Namurian in the Limburg area just northeast of the Brabant-Massif and is the lowermost member of the Epen Formation (Limburg Group). Other names for this basal unit of the Namurian are 'Hot Shales', 'Ampelite' and 'Hangende Alaunschiefer'. The type section is the depth interval of 926 to 992m in well Geverik-1 (GVK-01). The unit consists of dark-grey or black bituminous shaly claystones, with intercalations of siltstones and very fine-grained sandstone. The age of the member is Pendleian (to Early Arnsbergian ?), Namurian A. These black shales have been interpreted as having settled from suspension in an anoxic marine basin with restricted circulation. In the type section a gradual transition can be observed from the limestone-shale alternation of the Carboniferous Limestone Group into the marly basal interval of the Geverik Member. Elsewhere, the member is usually found to rest unconformably on massive Dinantian carbonates. Due to the very high degree of coalification only black to very dark brown organic debris has been encountered.

In certain parts of the basin the Westphalian directly overlies the Dinantian (Cameron & Ziegler, 1997). In the U.K. and in Dutch well E02-01 the Westphalian overlying Dinantian strata is relatively young Westphalian C-D to Stephanian. In the well O18-01, on the margin of the London Brabant Massif, early Westphalian A directly overlies the Dinantian.

Our observations for the Namurian show that a two-fold division can be recognised: Pendleian - "Middle" Arnsbergian and latest Arnsbergian – Yeadonian respectively. The top of the latest Arnsbergian - Yeadonian sequence coincides with the top of the Namurian. Based on the present data, the Pendleian is present in a large number of wells. This suggests that time equivalent strata of the Geverik "hot shales" are present throughout the basin (draping effect). However, the TOC value for this shaly layer varies significantly. This interval is time-equivalent to the Bowland, Edale and Pendle Shales in the UK. A major hiatus is present in the Namurian in most wells. This hiatus is visible as an unconformity near the Nagele-1 and Emmeloord-01 wells on seismic lines (Appendix E18) and near well Tjuchem-2 (Appendix E17). Biostratigraphically, the hiatus is characterised by the absence of a part of the lower interval. In general, middle Arnsbergian and older strata may be missing. The Late Namurian (Kinderscoutian and younger) is (mostly) present. This hiatus is also confirmed by the fact that the lower interval (Pendleian - "middle" Arnsbergian) is significantly thinner developed in most areas than the upper part while it contains much more time (ca. 8 Ma). The duration of the upper part (latest Arnsbergian - Yeadonian) is significantly less (ca. 2 Ma). This is in particular the case in the distal parts of the basin (Areas 1 and 2). In the proximal parts a thick lower sequence may be present (Areas 3&4: compare wells Nagele-1 and Tjuchem-2, Enclosure 3). Despite the clear indications of a hiatus it is not possible to pick the exact position of this hiatus by well log information only. Based on the present dataset, it is difficult to further subdivide the two intervals on biostratigraphic data. This is due to the relatively high maturation in most wells, the poor preservation of (micro)fossils and lack of good samples.

For additional reading on the Pre-Westphalian development, please see De Vos et al., 1993; Dreesen et al., 1987; Drozdowski et al., 1998; Helsen et al., 1997; Langenaeker, 2000; Mathes-Schmidt & Elfers, 1998; McKerrow et al., 2000a; McKerrow et al., 2000b; Munchez & Langenaeker, 1993; Oncken et al., 2000; Pharaoh, 1999; Pharaoh et al., 1993; Pharaoh et al., 1995; Poty, 1982; Ribbert, 1998a; Ribbert, 1998b; Ribbert, 1998c; Vandenberghe, 1984; Verniers et al., 2002; Wolburg, 1970; Woodcock & Pharaoh, 1993.

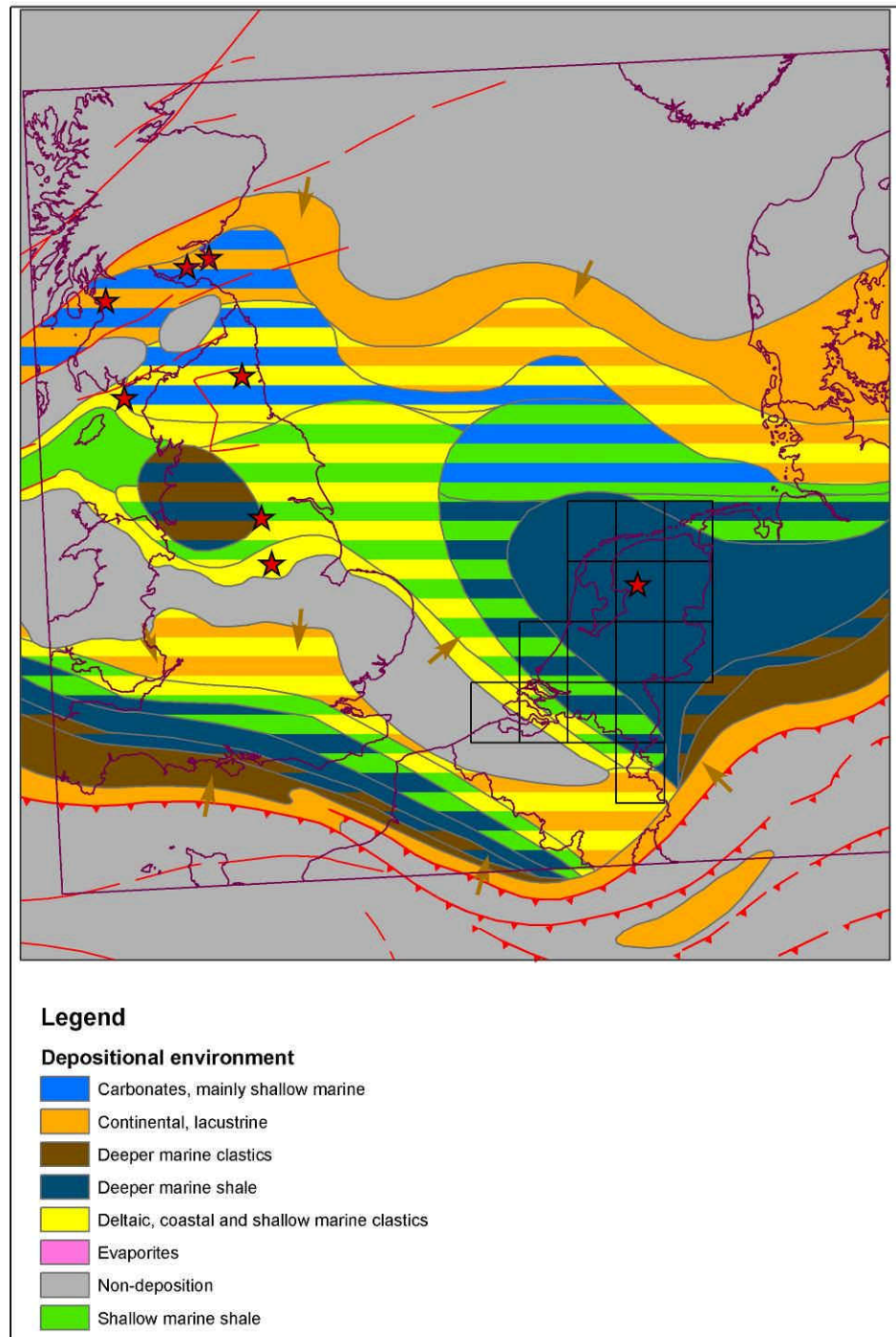


Figure 2.13 Paleogeographical map of the Early Namurian depositional environments, after Ziegler (1990)

2.3 Stratigraphic units

The newly available biostratigraphic data warranted an updated stratigraphic framework that could be used for the entire study area (both onshore and offshore). The existing lithostratigraphic framework (Van Adrichem Boogaert and Kouwe, 1993-1997) was considered less suitable, because of the fact that units cannot be easily correlated from one area to the other. In this project we have dealt with this problem by making an updated framework, dominated by chronostratigraphic interpretations.

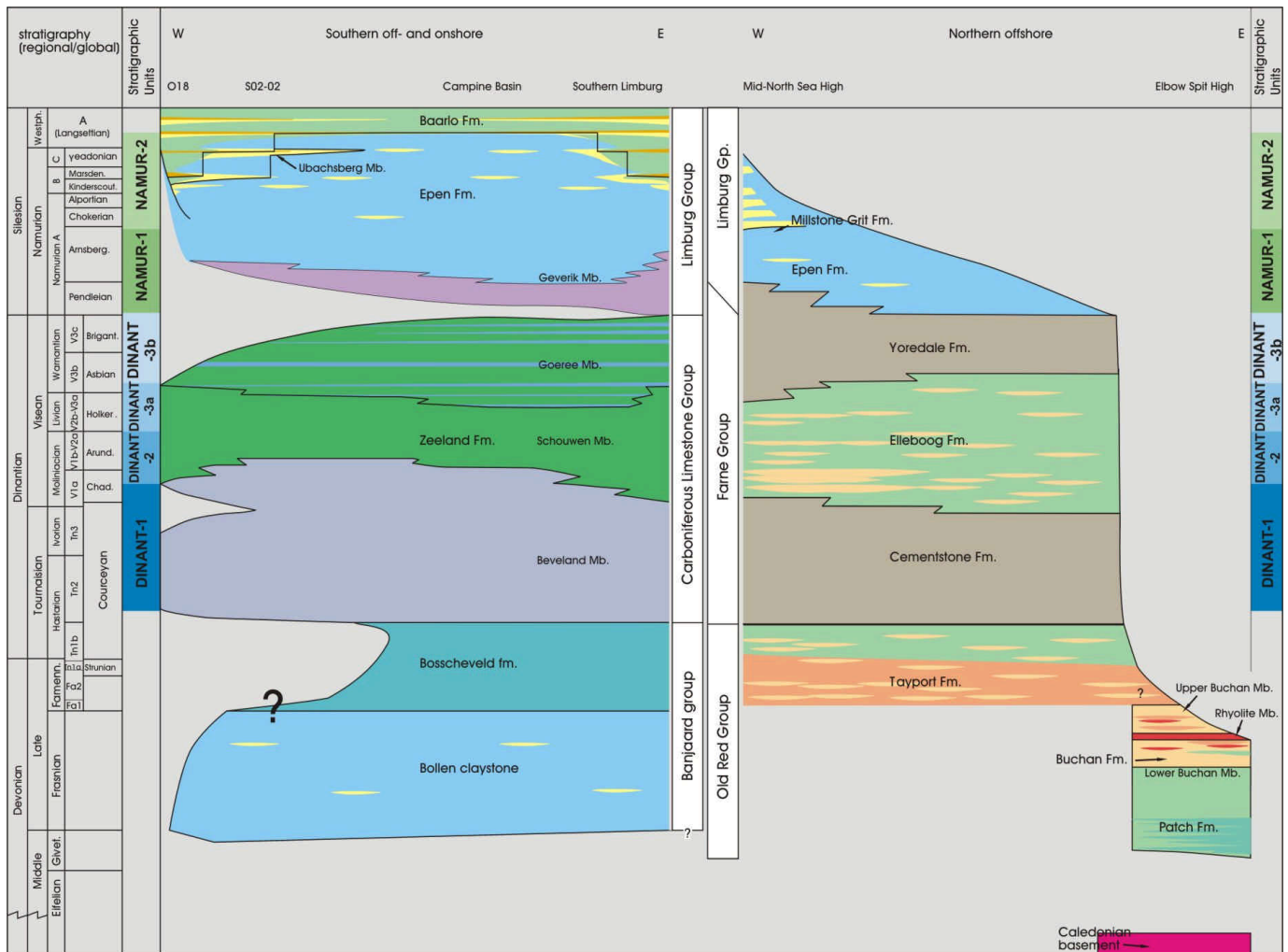


Figure 2.14 Updated stratigraphic chart showing the correlated Namurian and Dinantian intervals discussed in this section. Please note that with respect to the original version of this chart (Van Adrichem Boogaert and Kouwe, 1993-1997) we have changed the relationships between the lithostratigraphic units and the timing

All biostratigraphic data have been combined with log information and lithostratigraphic data in a Petrel project. Despite the lack of information in certain areas the data integration gave us a new opportunity to subdivide the Early Carboniferous sediments. The most important available logs used in the correlation are the sonic and gamma-ray logs. Based on the log values for specific depths a simple lithology prediction macro for Petrel was written.

This macro specifies the following lithologies using the matching rules:

Sand:	GR < 75 API
Silt:	75 < GR < 100 API
Shale:	GR > 100 API and DT < 90 μ s
Limestone:	GR < 75 API and DT < 55 μ s
Coal:	DT > 90 μ s

The combination of lithology display colours and the biostratigraphic data provides a good visual tool to gain insight into the distribution of Early-Carboniferous sediments (Enclosures 1, 2 and 3). Two units have been defined in the Namurian and four units in the Dinantian.

The subdivision of the Dinantian and Namurian is described separately in the following sections. The wells used in this correlation are shown in Figures 2.15 and Figure 2.16. For well correlations we refer to the Enclosures 1, 2 and 3.

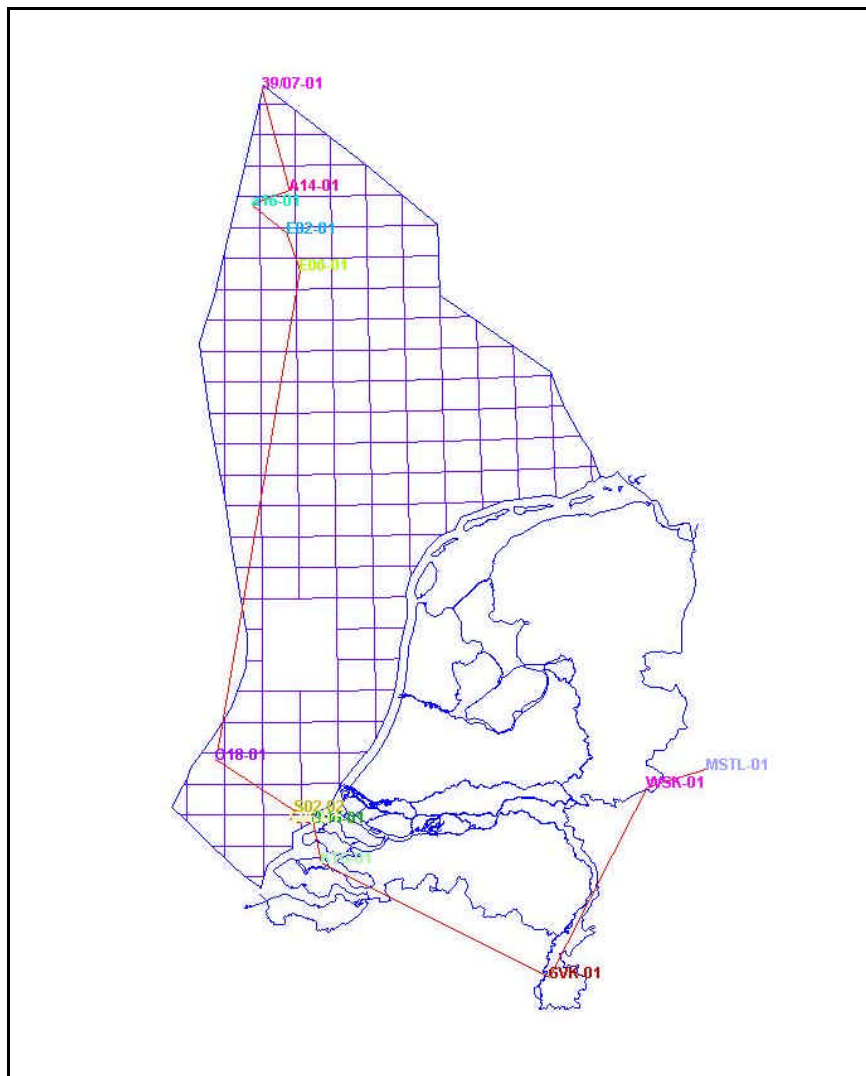


Figure 2.15 Wells used for the Dinantian well correlation

2.3.1 *Dinantian subdivision*

The Dinantian sediments was divided into 4 units mainly based on biostratigraphic data and on the carbonate contents. From old to young, the following names have been used to subdivide the Dinantian:

Dinant-1, Dinant-2, Dinant-3a and Dinant-3b (see Figure 2.14). There is some difficulty in correlating the clastic sediments from the Northern offshore to the limestones in the south (Carboniferous Limestone Group). The distance between the wells E06-01 and O18-01 is 295 km. Therefore, the correlation is mainly based on biostratigraphic information and the presence of limestones in the clastic northern sediments. Clastic units containing limestones have been correlated with the purest limestone units in the south. Vice versa, more clayey limestone units in the south have been correlated to the most purest clastic units in the north. An alternation of more clastic units and more calcareous units is the result.

Dinant-1

The sediments of unit Dinant-1 were deposited during the Courcayan (Tournaisian) and Early Chadian. In the south the lower limit of this unit can easily be recognised as a sharp transition from Devonian clastic sediments to the Dinantian limestones. These limestones contain clay at several levels. In Area 1 unit Dinant-1 coincides with the lithostratigraphic Beveland Member of the Zeeland Formation.

In the Northern offshore the lower limit of unit Dinant-1 was only drilled by well E06-01 and is more difficult to pick. Despite the reddish colour of the cuttings, biostratigraphic data confirms a Dinantian (Tournaisian) age for most of lower part of the Dinantian section in this well. That section was taken to belong to the Tayport formation of the Old Red Group by Van Adrichem Boogaert and Kouwe (1993-1997). The sediments of this unit consist mainly of silt and clay, with minor sand. The sand layers are thin when compared to those of the other units. The boundary between the Devonian and Dinant-1 was picked purely on biostratigraphic information. In Area 2 unit Dinant-1 roughly corresponds to the upper part of the lithostratigraphic Tayport Formation and may also include the Cementstone Formation (of Early Chadian age) of the Farne Group.

On seismic lines we observe that the 'top Devonian' marker picked in E06-01 (purely on biostratigraphic information) coincides with the seismic event 'top Patch Formation' which we have defined on the seismic lines across well A17-01. The Patch Fm constitutes the lowest section of the Old Red Group drilled in A17-01, see Annex B-1 in the Stratigraphic Nomenclator (Van Adrichem Boogaert and Kouwe, 1993-1997). If both the seismic interpretation and the interpretation of well E06-01 are correct, this raises the question what happened to the Buchan Formation of the Old Red Group. In well A17-01 the Patch Formation is overlain by 633 m of the younger sandstone dominated Buchan Formation (including some 150 m of igneous rocks). According to (Van Adrichem Boogaert and Kouwe, 1993-1997) the Buchan Formation could not be dated because no distinct biomarkers have been recovered. They assumed a Frasnian to Famennian age based on the position between the Tayport and Patch formations. Since the Tayport formation (corresponding to our Dinant-1) is interpreted to be mainly of Tournaisian age, this leaves space for different assumptions about the Buchan formation as interpreted in well A17-01. It may belong in its entirety to the Devonian, or alternatively, part of it may be of Tournaisian age.

A striking observation is that the seismic sequence bounded by the top Patch and the top Kyle events (corresponding to a large part of the Devonian Old Red) significantly increases in thickness moving from A17-01 to the SE, whereas the units younger than the top Patch event remain more or less constant in thickness. This would suggest an intra-Devonian structural unconformity. This event may however be of local significance only if it is only related to the movements of the plutonic body drilled near the TD of well A17-01 (Appendices E6 and E8). It is postulated that the rocks younger than our top Patch Fm interpretation have not been affected by any structural doming.

Dinant-2

The sediments of unit Dinant-2 were deposited during the Chadian and Arundian. This unit is a more calcareous unit than Dinant-1. The limestones in the south (Area 1) are pure with little clastic intercalations. The base of Dinant-2 in Area 1 is mainly picked at a change in the expression of the GR log. The timing of this change is in the Chadian (e.g. well S05-01). In Area 1 the unit roughly corresponds to the Schouwen Member of the Zeeland Formation, but there are minor differences: in wells S05-01 and Geverik-1 the upper part of the Schouwen Member belongs to our Dinant-3a. The clastic sediments in Area 2 (Northern offshore) of this time interval show an alternation of limestones and clastic sediments. Abundant limestone layers have been observed in well E06-01 in the lower part of this unit. The alteration of clastic and limestone layers results in a different seismic facies (higher amplitudes, high frequency) of the unit in Area 2. In Area 2 unit Dinant-2 approximately corresponds to the Cementstone Formation and part of the Elleboog Formation (Farne Group). Some coal layers are present in the 39/07-01 UK well. The clastic lower part of the Elleboog Formation is known in the UK as the Fell Sandstone Formation, which has been well described by Maynard & Dunay (1999). It ranges in age from Chadian to Holkerian. In Area 2 the Fell Sandstone Fm would correspond roughly to the upper part of Dinant-2 and lower part of Dinant-3a. In the UK offshore the Fell Sandstone was deposited at a time of high sediment supply, resulting in a thick (300m) succession of fluvial sandstones. Its distribution is closely linked to the accommodation space developed in the hanging walls of contemporaneous faults (Maynard & Dunnay, 1999).

Dinant-3

Sediments of unit Dinant-3 were deposited during the uppermost Dinantian (Holkerian, Asbian and Brigantian). Dinant-3 is characterised in UK well 39/07-01 as a sequence of silt- and sandstones with some calcareous intervals. In Area 2 it would correspond to the upper part of the Elleboog Formation and the Yoredale Formation (Van Adrichem Boogaert and Kouwe, 1993-1997). In the south of Area 2 (A16-01, E02-01 and E06-01) a subdivision can be made between a pure clastic sequence (Dinant-3a) and an overlying clastic sequence containing also calcareous deposits (Dinant-3b). In well E06-01 the unit Dinant-3a corresponds to the Elleboog Formation and the unit Dinant-3b corresponds to the Yoredale Formation. According to Maynard & Dunay (1999) a second level with reservoir potential (in addition to the Fell Sandstone) would be the Whitby Member, which they place in the late Asbian. This would correspond to our unit Dinant-3a, which also in well E06-01 shows thick sandstones.

The subdivision between Dinant-3a en Dinant-3b can also be made in the limestones of Area 1, where Dinant-3b shows the purest limestones and Dinant-3a consists of an alternation of shales and limestones (e.g. O18-01). In Area 1 the top of Dinant-3 is marked by a sharp transition from calcareous sediment to clastic sediments. Dinant-3

roughly includes the Goeree Member of the Zeeland Formation, but also part of the Schouwen member in some wells (S05-01 and Geverik-1). Dinant-3 thins remarkably towards the London Brabant massif, where it eventually disappears (e.g. well Kortgene-1, see Enclosure 2). In the eastern Area 4 (well Winterswijk-1) a calcareous clay has been deposited which was correlated to the Dinant-3a unit. In the southern area the top of the Dinant-3 unit is marked by a sharp transition from calcareous sediment to clastic sediments.

2.3.2 *Namurian subdivision*

The Namurian has been subdivided into two units: Namur-1 and Namur-2. Unlike the subdivision of the Dinant described above, the subdivision of the Namurian shows only weak links to the lithostratigraphic subdivisions of Van Adrichem Boogaert and Kouwe (1993-1997).

The transition from the Dinantian to the Namurian is characterised by a marked drop in carbonate sedimentation in NW Europe and, in particular, in the Southern North Sea. Because the clastic sediment input in the earliest Namurian remained low, the lack of carbonates instigated sedimentation of only clays and organics. Namurian sediments are characterised by very thick shale deposits in the south and east and much thinner but coarser clastic deposits in the north-western area (Area 2). The subdivision of the Namurian is mainly based on biostratigraphic data and on the more frequent occurrence of sand bodies in the upper part of the Namurian. The wells used for the correlation are presented in Figure 2.16. Van Adrichem Boogaert and Kouwe (1993-1997) also made a distinction between the more sandy parts (Millstone Grit in Area 2 and Ubachsberg member in Areas 1 and 3) and the clayey sequences (mainly Epen Formation). The boundaries between these units are however very diachronous. Our Namur-2 consists of the upper part of the Epen Formation and the lower part of the Baarlo Formation.

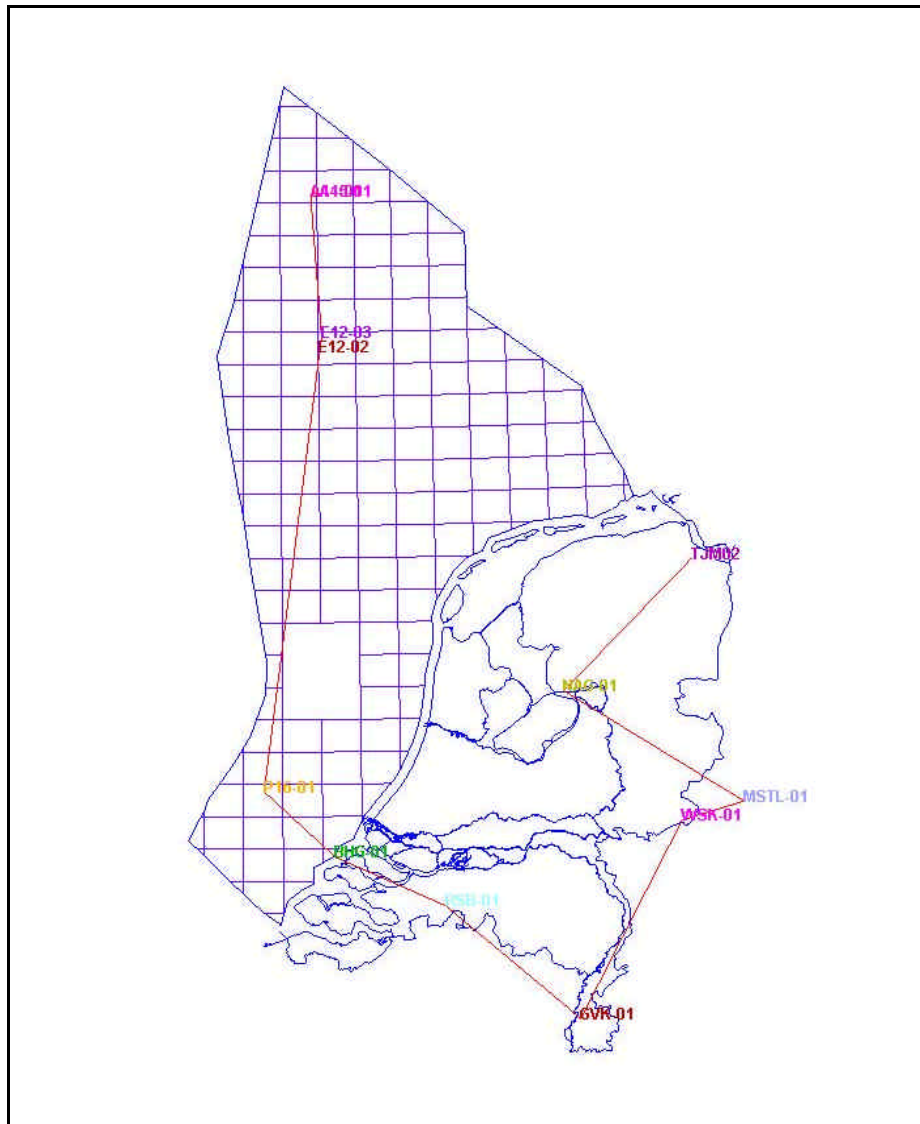


Figure 2.16 Wells used for the Namurian well correlation

Namur-1

The sediments of unit Namur-1 were mainly deposited during the Pendleian to Cholerian. In well A14-01 the base of Namur-1 is characterised by a sharp drop in the sand content. The same pattern is visible in wells E12-03 and E12-02. The top of the unit is characterised by the first occurrence of massif sandstone beds belonging to the Millstone Grit Formation. The deposition of Namurian sediments in Area 1 is very much restricted, probably as a result of a paleorelief. Only relatively thin sections of the Namur-1 unit have been found in P16-01 and Brouwershavense Gat-1. More to the east in Area 1 a very thick section of a clayey Namur-1 is present in the Rijsbergen-1 well. The lowest part of the Namur-1 is dominated by a clay with a very high TOC also known as the Geverik Member (type location: Geverik-1). The top of the Namur-1 unit in Area 1 defined by the occurrence of sand bodies however these bodies are much less pronounced compared to those in Area 2.

During the Namur-1 accommodation space was highest in Areas 3&4 resulting in a thick sequence of silts and clays belonging to the Epen Formation. A pronounced

unconformity has been found on seismic in the area of the Nagele-1 and Tjuchem-2 well.

Namur-2

The sediments of unit Namur-2 were mainly deposited during the Yeadonian and Marsdenian, however the base of the Namur-2 unit in the eastern wells (Nagele-1 and Tjuchem-2) was found to be of Chokierian age. The total thickness of the unit in Area 2 changes rapidly over relative short distances (compare E12-03 to E12-02) which may indicate the presence of a paleo-relief.

In Area 1 both the thickness and the sand content is smaller. In the eastern part of Area 1 the accommodation space was large, resulting in a thick sequence of clayey sediments with some sandier intercalations. The high gamma ray values in the well Rijsbergen-1 in the lowermost part of the Namur-2 unit can be explained by the occurrence of calcareous cement. The south-eastern part of Area 3 shows a very thick sequence of clayey sediments with some sand bodies. The amount of sands and silts increases further in the northern part of Areas 3&4 (Nagele-1 and TJM-01).

2.4 Lithology distribution maps

Based on the stratigraphic framework described above, lithology distribution maps of the six stratigraphic units mentioned above were composed for two different modelling scenarios. These maps are interpretations based on literature data (Lokhorst, 1998; Ziegler, 1990; Pagnier *et al.* 2002) and on a lithology calculation performed in Petrel. As an example of the well input data Figure 2.17 shows the lithology distributions in the wells for the Namur-2 unit. Similar plots are given for all units in Appendix C.

We have used two scenarios for the constructions of the maps. The maps serve as input for the PetroMod modelling. A good understanding of the paleorelief during the deposition of Early Carboniferous sediments is difficult due to the present depth of these sediments and the overprint by later tectonic pulses. Therefore, several models were proposed by different authors. Paleogeographical maps found in literature show two models for facies distribution of Carboniferous sediments. *Scenario 1* is based on a simple flexural ramp model (Ziegler, 1990) for both the northern and southern part of the basins (Figure 2.18). *Scenario 2* is based on the presumed existence of highs and lows bounded by normal faults (Pagnier *et al.*, 2002).

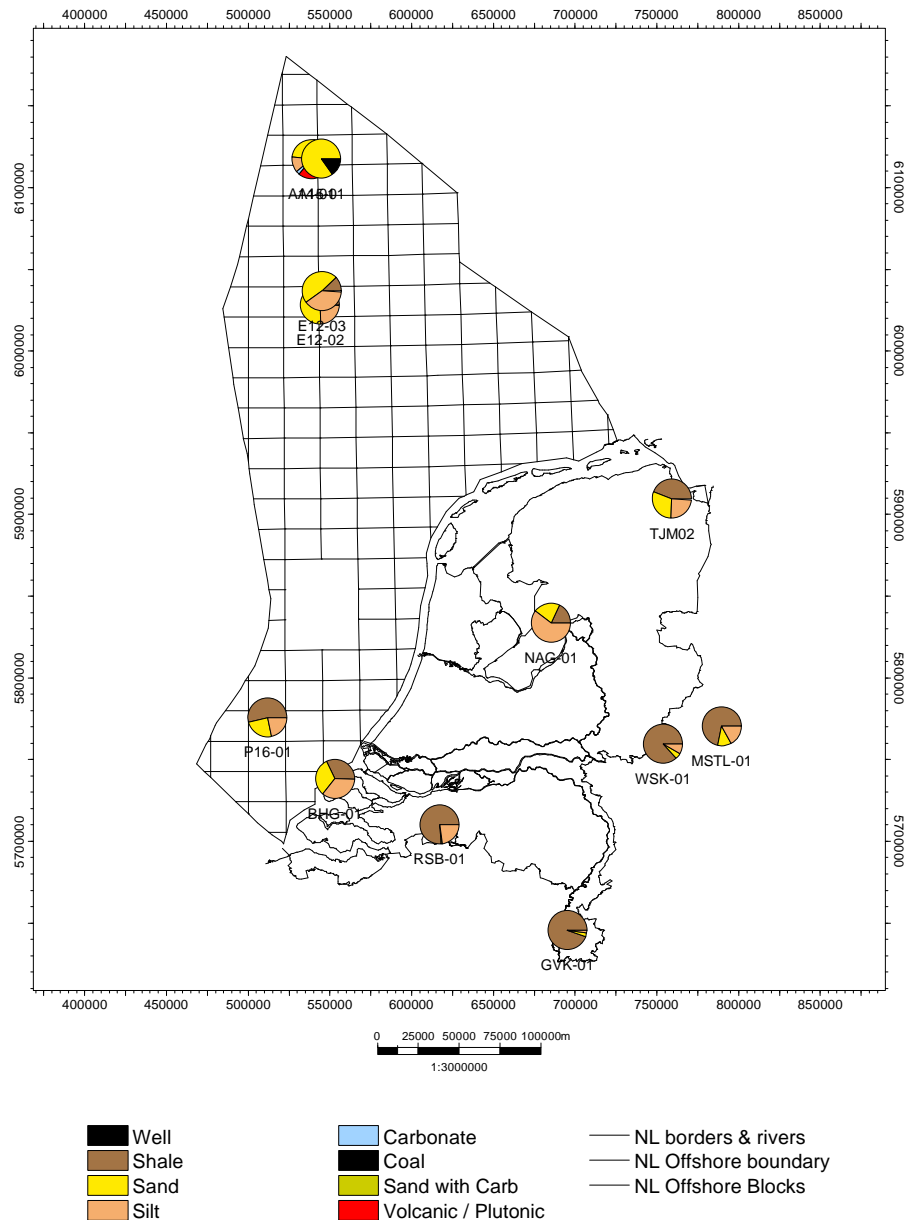


Figure 2.17 Distribution of lithologies in the wells for the Namur-2 unit. This information was input for the construction of the lithology distribution maps needed for the 3D basin modelling. Similar plots for the other pre-Westphalian units are given in Appendix C

2.4.1 Scenario 1

This is one of scenarios also adapted by Collinson Jones Consulting (1995). The simplest scenario was first proposed by Ziegler (1990), and later refined by (Lokhorst *et al.*, 1998). It shows a basin with flexural ramps towards the south and the north (Figure 2.18). This means that the distribution of lithologies is characterised by large sheet-like deposits. For instance during the Dinantian, shales and shaly limestones can be found throughout a large part of the basin.

We have used the maps of the Lokhorst *et al.* (1998) and plotted the lithologies of the individual units on these maps. Using this information the maps were refined and adapted. The maps are limited to the Netherlands situation only. In total 6 maps were

produced based on this model and these maps are described in following sections. It has been argued by Collinson Jones Consulting (1995) that this scenario is to be the least likely one for the UK offshore situation because no onshore analogues have been found.

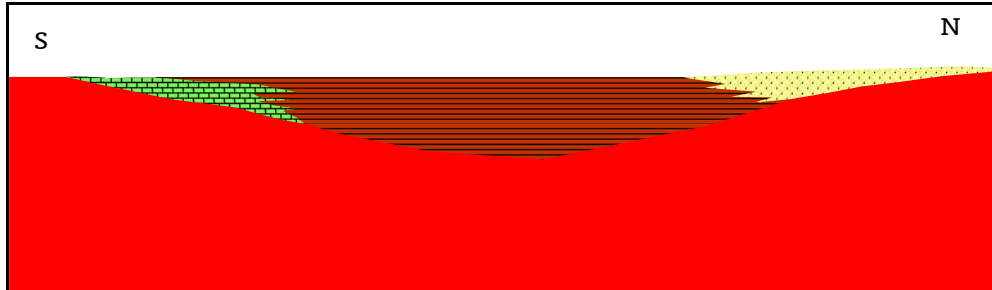


Figure 2.18 Impression of Scenario 1: flexural ramp model

2.4.2 Scenario 2: Block and basin model

This scenario is mainly based on the ideas of Pagnier *et al.* (2002), who adapted it from a scenario presented by Collinson Jones Consulting (1995) for the UK sector. The principle of this scenario is the existence of relief forming highs and lows influencing the deposition of platform limestones during the Dinantian. The structural highs may already have been formed during pre-Carboniferous times and would be bounded by normal faults which remained active during the Early Carboniferous. A schematic profile is shown here as Figure 2.19. The postulated framework presented by Pagnier *et al.* (2002) is given as Figure 2.20.

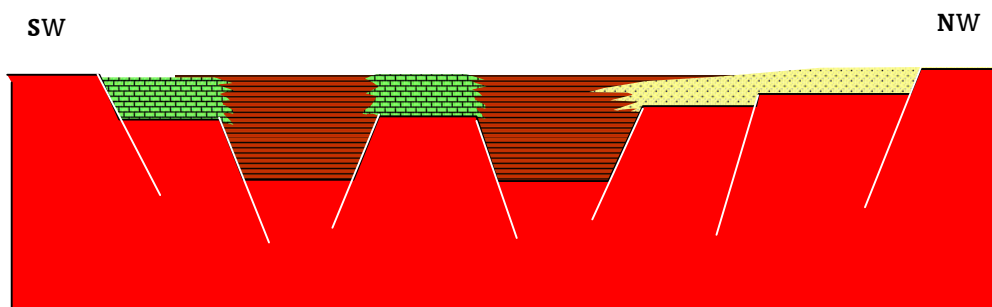


Figure 2.19 Impression of Scenario 2: block and basin model

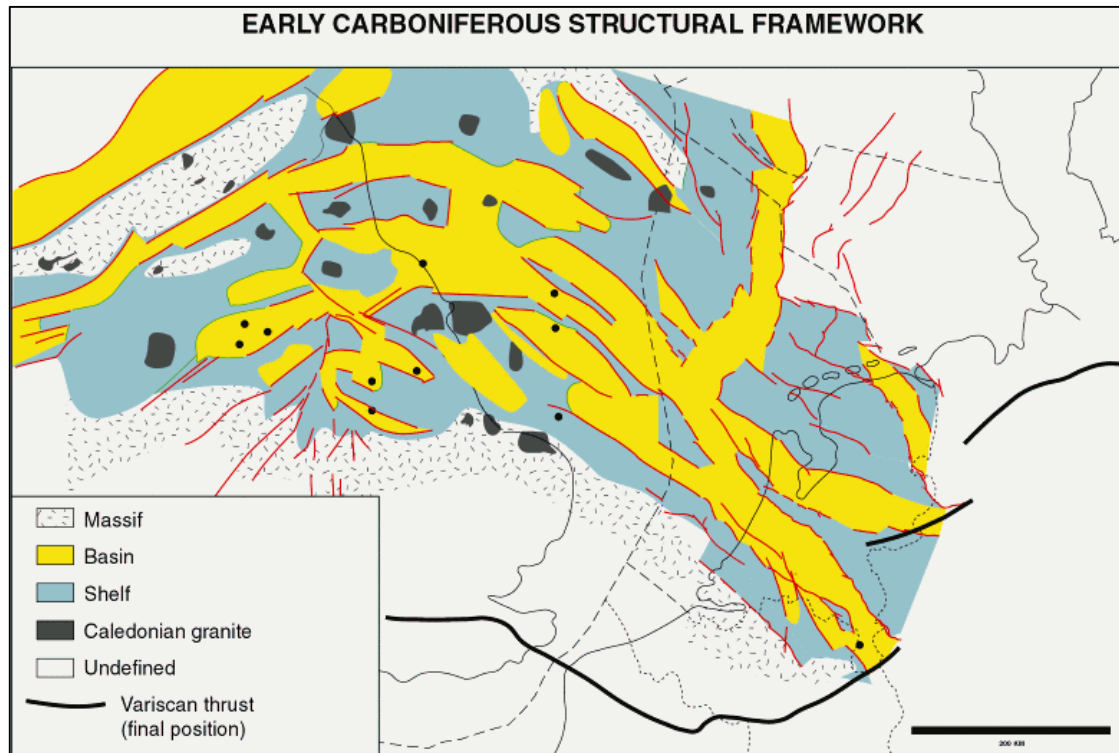


Figure 2.20 Application of the model of Scenario 2 (Figure 2.19) to the Netherlands on- and offshore as presented by Pagnier et al. (2002), after e.g. Besly (1998)

The implicate assumption in Figure 2.20 is that much of the structural framework as it can be witnessed today (e.g. Broad Fourteens Basin, Central Netherlands Basin, West Netherlands Basin/Roer Valley Graben, Lauwerszee Trough and Dutch Central Graben) already had an early expression during the Early Carboniferous.

Shales were deposited in the structural lows. A distinction is made in the amount of limestone in these Dinantian shales because of higher clastic influx from the north. This means that the southern lows contained mainly shaly limestone, whereas the northern lows have been filled with calcareous shales. The faulted boundaries also imply the possibility of the occurrence of turbiditic facies during the Namurian. This idea has been adapted for the Namur-2 period when coarser clastic material prograded from the north. Around the northern and southwestern boundary faults an area with turbiditic silts and sands has been defined. The existence of these turbidites has however not been proven yet for the Dutch area.

Using this model we have constructed the lithology distribution maps. A comparison was also made with the residual gravity map (Figure 2.21). The residual gravity field was obtained by subtracting the gravity effect of the post-Carboniferous overburden from the observed Bouguer gravity anomaly map (Appendix K). The gravity anomalies more or less correspond to the pattern in Figure 2.20: high values are observed in the basins. As is explained in Appendix K, this coincidence in itself is not a lot of proof, because the gravity anomalies in the basins may simply be the result of the fact that the crust is thinner under the basins. In that case stripping the post-Carboniferous overburden does not remove all of the anomalies in the measured gravity field.

In general, it is very difficult to model the location of important pre-Westphalian boundary faults with any degree of certainty. Therefore, the following maps should be regarded as conceptual models only. Their main purpose was to represent an indicative idea of the distribution of lithologies which was input to the 3D modelling (Appendix I).

All things considered it is believed that the conceptual model presented here as Scenario 2 is more realistic than the model of Scenario 1 which assumes a quiet sag basin during the Dinantian and Namurian.

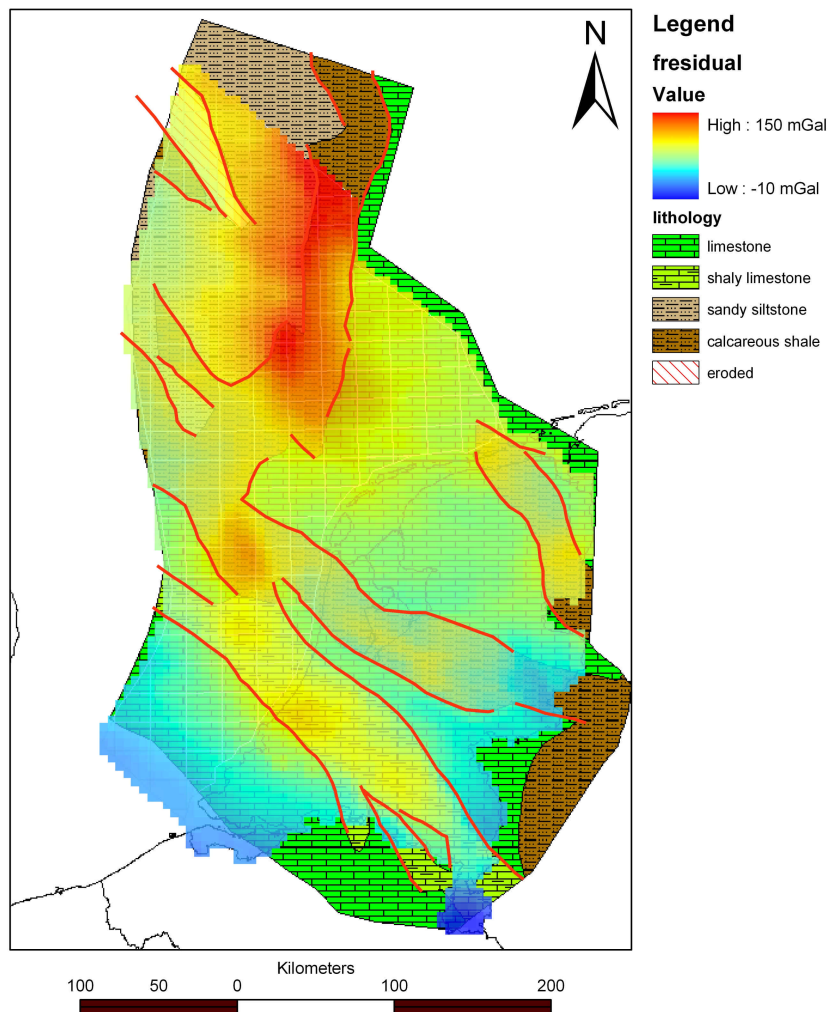


Figure 2.21 Dinant-1 structure map combined with the residual gravity field (subtracting the summed gravity effect of the overburden)

Dinant-1

The distribution map of Dinant-1 shows fine grained sandy sediments mainly deposited in the north and east. Source areas during this time are the Mid German High in the south east and the Fenno Scandian High in the north (Ziegler 1990). No limestones were observed in wells from these areas. The south is dominated by limestones. The runoff from the London-Brabant Massif is therefore limited during this time. It is expected that calcareous shales were deposited in de deeper parts of the basin (east and north east).

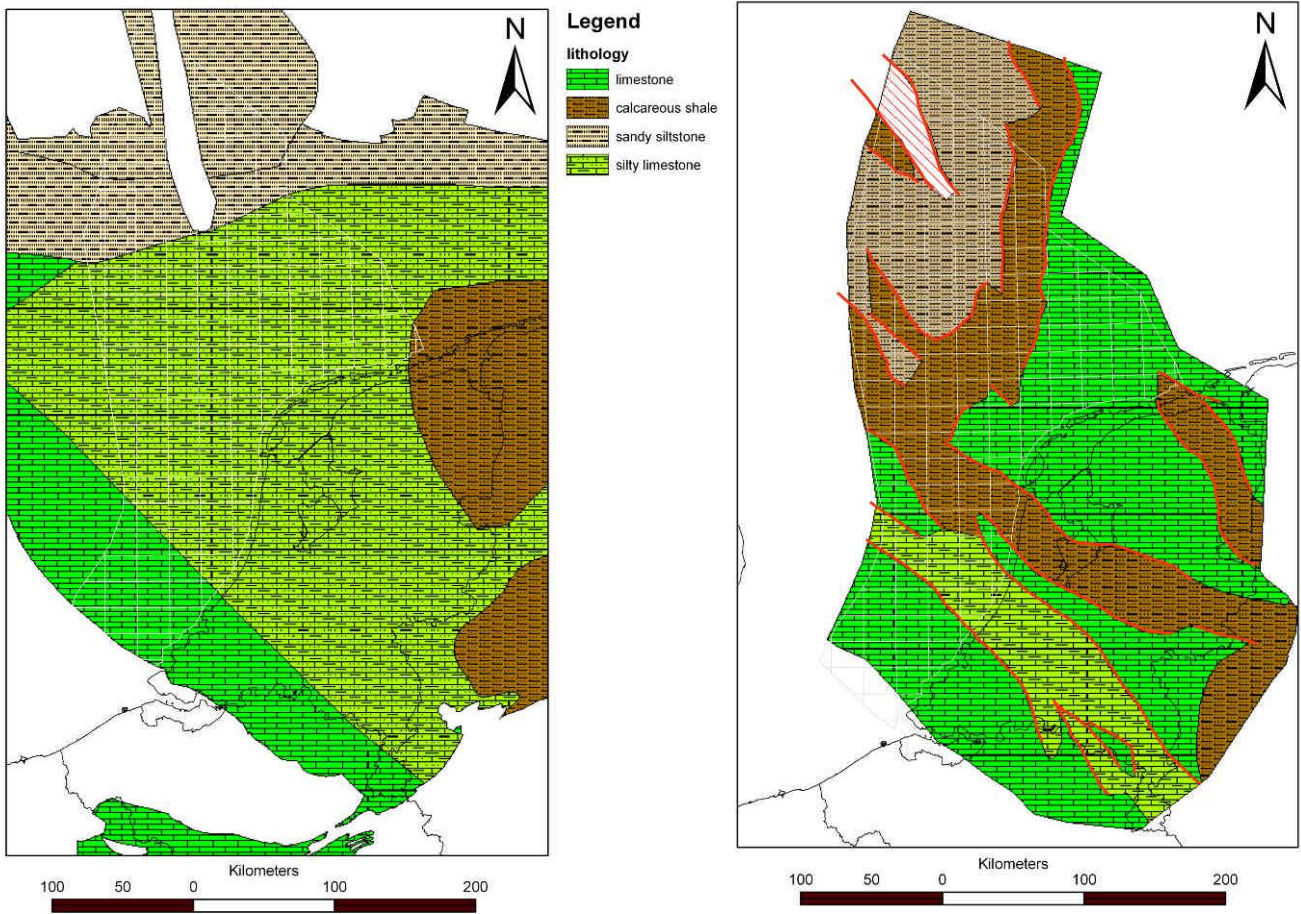


Figure 2.22 Distribution maps of unit Dinant-1 for respectively Scenario 1, sag model (left) and Scenario 2, a block and basin model (right)

Dinant-2

Based on the well information it is to be expected that there was less clastic influx in this period from the south east. In the east only limestones have been observed. Sourcing was now only from the north (Fenno Scandian High). This can be interpreted as a prograding system as the grain size is coarser than in the Dinant-1 unit. In the deeper parts of the basin mainly calcareous shale can be found.

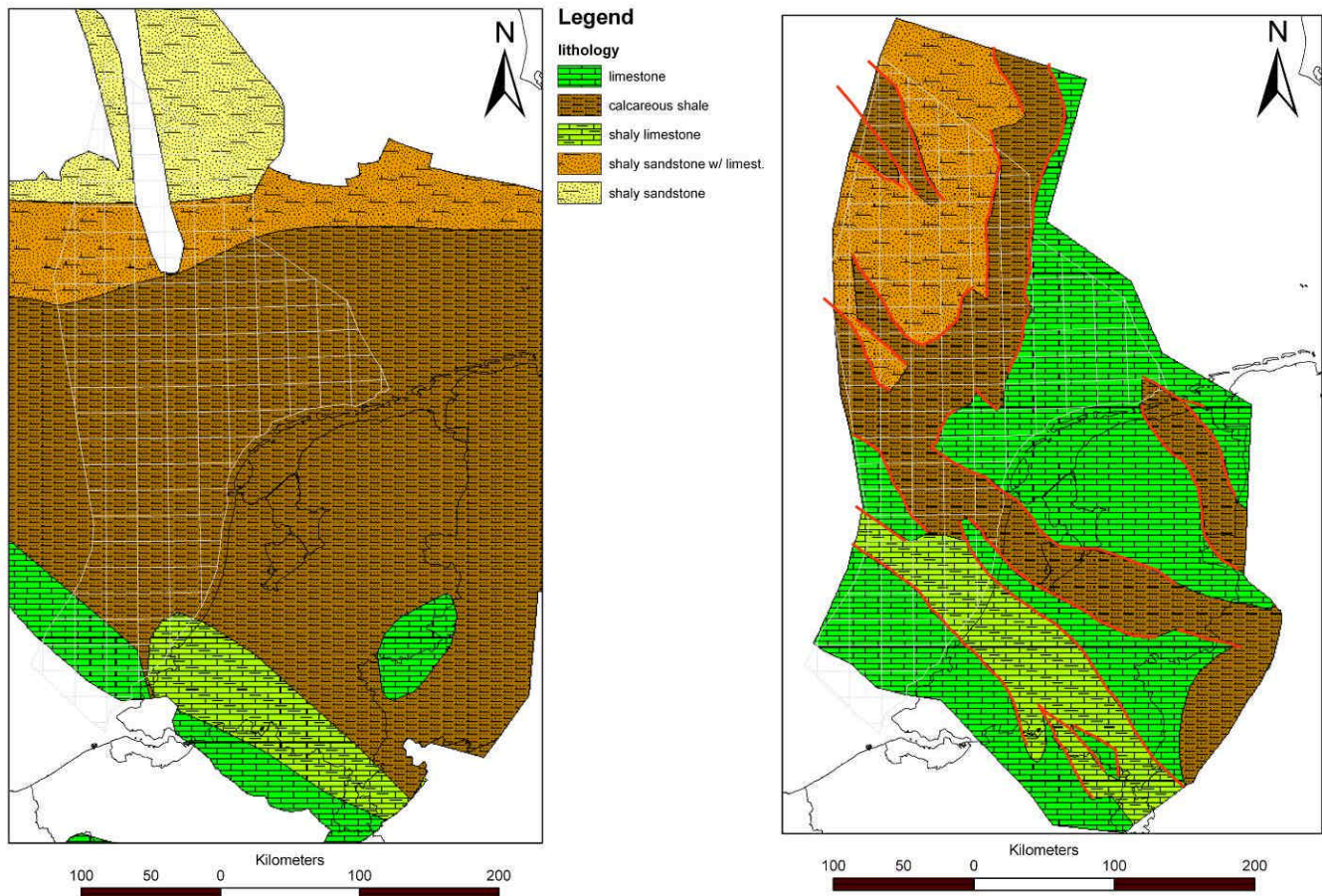


Figure 2.23 Distribution maps of unit Dinant-2 for respectively Scenario 1, sag model (left) and Scenario 2, a block and basin model (right)

Dinant-3a

Dinant-3a was again a period of more clastic influx from the north and south east. The northern prograding clastic systems (Yoredale Formation) have probably reached the K and L blocks. Pure limestones have only been found in the most southwestern part. It is likely during this period that mainly calcareous shales were deposited in the central part of the basin.

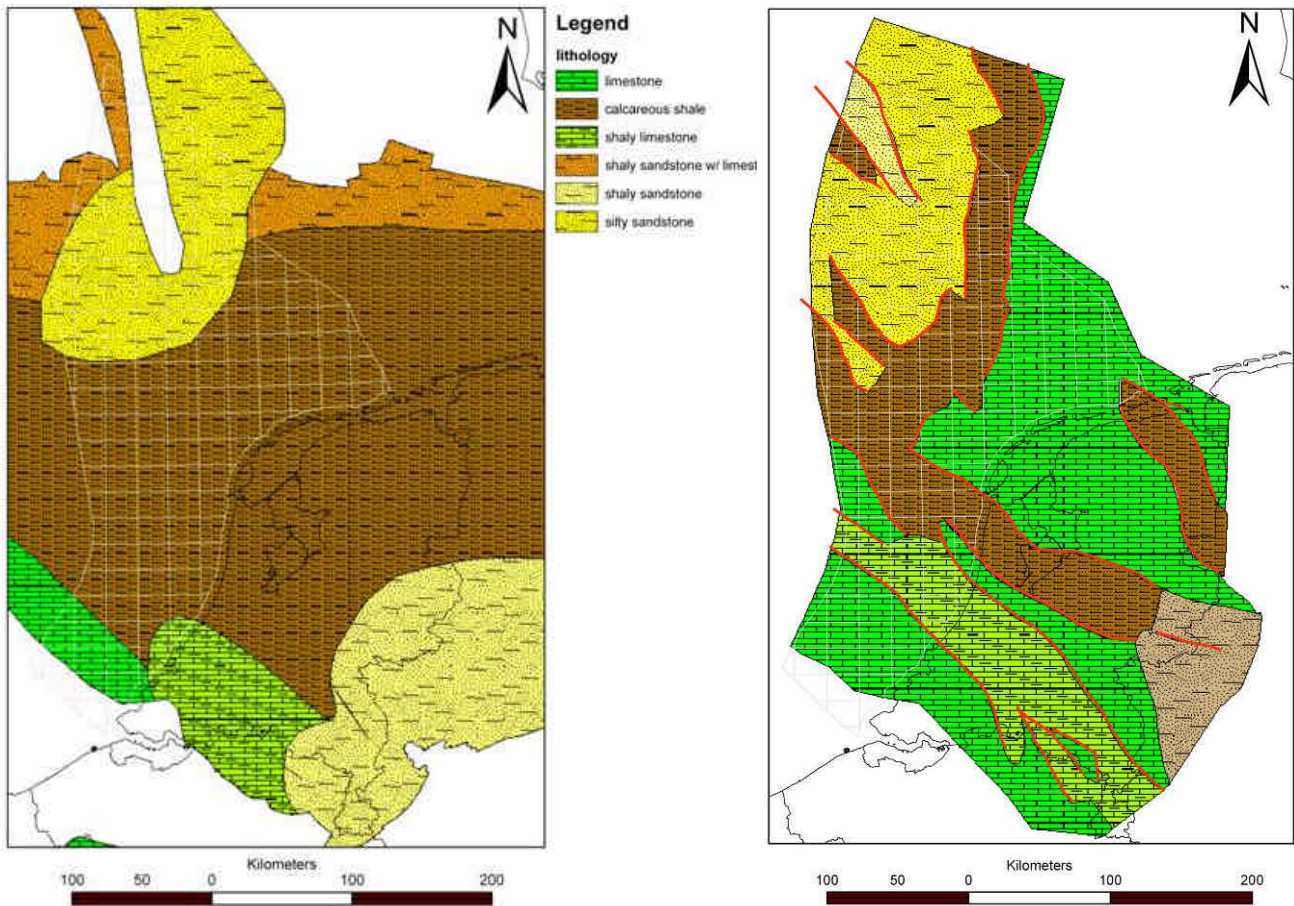


Figure 2.24 Distribution maps of unit Dinant-3a for respectively Scenario 1, sag model (left) and Scenario 2, a block and basin model (right)

Dinant-3b

The sand-to-shale ratio was reduced in this period which can be interpreted as a lower clastic influx from the Mid German High and Fenno Scandian High. More calcareous sediments can be found in south eastern area. The same trend can be observed in the Northern offshore when compared with Dinant-3a. More limestones are found in e.g. well E06-01 and other northern wells, while limestone is absent in the Dinant-3a unit. It is therefore supposed that deposition of limestones is again more dominant during this period.

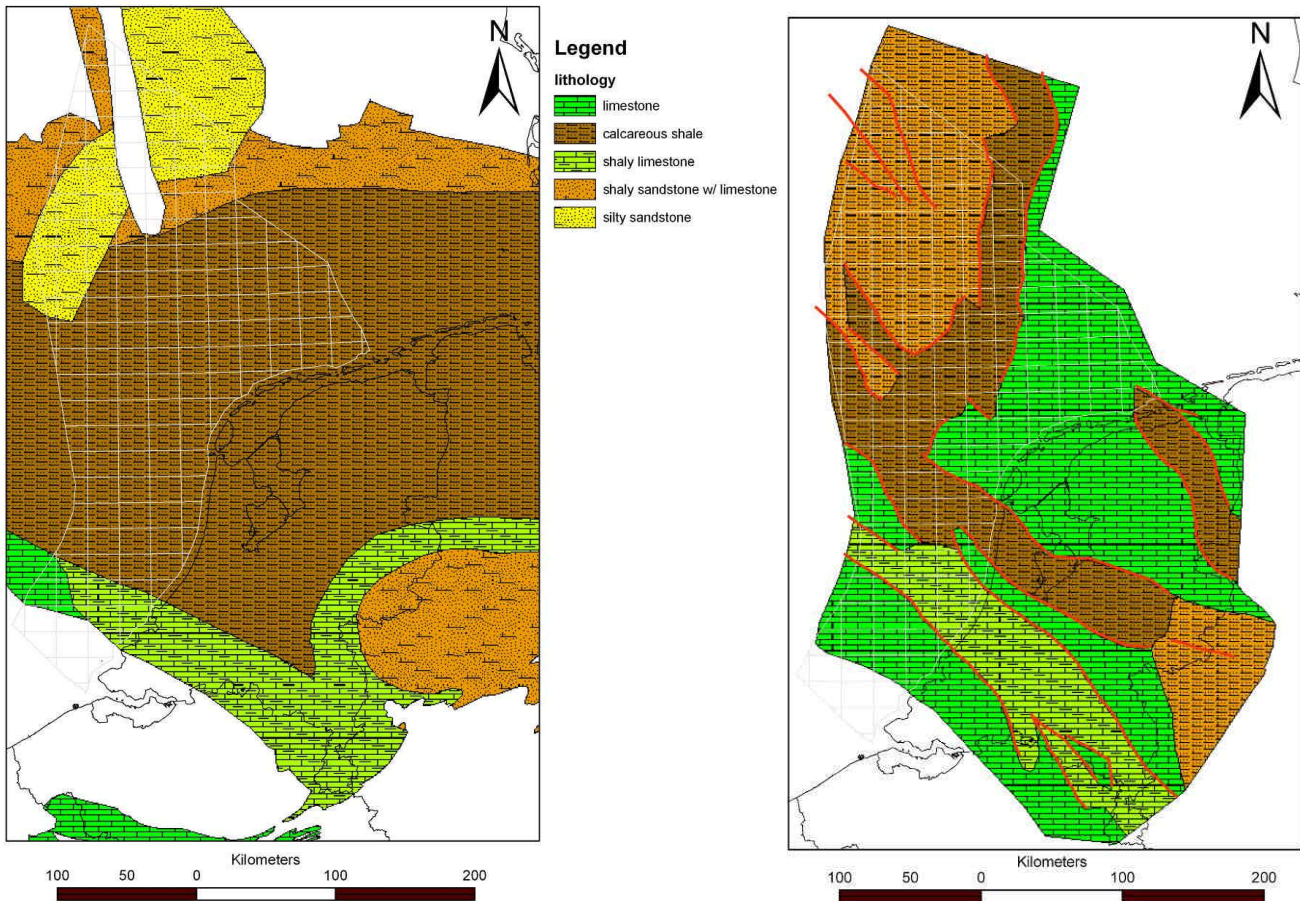


Figure 2.25 Distribution maps of unit Dinant-3b for respectively Scenario 1, sag model (left) and Scenario 2, a block and basin model (right)

Namur-1

The Fenno Scandian High (Ziegler, 1990) still remained an active source for clastic sediments during the Namurian, however the progradation of coarser sediments during the Dinant-3b and the Namur-1 ceased in Area 2. This oldest Namurian unit is dominated by the deposition of shales in a wide area. In the south the base of the shales is marked by the Geveik Member. Some silts can be found in the south-western part as a result of local runoff from the London Brabant Massif. The Mid German High was swallowed by the further development of the Variscan belt during the Namurian. As a result of this development the Variscan Foredeep Basin got closer to the borders of the present-day Netherlands which means an input of coarser clastics from the south east. In the north-east prograding systems from the northern Fenno Scandian High closed in the basin in the north-eastern part of the Netherlands from the north. The relatively coarse clastics found in the Tjuchem-2 and Münsterland-1 can either have a northern source or a south eastern source. In Figure 2.26 the interpretation of a northern source has been mapped.

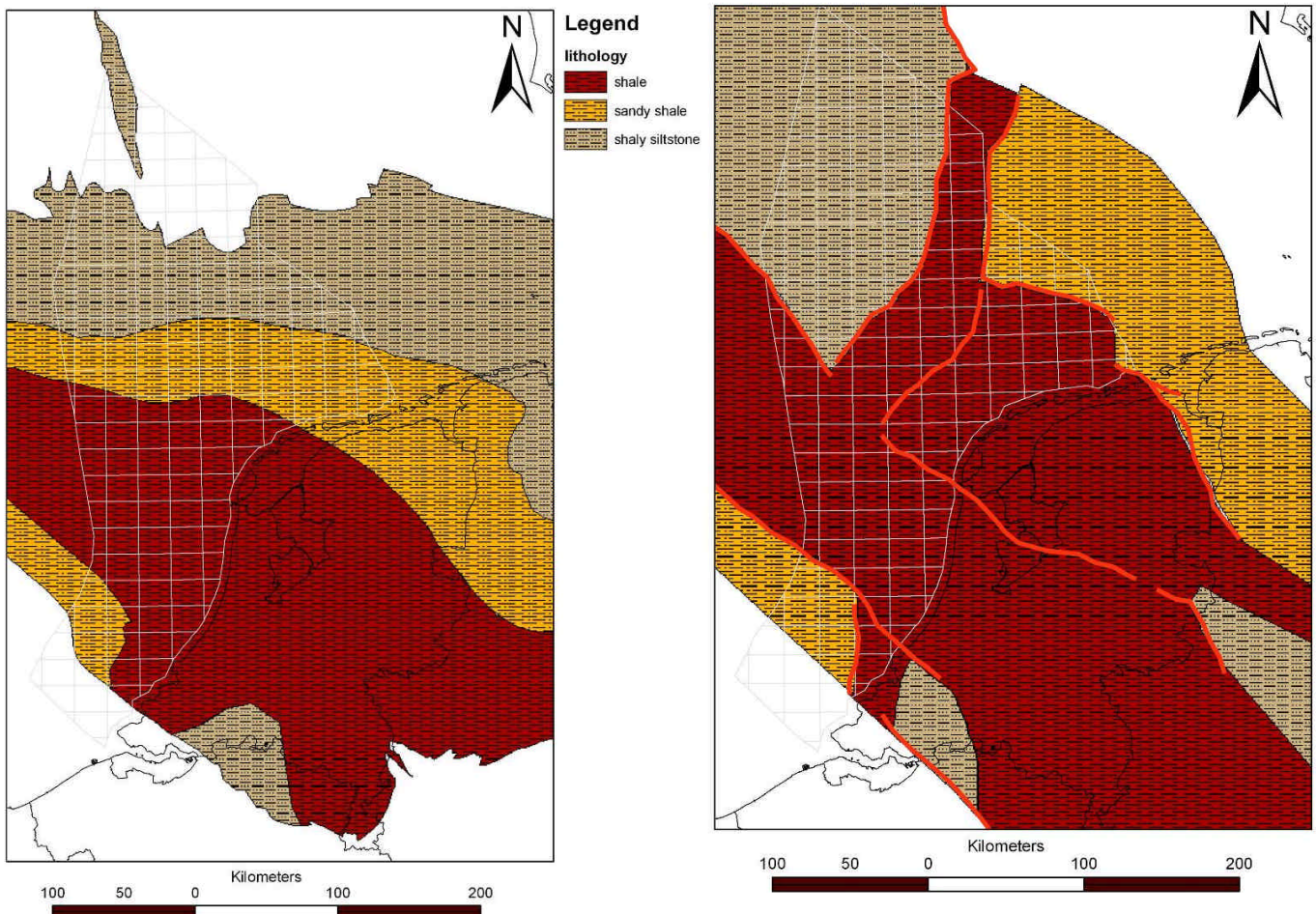


Figure 2.26 Distribution maps of unit Namur-1 for respectively Scenario 1, sag model (left) and Scenario 2, a block and basin model (right)

Namur-2

With proceeding time in the Namurian the influx of clastic material from the north increased. Also the runoff from the London Brabant Massif shows an increase of coarser sediments in the south-western part of the Netherlands. Net sand ratios are higher for all areas except the central part of the basin.

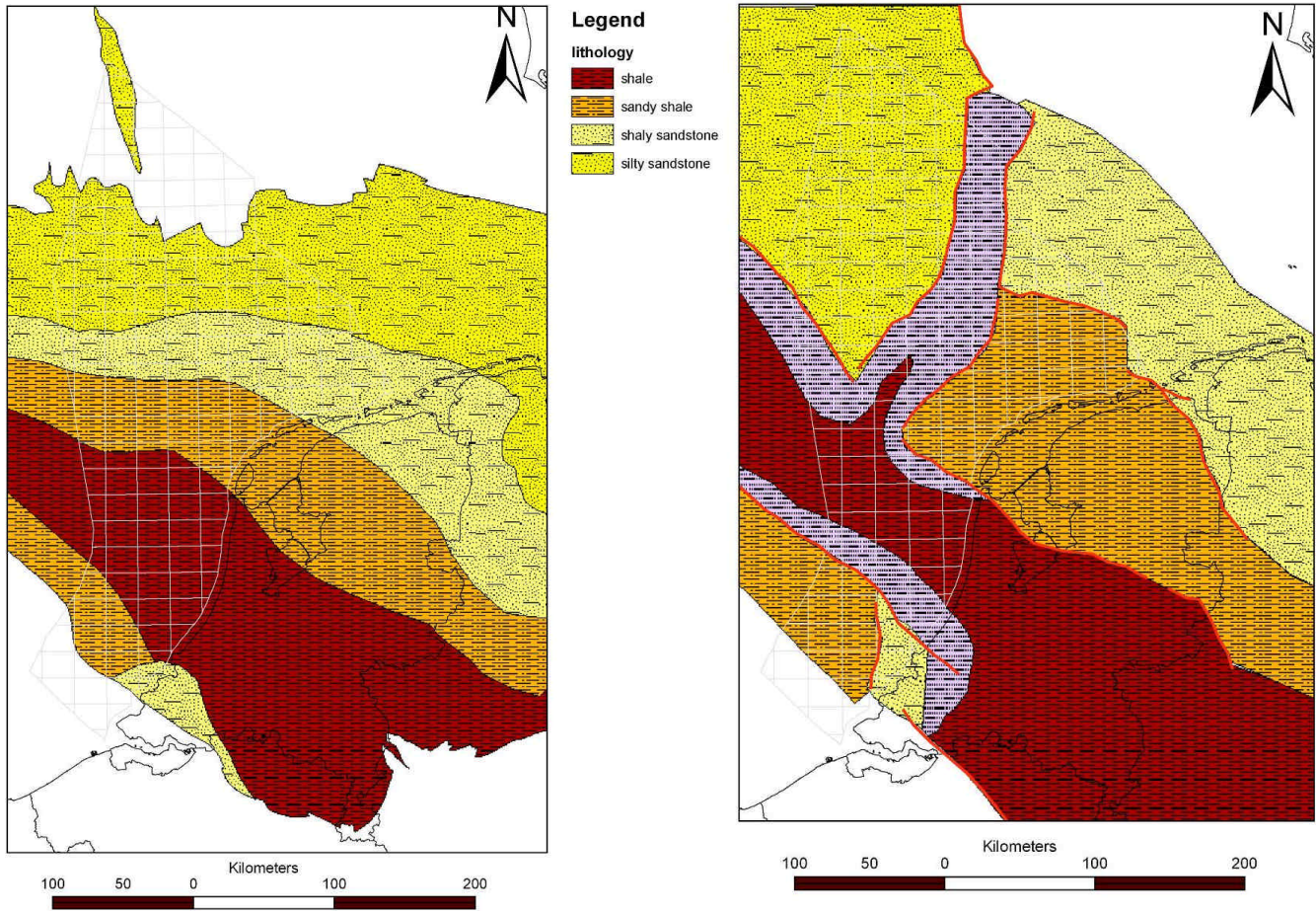


Figure 2.27 Distribution maps of unit Namur-2 for respectively Scenario 1, sag model (left) and Scenario 2, a block and basin model (right)

3 Pre-Westphalian source rocks and their maturity

Rocks are commonly considered as source rocks in case they are, may become, or have been able to generate petroleum (Tissot & Welte, 1984). The 'oilfield glossary' (Schlumberger, 2005) defines a source rock as a rock rich in organic matter which, if heated sufficiently, will generate oil or gas. Typical oil source rocks, usually shales or limestones, contain about 1.0 % organic matter and at least 0.5% total organic carbon (TOC), although a rich oil source rock interval might have as much as 10.0% organic matter. Source rocks for gas, often coal seams, consist for the major part of organic matter (~ 65% or higher), depending on the environmental setting.

Within this study rock samples with a high probability of having source rock potential have been collected from predominantly pre-Westphalian sediments and analysed in the laboratory. The source rock potential has been determined for these samples by considering three crucial variables:

- The amount of organic matter,
- The type of organic matter (kerogen type) and
- The maturity of the organic material

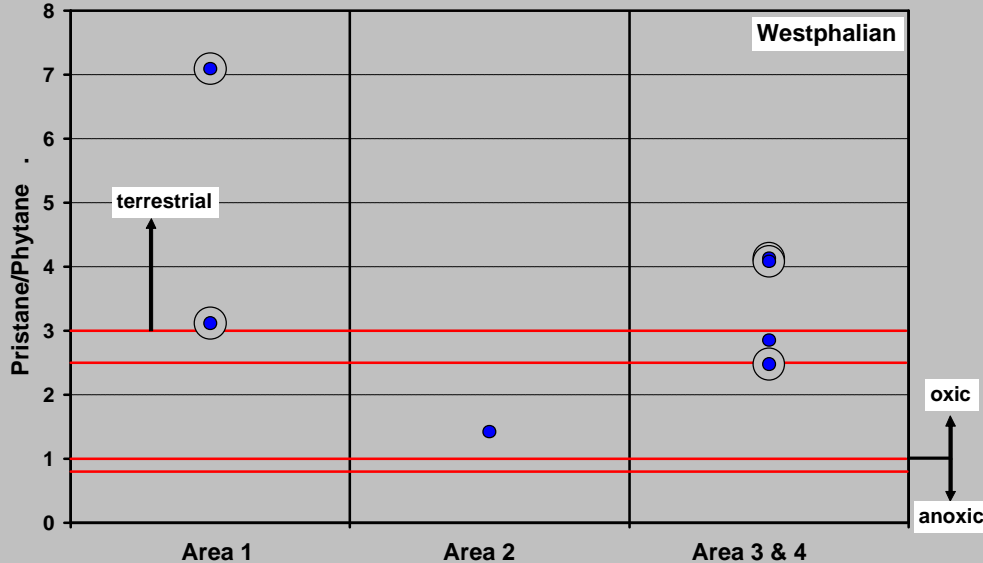
The first two variables are the result of sedimentation in a depositional environment, i.e. the facies. The depositional environment of organic rich rocks can be determined by sedimentological studies, palynological evaluations and the analyses of geochemical data (e.g. see textboxes 1 and 2), such as the studies performed in this project. Rocks of marine origin tend to be oil-prone, whereas terrestrial source rocks (such as coal) tend to be gas-prone. However, this distinction is not strict. Preservation of the deposited organic matter without degradation after sedimentation and burial is critical for the creation of a good source rock potential, and necessary for a complete petroleum system. The potential can be destroyed by oxidation, biodegradation or by thermal maturation. Thermal maturation is the process of converting the organic matter to hydrocarbons. This third variable depends mainly on the geological history of the sediments after deposition. Good source rocks reach the optimal maturity window at the right time, i.e. when generated hydrocarbons can accumulate in reservoirs that are preserved through geological times. Immature source rocks still have organic matter preserved, but have not yet contributed to petroleum occurrences, whereas overmature source rocks have lost their ability to generate hydrocarbons. The parameters that are measured to determine the level of maturity are influenced by the composition of the organic material. This is especially the case when bulk parameters are used. Since vitrinite reflectance is measured on one single organic component (vitrinite) its value is less dependent on the (bulk) composition of the sample.

This study aimed at the identification of source rocks in the pre-Westphalian deposits of the Southern North Sea Basin, especially in the Netherlands on- and offshore. Cambrian rocks are not known from wells in the Netherlands. Sediments of this age, the Alum Shale, are known to have source rock potential in Northern Europe and the Baltic States (e.g. Gérard *et al.*, 1993). However, even if similar rocks were deposited in the Southern North Sea, it is very unlikely that these could have contributed to present-day petroleum occurrences, because they would have lost their source rock potential as a result of several phases of deep burial, uplift and erosion (e.g. the Caledonian phases). Sediments of Silurian age have been drilled in the Southern North Sea basin. These

Text box 1: facies analysis by pristane/phytane ratio

The classical idea about the pristane/phytane ratio (Pr/Ph) is that it indicates the redox potential of the source sediments (Didyk *et al.*, 1978). According to these authors, Pr/Ph ratios less than unity indicate anoxic deposition, whereas ratios > 1 indicate oxic conditions (Peters and Moldowan, 1993). In the classical idea phytol is considered to be the only precursor of pristane and phytane. However, later research (Goossens *et al.*, 1984) revealed that other precursors (tocopherol, isoprenoid ethers from Archeobacteria) also play a dominant role. This implies that the Pr/Ph ratio is an indication for the absence or presence of certain organisms rather than a redox indicator (Tissot and Welte, 1984) gives an empirical relation between origin of the organic material and the Pr/Ph: Pr/Ph $\gg 1$ indicates terrestrial organic matter, Pr/Ph $\ll 1$ an evaporitic depositional environment, and Pr/Ph ≈ 1 marine organic material. Unfortunately, the Pr/Ph ratio is changed by thermal maturation (Connan, 1974; Ten Haven *et al.*, 1987; Albrecht *et al.*, 1976; Radke *et al.*, 1980; Brooks *et al.*, 1969; Connan, 1984). Ten Haven *et al.* (1987) found an increase in Pr/Ph with increasing maturity. According to Koopmans *et al.* (1996) the Pr/Ph becomes more or less constant after a certain maturity.

In samples of low thermal maturity, Pr/Ph ratios are not recommended to describe paleoenvironment (Volkman and Maxwell, 1986; Peters and Moldowan, 1993). Within the oil generative window, high Pr/Ph ratios (>3.0) indicate terrestrial organic matter input, and low values typify anoxic commonly hypersaline environments. For samples showing Pr/Ph in the range 0.8 to 2.5, it is not recommended to use Pr/Ph as an indicator of paleoenvironment (Peters and Moldowan, 1993). There is also a relation between maturity and Ph/*n*-C18, which decreases with increasing maturity (Ten Haven *et al.*; 1987).



Example of the use of *pr/ph* ratio. The analysed Westphalian coal samples (indicated by the circle) clearly indicate a terrestrial environment, while other Westphalian (shale) samples are less distinct.

rocks often have a dark colour, e.g. in well O18-01 which reached its final depth in dark, turbiditic claystones and sandy claystones of Late Silurian age (Van Adrichem Boogaert and Kouwe, 1993-1997). This dark colour of the Silurian rocks and the common lack of bioturbation indicate initially high TOC values (Cameron and Ziegler, 1997). However, due to the Caledonian (Acadian) deformation phase in the Early and Middle Devonian these rocks were already overmature at an early stage. This is also indicated by the slaty cleavage of these rocks found in the UK and Belgium (Cameron and Ziegler, 1997). These rocks are probably overmature throughout the basin, except on the stable Midland Massif in the UK part of the London-Brabant Massif (Cameron

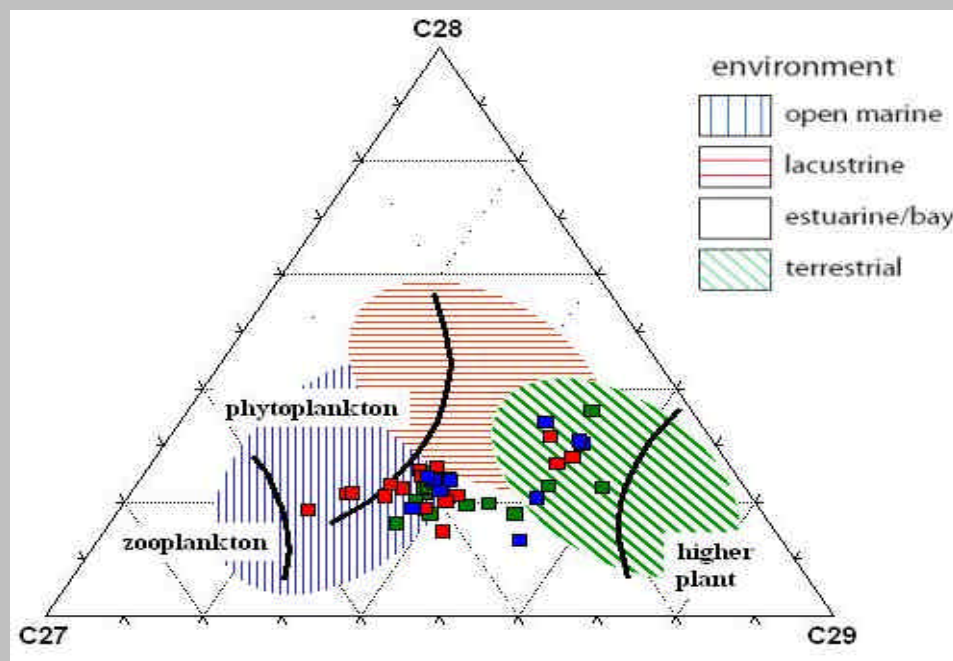
and Ziegler, 1997). Our analyses show that the organic rich shales of O18-01 are past their hydrocarbon generating potential. We therefore consider the source rocks potential of Silurian and older source rocks highly speculative. Given the lower maturity in area 2 (see below) there may be some source rock potential in the Silurian, but these rocks were never drilled.

Based on the above, it was decided at the onset of the study that the economic basement is formed by the low-grade metamorphic Cambrian to Silurian Caledonian succession and that sediments of these ages are not considered in this study.

Therefore, the potential was evaluated of the Devonian, the Dinantian, the Top Dinantian to Base Namurian transition, and the Namurian. All tables and figures used in this Chapter are extracted from the digital geochemical database accompanying this report. For details on geochemical methods, instruments and calculations reference is made to Appendices A, B and F.

Text box 2: facies analysis by sterane evaluation

The proportion of C27-C28-C29 steranes gives an indication for the depositional environment of a source rock. Dominance of C29 steranes indicates terrestrial depositional environment. C27 steranes are predominantly produced by zooplankton and are therefore a strong indicator for marine conditions. The ternary plot of the C27-C29 regular steranes describes the relationship between the sterane compositions in biological sources (marked by the thick lines in the diagram) and in open marine, lacustrine, estuarine or bay and terrestrial ecosystems (after Huang & Meinschein, 1979). The percentage distribution of the steranes is extracted from the geochemical database. The tic marks on the ternary plot represent 10 percent intervals. More information on source related biomarkers can be found in Peters et al. (2005)



Example of ternary plot of C27, C28 and C29 steranes. All samples are plotted without distinction of age. Green = Area 1, red = Area 2, blue = Area 3

3.1 Devonian

3.1.1 Facies and typing of organic matter

3.1.1.1 Area 1

The major part of the Netherlands on- and offshore was part of a cratonic high during the Early Devonian and deposition of source rocks during this time is therefore unlikely. From the Middle Devonian onwards, sediment accumulation started in Area 1 in a mostly continental to shallow marine setting (Ziegler, 1990). Potential source rocks in Area 1 can be found within the Late Devonian succession. In Area 1 this includes the marine strata of the Bollen claystone and the interbedded dark-grey, partly calcareous mudstones of the Bosscheveld Fm (Van Adrichem Boogaert and Kouwe, 1993-1997). The Bollen claystone has been encountered in the wells S05-01 (reference section, Van Adrichem Boogaert and Kouwe, 1993-1997), Brouwershavense Gat-1 (BHG-01), Kortgene-1 (KTG-01), S02-02 and Winterswijk-1 (WSK-01). It consists of dark mudstones and some intercalated, thin, white to greenish-grey, fine grained sandstones. The unit was deposited in a low-energy shelf, shoreface to transitional marine setting. (Van Adrichem Boogaert and Kouwe, 1993-1997).

Although no wells in Area 1 have encountered the Devonian directly north of the Zeeland Platform, marine source rocks could be present here as well. Cameron and Ziegler (1997) postulated that if marine source rocks are present, they should occur (based on the paleogeography) most likely in the UK Quadrants 48, 49, 53, and 54 and in the Dutch Quadrants K and P.

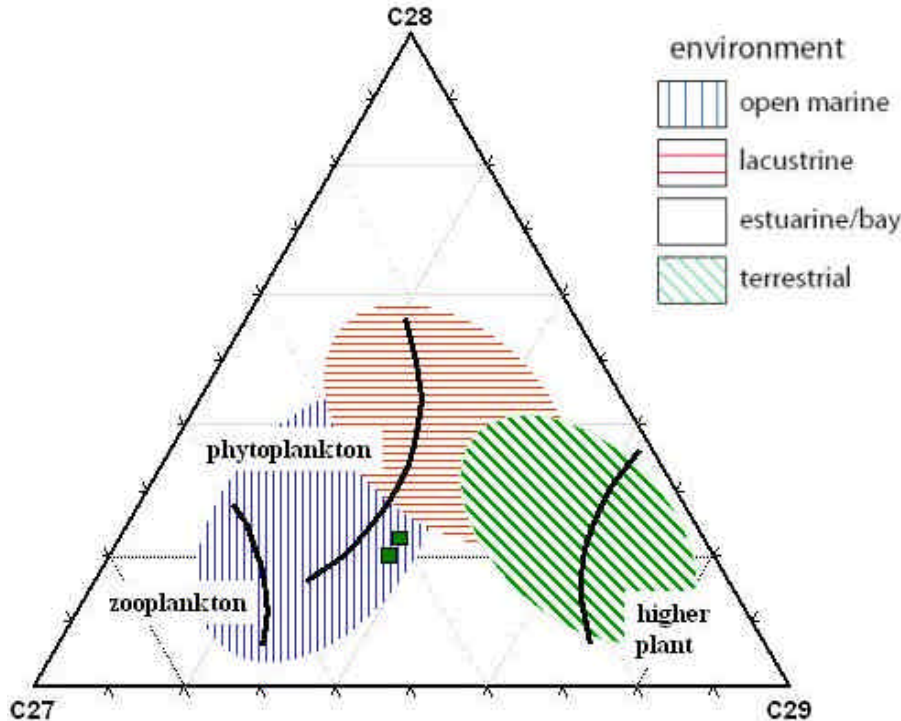


Figure 3.1 Devonian facies (based on GC-MS (SIM) data – biomarker analysis) on the basis of the proportion of C27-C28-C29 steranes. Dominance of C29 steranes indicates terrestrial depositional environment. C27 steranes are predominantly produced by zooplankton. Green squares = Area 1

Given the marine character of the deposits, organic rich Type II shales could be present in the Bollen Claystone. The evaluation of the sterane composition confirmed a merely marine environment (Figure 3.1). The pristane / phytane ratio is not very discriminative (Figure 3.2). However, Rock Eval measurements on the samples showed that Type II organic matter could not be confirmed for the Devonian (Figure 3.2). Some samples in Area 1 show higher Hydrogen Indices, which can indicate original Type II material. However, due to the present-day degree of coalification no source rock potential has remained.

Textbox 3:

It appears that in UK well 38/3-1 Devonian coal seams were drilled (UK Nomenclature; The Millenium Atlas, 2003). Several coal seams have been identified on the logs in the Devonian succession and cuttings of this well were sampled. These samples clearly show coal pieces, also confirmed by others (Marshall, pers. com.).

Several options are possible:

1. The host rock and the coal seams are indeed of Devonian age. This would change the perception of the Devonian sedimentary setting in area 2.

Palynological studies in the eighties showed that the coal-bearing section was, surprisingly, of Fammenian age (Besly, pers. com.). The palynology was subsequently done again, independently, with the same result (Besly, pers. com.). These results (Late Devonian – Devonian age) have been published (Glennie, 1998), by stating that the coal bearing section is a thick (c. 795 m) unit of very fine to fine-grained micaceous sandstones, with thin interbeds of shales and coals (Glennie, 1998). The latter are clearly visible on logs and in cuttings (Glennie, 1998), although others do not think that the log signature is convincing (Besly, pers. com.); Marshall, pers. com.).

The coal seams are about 0.5 – 1 m thick and to comprise 1 to 2 % of the total section (Glennie, 1998). Unfortunately, the apparent coal seams are not cored (Glennie, 1998).

2. The host rock is of Devonian age and the coal particles in the samples result from a lignite/coal mud additive or contaminant. This idea is supported by several workers who have evaluated this well (Besly, pers. com.). The occurrence of Frasnian coals is highly unusual, since these are unknown in the Scottish Old Red sandstones (as indeed is most organic matter; Marshall, pers. com.). The lithology of immature sandstone is also rather unusual for a coal facies (Marshall, pers. com.). Where we find thin Frasnian coals in Greenland the surrounding sandstones are rather different (Marshall, pers. com.).

Unfortunately, treatment of a picked coal sample in fuming nitric revealed nothing (no palynomorphs; Marshall, pers. com.).

The vitrinite reflectance was the same for the run of coals and again too low for local reflectance from kerogen isolates (Marshall, pers. com.).

Marshall (pers. com.) concluded that there was a lignite/coal mud additive (as this well was drilled decades ago) in a well with poor hole condition.

3. The host rock and the coal seams are of Carboniferous age. This seems unlikely, given the palynological evidence.

Clearly, the only possibility for a Devonian source rock is if option 1 would be the case. Glennie (1998) state that the coals in well 38/3-1 have very good source potential, largely from type III gas-prone kerogens. TOC measured on three picked-cuttings samples of coal lithologies range from 22 to 35% (30.5 % mean), and good potential yields are suggested by pyrolysis (Glennie, 1998). The source potential of these coals is limited by their low abundance in the sequence (1-2 %), although this is partly offset by the overall thickness of the coal-bearing interval (795 m; Glennie, 1998). Analysis of the shales in the section revealed minimal source rock potential (Glennie, 1998).

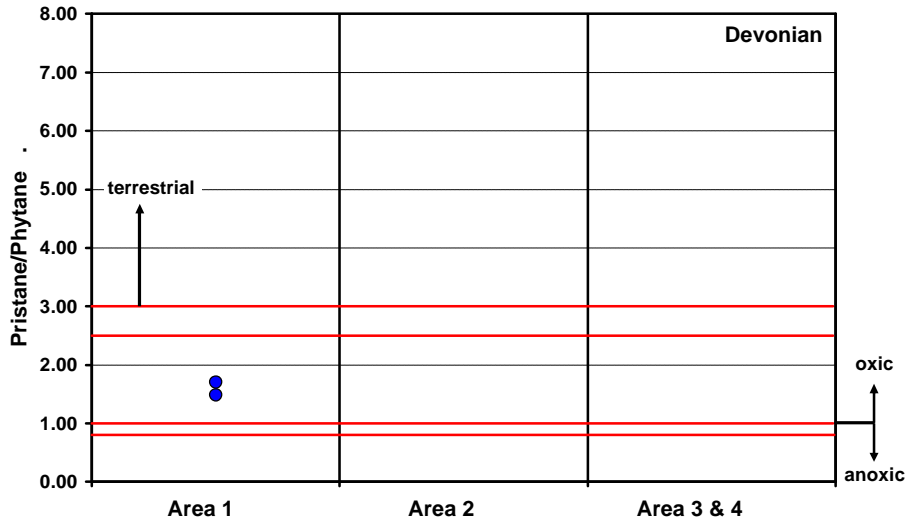


Figure 3.2 Variation in Pristane/Phytane ratio of the Devonian per area

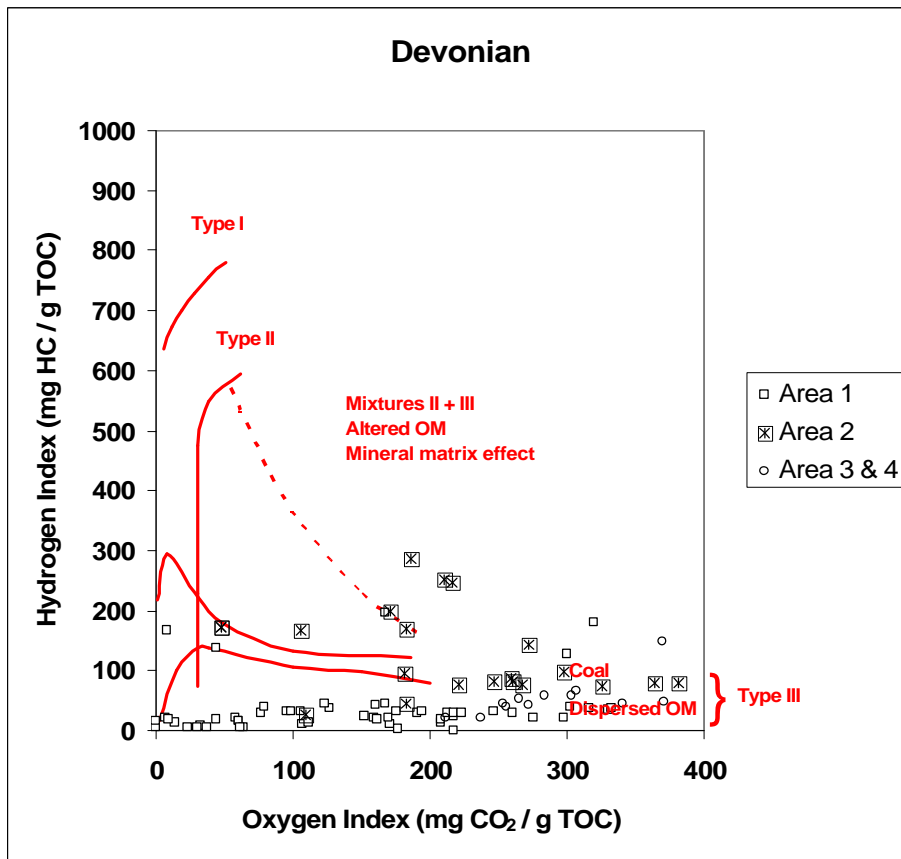


Figure 3.3 Pseudo-Van Krevelen diagram of the Devonian

3.1.1.2 *Area 2*

In Area 2, shelf carbonates, non-marine sediments and coastal-margin deposits were deposited during the mid-Devonian (Marshall and Hewett, 2003). The Kyle Group is known to have a mudstone unit in its upper part in other parts of the North Sea (Cameron, 1993; Millenium Atlas). The Kyle Group was not drilled in the Netherlands offshore area but was identified by seismic evaluation (Appendix E). The Kyle Group is covered by clastic sediments of the Old Red Group, that were deposited in a continental setting. Source rock quality of these rocks is expected to be low because they are barren of organic matter. The mudstone in the upper part of the Kyle Group may contain some organic matter, but this could not be confirmed. There are therefore, no direct indications for any source rock quality of this mudstone. Other Devonian source rocks in Area 2 are unlikely, or have negligible source rock potential (Glennie, 1998). North of Area 2, lacustrine mudstone source rocks are encountered in the Orcadian basin between Scotland and the Shetland Islands (Marshall and Hewett, 2003). Extension of these rocks into the Netherlands offshore is considered unlikely.

Although there are reports that in UK well 38/3-1 Devonian coal seams were drilled (UK Nomenclature; Marshall and Hewett, 2003), this is considered to be unlikely (see Textbox 3). However, Glennie (1998) did consider the organic matter in this well as potential Type III source rocks on the basis of HI and OI. The values for the HI and OI were confirmed in this study (Figure 3.3). However, the shape of the Rock Eval pyrogram is very irregular, and no reliable Tmax value could be deduced. This seems to confirm the possibility of contamination of the cuttings with an organic additive. This is also in agreement with earlier results of the analysis of atomic H/C ratio of a hand-picked coal sample. These showed a consistency with the idea of a contaminant (e.g. caving) and not an in situ coal (Marshall, pers. com.).

The other Devonian samples from Area 2 show a high OI and HI (up to circa 150). These data indicate Type III organic matter in Area 2, which is in agreement with the terrestrial environment of the Old Red Group deposits.

3.1.1.3 *Area 3&4*

The deposits of Devonian age in Area 3 & 4 are part of the Banjaard Group. Sediments of this group were encountered in wells Winterswijk-1, Munsterland-1 and Isselburg-3 (NITG-TNO, 1998). In this area, the Banjaard Group is divided into the Banjaard clastics, the Bollen Claystone and the Bosscheveld Fm. The clastic deposits were deposited in a shallow marine environment. The Bollen Claystone and the Bosscheveld Fm were deposited during an important transgression (NITG-TNO, 1998). Source rock occurrences were not found, but if present they are expected to be originally of Type II organic matter due to its marine origin.

3.1.2 *Total Organic Carbon*

3.1.2.1 *Area 1*

Shale intervals of the Bollen claystone were sampled for geochemical analysis. In addition, the Bosscheveld Fm was sampled, preferentially the shales, and Devonian sediments from Belgian wells were also sampled. The data show that there is some source rock potential in the Devonian. One Devonian sample of well Brouwershavense Gat-1 has a TOC of 2.14%. In general, the TOC is relatively low, although, given the maturity of the Devonian in this area, the initial TOC would have been higher. The

contribution of Devonian source rocks in Area 1 to hydrocarbon accumulations seems limited but the possibility of some potential can not be excluded.

3.1.2.2 Area 2

In the northern offshore of the Netherlands the Devonian succession was drilled in wells A17-01 and E06-01. Samples were taken from both wells. The analytical results show that the present-day TOC content of these samples of Devonian rocks is negligible, although at a depth of 2883 m a high TOC value (5.8 %) was encountered in well A17-01, which was confirmed by a second measurement on the same sample. It seems, however, likely that this high TOC content is due to contamination (see Textbox 3 and 3.1.1.2).

3.1.2.3 Area 3&4

The TOC values of the samples taken from wells in Area 3 & 4 are low, and comparable to the values in Area 1 and 2.

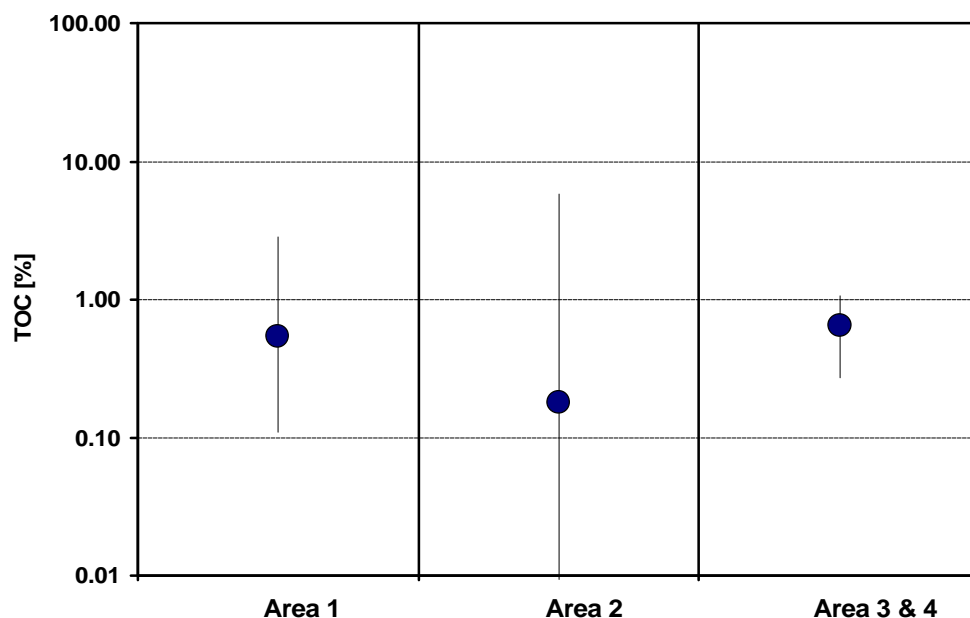


Figure 3.4 Distribution of TOC values in the Devonian per area, with the range and median. Generally the TOC is well below 1.0 %.

3.1.3 Maturity

3.1.3.1 Area 1

The maturity of the Devonian samples in Area 1 ranges from 1.5 to 3.0 %Rr (Figure 3.5) and this would position the organic material within the stage of gas generation. Whether gas generation is actually taking place depends on the amount and type of organic material present.

3.1.3.2 Area 2

In Area 2 the Devonian deposits have maturities ranging from 0.7 to 1.5 %Rr, significantly lower than in Area 1 (Figure 3.5). The organic material in the Devonian deposits at the locations of the wells are currently in the late oil window to early gas window. However, the low TOC of the material implies poor source rock quality.

3.1.3.3 Area 3&4

The Devonian deposits in Area 3&4 are overmature, with maturity values well over 4.0 %Rr. Reconstruction of the burial history will show the timing of maturation at these locations.

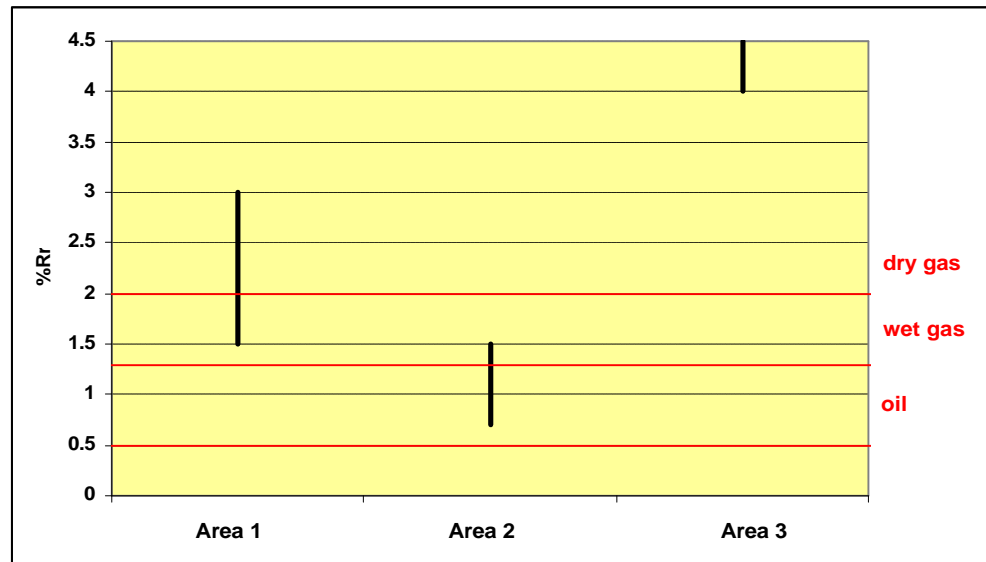


Figure 3.5 Variation in measured maturity of the Devonian samples per area

3.2 Dinantian

3.2.1 Facies and typing of organic matter

3.2.1.1 Area 1

The Dinantian deposits in Area 1 (the Zeeland Fm.) are mainly carbonates. In the UK onshore area Brigantian intrashelf basinal carbonates have been identified as possible Dinantian source rocks (Gutteridge, 2002). Therefore, Dinantian deposits, and especially shales, are being considered as possible source rocks. The Zeeland formation (Carboniferous Limestone Group) consists of three members (Fig. 2.16; Van Adrichem Boogaert and Kouwe, 1993-1997) that correspond to our Dinant-1, Dinant-2 and Dinant-3 respectively (Chapter 2):

- **Dinant-1** (~The Beveland Mb), a succession of medium–grey or brown-grey to darkbrown or brown black, coarse crystalline dolomites, often containing black organic intergrain residues. In places minor grey to dark-grey limestone intercalations occur, as well as minor quantities of dark-brown to blackish siltstone and shaly claystone. Dark beds of silicified dolomite are occasionally present. This member has been encountered in well Kastanjelaan-02.
- **Dinant-2** (~The Schouwen Mb), a thick succession of light to dark-grey, dark-to yellowish-brown and brownish black, and light yellowish-brown to dusty yellow-brown limestones. Intergranular bituminous, organic material is present. This member has been encountered in well Geverik-1.

- **Dinant-3** (~The Goeree Mb), a succession of grey to dark grey and black limestones, thin- to thick-bedded and often partly silicified. The limestones often grade into calcareous and/or silicified black shales (see “Namurian source rocks” below) or black cherts towards the top. This member has been encountered in well Geverik-1.

Evaluation of the sterane proportions in Area 1 indicates that the organic material is a mixture of terrestrial and marine organic matter (Figure 3.6). The most distinct terrestrial signal was found in well S05-01. The samples indicated in this figure represent mainly the shales that are found within the carbonate succession. It must be emphasized that in the selection of the samples, shale intervals with a high gamma ray signal were preferentially sampled. However, the data are slightly biased by the availability of sample material. For example, samples in well O18-01 were taken from a pure carbonate core. At other depths in this well shale intervals with high gamma ray were identified, but these were not sampled.

Given the sedimentological description above, a terrestrial input was not expected. This possible terrestrial input could neither be confirmed by the pristane / phytane ratio, which shows non-discriminative values (Figure 3.7).

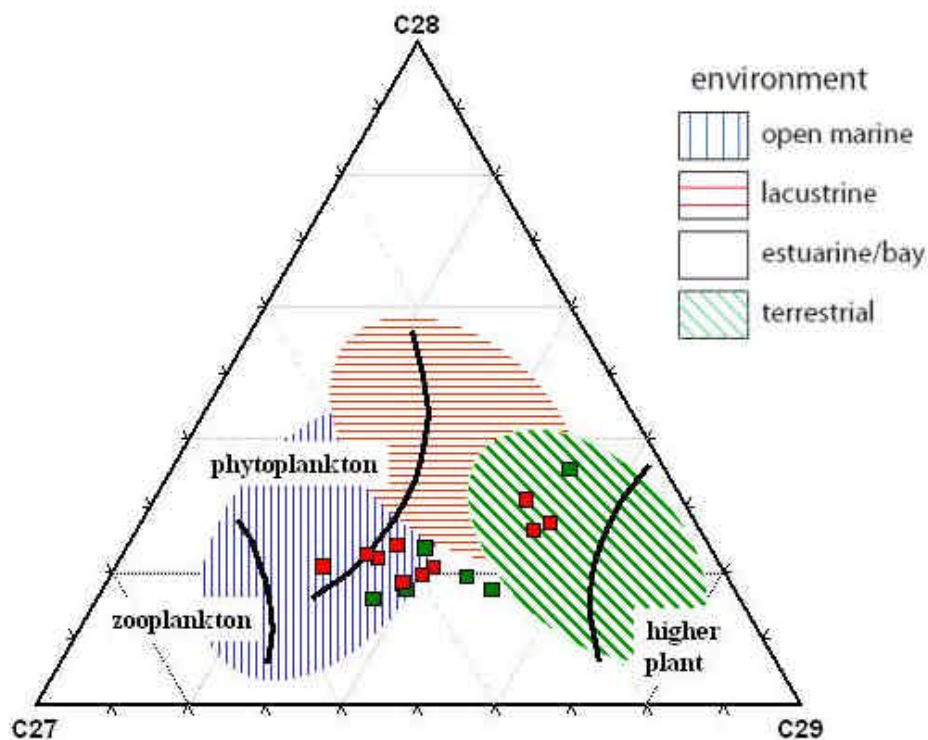


Figure 3.6 Dinantian facies (based on GC-MS (SIM) data – biomarker analysis) on the basis of the proportion of C27-C28-C29 steranes. Dominance of C29 steranes indicates terrestrial depositional environment. C27 steranes are predominantly produced by zooplankton. Green squares = Area 1, red squares = Area 2

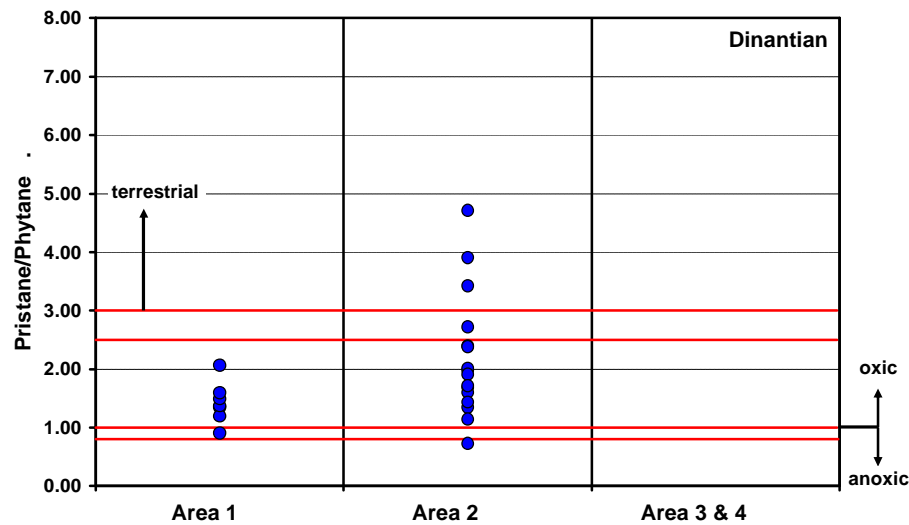


Figure 3.7 Variation in Pristane/Phytane ratio of the Dinantian per area

Based on the sedimentological description, Type II organic matter was expected to dominate. However, only few samples showed a HI of more than 200 (at relatively high OI). Analyses in this study showed mainly Type III organic matter in Area 1 (Figure 3.8). This is in agreement with the indication of the steranes of a terrestrial contribution.

The black organic intergrain residues of Dinant-1 (the Beveland member) do not seem to have much source rock potential. Similar stylolites have been extensively investigated in well O18-01, without indications for source rock potential.

In view of these analyses, the most likely occurrence of intra-Dinantian source rocks in Area 1 are the bituminous sediments of the Schouwen Mb (approximately coinciding with our unit Dinant-2).

3.2.1.2 Area 2

In Area 2 the Dinantian deposits correspond to the Farne Group (Van Adrichem Boogaert and Kouwe, 1993-1997), which consists of the Cementstone Formation, the Elleboog formation and of the Yoredale Formation (Chapter 2).

The Cementstone Fm is formed by a cyclic alternation of carbonates, claystones, sandstones and minor coal seams. The carbonates occur as limestone, dolomitic limestone beds. The unit was deposited under paralic conditions with repeated marine incursions, during which marine limestones and claystones were formed.

The Elleboog Fm comprises a sequence of alternating claystones, sandstones and minor amounts of coal, with a few calcareous or dolomitic intercalations. The formation was deposited in a paralic and fluvial setting.

The Yoredale Fm is formed by a cyclic alternation of limestones, claystones, sandstones and rare coal seams. The number of limestone beds is variable. The formation was deposited under paralic conditions. Frequent marine incursions resulted in the formation of marine limestones and claystones (Van Adrichem Boogaert and Kouwe, 1993-1997).

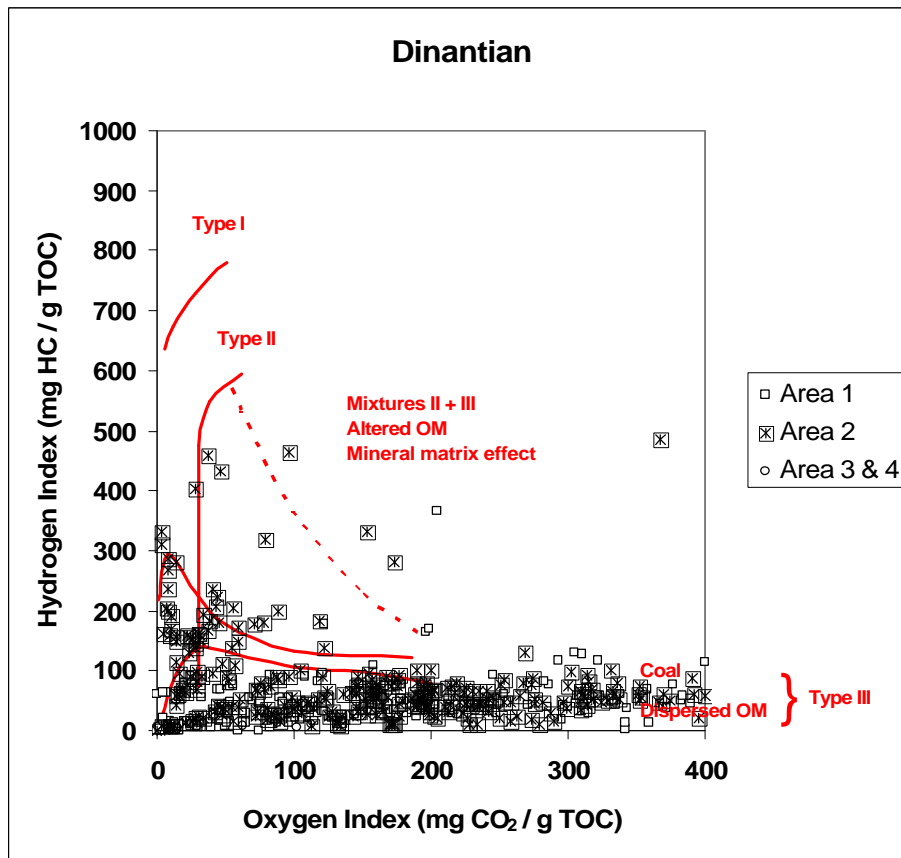


Figure 3.8 Pseudo-Van Krevelen diagram of the Dinantian

The sterane composition of the investigated rock samples in Area 2 indicate both a marine and terrestrial depositional environment. This is in agreement with the character of the transgressive cyclothems with marine influences at the base, as shown above (Figure 3.6). Evaluation of the pristane / phytane ratio shows also a clear distinction between the investigated samples: while the coal samples have a clear terrestrial signature, the shale samples show marine influences (Figure 3.7). Plotting the geochemical results vs. depth shows that the cyclothems are indeed recognized in the geochemical data (Figure 3.9). The coal seams are deposited in a terrestrial setting, and are most likely gas-prone (Type III).

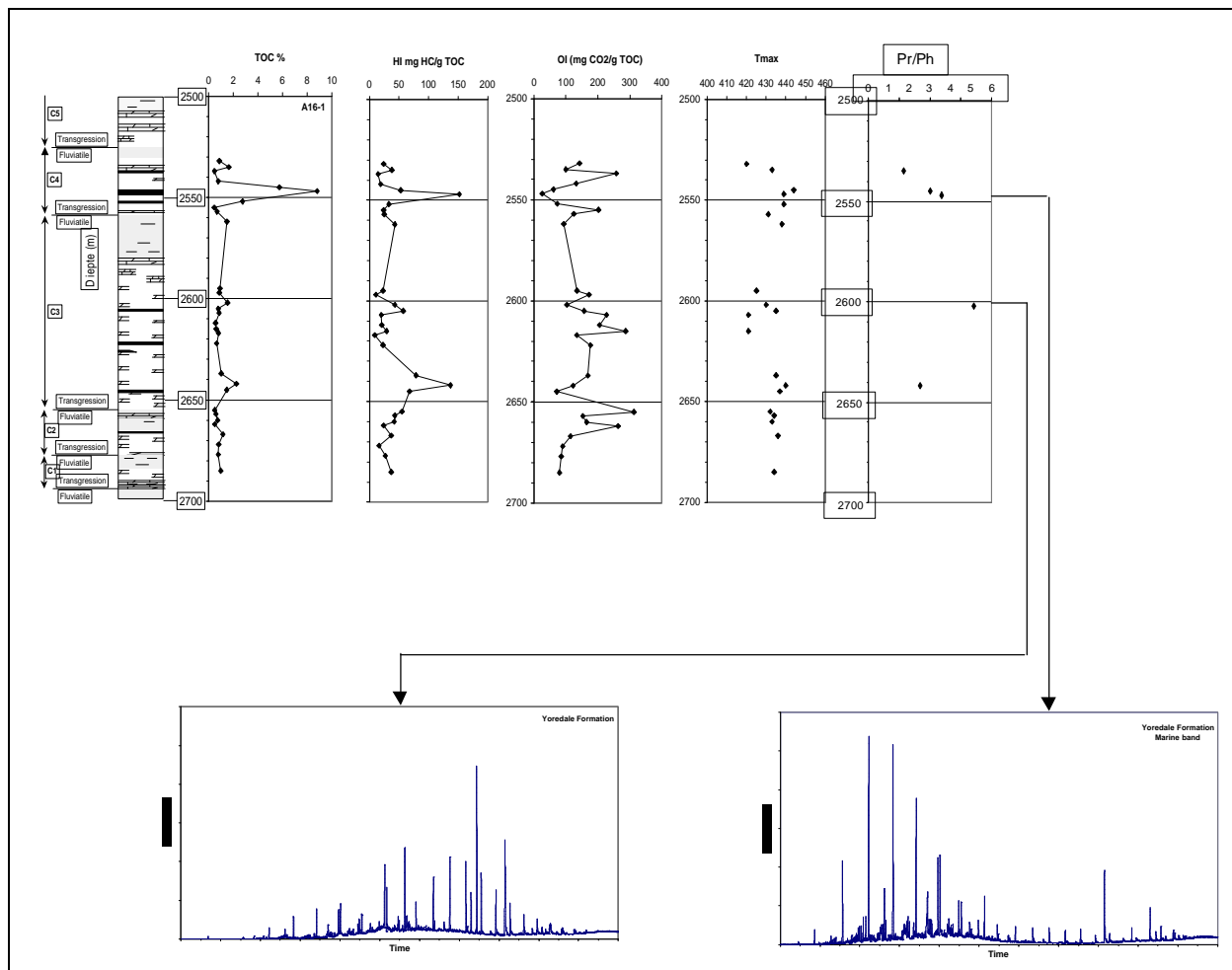


Figure 3.9 Lithology, TOC, HI, OI, Tmax and Pr/Ph in the Yoredale facies in well A16-01 (from Graf Pannatier *et al.*, 2000; data included in this study)

The analyses of samples from Dutch wells did not indicate Type II kerogen. However, the analysed samples from the Yoredale deposits in some of the UK wells do show indications of Type II source rocks near our Area 2 (Figure 3.8). Marine oilprone source rocks are possibly present within parts of the Yoredale succession, probably due to marine influences during transgressions.

Marine oilprone rocks may possibly also be present in the center of the Dinantian basin between the Elbow Spit and Cleaver Bank Highs and the London Brabant Massif. This central offshore area was geographically remote from the Yoredale delta. Anoxic bottom conditions are expected to have existed in this area, at least during part of the time (Cameron and Ziegler, 1997). Therefore, these basins probably were the sites of deposition of shales, organic-rich shales and chert layers that have developed on top of drowned platforms. Black shales with oil-generating potential have been observed in several parts of the Variscan foreland, mainly at the base of the Namurian (Cornford, 1998). Similar shales may be present within the Dinantian sequence. However, these deposits were never drilled.

3.2.1.3 Area 3&4

Well Winterswijk-1 (WSK-01) in Area 4 has penetrated 185 m of Dinantian rocks. The deposits found here consist of carbonates with intercalated shale deposits (NITG-TNO, 1998). These deposits are probably present throughout the eastern part of the Netherlands and into Germany. In the south-eastern part of Area 3 & 4 in Germany, the Dinantian deposits consist of a condensed sequence of deep basin sediments (Fig. 3.10). Relevant wells that have encountered the Dinantian include the wells Münsterland-1, Isselburg-3, Wachtendonk-1 and Schwalmthal-1001.

Typing of organic matter of the samples from wells Münsterland-1 and Schwalmthal-1001 was not possible due to high maturation (Figure 3.12). Based on the marine character of the rocks Type II is expected.

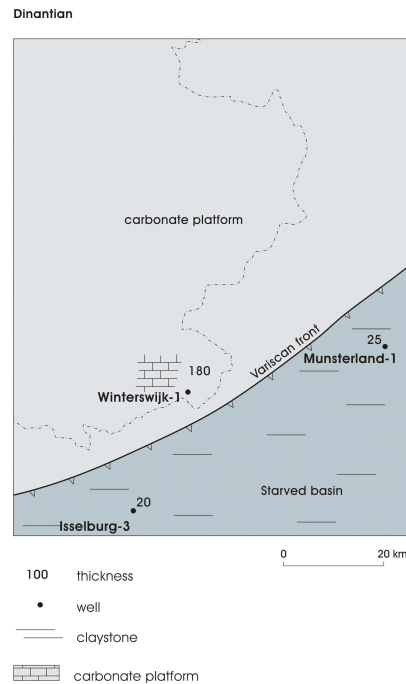


Figure 3.10 Paleogeographical map during deposition of the Dinantian (adapted after NITG-TNO, 1998). The carbonate platform that was present at the location of well Winterswijk-1 is bounded to the south by a deep starved basin with a condensed sequence (NITG-TNO, 1998).

3.2.2 Total Organic Carbon

3.2.2.1 Area 1

Based on the TOC (up to 2%), some source rock potential is present in the Dinantian in Area 1 (Figure 3.11). The analytical results of the samples from intra-Dinantian shales that from well 53/12-02, west of the Dutch sector, indicate that the TOC can be higher, up to circa 2.7 %. The analyses of samples from the Belgian wells also show that specific intervals are enriched in organic matter. South of the London-Brabant Massif, there are some organic rich intervals in the Dinantian 1 unit (Tournaisian, well Rollegem-Tombroek).

3.2.2.2 Area 2

The evaluation of the organic content of the Yoredale facies (Area 2) of 15 wells shows that the organic matter is concentrated in the coal seams. Thin coal seams (up to 1 m) are found throughout the whole succession. TOC contents are generally between 0.89 and 1.87 % (Gerling et al., 1999), but locally almost up to 9.0% (Graf Pannatier et al., 2000; data included in this study). These observations have probably resulted from analyses of cuttings; the TOC of cores of the coal seams are higher. Some of these coal seams are relatively pure, with TOC values of 50 – 70 %. Some of the shales have TOC values in the order of 3.0 %.

3.2.2.3 Area 3&4

The samples from Area 3&4 show moderate values of TOC. This is still relatively high, considering the maturity of the analysed samples (see below).

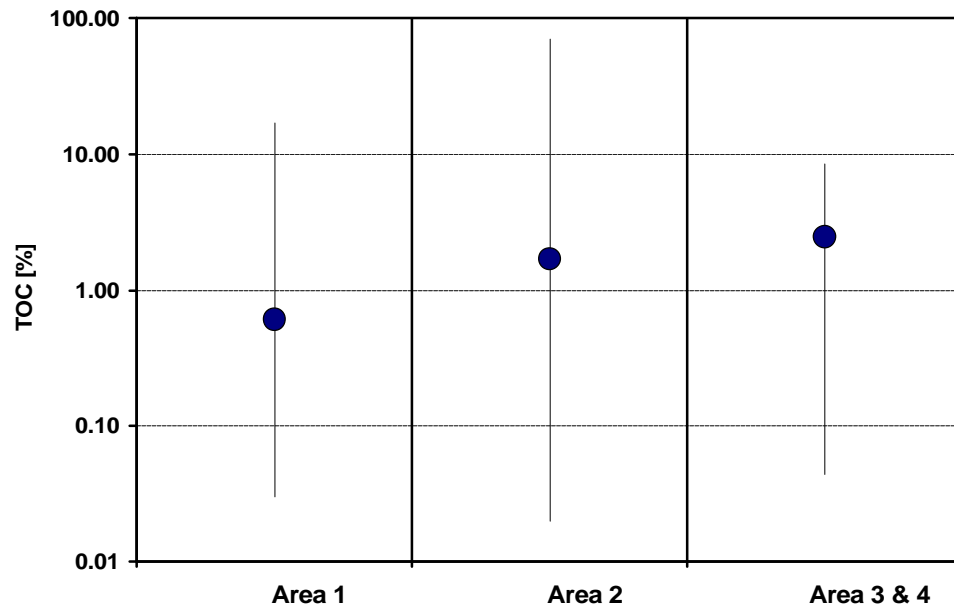


Figure 3.11 Distribution of TOC values in the Dinantian per area, with the range and median.

3.2.3 Maturity

3.2.3.1 Area 1

The maturity of the Dinantian of the Netherlands in Area 1 ranges from 0.8 to 2.0 %Rr (Figure 3.12). Depending on the type of organic matter these deposits could be generating both oil and gas.

3.2.3.2 Area 2

In most wells in Area 2 this maturity generally falls within the 0.5 – 1.4 %Rr range. This implies immature to mature organic matter with respect to oil generation and immature to early mature with respect to significant gas generation. Well 41/24a-02 and well 43/17b-02 are exceptions with a higher degree of coalification in the Dinantian.

3.2.3.3 Area 3&4

The samples taken from Dinantian deposits in Area 3&4 are, like those from the Devonian in those areas, overmature with maturity values well over 4.0%Rr.

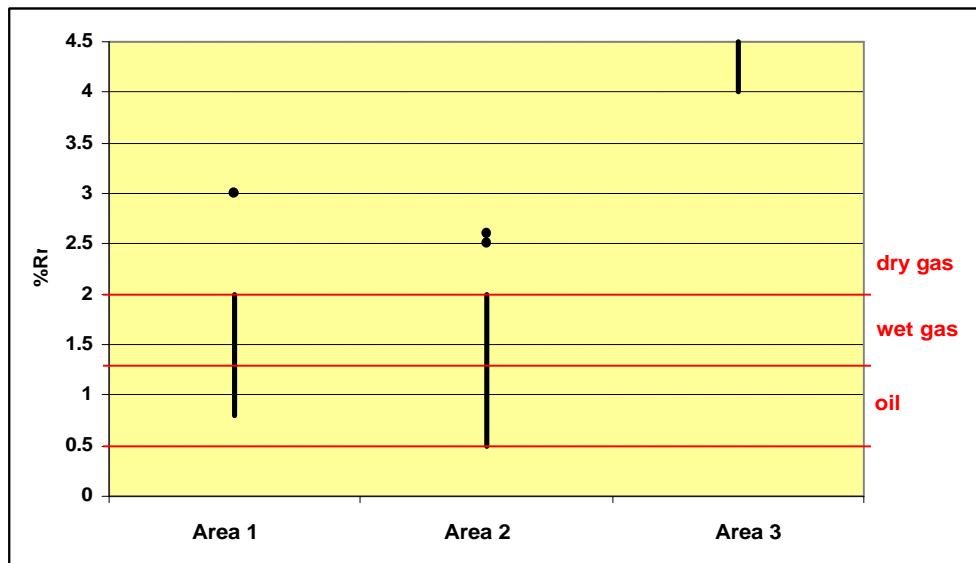


Figure 3.12 Variation in measured maturity of the Dinantian samples per area

3.3 Top Dinantian – base Namurian

3.3.1 Facies and typing of organic matter

Organic rich shales have been deposited near the boundary between the Dinantian and the Namurian. This boundary indicates the change to a regressive system in the Namurian-Westphalian. The sediments of this period were only developed in the fully marine parts of the basins, because of the restricted circulation of the water during deposition.

The beginning of shale deposition in the basins is not completely synchronous with the Dinantian-Namurian boundary: in the U.K. (and possibly in the Netherlands) Dinantian organic rich shales were deposited in basins chronologically equivalent to carbonate platform deposits. Chapter 2 describes that based on, among others, these observations a major deepwater, shale basin was postulated for much of the Namurian in the southern North Sea, essentially in the same basin as the Dinantian (Cameron, 1993; Gerling et al., 1999; Cameron and Ziegler, 1997). This was considered as model 1 in Chapter 2. Possibly, carbonate platforms acted as barriers that prevented terrestrial influx into the intra-platform basins (model 2). If these intra-platform basins existed in the Namurian, they might have also contained these basal Namurian source rocks. These rocks are referred to as 'Geverik Member', 'Hot Shales', 'Ampelite', 'Bowland Shale', 'Edale Shale' and 'Hängende Alaunschiefer' in Germany.

3.3.1.1 Area 1

In area 1, the Dinantian-namurian boundary was cored in well Geverik-1. The high TOC shale interval at the base of the Namurian 1 unit in this well is the type section for the Geverik Member (Van Adrichem Boogaert and Kouwe, 1993-1997). This member constitutes the base Namurian in the Limburg area just northeast of the Brabant-Massif. The unit consists of dark-grey or black, bituminous, shaly claystones, with intercalations of siltstones and very fine-grained sandstone. The age of the member is Alportian to Arnsbergian (Namurian A). These black shales have been interpreted as

having settled from suspension in an anoxic marine basin with restricted circulation. In the type section a gradual transition can be observed from the limestone-shale alternation of the Carboniferous Limestone Group into the marly basal interval of the Geverik Member. The Geverik Mb has been identified in wells throughout area 1, where it is usually found to rest unconformably on massive Dinantian carbonates (see also Figure 2.12).

Evaluation of the sterane composition (Figure 3.13) and the pristane / phytane ratio (Figure 3.14) indicate a dominantly marine depositional environment, which agrees with the conclusion from the sedimentological evaluation. The sample with the highest terrestrial signal is from well P16-01. Typing of the organic matter in Area 1 is generally difficult because of the overmaturity of the section in most of the wells (section 3.3, figure 3.17). Due to the very high degree of coalification mostly only black to very dark brown organic debris has been encountered. However, the marine environment in this well was previously defined by microscopic kerogen typing. The deposited organic matter deposited in this marine environment was most probably initially oil-prone (Type II). An exception to the high coalification is well P16-01, with a moderate maturity at the transition between the Dinantian and the Namurian. The analysed samples of this well show low HI and are therefore classified as predominantly Type III material (Figure 3.15). This confirms that the depositional environment at the location of well P16-01 was not fully marine as it was e.g. in well Geverik-1. This agrees with the facies typing by the sterane composition.

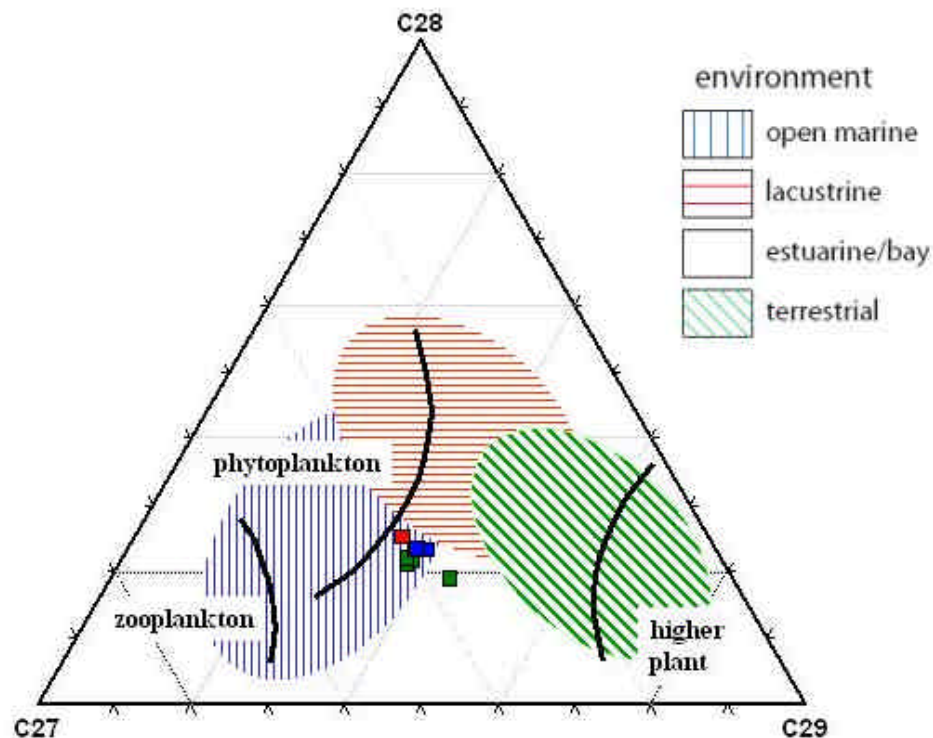


Figure 3.13 Top Dinantian – Base Namurian facies (based on GC-MS (SIM) data – biomarker analysis) on the basis of the proportion of C27-C28-C29 steranes. Dominance of C29 steranes indicates terrestrial depositional environment. C27 steranes are predominantly produced by zooplankton. Green = Area 1, red = Area 2, blue = Area 3

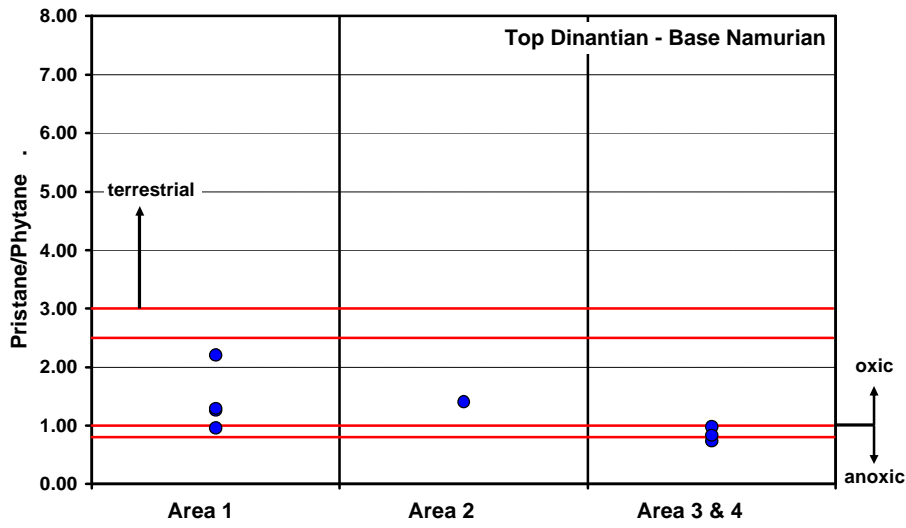


Figure 3.14 Variation in Pristane/Phytane ratio of the Top Dinantian – Base Namurian per area

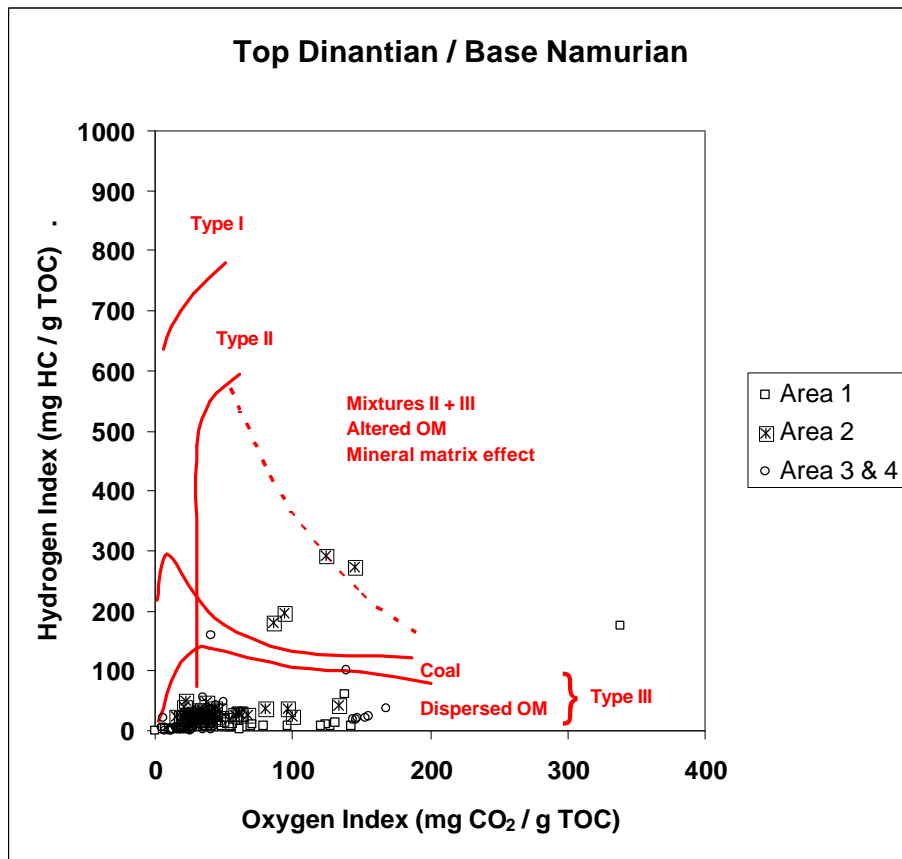


Figure 3.15 pseudo-Van Krevelen diagram of the Top Dinantian – Base Namurian

3.3.1.2 Area 2

The organic rich Dinantian-Namurian transition (Bowland Shale) was not drilled in Area 2, but was encountered in the U.K. sector east of Area 2 (Figure 3.16). In the UK on- and offshore the shales near the top of the Dinantian and the base of the Namurian are generally considered to be important source rocks, especially when onlapping onto

carbonate platforms (Gutteridge, 2002; Cornford, 1998; Gerling *et al.*, 1999; Fraser *et al.*, 1990; Pering, 1973; Walkden and Williams, 1991; Lawrence *et al.*, 1987; Hardman *et al.*, 1993; Cameron and Ziegler, 1997; Leeder *et al.*, 1990; Leeder and Hardman, 1990; Leveille *et al.*, 1997; Bernard and Bouché, 1991). In the East Midlands oil is produced from fields possibly sourced by Lower Namurian shales (Cornford, 1998). Samples were taken from the Bowland Shale in the UK sector, which is assumed to be comparable to the Geverik Mb although the age of this deposit is Late Dinantian (e.g. well 41/24a-2). There are not enough published wells to define the extent of deepwater Bowland Shale Formation (Cameron *et al.*, 1992; Cameron, 1993). However, their presence and regional development can be assumed (Maynard and Dunay, 1999).

Evaluation of the sterane composition (Figure 3.13) and the pristane / phytane ratio (Figure 3.14) indicate a dominating marine depositional environment, which is comparable to Area 1. This suggests Type II organic matter. However, this could not be confirmed by the analyses of the sampled shales, although elevated HI's were measured up to circa 300 (Figure 3.15).

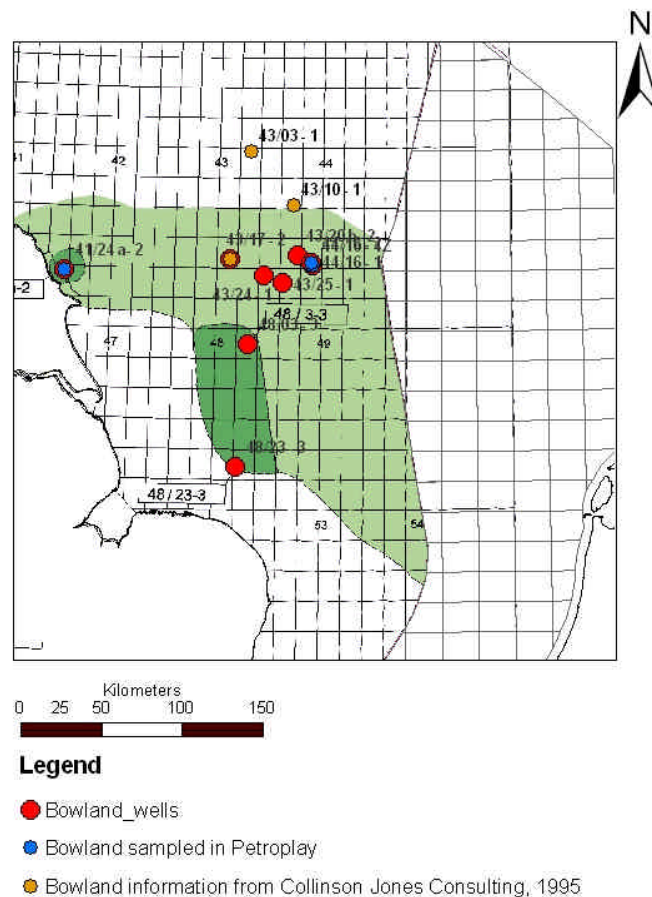


Figure 3.16 Overview of UK offshore area where the Bowland Formation is encountered (dark green) and where the Bowland Formation is probably present at depth (light green), after the UK Nomenclature. Also indicated are the wells where the Bowland Formation is reported to be present (in red), the wells where the Bowland Formation was sampled for this study (in blue), and the wells where information was included from Collinson Jones Consulting (1995)

3.3.1.3 Area 3&4

In this area samples were taken from the 'Hängende Alaunschiefer' in wells Münsterland-1 and Schwalmtal-1001. The sterane composition (Figure 3.13) and the pristane / phytane ratio (Figure 3.14) indicate a dominating anoxic marine depositional environment. Despite the high maturity, elevated HI were measured (Fig 3.15), which gives indications of Type II organic matter.

3.3.2 Total Organic Carbon

3.3.2.1 Area 1

The TOC content of the organic rich shale at the base of the Namurian in well Geverik-1 showed relatively high TOC content. This indicates, taking into consideration that these rocks are overmature, very high initial TOC values during deposition. These observations are confirmed for some of the Belgian wells. Especially, the samples from well Turnhout show high values of up to 12% (Figure 3.17) at high maturation (see below). The data show an increase in TOC values from the Zeeland Platform (Brouwershavense Gat-1) to the basin (Geverik-1). Well P16-01 is located in the transition (Zeeland Platform) from massif to basin and shows intermediate TOC values.

3.3.2.2 Area 2

Samples from the Base Namurian and Top Dinantian deposits in the UK sector show an average TOC of 3%, with maxima around 6% (Figure 3.17). This qualifies, on the basis of the TOC, this rock as a good source rock.

3.3.2.3 Area 3&4

The TOC values of the German wells (Münsterland-1 and Schwalmtal-1001) in Area 4 show relatively high values (up to 10%; Figure 3.17) at high coalification. Initial TOC during deposition must have been much higher.

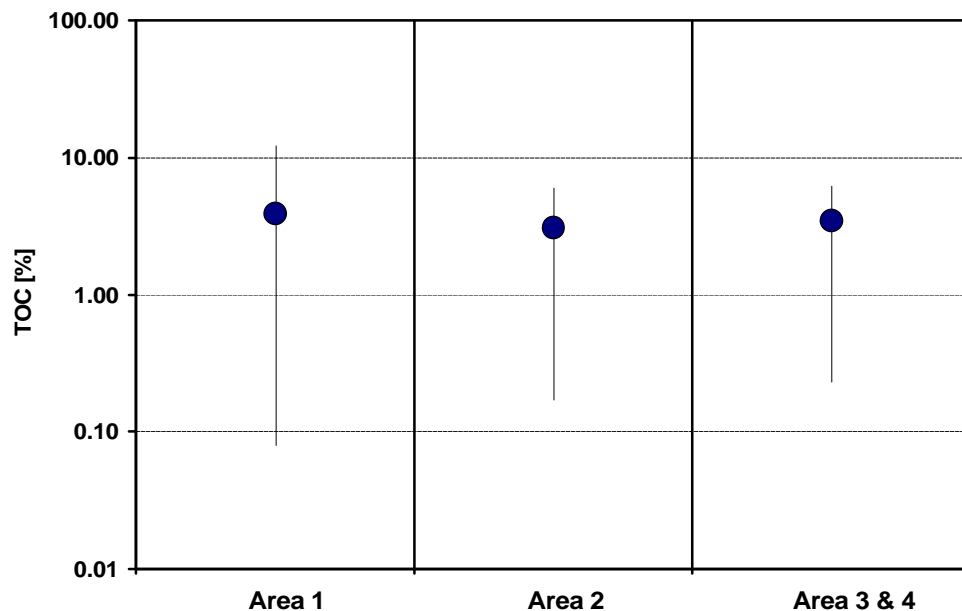


Figure 3.17 Distribution of TOC values of samples from the interval top Dinantian – base Namurian per area, with the range and median..

3.3.3 Maturity

3.3.3.1 Area 1

The maturity of the Dinantian to Namurian transition in area 1 is clearly different in the north-west compared to the south-eastern part of the area. The transition is overmature in the south-eastern part of the area (well Geverik-1 and Belgian wells) while it is in the late oil window to early gas window in the north-western part of the area (wells Brouwershavense Gat-1, O18-01, P16-01; Figure 3.17).

3.3.3.2 Area 2

In Area 2 the variation in the maturity of the Top-Dinantian to Base Namurian is also substantial. The locations of the investigated wells are currently within the oil window to early gas window.

3.3.3.3 Area 3&4

The Dinantian to Namurian transition in Area 3&4 is overmature and burial history reconstruction will show the timing of maturation at these locations (see Chapter 6 and Appendix H).

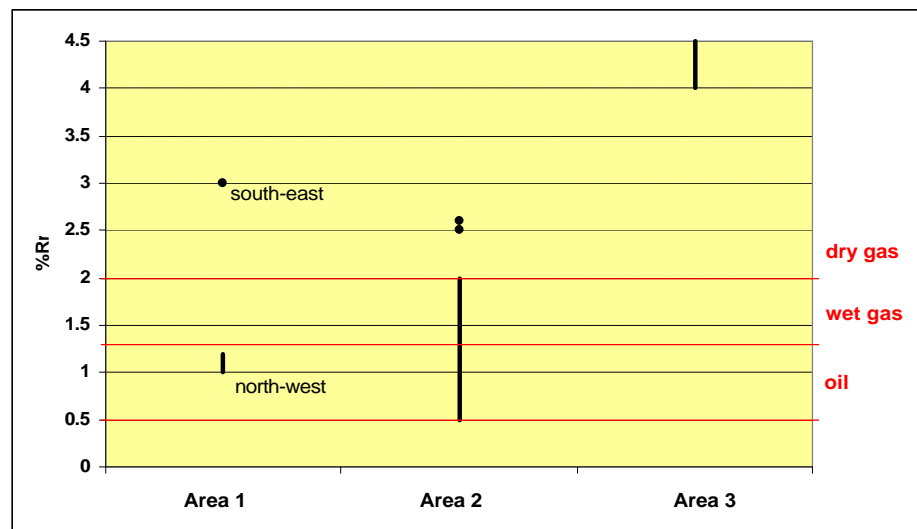


Figure 3.18 Variation in measured maturity of the samples from the interval top Dinantian – base Namurian per area

3.4 Namurian

3.4.1 Facies and typing of organic matter

3.4.1.1 Area 1

The Namurian succession (Epen Formation) in Area 1 is assumed to consist of dark-grey to black mudstones with a few intercalations of sandstones, as for example drilled in well Rijsbergen-1. Brief marine incursions are expected to have occurred during the deposition of the Namurian, that may be represented by elevated TOC values, and therefore source rock potential. Source rocks are possibly also found in mudstone-dominated intervals with thin silt- and fine-grained sandstone intercalations, which can be up to 100 m thick.

Contrary to Van Adrichem Boogaert and Kouwe (1993-1997), who stated that coal seams are absent in the Namur-1 and -2 (Epen Fm) it was found that coal seams are present in the Namurian. A review of the well logs of well Rijsbergen-1 indicated the occurrence of some thin coal seams in the upper part of the Namur-2, which is an indication of increased terrestrial influence. This is also confirmed by the upper Namurian succession in Zuid-Limburg, among others in well Geverik-1 which contains various intervals with thin (impure) coal seams (see e.g. TNO-NITG, 1999). These seams occur in the upper part of the Namurian 2 (RGD, 1986). These coal seams were not sampled.

Facies analysis by the sterane composition show that the sampled rocks (mostly shales) have a merely marine signature although a lacustrine origin can not be excluded (Figure 3.19). However, the pristane / phytane ratio of one of the samples shows a relatively high value, indicating some terrestrial influence (Figure 3.20).

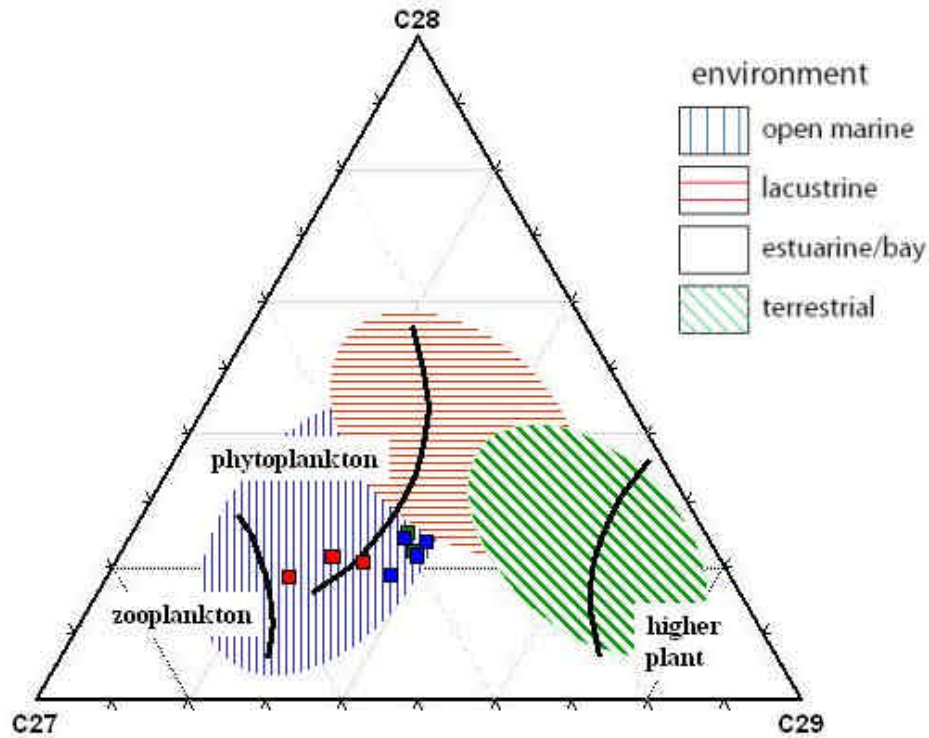


Figure 3.19 Namurian facies (based on GC-MS (SIM) data – biomarker analysis) on the basis of the proportion of C27-C28-C29 steranes. Dominance of C29 steranes indicates terrestrial depositional environment. C27 steranes are predominantly produced by zooplankton. Green = Area 1, red = Area 2, blue = Area 3

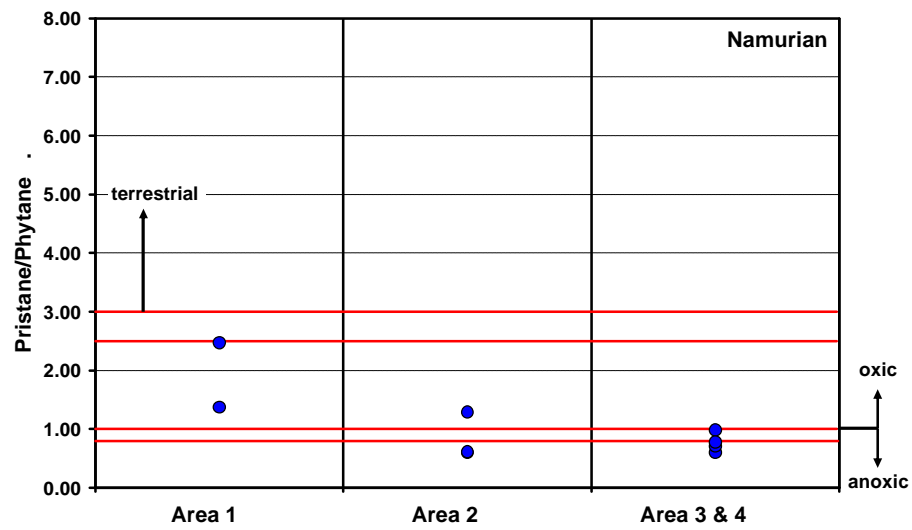


Figure 3.20 Variation in Pristane/Phytane ratio of the Namurian per area

Given the marine character of these rocks, the organic matter is expected to be predominantly Type II. Indeed, there are strong indications that Type II organic matter is present within the Namurian interval (Figure 3.21). However, the analytical results of many samples from the Namurian show Type III rather than a Type II characteristics. In conclusion, both gas- and oil-prone source rocks were identified in the Namurian succession of Area 1.

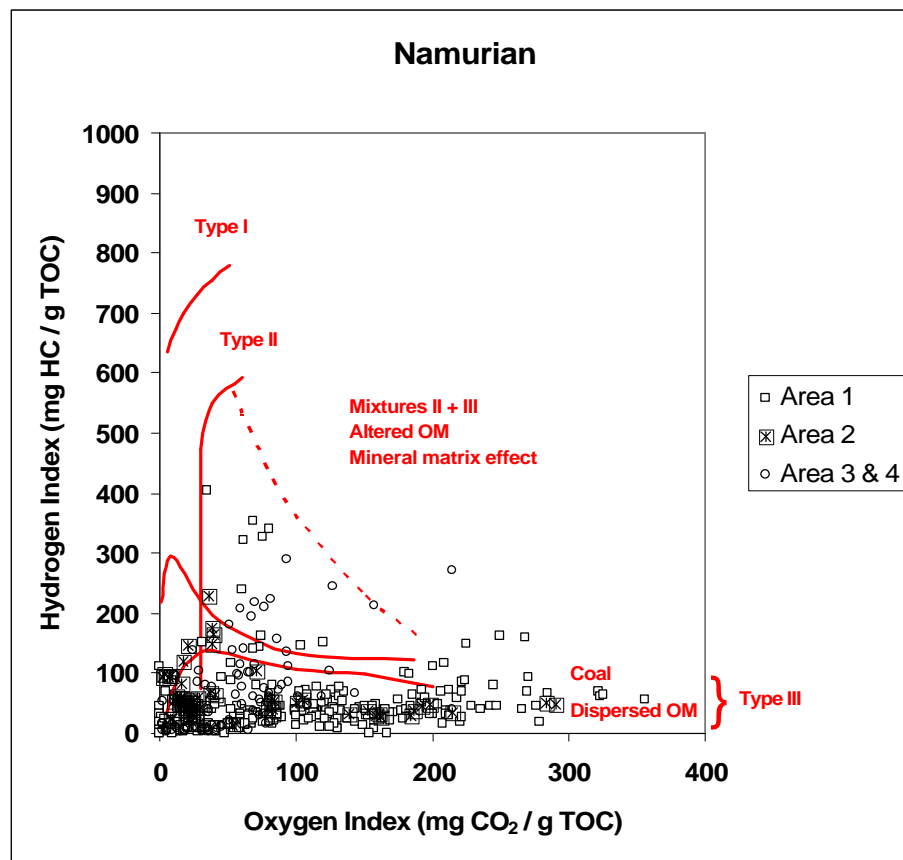


Figure 3.21 Pseudo-Van Krevelen diagram of the Namurian

3.4.1.2 *Area 2*

The Namurian succession in Area 2 is formed by the Namurian 1 (Epen Formation) and by the Namurian 2 (Millstone Grit Formation). The Millstone Grit Formation is defined in the UK offshore as a succession of interbedded grey, white and brown sandstones, and dark-grey, partly carbonaceous mudstones and siltstones (summarised after Cameron, 1993). The formation consists of stacked coarsening-upward cycles, generally starting with a basal marine interval (Van Adrichem Boogaert and Kouwe, 1993-1997). At some locations, deposition of the Klaverbank Formation already started in the Namurian B/C, i.e. the last deposition of Namurian 2 does not correspond with the end of the Namurian. The Klaverbank Formation contains coal seams (Van Adrichem Boogaert and Kouwe, 1993-1997). Some Namurian coal seams were sampled.

The selected Namurian shale samples taken from wells in Area 2 indicate a strong marine depositional setting (Figure 3.19), much more distinct than the samples from Area 1. This seems to be confirmed by the pristane / phytane ratio, which carries no terrestrial signal.

Based on the above, oilprone Type II organic matter would be expected. However, this could not be confirmed by the analyses (Figure 3.21). Possibly, this is due to the degree of coalification (see below). The sampled Namurian coal seams are characterised as Type III organic matter, and gas-prone.

3.4.1.3 *Area 3&4*

In Area 3&4 four samples were geochemically evaluated. Three of these samples are from shales, whereas one sample was taken from a Namurian C coal. Remarkably, the sterane composition suggests a marine depositional environment for all analysed samples (Figure 3.19). Also, the pristane / phytane ratio does not indicate a terrestrial input for the Namurian coal (Figure 3.20). Although this could indicate a marine influence on the coal, care should be taken when drawing conclusions for these high maturity samples. The analyses show a mixing between Type II and Type III organic matter in the Namurian succession in Area 3&4. Both oil and gas may have been generated from this kind of kerogen.

3.4.2 *Total Organic Carbon*

3.4.2.1 *Area 1*

The geochemical analyses show that at some locations in Area 1 shale intervals with relatively high TOC values are present (Figure 3.22). The analyses of the intra-Namurian deposits in some Belgian wells show that the major part of the Namurian sequence has moderate to low TOC values. However, some intra-Namurian shale intervals show high TOC values, such as shown in well Turnhout.

3.4.2.2 *Area 2*

The analysed samples in Area 2 include cored coal seams (e.g. well 44/16-1z), as is shown by some high TOC values. In the Namurian also some shales are present with high organic matter content, up to 6%.

3.4.2.3 Area 3&4

In Area 3&4 Namurian samples were taken from both shales and from coal seams (e.g. in well Münsterland-1). The latter show a high value of TOC. Shale samples have, despite their maturity (Figure 3.23), relatively high values of TOC.

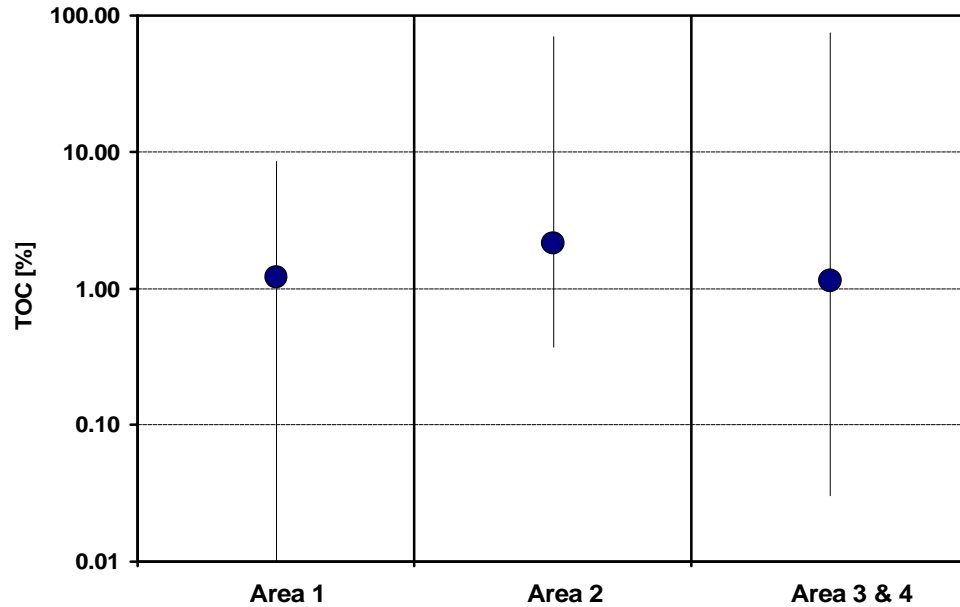


Figure 3.22 Distribution of TOC values of samples from the Namurian per area, with the range and median.

3.4.3 Maturity

3.4.3.1 Area 1

The maturity of the Namurian sediments in Area 1 shows a wide range from 0.5 %Rr (immature) to 5.0 %Rr (overmature). Within Area 1 a geographic distinction can be made with respect to the maturity (Figure 3.23). The south-eastern part of the area is overmature whereas the Namurian is in the late oil window to early gas window in the north-west of the area.

3.4.3.2 Area 2

The maturity of the Namurian succession in Area 2 has a relatively wide range from 0.5 %Rr to approximately 2.0 %Rr. In the Dutch part of the area the maturity does not go beyond approximately 1.3 %Rr, implying that the organic matter is currently positioned within the oil window and has not reached the stage of significant gas generation. The UK area near Area 2 may be considered mature with respect to gas generation.

3.4.3.3 Area 3&4

The Namurian sediments in Area 3&4 have, in comparison to those of Area 1 and 2, a relatively high maturity. The larger part of the Namurian is overmature, but at some locations the top of the Namurian is still in the wet gas to early dry gas window.

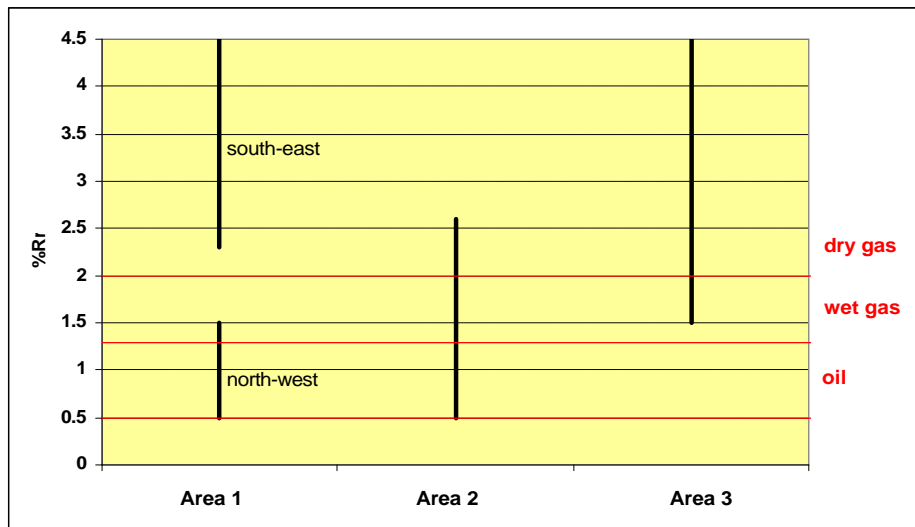


Figure 3.23 Variation in measured maturity of the Namurian samples per area

3.5 Evaluation of potential source rocks

An excellent source rock can be defined as a rock with an initially high content of organic matter that is reaching the appropriate maturity (oil window for Type II, gas window for Type III) at the correct time, i.e. when generated hydrocarbons can accumulate in a reservoir (critical moment, see following chapters). In order to evaluate the quality of the potential pre-Westphalian source rocks, an overview was made of the most important characteristics: TOC, Type of organic matter, and maturity (Table 3.1).

Based on this table it can be concluded that source rocks with a fair to good initial potential were distributed in all areas from the Devonian to the Namurian. Source rocks with an initial excellent potential were deposited during the transition from the Dinantian to the Namurian in Area 1 and Area 3&4. However, these source rocks are currently overmature. Burial history reconstruction must identify at what moment in geological history generation and expulsion of hydrocarbons took place. Areas in which the source rocks reached the stage of oil or gas generation in (sub-)recent times will have the highest prospectivity.

At present, source rocks with fair potential still exist in pre-Westphalian deposits. This is true in Area 1, but even more so in Area 2, where source rocks with fair potential were identified in the Dinantian, the Dinantian to Namurian transition, and the Namurian. Possible contribution to hydrocarbon accumulations depends on the timing of the maturity (thermal history) and on the total volume of source rock present. The source rocks of the Dinantian in area 2 are the Yoredale coal seams, generally up to 1 m thick, and the marine intervals. In the Namurian the main source rocks are organic rich shales and coal seams. Although the individual thicknesses of organic rich layers are relatively small, the cumulative thickness of all the seams may have generated significant amounts of hydrocarbons. 3D basin modelling was performed to establish whether the total volume of source rock is sufficient to have generated significant amounts of hydrocarbons (Appendix I).

Table 3.1: Summary table for the evaluation of the potential source rocks (SR).

Age of units	Area	Type	TOC median [%]	TOC max [%]	Maturity [%Rr]	Initial SR potential	Present-day SR potential
Devonian	Area 1	III + (II)	0.5	2.9	1.5 - 3.0	fair	low
	Area 2	III + (II)	0.2	5.8	0.7 - 1.5	fair	fair to low
	Area 3 & 4	(II)	0.7	1.1	4.0 - 5.0	low to fair ?	low
Dinantian	Area 1	III + (II)	0.6	16.9	0.8 - 2.0	fair	fair to low
	Area 2	III + II	1.2	68.2	0.5 - 2.0	fair to good	fair
	Area 3 & 4	(II)	2.7	8.7	4.0 - 5.0	low to fair ?	low
Top Dinantian - Base Namurian	Area 1	II + III	2.5	12.1	1.0 - 1.2 (NW)	good to fair	fair
					3.0 - ? (SE)	excellent	low
	Area 2	III + (II)	3.2	6.0	0.5 - 2.0	good	good
Area 3 & 4	II	3.5	6.2	4.0 - 5.0	excellent	low	
Namurian	Area 1	III + II	1.1	4.5 (21.5)	0.5 - 1.5 (NW)	fair	fair
					2.3 - 5.0 (SE)	fair	low
	Area 2	III + (II)	2.2	72.1	0.5 - 2.6	fair	fair
Area 3 & 4	III + II	1.3	77.1	1.5 - 4.5	good	low	

Of course, the results described above are biased, due to the limited number of wells at selected locations (mostly present-day structural highs). Based on the preferred block-and-basin setting, other pre-Westphalian source rocks may be present. However, there are no direct indications for this since these were never drilled. Nevertheless, oilprone source rocks with high organic matter content can be presumed to be deposited in the "deeper" intra-platform basins that were characterised by restricted circulation (model 2, see chapter 2). Scenarios including these source rocks were modelled in 3D in order to evaluate the possibility of a contribution of these source rocks to hydrocarbon accumulations (Appendix I).

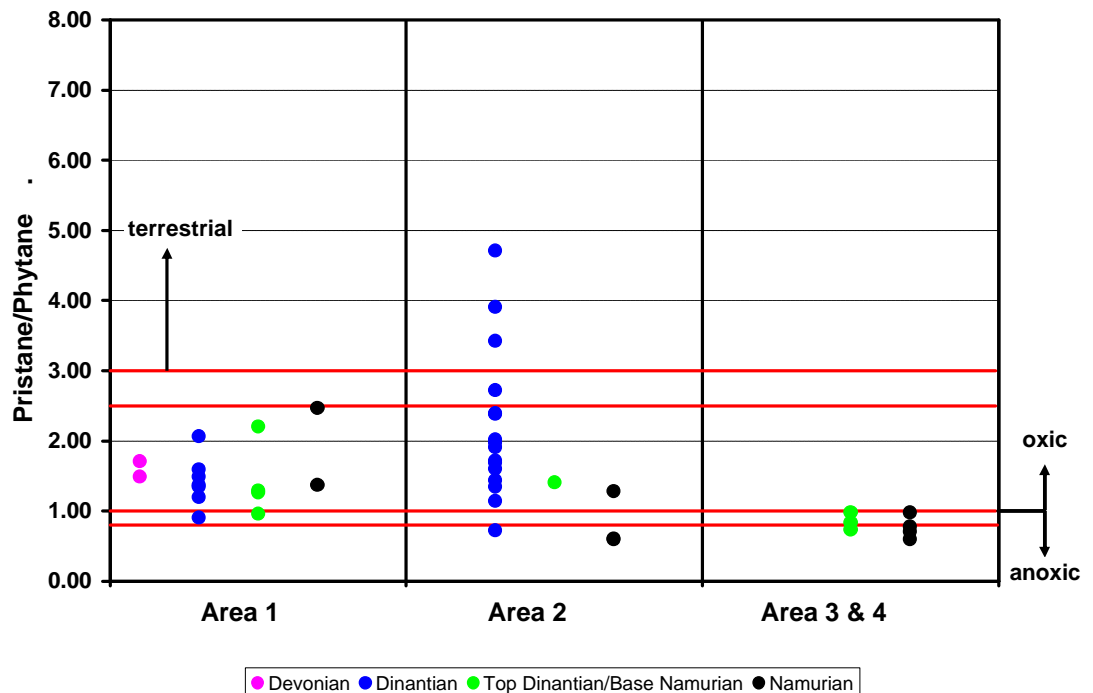


Figure 3.24 Summary plot of measured Pristane/Phytane ratios

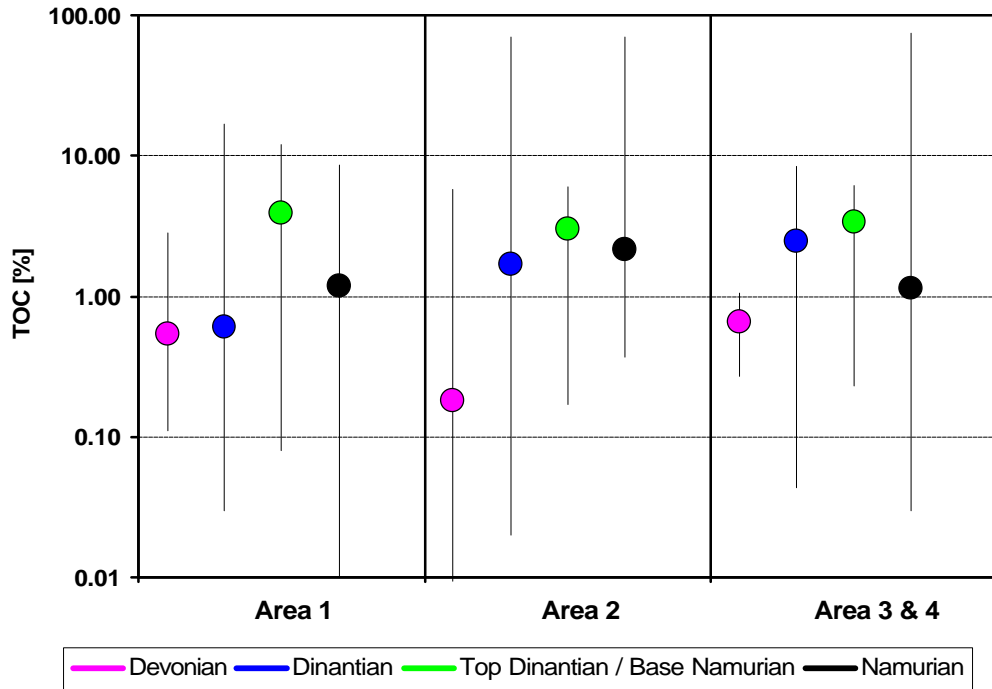


Figure 3.25 Summary plot of measured TOC values, with range and median

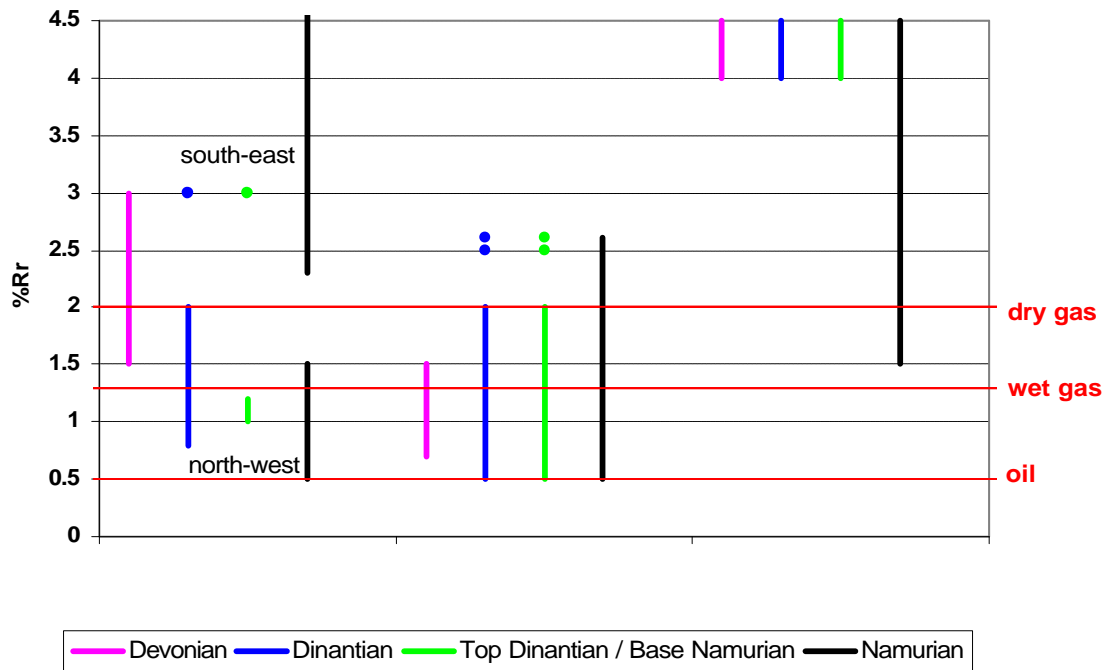


Figure 3.26 Summary plot of range of vitrinite reflectance measurements

4 Hydrocarbon potential of Area 1

4.1 Geological and seismic interpretation

Area 1 is the area on the northeastern margin of the London-Brabant Massif (Figure 1.1). It consists of a Dutch offshore part in the west and the southernmost part of the Netherlands onshore, previously mapped for the national 1 : 250.000 mapping programme (TNO-NITG, 2003).

4.1.1 Well correlations

Figure 4.1 shows the well correlation panel for Area 1, correlating (from west to east) wells O18-01, P16-01, S02-02, S05-01, Brouwershavense Gat-1, Kortgene-1, Rijsbergen-1 and Geverik-1. These wells were selected at the start of the project as key wells, because they all reached pre-Westphalian sediments. Five of the eight wells reached the Devonian (in O18-01 and Kortgene-1 even Silurian is interpreted near the TD of the wells), one well (Geverik-1) has its TD in the Dinant-3 (Late Asbian – Brigantian), and the remaining two wells reached rocks of Namurian age (unit Namur-1).

4.1.2 Seismic interpretation

The onshore part of Area 1 had recently been mapped by TNO-NITG for the national 1 : 250.000 mapping programme "*The Geological Atlas of the subsurface of the Netherlands*" (TNO-NITG, 2001; TNO-NITG, 2003). In this previous project Belgian well information was also used. About 40 Belgian wells had reached Dinantian or older rocks. For the Petroplay project we decided to simply use the top Dinantian depth grid resulting from the 1 : 250.000 mapping programme and we only interpreted additional offshore 2D lines. Figure 4.2 shows the seismic basemap for these offshore lines.

The offshore seismic data used was all shot between 1974 and 1989. The mapped reflectors form the boundaries between the lithostratigraphic units (groups and formations). The seismic data were calibrated against a number of wells, by means of acoustic logs and check-shot surveys. The interpreted seismic horizons are the bases of: Upper North Sea Group, North Sea Supergroup, Chalk Group, Rijnland Group, Schieland Group, Altena Group, Permo-Triassic groups, Limburg Group and Carboniferous Limestone Group. The latter two horizons correspond respectively to the Top Dinant-1 and the Top Devonian of the stratigraphic framework introduced in this project.

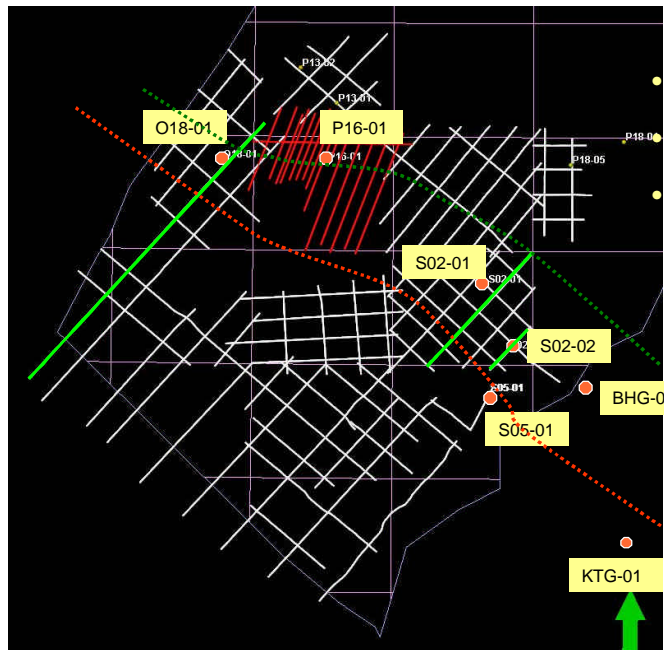


Figure 4.2 Seismic basemap for the offshore part of Area 1. In white: analogue lines; in red: digital lines; in green lines shown in Appendix E of this report; Red dashed line is subcrop Namurian

The base of the Limburg Group (Top Dinant-3b) has been interpreted on a large number of seismic lines. This horizon can frequently be traced as a strong, prominent reflector as a result of the transition from limestones to shales, on top of which onlap is observed in places. A number of seismic lines show the underlying deposits of the Carboniferous Limestone Group, as an acoustically transparent unit characterised by discontinuous reflectors (Figure 4.3). The depth to the top of the Carboniferous Limestone Group increases in a north-easterly direction from some 1000 to 6500 m. The thickness of the Carboniferous Limestone Group varies from 500 to 1300 m. The base of the Carboniferous Limestone Group (Top Devonian) also shows as a strong, sometimes very wide, prominent reflector, characterised by an angular unconformity.

From the seismic profiles (Figure 4.3 and Appendices E1-E4) a relatively simple structural pattern emerges, at least if viewed at the regional scale. The pre-Westphalian units are dipping uniformly to the northeast, offset by NE dipping normal faults. The pre-Westphalian sediments are covered by omnipresent Chalk or by the Late Cretaceous Rijnland Group more to the NW.

Replace these two pages by

Fig-4-1-Area1 well section_A3-size.pdf

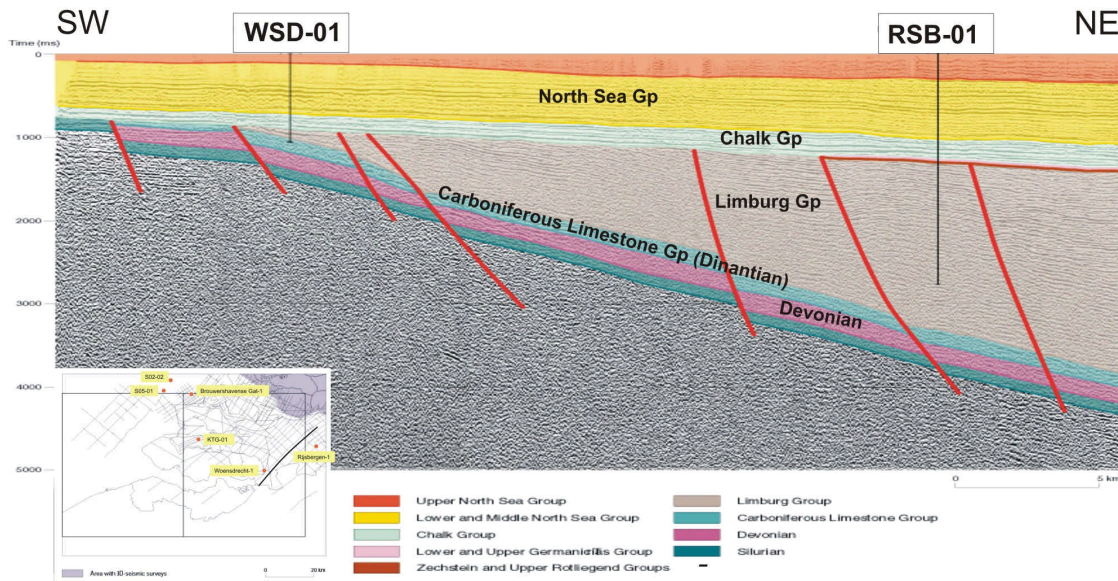


Figure 4.3 Representative seismic profile (2D line 846014, from TNO-NITG, 2003) with the projections of wells Woensdrecht-01 and Rijsbergen-1. Appendices E2-E4 show more SW-NE profiles from the offshore part of Area 1

Using the already available grids for the onshore part, together with newly constructed grids for the offshore part, a regional depth map of Top Dinantian was made (Figure 4.4). The seismic interpretations of the lines shown in Figure 4.2 were digitised. Since only a regional picture of the depth of the horizon was needed, it was decided not to digitise the offshore faults. On Figure 4.4 also the subcrop (to Mesozoic strata) lines of the Dinantian, the Devonian and the Cambro-Silurian are plotted. The latter was obtained from Belgian well information only.

The Top Dinantian depth map shows where Dinantian units are present (NE of the subcrop line) and buried not deeper than some 5000 m. Both conditions are met within a zone with a width of approximately 40 kms from the border of Noord-Brabant with Belgium extending to the NW. This zone roughly includes eastern Noord-Brabant, the northeastern part of Zeeland, southernmost Zuid-Holland and the offshore blocks O15, O18, P13, P16, P17, S02 and S03.

Obviously, possibly prospective Namurian intervals are present and slightly less deep buried also somewhat more to the northeast.

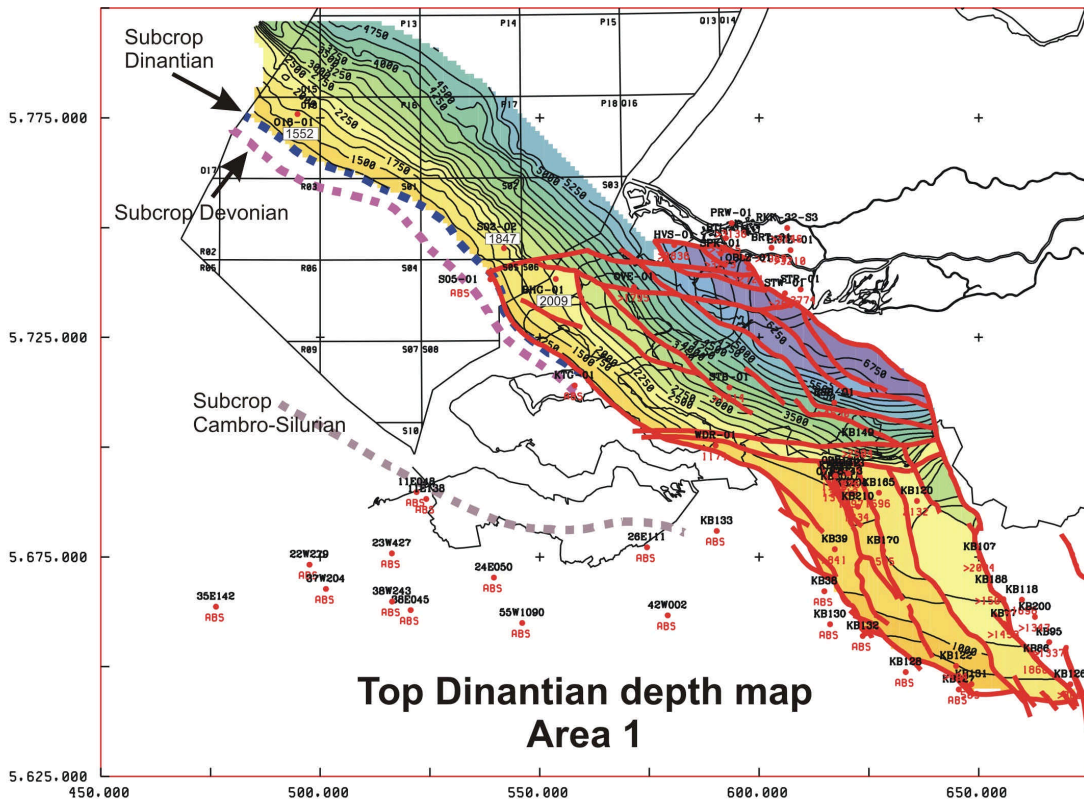


Figure 4.4 Top Dinantian depth map for Area 1 resulting from the seismic interpretation

4.2 Source rocks

The most promising source rocks in Area 1 are those around the Dinantian to Namurian transition (Chapter 3 and Table 3.1). Initially they must have had good to excellent source rock potential. In addition, there also is some source rock potential within the Dinantian and Namurian sequences.

In a large part of the area, especially the southeast, the pre-Westphalian source rocks are highly mature. Still, at the margin of the structural high areas, especially in the P-blocks, some source rock potential may have survived until the Tertiary (see section 4.5).

4.3 Reservoirs

4.3.1 Devonian reservoir potential in Area 1

The Devonian deposits in Area 1 comprise the Bollen Claystone (~ of Frasnian age) and the Bosscheveld Formation of Famennian to Early Tournaisian age (Figure 2.2; Van Adrichem Boogaert and Kouwe, 1993-1997).

The Bollen Claystone is composed of shales and has no reservoir potential. However, in the Booischoot well in Belgium 388 m of non-marine conglomerates, partly of Frasnian age, were encountered. It is unlikely that these conglomerates extend to the north.

The Bosscheveld Fm consists of interbedded dark-grey, partly calcareous mudstones, fine-grained sandstones and often nodular limestones. The Bosscheveld Fm has been found in the well Kastanjelaan-02 (Van Adrichem Boogaert and Kouwe, 1993-1997) in Zuid-Limburg and in the western wells Brouwershavense Gat-1, Kortgene-1, S02-02, S05-01 and O18-01 (see Figure 4.1). Only thin sandstone beds are present in these wells. In the Famennian sections of all these wells mudstones and siltstones dominate.

Based on the currently available data we therefore consider the reservoir potential of the Devonian sediments in Area 1 to be low and highly speculative.

4.3.2 *Dinantian reservoir potential in Area 1*

The sediments of Dinantian age in Area 1 are marine carbonates, almost exclusively deposited on a carbonate platform. Figure 4.1 shows the subdivision made into the units Dinant-1, -2, -3a and -3b. In Area 1 this corresponds to the lithostratigraphic Zeeland Formation of the Carboniferous Limestone Group (Van Adrichem Boogaert and Kouwe, 1993-1997), which is subdivided into three members: the Beveland Mb, the Schouwen Mb and the Goeree Mb (Van Adrichem Boogaert and Kouwe, 1993-1997).

In some wells the uppermost unit Dinant-3b is not or not fully developed. This can obviously be the result of erosion, but it is also possible that it relates to the sedimentation patterns at the carbonate platforms. The Dinantian succession in well Geverik-1 (GVK-01) was described in the OPAC report (RGD, 1986). Nine “macro-trends” were distinguished in the sedimentation pattern, based on thickening and thinning of beds. The sediments show a transgressive character: the lithology changes from carbonates at the bottom of the succession to shales at the top. The sedimentological transition from transgressive in the Dinantian to regressive in the Namurian-Westphalian occurs later (at circa 860 m depth in the well) than the stratigraphic change (at circa 980 m). A similar observation was made for well Wachtendonk on the Krefeld High in Germany. The transition from Dinantian to Namurian in well Geverik-1 does not show a large hiatus.

The development of a thick sequence of Dinant-3 unit in well Geverik-1 (in comparison to the other wells closer to London-Brabant Massif and Zeeland Platform) indicates that there was more accommodation space at this location. Probably, this was related to a block north of the massif, bounded by step-faults, that started to subside from the Late Holkerian onwards. It is anticipated that similar (tilted) blocks were present north of the London-Brabant Massif throughout Area 1.

Gutteridge (2002) gave an overview of onshore Dinantian reservoir types (Figure 4.5) associated with the Derbyshire carbonate platform. This could be an analogue for offshore carbonate platforms in Area 1. He listed a number of reservoir types associated to the setting.

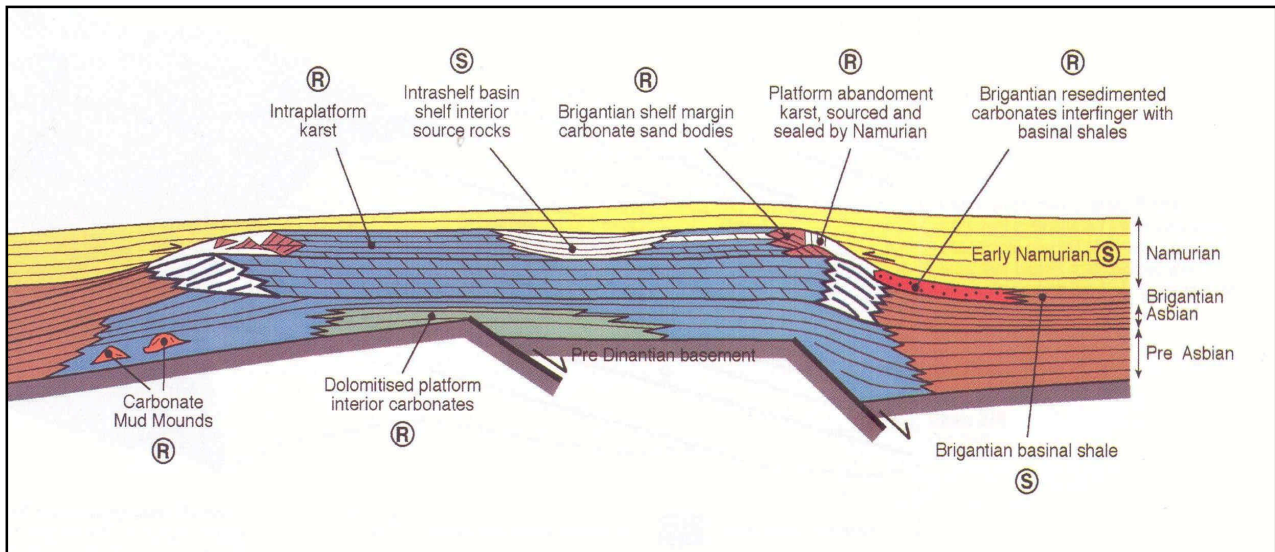


Figure 4.5 Potential reservoirs and source rocks associated with the Derbyshire carbonate platform (from Gutteridge, 2002)

1) Platform interior carbonates: Intraplatform karst

Intraplatform karst systems formed during carbonate platform sedimentation during 4th or 5th order eustatic sea level low stands. The pore system comprises channels and large vugs, superimposed on a moderate to poor matrix porosity representing relict depositional porosity. The reservoir is highly layered with karst systems extending few metres into the carbonate platform interbedded with impermeable shelf limestones.

2) Carbonate platform margins: Carbonate platform abandonment karst

This reservoir type occurs at the carbonate platform margin and upper marginal slope. A dual porosity system is present (sub-vertical fractures superimposed on a matrix pore system comprising intergranular and occasional vuggy pores). Down-slope karstic collapse of the shelf margin has produced a boulder bed that contains large-scale channel and vuggy porosity.

3) Post-platform karst systems

Post-platform karst systems formed after the cycle of basin development and sedimentation in which the Dinantian carbonate platform accumulated. Examples include sub-Triassic and sub-Cretaceous karst. The pore system is a combination of high permeability fractures and large vugs, possibly up to several metres in diameter.

4) Carbonate platform margins: Shelf margin bioclastic carbonate sand bodies

Carbonate sand bodies occur at the shelf edge in a belt some 1-2 km wide. The width and thickness of these carbonate sand bodies is controlled by the relief on the carbonate platform margin. The carbonate sand body is layered at a scale of up to 15-20 m. These are separated by thin impermeable karsted and calcretised horizons.

5) Carbonate platform margins: Carbonate turbidite systems fed by high stand shedding of carbonate sand from platforms

These carbonate sand bodies form sheet, fan or apron deposits draped over the base of the carbonate platform marginal slope and extend into the basin. These reservoirs comprise amalgamated carbonate sand bodies adjacent to the platform margin

becoming progressively more layered and interbedded with impermeable shales in the basin. Carbonate turbidite systems are fed from shelf margin carbonate sand bodies and are therefore associated with footwall carbonate platform margins.

6) Platform interior carbonates: dolomitised platform carbonates

Reservoir potential is present in dolomitised platform interior carbonates. Dolomitisation took place in the presence of Mg-rich pore fluids expelled from surrounding shale-rich successions during Upper Carboniferous burial. Intercrystal porosity is moderate to good and borehole evidence shows that porosity is preserved in the subsurface.

7) Dinantian basinal successions

Carbonate mud mounds form potential reservoirs in the basinal parts. They form mound, or bank-like features often up to several hundreds of metres thick and lateral spreads of several hundred metres to kilometres extent. Carbonate mud mounds are surrounded by flank facies comprising grainstone with good depositional porosity.

Not all of the reservoir types listed above are equally likely to occur in Area 1. Good candidates in Area 1 are the three different types of karstified reservoirs (types 1, 2 and 3). In the UK, there are indications that certain karst surfaces have formed at intervals of 30.000 to 100.000 years, suggesting that they are linked to Milankovitch-controlled glacio-eustacy (Walkden, 1974). Other models suggest that tectonic uplift played a major role (Bless *et al.*, 1980). Our own examination of cores (e.g. O18-01) showed that karstified zones are present in the Dinantian sections. Also, karstified horizons in the Dinantian are reported in the S-blocks (wells S02-01 and S05-01). In wells Turnhout and Halen (Belgium) "collapsed" breccias in Dinantian strata indicate karstification. In Zuid-Limburg (and in the Belgium Campine Basin) strongly karstified limestones are interpreted from diffraction hyperbola on seismic lines. Near the town of Loenhout (Belgium) gas is stored in karstified Dinantian carbonates. These karst zones are attributed to post-Carboniferous phases.

With respect to type 4 of Gutteridge (2002) (the shelf margin deposits) it is believed that this reservoir type may also occur, although this has not yet been proven in Dutch wells. Carbonate debris indicating ramp slumps were not yet encountered in the Netherlands (on- and offshore) areas. According to Cameron and Ziegler (1997) the progradational wedges of the Namurian shales, analogue to those capping the onshore Dinantian blocks of Northern England, may also have developed on the margins of the highs. At the Petroplay excursion held in 2005 in Derbyshire it was demonstrated that reef talus deposits can occur at the margins and can result in reservoir potential. An example is the 'Blue John' occurrence in the Peak District (Collinson, 2005).

With respect to the other three types listed by Gutteridge (2002), 5, 6 and 7, we believe there is much less potential in Area 1. In the Netherlands (on- and offshore) areas there are so-far no indications (seismic or wells) for carbonate turbidites (type 5) and if they would occur, porosity and permeability would be low. Likewise, dolomitized platform carbonates do not seem very promising. Most wells in Area 1 do show a partial dolomitization, especially in the lower part of the Dinantian (Dinant-1), but in well Geveirik-1 it was demonstrated that secondary dolomitization is related to fault zones (RGD, 1986).

4.3.3 *Namurian reservoir potential in Area 1*

The Namurian in Area 1 mainly consists of mudstones alternated with thin sandstone layers. The Namur-1 sequence as a whole resembles a classic regressive megasequence, similar to the ones encountered in North Derbyshire. Likewise, the mud-prone lower part of the Namurian might contain turbidite packages similar to the Mam Tor sandstone. Individual beds rarely exceed one meter in thickness, but such a sandy interval can easily attain thicknesses of more than 100 m (Collinson, 2005) and could form potential reservoir rocks.

Several wells in Area 1 have encountered thin sandstones which can be interpreted as turbidites, but porosities in these sandstones were extremely low.

In several wells in Area 1 the regressive megasequence culminates in a sandstone sheet (e.g. the Ubachsberg Mb, Van Adrichem Boogaert and Kouwe, 1993-1997). These sheet sandstones can be considered as analogues of the Chatsworth Grit at Stanage Edge (Petroplay excursion, 2005). Deposited in very broad, low-relief paleovalleys, connectivity would not be a problem in these fluvial sheet sands. They form an interesting reservoir rock in areas where porosity has been preserved.

In the upper part of the Namur-2 section in well Rijsbergen-1 (RSB-01) deltaic sequences have been interpreted topped by thin sheet sandstones. A sheet sandstone that could be considered as the Ubachsberg Mb has been identified in well P16-01. In addition, regular sandstone layers are present in the Namurian succession in well P16-01. These sandstones are however tight and show little reservoir properties. The lowest section of the Namur-2 unit in well Brouwershavense Gat-1 contains a sandstone which may have reservoir properties.

4.4 Seals

The thick shale deposits of the Namurian can be excellent seals where present. The seal of the gas storage site in Loenhout (Belgium) in karstified Dinantian carbonates is also formed by Namurian shales. Detailed information on the seal quality is currently unknown to the authors, e.g. pressure data were unavailable.

At those locations where the Westphalian directly overlies the Dinantian or where the basal Namurian contains turbiditic or deltaic sandstones, intra-Westphalian shales might provide a seal, but it is frequently argued that such a seal has not really proven itself yet. Sealing could be problematic at those locations where the Dinantian is covered by Upper Cretaceous.

500 m of anhydrites have been encountered in Belgium in the St Ghislain borehole, south of the London Brabant Massif (Bless et al., 1980). Also, in the Namur Basin, several outcrops with indications for the existence of evaporites can be observed (Bless et al., 1980). These evaporites are thought to be limited to the marginal parts of the Dinant Basin where they possibly developed under lagoonal conditions. If and how far these evaporitic deposits extend to the north is not known. The residual gravity field shows a gravity low in southern Limburg (Dortland, 2003; accompanying report to this study). The negative values of the residual in southern Limburg indicate that there are sediments present with a density lower than the reference density of 2.67 g/cm³. In 1979, a gravity survey in southern Limburg and surroundings established some negative gravity anomalies near Maastricht (Bless et al. 1980). Several working models explained these gravity lows as caused by evaporite accumulations of either Middle

Visean or pre-Middle Visean age (Stoppel et al. 1981). Nevertheless, at this stage the presence of pre-Westphalian evaporites in the Netherlands seems highly speculative.

4.5 Hydrocarbon generation and its timing

In Area 1 hydrocarbon generation took place throughout the geological history, with a major generation peak during the Carboniferous (Figure 4.6). After the main phase of hydrocarbon generation at the end of Carboniferous, minor amounts were generated during the Triassic. At the end of the Jurassic, shortly before the Late Kimmerian 1 uplift and erosion, another generation phase took place. Generation ceased during Early Cretaceous time to start again during the Upper Cretaceous. Although only minor amounts were generated, generation from the base Namurian kerogen Type II source rock took place continuously until present-day in Area 1 (Figure 4.6). This figure demonstrates that the critical moment for Area 1 dates back to Carboniferous.

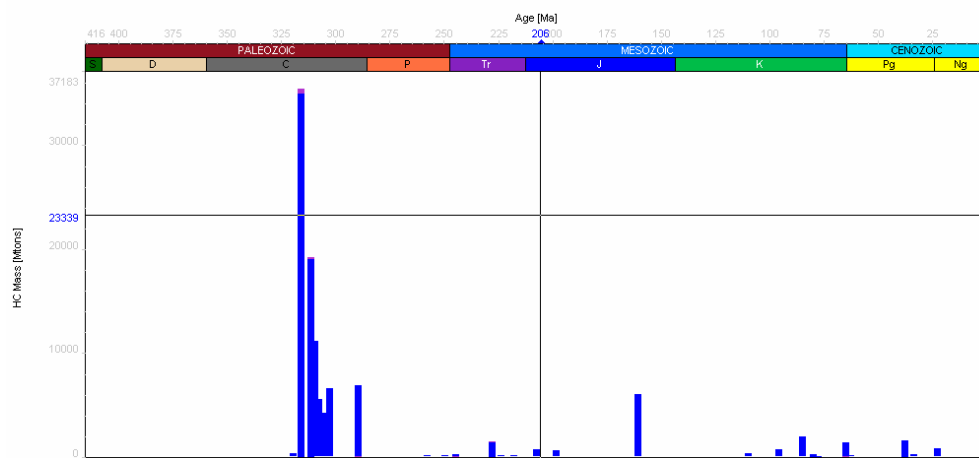


Figure 4.6 Generated (magenta) and expelled (blue) hydrocarbons per time period for base Namur-1 (Geverik Member equivalent) of Area 1 (Burnham 1989_T2 kinetics). Expulsion in the model occurs directly after generation, therefore the bars in the graph are overlapping.

The hydrocarbon generation through time is a function of the differential burial history for different parts of Area 1. From the 3D model maps were extracted that show the transformation ratio of the organic matter for several moments in geological time (Appendix I). It is observed that generation during the Carboniferous started in the south eastern part of Area 1. In the centre of the West Netherlands Basin the transformation already reached 100 % by the end of the Carboniferous. During the Triassic and Jurassic the area of transformation was further extended towards the northwest and the zone of active transformation became smaller. In the latest 60 Ma transformation took place mainly in the northwestern part of Area 1.

From the 3D model burial history plots and generation vs time diagrams have been extracted for a number of pseudowells along 3 different profiles (Figure 4.7) in order to illustrate the generation pattern through time for a basal Namur-1 Type II source rock. Along each of these three profiles 5 or 6 pseudowells were defined. For the pseudowells the burial history graphs (depth vs time) and the generation vs time diagrams have been extracted.

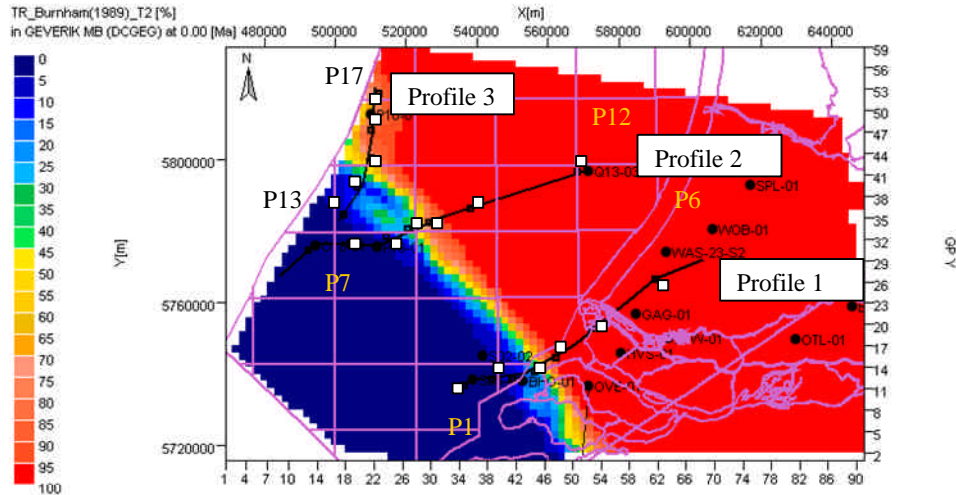


Figure 4.7 Location of the 3 profiles and pseudowells in Area 1. Pseudowells are marked with numbers (P1 to P6). Profile 1 is situated in the southern part of Area 1 and passes across wells S05-01 and BHG-01 and continues further to well GAG-01. Profile 2 is situated further to the northwest and starts close to key well O18-01 running to wells P16-01 and Q13-03. Profile 3 is situated at the western edge of Area 1. The number of the pseudowells corresponds to the number of the burial history graph. The hydrocarbon generation diagrams are shown in Figures 4.10, 4.13 and 4.16.

Profile 1

At the margin of the London-Brabant Massif (pseudowells 1 and 2), the base Namurian source rock has never been deeply buried and therefore only minor generation took place during Carboniferous, when this area was at deepest burial (Figure 4.8). This can be seen from Figures 4.9 and 4.10, which display the bulk generation rate through time. Further towards the West Netherland Basin (pseudowells 3 and 4) recent subsidence caused minor hydrocarbon generation from about 30 Ma onwards. Further towards the centre of the West Netherlands Basin (pseudowells 5 and 6), the source rock already reached maximum generation at the Carboniferous and no more hydrocarbons were generated throughout the subsequent geological history.

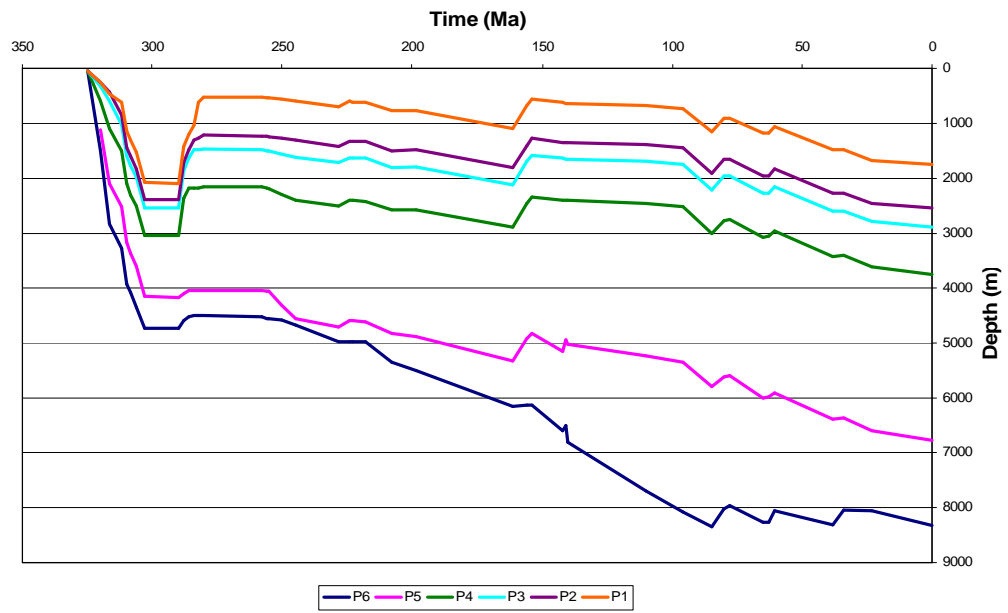


Figure 4.8 Burial history diagrams of the pseudowells along Profile 1 in the southern part of Area 1. Pseudowells are marked with numbers (P1 to P6)

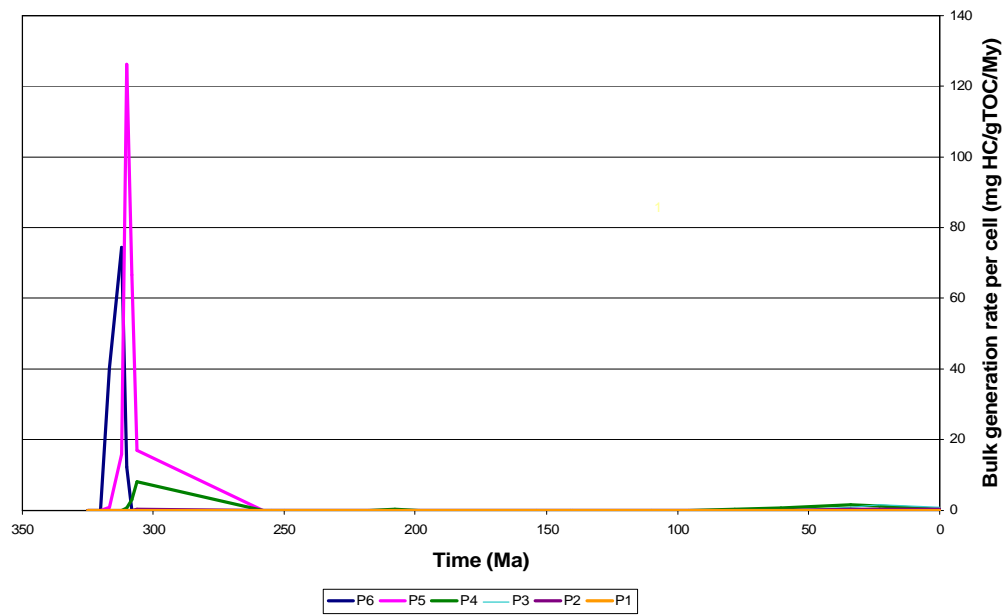


Figure 4.9 Hydrocarbon generation per event for the pseudowells along Profile 1 of Area 1. Pseudowells are marked with numbers (P1 to P6)

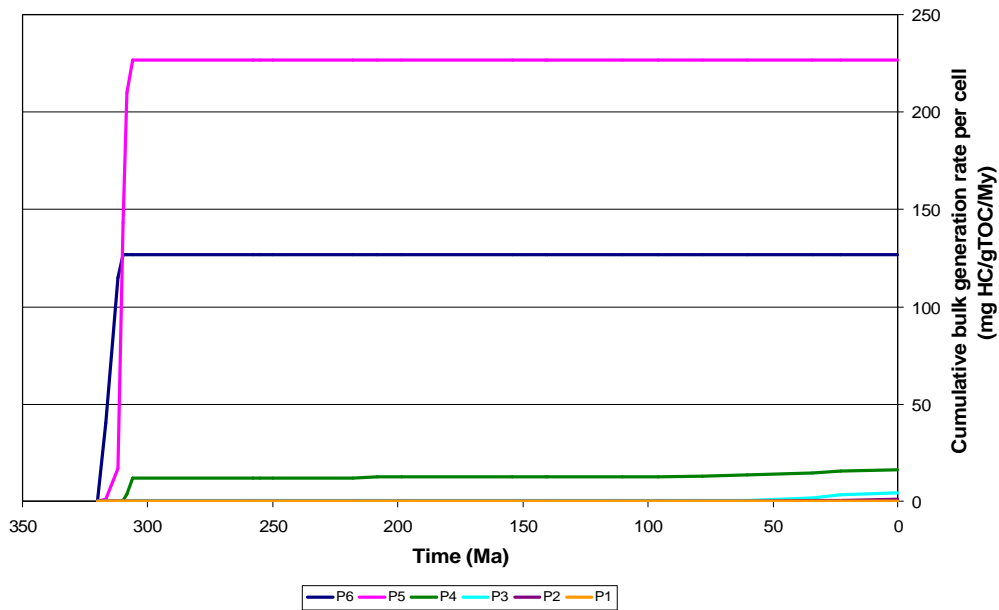


Figure 4.10 Cumulative hydrocarbon generation for the pseudowells along Profile 1 of Area 1. Pseudowells are marked with numbers (P1 to P6)

Profile 2

The burial history of six pseudowells are given in Figure 4.11. Pseudowells 7 and 8 in the vicinity of the London-Brabant Massif show a similar burial history as pseudowells 1 and 2. Pseudowells 9 and 10 show minor generation during the Jurassic, but the main phase of hydrocarbon generation is taking at present, at the time of deepest burial (Figures 4.12 and 4.13). A slightly different pattern can be observed for pseudowell 11. Here some major generation also took place at about 90 Ma. This is probably an effect of local subsidence in the area. Pseudowell 12 had its major hydrocarbon generation during the Carboniferous after which no further generation took place.

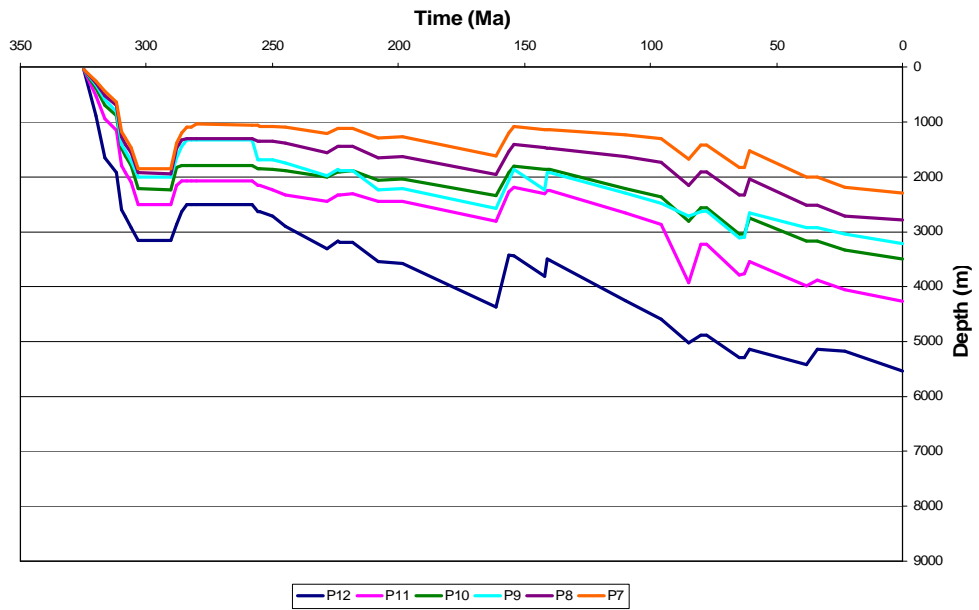


Figure 4.11 Burial history diagrams of the pseudowells along Profile 2 of Area 1. Pseudowells are marked with numbers (P7 to P12)

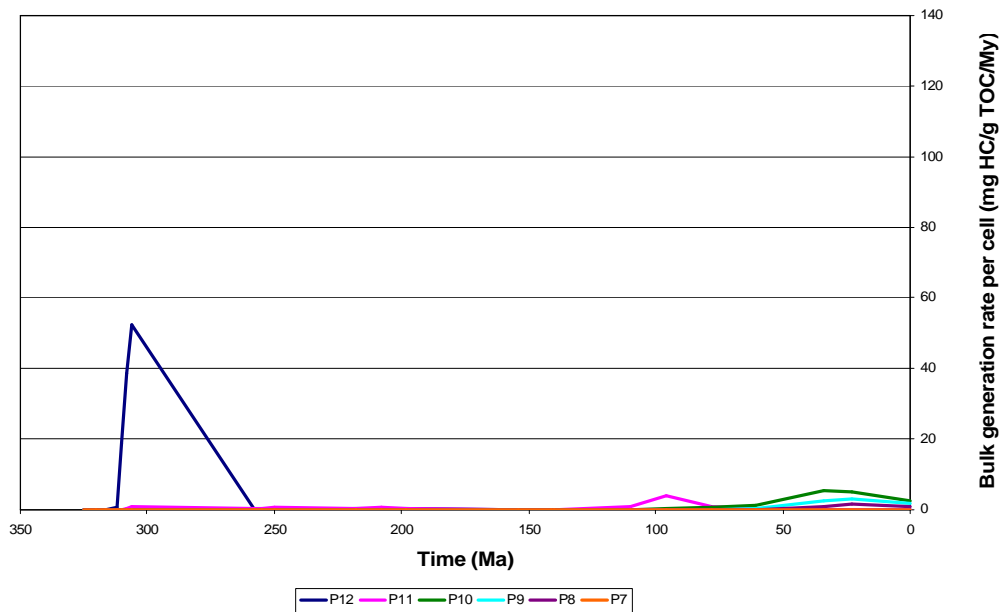


Figure 4.12 Hydrocarbon generation per event for the pseudowells along Profile 2 of Area 1. Pseudowells are marked with numbers (P7 to P12)

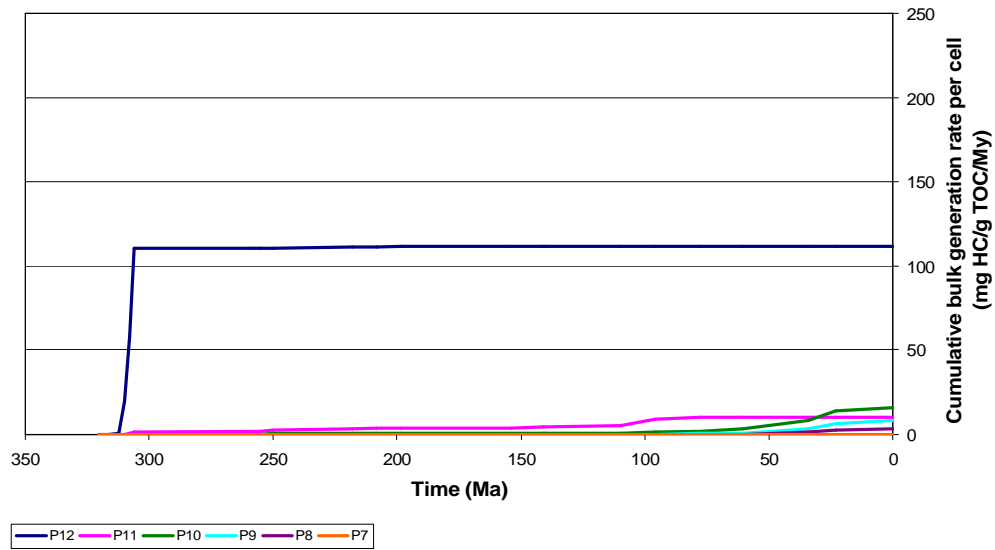


Figure 4.13 Cumulative hydrocarbon generation for the pseudowells along Profile 2 of Area 1. Pseudowells are marked with numbers (P7 to P12)

Profile 3

The western area is characterised by three phases of hydrocarbon generation (Figure 4.14). The first phase occurred during the Carboniferous, where minor amounts of hydrocarbons were generated (Figures 4.15 and 4.16). The second phase of hydrocarbon generation occurred during the Lower Cretaceous, induced by a rapid burial of the Namurian source rock. The Laramidian uplift interrupted the hydrocarbon generation shortly, but generation resumed and continues until today, with a peak of generation at about 23 Ma.

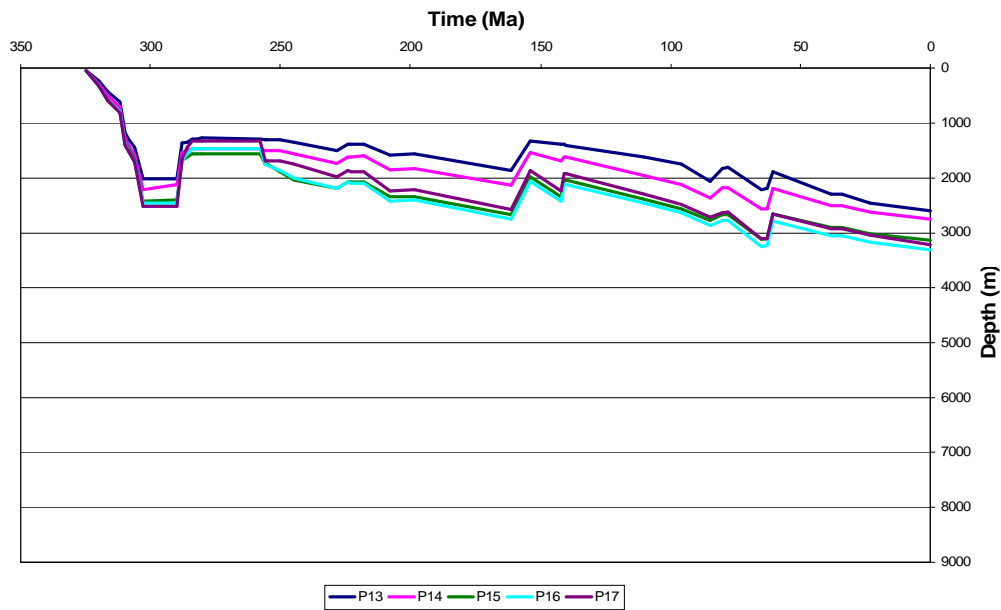


Figure 4.14 Burial history for the pseudowells along Profile 3 of Area 1. Pseudowells are marked with numbers (P13 to P17)

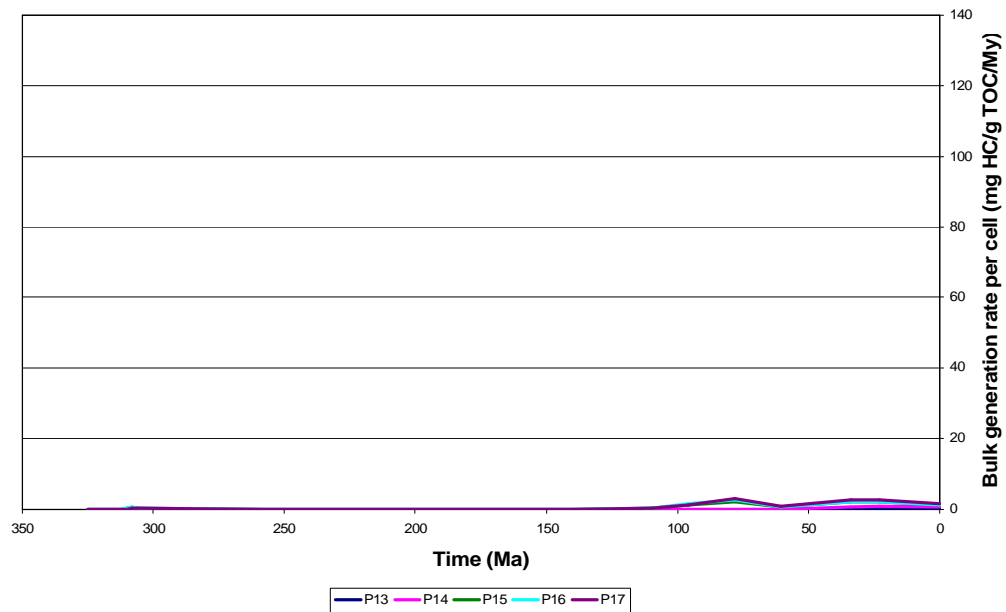


Figure 4.15 Hydrocarbon generation for the pseudowells along Profile 3 of Area 1. Pseudowells are marked with numbers (P13 to P17)

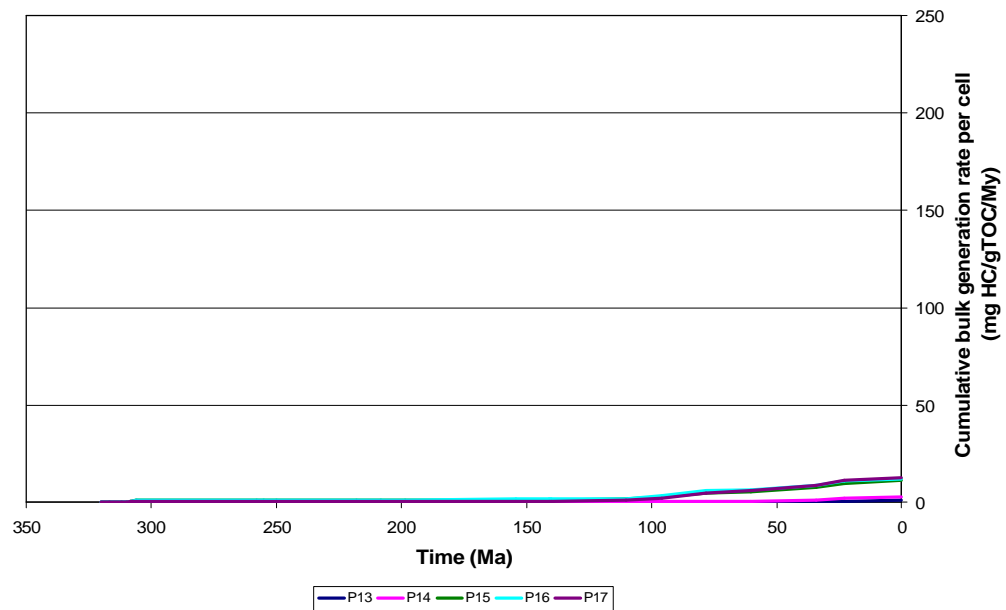


Figure 4.16 Cumulative hydrocarbon generation for the pseudowells along Profile 3 of Area 1. Pseudowells are marked with numbers (P13 to P17)

From the evaluation of the pseudowells of the two southernmost profiles in Area 1 we observe, that there is only a narrow zone along the margin of the London-Brabant Massif where present-day generation is taking place. On the Massif the source rock has been eroded. Towards the central part of the West Netherlands Basin the main phase of generation already took place during the Carboniferous. In that area all organic matter has been transformed to hydrocarbons already early in the geological history and no further generation is possible.

Within Area 1 the narrow prospective zone widens slightly toward the northwest, where deepest burial was recently reached and hydrocarbon generation from a Namurian source is modelled. The prospective zone can be somewhat broader if the possibility of a large lateral component in the migration path is taken into account.

Depending on the chosen kinetic approach, the location of this zone of recent hydrocarbon generation differs slightly. More information about the implication for the present-day transformation ratio is given in Appendix I.

4.6 Possible play concepts

The most likely source rocks in Area 1 are the Namurian source rocks (Base Namur-1, i.e. Geverik Mb equivalent hot shales). The 3D basin modelling has shown that the majority of the hydrocarbons throughout the area was generated at the end of the Carboniferous. The preservation of possible reservoirs that were filled at this time until recent time is not probable. The chance for preservation is highest on the relatively stable London Brabant Massif, where updip migrated hydrocarbons may have accumulated.

Still, although much of the hydrocarbon generation has been early, narrow zones can be expected where the timing is later and more favorable. In these narrow zones, generation of hydrocarbons still occur during the Cretaceous and Tertiary. The hydrocarbons that are generated at his times could have been accumulated in pre-Westphalian reservoirs, but also in reservoirs of younger age. Figure 4.17 shows a schematic overview of the possible pre-Westphalian reservoir types into which hydrocarbons generated from lower Namurian source rocks may have migrated.

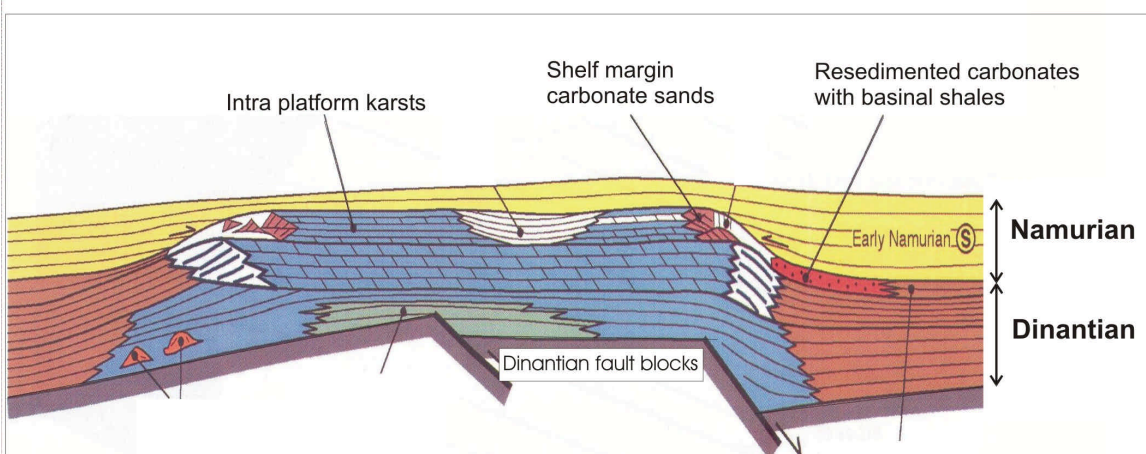


Figure 4.17 Play concepts for Area 1 (modified after Gutteridge, 2002)

From the overview given in section 4.3.2 the following most promising reservoir types can be selected for the hydrocarbon plays in Area 1 (Figure 4.18):

- Karstified upper parts of the Dinantian (most likely Dinant-3)
- Shelf margin carbonate sands over the ramps, e.g. reef talus of the 'Blue John' kind
- Namur-1 or -2 sandstones (not sketched in Figure 4.17)

The Namurian shales constitute a good seal to any hydrocarbons trapped in the Dinantian reservoirs.

In summary, two sorts of play concepts can be distinguished:

- 1) An 'early' play consisting of a Dinantian carbonate reservoir, source from 'Geverik equivalent shales' during the Late Carboniferous and sealed by Namurian shales. The main risks would be preservation of hydrocarbons in the structures.
- 2) A 'late' play with the same source, and either Dinantian or Namurian (or even Permian or Mesozoic) reservoirs filled during the Late Mesozoic. The risks are both the seal and the longer migration distances.

5 Hydrocarbon potential of Area 2

5.1 Geological and seismic interpretation

Area 2 consists of the northernmost part of the Netherlands offshore (Figure 1.1) including the A-blocks, the westernmost B-blocks and the northern E-blocks of the Netherlands North Sea Sector. In this Area the following key wells were defined at the start of the project: A11-01, A14-01, A15-01, A16-01, A17-01, E02-01, E02-02, E06-01, E12-02, E12-03 (gamma ray and sonic logs displayed in Figure 5.1). The wells were selected because they reached pre-Westphalian rocks. In addition to these ten wells information from the foreign wells 39/07-01, 38/25-01 and B10-02 was used for the seismic interpretation.

5.1.1 Well correlations

Figure 5.1 shows the well correlation panel for Area 2, a correlation from well 39/07-01 in the north to E12-03 in the south. Of the ten key-wells the wells A17-01 (950 m of Devonian – Tournaisian age Old Red Group encountered below the base Chalk unconformity) and E06-01 have reached Devonian rocks. Most of the other wells drilled into the Dinantian (all except A11-01, A15-01 and E12-03), but E06-01 is the only one with a complete Dinantian section.

Likewise, there is only one well with the complete Namurian section: E12-02, which is the only well in Area 2 where the stratigraphic top Namur-2 has been preserved from erosion. In the other wells of Area 2 the Top Namur-2 marker, if interpreted, does not represent the true stratigraphic top. In E12-02 the Namur-1 section deposited during the Pendleian – Arnsbergian is not quite as thick as it can be in Area 1. The thickness variations of in particular the Early Namurian basinal and prodelta parts of the Namurian infill vary across the basin from north to south as can be seen in Figure 5.2, a sketch copied from Cameron *et al.* (1992).

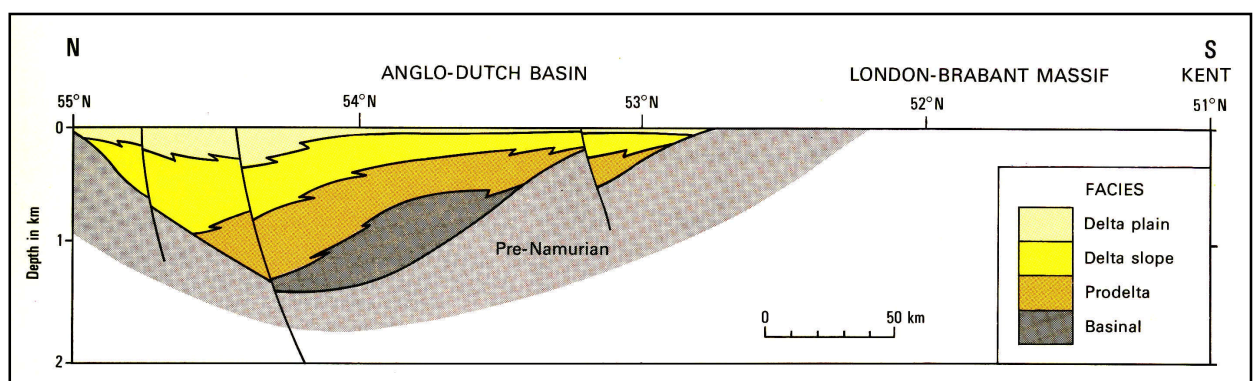


Figure 5.2 Schematic distribution of Namurian sediments between 55° N and 51° N in the southern North Sea according to Cameron *et al.* (1992). This schema is relevant to Area 2, but not accurate in Area 1.

UK well 43/25-1 proved that Namurian sediments are locally more than 1250 m thick in the north-central part of the Anglo-Dutch basin (Cameron *et al.*, 1992). In general, a large-scale shallowing upward of sedimentary facies can be observed in the Namurian.

Replace these two pages by file
Fig-5-1-Area2 well section_A3-size.pdf

The Namur-2 section in well E12-2, coinciding approximately with the Chokerian – Yeadonian, represents the fluviodeltaic and fluvial upper parts of the Namurian containing the better reservoir sands.

Several wells in Area 2 have drilled igneous rocks in the pre-Westphalian. Within the Namurian successions intrusive rocks were found in both wells A14-01 and A15-01. To our knowledge these have not been dated. Also within the intra-Namurian succession is the doleritic sill found in well E12-03. Again, the dating is unknown, which leaves the possibility that this igneous rock may be of Namurian age. Well A17-01 has drilled into a granite, now dated (within constraints of the measurement) at 410 ± 8 Ma, as discussed in Chapter 2, but also found volcanic rocks in the Dinant-1 (Tournaisian) upper part of its Old Red succession. The igneous rock found in E06-01 is reported to have been dated as Permian (Sissingh, 2004). All in all, there are two equally likely possibilities: the igneous rocks of wells A14-01, A15-01 and E12-03 are of Permian age, or alternatively one or more of these bodies are of Namurian age, similar to what has been dated at well Nagele-1 (see Chapter 6).

5.1.2 Seismic interpretation

Figure 5.3 shows the locations of the 2D seismic profiles used for the seismic interpretation. Digital copies of these lines were available and loaded into a separate Petrel project for Area 2. The lines belong to three regional 2D surveys of 1983, 1987 and 1991 vintage respectively.

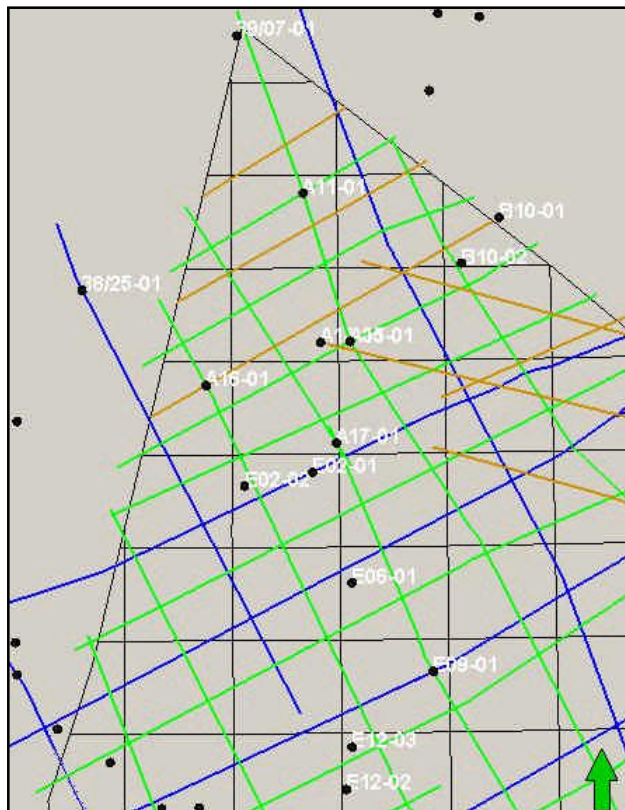


Figure 5.3 2D seismic lines of surveys SNST83 (blue), SNST87 (green) and ABT-91 (brown) used for the seismic interpretation of Area 2

The data quality of this seismic is generally fair to good. More detailed interpretations could however be obtained in the future by using the later 3D surveys acquired in the area. Appendices E5-E12 of this report are copies of selected interpreted lines of Area 2, mainly crossing or passing close to the key wells. These plots can be used to assess the general quality of the seismic data, the correlations made with the well picks overall structural geological configuration in the area.

The Base North Sea and the Base Chalk are the two regional horizons, which can be interpreted easily all over the whole area. Base Chalk constitutes a major erosional unconformity. Locally thin sections of Lower Cretaceous, Zechstein and Silverpit are preserved. The most prominent pre-Westphalian horizons that could be mapped were Top Namur(-2), Top Dinant(-3b) and Dinant-1 (Figure 5.4). It should be noted that over part of the Elbow Spit High the Top Dinant horizon was interpreted to coincide with the base Zechstein, where actually erosion has cut slightly into the Dinant-3 (e.g. Appendix E10). This practical decision was made in order to make the top Dinantian depth map (Figure 5.6). In a small area around well A17-01 the Dinantian is completely absent due to erosion (see Enclosure E6). This was ignored in the contouring of Figures 5.5 and 5.6.

Soon after the start of the interpretation it was found out that in addition, a deeper, but very clear and remarkable seismic event could be mapped in almost the entire area. This horizon has not been drilled by any of the wells in the area. The sequence immediately below this horizon has a very distinct high amplitude low, frequency seismic facies. Comparison with existing literature (Gatliff *et al*, 1994; Marshall & Hewett, 2003) makes it very likely that this horizon represents the top of Mid Devonian limestones that are overlain by the Old Red Group. The name for these limestones in the UK is the Kyle Group (UK wells 37/12-1 and 38/3-1). Well 30/16-5 drilled through this sequence and encountered deformed rocks of Ordovician age (Marshall and Hewett, 2003).

On the Elbow Spit High the major regional unconformity Base Chalk has eroded deeply into the pre-Westphalian stratigraphy. Locally, rocks of Devonian age subcrop the Base Chalk. Moving away from the centre of the Elbow Spit High, younger pre-Westphalian units start subcropping the Base Chalk. The Eastern Boundary Fault of the Elbow Spit High constitutes a very abrupt structural boundary, east of which pre-Westphalian rocks hardly recognisable on seismic data. Moving to the west the deepening of the pre-Westphalian units is more gradual.

On some lines pre-Westphalian units can be distinguished based on their distinct seismic facies. E.g. the unit Dinant-3b (see Figure 5.1, wells E02-02 and E06-01), containing calcareous beds, has a higher amplitude seismic facies than unit Dinant-3a, which contains less carbonates. This is illustrated in Figure 5.4, a seismic section across wells E06-1, displaying the gamma ray log of the Dinantian sequences on top of the seismic section.

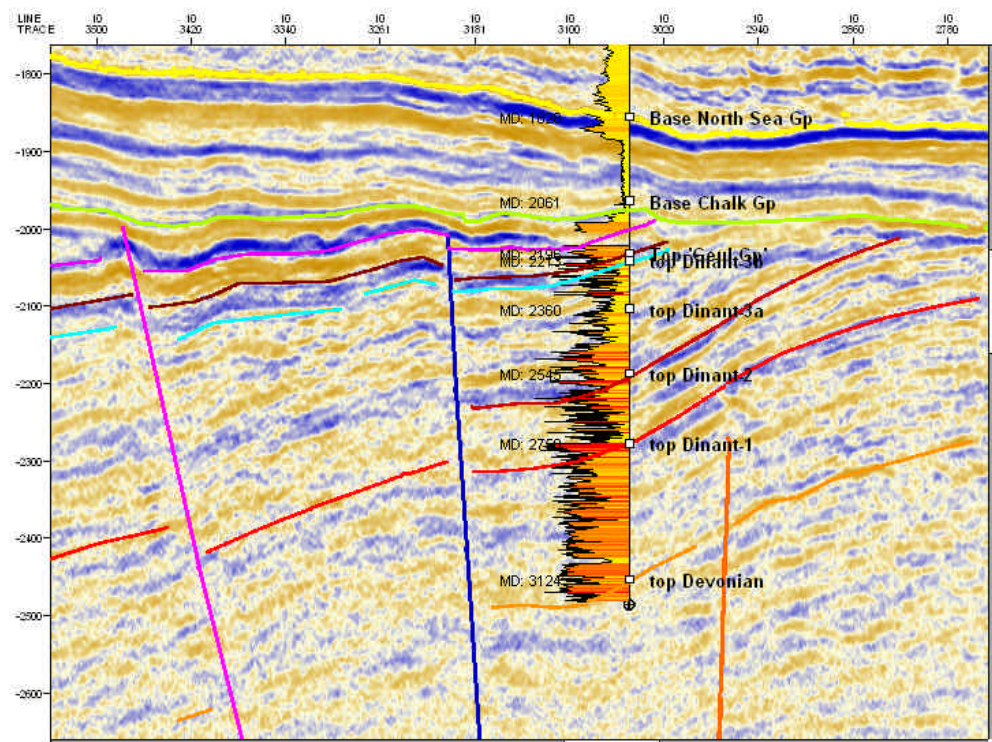


Figure 5.4 Seismic section NW of well E06-01 showing the correlation, seismic facies (higher amplitudes in Dinant-3) and the well's gamma ray log (high values plotted to the left)

Another important observation that can be made (e.g. on Appendix E8) is the fact that on this part of the Elbow Spit High there can be rapid lateral variations in terms of the overburden of the pre-Westphalian. At the location of E02-02 a thick Zechstein sequence (including rock salt), capable of providing a good seal, is present, whereas a few kilometres to the northeast the Zechstein is absent.

5.2 Source rocks

The geochemical evaluation presented in Chapter 3 resulted in the identification of good present-day source rock potential of sequences near the Dinantian – Namurian transition and fair potential for intra-Dinantian and intra-Namurian source rocks (Table 3.1).

This most promising source rock from the Dinantian – Namurian transition can be expected to be preserved to the south (i.e. blocks E04, E05 and E06) of the interpreted Namurian subcrop line (see map in Appendix E10) and east of the subcrop line on the Elbow Spit High and immediately adjacent to the High in the A blocks.

The geochemical analyses indicated mainly gas prone (Type III) source rocks in the Dinant-2 and -3 (Yoredale Fm. equivalent). However, given the expected block and basin structure of the basin, the presence of Type II source rocks is expected that might be within the gas window at present-day near the margins of the structural highs. The potential source rocks are, however, not yet encountered by wells.

Top Dinantian time map

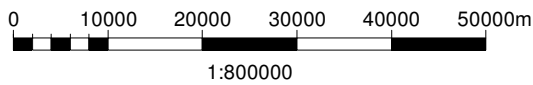
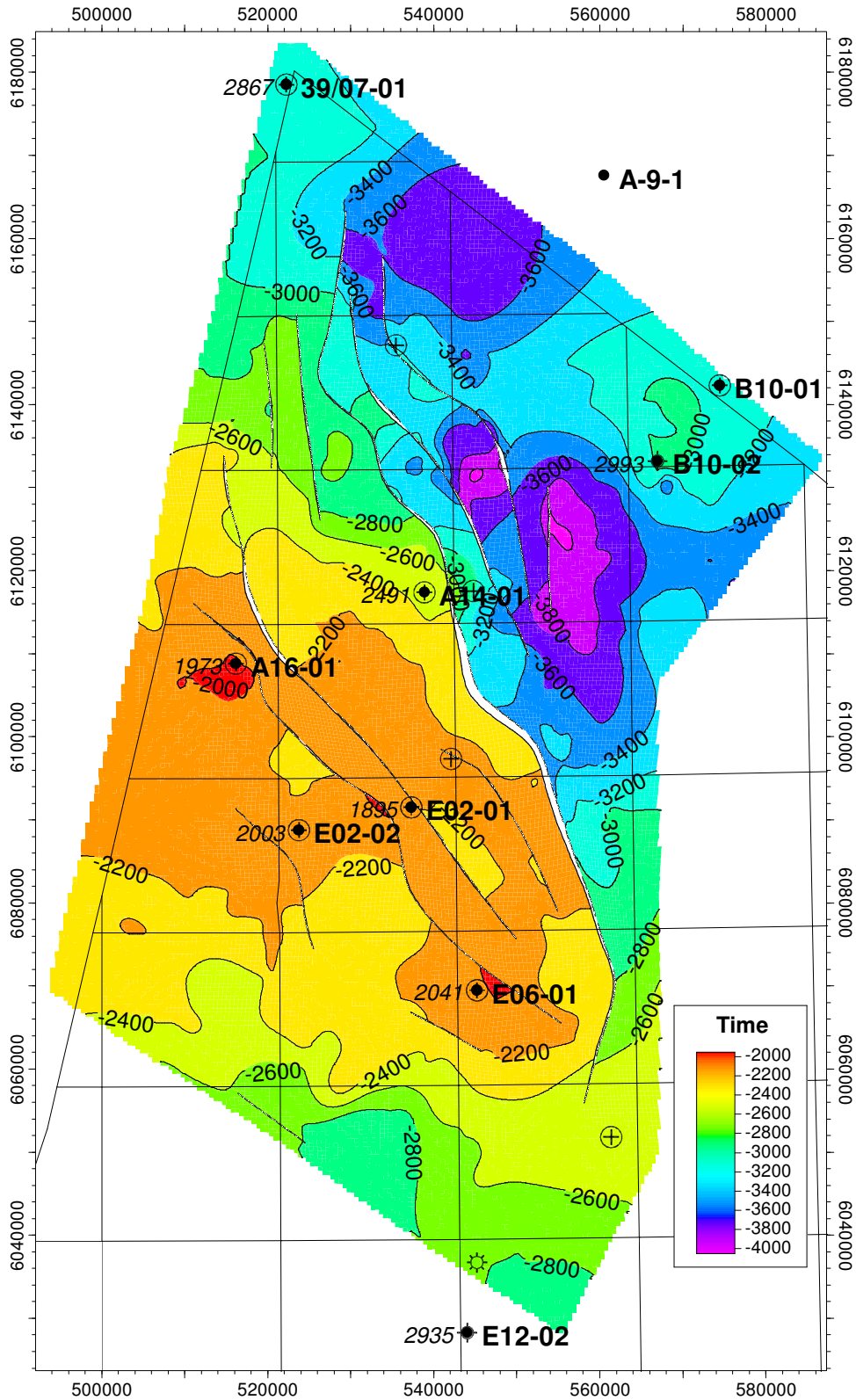


Figure 5.5

Area 2	Scale 1:800000
[msec] TWT	Contour inc 200
Top Dinant	Date 12/19/2005



Top Dinantian depth map

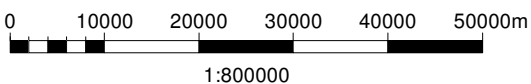
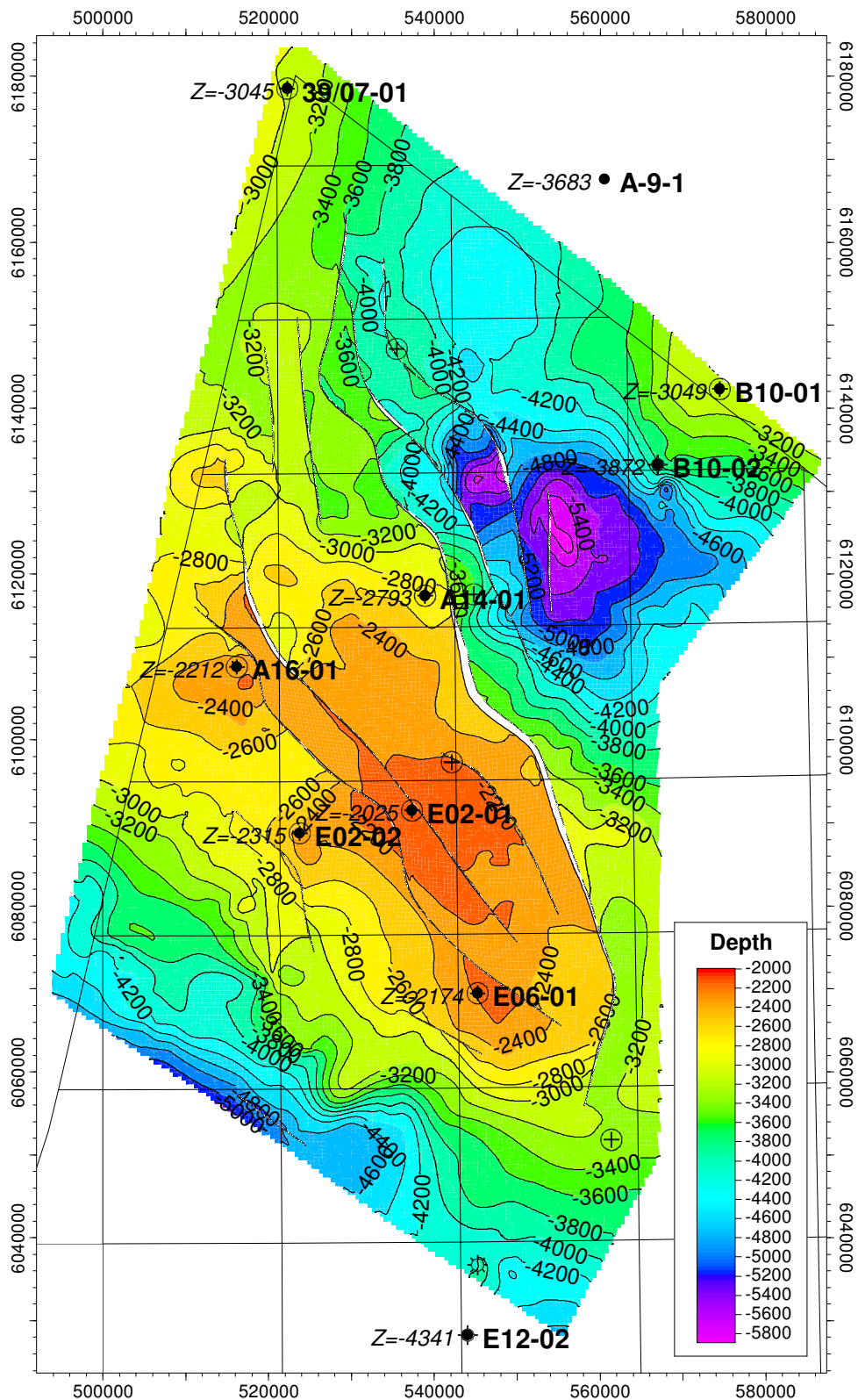


Figure 5.6

Area 2	Scale 1:800000
[m] below MSL	Contour inc 200
Top Dinant	Date 12/19/2005



5.3 Reservoirs

5.3.1 *Devonian reservoir potential in Area 2*

There are two possible Devonian reservoirs that can be identified in Area 2: the Mid-Devonian carbonates (Kyle Group equivalent) and the sandstones of the Old Red Group. As mentioned before, Middle Devonian carbonates have been encountered in the UK offshore (wells 38/3-1 and 37/12-1) and in Germany onshore (Münsterland-1) but were not drilled in the Netherlands. Nevertheless, seismic interpretation of Area 2 seems to confirm their presence. These carbonates are overlain by terrestrial deposits, which could indicate that these rocks have been exposed to karstification.

Both the Buchan and the Tayport Formations in the Old Red Group contain thick and often well developed sandstones (Van Adrichem and Boogaert, 1993-1997). These sandstones are also reservoir candidates in Area 2. They have only been drilled in well A17-01. It is unclear what their extension is towards the south. North of the Mid North Sea High the Auk, Argyll, and Embla fields show Old Red reservoir with low permeability fluvial sandstones. Noteworthy is that the low permeability, possibly problematic during production, is enhanced by a network of open fractures

All things considered, given the limited amount of data, we regard the quality of the Devonian reservoirs as highly speculative.

5.3.2 *Dinantian reservoir potential in Area 2*

The units Dinant-1, -2 and -3 consist of a cyclic alternation with carbonates, claystones, sandstones and coal seams. Obviously, the reservoir potential is formed by the sandstones in these cycles. Maynard & Dunay (1999) identify two potential reservoirs for the Dinantian play at the northern margin of the Southern Gas Basin (which includes our Area 2): the Fell Sandstone Formation and the Whitby member. The Fell sandstone Fm corresponds roughly to our Dinant-2 and Dinant-3a units, whereas the Whitby member of the Scremerston Fm relates to the lower part of Dinant-3b (of Asbian to Brigantian age). The Fell Sandstone was deposited at a time of high sediment supply, resulting in a thick (300m) succession of fluvial sandstones. Its distribution is closely linked to the accommodation space developed in the hanging walls of contemporaneous faults. The Whitby Member was deposited during the Asbian at a time of lower sediment supply which enabled relative sea-level changes to control the vertical distribution of sandstone bodies. It could have infilled a paleovalley. If active faulting continued throughout this time than a similar hanging wall concentration of sandbodies, as is seen in the Fell Sandstone Formation, could be expected (Maynard & Dunnay, 1999).

5.3.3 *Namurian reservoir potential in Area 2*

In Area 2 Namurian sequences have been drilled in at least wells A11-01, B10-02, A14-01, A15-01, E12-02 and E12-03. The sandstones in unit Namur-2 belong to the Millstone Grit Formation. Individual sandstone beds are more than 10 m thick, but stacked beds can amount up to 80 m. The sands are fine to medium-grained, with occasional gravelly intercalations. Sandstone beds can have sharp tops and bottoms, or

grade into mudstones. Most of these sandstones were deposited by sheet-delta systems (Collinson, 1988). The sandstones have been interpreted as delta-front deposits: mouth bars, and distributary-channel fills. Their amalgamation during delta progradation has resulted in sheets of great lateral continuity. Intercalated fines reflect periods of higher sea/lake level, and were deposited as prodelta turbidites, or settled from suspension (Van Adrichem Boogaert and Kouwe, 1993-1997). In well E12-03 gas-bearing fluvial sandstones occur in unit Namur-2 (Figure 5.1 and Enclosure 3). The fact that these sands contain gas in block E12 are proof of their reservoir potential.

In a block and basin setting, as described in Chapter 2, Namurian slope settings (turbidites) may be anticipated. Such Namurian turbidites have been found in well 43/17-2, where they are positioned above the Bowland Shale (Maynard and Dunnay, 1999). Also Cameron *et al.* (1992) show examples of wells with Namurian turbidites in the Anglo-Dutch basin (well 48/3-3 where they are of Marsdenian age). The reservoir potential of the turbidites is probably less than that of the fluvial sands. In the Dutch part of Area 2 no examples were found of Namurian turbidites with any significant reservoir potential. The lowest part of Namur-1 section in well A14-01 may represent a silty turbiditic sequence, but its reservoir potential is poor.

5.4 Seals

The best seal present in Area 2 is formed by the Zechstein evaporites. Caution is needed however, because the Zechstein, though present over most of the area is not present or thick enough everywhere. This is e.g. illustrated by Figure 5.3 and Appendices E10 and E11. In general, sufficiently thick Zechstein (including rock salt) is present at the southern margin of the Elbow Spit High and at the eastern margin once a bit farther east than the main bounding fault. On the High itself and off the High but too close to the eastern bounding fault a Zechstein seal cannot be relied upon. In those cases any Dinantian reservoirs may still be sealed by Namurian shales or Rotliegend sections if present.

5.5 Hydrocarbon generation and its timing

In Area 2 hydrocarbon generation took place throughout the geological history, as a function of burial history. Figure 5.8 presents an overview of hydrocarbon generation from the source rocks in units Dinant-3 (Yoredale Fm equivalent) and Namur-1. The first phase of hydrocarbon generation started already at the end of the Carboniferous, followed by more generation during the Triassic and Jurassic. At the end of the Jurassic a major phase of hydrocarbon generation occurred. Generation ceased during the Early Cretaceous and resumed during the Late Cretaceous, increased substantially from about the beginning of Paleocene until present.

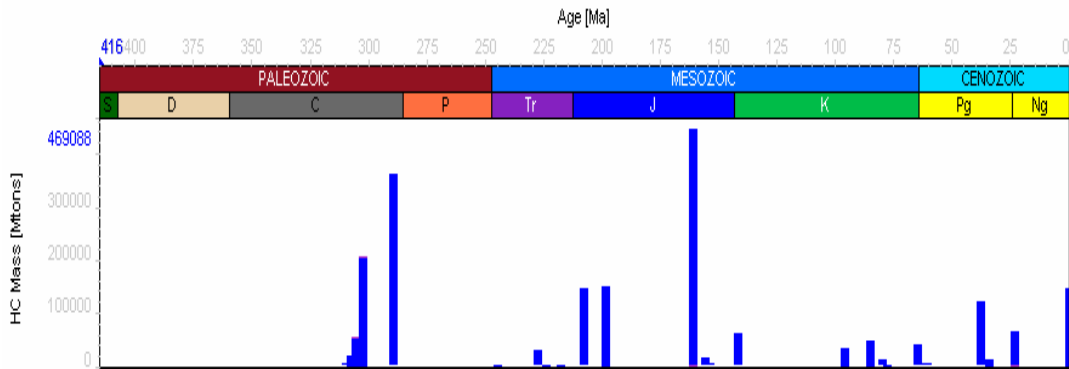


Figure 5.8 Generated and expelled hydrocarbons per event for all source rocks in Dinant-3 (Yoredale Fm equivalent) and Namur-1 in Area 2 (Burnham 1989_T2 & Burnham 1989_T3 kinetics)

From the 3D model, maps showing the transformation ratios have been extracted (Appendix I) for several moments in geological time. Generation during the Carboniferous started in the western and southern parts of Area 2 and continued until the Triassic. During the Jurassic generation occurred at the southern and eastern margins of the Elbow Spit High, where in some parts hydrocarbon generation occurred to a larger extent. Only minor transformation of organic matter occurred during the Early Cretaceous. Significant generation started again during the Late Cretaceous and increased from about 34 Ma onwards, when the eastern margins of the Elbow Spit High underwent strong subsidence.

From the 3D model, burial history plots and generation vs time diagrams have been extracted for six pseudowells along a profile across the Elbow Spit High (Figures 5.9 and 5.10). These diagrams illustrate the generation pattern through time for a base Namurian 1 Type III source rock. It can be assumed that the slightly deeper buried source rocks of the Dinantian show a similar burial and hydrocarbon generation pattern.

In the south-western part of the area (Figure 5.9, pseudowells 1 and 2), deep burial already occurred during the Carboniferous. The deep burial initiated the first phase of hydrocarbon generation (Figure 5.10). As this area was part of the Southern Permian Basin, subsidence continued after the Saalian uplift during the Zechstein and Triassic. Towards the end of the Jurassic a new phase of significant hydrocarbon generation occurred, especially in the southern part (Figure 5.10). After the Late Kimmerian 1 tectonic phase, which caused severe uplift, the area subsided regularly, interrupted by minor phases of uplift and erosion until present. A third phase of hydrocarbon generation occurred at the end of the Cretaceous.

The western margin of the Elbow Spit High (Figure 5.9, pseudowell 3) shows a strong subsidence during Carboniferous times and a first phase of hydrocarbon generation during Carboniferous. The western margin of the Elbow Spit High did not undergo major burial during the Mesozoic. However, prior to the Late Kimmerian 1 tectonic phase a second phase of hydrocarbon generation occurred. After uplift and erosion during the Late Kimmerian tectonic phase, which was one of the major tectonic events after the Saalian tectonic event in this area, the area started to subside again and reached the strongest subsidence from about 60 Ma to present. After a minor effect of the

Pyrenean tectonic phase, the major phase of hydrocarbon generation started at about 30 Ma and continues until present day (Figures 5.10 and 5.11).

The area of the Elbow Spit High (Figure 5.9, pseudowell 4) also underwent comparably strong subsidence during the Carboniferous, but the Saalian unconformity removed about 2000 m of sediments. The Elbow Spit High only received marginal sedimentary load during the Mesozoic. The strongest subsidence started about 60 Ma. Since the Elbow Spit High was never deeply buried and just recently reached the deepest burial, only marginal amounts of hydrocarbons have been generated though time 9 (Figures 5.10 and 5.11).

At the eastern margin of the Elbow Spit High (Figure 5.9, pseudowells 5 and 6) the Mesozoic subsidence only marginally succeeded the Carboniferous subsidence. Carboniferous subsidence was smaller than in the southern part of the Elbow Spit High and therefore only minor amounts of hydrocarbons were generated. Also the amounts of hydrocarbons generated during the Mesozoic were small. This northeastern margin of the Elbow Spit High is regularly subsiding from about 60 Ma onwards and especially during the last 23 Ma the area is subsiding rapidly. As a consequence of the geological history, the main phase of hydrocarbon generation started about 50 Ma and continues until present (Figure 5.10 and 5.11). The highest generation rate is reached in the direct vicinity of the Elbow Spit High.

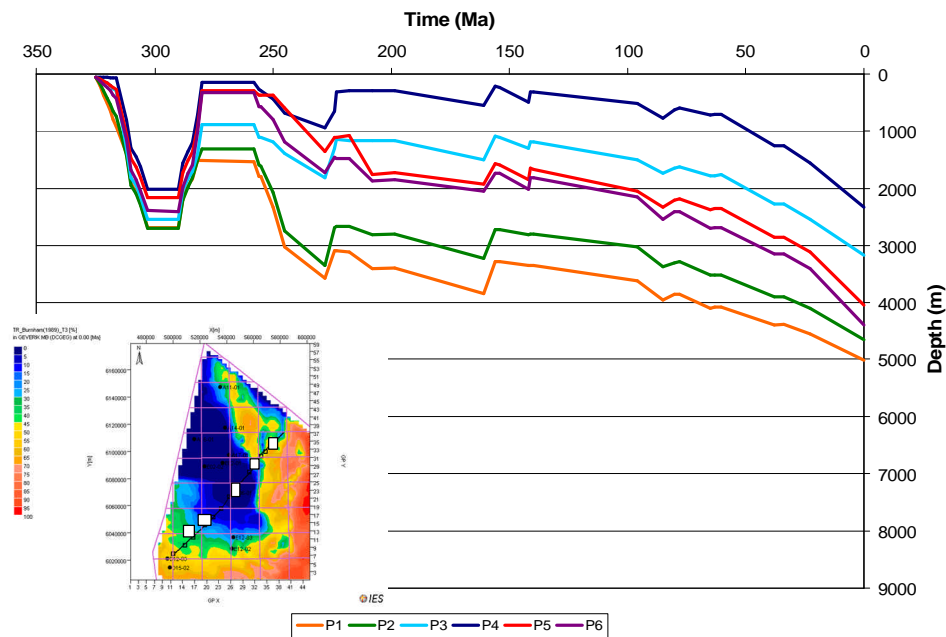


Figure 5.9 Burial history diagrams for six pseudowells along a profile across the Elbow Spit High. Pseudowells are marked with numbers (starting with pseudowell 1 in the SW and ending with pseudowell 6 in the NE). Colours on the inset map represent depth

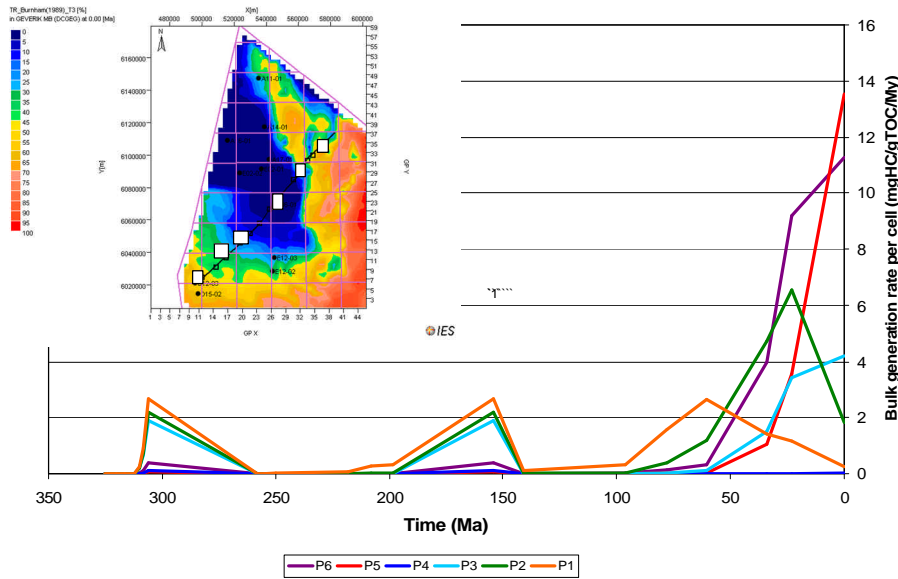


Figure 5.10 Hydrocarbon generation diagram per event diagrams for six pseudowells along a profile across the Elbow Spit High. Pseudowells are marked with numbers (P1 in the SW to P6 in the NE). Colours on the inset map represent the Transformation Ratio

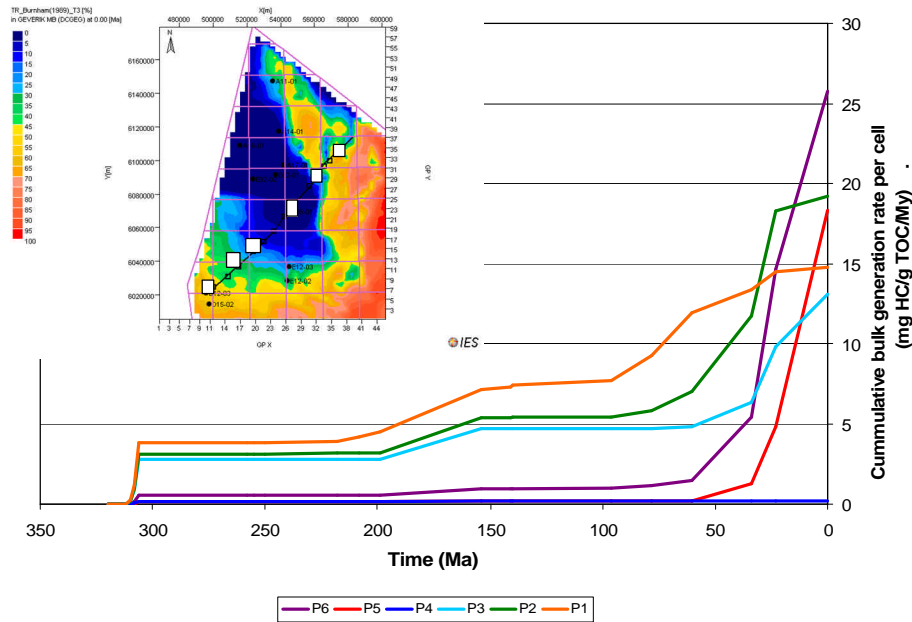


Figure 5.11 Cumulative hydrocarbon generation for six pseudowells along a profile across the Elbow Spit High. Pseudowells are marked with numbers (P1 in the SW to P6 in the NE). Colours on the inset map represent the Transformation Ratio

In the modelling the amount and timing of hydrocarbon generation also strongly depends on the chosen kinetic approach. More information about the implication for the present day transformation ratio is given in Appendix I.

5.6 Possible play concepts

The evaluation of the timing of maturation showed that generation and expulsion of hydrocarbons occurred throughout geological history. This implies that the prospectivity of the area is strongly dependent on other critical factors such as the reservoir quality and the presence of an adequate seal at specific locations in the area. Figure 5.12 summarises the most probable play concepts for Area 2. Given Namur-1 or Dinantian source rocks, migration into several possible reservoirs is sketched. Possible reservoirs are in the Dinant-1, -2 and -3 and in the Namur-2. The best seal present is formed by Zechstein evaporates.

Going south from the Elbow Spit High, the Namurian and Dinantian sections can be seen on seismic lines to rapidly move to greater depths. Moving south through the E-blocks thicker and thicker Westphalian sequences are present on top of the Namurian. As a consequence of the deeper burial, the pre-Westphalian probably loses its hydrocarbon potential somewhere half-way in the E quadrant.

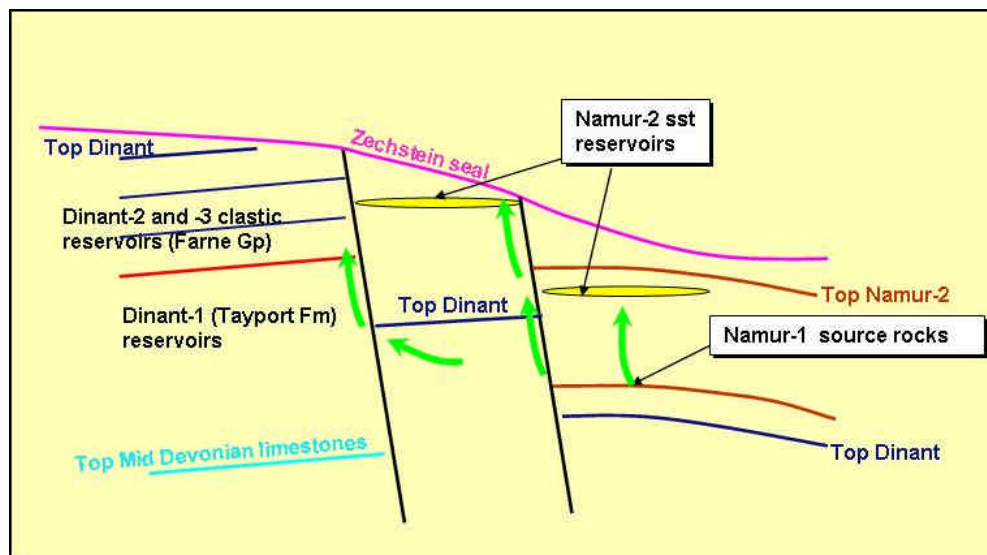


Figure 5.12 Play concepts for Area 2

The same is true moving away from the Elbow Spit High to the east. Reference is made to Figure 5.6, the depth map for the top of the Dinantian. In terms of maturity the most promising part of Area 2 consists of a rim around the southern and eastern margins of the Elbow Spit High (Figure 5.13).

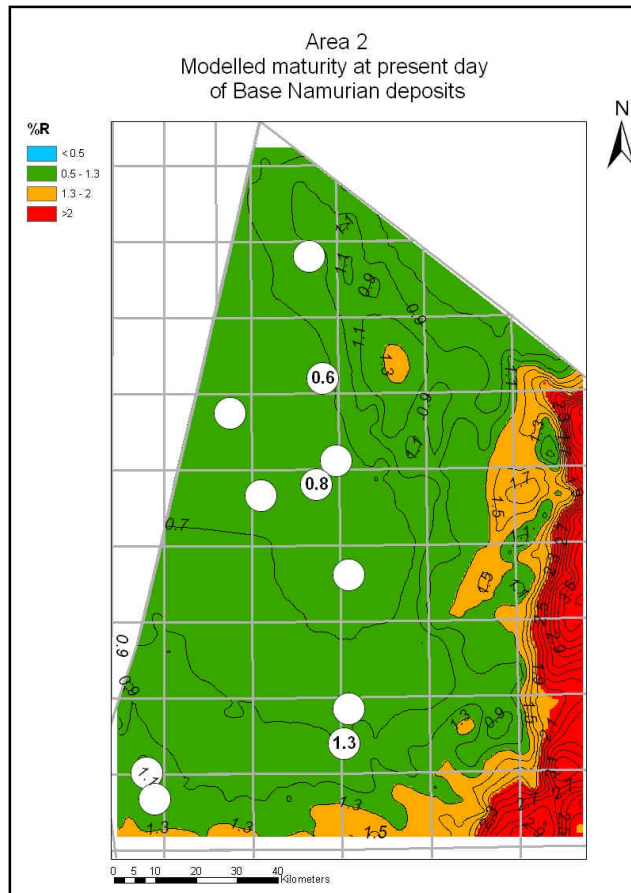


Figure 5.13 Maturity of a near base Namurian source rock at present (from Appendix J)

It is not known what stratigraphic level represented the source for the gas found in well E12-03, but the structural configuration (Appendix E12) suggests that there is very little Westphalian section present in the immediate vicinity of both E12 wells. Therefore, the if sourced from the Westphalian must have laterally migrated, or alternatively, the gas found in E12-03 had a Namurian source. Figure 5.14 indicates that the present-day maturity in block E12 is close to, but not yet in the gas window.

In summary, the most promising play concept for Area 2 implies:

- Late generation of hydrocarbons (Tertiary) from a (near) base Namurian shale and charging either Devonian, clastic Dinantian or Namurian reservoirs, sealed by Zechstein rock salt. The main risks are reservoir quality and migration path. In those parts of Area 2 where maturation is still insufficient, lateral migration is required.

6 Hydrocarbon potential of Areas 3 & 4

6.1 Geological and seismic interpretation

6.1.1 Well correlations

The key wells used in Area 3&4 are: Winterswijk-1 (WSK-01), Munsterland-01 (Münsterland-1 in Germany), Nagele-1 (NAG-01), Emmeloord-01 (EMO-01) and Tjuchem-2 (TJM-02). Figure 6.1 shows the well correlations panel made between these wells from south to north. Both wells in Area 4 (Winterswijk-1 and Münsterland-1) have reached Devonian sediments, in the latter case even Middle Devonian (Givetian) carbonates. The other three wells have their TD in the Namurian, with Nagele-1 and Tjuchem-2 reaching into the Namur-1 deposits, but Emmeloord-1 only penetrating the Namur-2.

6.1.2 Seismic interpretation

The Areas 3 & 4 as defined at the start of the Petroplay project are taken as one study area. Figure 6.2 shows the extent of this area.

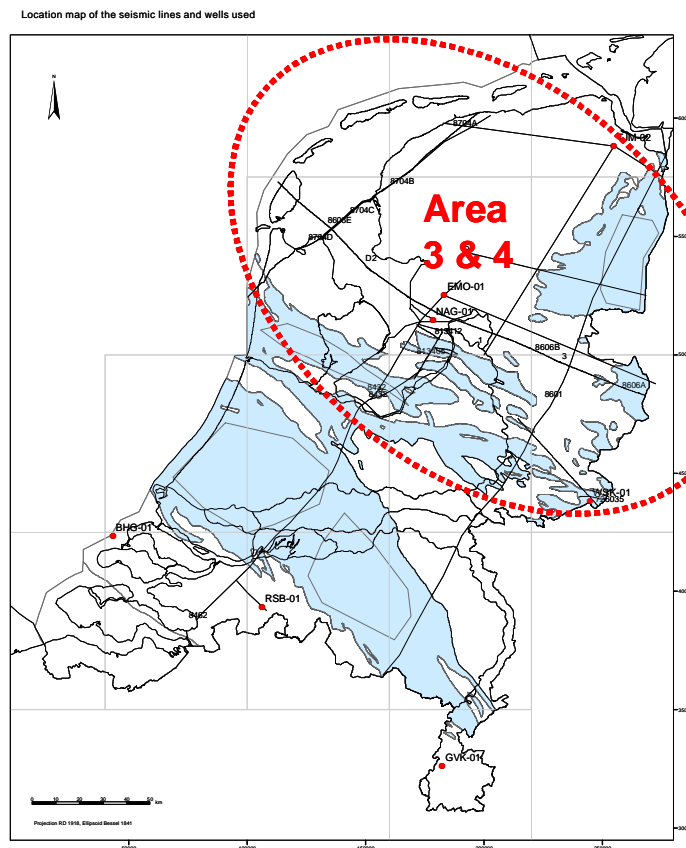


Figure 6.2 Location map onshore Areas 3 & 4 showing the 2D seismic lines used for the seismic screening. Basins are shown in blue

Replace these two pages by file

Fig-6-1-Area3 well section_A3-size

The main objective of the seismic screening was to establish if pre-Westphalian seismic events could be interpreted and correlated at a regional scale. The stratigraphic interpretations of the four wells Winterswijk-1, Emmeloord-1, Nagele-1 and Tjuchem-2 were tied to some regional seismic lines.

The best available regional onshore seismic grid is that of the lines shot in 1986 and 1987 by Delft Geophysical for the nation-wide 'Deep Seismic' research project conducted by RGD. The main lines of interest are 8601, 8606 and 8704. Digital copies of these lines were loaded into a separate Petrel project. Compared to the quality of the available offshore seismic data in Areas 1 & 2, the quality of the available onshore seismic data is generally poor at pre-Westphalian levels. In contrast to the other two Areas, described in Chapters 4 and 5, therefore no attempt was made to construct top Dinantian depth grids on the basis of seismic information. The depth grids used in the basin modelling were mainly based on regional trends and well information.

In order to tie the well interpretations to the seismic grid some additional 2D lines crossing the wells were selected. Digital copies of 2D lines 726035, 803007, 803012, 813405 en 813412, provided by NAM, were used to tie the wells Winterswijk-1, Emmeloord-1 and Nagele-1 to the main grid. A number of random lines was generated (by NAM) out of the regional 3D seismic compilation and digital copies of these lines were loaded into the Petrel project. Tjuchem-2 was tied to these lines. Unfortunately, the random lines out of the 3D area had a trace length of only 3.5 secs.

Starting with the well interpretations in Winterswijk-1 on line 726035 (see Appendix E13) an attempt was made to correlate the interpretations of top Dinant-3b and top Namur-2 to the rest of the seismic grid. The quality of line 726035 is rather poor. Nevertheless, at the location of the well Winterswijk-1 a strong high amplitude reflection is observed near top Dinantian level. Since the logs show an intrusive body in the lowest part of the Namurian (see Figure 6.1) this high amplitude event, at least locally, corresponds also to the igneous rocks. Moving from the well along the line to the NW, a few more patches of this reflector were seen (between 2000 and 2500 msec TWT) and an attempt was made to bring this interpretation to the intersection point with regional line 8601-C. Moving to the north along lines 8601D and C (through the province of Overijssel) the top Dinantian interpretation seems to gradually deepen to a TWT 'depth' of about 3000 msec at the intersection point with line 8606A. The interpretation is difficult, but guided by the more clearly dipping Westphalian seismic events above.

Of the lines 8606A and 8606B only paper copies were available. The presumed top Dinantian event remains more or less constant at a 'depth' of about 3000 msec until halfway on line 8606B (i.e. approximately north of Zwolle). At that point there is an indication for a large regional fault offsetting the Carboniferous a few hundred msec deeper to the west.

Line 8606NC is included as Appendix E18. The interpretation of top Dinantian (correlated all the way from Winterswijk-1) can be tied to the interpretation taken from well Nagele-1. The Top Dinantian is found at about 3000 msec in the east and is dipping to 3250 msec in the west. It is observed that the total 'thickness' of the Namurian sequences has increased to about 1000 msec (some 2250 meters, given an average velocity of 4500 msec). Another interesting observation is a clear intra-Namurian regional unconformity on which the younger Namurian sequences are

onlapping. The surface also represents an erosional unconformity. When tied to well Nagele-1 on line 803012 the unconformity can be dated as of Late Arnsbergian age. It also plots very close to the extrusions found in Nagele-1 and dated at 327 ± 8 Ma.

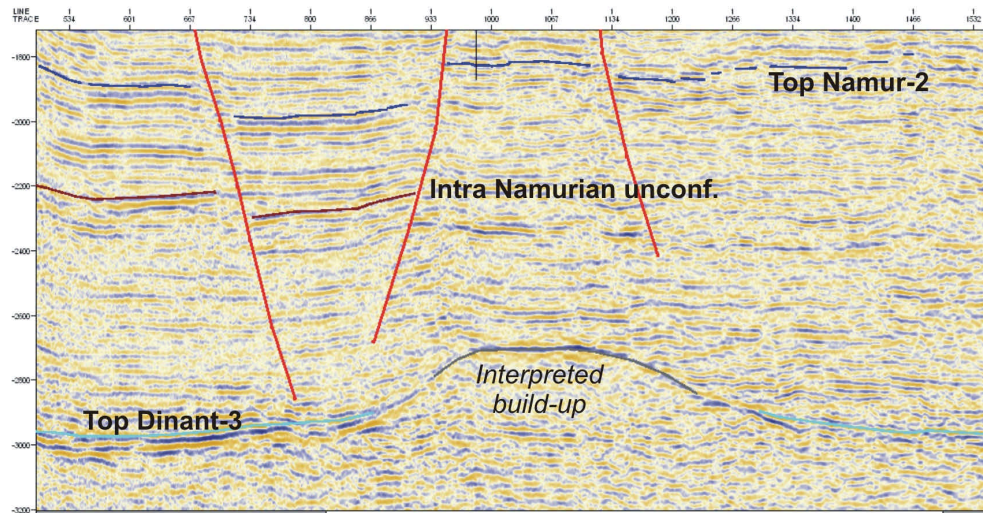


Figure 6.3 Part of line 803007 (see also Appendix E15) with the interpreted carbonate build-up

Figure 6.3 shows part of line 803007, which runs across well Emmeloord-1. At greater depth than the TD of the well a structure is visible which we interpret as a Dinantian carbonate build-up. Its dimensions are estimated to be 600 m high and 5000 m wide.

The well picks of well Tjuchem-2 have been tied to the random lines obtained from NAM, which have been extracted from their regional 3D compilation. The quality of the merged 3D survey has been degraded because only every fourth trace was used. The northernmost part of the line runs across Tjuchem-2 (Appendix E17). At the well the top of the Namur-2 is at about 2200 msec. Moving along a NW-SE line to the SW (Appendix E16) this depth of the top Namurian is observed to increase gradually. We observe that in fact at any location in between the Noordoostpolder and the location of well Tjuchem-2 the pre-Westphalian units are at present buried deeper than near the well itself.

6.2 Source rocks

The main intervals with initial high source rock potential are found near the base Namur-1 (Geverik Mb equivalent) and within the Namurian. Pre-Westphalian source rocks in Area 3&4 are generally over-mature (see Chapter 3). Generation will have occurred early in geological history, mainly due to a higher heatflow at several instances in time (see Appendix H and section 6.5).

6.3 Reservoirs

6.3.1 Devonian reservoir potential in Area 3&4

In well Winterswijk-1 some 300 m of sandstone was drilled in the Devonian (Figure 6.1 and Enclosure 2). This interval corresponds to the Bosscheveld Fm. (Van Adrichem

Boogaert and Kouwe, 1993-1997) and is considered to be a possible time-equivalent of the Condruz Sandstone which occurs on the southern rim of the London Brabant Massif in Belgium and Germany. These sandstones may have some reservoir potential, but the sonic log indicates that in Winterswijk-1 the sandstone is probably tight.

6.3.2 Dinantian reservoir potential in Area 3&4

The seismic screening of Area 3&4 revealed an elevated feature in the pre-Westphalian deposits underneath well Emmeloord-01 (EMO-01). Well Emmeloord-1 was unfortunately not deep enough to penetrate this feature. However, there seem to be similarities with carbonate build-ups as encountered in Belgium, U.K., and Ireland (Mucchez *et al.*, 1990; Grayson & Oldham, 1987). In the U.K. and Ireland, mud-mounds were formed throughout the Dinantian, but most of them were formed in either the Early or the Late Dinantian (Bridges *et al.*, 1995; Figure 6.4).

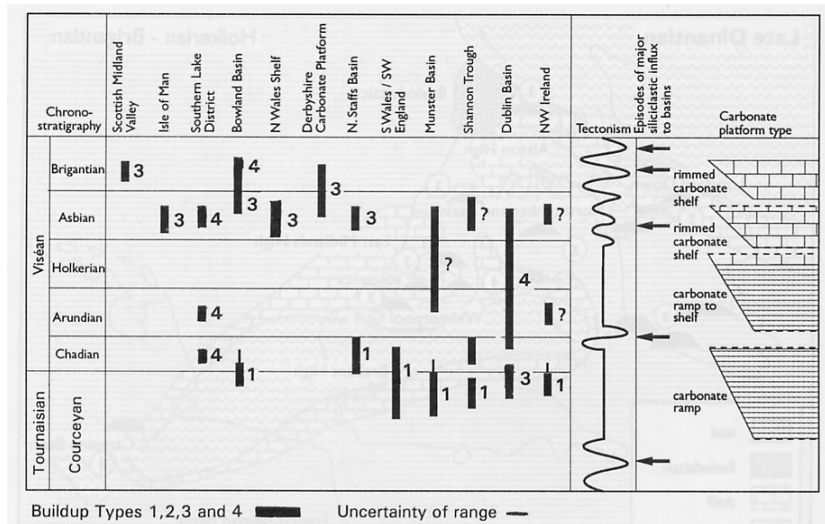


Figure 6.4 Plot of occurrence of Early Carboniferous buildups in the British Isles against stratigraphic age. Two phases of development can be recognized. The first phase, dominated by Type 1 buildups, occurred during a time of relative tectonic quiescence, and was terminated by tectonic activity. The second, dominated by type 3, occurred during a time of tectonic activity and terminated as siliciclastics, derived from the north, were delivered to the contemporary platforms (after Bridges, 1995). The numbers in the picture refer to the type of buildup, as explained in Figure 6.5.

Carbonate mud-mounds that were formed at the Early Dinantian are often referred to as Waulsortian mud-mounds as e.g. studied in Belgium. There are important differences in the depositional setting and internal complexity between these Early and Late Dinantian mud-mounds, as e.g. the Derbyshire carbonate platform in the U.K. (Gutteridge, 1995). However, instead of using the term Waulsortian, which has not always been used consistently, Bridges *et al.* (1995) proposed five types of Early Carboniferous buildups (Figure 6.4 and 6.5). In general, the type of depositional setting changes from carbonate ramp deposits in the Early Dinantian to rimmed carbonate shelf in the Late Dinantian. This change was related to a change from a quite tectonic activity to a period of active tectonics (Bridges *et al.*, 1995; Figure 6.4). Sea-level variations are expressed in deep-water carbonate mudmounds by changes in their microfacies and grain assemblages (Bridges *et al.*, 1995). Late Dinantian carbonate mud-mounds were deposited on carbonate shelves and shelf margins were within the range of fourth- and fifth-order sea-level variations. The growth of carbonate mud-mounds in carbonate shelf settings was

often terminated by subaerial exposure, resulting in karstic surfaces (Bridges *et al.*, 1995).

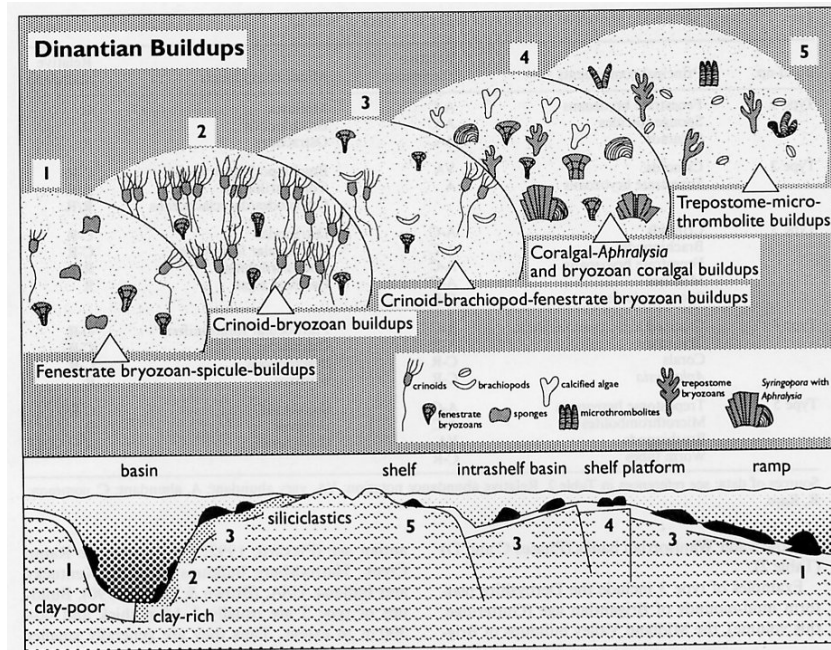


Figure 6.5 The five types of early Carboniferous buildup and their characteristic environmental settings: 1) fenestrate bryozoan-sponge spicule buildups, 2) crinoid-bryozoan buildups, 3) crinoid-brachiopod-fenestrate bryozoan build-ups, 4) coralgal-Aphralysia and bryozoan-coralgal buildups, 5) trepostome-microthrombolite buildups. The buildup types are distinguished by the principal skeletal components. After Bridges *et al.*, 1995

Carbonate buildups in area 3&4 were until now not reported in literature for both the Early and the Late Dinantian deposits (Figures 6.6 and 6.7). Because the structure was not penetrated, the age and the type of the buildup are not known with certainty. However, given the stratigraphic position the buildup appears to occur at the Dinantian to Namurian transition (see Section 6.1.2). This makes a Late Dinantian age of the structure more likely than an Early Dinantian age. From a reservoir point of view, this is more favorable. The Early Dinantian buildups were, in general, deposited in a muddy environment with fine grained matrix with a lower initial reservoir quality. The Late Dinantian buildups have an open carbonate framework and have initially higher porosities. However, given the deep burial and diagenetical changes in the Netherlands, the reservoir quality will be highly dependent on the secondary porosity developed through time (e.g. karstification).

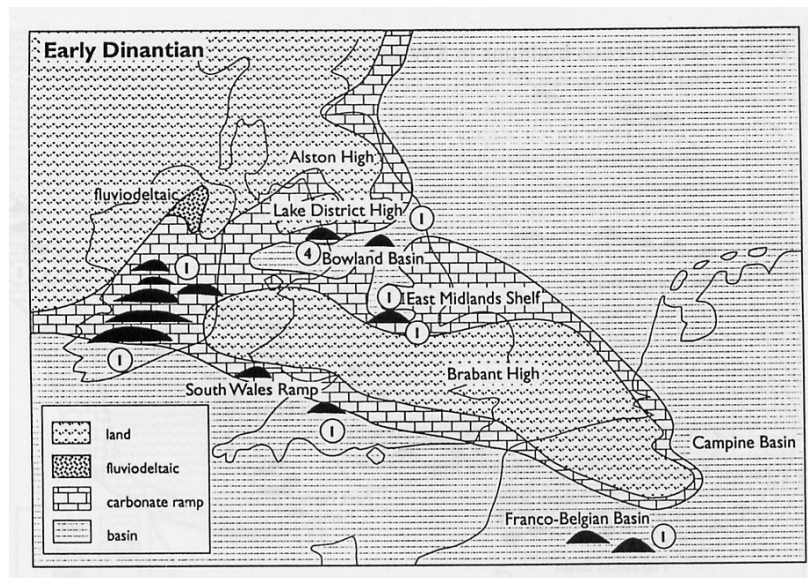


Figure 6.6 Early Dinantian buildups in Belgium and the British Isles. Most of the buildups belong to type 1 and formed in mid- and distal ramp and basinal settings. After Bridges *et al.*, 1995

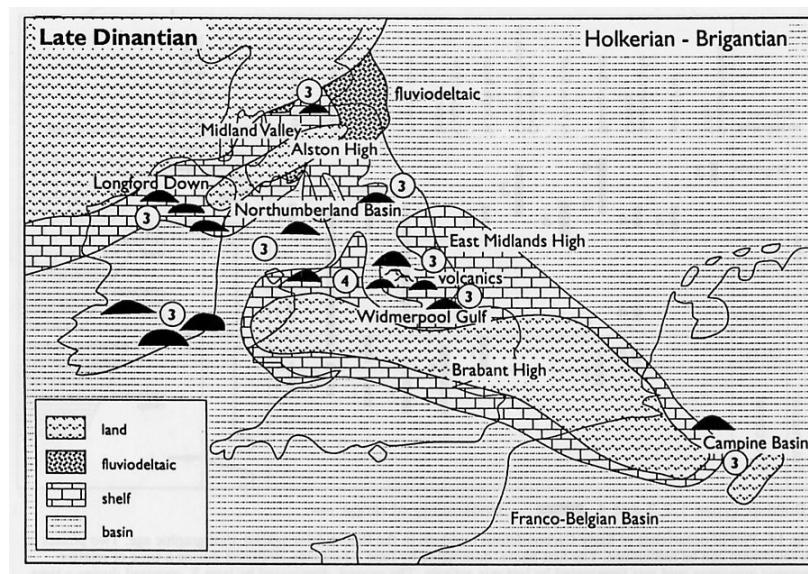


Figure 6.7 Late Dinantian buildups in Belgium and the British Isles. Most of the buildups belong to type 3 and formed on shelf margins and in intraplatform basin settings. After Bridges *et al.*, 1995

In the Belgian Campine Basin a number of these Late Dinantian build-ups have been extensively studied for gas storage purposes. The Heibaart and Poederlee build-ups are regarded as microbial build-ups (Muechez *et al.*, 1987, 1990), essentially consisting of pelletoidal, micritic limestone with little or no initial porosity. Reservoir properties were greatly enhanced by early karstification at the end of the Dinantian, formation of fracture networks, and paleokarst reactivation. This resulted in the Heibaart case in average porosities of 2-3 % and permeabilities up to 3 Darcy. It has been suggested (Muechez *et al.*, 1990) that the Heibaart and Poederlee build-ups formed on fault-bounded, periodically uplifted domal structures (Figure 6.8), which resulted in a higher elevation in the first place, but also favoured the initial karstification.

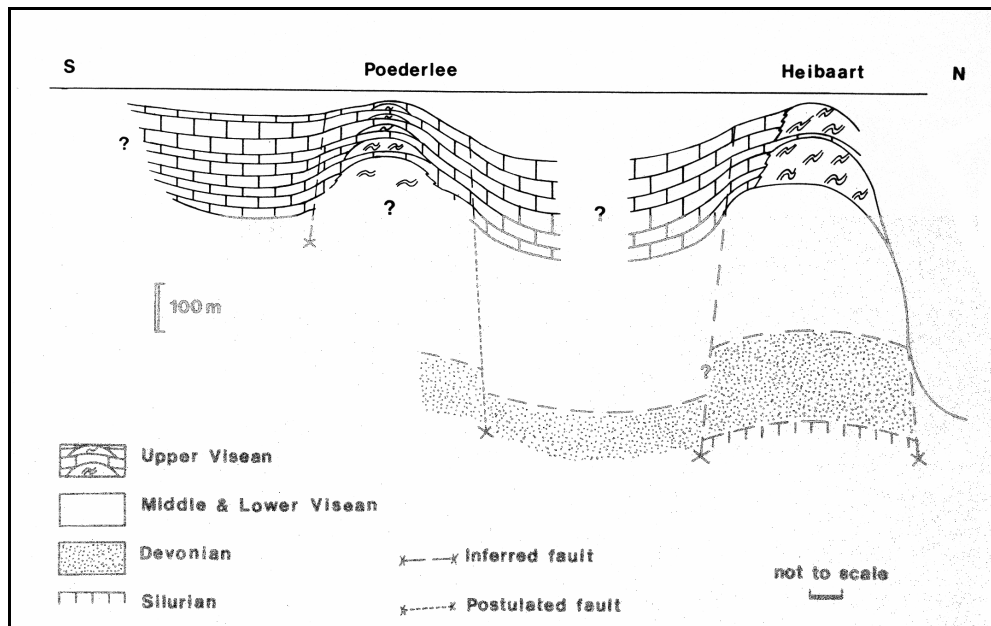


Figure 6.8 N-S paleogeographical section through the Lower Carboniferous and Devonian of the Campine Basin, illustrating the fault-bounded domal structures of the Poederlee and Heibaart buildups (from Muchez *et al.*, 1990)

This opens perspectives for similar structures in Area 3&4, like e.g. the Emmeloord structure. Areas with similar deep-seated fault-bounded domal structures have potential for a) having well-developed microbial buildups and b) paleokarst and/or tectonic fracturing.

6.3.3 Namurian reservoir potential in Area 3&4

Sandstones within the Namurian units Namur-1 and -2 were found in wells Münsterland-1, Nagele-1 and Tjuchem-2 (Figure 6.1). Their reservoir quality seems to be variable. The sonic logs indicate that the thick Namur-2 sandstone in Münsterland-1 is probably tight, that some of the thinner sandstones in Nagele-1 may have some porosity and that the best candidates are found in well Tjuchem-2, both in the Namur-1 and Namur-2 unit. The better Namurian reservoir potential in Tjuchem-2 may be explained by the shorter distance to either a northerly or north-easterly source, as also indicated in Figure 2.24.

6.4 Seals

Devonian or Dinantian reservoirs can easily be sealed by the thick Namurian shales (demonstrated to be present in wells Winterswijk-1, Nagele-1, Münsterland-1 and Tjuchem-2). In case of a Late Dinantian carbonate build-up near well Emmeloord-1, both the side seals and the top seal are likely to be formed by Namurian shales. For the Namurian reservoirs either intra-Namurian or younger seals are required.

6.5 Hydrocarbon generation and its timing

From the 3D model, burial history plots have been extracted for six pseudowells along a profile (Figure 6.9). The burial history plots are given for the base Namur-1 source rock. It can be assumed that the slightly deeper buried source rocks of the Dinantian show a similar burial and hydrocarbon generation pattern. In the southwestern part of

the area the source rock reached its deepest burial during the Jurassic, shortly before the Late Kimmerian 1 uplift and erosion (Figure 6.10, pseudowells 1, 2, and 3), whereas in the northeastern part deepest burial is reached at present (pseudowells 3, 4 and 5). The northeastern part of the area has been much deeper buried throughout time than the southwestern part. In the northeastern part the source rock reaches depths of about 6500 m at present, whereas in the southwestern part their present day depth of burial ranges between 4500 and 5000 m.

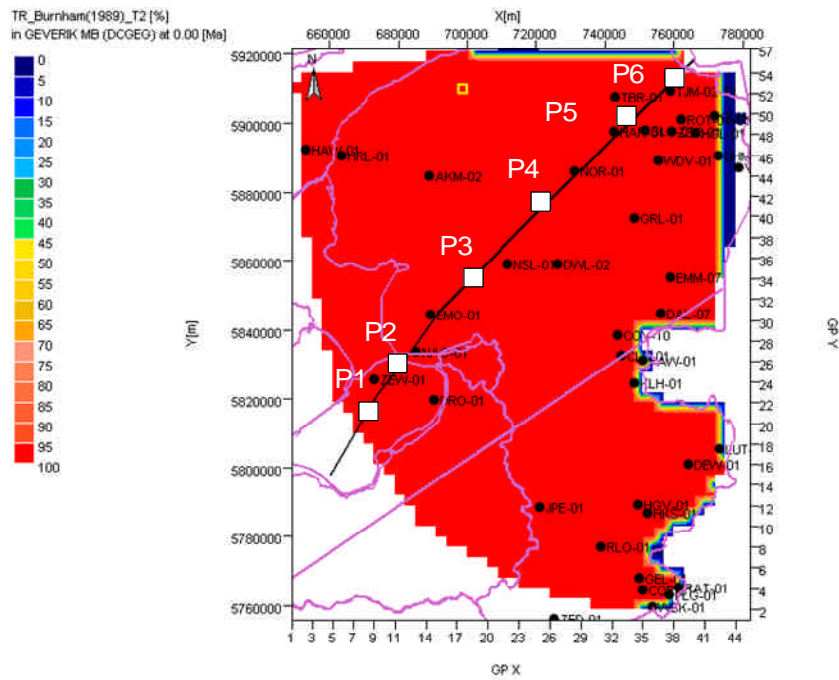


Figure 6.9 Transformation ratio of a base Namurian source in Area 3&4, showing a profile with six pseudowells

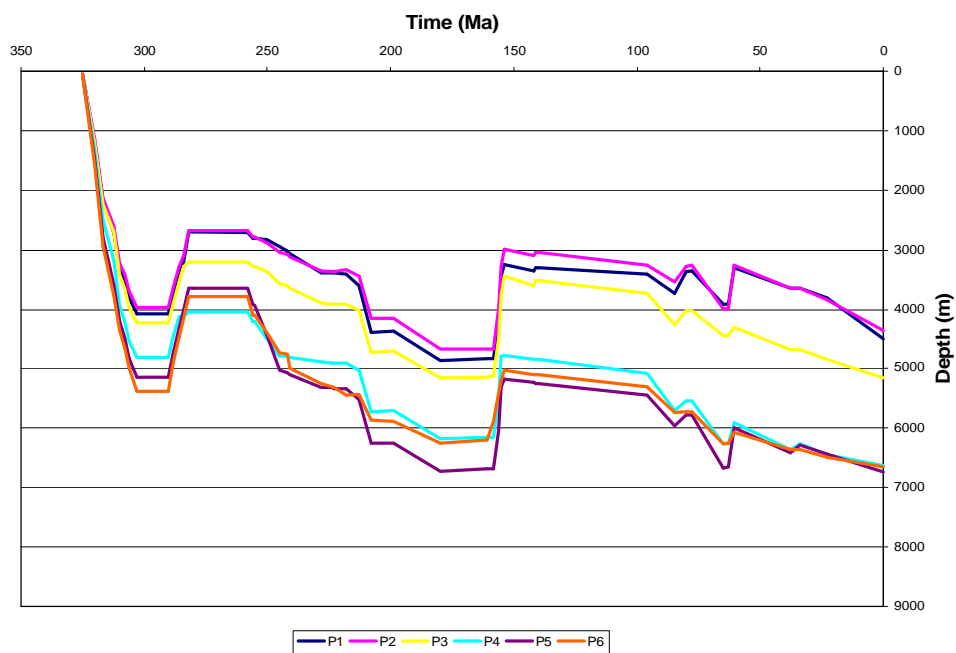


Figure 6.10 Burial history graph for the pseudowells along a profile. Pseudowells are marked with numbers (P1 in the SW to P6 in the NE)

The maturation and hydrocarbon generation in Area 3&4 were simulated for two source rocks: an intra-Dinantian and a basal Namur-1 source rock. The potential Type III source rock in the top of the Namur-2, as encountered in well Emmeloord-1 (chapter 3), was not taken into consideration. Lateral distribution and the timing of maturation (and therefore hydrocarbon generation) in Area 3&4 depend not only on the temperature increase due to burial, but also largely on spatial variations in heatflow during time (Figure 6.11). These high heatflow values needed to be applied in the modelling in order to fit the vitrinite reflectance data of the wells (see Appendices H and I). Higher heatflows were applied during the Carboniferous and also during the Jurassic (see Appendix H). The applied higher heatflows resulted in temperatures between 170 and 270°C during the Carboniferous.

The effect of higher temperatures on vitrinite reflectance is best shown by pseudowell 2, where the maturation is obviously strongly affected. This leads to high vitrinite reflectance values of almost 4.5 %R, although the source rock has not been deeply buried (Figure 6.12). Vitrinite reflectance of the source rock at pseudowells 1, 2 and 3 reached its highest values at the end of Jurassic (Figure 6.12). The values for the vitrinite reflectance of pseudowell 1 and 3 are lowest and vary from 2.7 and 3.5 %. Pseudowells 4, 5 and 6 show a slight increase of vitrinite reflectance during the latest 30 Ma, but the values of vitrinite reflectance are already high (between 4 and 5 %) before the onset of the increase. This will therefore have limited influence on the further generation of hydrocarbons.

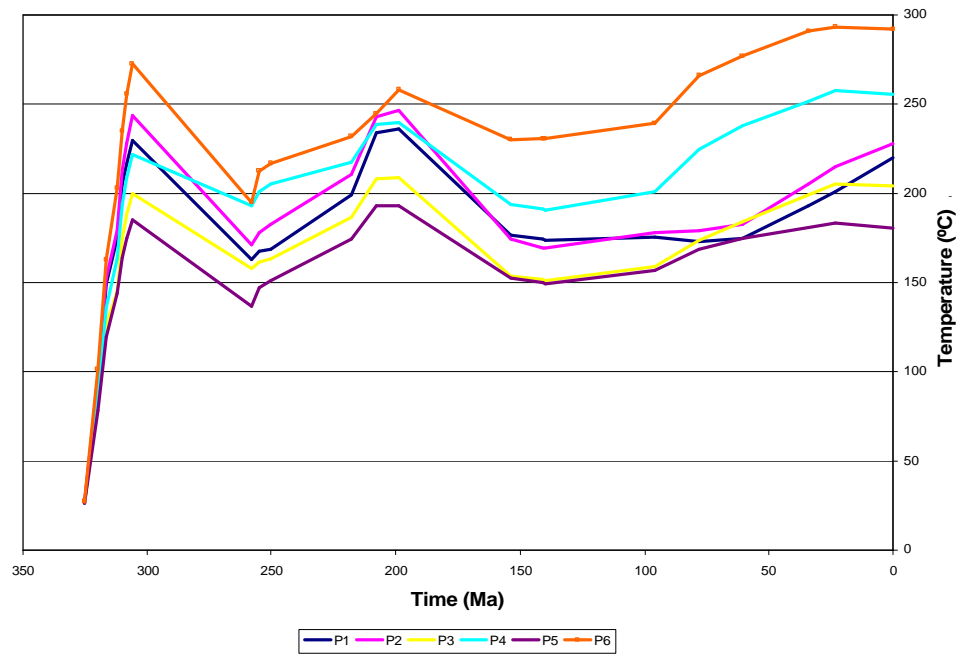


Figure 6.11 Temperature profile through time for the pseudowells along a profile. Pseudowells are marked with numbers (P1 in the SW to P6 in the NE)

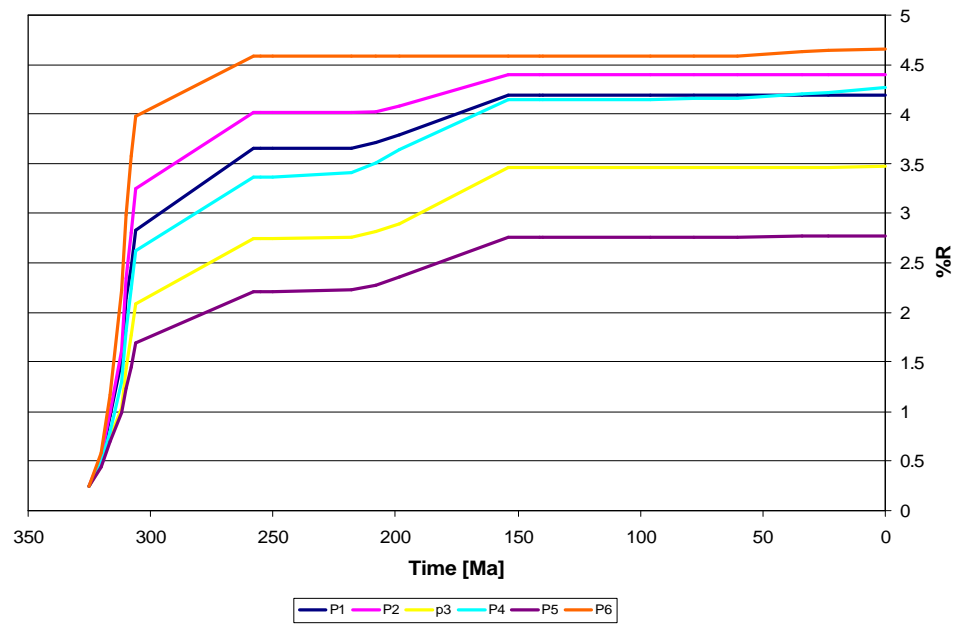


Figure 6.12 Vitrinite reflectance through time for the pseudowells along a profile. Pseudowells are marked with numbers (P1 in the SW to P6 in the NE)

Generation of hydrocarbons from the kerogen in the Namurian and older source rocks took place already during the Carboniferous (Figures 6.13 and 6.14). The transformation was completed at the end of the Carboniferous; no more hydrocarbons could be generated (e.g. see Figure 6.9). There are no signs for a coalification jump between the Namur-1 and Namur-2, therefore a similar conclusion can be drawn for the potential Type III source rock in the top of the Namur-2.

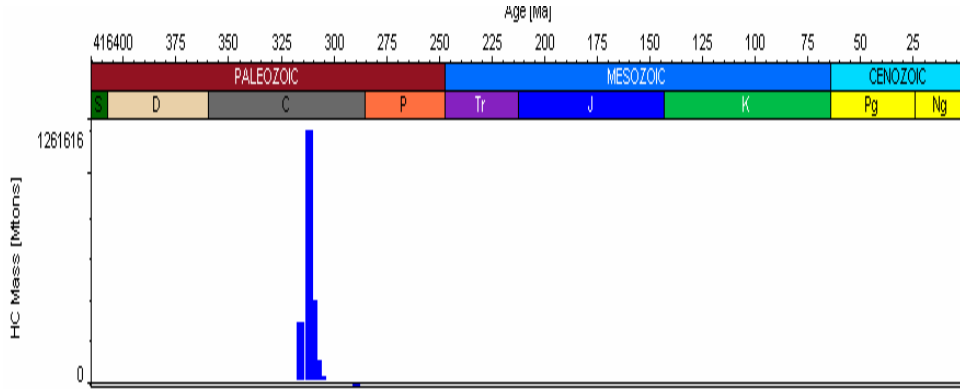


Figure 6.13 Generated and expelled hydrocarbons per event for all source rocks in Area 3&4 (Burnham 1989_T2 kinetics)

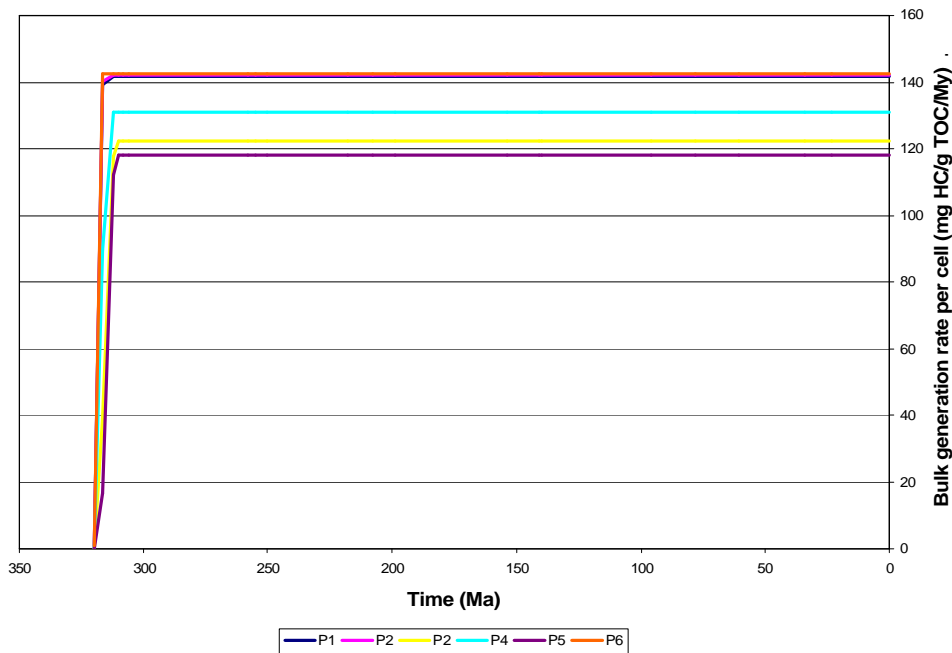


Figure 6.14 Cumulative hydrocarbon generation diagrams of the pseudowells along a profile. Pseudowells are marked with numbers (P1 in the SW to P6 in the NE)

The prospectivity of the pre-Westphalian in the region is therefore strongly dependent on the preservation of the hydrocarbons from the Carboniferous onwards. This implies that accumulation space, the reservoir, and a good seal were present at the end of the Carboniferous and were preserved throughout geological times.

The Dinantian reef structure (Section 6.3.2) was considered to have the highest potential for preservation. It was assumed that if the structure has a fair to good reservoir quality, this resulted from early karstification processes during excavation. Given the apparent coverage of the structure by marine Namurian shales, karstification must have taken place before the deposition of these Namurian deposits. Reservoir and seal were thus already in place at the time of generation. In order to simulate this, a conceptual mound-shaped structure (as an example), was included in the model (see Appendix I) in the vicinity of well Emmeloord-1. The porosity of the structure was intentionally fixed in order to simulate preservation of the porosity through time. The modelling shows that the hydrocarbons generated during the Carboniferous accumulated in many locations in the area, including the structure. These accumulations are predicted to have consisted of both liquid and vapour (Fig. I-15). Already at the end of the Carboniferous the liquid accumulations were transformed to vapour accumulations and the size and amount decreased (I-16). At 250 Ma almost all hydrocarbon accumulations had disappeared. However, under the constraints and assumptions of the model, a small vapour accumulation is predicted to be preserved until present day (Fig. I-17). It must be emphasised that leakage of hydrocarbons through faults was not considered in the model, only diffusion through the seal.

6.6 Possible play types

The geochemical analyses revealed Upper Namurian Type III source rocks in well Emmeloord-1. The results from the maturity modelling imply that any pre-Westphalian source rocks in Area 3&4 have generated hydrocarbons already during the Carboniferous and that after that very little generation has occurred (Figure 6.13). The source rocks are generally over mature. This is partly due to the high geothermal gradient.

Only under specific conditions there could locally be hydrocarbon potential as an exception to the general trend. Such conditions could be the early trapping of gas in structures which have remained in tact throughout geological history or a local exception to the high heat flow. Since only data is available from 5 wells, the possibility is still there that such lower heat flow occurs at locations which have not yet been sampled.

Dinantian carbonate build-ups similar the one observed in the Noordoostpolder are a candidate for play type. In addition, Namurian sandstones as found in Tjuchem-2 could be a target. Both plays are considered very high risk.

7 Conclusions

This study confirmed that there is hydrocarbon potential for pre-Westphalian sediments in the Netherlands on- and offshore. In particular, the widespread occurrence of potential source rocks was established. Timing of generation and expulsion together with reservoir and seal quality are the most crucial factors that determine the prospectivity in any particular area. It was found that these factors are highly variable throughout the investigated areas.

The Petroplay project resulted in the first nation-wide inventory and overview of geological and geochemical data of the pre-Westphalian sedimentary sequences, covering both the Netherlands onshore territory and the Dutch North Sea Sector. In addition to existing data, new data were acquired through new biostratigraphic and geochemical analyses. New data from the surrounding areas (U.K., Belgium, Germany) were also integrated in the database and interpretations. Also, new geological and geophysical interpretations were made using both the existing and the new information.

The main focus of the project was the source rock potential and hydrocarbon generating potential throughout geological time of the various intra-Dinantian and intra-Namurian potential source rocks. Therefore, geochemical analyses and interpretation and 1D and 3D maturity modelling constituted a core activity within the project. The results of these analyses and modelling efforts were used in conjunction with other geological and geophysical interpretations in order to arrive at a synthesis of geochemistry, (bio-)stratigraphy, geology and geophysics. The synthesis implied an assessment of feasible hydrocarbon play concepts depending on pre-Westphalian source rocks. Three distinct areas in the Netherlands on- and offshore were studied in more detail. The selection of these areas was mainly based on the depth of the pre-Westphalian sediments. For each of these areas the hydrocarbon generation potential throughout geological time of pre-Westphalian source rocks was examined by 3D basin modelling.

The geological study revealed some features in the pre-Westphalian deposits that were known from the surrounding areas but were so far not reported in literature for the Netherlands on- and offshore. Most important features are the presence of the Mid-Devonian carbonates in the northern offshore, the interpreted carbonate buildup and the intra-Namurian unconformity in Area 3&4.

Based on the geological evaluation, it was concluded that a "block-and-basin" tectonic setting is more likely to have existed during the Dinantian than the simple basin model. This suggests that source rock intervals were deposited in patches throughout the research area, possibly at slightly different time intervals, rather than as one continuous source rock layer.

Based on geochemical analyses and interpretation it is concluded that the pre-Westphalian sequences contain source rocks with good initial potential in all areas. This conclusion is supported by the observation of TOC rich zones at different levels. The most promising source rock level of all are deposits near the base Namurian, containing TOC rich shales equivalent to the Geverik Member and the Bowland Shale Formation in the UK. In addition, other potential source rocks were found within the Dinantian and Namurian sequences. We conclude that within the pre-Westphalian sequences levels

with initially good source rock potential are almost omni-present throughout the areas studied.

In Area 1 (the northern margin of the London-Brabant Massif) hydrocarbon generation has occurred pre-dominantly during the Carboniferous, but has continued at a lower level throughout geological history until recently. Depending on the local circumstances this leaves scope for exploration in parts of Area 1. The prospectivity for hydrocarbons generated by pre-Westphalian can be narrowed down to a rather limited elongated area parallel to the trend of the London-Brabant Massif.

In Area 2 (the northern offshore, including the A, the western B and northern E blocks) hydrocarbon generation is generally later, until recent. The most prospective parts of Area 2 are the eastern and southern margins of the Elbow Spit High, because there the pre-Westphalian source rocks have been buried deep enough to become mature. In addition, in those margins adequate seals for trapped hydrocarbons are most likely to be present. The main risks in Area 2 are reservoir quality and migration path.

The geochemical analyses and 3D basin modelling demonstrated that in Area 3&4 (the central to eastern and north-eastern Netherlands onshore) source rocks are generally over-mature. This is partly due to a higher than average heat flow which needs to be assumed in order to fit all data in the 1D and 3D basin modelling. Only under specific and probably very local circumstances could some hydrocarbon accumulations be preserved in Area 3&4. One of those conditions could e.g. be the occurrence of a lower heat flow in areas not penetrated by wells to date. Another one may be the very early trapping of hydrocarbons into a structure which has not been disturbed since the Carboniferous. Using seismic interpretation the presence of an intra-Namurian unconformity was interpreted at approximately Late Arnsbergian level. Also from seismic data the presence of at least one Dinantian carbonate build-up was interpreted in the Noordoostpolder.

Various products have been produced by the project. An overview of the availability and quality of existing biostratigraphic data together with some additional new interpretations lead to a newly proposed chronostratigraphic framework, which links the Devonian, Dinantian and Namurian stratigraphy of the northern offshore to that of the southern offshore and onshore areas. A second product was a new geochemical database for the pre-Westphalian data available. This database is attached to this report as a MS-Excel file. It includes the analyses of samples from all available Dutch wells, completed with a large number of Belgian, German and offshore UK wells.

8 Acknowledgements

This project was conducted in cooperation with the sponsors. During the semi-annual progress meetings and the geological excursion representatives of the sponsors provided useful input to the discussions. NAM provided digital seismic lines for Area 3&4. EBN, NAM, PetroCanada, Gaz de France, Wintershall and Total are thanked for providing and additional data and samples for the project.

The authors also thank the following TNO staff for their contributions to the project. Henk Pagnier, Cees Geel, Frank van de Belt (geology), Ed Duin, Hans Doornenbal, Joost Verbeek, Carla Elmers (seismic interpretation and mapping), Sterre Dortland (gravity modeling), Ymke van de Berg, Marta Reszak (1D basin modeling), Kenneth Rijdsdijk (biostrat), Kathrin Reimer, Bertil van Os, Rob van Galen, Piet Peereboon and Giovanni Dammers (geochemical analyses) and Harmen Mijnlief (review).

John Collinson is acknowledged for his splendid geological excursion in the Peak District in England.

The core houses and personnel that cooperated in the sampling campaign are greatly thanked for their support. These are DTI in Edinburgh, BGD in Brussels, Gaz de France in Lingen and Landesamt Krefeld.

9 Literature

Albrecht, P., Vandenbroucke, M., and Mandengue, M., 1976. "Geochemical studies on the organic matter from the Douala Basin (Cameroon). I. Evolution of the extractable organic matter and the formation of petroleum", *Geochimica et Cosmologica Acta*, Vol. 40, p. 791-799.

Allen, P.A. and Allen, J.R., 1990. *Basin analysis: principles and applications*. Blackwell publications, Oxford.

Bérnard, F. and Bouché, P., 1991. Aspects of the petroleum geology of the Variscan foreland of western Europe. In: Spencer, A.M. (ed.) *Generation, accumulation and production of Europe's Hydrocarbon*. Special Publications of the European Association of Petroleum Geoscientists, 1. Oxford University Press, Oxford, p. 1119-138.

Best, G., Kockel, F. and Schöneich, H., 1983. Geological history of the southern Horn Graben. *Geologie en Mijnbouw* 62, p. 25-34.

Besly, B.M., 1998. Carboniferous. In: Glennie, K.W. (ed) *Petroleum Geology of the North Sea*, Basic concepts and recent advances (fourth edition), 104-136.

Bless, M.J.M., Bouckaert, J., Bouzet, PH., Conil, R., Cornet, P., Fairon-Demaret, M., Groessens, E., Paproth, E., Pirlet, H., Streel, M., Amerom, H.W.J. van and Wolf, M., 1976. Dinantian rocks in the subsurface North of the Brabant and Ardenno-Rhenisch massifs in Belgium the Netherlands and the Federal Republic of Germany. *Meded. Rijks Geol. Dienst Nieuwe Serie*, 27-3, p. 81-195, Rijks Geologische Dienst.

Bless, M.J.M., Bouckaert, J., Paproth, E., 1980. Pre-Permian around the Brabant massif in Belgium, the Netherlands and Germany. *Meded. Rijks Geol. Dienst*, 32-1/14, pp. 179, Rijks Geologische Dienst.

Bless, M.J.M., P. Boonen, J. Bouckaert, R. Conil, M. Duser, P.J. Felder, W.M. Felder, H. Gökdag, F. Kockel, M. Laloux, H.R. Langguth, C.G. Van der Meer Mohr, J.P.M.TH. Meessen, F. Op het Veld, F. Paproth, H. Pietzner, J. Plum, E. Poty, A. Scherp, R. Schulz, M. Streel, J. Thorez, P. Van Rooijen, M. Vanguetaine, J.L. Vieslet, D.J. Wiersma, C.F. Winkler Prins and M. Wolf, 1981. Preliminary report on lower Tertiary-upper Cretaceous and Dinantian-Famennian rocks in the boreholes Heugem-1/1a and Kastanjelaan-2 (Maastricht, the Netherlands). *Mededelingen Rijks Geologische Dienst*, 35-15, pp. 333-415, Rijks Geologische Dienst.

Boreham, C.J., Crick, I.H., and Powell, T.G., 1988. Alternative calibration of the Methylphenanthrene Index against vitrinite reflectance: Application to maturity measurements on oils and sediments, *Organic Geochemistry*, 12, p. 289-294.

Bray, E.E. and Evans, E.D., 1961. Distribution of n-paraffins as a clue to recognition of source beds: *Geochim. Cosmochim. Acta*, 22, p. 2-15.

Bridges P.H., Gutteridge, P., and Pickard, N.A.H., 1995. The environmental setting of Early Carboniferous mud-mounds, *Spec. Publ. Int. Ass. Sediment.*, 23, 171-190

Brooks, J.D., Gould, K., and Smith, J.W., 1969. Isoprenoid hydrocarbons in coal and petroleum", *Nature*, 222, p.257-259.

Bruce, D.R.S. and Stemmerik, L., 2003. Carboniferous. 83-89 *In*: Evans, D., Graham, C., Armour, A. & Bathurst, P. (eds.). The Millennium Atlas, Petroleum Geology of the Central and Northern North Sea. The Geological Society of London.

Burnham, A.K., 1989. A simple kinetic model of petroleum formation and cracking. - Lawrence Livermore National Laboratory Report UCID- 21665, 11p.

Burnham, A.K. and Sweeney, J.J., 1989. A chemical kinetic model of vitrinite maturation and reflectance. - *Geochimica et Cosmochimica Acta*, **53**: 2649-2657.

Cameron, N. and Ziegler, T., 1997. Probing the lower limits of a fairway: further pre-Permian potential in the southern North Sea. *In*: Ziegler, K., Turner, P. & Daines, S.R. (eds.) Petroleum Geology of the Southern North Sea: Future Potential. Geological Society London, Special Publication 123, p. 123-141.

Cameron, T.D.J., 1993. Carboniferous and Devonian of the Southern North Sea. *In* Knox, R.W.O.B. & Cordey, W.G. (eds.) Petroleum Geology of the Continental Shelf of North-West Europe. Institute of Petroleum, London, p. 301-309.

Cameron, T.D.J., Crosby, A., Balson, P.S., Jeffery, D.H., Lott, G.K., Bulat, J. and Harrison, D.J., 1992. The geology of the southern North Sea (Chapter 5: Carboniferous). United Kingdom Offshore Regional Report, p. 23-37, British Geological Survey.

Clayton, G., Coquel, R., Doubinger, J., Loboziak, S., Owens, B. & Streel, M., 1977. Carboniferous miospores of western Europe: illustration and zonation. *Mededelingen Rijks Geologische Dienst*, 29, p. 1-72

Cocks, L.R. & Torsvik, T.H., 2005. Baltica from the late Precambrian to mid-Palaeozoic times: The gain and loss of a terrane's identity. *Earth-Science Reviews* 72: 39-66.

Collinson, J.D., Jones, C.M., Blackburn, G.A., Besly, B.M., Archard, G.M., and McMahon, A.H., 1993. Carboniferous depositional systems of the Southern North Sea. *In*: Petroleum Geology of Northwest Europe: Proceedings of the 4th Conference (edited by J.R. Parker), Geological Society, London, p. 677-687

Collinson Jones Consulting 1995. Source-rock potential of the Sub-Westphalian Carboniferous of the Southern North Sea, January 1995.

Collinson, J.D., 1988. Controls on Namurian sedimentation in the Central Province basins of Northern England. Sedimentation in a synorogenic basin complex: the Upper Carboniferous of Northwest Europe (Edited by: Besly, B.M. & Kelling, G.), p. 85-101, Blackie, Glasgow.

Collinson, J.D., 2005. Dinantian and Namurian facies architecture of North Derbyshire, a field trip for TNO/Petroplay, 19-21 May, 2005.

Conil, R., Groessens, E., Laloux, M., Poty, E. and Tourneur, F., 1990. Carboniferous guide foraminifera, corals and conodonts in the Franco-Belgian and Campine basins: Their potential for widespread correlation. *Courier Forschungs Institut Senckenberg*, 130, p. 15-30.

- Connan, J.**, 1974. Diagenese naturelle et diagenese artificielle de la matière organique a element vegetaux predominants”, in: *Advances in Geochemistry 1973* (B.P. Tissot and F. Bienner, eds.), Éditions technip, paris, p. 73-95
- Connan, J.**, 1984. Biodegradation of crude oils in reservoirs”, in: *Advances in Petroleum Geochemistry, Vol. 1* (J. Brooks and D.H. Welte, eds), Academic Press, London, p. 299-335.
- Corfield, S.M., Gawthorpe, R.L, Gage, M., Frase, A.J. and Besly B.M.** 1996. Inversion tectonics of the Variscan foreland of the British Isles. *Journal of the Geological Society, London*, 153, p. 17-32.
- Cornford, C.**, 1998. Source rocks and hydrocarbons of the North Sea. *In: Glennie, K.W. (ed.) Petroleum Geology of the North Sea: Basic concepts and recent advances.* p. 376-462, Blackwell Science.
- Coward, M.P.**, 1990. The Precambrian, Caledonian and Variscan framework to NW Europe. *In : Hardman, R.F.P. and Brooks, J. (eds) Tectonic Events Responsible for Britain’s Oil and Gas Reserves.* Geological Society, London, Special Publication, 55, p. 1-34.
- Coward, M.P.** 1993. The effect of Late Caledonian and Variscan continental escape tectonics on basement structure, Paleozoic basin kinematics and subsequent Mesozoic basin development in NW Europe. *In: Parker, J.R. (ed.) Petroleum Geology of Northwest Europe: proceedings of the 4th Conference.* Geological Society, London, p. 1095-1108.
- De Vos, W., Verniers, J., Herbosch, A. & Vanguetstaine, M.**, 1993. A new geological map of the Brabant Massif, Belgium. *Geological Magazine* 130: 605--611.
- Didyk, B.M., Simoneit, B.R.T., Brassell, S.C., and Eglinton, G.**, 1978. Organic geochemical indicators of paleoenvironmental conditions of sedimentation”, *Nature*, Vol. 272, p.216-222
- Dirkzwager, J.B.**, 2002. Tectonic modelling of vertical motion and its near surface expression in the Netherlands. PhD thesis, Vrije Universiteit Amsterdam, the Netherlands, 156 p.
- Doornenbal, J.C.**, 2001. Regionale snelheidsmodellen van het Nederlandse territor. TNO report NITG 01-116-B.
- Dortland, S.**, 2003. Forward gravity modelling of the onshore Dutch subsurface to obtain a residual gravity field for the pre-Permian sedimentary succession. TNO report NITG 03-155-B.
- Dreesen, R., Bouckaert, J., Duser, M., Soille, P. & Vandenberghe, N.**, 1987. Subsurface structural analysis of the late Dinantian carbonate shelf at the northern flank of the Brabant Massif (Campine Basin, N-Belgium). *Toelichting Verhandelingen Geologische kaart en Mijnkaart van België* 21: 37 pp.
- Drozdowski, G., Klostermann, J., Ribbert, K.-H., Wrede, V. & Zeller, M.**, 1998. Sedimentation und Tektonik im Paläozoikum und postpaläozoikum der Niederrheinischen Bucht. *Fortschritte Geologie Rheinland und Westfalen* 37: 573--583.
- Duin, E.J.Th., R.H.B. Rijkers, and Remmelts, G.**, 1995. Deep seismic reflections in the Netherlands, an overview. *Geologie en Mijnbouw*, 74, p. 191-197.
- Eckardt, C.B.**, 1989. Organisch-geochemische Untersuchungen am Kupferschiefer Nordwestdeutschlands”, *Diss. Tech. Hochsch., Aachen.*

- Espitalié, J., Ungerer P., Irwin H. & Marquis, F.**, 1988. Primary cracking of kerogen. Experimenting and modelling C₁, C₂-C₅, C₆-C₁₅ and C₁₅₊ classes of Hydrocarbons Formed. Org. Geochem., 13, 893-899.
- Ewbank, G., Manning, D.A.C. and Abbott, G.D.**, 1993. An organic geochemical study of bitumens and their potential source rocks from the South Pennine Orefield, Central England. Org. Geochem., 20(5), p. 579-598.
- Ewbank, G., Manning, D.A.C. and Abbott, G.D.**, 1995. The relationship between bitumens and mineralization in the South Pennine Orefield, central England. Journal of the Geological Society, London, 152: 751-765.
- Espitalié, J., Deroo, G. and Marquis, F.**, 1985/1986. La pyrolyse Rock-Eval et ses applications. Rev. IFP, 40(5): p. 563-579; 40(6): p. 755-784; 41(1), p. 73-89.
- Forbes, P.L., Ungerer, A.B., Kuhfuss, F., Riis, F., Eggen, S.**, 1991. Compositional modelling of petroleum generation and expulsion: trial application to a local mass balance in the Smorbukk Sor field, Haltenbanken area, Norway. AAPG Bulletin, 75, p 873-893.
- Fraser, A.J. and Gawthorpe, R.L.**, 1990. Tectono-stratigraphic development and hydrocarbon habitat of the Carboniferous in northern England. In : Hardman, R.F.P. and Brooks, J. (eds) Tectonic Events Responsible for Britain's Oil and Gas Reserves. Geological Society, London, Special Publication, 55, p. 49-86.
- Fraser, A.J., Nash, D.F., Steele, R.P., and Ebdon, C.C.**, 1990. A regional assessment of the intra-Carboniferous play of Northern England", in: Brooks, J., (ed.), Classic Petroleum Provinces., The Geological Society, London, Special Publications, 50, p. 417-440.
- Gardner, G.H.F., L.W. Gardner, and Gregory, A.R.**, 1974. Formation velocity and density – the diagnostic basics for stratigraphic traps. Geophysics, 39, p. 770-780.
- Gatliff, R.W., Richards, P.C., Smith, K., graham, C.C., McCormac, M., Smith, N.J.P., Long, D., Cameron, T.D.J., Evans, D., Stevenson, A.G., Bulat, J. and Ritchie, J.D.**, 1994. The geology of the Central North Sea. United Kingdom Offshore Regional Report, British Geological Survey.
- Gawthorpe, R.L.**, 1987. Tectono-sedimentary evolution of the Bowland Basin, N. England. Journal of the Geological Society, London, 144, p. 59-72.
- Gérard, J., Wheatley, T.J., Ritchie, J.S., Sullivan, M., Bassett, M.G.**, (1993). Permo-Carboniferous and older plays, their historical development and future potential. In: Parker, J.R (ed.): Petroleum Geology of Northwest Europe: Proceedings of the 4th Conference, 1992, p. 641-650
- Gerling, P., Geluk, M.C., Kockel, F., Lokhorst, A., Lott, G.K. and Nicholson, R.A.**, 1999. NW European Gas Atlas' - new implications for the Carboniferous gas plays in the western part of the Southern Permian Basin. Petroleum geology of North West Europe: Proceedings of the fifth conference, 1997 (Edited by: Fleet, A.J. & Boldy, A.R.), 2, p. 799-808, Geological Society, London.
- Glennie, K.W.**, (ed.) 1998. Petroleum Geology of the North Sea, Fourth Edition, Blackwell Science.

- Glennie, K.W.**, 2005. Regional tectonics in relation to Permo-Carboniferous hydrocarbon potential, Southern North Sea Basin. *In: Collinson, J., Evans D., Holliday, D. & Jones, N. (eds.) Carboniferous hydrocarbon geology, the Southern North Sea and surrounding onshore areas.* Yorkshire Geological Society Occasional Publication 7, 2005.
- Goossens, H., De Leeuw, J.W., Schenck, P.A., and Brassell, S.C.**, 1984. Tocopherols as likely precursors of pristane in ancient sediments and crude oils, *Nature*, 312, p. 440-442.
- Gradstein, F., Ogg, J., and Smith, A.**, 2005. *The Geological Time Scale—Recent Developments and Global Correlations*, Cambridge University Press.
- Graf Pannatier, E., Van Bergen, F., David, P., Reimer, K.**, 2000. Contribution of pre-Westphalian source rocks to hydrocarbon accumulations in the Southern North Sea, TNO-report: NITG 00-291-A.
- Grayson, R.F. and Oldham, L.**, 1987. A new structural framework for the northern British Dinantian as a basis for oil, gas, and mineral exploration. *In: Miller, J., Adams, A.E., and Wright, V.P (eds): European Dinantian Environments*, John Wiley and Sons Ltd, New York: p. 38-59.
- Gutteridge, P.**, 1995. Late Dinantian (Brigantian) carbonate mud-mounds of the Derbyshire carbonate platform, *Spec. Publ. Int. Ass. Sediment.*, 23, p. 289-307.
- Gutteridge, P.**, 2002. Late Dinantian evolution of the northern margin of the Derbyshire Carbonate platform, Castleton, Field trip guide of the conference on the Hydrocarbon resources of the Carboniferous, Southern North Sea and surrounding *onshore areas*, Yorkshire Geological Society, 13-15th of September 2002, Sheffield.
- Halliburton**, 1993. *The Petroleum Geology of the Five Countries Area, Central Graben, North Sea, a hydrocarbon exploration study*, October 1993.
- Hardman, M., Buchanan, J., Herrington, P. and Carr, P.**, 1993. Geochemical modelling of the East Irish Sea Basin: its influence on predicting hydrocarbon type and quality. *Petroleum geology of North West Europe: Proceedings of the fourth conference* (Edited by: Parker, J.R.), p. 809-821, Geological Society, London.
- Harland, W.B., Armstrong, R.L., Cox, A.V., Craig, L.E., Smith, A.G. and Smith, D.G.**, 1990. *A geologic time scale 1989*. 262 pp. Cambridge University Press.
- Helsen, S., Fairon-Demaret, M. & Bultynk, P.**, 1997. Enigmatic plant mesofossil from the Viséan of the Kortgene-1 well (southern Netherlands). *Bulletin Institut Royal Science Naturelles de Belgique* 67: 79--82.
- Hollywood, J.M. and Whorlow, C.V.**, 1993. Structural development and hydrocarbon occurrence of the Carboniferous in the UK Southern North Sea Basin. *In: Parker, J.R. (ed.) Petroleum Geology of Northwest Europe: proceedings of the 4th Conference.* Geological Society, London, p. 689-696.
- Horscroft, R., Lee, M.K., Sutton, E.R., Rollin, K.E., Davidson, K. and Williamson, J.P.**, 1992. The pre-Permian (Carboniferous) of the southern North Sea from 3D modelling and image analysis of potential field data: 61st meeting of the European Association of Exploration Geophysicists, extended abstract, EAGE, p. 328-329.

- Huang, W.Y. & Meinschein, W.G.**, 1979. Sterols as ecological indicators. *Geochim. Cosmochim. Acta*, 43: 739-745.
- Hunt, J.M.**, 1991. Generation of gas and oil from coal and other terrestrial organic matter: Organic geochemistry. V. 17, p. 673-807.
- ISO 7404 Part 2**, 1982. Methods for the petrographic analysis of bituminous coal and anthracite: Methods of preparation of coal samples for petrographic analysis. ISO/TC 27, 9 pp. (draft dd. 1982-11-25).
- ISO 7404 Part 5**, 1982. Methods for the petrographic analysis of bituminous coal and anthracite: Method of determining microscopically the reflectance of vitrinite. ISO/TC 27, 11 pp. (draft dd. 1982-04-08).
- Kappelmeyer, O. and Haenel, R.**, 1974. Geothermics with special reference to application: Gebrueder Boertraeger, Berlin, 240 p.
- Katz, B.J., Royle, R.A., Mertani, B.**, 1990. Southeast Asean and Southwest Pacific coals contribution to the petroleum resource base. Proceedings Indonesian Petroleum Association, 19th Annual Convention: p 299-2-329.
- Kertz, W.** (1969): Einfuehrung in die Geophysik1: B.I. Wissenschafts Verlag, Mannheim, 232 p.
- Klemperer, S. and Hobbs, R.**, 1991. The BIRPS Atlas: Deep seismic reflection profiles around the British Isles. Cambridge University Press, p. 124.
- Koopmans, M.P., De Leeuw, J.W., Lewan, M.D., Sinninghe Damste J.S.**, 1996. Impact of dia- and catagenesis on sulphur and oxygen sequestration of biomarkers as revealed by artificial maturation of an immature sedimentary rock. *Organic Geochemistry* (25)5-7, p. 391-426.
- Krevelen, D.W. van**, 1993. Coal.- Elsevier, Amsterdam.
- Kus, J., Cramer, B. and Kockel, F.**, 2005. Effects of a Cretaceous structural inversion and a postulated high heat flow event on petroleum system of the western Lower Saxony Basin and the Charge history of the Apeldorn gas field. *Netherlands Journaal of Noble, R.A., Wu, C.H., Atkinson, C.D.* (1991): Petroleum generation and migration from Talang Akar coals and shales offshore N.W. Java, Indonesia. – *Organic Geochemistry*, 17, p. 363-374.
- Kvalheim, O.M, Christy, A.A., Telnæs, N., and Bjørseth, A.**, 1987. Maturity determination of organic matter using the methylphenanthrene distribution, *Geochimica et Cosmochimica Acta*, 51, p. 1883-1888.
- Langenaeker, V.**, 2000. The Campine Basin. Stratigraphy, structural geology, coalification and hydrocarbon potential for the Devonian to Jurassic. *Aardkundige Mededelingen* 10: 1--142.
- Lawrence, S.R., Coster, P.W. and Ireland, R.J.**, 1987. Structural development and petroleum basin (Carboniferous), North-west England. *Petroleum geology of North West Europe* (Edited by: Brooks, J & Glennie, K.W.), p. 217-224, Graham and Trotman, London.

Leekie, G.G., Spencer, A.M. and Chew, K.J., 1995. North Sea hydrocarbon plays and their resources. 57th EAGE conference and technical exhibition, Glasgow, 29 May-2 June 1995, Oral and Poster presentations. Extended abstracts, 2, F018.

Leeder M.R., 1982. Upper Palaeozoic basins of the British Isles: Caledonide inheritance versus Hercynian plate margin processes. *Journal of the Geological Society, London*, 139, p. 479-491.

Leeder, M.R., 1982. Recent developments in Carboniferous geology: a critical review with implications for the British Isles and N.W. Europe. *Proceedings of the Geologists' Association*, 99, p. 73-100.

Leeder, M.R. and Hardman, M., 1990. Carboniferous of the Southern North Sea Basin and Controls on hydrocarbon prospectivity. *In: Hardman R.F.P. & Brooks, J. (eds.) Tectonic Events responsible for Brian's Oil and Gas Reserves. The Geological Society, London, Special Publications*, 55, p. 87-105.

Leeder, M.R., Raiswell, R., Al-Batty, H., McMahon, A. and Hardman, M., 1990. Carboniferous stratigraphy, sedimentation and correlation of well 48/3-3 in southern North Sea Basin: integrated use of palynology, natural gamma/sonic logs and carbon-sulphur geochemistry. *Journal of the Geological Society, London*, 147, p. 287-300.

Lees, A. and Miller, J., 1985. Facies variation in Waulsortian buildups, Part 2: Mid-Dinantian buildups from Europe and North America. *Geological Journal*, 20, p. 159-180.

Lees, A., Hallet, V. and Hibo, D., 1985. Facies variation in Waulsortian buildups, Part 1: A model from Belgium. *Geological Journal*, 20, p. 133-158.

Leveille, G.P., Primmer, T.J., Dudley, G., Ellis, D., and Allinson, G.J., 1997. Diagenetic controls on reservoir quality in Rotliegendes sandstones, Jupiter Fields area, southern North Sea. *In: Ziegler, K., Turner, P. & Daines, S.R (eds.) Petroleum Geology of the Southern North Sea: Future Potential, Geological Society, London, Special Publications*, 123, p. 123-141.

Lithostratigraphic Nomenclature of the U.K. North Sea, CD-ROM.

Littke, R., Büker, C, Hertle, M., Karg, H., Stroetmann-Heinen, V., Oncken, O., 2000. Heat flow evolution, subsidence and erosion in the Rheno-Hercynian orogenic wedge of central Europe. *In: Franke, W., Haak, V., Oncken, O. & Tanner, D. (eds.) Orogenic Processes: Quantification and Modeling in the Variscan Belt. Geological Society, London, Special Publications*, 179, p. 231-255.

Lokhorst, A. (ed.), 1998. The Northwest European gas atlas (CD-ROM). Netherlands Institute of Applied Geoscience TNO (Haarlem); ISBN 90-72869-60-5.

Marshall, J.E.A. and Hewett, A.J., 2003. Devonian. 65-81 *In: Evans, D., Graham, C., Armour, A. & Bathurst, P. (eds.) The Millennium Atlas, Petroleum Geology of the Central and Northern North Sea. The Geological Society of London.*

Martinsen, O.J., Collinson, J.D., Holdsworth, B.K., 1995. Millstone Grit cyclicity revisited, II: sequence stratigraphy and sedimentary responses to changes of relative sea-level. *In: Sedimentary Facies Analysis (Eds Plint, A.G.), Spec. Publ. int. Ass. Sediment.*, 22, p. 305-326.

Mathes-Schmidt, M. & Elfers, H., 1998. Mikrofazielle Untersuchungen im Unterkarbon (Visé) und tieferen Oberkarbon (Namur A) der Bohrung Schwalmtal 1001. *Fortschritte Geologie Rheinland und Westfalen* 37: 439--457.

Maynard, J.R. and Dunay, R.E., 1999. Reservoirs of the Dinantian (Lower Carboniferous) play of the Southern North Sea. *In: Fleet, A.J. & Boldy, S.A.R. (eds.) Petroleum Geology of Northwest Europe: Proceedings of the 5th Conference*, p. 729-745. Geological Society, London.

Maynard, J.R., Hofman, W., Dunay, R.E., Bentham, P.N., Dean, K.P. and Watson, I., 1997. The Carboniferous of western Europe: the development of a petroleum system. *Petroleum Geoscience*, 3, p. 97-115.

McKenzie, D.P., 1978. Some remarks on the development of sedimentary basins. *Earth and Planetary Science Letters*, 40, p. 25-32.

McKerrow, W.S., Mac Niocaill, C. & Dewey, J.F., 2000a. The Caledonian orogeny redefined. *Journal of the Geological Society (London)* 157, p. 1149--1154.

McKerrow, W.S., Mac Niocaill, C., Ahlberg, P., Clayton, G., Cleal, C. & Eagar, R., 2000b. The Late Palaeozoic relations between Gondwana and Laurussia. *In: Franke, W., Haak, V., Oncken, O. & Tanner, D. (eds): Orogenic processes: Quantification and Modelling in the Variscan Belt. Geological Society Special Publication* 179, p. 9-20.

Meissner, R., P. Sadowiak, and Thomas, S.A., 1994. East Avalonia, the third partner in the Caledonian collisions: evidence from deep seismic reflection data. *Geologische Rundschau*, 83, p. 186-196.

Menning, M., Weyer, D., Drozdowski, G., and Wendt, I., 2001. More radiometric ages for the Carboniferous time-scale. *Newsletter on Carboniferous Stratigraphy*, 19, p. 16-18

Millenium Atlas, 2003. *Petroleum Geology of the Central and Northern North Sea*. Organised by Armour, A., Bathurst, P., Evans, D., Gammage, J. & Hickey, C. Published by the Geological Society of London.

Muchez, Ph., Conil, R., Viaene, W., Bouckaert, J., and Poty, E., 1987. Sedimentology and biostratigraphy of the Viséan carbonates of the Heibaart (DzH1) borehole (northern Belgium). *Ann. Soc. Géol. Belg.* 110:199-208.

Muchez, Ph., Viaene, W., Bouckaert, J., Conil, R., Dusar, M., Poty, E., Soille, P. and Vandenberghe, N., 1990. The occurrence of a microbial buildup at Poederlee (Campine Basin, Belgium): Biostratigraphy, sedimentology, early diagenesis and significance for early Warrantian paleogeography. *Ann. Soc. Géol. Belg.* 113:329-339.

Muchez, Ph. & Langenaeker, V., 1993. Middle Devonian to Dinantian sedimentation in the Campine Basin (northern Belgium) in relation to Variscan tectonics. *Special Publication International Association of Sedimentologists* 20: 171--181.

Oncken, O., Plesch, A., Weber, J., Ricken, W. & Schrader, S., 2000. Passive margin detachment during arc-continent collision (Central European Variscides). *In: Franke, W., Haak, V., Oncken, O. & Tanner, D. (eds): Orogenic processes: Quantification and Modelling in the Variscan Belt. Geological Society Special Publication* 179: 199--216.

- Pagnier, H.J.M., Belt, F.J.G. van den, Mijnlief, H.F., Bergen, F. van, Verbeek, J.**, 2002. An overview of the Carboniferous structural and sedimentary evolution of the Southern North Sea with a discussion of hydrocarbon fields and play concepts in the Dutch sector. *In: Hydrocarbon resources of the Carboniferous, Southern North Sea & surrounding onshore areas (abstracts)*, Yorkshire Geological Society, Sheffield, 13-15 September 2002.
- Paproth, E., Dreesen, R. and Thorez, J.**, 1986. Famennian paleogeography and event stratigraphy of northwestern Europe. *Annales de Société Géologique de Belgique*, 109, p. 175-186.
- Passey, Q.R., S. Creaney, J.B. Kulla, F.J. Moretti, and Stroud, J.D.**, 1990. A practical model for organic richness from porosity and resistivity logs. *AAPG Bulletin* 74, p.1777-1794.
- Pepper, A.S. & Corvi, P.J.**, 1995a. Simple kinetic models of petroleum formation. Part I: oil and gas generation from kerogen. – *Marine and Petroleum Geology*, 12(3): 291-319.
- Pepper, A.S. & Corvi, P.J.**, 1995b. Simple kinetic models of petroleum formation. Part II: oil-gas cracking. – *Marine and Petroleum Geology*, 12(3): 321-340.
- Pepper, A.S. & Corvi, P.J.**, 1995c. Simple kinetic models of petroleum formation. Part III: Modelling and open system – *Marine and Petroleum Geology*, 12(4): 417-452.
- Pering, K.L.**, 1973. Bitumens associated with lead, zinc and fluorite ore mineral in North Derbyshire, England. *Geochemica et Cosmochimica Acta*, 37, p. 410-417.
- Peters, K.E.**, 1986. Guidelines for evaluating petroleum source rocks using programmed pyrolysis. *AAPG Bulletin*, 70, p. 318-329.
- Peters, K.E., Walters, C.C., and Moldowan, J.M.**, 2005. *The Biomarker Guide. Volume II. Biomarkers and Isotopes in Petroleum Systems and Earth History.* Cambridge University Press, 1155 pp.
- Pharaoh, T.**, 1999. Palaeozoic terranes and their lithospheric boundaries within the Trans-European Suture Zone (TESZ): a review. *Tectonophysics* 314, p. 17-41.
- Pharaoh, T., Molyneux, S., Merriman, R., Lee, M. & Verniers, J.**, 1993. The Caledonides of the Anglo-Brabant Massif reviewed. Special issue on the Caledonides of the Anglo-Brabant Massif. *Geological Magazine* 130, p. 561-562.
- Pharaoh, T., England, R. & Lee, M.**, 1995. The concealed Caledonide basement of Eastern England and the Southern North Sea – a review. *Studia geophysica et geodaetica* 39, p. 330--346.
- Poty, E.**, 1982. Paléokarst et brèches d'effondrement dans le Frasnien moyen des environs de Visé. Leur influence dans la paléogéographie dinantienne. *Annales de la Société géologique de Belgique* 105: 315--337.
- Poty, E., Hance, L., Lees, A. and Hennebert, M.**, 2001. Dinantian lithostratigraphic units (Belgium). *Geologica Belgica*, 4, p. 69-94.

Powell, T.G. (1988) Developments in concepts of hydrogen generation from terrestrial organic matter: Petroleum resources of China and related subjects, Texas, CircumPacificCouncil of Energy and Mineral Resources. Earth Sciences Series, 10, p 807-824.

Prinzhofer, A.A. & Huc, A.Y., 1995. Genetic and post-genetic molecular and isotopic fractionations in natural gases. Chemical Geol., 126:281-290.

Püttmann, W., Eckardt, C.B., Schaefer, R.G., 1988. Analysis of hydrocarbons in coal and rock samples by on-line combination of thermodesorption, gas chromatography and mass spectrometry. Chromatographia 25 (1988), p. 279-287.

Püttmann, W. and Schaefer, R.G., 1989. The composition of aromatic hydrocarbons trapped in coals and its relation to carbonization properties. In: Proceedings of the 1989 International Conference on Coal Science, Tokio, Japan 1, p. 75-78.

Püttmann, W. and Schaefer, R.G., 1990. Assessment of carbonization properties of coals by analysis of trapped hydrocarbons, Energy and Fuels 4 (1990), p. 339-346.

Quigley, T.M., MacKenzie, A.S. & Gray, J.R., 1988. Kinetic theory of petroleum generation. – Proc. Conf. on Migration of hydrocarbons in sedimentary basins, Bordeaux, June 1987. Editions Technip, Paris, 649-665.

Quirk, D.G., 1993. Interpreting the Upper Carboniferous of the Dutch Cleaver Bank High. *In:* Parker, J.R. (ed.) Petroleum Geology of North West Europe: Proceedings of the 4th Conference, p. 697-706. Geological Society, London.

Radke, M., 1987. Organic geochemistry of aromatic hydrocarbons, in: Advances in Petroleum Geochemistry (J. Brooks and D. Welte, eds.), Academic press, New York, p. 141-207

Radke, M., Schaefer, R.G., Leythaeuser, D., and Teichmüller, M., 1980. Composition of soluble organic matter in coals: relation to rank and liptinite fluorescence. Geochimica et Cosmochimica Acta, Vol. 44, p. 1787-1800.

Radke, M., and Welte, D.H., 1983. The Methylphenanthrene Index (MPI). A maturity parameter based on aromatic hydrocarbons. *In:* advances in organic Geochemistry 1981 (M.Bjørøy et al., eds.), J. Wiley and sons, New York, p. 504-512.

Radke, M., Welte, D.H., and Willsch, H., 1986. Maturity parameters based on aromatic hydrocarbons: Influence of the organic matter type: Organic Geochemistry, 10, p. 51-63.

Radke, M., Garrigues, P., and Willsch, H., 1990. Methylated dicyclic and tricyclic aromatic hydrocarbons in crude oils from the Handil field, Indonesia, Organic Geochemistry, 15, p. 17-34.

Ramsbottom, W.H.C., Calver, M.A., Eagar, R.M.C., Hodson, F., Holliday, D.W., Stubblefield, C.J., and Wilson, R.B., 1978. A Correlation of Silesian Rocks in the British Isles. Geological Society of London Special Report, 10, p. 1-81.

Ribbert, K.-H., 1998a. Devonischen Schichtenfolgen im Untergrund der Niederrheinischen Bucht. Fortschritte Geologie Rheinland und Westfalen 37, p. 9-47.

Ribbert, K.-H., 1998b. Die devonische Karbonatfazies und die Honseler Fazies im Bereich der Krefelder Achsenauwölbung und ihrer Randgebiete. Fortschritte Geologie Rheinland und Westfalen 37, p. 109-139.

Ribbert, K.-H., 1998c. Das Famenne im Untergrund der Niederrheinischen Bucht. Fortschritte Geologie Rheinland und Westfalen 37, p. 81--107.

Rijks Geologische Dienst, 1986. Onderzoeksresultaten van de boring Geverik-1, Rapport GB 2144/GD10167.

Schlumberger, 2004. Oilfield Glossary. <http://www.glossary.oilfield.slb.com>.

Schoell, M., Teschner, M., Wehner, H., Durand, B., and Oudin, J.L., 1983. Maturity related biomarker and stable isotope variations and their application to oil/source rock correlation in the Mahakam Delta, Kalimantan. In: *Advances in Organic Geochemistry 1981* (M. Bjorøy et al., eds.), J. Wiley and Sons, New York, p. 156-163.

Schroot, B.M. and de Haan, H.B., 2003. An improved regional structural model of the Upper Carboniferous of the Cleaver Bank High based on 3D seismic interpretation. In: *Nieuwland, D.A. (ed.) New Insights into Structural Interpretation and Modelling*. Geological Society, London, Special Publications, 212, p. 23-37.

Sissingh, W., 2004. Paleozoic and Mesozoic igneous activity in the Netherlands: a tectonomagmatic review. *Netherlands Journal of Geosciences / Geologie en Mijnbouw* 83(2), p. 113-134.

Soper, N.J., Webb, B.C and Woodcock, N.H., 1987. Late Caledonian (Acadian) transpression in north-west England: timing, geometry and geotectonic significance. *Proceedings of the Yorkshire Geological Society*, 47 (3), p. 175-192.

Starostenko, V.I., and O.V. Legostaeva , 1998. Calculation of the gravity field from an inhomogeneous, arbitrarily truncated vertical rectangular prism. *Izvestiya, Physics of the solid Earth*, 12, p. 991-1003.

Stoppel, D. et al., 1981: Possible explanation of the gravity low between Hermalle-sous-Argenteau and Heugem. Appendix in Bless et al. (1981), *Mededelingen Rijks Geologische Dienst*, vol. 35, no. 15, p. 371.

Sweeney, J. J. and Burnham, A. K., 1990. Evaluation of a Simple Model of Vitrinite Reflectance Based on Chemical Kinetics. - *Journal of The American Association of Petroleum Geologists Bulletin*, 74 (10), p. 1559-1570.

Teichmüller, M. and Durand, B., 1983. Fluorescence microscopical rank studies on liptinites and vitrinites in peat and coals, and comparisons with results of the Rock-Eval pyrolysis. *Int. J. Coal Geol.*, 2, p. 197-230.

Ten Haven, H.L., de Leeuw, J.W., Rullkötter, and J. Sinninghe Damsté, J.S, 1987. Restricted utility of the pristane/phytane ratio as a palaeoenvironmental indicator. *Nature*, 330, p. 641-643.

Tissot, B. and Espitalié, J., 1975. L'évolution thermique de la matière organique des sédiments: application d'une simulation mathématique. – *Rev. Inst. Fr. Pét.*, 30: p. 743-777.

Tissot, B.P., R. Pelet and Ungerer, P., 1988. Thermal history of sedimentary basins, maturation indices, and kinetics of oil and gas generation. - *AAPG Bull.*, 71, p. 1445-1466.

Tissot, B.P., and Welte, D.H., 1984. Petroleum formation and occurrence, Springer Verlag, New York, 699p.

TNO-NITG, 1999. Geological Atlas of the Subsurface of the Netherlands (1 : 250 000), Explanation to Map Sheet XV Sittard-Maastricht. Netherlands Institute of Applied Geoscience - TNO (Utrecht) 127 pp.

TNO-NITG, 2001. Geological Atlas of the Subsurface of the Netherlands (1 : 250 000), Explanation to map sheets XIII and XIV: Breda-Valkenswaard and Oss-Roermond. Netherlands Institute of Applied Geoscience - TNO (Utrecht) 149 pp.

TNO-NITG, 2003. Geological Atlas of the Subsurface of the Netherlands (1 : 250 000), Explanation to map sheets XI & XII: Middelburg-Breskens and Roosendaal-Terneuzen. Netherlands Institute of Applied Geoscience - TNO (Utrecht) 149 pp.

TNO-NITG, 2004. Geological Atlas of the Subsurface of the Netherlands – onshore. TNO-NITG, Utrecht.

Ungerer, P., 1990. State of the art of research in kinetic modelling of oil formation and expulsion. – Org. Geochem., 16(1-3), p. 1-25.

Van Adrichem Boogaert, H.A. and Kouwe, W.F.P., 1993-1997. Stratigraphic nomenclature of the Netherlands; revision and update by the RGD and NOGEP. *Mededelingen Rijks Geologische Dienst*, 50.

Vandenbergh, N., 1984. The subsurface geology of the Meer area in north Belgium, and its significance for the occurrence of hydrocarbons. *Journal of Petroleum Geology* 7, p. 55-66.

Vandenbroucke, M., Behar, F. & Rudkiewicz, J.L., 1999. Kinetic modelling of petroleum formation and cracking: implications from the high pressure/high temperature Elgin Field (UK, North Sea). – Org. Geochem., 30, p. 1105-1125.

Van Balen, R.T., Van Bergen, G., De Leeuw, C., Pagnier, H., Simmelink, H., Van Wees, J. D., and Verweij, J. M., 2000. Modelling the hydrocarbon generation and migration in the West Netherlands Basin, the Netherlands. *Geologie en Mijnbouw / Netherlands Journal of Geosciences*, 79, p. 29 - 44.

Van den Belt, F.J.G. and David, P., 2002. A general evaluation of the hydrocarbon potential of the Dinantian of the southern Dutch offshore, TNO report NITG 02-199-C.

Van den Belt, F.J.G., 2002. Reference guide to the Dinantian (Lower Carboniferous) of Western Europe, TNO report NITG 02-202-C.

Verniers, J., Pharaoh, T., André, L., Debacker, T., De Vos, W., Everaerts, M., Herbosch, A., Samuelson, J., Sintubin, M. & Vecoli, M., 2002. The Cambrian to mid Devonian basin development and deformation history of Eastern Avalonia, east of the Midlands Microcraton, new data and a review. In: Winchester, J.A., Pharaoh, T.C. & Verniers, J. (eds): *Palaeozoic Amalgamation of Central Europe*. Geological Society Special Publication 201, p. 47--93.

Volkman, J.K and Maxwell, J.R., 1986. Acyclic isoprenoids as biological makers. In: *Biological Markers in the Sedimentary Record* (R.B. Jones, ed.). Elsevier, New York, p. 1-42.

- Walkden, G.M. and Williams, D.O.**, 1991. The diagenesis of the late Dinantian Derbyshire-East Midland Carbonate shelf, central England. *Sedimentology*, 38, p. 643-670.
- Walkden, G.M.**, 1974. Paleokarstic surfaces in the Upper Visean (Carboniferous) limestones of the Derbyshire Block, England. *Journal of Sedimentary Petrology*, 44, p. 1234-1247.
- Waples, D.W.**, 1985. Kerogen. In: *Geochemistry in Petroleum Exploration*, IHRDC, Boston, p. 31-41.
- Wolburg, J.**, 1970. Zur Paläographie des Unterkarbons und Namurs im Münsterland. *Neues Jahrbuch Geologie Paläontologie Monatsheft* 12, p. 735-740.
- Woodcock, N.H. & Pharaoh, T.C.**, 1993. Silurian facies beneath East Anglia. *Geological Magazine* 130, p. 681--690.
- Wygrala, B.P.**, 1989. Integrated study of an oil field in the southern Po Basin, Northern Italy. - Ph.D. thesis, University of Cologne, West Germany.
- Ziegler, P.A.**, 1978. North-Western Europe: Tectonics and basin development. *In*: A.J. van Loon (ed.): key-notes of the MEGS-II (Amsterdam, 1978). *Geologie en Mijnbouw*, 57, p. 589-626.
- Ziegler, P.A.**, 1982. *Geological Atlas of Western and Central Europe*. Shell Internationale Petroleum Maatschappij, Elsevier, 130 p.
- Ziegler, P.A.**, 1987. Late Cretaceous and Cenozoic intra-plate compressional deformations in the Alpine foreland – a geodynamic model. *In*: Ziegler, P.A. (ed): *Compressional intra-plate deformations in the Alpine foreland*. *Tectonophysics*, 137, p. 389-420.
- Ziegler, P.A.**, 1990. *Geological Atlas of Western and Central Europe* (second and completely revised edition). Shell Internationale Petroleum Maatschappij, Elsevier, Amsterdam, 23.

10 Signature

Utrecht, 24 February 2006

TNO Bouw en Ondergrond

B.C. Scheffers
Team Group leader Oil&Gas

B.M. Schroot
Author

A Description of analytical methods

In this Appendix an overview is given of the analytical methods and the quality assurance procedures that were used to collect the geochemical data. In addition, a brief description is given of the procedures that were applied for the interpretation of the data.

The following procedures are described:

- A.1 Quality assurance
- A.2 Sample and data collection
- A.3 Carbon and sulphur analysis (Leco CS)
- A.4 Rock Eval VI analysis
- A.5 Vitrinite reflectance analysis
- A.6 Extraction and fractionation
- A.7 Gas Chromatography Mass Spectrometry (GC-MS)
- A.8 Gas Chromatography Isotope Ratio Mass Spectrometry (GC-IRMS)

A1 Quality assurance

In order to guarantee data quality and integrity each analysis is performed according to a standard operating procedure (SOP). These procedures are an integral part of the Quality Assurance (QA) manual of the geochemical laboratory of TNO.

Quality control (QC) practices consist of more focused, routine, day-to-day activities carried out within the scope of the overall QA program. QC is the routine application of procedures for obtaining data that are accurate (precise and unbiased), representative, comparable, and complete. QC procedures include activities such as identification of sampling and analytical methods, calibration and standardisation, and sample custody and record keeping. Audits, reviews, and complete and thorough documentation are used to verify compliance with predefined QC procedures.

A scheme of the analyses performed on the samples is given in Figure A-1 and an overview of the related standard operating procedures is presented in Figure A-2. The quality assurance protocols for individual techniques are given in the relevant sections.

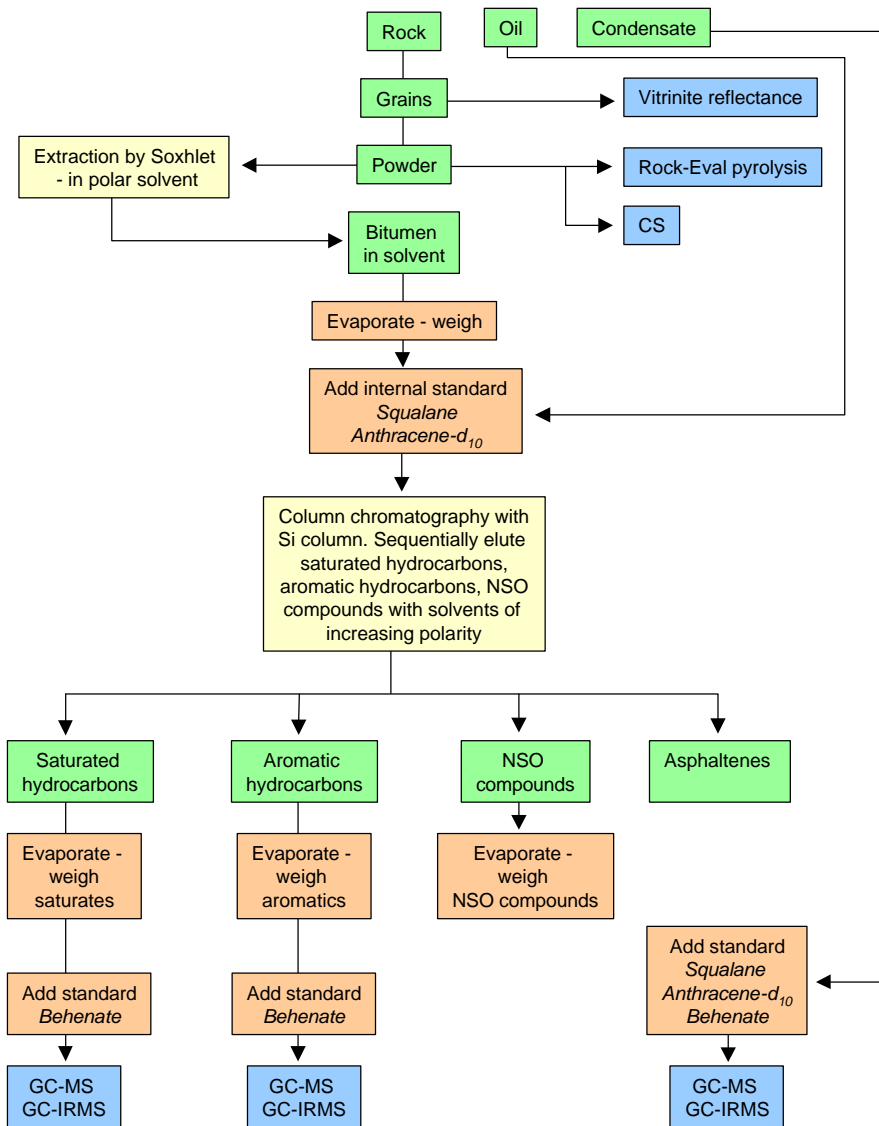


Figure A-1 Analytical scheme, showing the analyses that were used in the Petroplay project

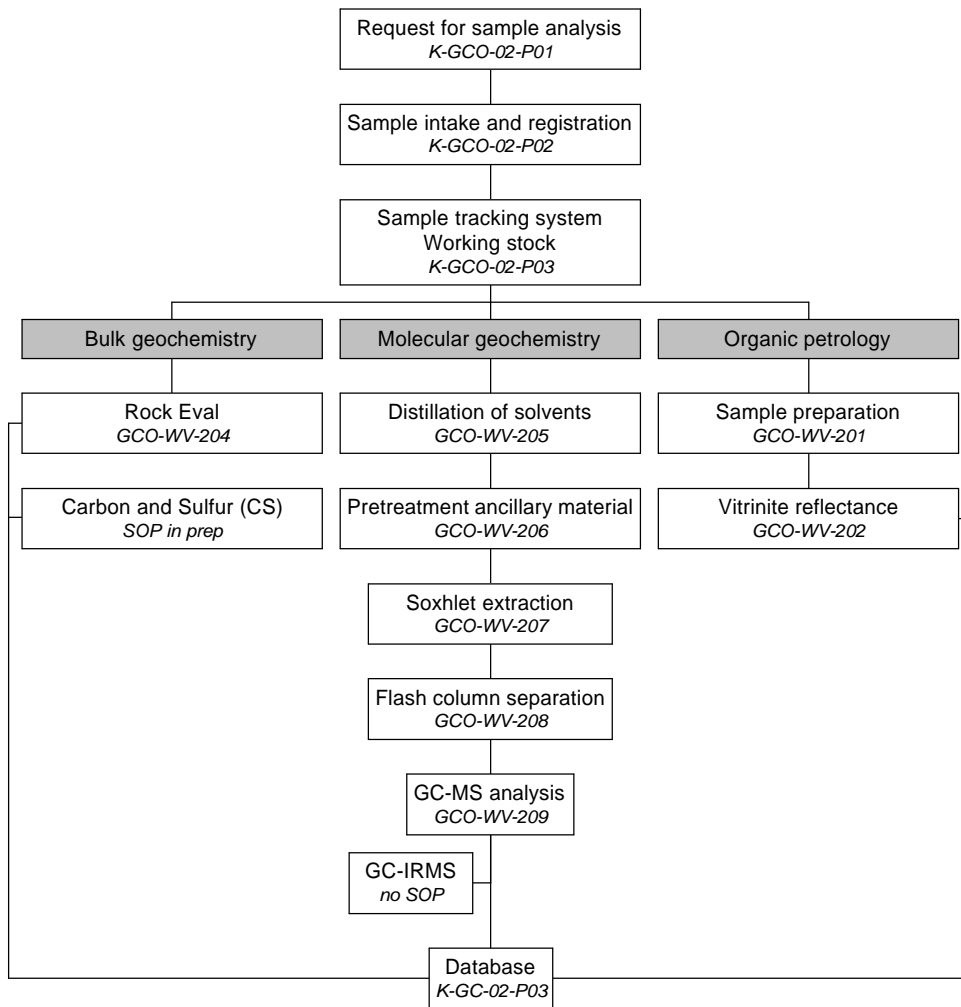


Figure A-2 Overview of the applied laboratory procedures within the Petroplay project

The data are stored in the DINO (Digitale Informatie Nederlandse Ondergrond) database of TNO. This database accommodates different types of data of the Dutch subsurface. For the Petroplay project geochemical data has been imported to the database and extracted in Excel format.

The DINO database contains all geochemical data as measured according to the standard operating procedures without interpretation or selection. This implies that the analytical quality of data is guaranteed, but also that data is stored in the database, which cannot directly be used for interpretation purposes, e.g. Rock Eval measurements that result in TOC values lower than 0.5 % often results in unreliable and erratic Tmax values and can therefore not be used in interpretations.

For visualisation and geological purposes, data are screened and interpreted. For example, Rock Eval analyses are performed in duplo and this duplo is averaged. This results in a second Excel file that contains only those data that are considered to be applicable in the further evaluation of the geologic models. In the descriptions of the individual analytical procedures these interpretations will be discussed in more detail.

A2 Sample and data collection

Samples were taken from cores, if available, and cuttings. Selection of samples was based on expected high Total Organic Carbon (TOC) values. It was anticipated that the likelihood of high TOC values in rocks is strongly related to a high gamma ray response. The gamma ray logs were therefore used to make a first selection. Prior to sampling, the lithology and colour of the samples were visually inspected (black clay samples or coal preferred).

In order to distinguish between the data from different sources, a label is introduced. The geochemical data are labelled with A, B or C.

The A labels are data produced within this study, the B labels are data produced earlier by the laboratory of TNO, and the C labels are data produced by other laboratory, mostly extracted from reports.

A3 Carbon and sulfur (CS)

Total carbon and sulfur are measured with a LECO SC 144DR. The total carbon content is analysed by total combustion of 0.2 – 0.3 gram of sample at 1350 °C while detecting the evading CO₂ and SO₂ by means of an infrared-detector. The amount of CO₂ and SO₂ is calibrated with a pure calcite standard and pure Ag₂SO₄ (Merck®), respectively. Relative standard deviations are less than 5%.

After the initial CS analysis, the total organic carbon content is determined on a selection of samples by measuring the sample after decalcifying with 1N HCl on a hotplate. About 0.2-0.3 gram of sample is weighed into a ceramic sample boat. The sample is placed on a hot plate at 90 °C and about 15 drops of HCl are added. After the sample is dry, a second aliquot of HCl is added to the sample. If there is still any visible reaction of the HCl with carbonates within the sample, the procedure is repeated.

The selection of samples is based on the total sulphur content. For samples with sulphur contents higher than approximately 1.50 % the total organic carbon content is determined with the Leco CS. For the other samples the total organic carbon content is determined with the Rock Eval. The reason for this pre-selection is the fact that high sulphur contents cause enhanced corrosion of the oxidation oven in the TOC module of the Rock Eval.

Quality control (QC) standards are analysed at the beginning and at the end of each analytical run and after every 20 unknown samples. QC charting and verification are carried out using Shewhart (1931) control charts constructed in Microsoft Excel, onto which are plotted the mean and standard deviation (s) of the QC data.

The calibration procedure will start again if the total organic C content of the ISE 921 is outside the ±2s limits.

A4 Rock Eval VI

Technique

Rock Eval pyrolysis is used to evaluate rapidly the petroleum-generating potential of rocks, and it provides information on the quantity, type, and thermal maturity of the organic matter in a rock.

Pyrolysis is the heating of organic matter in the absence of oxygen to yield organic compounds. Complete details of the Rock Eval pyrolysis technique and associated problems are given in Espitalié et al. (1985/1986) and Peters (1986). A schematic diagram of the Rock Eval is given in Figure A-3.

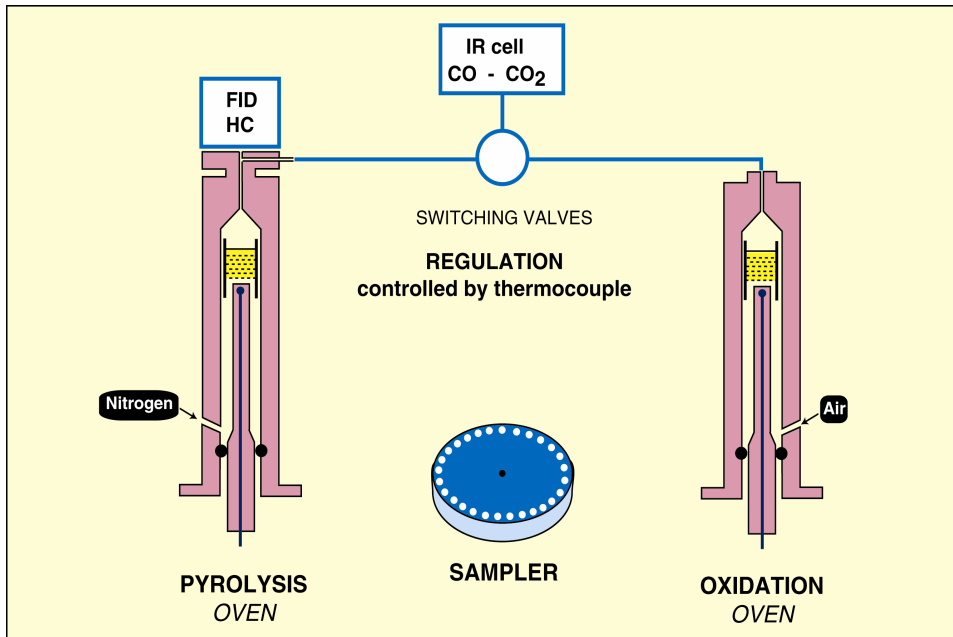


Figure A-3 Schematic overview of the Rock Eval, showing the two ovens for pyrolysis and oxidation. Detection of the generated hydrocarbons is done with a Flame Ionisation Detector and detection of the CO and CO₂ is done with an infrared cell

About 80 milligrams of ground rock sample are carefully weighed into a pyrolysis crucible and then heated to 300 °C to determine the amount of free hydrocarbons (S1). Next, the amount of pyrolysable hydrocarbons (S2) is measured when the sample is heated in an inert atmosphere which rises from 300 °C to 650 °C at a heating rate of 25 °C/minute. S1 and S2 are reported in mg HC/g sample. A typical pyrogram resulting from such a temperature programmed pyrolysis is given in Figure A-4.

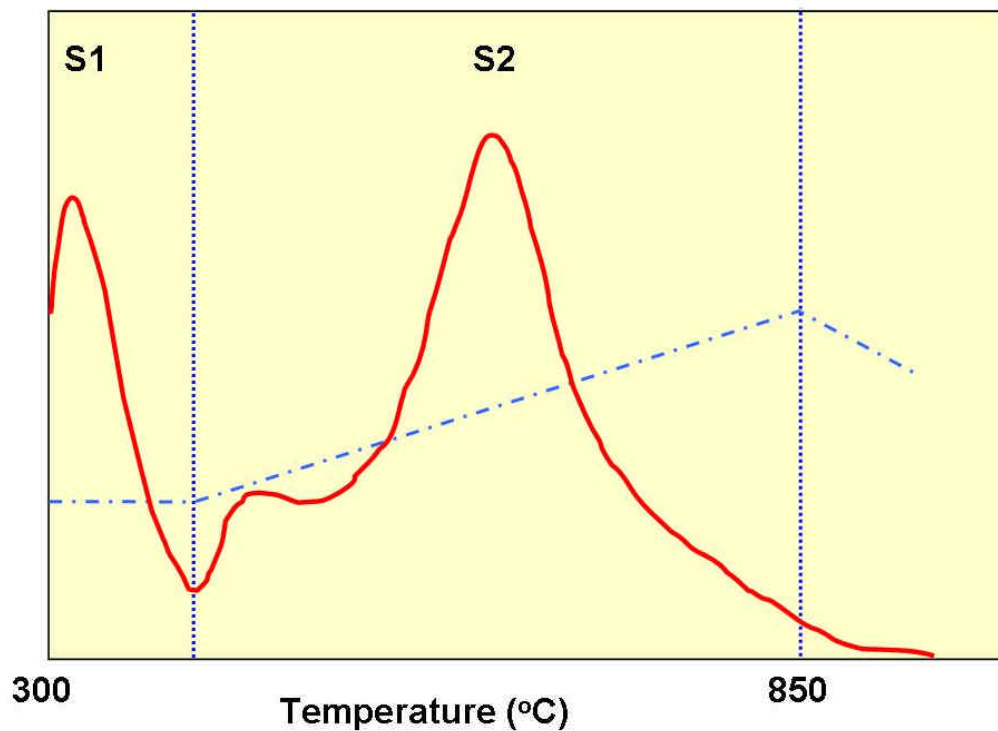


Figure A-4 Pyrogram of a Rock Eval VI pyrolysis showing the S1 and S2 peaks

The Rock Eval technique yields several measurements that determine the thermal maturity and hydrocarbon generation potential of source rocks. Total organic carbon content (TOC) is a useful parameter for evaluating the quantity of organic matter in a potential source rock. Total organic carbon was determined using the Rock Eval 6 instrument and is the sum of the carbon in the pyrolysate plus the carbon from the residual oxidised organic matter. In general (depending on the type of organic matter and lithology, fine-grained rocks having a total organic carbon content of greater than 0.5 percent are considered a potential hydrocarbon source rock.

Other Rock Eval measurements include the S1 peak, which is the amount of hydrocarbons that are thermally extracted from the rock; the S2 peak, the amount of hydrocarbons generated by pyrolytic degradation of the kerogen; and the S3 peak, the amount of carbon dioxide generated during heating to 400 °C.

Rock Eval pyrolysis also measures Tmax, the temperature at the culmination of the S2 peak; that is, the temperature of maximum hydrocarbon yields. Tmax can be used as a thermal maturity indicator because the temperature for maximum hydrocarbon yield increases as kerogen matures. Hydrocarbons begin to be generated between Tmax values of approximately 435 °C and 440 °C, and thermal cracking to gas and condensate occurs at about 460 °C (Tissot and Welte, 1984).

The hydrogen index (HI) is defined as the S2 yield (remaining hydrogen-generating capability of the organic matter) normalised to the total organic carbon content (TOC); in other words, the fraction of the total organic carbon that is generated as hydrocarbons. The hydrogen index is also useful in describing the type of organic matter present in the source rock. The oxygen index (OI) is the quantity of carbon

dioxide from the S3 peak normalised to the total organic carbon content and, if plotted against the HI, yields information about the type of organic matter in the source rock. The production index (PI), or transformation ratio, is defined as the ratio (S1/(S1+S2)), or the ratio of volatile hydrocarbon yield to total hydrocarbon yield. The production index can be used to evaluate thermal maturity because, if there is no migration of hydrocarbons, it increases with heating. In general, the beginning of generation is at a production index of about 0.08 – 0.10, and thermal cracking of oil to gas and condensate occurs at about production indices of 0.40 – 0.50.

An overview of all measured and calculated parameters from one Rock Eval VI analysis is given in Table A-1.

Table A-1 Overview of the measured and calculated Rock Eval VI parameters

Measured parameters			
	Detector/Oven	Unit	Name
S1	FID/Pyrolysis	mg HC/g rock	Free hydrocarbons
S2	FID/Pyrolysis	mg HC/g rock	Oil potential
TpS2	TC/Pyrolysis	°C	Temperature at maximum of S2 peak
S3	IR/Pyrolysis	mg CO ₂ /g rock	CO ₂ from organic source
S3'	IR/Pyrolysis	mg CO ₂ /g rock	CO ₂ from mineral source
S3CO	IR/Pyrolysis	mg CO/g rock	CO from organic source
S3'CO	IR/Pyrolysis	mg CO/g rock	CO from mineral source
S4CO	IR/Oxidation	mg CO/g rock	CO from organic source
S4CO ₂	IR/Oxidation	mg CO ₂ /g rock	CO ₂ from organic source
S5	IR/Oxidation	mg CO ₂ /g rock	CO ₂ from mineral source
Calculated parameters			
	Unit	Formula	Name
Tmax	°C	TpS2-STD Tmax	Tmax
PI		S1/(S1+S2)	Production Index
PC	% weight	$\frac{\left[(S1+S2) \times 0,83 \right] + \left[S3 \times \frac{12}{44} \right] + \left[\left(S3CO + \frac{S3'CO}{2} \right) \times \frac{12}{28} \right]}{10}$	Pyrolysable Carbon
RC CO	% weight	(S4CO x 12/44)/10	Residual Carbon CO
RC CO ₂	% weight	(S4CO ₂ x 12/44)/10	Residual Carbon CO ₂
RC	% weight	RC CO + RC CO ₂	Residual Carbon
TOC	% weight	PC + RC	Total Organic Carbon
HI	mg HC/g TOC	(S2 x 100)/TOC	Hydrogen Index
OI	mg CO ₂ /g TOC	(S3 x 100)/TOC	Oxygen Index

Procedure

The full analytical procedure is described in the standard operating procedure GL-WV 204 (Rock Eval analysis).

The Rock Eval is calibrated with a standard (55000) of known S2 and Tmax values provided by Vinci Technologies (Paris, France). The quality control (QC) standard (ISE 921) is analysed after every 10 unknown samples. QC charting and verification are carried out using Shewhart (1931) control charts constructed in Microsoft Excel, onto which are plotted the mean and standard deviation (s) of the QC data. All samples are measured in duplo and in case of strong differences between both analyses the sample is either rejected or analysed again.

All data that are stored in the database are measured according the standard operating procedures implying that the analytical quality is guaranteed. Yet, in the evaluation of the data in terms of maturity and kerogen type some restrictions are made. Figure A-5 gives the decision tree for the applicability of the Rock Eval data. Samples with a TOC less than 0.50% are rejected because in most of these cases the FID signal (S2) is too low, often resulting in erratic Tmax values. In some cases the S2 signal consists of more than one peak, implying more than one population or type of organic matter in the sample, each with its own Tmax value. On the basis of the general trend of Tmax values in a well it is sometimes possible to determine the 'true, Tmax value. In cases where the S2 signal is unresolved the resulting Rock Eval parameters will not be evaluated further. Unresolved S2 peaks are often the result of a low signal just above the baseline.

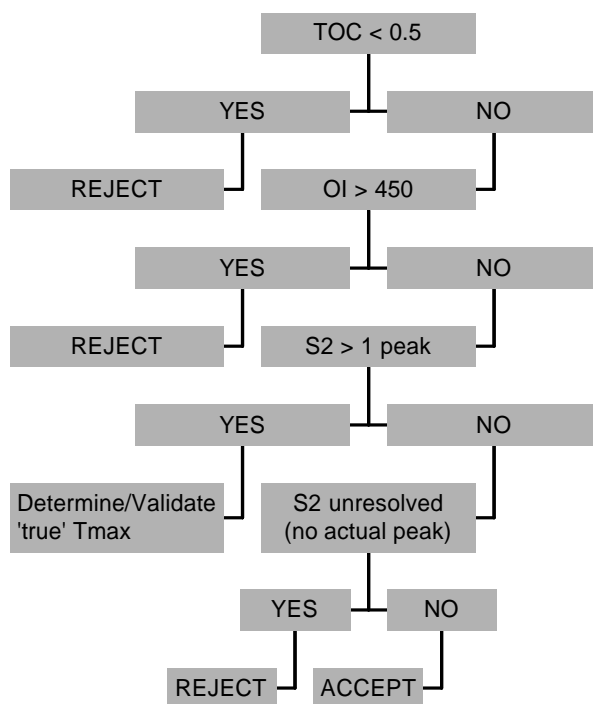


Figure A-5 Evaluation of the Rock Eval data for application in geological interpretations

A5 Vitrinite Reflectance

Technique

Vitrinite reflectance is an optical (microscopic) maturity parameter. Increasing vitrinite reflectance values are related to the progressive aromatisation of the kerogen with accompanying loss of hydrogen in the form of hydrocarbon gases with increasing time and temperature.

Vitrinite, a maceral derived from woody plant material, is common in coal and organic-rich shale. Vitrinite reflectance is a measure of the proportion of light reflected from a polished vitrinite grain. It is related to the degree of metamorphism of the vitrinite grain and can be related to other thermal maturity indicators. Since vitrinite changes predictably and consistently upon heating, its reflectance is a useful measurement of source rock maturity.

Vitrinite reflectance values have been correlated with oil and gas generation for potential source rocks. For example, Waples (1985) stated that, depending on the type of kerogen, oil generation begins over a range of vitrinite reflectance values – onset of oil generation ranges from about 0.45 percent Ro to 0.50 percent Ro for high-sulphur kerogen, to 0.60 percent Ro for marine kerogen, to 0.65 percent Ro for terrestrial kerogen (see Figure A-6).

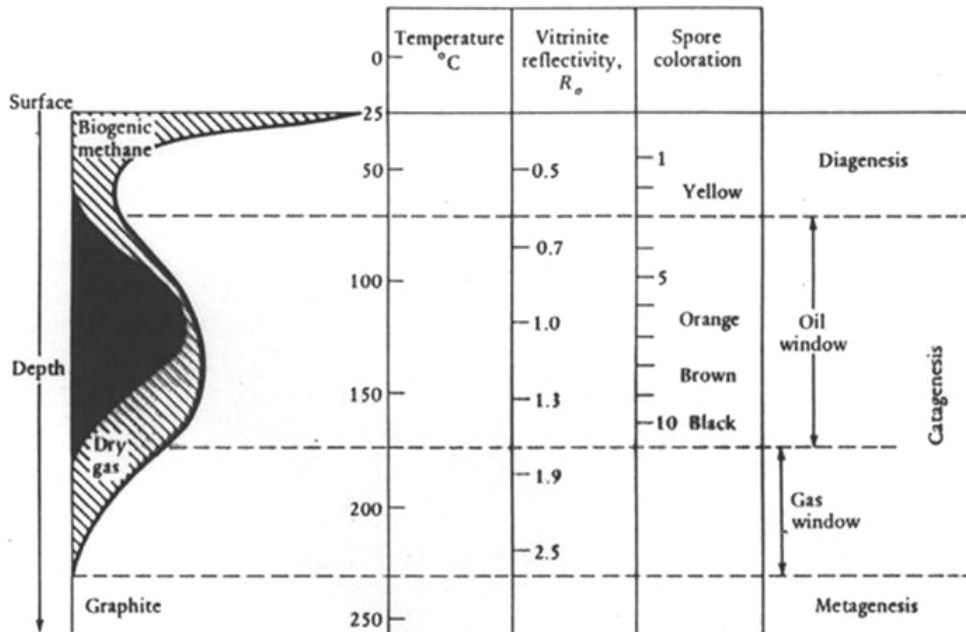


Figure A-6 Correlation between hydrocarbon generation, temperature, and some maturity indicators

Procedure

The full procedure for the measurement of vitrinite reflectance values is given in the standard operating procedures GL-WV 201 (sample preparation organic petrology) and GL-WV 202 (vitrinite reflectance).

Sample preparation and vitrinite reflectance measurements were performed according to international standard methods (ISO 7404-2, 1985 and ISO 7404-5, 1994) by an accredited petrographer (ICCP). For each sample hundred readings are randomly performed on vitrinite particles to obtain a statistically acceptable population. However,

for most of the samples the amount of suitable vitrinite particles was insufficient to measure the required hundred points, thereby reducing the accuracy of the measurement. The mean value of the readings per sample represents the vitrinite reflectance of the sample (%R_r or % R_{max}), the standard deviation indicates the uncertainty in the measurement.

As an integral part of the quality control system each measurement is recorded with a statement regarding the overall quality of the measured vitrinite particles.

For the following parameters labels are applied:

Parameter 1	IDENTIFICATION OF VITRINITE: coal or dispersed organic material, clear identification of the macerals is possible
Parameter 2	PARTICLE SIZE: does the measuring spot fits good / reasonably on the collotellinite particle
Parameter 3	QUALITY OF THE PARTICLE SURFACE: assessment of the measurement field (3* diameter of the measuring spot) regarding scratches, minerals, relief, oxidation

These parameters are assessed by the following labels:

+	Has a possible influence on the measurement
0	Has no influence on the measurement

An ideal or perfect sample is represented by the code 000.

On the basis of the quality code of the vitrinite in the sample, the number of measurements and the standard deviation a statement can be made on the 'reliability' of the measurement. This will always be a partially subjective assessment.

+	High reliability, (Stdv \leq 0.05; N \geq 40)
(no code)	Average reliability, (0.05 \leq Stdv \leq 0.10; 15 \leq N \leq 40)
-	Low reliability, (Stdv \geq 0.10; N \leq 15)
mp	More than one population of vitrinite reflectance values, possibly indicating reworking or caving

A6 Solvent extraction and fractionation

Procedure

The full procedure for the extraction and fractionation of hydrocarbons from (source) rocks is given in the standard operating procedures GL-WV 207 (soxhlett extraction) and GL-WV 208 (flash column)

The fraction of the organic matter that is soluble in organic solutes is extracted from the powdered samples (10-20 g) by soxhlett extraction with dichloromethane (DCM) and methanol (MeOH) (95:5 v.v.) for 24 hours. The solvent is evaporated by careful rotary evaporation and, after transfer of the liquid extract into small vials, by air drying in the

fume hut. After these steps the mass of the extractable organic matter (EOM) is determined.

The extract contains next to aliphatic-, aromatic- and NSO-components an amount of asphaltenes, which have to be removed from the extract prior to the GC-MS analysis.

The extract is separated in four hydrocarbon-groups using a flash-column (see Figure A-7). The stationary phase in this column is silica gel, which was activated for 1 hour at 150 °C.

Three fractions - aliphatic, aromatic, and NSO-components - are eluted with respectively n-pentane, dichloromethane and methanol (see also Figure A-1). The asphaltenes fraction is not dissolved and remains on the column. The mass of each fraction is determined. The fractions are diluted with n-pentane ($c = 1 \text{ mg/mL}$) and analysed by GC-MS or GC-IRMS.



A)



B)

Figure A-7 Equipment for extraction and fractionation of source rock derived hydrocarbons.

A) Rotary evaporator for the distillation of the organic solvents.

B) Flash column filled with silica gel for the fractionation of the extract into different hydrocarbon classes.

A7 Gas Chromatography Mass Spectrometry (GC-MS)

Technique

Mass spectrometry is used to identify unknown compounds and quantify known compounds. It is sensitive and selective and is commonly used in combination with a separation technique, such as gas or liquid chromatography, to analyze complex mixtures. After a molecule is introduced into the mass spectrometer, the molecule is first ionized, then fragmented. Following this, the ions can be selected and counted. The plot of the mass-to-charge ratio (m/z) of these ions, as a function of abundance, is a mass spectrum. Figure A-8 gives an example of a mass spectrum.

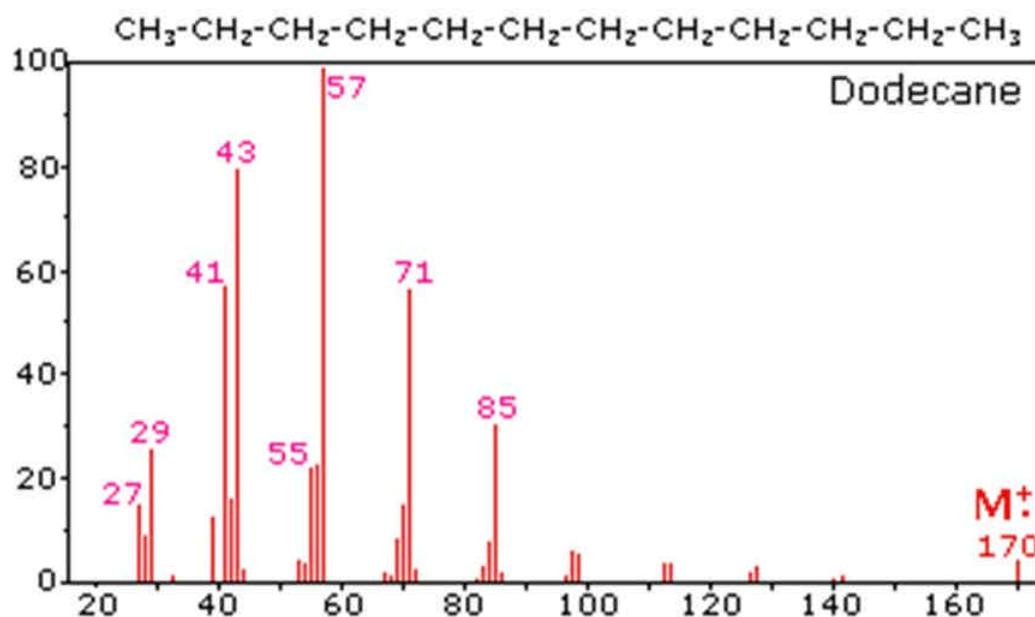


Figure A-8 Example of a mass spectrum of a common molecule in source rock extracts (n-C12)

A quadrupole mass filter can be operated in a scan mode (TIC) or select ion monitoring (SIM) mode.

In SIM, the mass filter is set to pass one selected m/z . This provides the greatest sensitivity and is used for quantitative applications. It is used when the analyst has prior knowledge of what ions to expect. In scan mode, the mass filter is set to sequentially pass a range of masses. It has lower sensitivity because most of the ions strike the rods during the scan, generating a Total Ion Current (TIC). For general unknowns, the selected mass may be at 100, then 101, then 102 and so on. This mode is used to collect spectra for interpretation or a library search.

When a sample contains several components, they may be separated (in time) using chromatographic techniques. After each component enters the mass spectrometer, its molecules are ionized, filtered, and detected to produce a unique mass spectrum. The individual spectra are used to identify the components.

Procedure

Gas chromatography – Mass spectrometry (GC-MS) has been performed on the aliphatic and aromatics fractions of the liquid extracts of the powdered sample material in TIC mode. For the biomarker analysis the mass spectrometer is set in SIM-mode in a second analysis. The sterane distribution in the samples is derived from the m/z 217 mass chromatogram and the terpane distribution in the samples is derived from the m/z 191 mass chromatogram from the SIM analysis.

The chromatogram of the aliphatic and aromatic fractions is scanned for the presence of predefined components. If a component is detected its peak is automatically integrated and its peak area is reported. Table A-2 gives an overview of the settings of the GC-MS system.

Table A-2 Summary of the GC-MS method (Total Ion Current mode)

Gas chromatograph	HP 6890 GC
Mass spectrometer	HP 5973 MSD
Injection volume	1 µL
Injector temperature	250°C
Carrier gas	Helium
Constant flow	1.5 mL/min
Column	J&W DB-1 (50 m x 0.25 mm x 0,5 µm) or comparable column
Oven temperature	30°C (20 min const.) with 2°C/min to 300°C (20 min const.)
Ion source temperature	230°C
Scan range	0-20 min: 2 scans/s between m/z 15.0 en 765.0 from 20 min, 2 scans/s between m/z 50.0 en 800.0
For WV209_EX.M	
Injection mode	Pulsed split less
For WV209_CO.M	
Injection mode	Split 150:1

A8 GC-IRMS*Technique*

Gas chromatography combustion isotope ratio mass spectrometry (GC/C/IRMS) is a highly specialised instrumental technique used to ascertain the relative ratio of light stable isotopes of carbon ($^{13}\text{C}/^{12}\text{C}$), hydrogen ($^2\text{H}/^1\text{H}$), nitrogen ($^{15}\text{N}/^{14}\text{N}$) or oxygen ($^{18}\text{O}/^{16}\text{O}$) in individual compounds separated from often complex mixtures of components. The ratio of these isotopes in natural materials varies slightly as a result of isotopic fractionation during physical, chemical and biological processes resulting, in some cases, with the relative isotopic ratio of specific compounds being highly diagnostic of key environmental processes. The primary prerequisite for GC-IRMS is that the compounds constituting the sample mixture are amenable to GC, i.e. they are suitably volatile and thermally stable. Polar compounds may require further chemical modification (derivatization) and in such cases the relative stable isotope ratio of the derivatization agent must also be determined.



Figure A-9 The GC-IRMS system that is used for the determination of the $^{13}\text{C}/^{12}\text{C}$ and $2\text{H}/1\text{H}$ stable isotope ratios for the straight-chain n-alkanes in the source rock extracts and oil

The term stable isotope refers to a given atom's mass. While the number of protons defines an element [e.g., carbon (6) vs. nitrogen (7) vs. hydrogen (1)], the number of neutrons defines which isotope (*i.e.*, of which mass) of the element is being referred to. As a most relevant example for present purposes, carbon-12 (denoted ^{12}C) has six protons and six neutrons. The addition of one more neutron makes ^{13}C . For reference, ^{12}C comprises 98.89% of all naturally occurring carbon and ^{13}C comprises 1.11%. To be useful as a tracer, one needs a pair of isotopes (*e.g.*, ^{12}C and ^{13}C) to form a ratio (*viz.*, $^{13}\text{C}/^{12}\text{C}$). (For perspective, note that the GC-IRMS averages the $^{13}\text{C}/^{12}\text{C}$ ratios of enormous numbers of individual $^{12}\text{CO}_2$ and $^{13}\text{CO}_2$ molecules to produce a single isotopic ratio.) The variation in that ratio is the tracer of interest here.

As the name of the instrument indicates, the gas chromatography/isotope-ratio mass spectrometer, the associated technique separates individual compounds by gas chromatography, combusts them into carbon dioxide peaks, and measures the isotopic composition of the resultant carbon dioxide peaks with a very precise isotope-ratio mass spectrometer (Fig. A-10). For hydrogen and oxygen a high temperature thermal conversion reactor is required (not shown). Water is then removed in a water separator by passing the gas stream through a tube constructed from a water permeable nafion membrane. The sample is then introduced into the ion source of the MS by an open split interface.

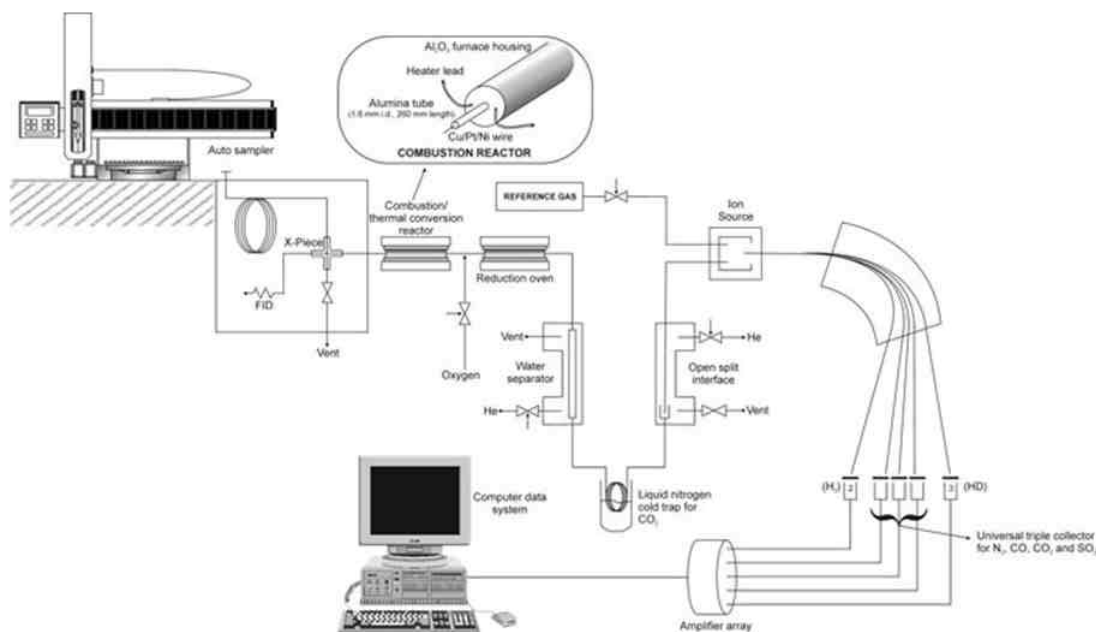


Figure A-10 A schematic of a typical GC-IRMS instrument (from: www.bris.ac.uk/nerclsmsf/techniques/gccirms.html)

The three major components of a GC-IRMS system include: (i) a gas chromatograph where organic compounds are separated into individual peaks, (ii) a high-temperature ($\sim 900^{\circ}\text{C}$) combustion oven where individual chromatograph peaks are combusted into CO_2 and H_2O , and (iii) an isotope ratio mass spectrometer (IRMS) where the resulting $^{13}\text{CO}_2$ and $^{12}\text{CO}_2$ are separated and measured to give isotopic ratios for individual compounds. For the measurement of the hydrogen isotopes the compounds are pyrolysed to form hydrogen gas and the resulting ratio of $^2\text{H}/^1\text{H}$ is determined. An example of the determination of both the stable carbon and the stable hydrogen isotope ratios on a number of straight-chain alkanes extracted from an oil sample is given in Figure A-11.

Just as for GC-MS the sample solution is injected into the GC inlet where it is vaporized and swept onto a chromatographic column by the carrier gas (usually helium). The sample flows through the column and the compounds comprising the mixture of interest are separated by virtue of their relative interaction with the coating of the column (stationary phase) and the carrier gas (mobile phase). To date it is still difficult to achieve a sufficient baseline separation of the individual components, which is major prerequisite for reproducible and accurate isotope data analysis. Condensates, oils, and source rock extracts are extremely complex mixtures of components, and the gas chromatographic separations often results in co-elution of several individual molecules.

Figure A-12 shows this co-elution for the straight-chain C_{14} alkane with an unknown molecule (probably a branched alkane). Co-elution of these compounds influences the isotope ratio of the C_{14} molecule

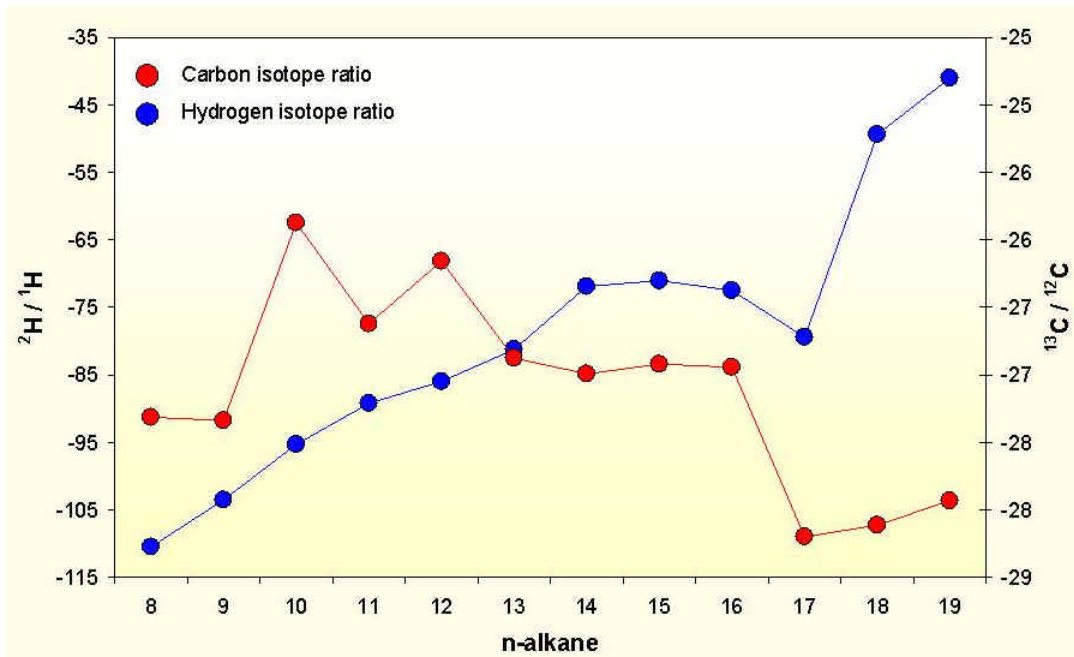


Figure A-11 The carbon and hydrogen isotope ratios of the straight-chain alkanes of a North Sea oil. These signatures can be used to characterise oils and source rock extracts for correlation purposes

The isotope ratios for both carbon and hydrogen are determined by integration of the C₁₄ peak. In the example of Figure A-12 automated integration of co-eluting peaks is not possible. Manual integration of all relevant peaks is highly time-consuming and not always reproducible. The resolution of the peaks can be enhanced by further fractionation of the aliphatic fraction into straight-chain and branched alkanes. This procedure is still in development

Therefore the isotope data of notably the source rock extracts should be used with care when used for interpretations in geological context.

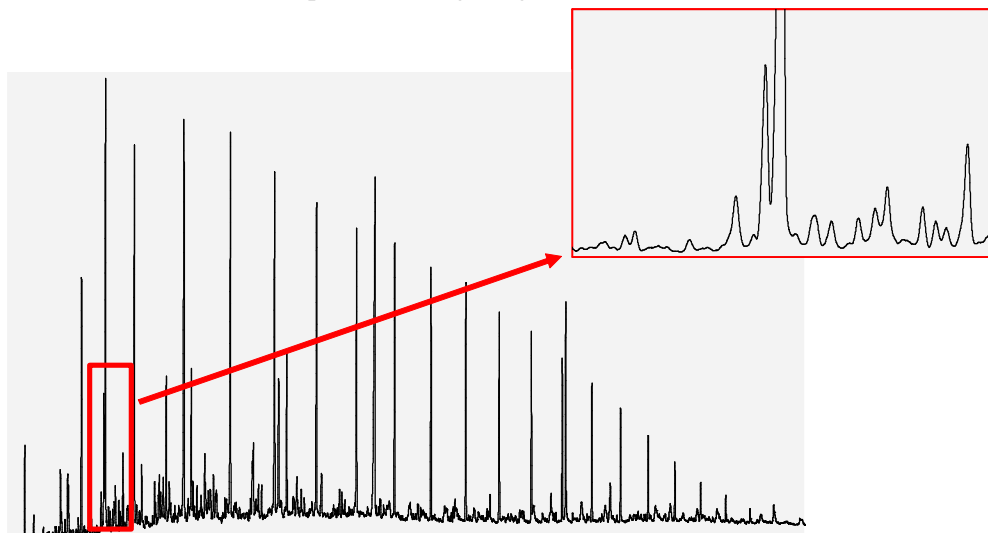


Figure A-12 Chromatogram of the aliphatic fraction of a source rock extract showing the co-elution of an unknown component with the straight-chain C₁₄ alkane

B Geochemical Database

Geochemical and organic petrological analyses have been performed to establish the type and maturity of potential pre-Westphalian source rocks. These analyses resulted in optical (vitrinite reflectance), bulk geochemical (Rock Eval), molecular and isotopic geochemical data that are stored in the digital geochemical database. The applied analytical methods are described in Appendix A. All analytical data as measured for the Petroplay project or collected from company reports are stored in the Petroplay database. In this section an overview is given of the data. The primary goal of the analyses is to establish the source rock potential of the collected material (maturity, kerogen type, etc.). In this section the evaluation of the data as derived from the different techniques will also be presented. These evaluated data (e.g. maturity trends) are used for the description of the source rock potential of the pre-Westphalian (see Chapter 3). The data are also used for the calibration of the basin modelling concepts.

Sample selection

The source rock samples were selected at several locations. The samples from the wells in the public domain in the Netherlands off- and onshore area were sampled at the core storage facility of TNO (offshore wells older than 10 years, onshore wells sampled with permission of the owner). In 2004 the core house of Gaz de France in Lingen was visited in order to acquire samples from well Munsterland-1. In 2005 the core houses of the Landesamt Krefeld in Krefeld and of the Belgian Geological Survey in Brussels were visited in order to acquire samples from relevant wells that have reached the pre-Westphalian. In Germany, only well Schwalmtal-1001 was in the public domain and could therefore be sampled. In Belgium, samples were taken from a total of 13 wells. Also wells south of the London Brabant Massif (LBM) were selected, because it was expected that the maturity of these wells was somewhat lower than north of the LBM.

It was decided to include also UK wells to get samples from specific (potential) pre-Westphalian source rocks. Several UK offshore wells were suggested for sampling. In august 2004 the DTI core house in Edinburgh was visited to take samples of selected wells, with a special focus on the Bowland shale (Geverik member equivalent) and the Yoredale deposits.. Core and cutting samples were taken from in total 10 wells of the UK.

Selection of samples was based on expected high total organic carbon (TOC) values. It was anticipated that the likelihood of high TOC- values in rocks is strongly related to high gamma ray response. The gamma ray logs were, if available, therefore used to make a first selection by applying the so-called 'Δ Log R method' see below). In addition, the lithology and colour of the samples were visually inspected (black clay samples or coal preferred) prior to the actual sampling.

The technique chosen in this study for the evaluation of the log patterns is the 'Δ Log R method' and is described in detail by Passey et al (1990). It makes use of commonly available well logs, viz. the gamma-ray, sonic, and deep resistivity logs. The principle of the method is straightforward. A shale interval at sufficient depth is thought to consist of a shale matrix, some porosity, and possibly hydrocarbons. The shale content is indicated by the gamma-ray log. The sonic log responds to the amount of porosity, but is only slightly affected by the presence of (light) hydrocarbons. A deep-reading

resistivity device however, will respond strongly to the presence of hydrocarbons, i.e. the resistivity will increase. If there are no hydrocarbons and there is only (saline) water present in the shale pores, the sonic and resistivity logs will overlay if they are properly scaled. In an organic-rich section, there will be a distinct separation between the sonic and resistivity logs. The amount of separation indicates the amount of organic material. In order to use this method, a few conditions have to be met. First of all, a baseline interval must be established. A baseline interval is a shaly interval with sufficient thickness where the sonic and resistivity logs run parallel. The suitable scales must be chosen for the logs, so that they overlay each other in the baseline interval. Their relative scales must however remain fixed. Then for every point the $\Delta \text{Log R}$ separation can be calculated. When the level of maturity for the interval is known, TOC can be calculated through the formula:

$$\Delta \text{Log R} = \log_{10}(R/R_{\text{baseline}}) + 0.02 \times (\Delta t - \Delta t_{\text{baseline}})$$

Passey et al. (1990) give some good examples of this method (Fig. B-1).

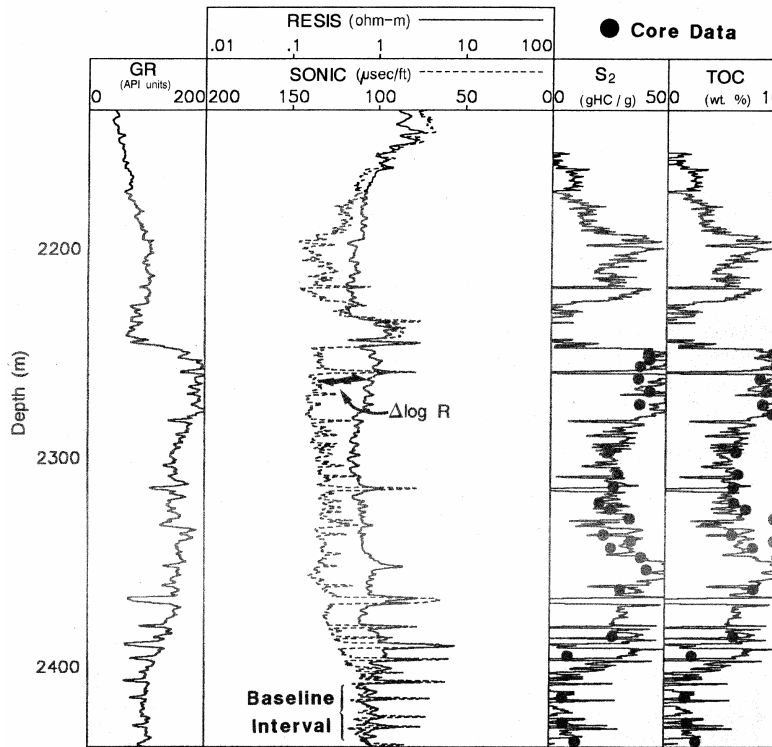


Figure B-1 An example of a well for which a log-derived TOC was calculated in comparison to laboratory determined TOC values. Sonic/resistivity overlay showing ? Log R separation in the organic-rich interval. The relative scaling of the sonic and resistivity curves is 50 µsec/ft corresponds to one tenth of resistivity. There is a remarkable agreement between the two organic carbon contents (from Passey et al., 1990)

Within this study the technique described above was applied to evaluate the possible organic rich strata. This evaluation showed that there is a fair similarity between the calculated and measured TOC, e.g. in the extensive shaly Namurian succession of well Tjuchem-2 (Fig.B-2). This method also shows that not all shales that are potentially rich in organic matter were sampled. Evaluation of well Geverik-1 confirmed the high content of organic matter in the Geverik Member,

while the underlying Dinantian carbonates are virtually void of organic material (Fig. B-3).

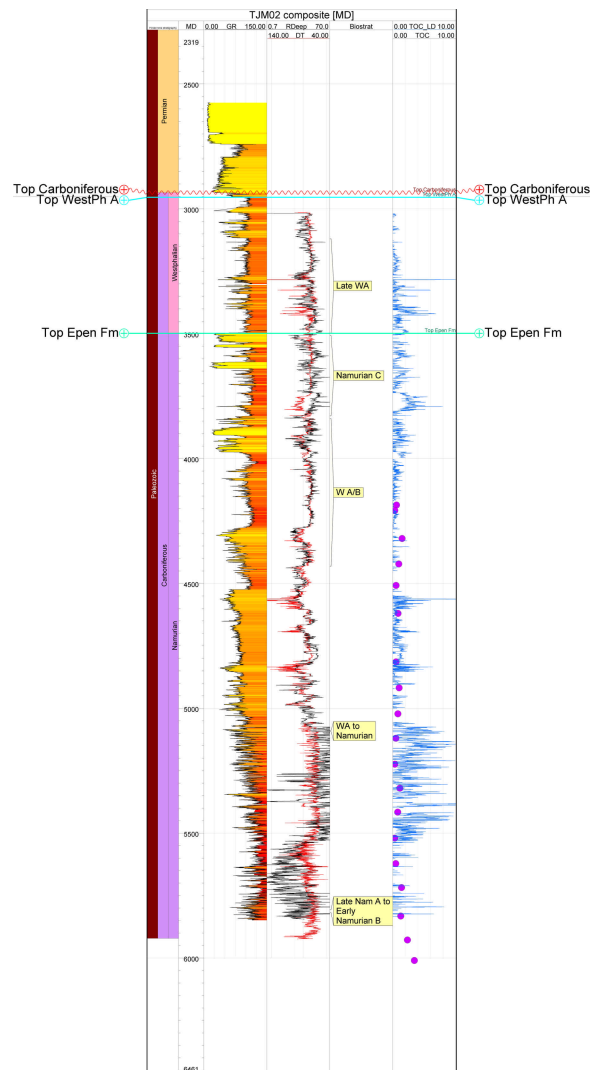


Figure B-2 Log-derived and measured TOC in well TJM-02(-S1), as an example of the evaluation following Passey et al. (1990).

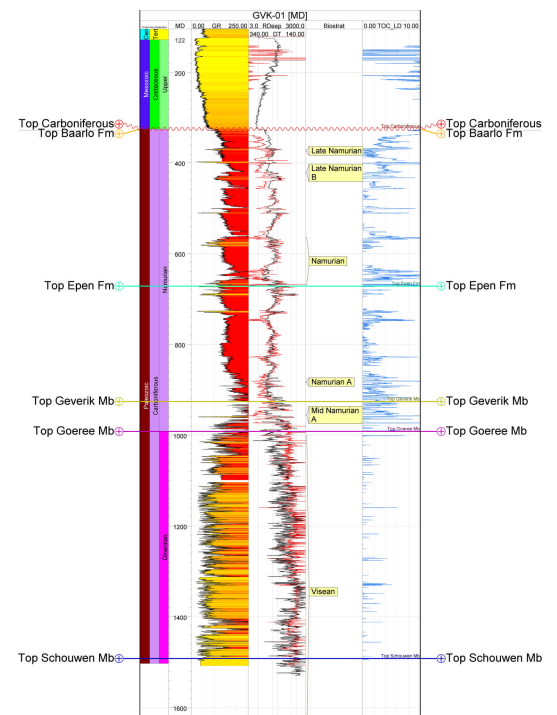


Figure B-3 Log-derived and measured TOC in well GVK-01, as an example of the evaluation following Passey et al. (1990) Note the high TOC values in the Geverik Member

Geochemical and organic petrological data

Tables B-1, B-2 and B-3 give an overview of all samples and analytical data as currently stored in the Petroplay database. The exact depth interval and stratigraphy of the selected samples are indicated in the digital data files. In order to distinguish between the data from different sources, a label is introduced. The analytical data are labelled with A, B or C. The A labels are data produced within this study, the B labels are data produced earlier by the laboratory of TNO, and the C labels are data produced by other laboratories, mostly resulting from reports. All samples collected specifically for this study (A-labels) were analysed on their carbon and sulphur content and with the Rock Eval. Optical (vitrinite reflectance) and molecular geochemical measurements

(GC-MS) have been executed on a selection of samples. In addition, a number of condensate samples were analysed by GC-IRMS in order to determine the carbon and hydrogen isotope ratios of the n-alkanes in these samples. These condensate samples were already present in the laboratory of TNO.

An overview of all the wells that were used in this study is given in Figure B-4.

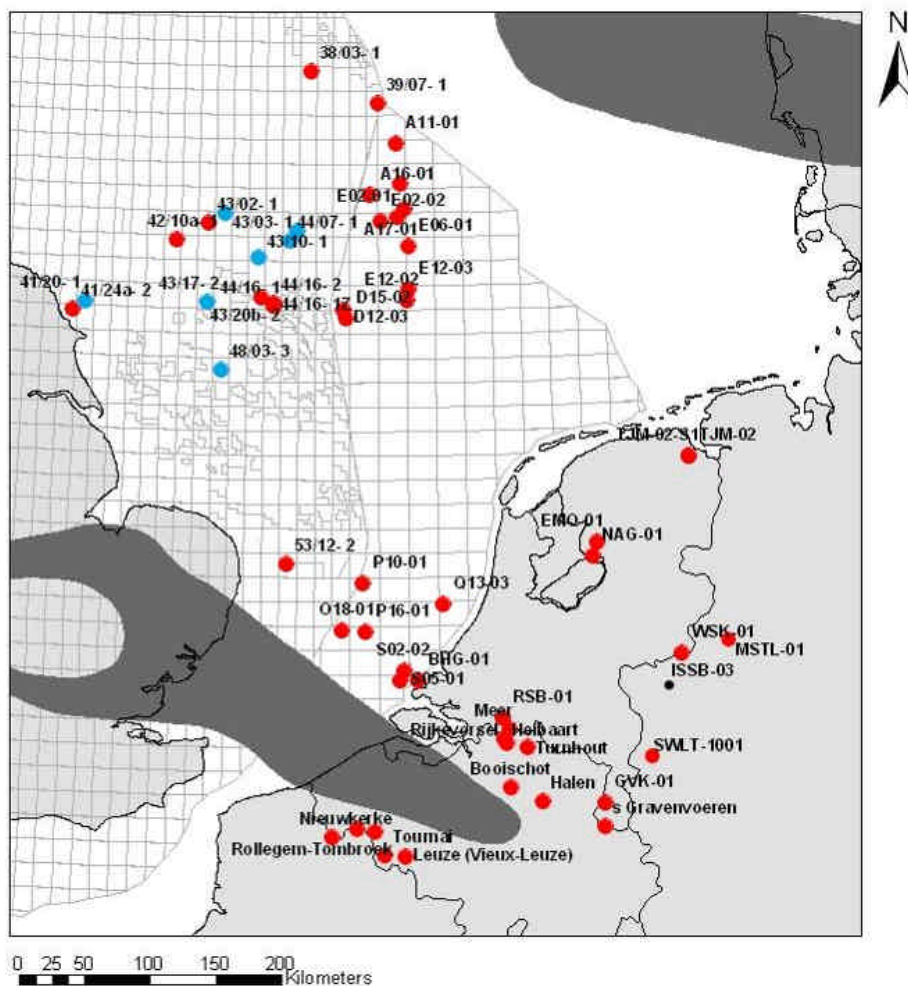


Figure B-4 Overview of wells that were sampled (in red). Data (after Collinson, 1995) from the wells indicated in blue are also included in the database

Table B-1 Summary of the number of samples in Area 1 for the geochemical and organic petrological analyses.

	Well	CS	Rock Eval			Vitrinite reflectance			TIC	SIM	IRMS	
			A	A	B	C	A	B				C
Area 1	NL	BHG-01		15	10	6	3	5		2	2	
		GVK-01			53			10				
		O18-01		3		9			13	1	1	1
		P10-01	10	10								
		P16-01	46	46		22	7		11	6	6	1
		Q13-03	7	7								
		RSB-01			16			21				
		S02-02			21	10		5	14			
		S05-01	53	53			7			7	7	3
	BE	17W KB-265 Merksplas	11	11								
		Booischoot-KB-132	3	3								
		DZH-01-Heibaart	5	5								
		Halen-KB-131	17	17								
		125E KB-298 Leuze	8	8								
		7E KB-205 Meer (Hoogstraten)	6	6								
		95W KB 152 Nieuwerkerke	3	3								
		16E KB-176 Rijkevorsel	11	11								
		Rollegem-Tombroek	3	3								
		's Gravenvoeren	2	2								
		124E KB-455 Tournai	8	8								
KB-120 Turnhout	29	29										
Wervik 1	4	4										
UK	53/12-2	3	3			2			1	1	1	

Table B-2 Summary of the number of samples in Area 2 for the geochemical and organic petrological analyses.

	Well	CS	Rock Eval			Vitrinite reflectance			TIC	SIM	IRMS	
			A	A	B	C	A	B				C
Area 2	NL	A11-01	6	6			2					
		A14-01			14				2			
		A16-01			33				5			
		A17-01	6	6								
		D12-03	6	6			2					
		D15-02	22	23			2					
		E02-01	26	26			3			4	4	3
		E02-02	58	58	3							
		E06-01			4	19			11			
		E12-02			8							
	E12-03	13	13	2								
	UK	38/3-01	7	7								
		38/16-01				5			13			
		39/7-01	5	5						2	2	1
		41/20-01				24			2			
		41/24a-02	32	32		5	2		9	2	2	2
		42/10-01 / 42/10A-01	24	24		38			9	2	2	
		43/03-01				16						
		43/10a-01				26						
		43/17b-02				8			3			
		43/20b-02	7	7						2	1	
		43/2-01	12	12						1	1	
		44/02-01				17			8			
		44/07-01				4			3			
		44/16-01	11	11			1			1	1	1
		44/16-01Z	5	5						2	2	
		44/16-02	2	2			1					
		48/03-03				6			2			
Welton A5 oil									1	1	1	

Table B-3 Summary of the number of samples in Area 3/4 for the geochemical and organic petrological analyses

	Well	CS	Rock Eval			Vitrinite reflectance			TIC	SIM	IRMS	
			A	B	C	A	B	C				
Area 3/4	NL	EMO-01		13			5			4	4	3
		NAG-01		2	32			10				
		TJM-02			21			6				
		TJM-02-S1	6	7								
		WSK-01		14	5		3	2		1	1	
		SLO-01 (Reference sample of Zechstein Coppershale)								1	1	
	GE	MSTL-01	18			14			80	6	6	1
		SWLT-1001	16						89			

The digital database includes all duplo and triplo measurements of the different techniques that were used. Table B-4 summarises the number of data currently present in the database.

Table B-4 Number of analyses currently stored in the Petroplay database

Technique	Number of analyses
Leco CS	1106
Rock Eval	1488
Vitrinite reflectance	391
GC-MS (TIC of aliphatic and aromatic fraction)	101
GC-MS (SIM for biomarkers)	45
GC-IRMS (carbon and hydrogen stable isotope ratios of n-alkanes in condensates and extracts)	95
Total number of analyses	3226

Total organic carbon (TOC)

The total organic carbon (TOC) is one of the primary indicators of source rock quality. However, it should always be realized that TOC is a function of maturity: the TOC content decreases when petroleum is generated and expelled. Unfortunately, reconstruction of initial TOC value appeared to be difficult and relatively unreliable. This was due to the relative high maturity of many of the samples.

The present-day TOC is determined either with a Rock Eval analysis (TOC module) and/or with a Leco CS analysis. In cases of high sulfur contents (> 1.50 %S) the organic carbon content is determined only with the Leco CS.

The correlation of total carbon as resulting from the Rock Eval and the LECO analysis is plotted in Figure B-5. Although there is some deviation towards higher values, it can be concluded that the methods are complementary and in good agreement.

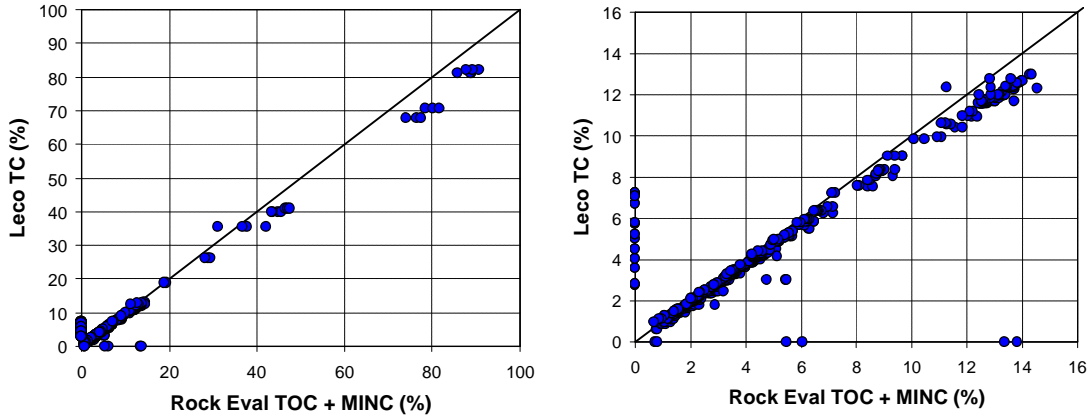


Figure B-5 Correlation between total carbon measured by Rock Eval and by LECO. Note the different scales in the left and right plots

Maturity indicators

Vitrinite reflectance is the most commonly applied maturity parameter in source rock evaluations. The quality of the measurement is strongly related to the ability to microscopically identify vitrinite particles in the sample. Vitrinite is a maceral that originates from the wood of land plants. Obviously, excellent reflectance values can be obtained from organic rich source rocks that were deposited in a terrigenous environment, such as coal in which vitrinite generally is the most abundant component. However, determination of vitrinite particles is often difficult in marine source rocks (type II kerogen). For Type II source rocks other (generally geochemical) maturity indicators are used. For this reason, several of these parameters have been evaluated (e.g. Tmax, Production Index, CPI, sterane and hopane isomerisation, ratios of methylphenantrenes).

It is obvious that any single parameter has its uncertainties and limitations in use. By using only one single technique for the determination of the level of maturity, especially when marine samples are concerned, a certain degree of uncertainty will remain. By using multiple indicators a more validated value for maturity can be obtained.

However, the use of most of the indicators was, for the purposes of this study, limited. Only vitrinite reflectance, Tmax and some of the methylphenantrene ratios were considered useful in the current project. The Tmax and the MPR are translated into so-called vitrinite reflectance equivalents by establishing correlation diagrams. For completeness, all evaluated maturity indicators are shortly addressed.

A (linear) correlation between measured vitrinite reflectance values and Tmax was established based on historic data from the Netherlands on- and offshore area (Fig. B-6). These (public-domain) historic data result from earlier studies, especially

from the TNO mapping projects of the deep subsurface. This dataset comprises analyses from samples from varying geological ages.

This relation between vitrinite reflectance and Rock Eval Tmax is approached by the following equation:

$$\%Rr = 0.0138 \times Tmax - 5.2$$

It must be noted that this relation varies to some extent from published values for other basins, e.g. Teichmüller & Durand (1983).

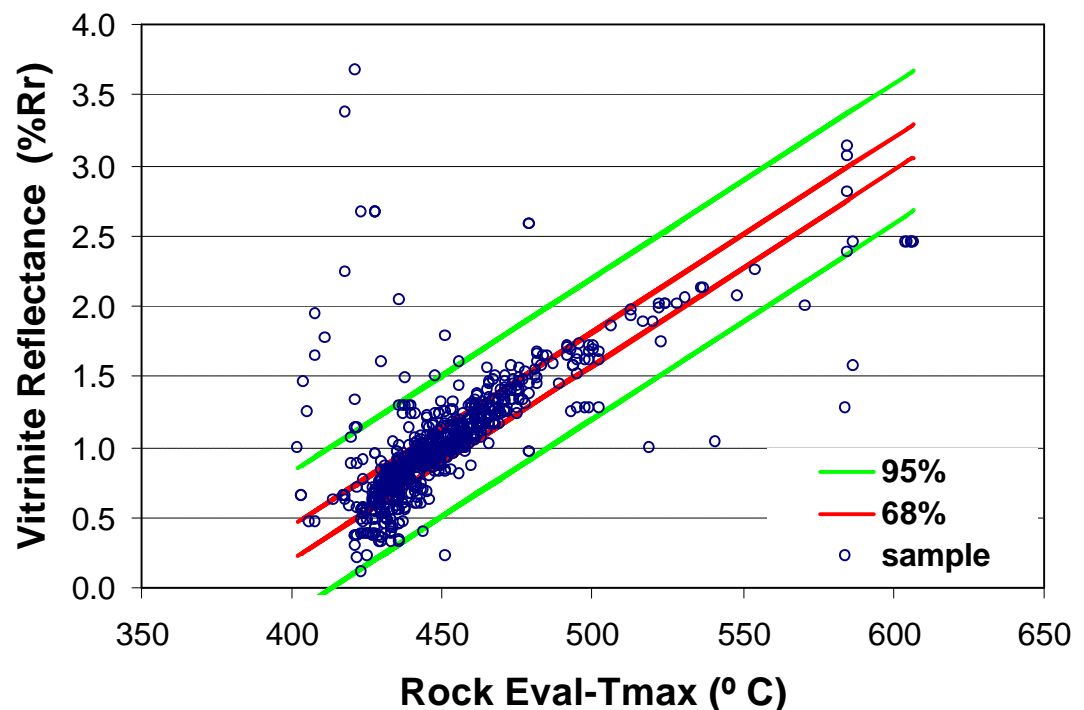


Figure B-6 Correlation between measured vitrinite reflectance and Tmax for samples from the Dutch subsurface. This figure also shows the 95% and 68% confidence intervals, i.e. the intervals that include, respectively 95% and 68% of the data points

The newly acquired Rock Eval data (A-label) allow for a more detailed data quality control. This is required because often the measurement as such is reliable, while the deduced parameters (especially Tmax) are not. In the maturity evaluation each pyrogram as derived from a Rock Eval analysis was checked with regard to the applicability of the Tmax value in the calculation of maturity trends. Some examples of this are given below. The first panel in Figure B-7 shows a pyrogram that will result in a highly reliable Tmax value (labeled “high reliability”), the pyrogram in the second panel will result in much less reliable Tmax values (labeled “low reliability”), and the data derived from the pyrogram in the third panel will be rejected (labeled “non reliability”). Other quality control procedures are described in Appendix A. The vitrinite reflectance equivalents as calculated from the Tmax values are reported in the digital database.

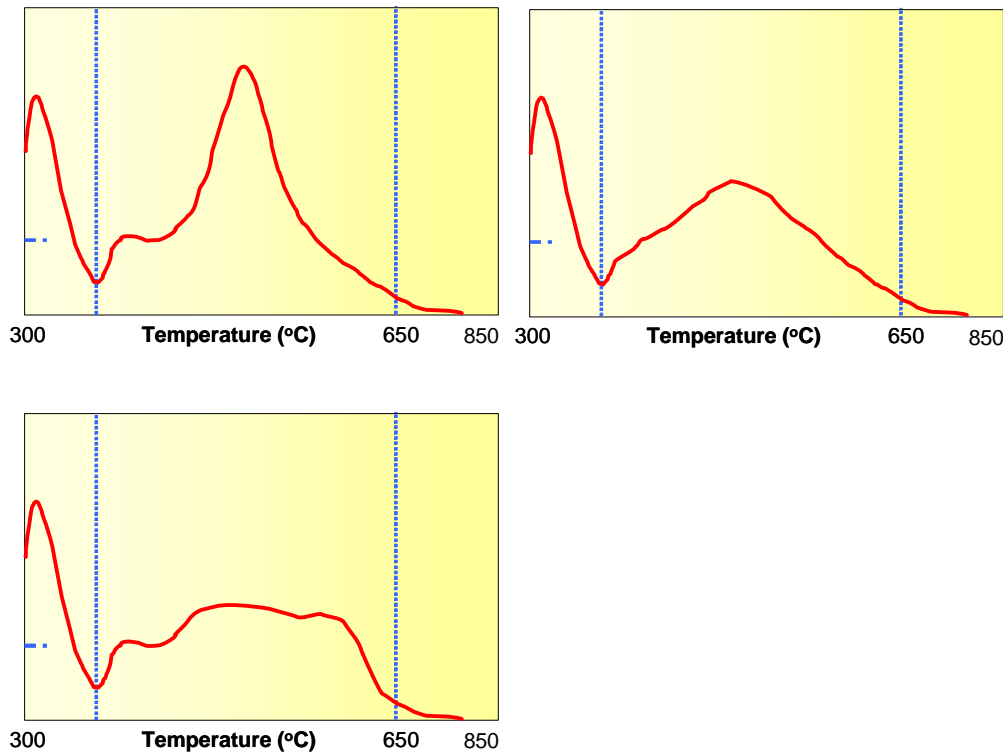


Figure B-7 Examples of pyrograms as derived from a Rock Eval analysis. Tmax values derived from the last panel are generally not used in the evaluation of maturity trends

The Production Index (PI), determined by $S1/(S1+S2)$, is a crude measure of thermal maturity derived from a Rock Eval analysis, that is also affected by other factors like type of organic matter (Peters *et al.*, 2005) or the presence of migrated hydrocarbons. An input of migrated oil to the source rock will increase the PI of that rock, because the impregnated hydrocarbons contribute to the S1 peak. Dependent on the amount of oil impregnated the PI can increase to nearly 1.00 due to this phenomenon. Impregnation of hydrocarbons in vitrinite can result in lower reflectance values. Further, care must be taken with source rocks that are expelling, because the S1 of these rocks does not further increase, and usually some S1 will remain as adsorbed dry gas, even in highly post mature rocks (Peters *et al.*, 2005).

According to Peters *et al.*, 2005 a PI less than about 0.10 indicates immature organic matter that has generated little or no petroleum. Peak oil generation occurs at a PI of 0.25, and the end of the oil window is reached at a PI of approximately 0.40 (Peters *et al.*, 2005; Miles, 1994). Further, Peters *et al.*, 2005 postulate that the PI increases from 0.40 to 1.00 when the hydrocarbon-generative capacity of the kerogen has been exhausted.

Historic data for the Netherlands onshore and offshore data can not exactly confirm the values for the indications of the oil window. However, a positive trend between maturity (Tmax) and Production Index is confirmed by these historic data. The use of the PI in this study appeared to be limited.

The Carbon Preference Index (CPI), as defined by Bray and Evans (1961), indicates preference of odd-numbered alkanes over even-numbered alkanes. The CPI can be correlated to maturity. With higher maturity the CPI approaches 1.0.

Two ratios of CPI are calculated:

$$\begin{aligned} \text{CPI(1)} &= 0.5 * \{[(nC25 + nC27 + nC29 + nC31 + nC33) / (nC24 + nC26 + nC28 + nC30 + nC32)] + [(nC25 + nC27 + nC29 + nC31 + nC33) / (nC26 + nC28 + nC30 + nC32 + nC34)]\} \\ \text{CPI (2)} &= 2 * nC29 / (nC28 + nC30) \end{aligned}$$

The use of the CPI in this study appeared to be limited.

Methylphenantrenes are methylated aromatic hydrocarbons, which occurrence in source rocks is almost independent on the type of organic matter. This characteristic makes methylphenantrene indices as maturity indicators very valuable for modelling of time-temperature history (Boreham et al., 1988). Another advantage is that they are present and can be measured in all source rocks. For this use various isomer ratios have been developed (e.g Radke *et al.*, 1980; Radke and Welte, 1983; Radke *et al.*, 1986; Radke, 1987; Radke *et al.*, 1990), such as the Methylphenanthrene Index (MPI-1 and MPI-2), the Methylphenanthrene Ratio (MPR), and the Methylphenanthrene Distribution Factor (MPDF). Although the indices are reported to be independent on the type of organic matter their correlations with vitrinite reflectance are only properly calibrated for Type III.

The Methyl Phenanthrene Index-1 (MPI-1) is defined as follows (Radke & Welte, 1983):

$$\text{MPI-1} = 1.5 * (2\text{MP} + 3 \text{MP}) / (\text{P} + 1\text{MP} + 9\text{MP})$$

where P is the concentration of phenanthrene and 2MP, 3MP, 1MP, and 9MP are the concentrations of 2-, 3-, 1-, and 9-methylphenanthrenes, respectively (Boreham *et al.*, 1988).

In several publications (Radke et al., 1982; Radke, 1988; Farrington et al., 1988) it is reported that the methylphenantrene index (MPI-1) is equivalent or superior to vitrinite reflectance as a maturity parameter in some field studies (Peters and Moldowan, 1993). The observed relationship between vitrinite reflectance and MPI-1 differs for different ranges of the vitrinite reflectance values, one for the range of 0.65-1.35 %Rr, and one for above 1.35 %Rr (Radke and Welte, 1983). Boreham *et al.* (1988) could extend the relation, although slightly different in their case, to levels of lower maturation (0.50 %Rr).

The Methyl Phenanthrene Index - 2 (MPI-2) is defined as follows (e.g. Radke *et al.*, 1982):

$$\text{MPI 2} = 3 * (2\text{MP}) / (\text{P} + 1\text{MP} + 9\text{MP})$$

where P is the concentration of phenanthrene and 2MP, 1MP, and 9MP are the concentrations of 2-, 3-, 1-, and 9-methylphenanthrenes, respectively.

The Methyl Phenanthrene Ratio (MPR) is the ratio between the concentrations of 2- and 1-methylphenanthrene (e.g. Radke *et al.*, 1982). A relation between MPR and vitrinite reflectance was determined, based on historic data from the Netherlands

on- and offshore area. These relations were validated up to circa 1.5 % vitrinite reflectance.

Figure B-8 shows that the MPR data of the analysed samples plot fairly well in the 95% confidence level (blue line). The relation between vitrinite reflectance and MPR is fairly good until 1.5 % vitrinite reflectance. Above this value (thus above an MPR of approximately 3) there is apparently another relation. A similar change in relationships above certain values is known in literature for the MPI-1 (see above). The MPR proved to be a strong maturity indicator in this study.

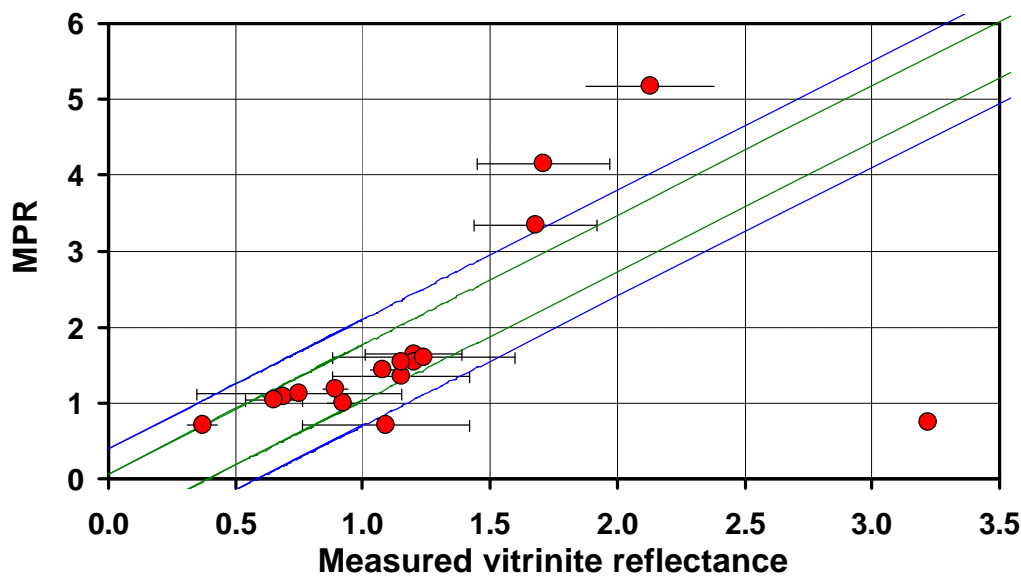


Figure B-8 Correlation between vitrinite reflectance and MPR as extracted from the TNO database (historic data)

The Methyl Phenanthrene Distribution Factor (MPDF) is defined as follows:

$$\text{MPDF} = (2\text{MP} + 3\text{MP}) / (1\text{MP} + 2\text{MP} + 3\text{MP} + 9\text{MP})$$

where 1MP, 2MP, 3MP, and 9MP are the concentrations of 1-, 2-, 3-, and 9-methylphenanthrenes, respectively (Kvalheim, 1987).

A good correlation can also be demonstrated between MPDF and measured vitrinite reflectance, see Figure B-9. From the historic data of the Netherlands on- and offshore it is known that there is a stable value of around 0.50 up to a vitrinite reflectance of 1.0 %Rr. Figure B-9 shows that the MPDF increases at higher maturities. However, no historic data and therefore no relation is yet available for higher maturities. Figure B-10 shows a strong correlation between MPDF and the MPR.

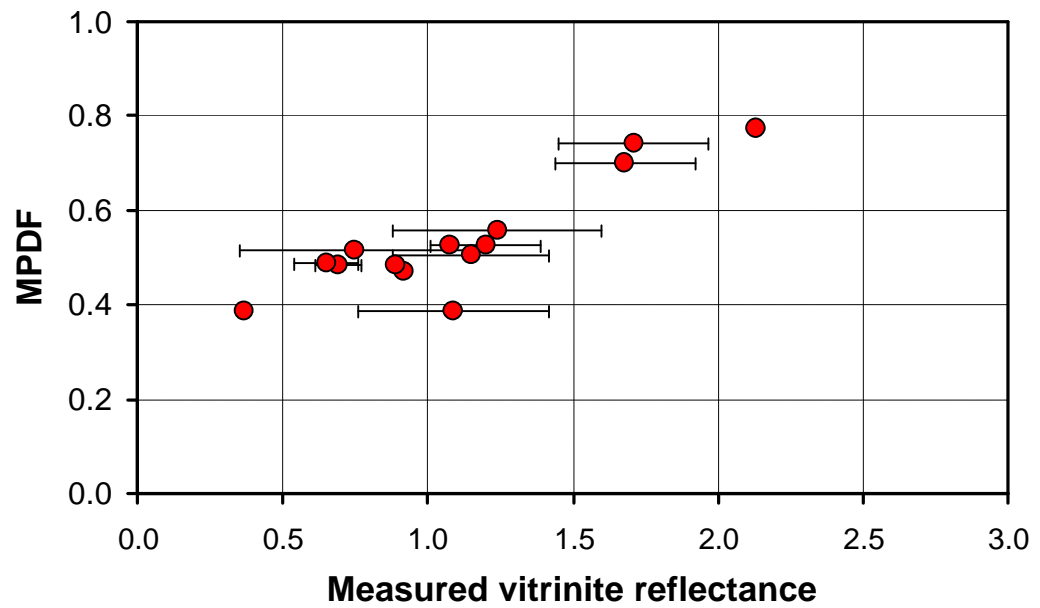


Figure B-9 Correlation between measured vitrinite reflectance (%Rr) and MPDF

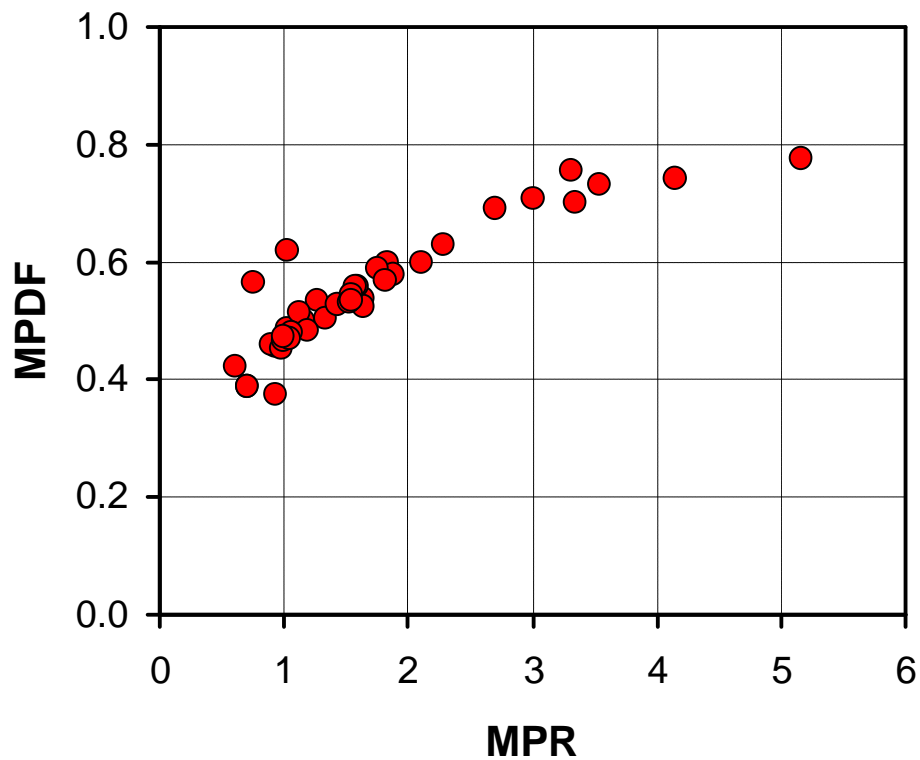


Figure B-10 Correlation between MPDF and MPR

The natural, although thermally not the most stable, configuration of hopanes is 17β(H), 21β(H), 22(R). During diagenesis (thermal stress), isomerisation occurs, which mainly

forms 17 β (H), 21 β (H) and to a lesser extent 17 β (H), 21 α (H) hopanes. Further, although much slower, isomerisation occurs at C₂₂, until equilibrium is reached between 22(R) and 22(S) isomers. The 22(R) configuration of the biological precursor of hopane is gradually converted to a mixture of 22(R) and 22(S) diastereomers. In the range C₃₁ to C₃₅ these are called homohopanes (Peters *et al.*, 2005).

The homohopane isomerisation is used to define the maturity of the source rocks. Because this isomerisation occurs earlier (during diagenesis) than the isomerisation of many other biomarkers it is highly specific for the immature to early mature stages of oil generation (Peters *et al.*, 2005). After reaching the equilibrium at the stage of early oil generation, no further maturity information can be derived from these ratios because the 22S / (22S + 22R) ratio remains constant. Schoell *et al.* (1983) showed that equilibrium for the C₃₂ hopanes occurs at a vitrinite reflectance of approximately 0.50 %Rr in the Mahakam Delta rocks (Peters *et al.*, 2005). The inflection point can be used to calibrate the onset of oil generation (Tissot and Welte, 1984; Püttmann *et al.*, 1988; Peters *et al.*, 2005). According to Peters *et al.* (2005) typically the C₃₁- or C₃₂-homohopane ratios are used, which rise from 0.0 to about 0.6. They report values of 0.50 to 0.54 to indicate immature source rocks, whereas values from 0.57 to 0.62 indicate that the main phase of oil generation has been reached or surpassed.

The epimer ratios increase slightly for the higher homologs from C₃₁ to C₃₅. Zumberge (1987) calculated the average equilibrium ratio for low maturity oils at C₃₁, C₃₂, C₃₃, as 0.55, 0.58, and 0.60, respectively (Peters *et al.*, 2005).

Historic data from the Netherlands onshore and offshore area show a fairly large scattering, but still a trend towards equilibrium of circa 0.60 - 0.65 can be observed in these data.

A maturity parameter that can also be used in the post mature range is the ratio between C₂₇ 17 α (H)-trisorhopane (Tm or 17 α (H)-22,29,30-trisorhopane) and C₂₇ 18 α (H)-trisorhopane II (Ts or 18 α (H)-22,29,30-trisorhopane). Because Tm shows lower relative stability during catagenesis (Peters *et al.*, 2005), the Ts/Tm ratio increases with increasing maturity.

Caution must be taken using the ratio, because it is also source-dependent. Further, Tm and Ts commonly co-elute with tricyclic or tetracyclic terpanes on the m/z 191 mass chromatogram, resulting in spurious ratios (Peters *et al.*, 2005). According to Peters *et al.* (2005) the Ts/(Ts + Tm) ratio is most reliable as a maturity indicator when evaluating oils from a common source with a consistent organic facies. The use of the hopane isomerisation in this study appeared to be limited, mostly due to the high maturity of most of the samples.

Several other maturity indicators based on sterane ratios were calculated and plotted, e.g. the diasterane index (Eckardt, 1989; Püttmann and Schaefer, 1989; 1990; Peters *et al.*, 2005), and the diasterane/diasterene ratio (e.g. Püttmann *et al.*, 1988). However, these evaluations were considered invalid for the investigation of the selected mostly high mature samples.

Analytical data

By using the relations described above, the maturity for each individual sample was calculated and translated into vitrinite reflectance equivalents. The results of the maturity analyses will be presented as maturity vs. depth trends in the next section. In the tables below an overview is given of the maturity resulting from these trends, subdivided into the three investigated areas. Additionally, for each stratigraphic unit the averaged total organic carbon content is given.

Table B-5 Maturity (%Rr) of Devonian potential source rocks. The Rock Eval analyses on seven samples from the Devonian interval of well 38/03-01 yielded unreliable maturity data, most likely due to the low TOC content or because they were an additive. No vitrinite reflectance measurements were carried out on this material.

Area	Well	Devonian	Remark
1	BHG-01	1.5 - 2.0	Deviations from maturity trend present
	O18-01	2.5 – 3.0	Possible coalification jump at the top of the Devonian
	S02-02	1.8 – 2.0	Wide scatter of maturity data
	S05-01	1.8 – 2.0	
	Leuze	X	Data scatter
	Nieuwkerke	X	Data scatter
	Tournai	X	Data scatter
	Total range	1.5 – 3.0	
2	38/03-01	X	No reliable maturity data
	A17-01	0.7 – 1.0	Maturity data unreliable
	E02-01	0.8 – 1.5 (?)	Maturity trend not well-established, maturity value based on extrapolation from post-Devonian
	E06-01	0.9 – 1.1	Intrusion present, maturity value based on trend without intrusion
		Total range	0.7 – 1.5
3 / 4	WSK-01	> 4.0	
	MSTL-01	~ 4.5	
		Total range	> 4.0

Table B-6 Maturity (%Rr) of Dinantian potential source rocks

Area	Well	Dinantian	Remark
1	GVK-01	> 3.0	
	BHG-01	1.2 - 1.5	Deviations from maturity trend present
	O18-01	1.0 – 1.5	
	P16-01	>1.0	Apparent coalification jump at the top of the Dinantian
	S02-02	1.0 – 2.0	Wide scatter of maturity data
	S05-01	1.0 – 1.5	
	53/12-02	0.7 – 1.3	
	Halen	X	Data scatter, probably high maturity
	Leuze	X	Data scatter, probably high maturity
	Rollegem-Tombroek	0.5 – 1.0	
	's Gravenvoeren	X	
	Tournai	? 0.3	Probably high maturity
	Wervik	0.5 – 1.0	
	Total range	0.8 – 2.0	
2	38/16-01	0.6-1.0	
	39/07-01	0.8 – 1.0	
	41/20-01	2.6 - ?	
	41/24a-02	1.2 – 2.0	Deviations from maturity trend present
	42/10a-01	0.7 – 1.0	
	43/02-01	0.6 – 1.1	
	43/17b-02	>2.5	
	44/02-01	0.4 – 1.0	
	A14-01	0.6 – 0.8	Intrusion present
	A16-01	0.5 – 0.8	
	E02-01	0.8 – 1.3	Maturity trend not well-established
	E02-02	0.6 – 0.7	
	E06-01	0.8 – 0.9	Intrusion present
	E12-02	1.3 – 1.4	
Total range	0.5 – 2.0		
3 / 4	WSK-01	> 4.0	
	MSTL-01	~ 4.5	
	SWLT-1001	> 4.5	
	Total range	> 4.0	

"Hydrocarbon potential of the Pre-Westphalian in the Netherlands on- and offshore"

Table B-7 Maturity (%Rr) of Top Dinantian – Base Namurian potential source rocks

Area	Well	Top Dinantian / Base Namurian	Remark
1	GVK-01	~ 3.0	
	BHG-01	~ 1.2	Deviations from maturity trend present
	O18-01	~ 1.0	
	P16-01	~ 1.0	
	Beerse-Merksplas	X	Probably high maturity
	Booischoot	X	Probably high maturity
	DZH-01-Heibaart	X	Probably high maturity
	Turnhout	X	Data scatter
	Total range	1.0 – 3.0	
2	A14-01	~ 0.6	Intrusion present, maturity based on trend without intrusion
	E02-01	~ 0.8	Maturity trend not well-established
	E12-02	~ 1.3	
	39/07-01	~ 0.8	
	41/20-1	~ 2.6	
	41/24a-02	~ 1.2	Deviations from maturity trend present
	43/03-01	0.8 – 1.0	
	43/10a-01	0.5 – 1.0	
	43/17b-02	~ 2.5	
	44/16-01	1.6 – 2.0	
	Total range	0.5 – 2.5	
3 / 4	WSK-01	4.0 – 4.5	
	TJM-02	~ 4.5	
	NAG-01	~ 4.5	
	MSTL-01	~ 4.5	
	SWLT-1001	~ 4.5	
Total range	4.0 – 4.5		

Table B-8 Maturity (%Rr) of Namurian potential source rocks

Area	Well	Namurian	Remark
1	GVK-01	2.3 – 3.0	
	BHG-01	0.5 – 1.2	Deviations from maturity trend present
	O18-01	0.8 – 1.0	
	P10-01	~ 1.0 – ?	
	P16-01	0.8 – 1.0	Based on extrapolation
	Q13-03	> 1.0	Based on extrapolation
	RSB-01	1.8 – 5.0	Deviations from the maturity trend present
	S02-02	0.8 – 1.5	Wide scatter of maturity data
	Beerse-Merksplas	X	Probably high maturity
	Halen	X	Probably high maturity
	Meer	~ 3 – 4	
	Rijkevorsel	X	Probably high maturity
	Turnhout	? 2-4	Data scatter, probably high maturity
	Total range	0.5 – 5.0	
2	39/07-01	0.6 – 0.8	
	41/20-01	1.7 – 2.6	
	41/24a-02	0.8 – 1.2	Deviations from maturity trend present
	43/17b-02	1.0 – 2.5	
	43/20b-02	1.0 – 2.0	No maturity trend established
	44/16-01	1.2 – 2.0	
	44/16-02	1.0 – 1.6	
	44/16-1Z	1.0 – 2.0	
	48/03-03	1.0 – 2.0	
	A11-01	1.0 – 1.2	
	A14-01	0.5 – 0.6	Intrusion present
	E02-01	0.7 – 0.8	Maturity trend not well-established
	E12-02	0.9 – 1.3	
	E12-03	1.0 – 1.2	
Total range	0.5 – 2.6		
3 / 4	EMO-01	> 1.8	
	NAG-01	1.0 – 4.5	Intrusion present, maturity based on trend without intrusion
	WSK-01	2.2 – 4.0	
	TJM-02	1.5 – 4.5	
	MSTL-01	2.0 – 4.5	
	SWLT-1001	3.0 – 4.5	
	Total range	1.0 – 4.5	

Table B-9 TOC values of the Devonian from geochemical analyses.

Area	Stratigraphy	Well	Depth interval [m]	Sample type	Minimum	Median	Maximum	No. of samples	Remark
1	Bollen Claystone Mb.	BHG-01	2660 - 2888	CU	0.69	1.89	2.88	4	Outlier of 18,99% (B) deleted, (analytical error as confirmed by duplo measurement)
		S02-02	2878	CU		0.20		1	
		S05-01	2018 - 2225	CU CO	0.14	0.58	0.92	13	
	Bosscheveld Mb.	BHG-01	2890 - 2892	CU		2.23		1	
		S05-01	2000 - 2005	CU	0.46	0.54	0.61	2	
	Devonian undiff.	Tournai	359	CO		0.15		1	
	Devonian undiff.	Leuze	658	CO		0.25		1	
	Devonian undiff.	Nieuwkerke	207 - 216	CO	0.43	0.42	0.52	3	
Devonian total					0.14	0.54	2.88	26	
2	Devonian undiff.	38/3-1	3082 - 3657	CO CU	0.03	0.28	0.39	6	Organic matter probably contamination, see textbox
	Devonian undiff.	A17-01	2136 - 2920	CU	0.54	1.51	5.79	6	
	Devonian total					0.03	0.18	5.79	12
3&4	Devonian undiff.	WSK-01	4602 - 4980	CU	0.28	0.67	1.06	8	
	Devonian undiff.	MSTL-	5930	CO		0.51		1	
	Devonian total					0.28		1.06	9

Table B-10 TOC values of the Dinantian from geochemical analyses. The relatively very high maximum values in the table (4.27 and 16.88) are both historic data "B" which were thus not measured according to current protocols.

Area	Stratigraphy	Well	Depth interval [m]	Sample type	Minimum	Median	Maximum	No. of samples	Remark	
1	Zeeland Fm., Member not identified	P16-01	2455 - 2464	CU	0.41	0.95	2.01	7		
		53/12-02	1890 – 2268	CU	1.58	2.13	2.18	3		
	Beveland Mb.	Brouwershavensgat-01	2362 - 2526	CU	0.41	1.32	4.78	7		
		S02-02	2650 – 2775	CU	0.19	0.77	1.63	3		
		S05-01	1792 - 1990	CU CO	0.07	0.75	2.32	27		
	Schouwen Mb.	S02-02	2155 - 2565	CU	0.20	0.37	0.60	4		
		S05-01	1233 - 1679	CU CO	0.17	0.60	1.10	11		
	Goeree Mb.	Brouwershavensgat-01	2190 - 2252	CU	1.15	1.44	1.77	4	Outlying (C) value of 47.12% deleted	
		Geverik-01	1000 - 1325	CU CO	0.03	1.24	16.96	18		
		O18-01	1601 – 1603	CO	0.05	0.09	0.15	9		
		S02-02	1890 - 2045	CU CO	0.40	0.55	1.51	6		
	Dinantian undiff.	s' Gravenvoeren	363 – 842	CO	0.15	0.21	0.26	2		
		Rijkevorsel	1324 – 1335	CU	0.24	1.28	2.32	2		
	Dinantian – Visean	Leuze	189 – 240	CO	0.40	0.90	2.38	3		
	Dinantian – Tournaisian	Leuze	395 – 617	CO	0.65	0.79	0.96	4		
		Tournai	65 – 269	CO	0.39	0.61	1.06	7		
		Rollegem-Tombroek	147 – 167	CO	0.60	0.77	9.73	3		
		Wervik-1	173 – 179	CO	1.05	1.47	1.84	4		
	Dinantian total					0.03	0.60	16.96	124	

Table B-10 (continued)

Area	Stratigraphy	Well name	Depth interval [m]	Sample type	Minimum	Median	Maximum	No. of samples	Remark
2	Dinantian undiff.	41/20-01	3379 - 3451	CU	0.02	1.39	4.70	7	
	Dinantian undiff.	43/03-01	3078 - 3157.7	CU	0.78	1.62	1.90	8	
	Dinantian undiff.	43/10A-01	2822 - 2982	CU	0.02	3.36	19.90	15	
	Dinantian undiff.	44/2-1	2789 - 3453	CU	0.04	0.55	30.49	16	
	Dinantian undiff.	44/7-1	2981 - 3018	CU	3.27	5.79	8.66	4	
	Dinantian undiff.	48/3-3	3795	CU		3.34		1	
	Yoredale	41/24a-2	2452 - 3052	CU CO	1.29	2.12	3.94	11	partly Yoredale
	Yoredale	39/7-1	3349 - 3593	CU	0.33	20.20	23.33	5	
	Yoredale	42/10a-1	2502 - 2992	CU CO	0.15	2.74	57.16	40	
	Yoredale	A16-01	2442 - 2685	CU	0.42	0.80	8.82	33	
	Yoredale	E02-01	2134 - 2350	CU	0.23	0.88	2.81	26	
	Yoredale	E02-02	2355 - 2648	CU	0.40	1.37	4.58	58	
	Yoredale	E06-01	2230 - 2710	CU	0.02	0.68	2.25	17	
	Yoredale	43/2-1	2908 - 2996	CU CO	0.77	4.17	68.18	12	Deepest samples are Scremerton
	Yoredale	A14-01	2820 - 3010	CU	0.19	1.59	3.26	14	
	Dinantian total				0.02	1.68	68.18	267	
3&4	Dinantian undiff.	SWLT-1001	1763 - 1769	CO	0.06	3.48	8.73	11	
		WSK-01	4434	CU		0.11		1	
		Dinantian total			0.06	3.25	8.73		

Table B-11 TOC values of the Top Dinantian- Base Namurian from geochemical analyses

Area	Stratigraphy	Well	Depth interval [m]	Sample type	Minimum	Median	Maximum	No. of samples	Remark
1	Geverik Mb.	Brouwershavensgat-01	2124	CU		2.08		1	
		Geverik-01	937 - 988	CO CU	1.99	3.71	6.66	6	Outlying (B) value of 65.59% deleted, probably due to analytical error
		P16-01	2335 - 2450	CU	1.51	2.42	4.97	29	
	Top Dinantian – Base Namurian	Beerse-Merksplas	1611 – 1627	CU	0.22	1.76	3.52	4	
		Turnhout	2143 – 2175	CO	0.28	4.94	12.12	13	
		DZH-01-Heibaart	1061 – 1100	CO	0.67	1.15	2.49	5	
		Booischoot	510 – 525	CO	0.08	0.29	1.35	3	
	Top Din / Base Nam. total					0.08	3.89	12.12	61
2	Base-Namurian	44/16-1	4567 - 4568	CO	0.21	0.28	0.34	2	
		44/16-2	4345 - 4353	CO	2.05	2.49	2.93	2	
	Base Namurian / top Dinantian	43/17B-02	4420 - 5584	CO	2.56	3.85	5.26	6	
		43/10A-01	2672 - 2818	CO	0.39	2.43	5.86	11	
	Dinantian-Bowland	41/24a-2	2454 - 2500	CO	1.76	3.51	4.43	21	
	Top-Dinantian	43/03-01	2969 - 3063	CO	0.17	1.25	5.96	8	
	Top Din / Base Nam. total					0.17	3.03	5.96	50
3&4	Base-Namurian	NAG-01	4228 - 4298	CO	0.53	0.61	0.97	5	
		SWLT-1001	1593 - 1638	CO	2.37	4.10	6.17	8	
		TJM-02 / TJM-02-S1	5808 – 6010	CU CO	1.27	1.83	3.43	4	
		MSTL-01	5388 – 5484	CU	1.34	4.79	5.57	5	
		WSK-01	4232 – 4282	CU CO	1.42	2.41	6.07	5	
	Top Din / Base Nam. total					0.53	3.41	6.17	27

N.B.: The organic rich deposits of the Geverik Mb. should not be confused with the black cherts towards the top of the Goeree Mb. These black cherts, considered to be erosional residues, often look like source rocks by their color, but have in fact a very low TOC value. This was recently shown by Rock Eval analysis of samples from a groundwater well that encountered the top of the Dinantian in Zuid-Limburg. The Geverik Mb was not encountered in this well.

Table B-12 TOC values of the Namurian from geochemical analyses

Area	Stratigraphy	Well	Depth interval [m]	Sample type	Minimum	Median	Maximum	No. of samples	Remark	
1	Epen Fm.	Brouwershavensgat-01	1595 - 2070	CU	0.77	1.13	1.59	6		
		Geverik-01	422 - 925	CU CO	0.23	0.68	4.05	27		
		P16-01	2075 - 2320	CU	1.06	1.43	4.57	14		
		Rijsbergen-01	2704 - 4266	CU	0.99	1.98	25.90	7		
	Intra-Namurian	Halen	366 - 952	CO CU	0.12	0.78	1.75	17		
		Meer	2250 - 2513	CU	0.82	0.87	1.02	6		
		Beerse-Merksplas	1295 - 1611	CU	0.40	0.97	1.88	7		
		Rijkevorsel	1085 - 1320	CU	0.50	0.92	2.29	9		
		Turnhout	1669 - 2140	CO	0.53	0.95	8.49	11		
	Namurian total					0.12	1.19	25.90 (8.49)	104	
	2	Intra-Namurian	41/20-01	3015 - 3026	CU	0.37	1.27	2.22	5	
43/17B-02			3459 - 3962	CU	3.00	3.39	3.78	2		
43/20b-2			3806 - 4396	CO	1.21	1.31	2.65	3		
44/16-1			4267 - 4279	CO	0.78	1.98	2.42	9		
44/16-1Z			4328 - 4346	CO	2.04	2.79	72.07	5		
48/03-03			3795 - 4584	CU	3.02	5.60	14.99	5		
E12-03			3506 - 3865	CO CU	0.89	1.89	7.22	14		
Namurian total					0.37	2.16	72.07	43		
3&4	Intra-Namurian	WSK-01	3404 - 3507	CU CO	0.39	0.90	2.42	4		
		TJM-02 / TJM-2-S1	3976 - 5718	CU	0.31	0.82	66.46	22		
		SWLT-1001	843 - 1526	CU CO	0.91	1.06	2.34	5		
		NAG-01	2145 - 4174	CO CU	0.31	1.02	2.55	26		
		MSTL-01	2918 - 5106	CU	1.09	1.57	77.15	8		
Namurian total					0.31	1.14	77.15	65		

B3 Maturity trend evaluation of wells

Maturity vs. depth curves were made for the selected key wells by plotting actual vitrinite reflectance values and vitrinite reflectance equivalents as derived from the other maturity indicators on the well logs.

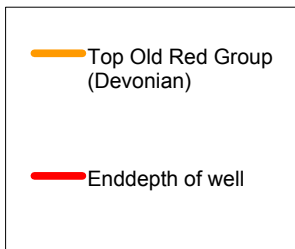
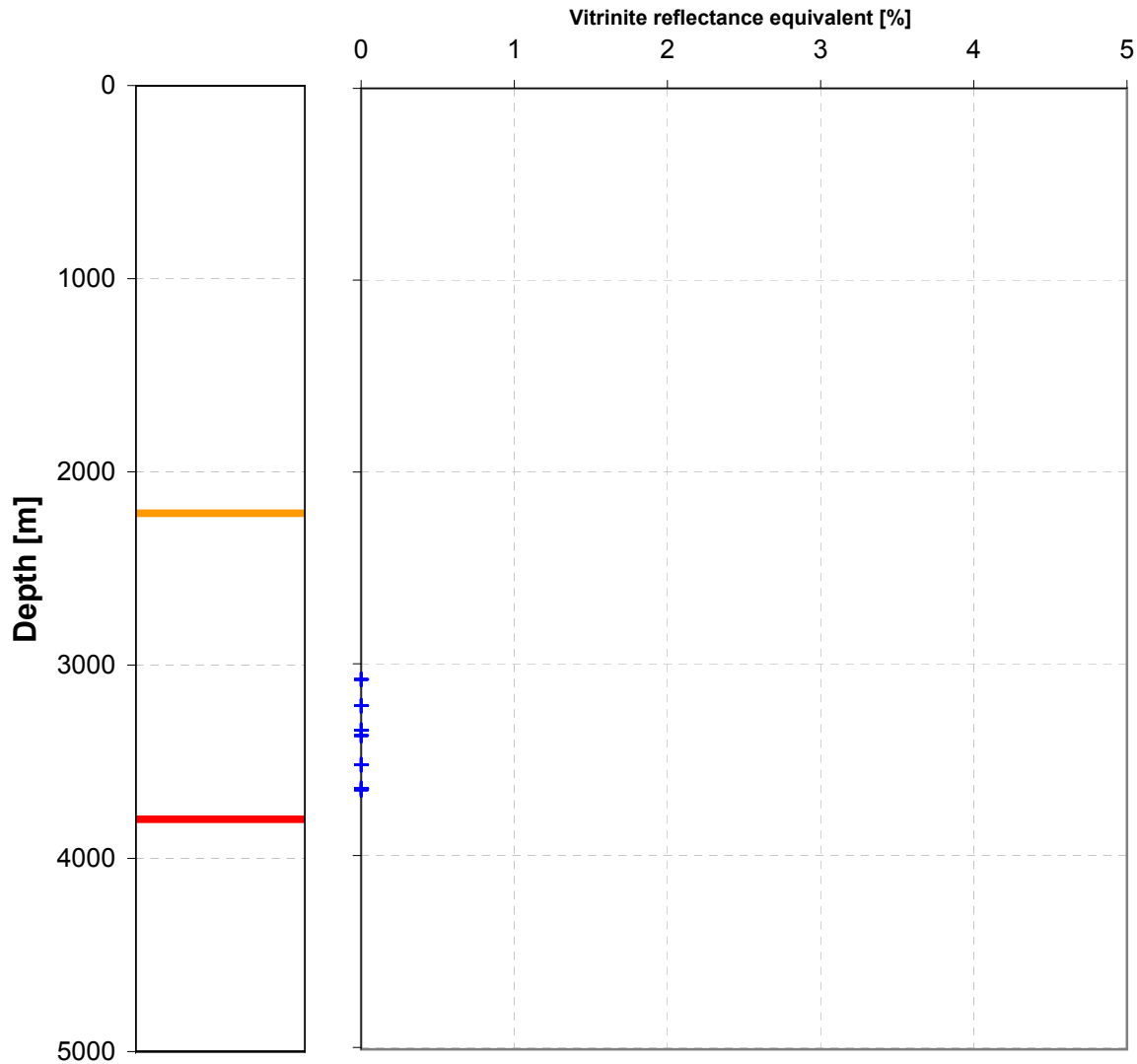
The following pages show these plots.



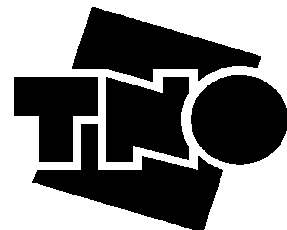
Joint Industry Project Petroplay

Quality controlled data

38/03-01



- A) Vitrinite reflectance
- B) Vitrinite reflectance
- C) Vitrinite reflectance
- B) Tmax-VR equivalent
- C) Tmax-VR equivalent
- A1) Tmax-VR equivalent - highly reliable
- ◆ A2) Tmax-VR equivalent - low reliability
- + samples

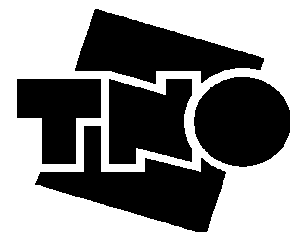
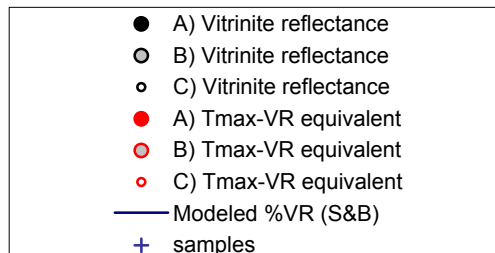
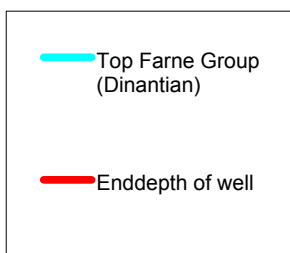
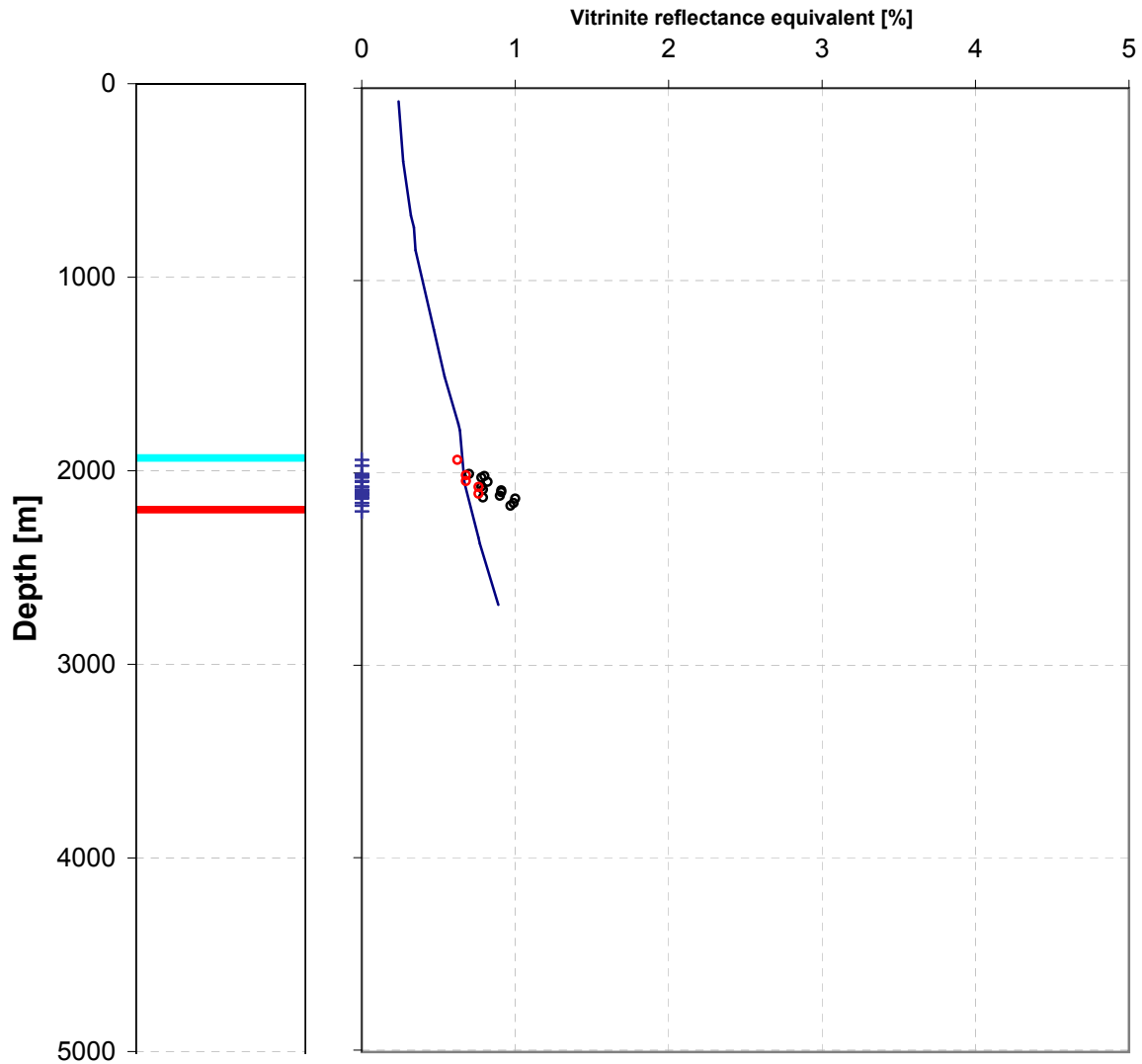




Joint Industry Project Petroplay

Raw data

38/16-01

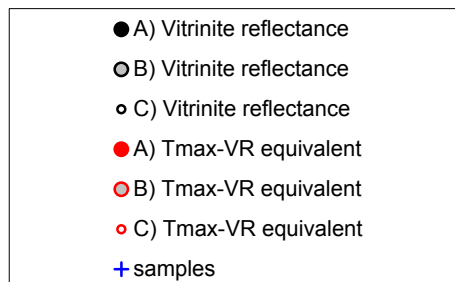
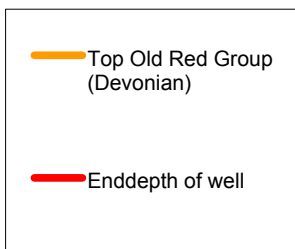
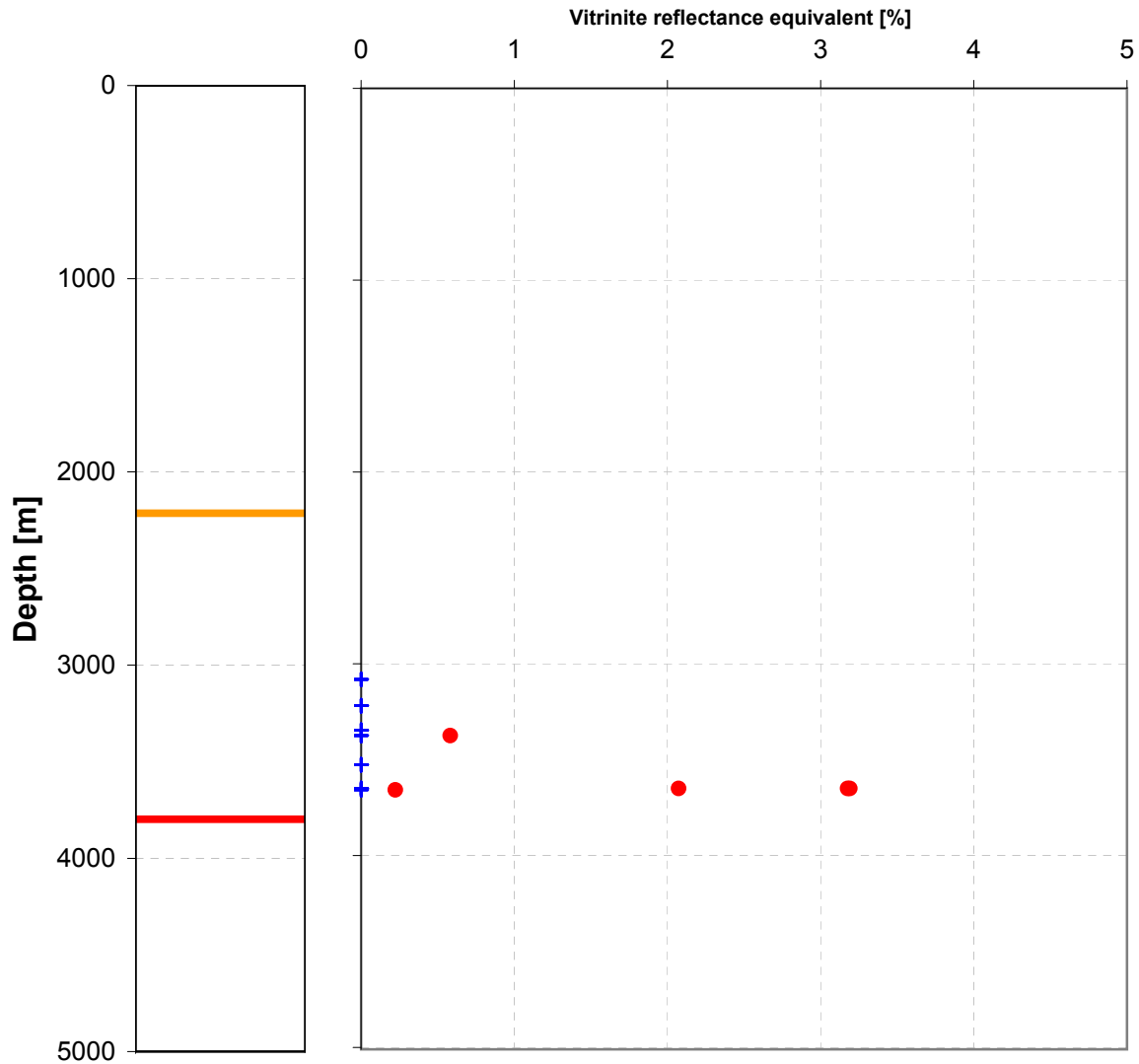




Joint Industry Project Petroplay

Raw data

38/03-01

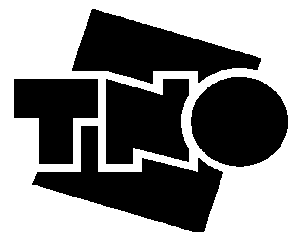
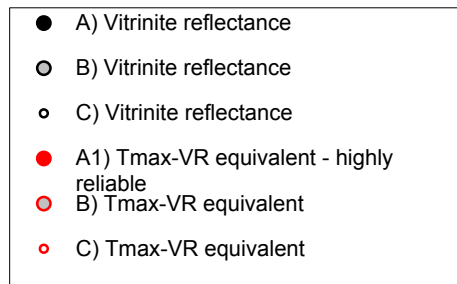
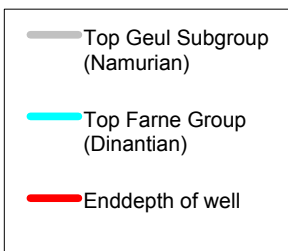
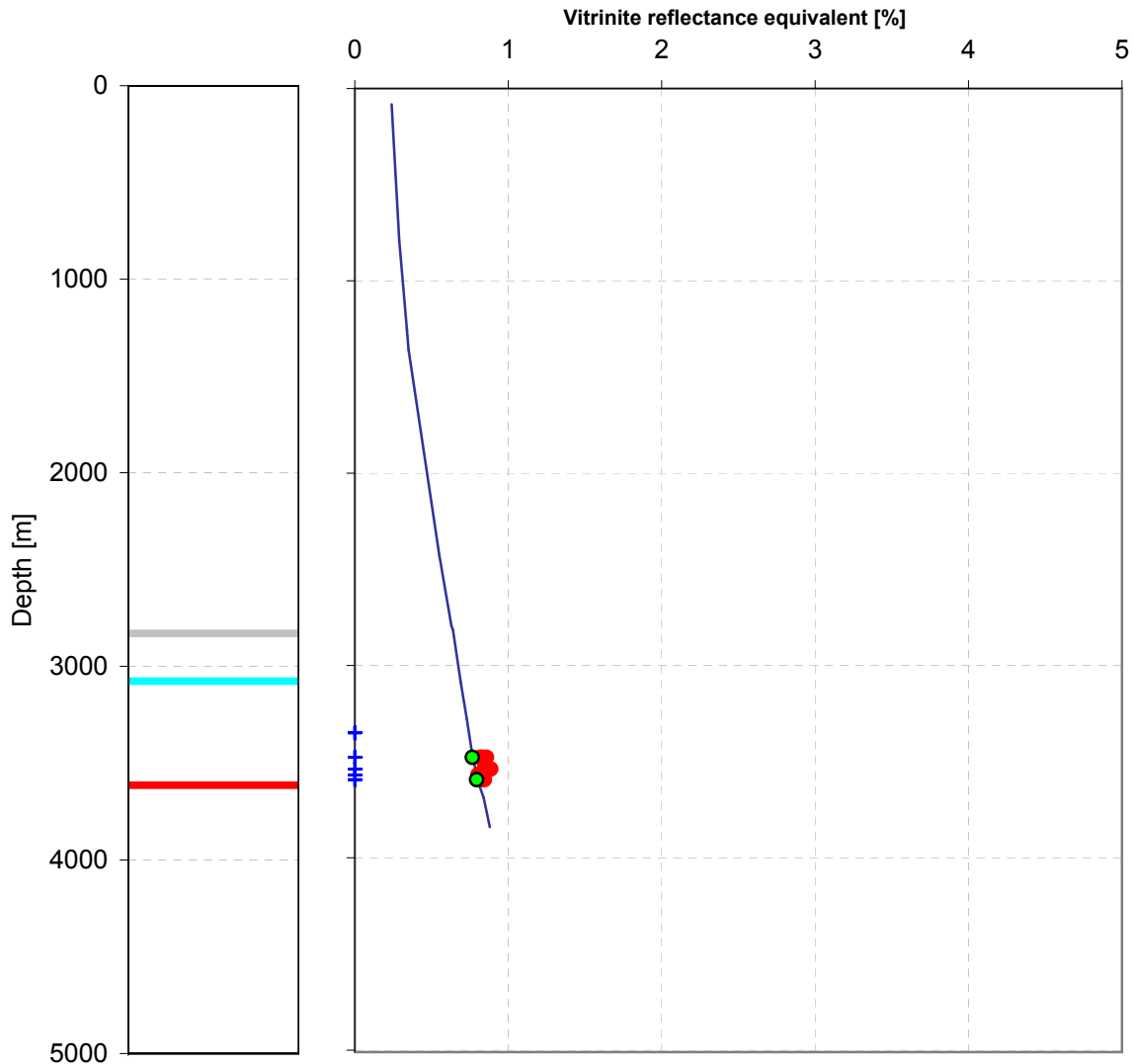




Joint Industry Project Petroplay

Quality controlled data

39/07-01

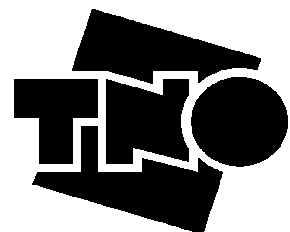
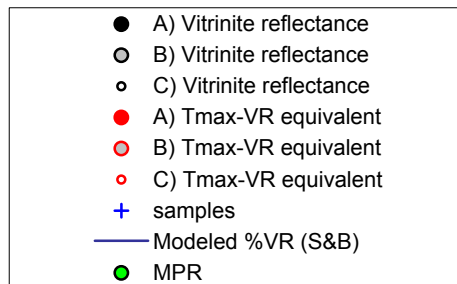
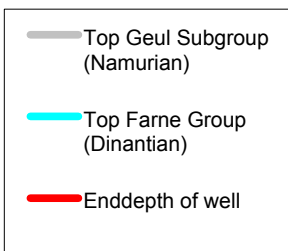
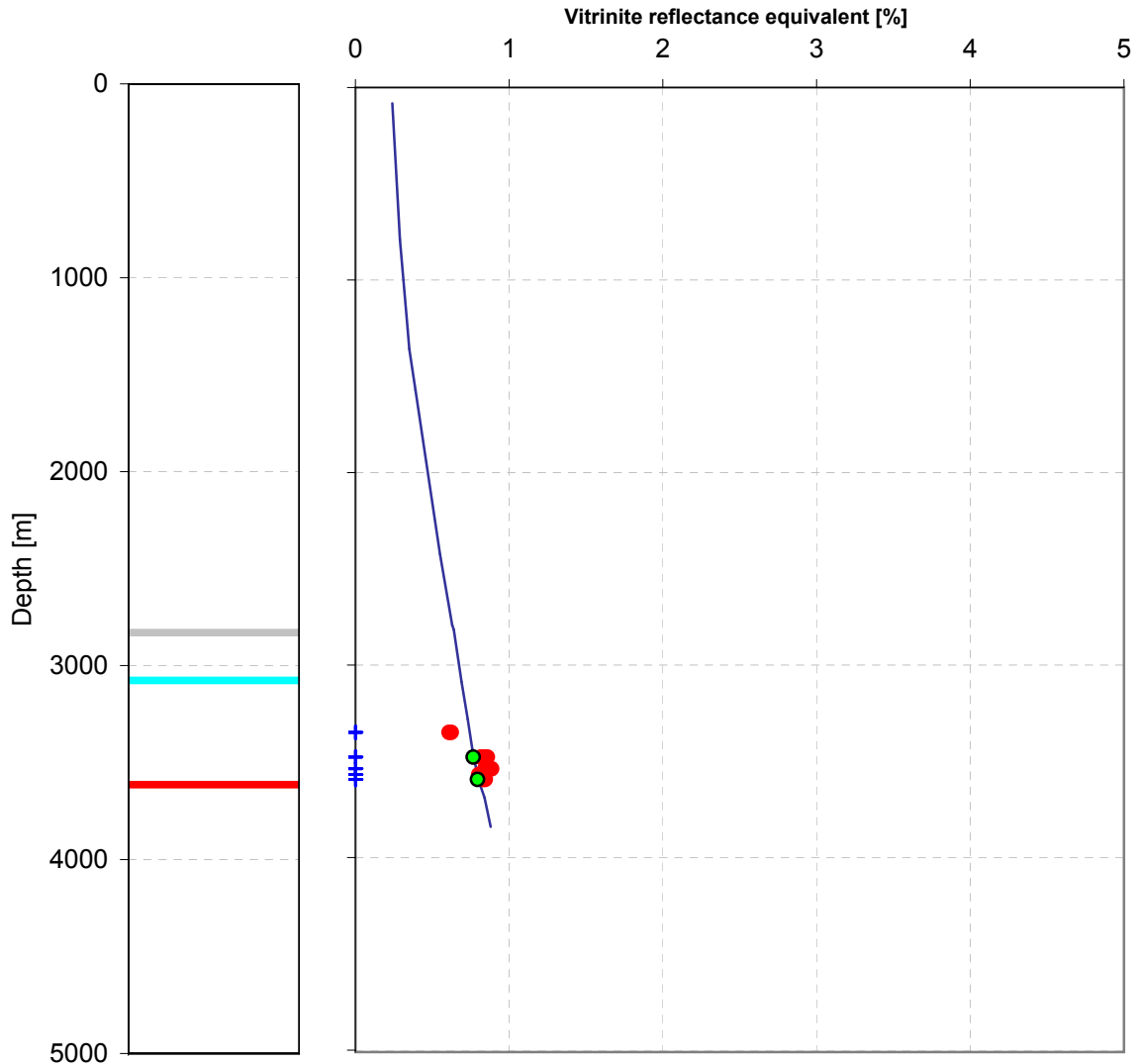




Joint Industry Project Petroplay

Raw data

39/07-01

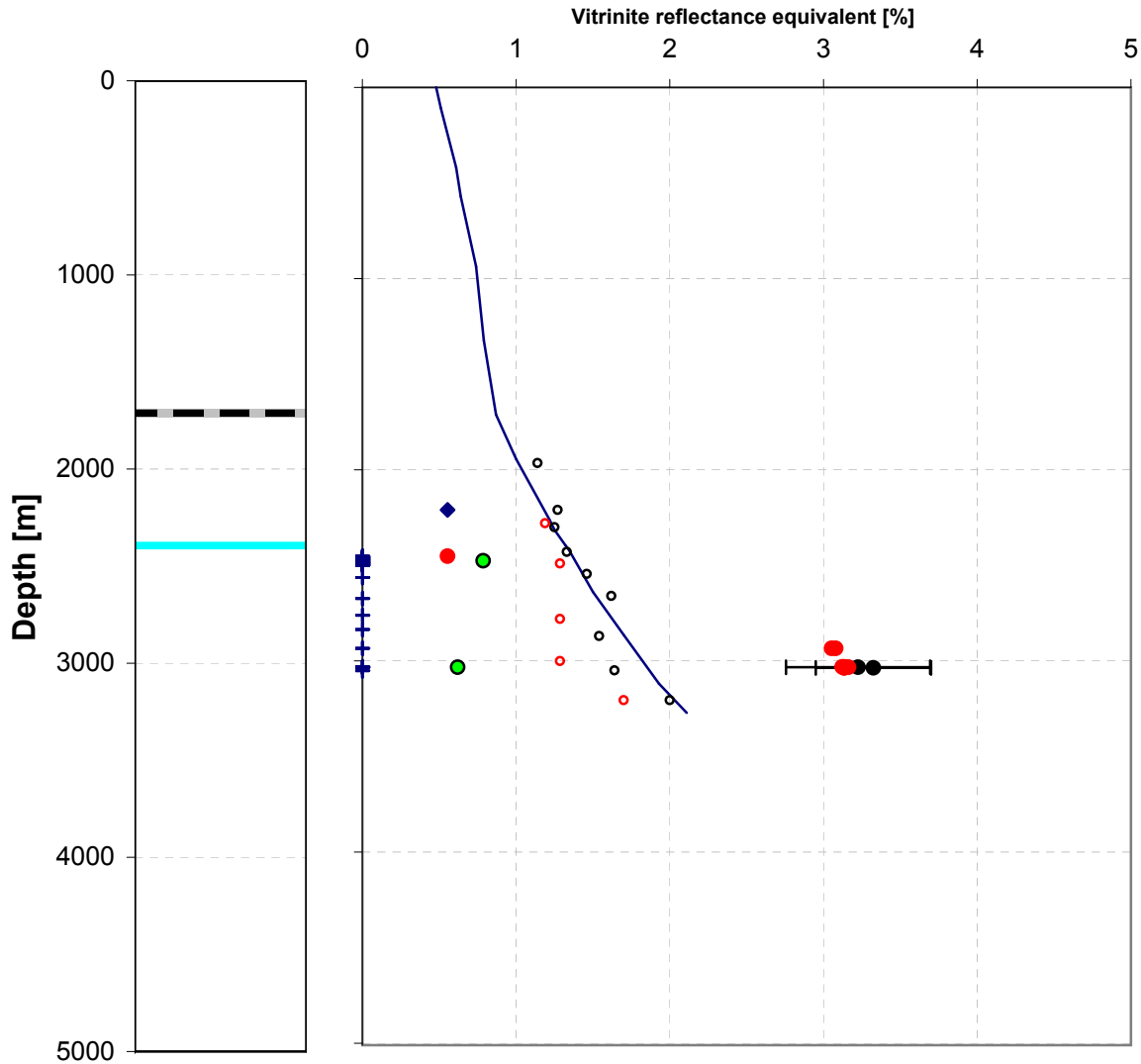




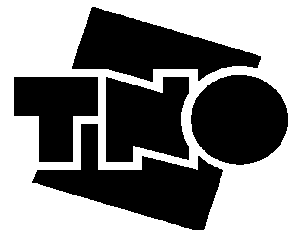
Joint Industry Project Petroplay

Quality controlled data

41/24a-2



- A) Vitrinite reflectance
- B) Vitrinite reflectance
- C) Vitrinite reflectance
- A1) Tmax-VR equivalent - highly reliable
- B) Tmax-VR equivalent
- C) Tmax-VR equivalent
- ◆ A2) Tmax-VR equivalent - low reliability
- + samples
- Modeled %VR (S&B)
- MPR

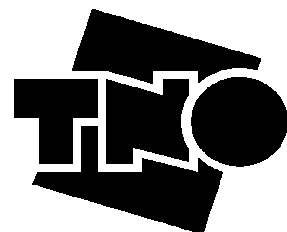
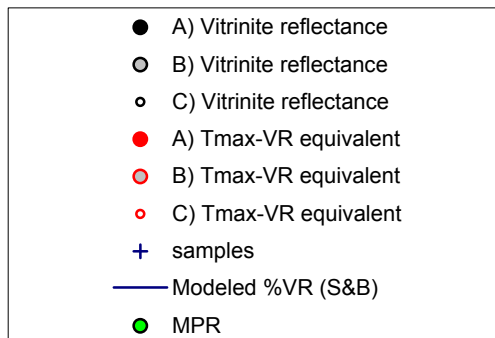
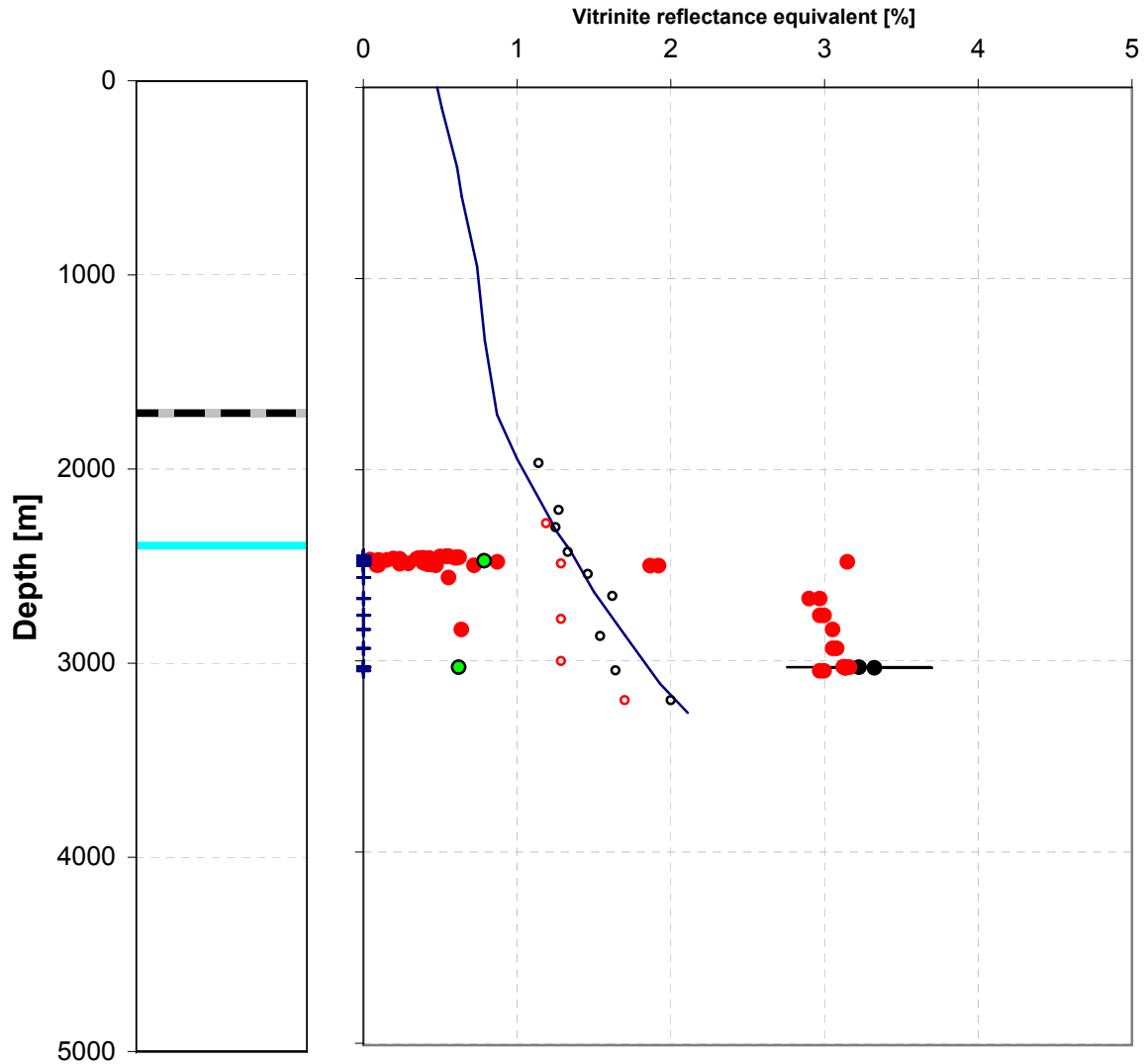




Joint Industry Project Petroplay

Raw data

41/24a-2

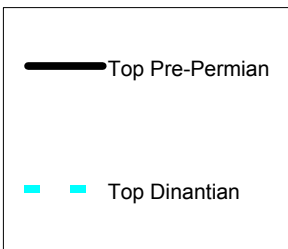
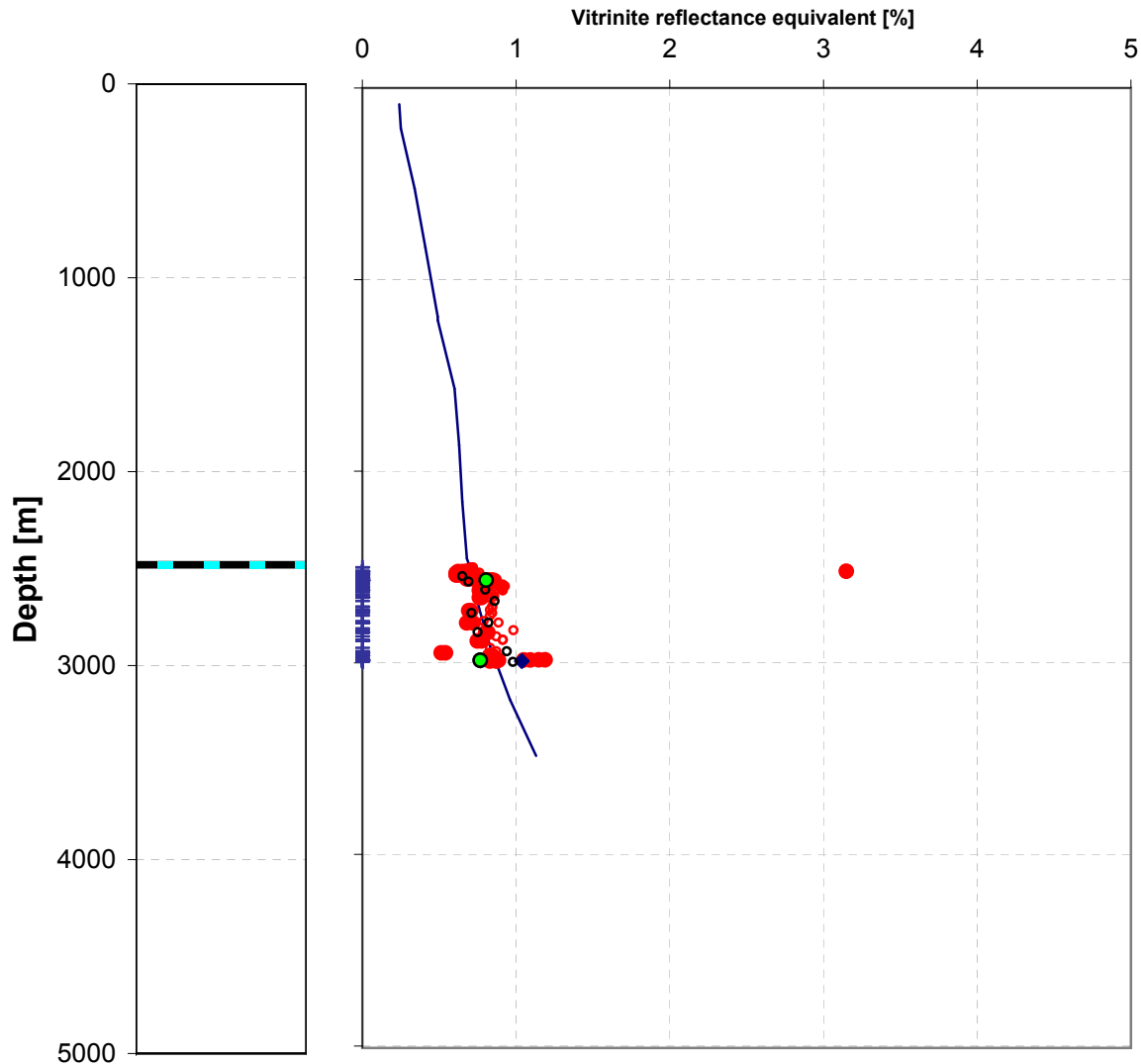




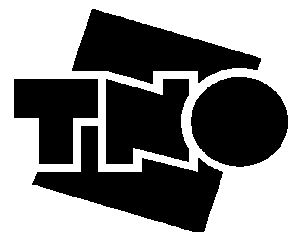
Joint Industry Project Petroplay

Quality controlled data

42/10a-01 (42/10-01)



- A) Vitrinite reflectance
- B) Vitrinite reflectance
- A1) Tmax-VR equivalent - highly reliable
- B) Tmax-VR equivalent
- C) Tmax-VR equivalent
- ◆ A2) Tmax-VR equivalent - low reliability
- C) Vitrinite reflectance
- Modeled %VR (S&B)
- + samples
- MPR

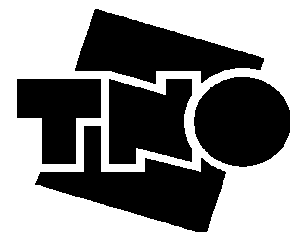
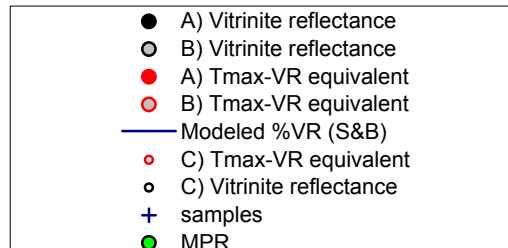
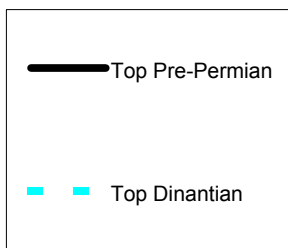
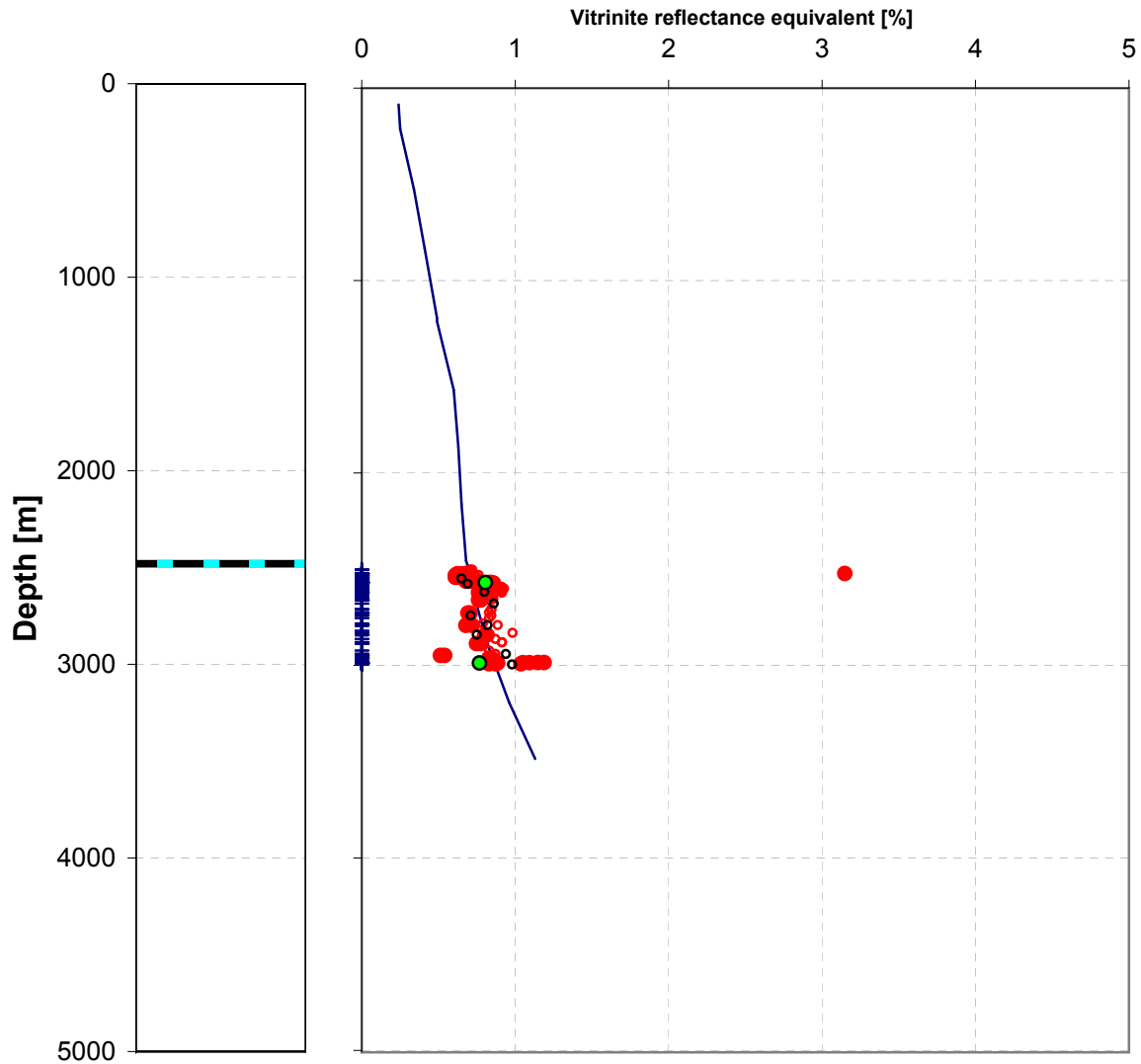




Joint Industry Project Petroplay

Raw data

42/10a-01 (42/10-01)

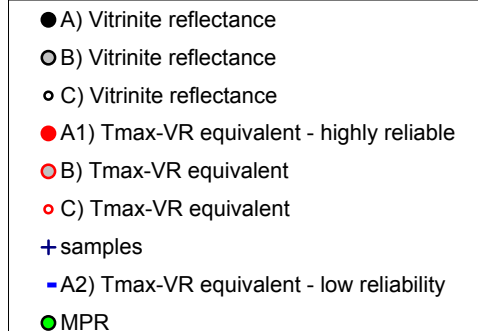
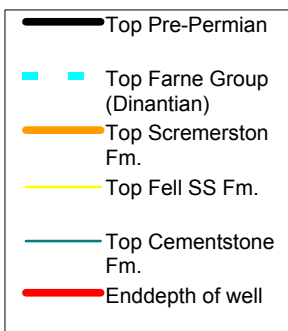
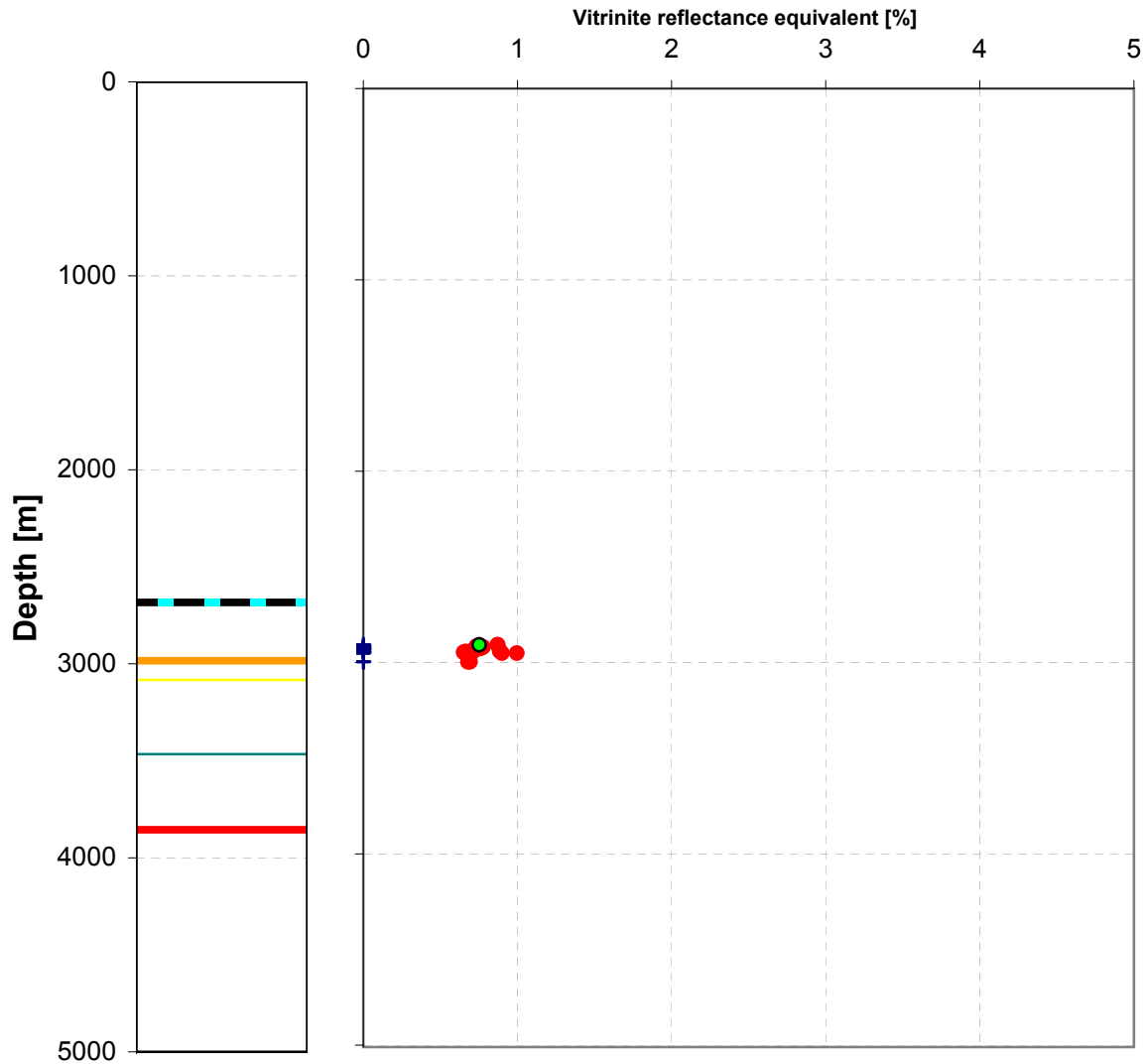




Joint Industry Project Petroplay

Quality controlled data

43/02-01

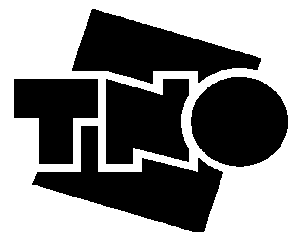
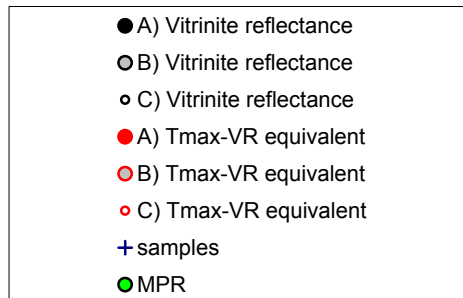
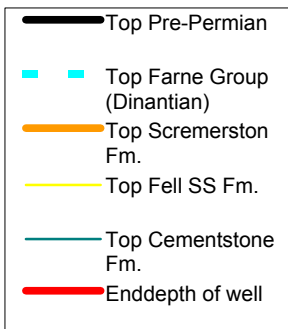
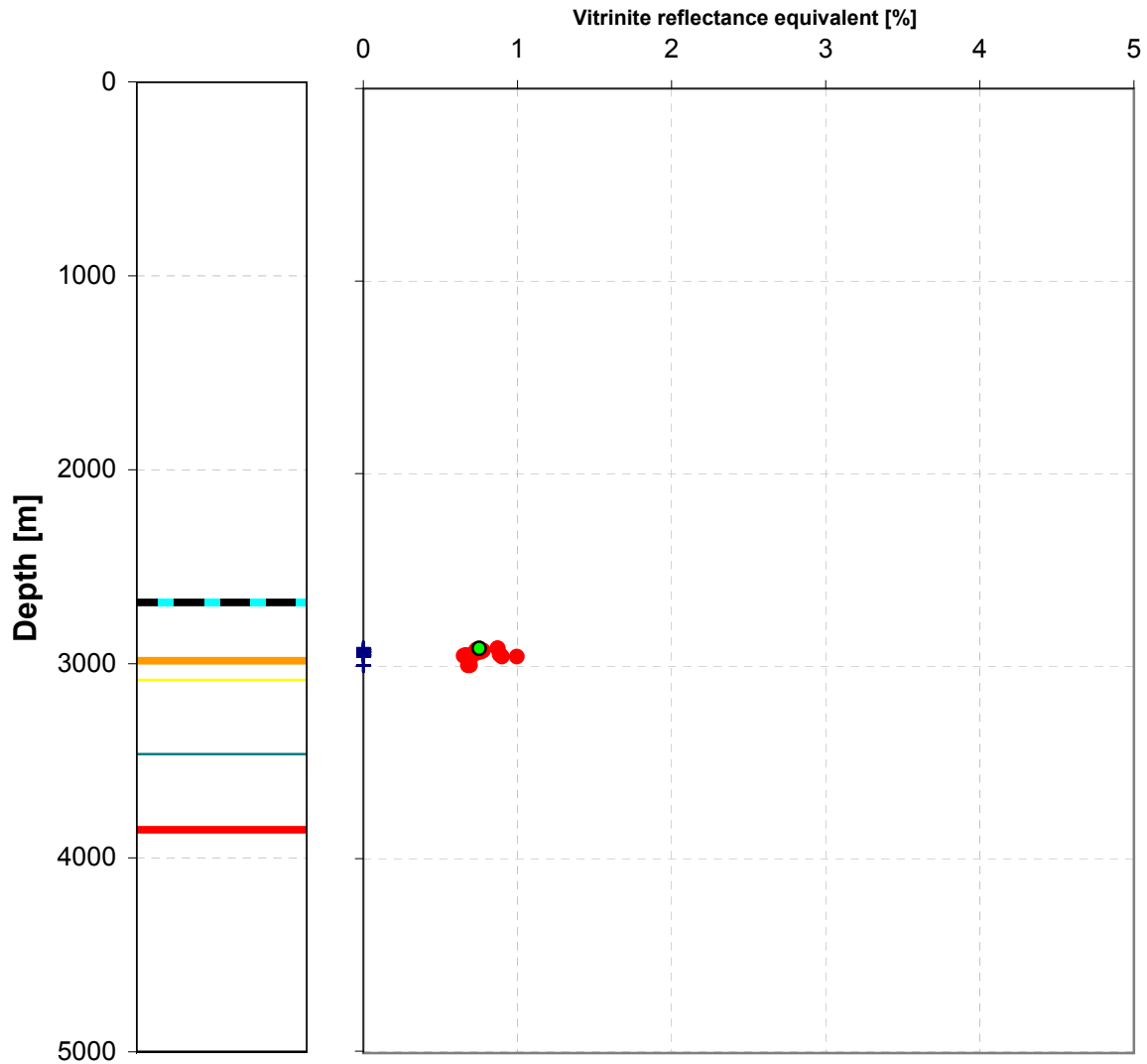




Joint Industry Project Petroplay

Raw data

43/02-01

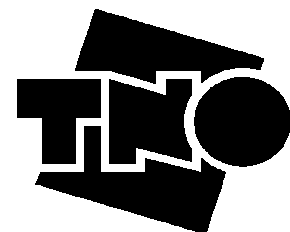
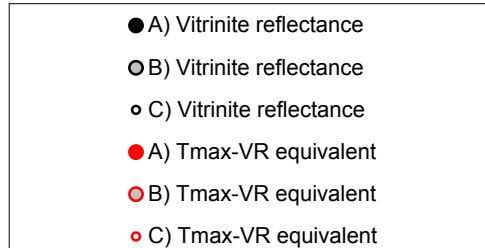
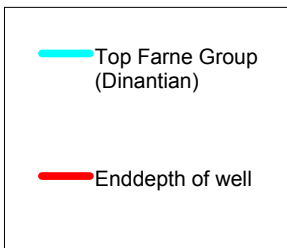
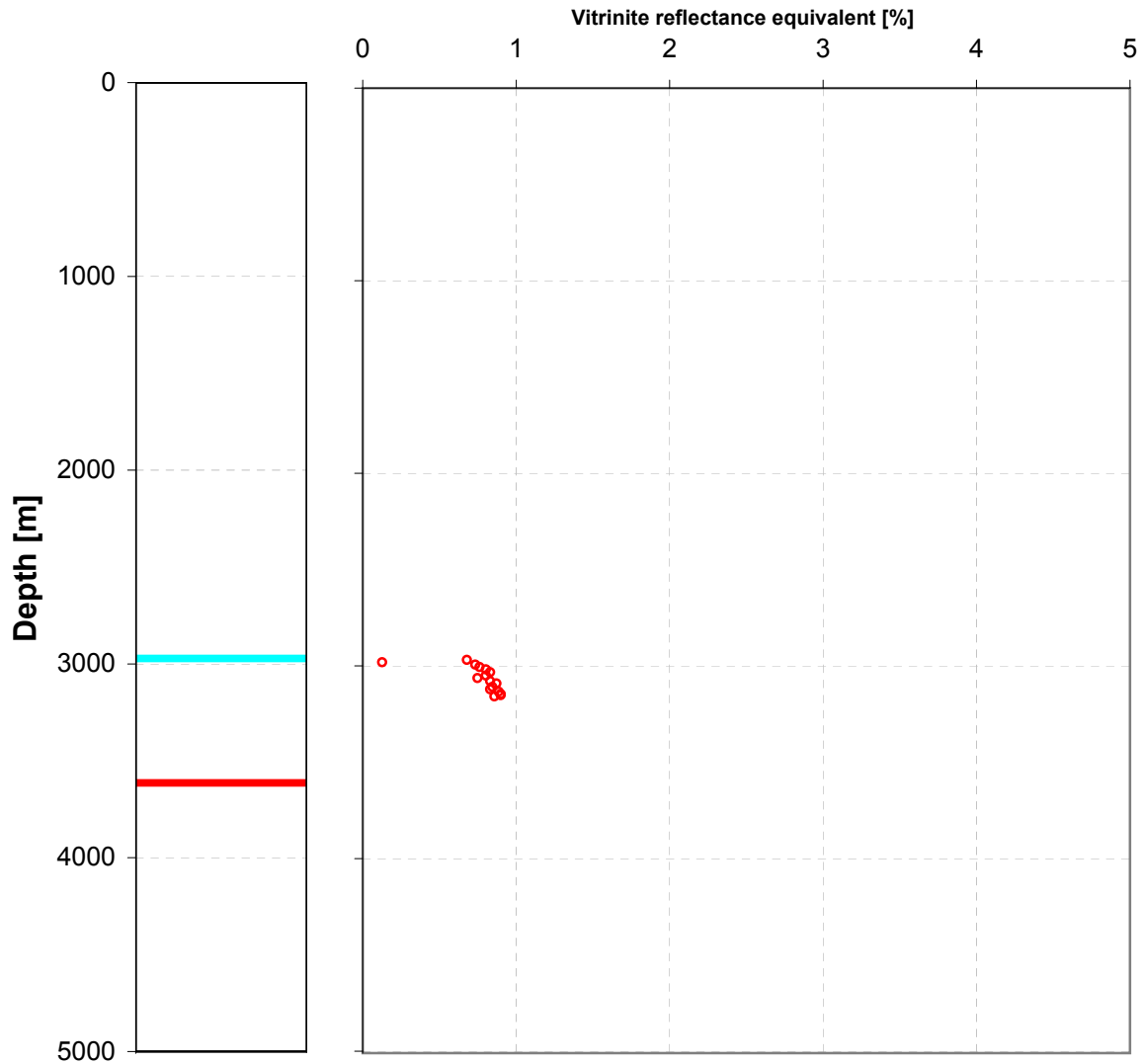




Joint Industry Project Petroplay

Raw data

43/03-01

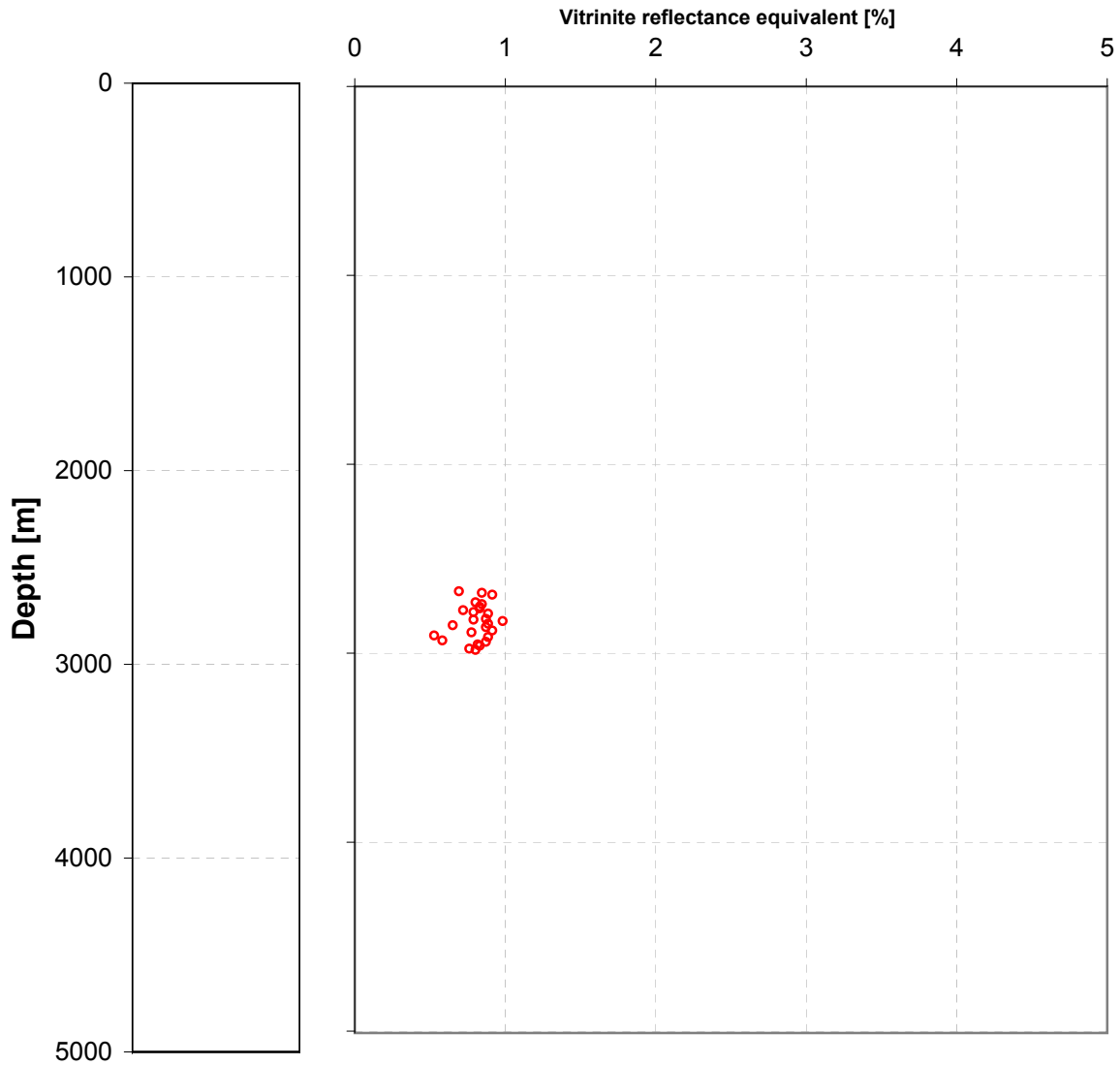




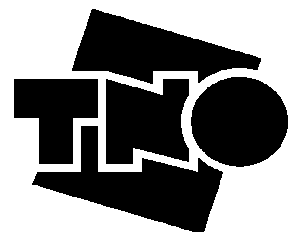
Joint Industry Project Petroplay

Raw data

43/10a-01



- A) Vitrinite reflectance
- B) Vitrinite reflectance
- C) Vitrinite reflectance
- A) Tmax-VR equivalent
- B) Tmax-VR equivalent
- C) Tmax-VR equivalent

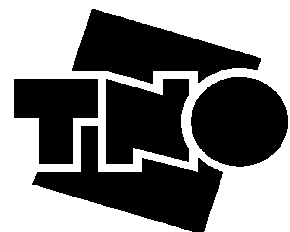
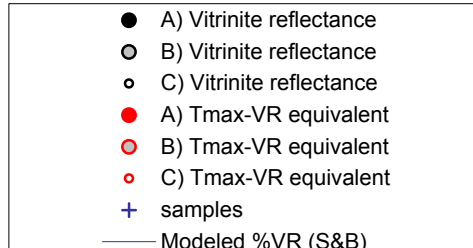
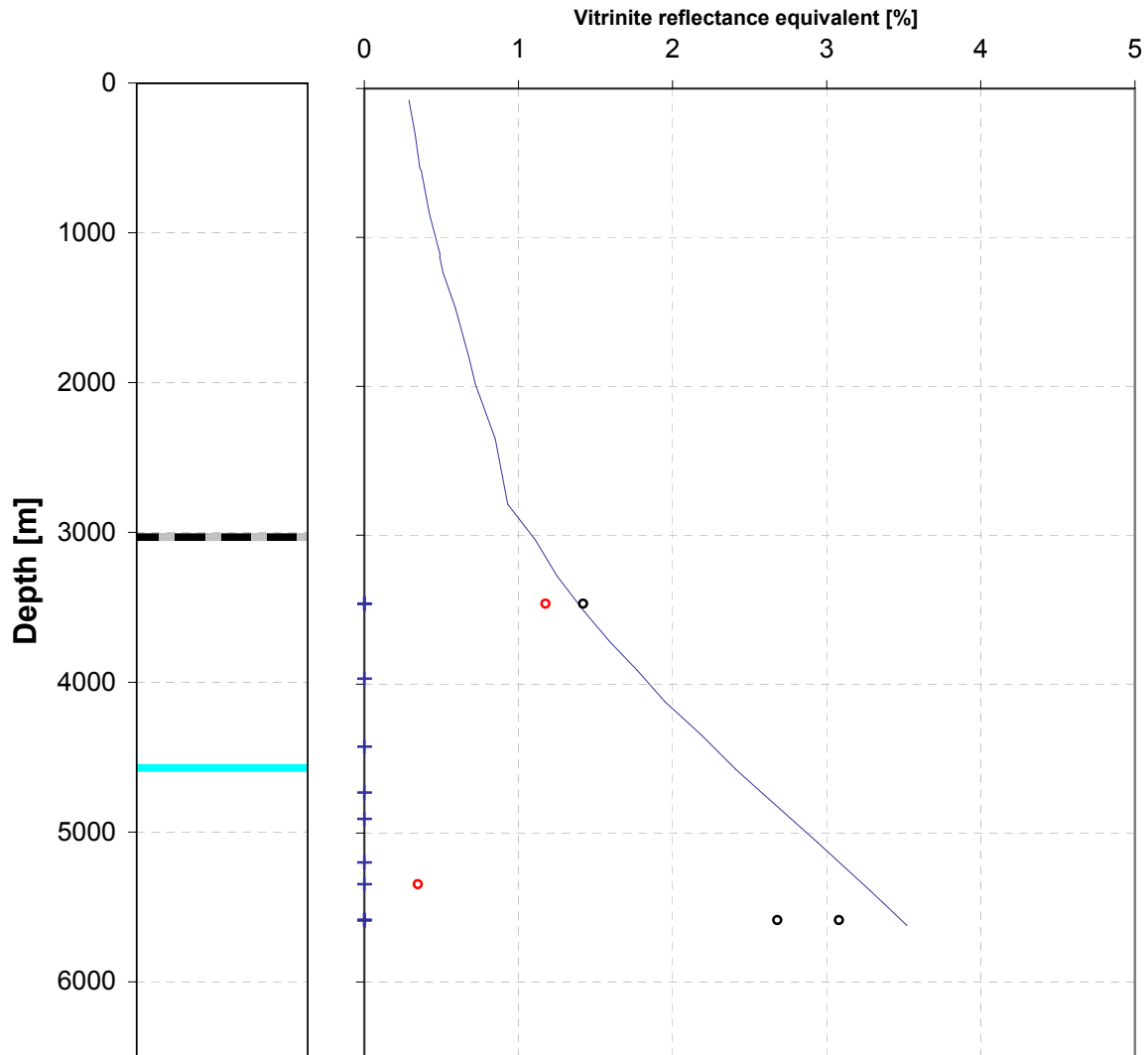




Joint Industry Project Petroplay

Raw data

43/17b-02

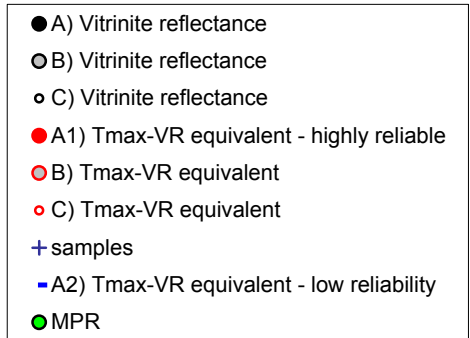
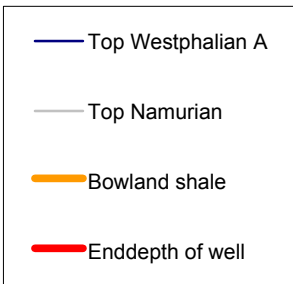
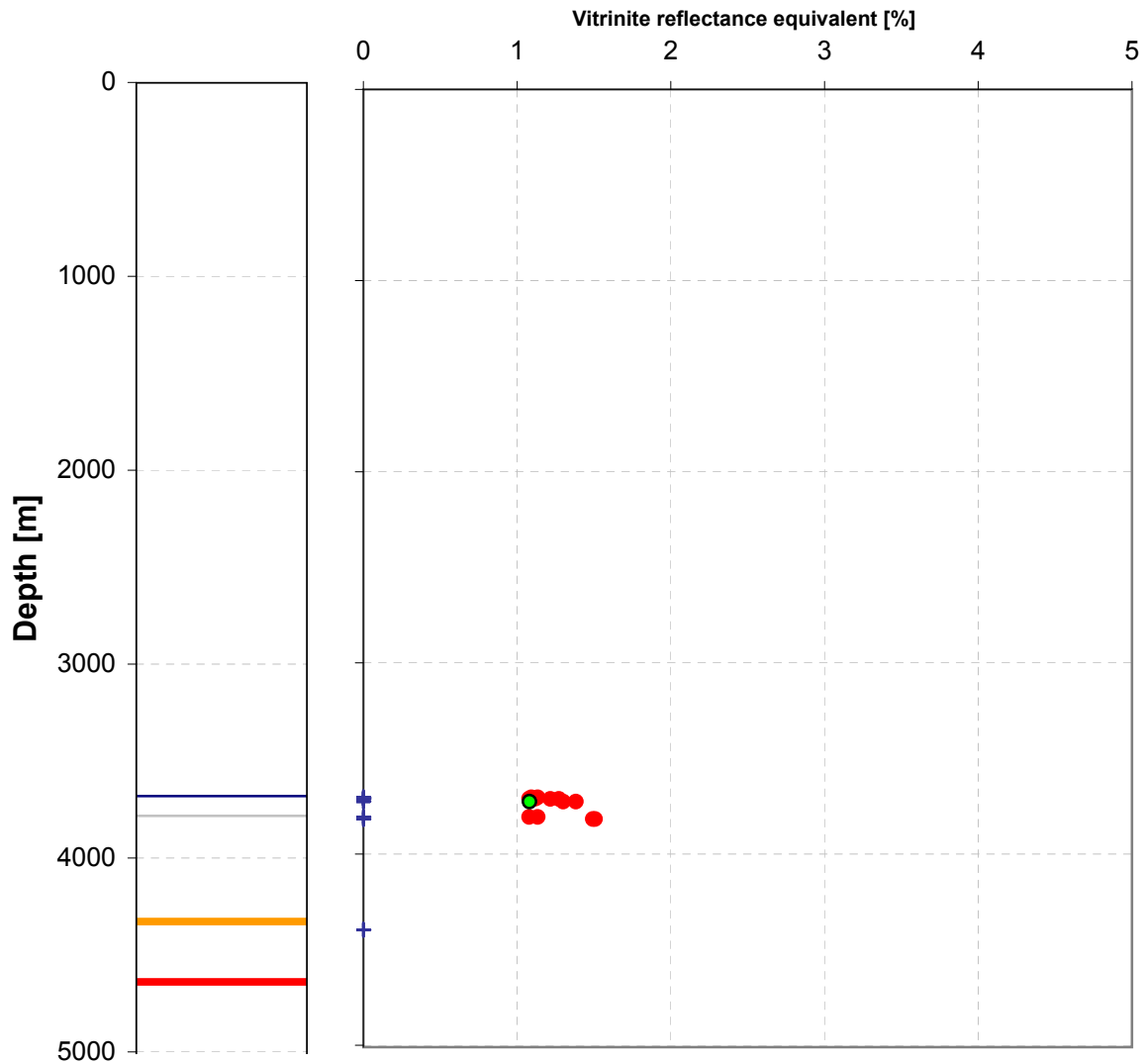




Joint Industry Project Petroplay

Quality controlled data

43/20b-02

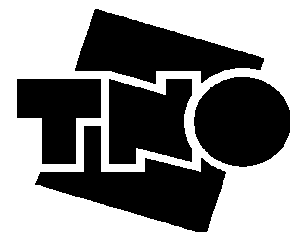
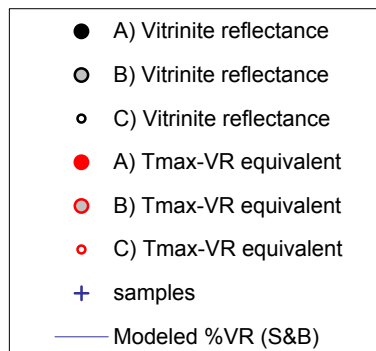
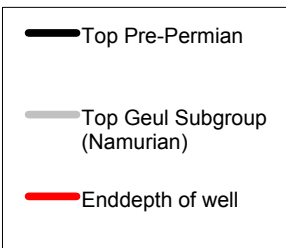
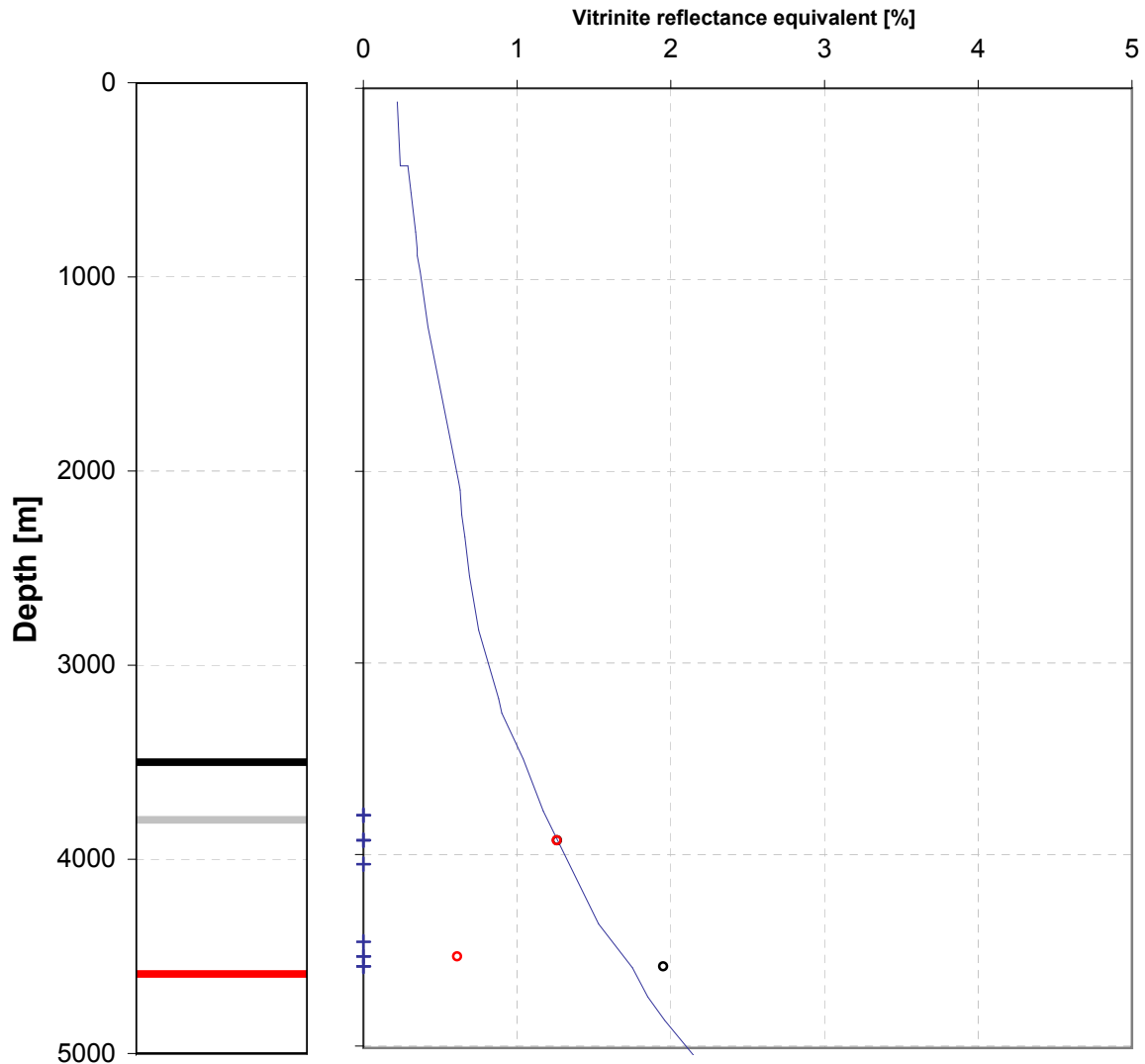




Joint Industry Project Petroplay

Raw data

48/03-03

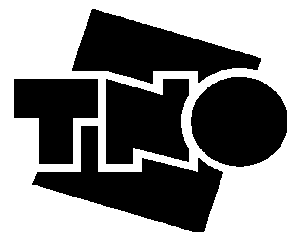
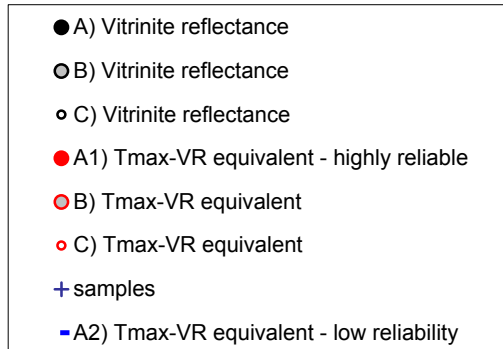
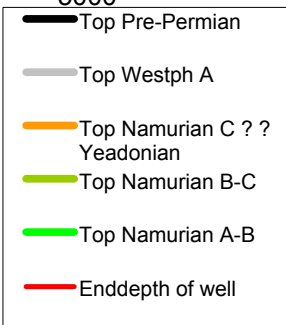
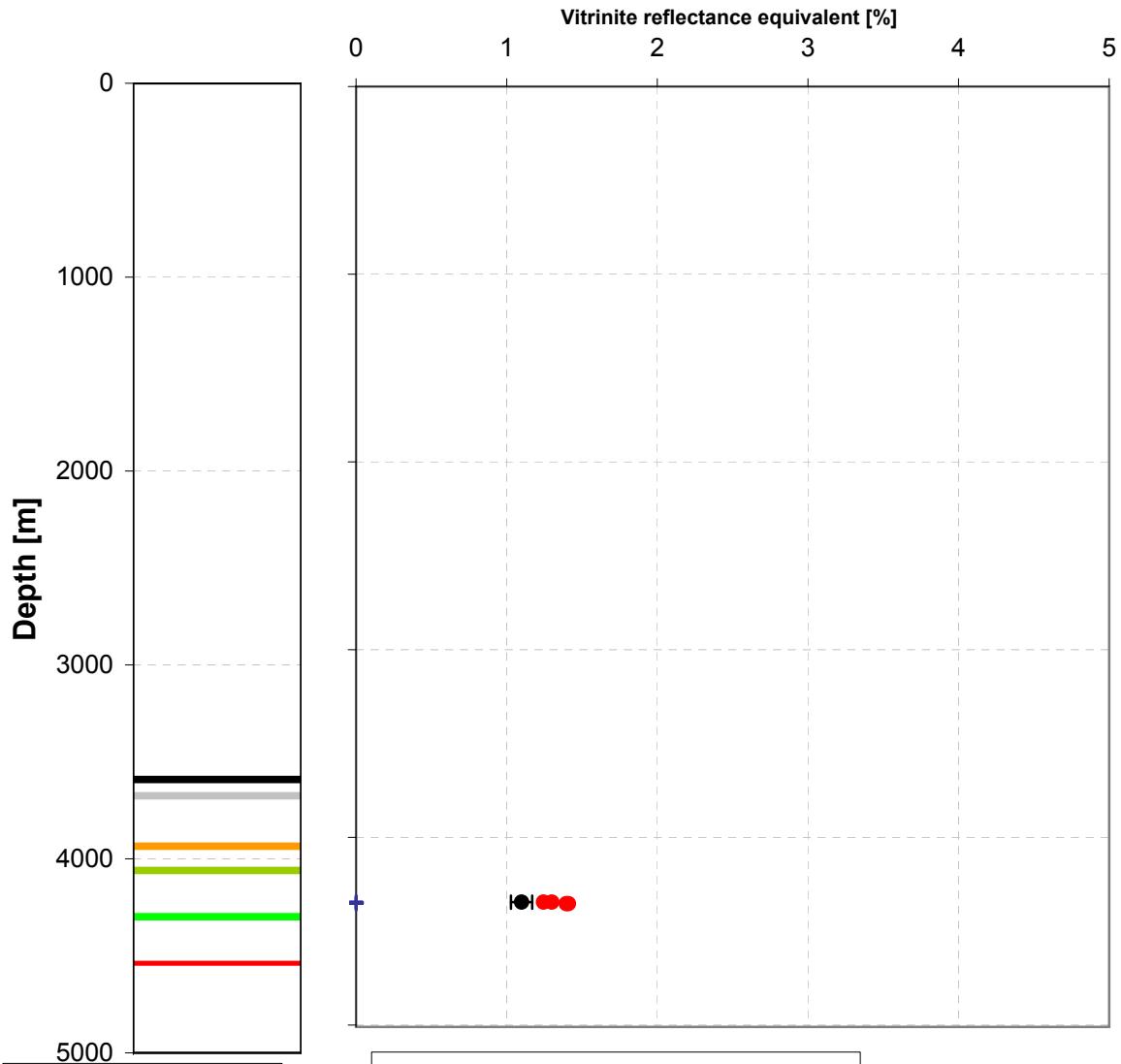




Joint Industry Project Petroplay

Quality controlled data

44/16-02

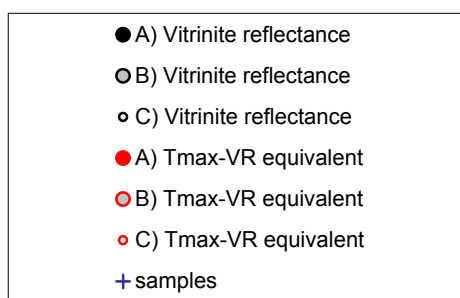
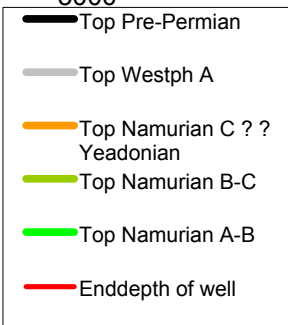
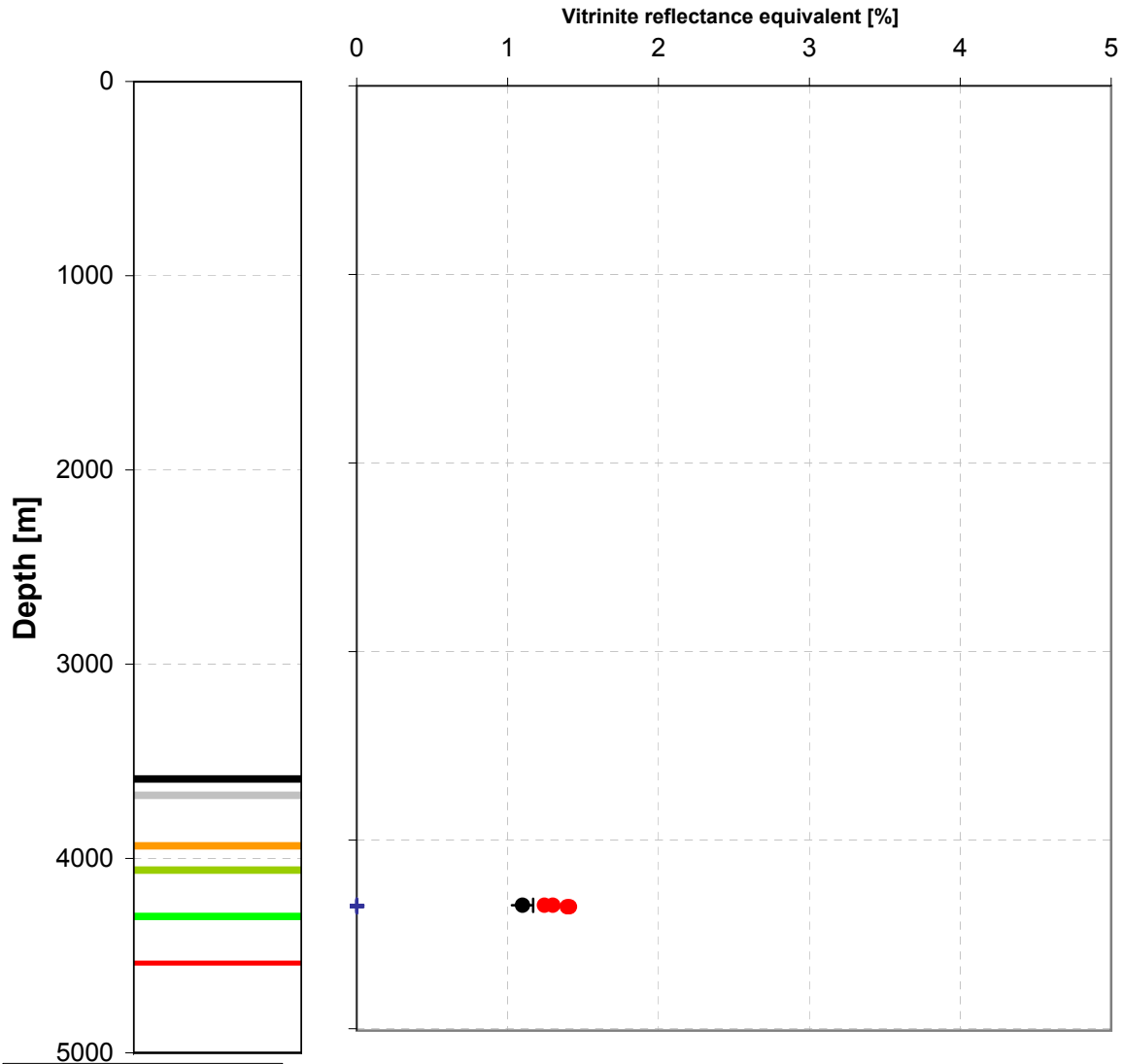




Joint Industry Project Petroplay

Raw data

44/16-02

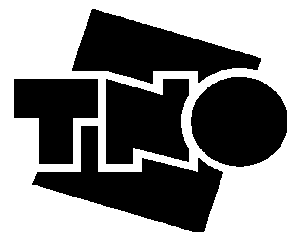
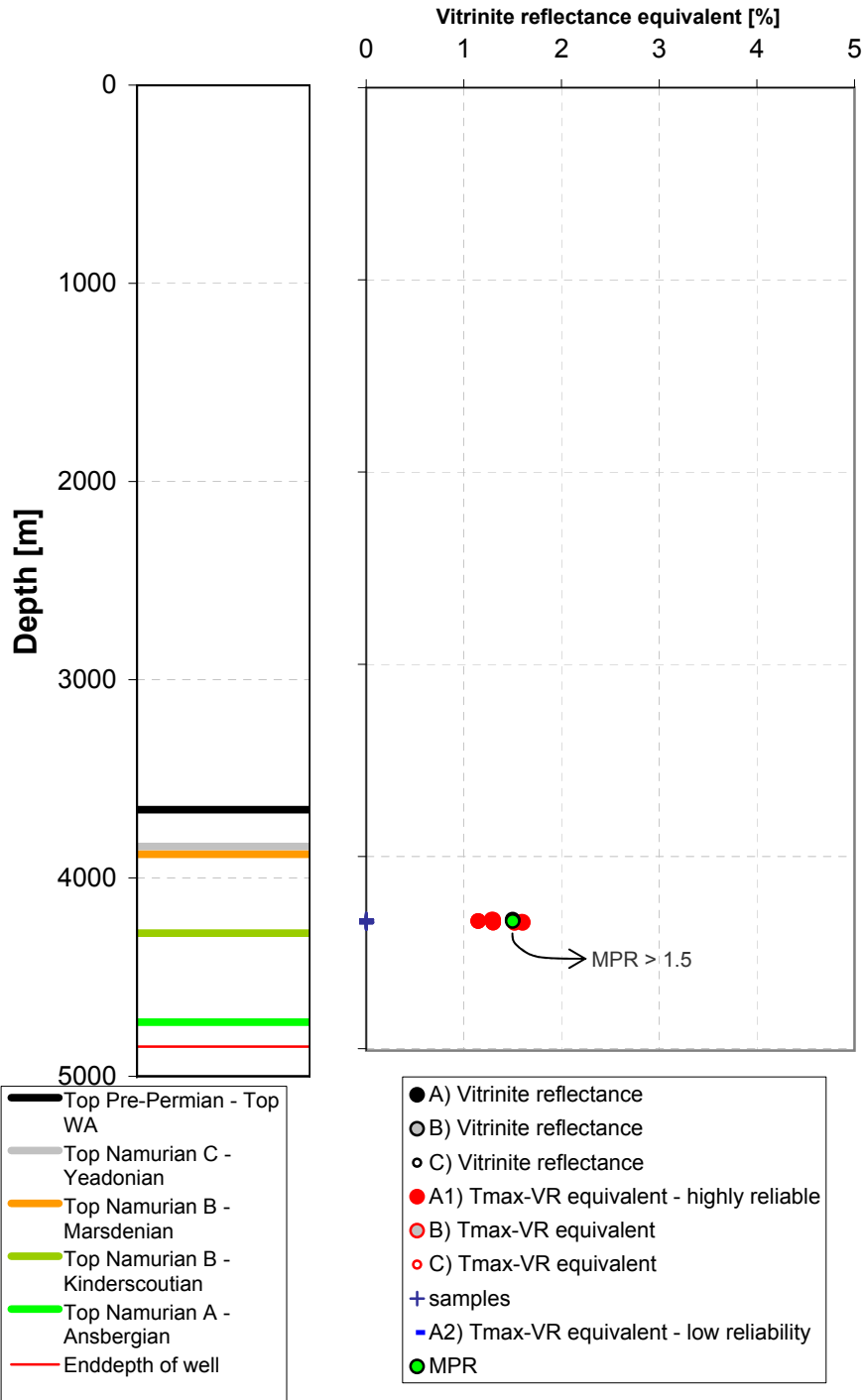




Joint Industry Project Petroplay

Quality controlled data

44/16-01Z

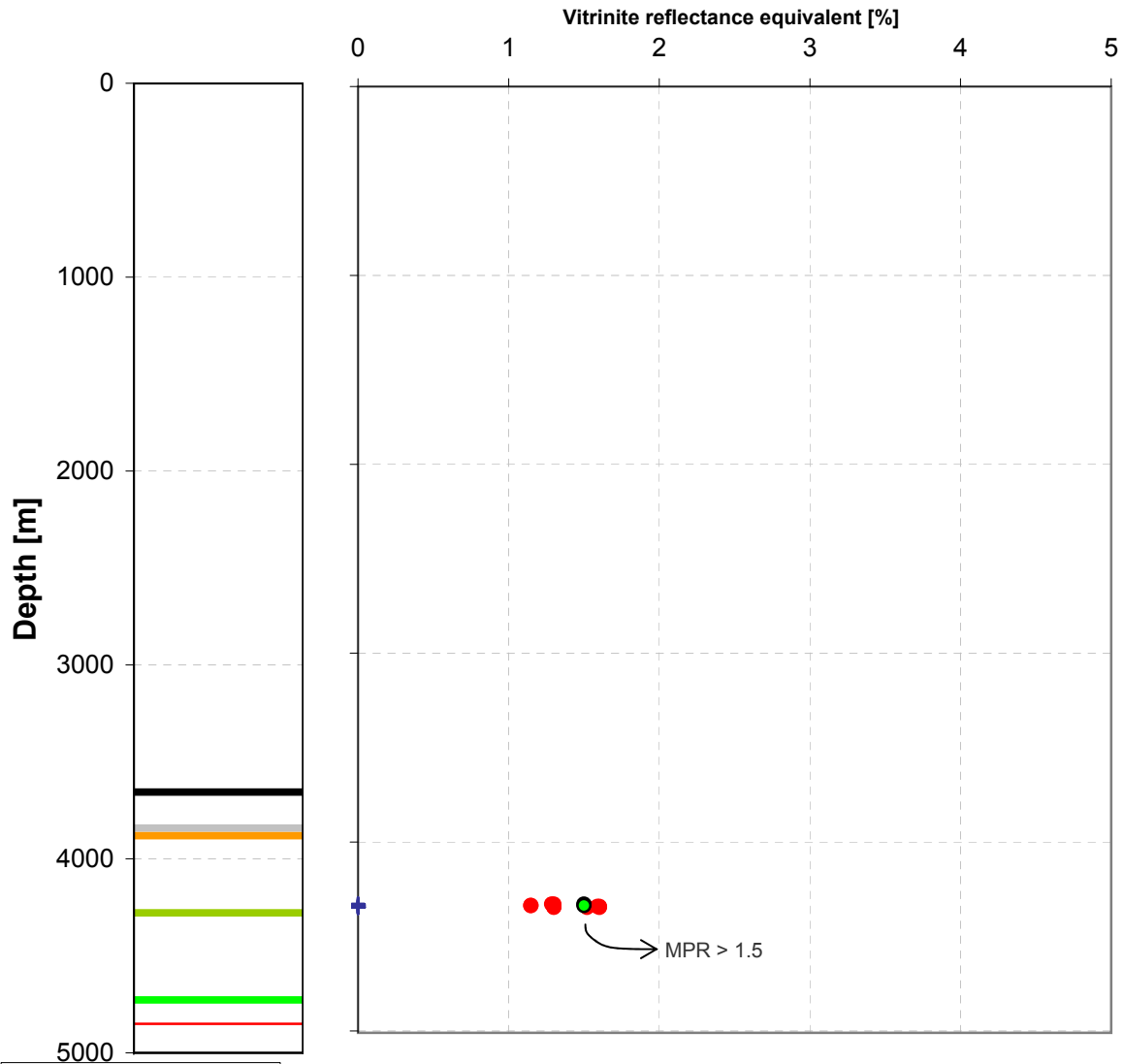




Joint Industry Project Petroplay

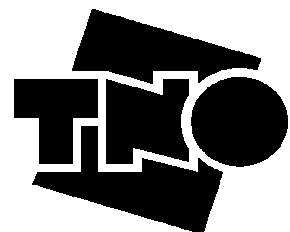
Raw data

44/16-01Z



- Top Pre-Permian - Top WA
- Top Namurian C - Yeadonian
- Top Namurian B - Marsdenian
- Top Namurian B - Kinderscoutian
- Top Namurian A - Ansbergian
- Enddepth of well

- A) Vitrinite reflectance
- B) Vitrinite reflectance
- C) Vitrinite reflectance
- A) Tmax-VR equivalent
- B) Tmax-VR equivalent
- C) Tmax-VR equivalent
- + samples
- MPR

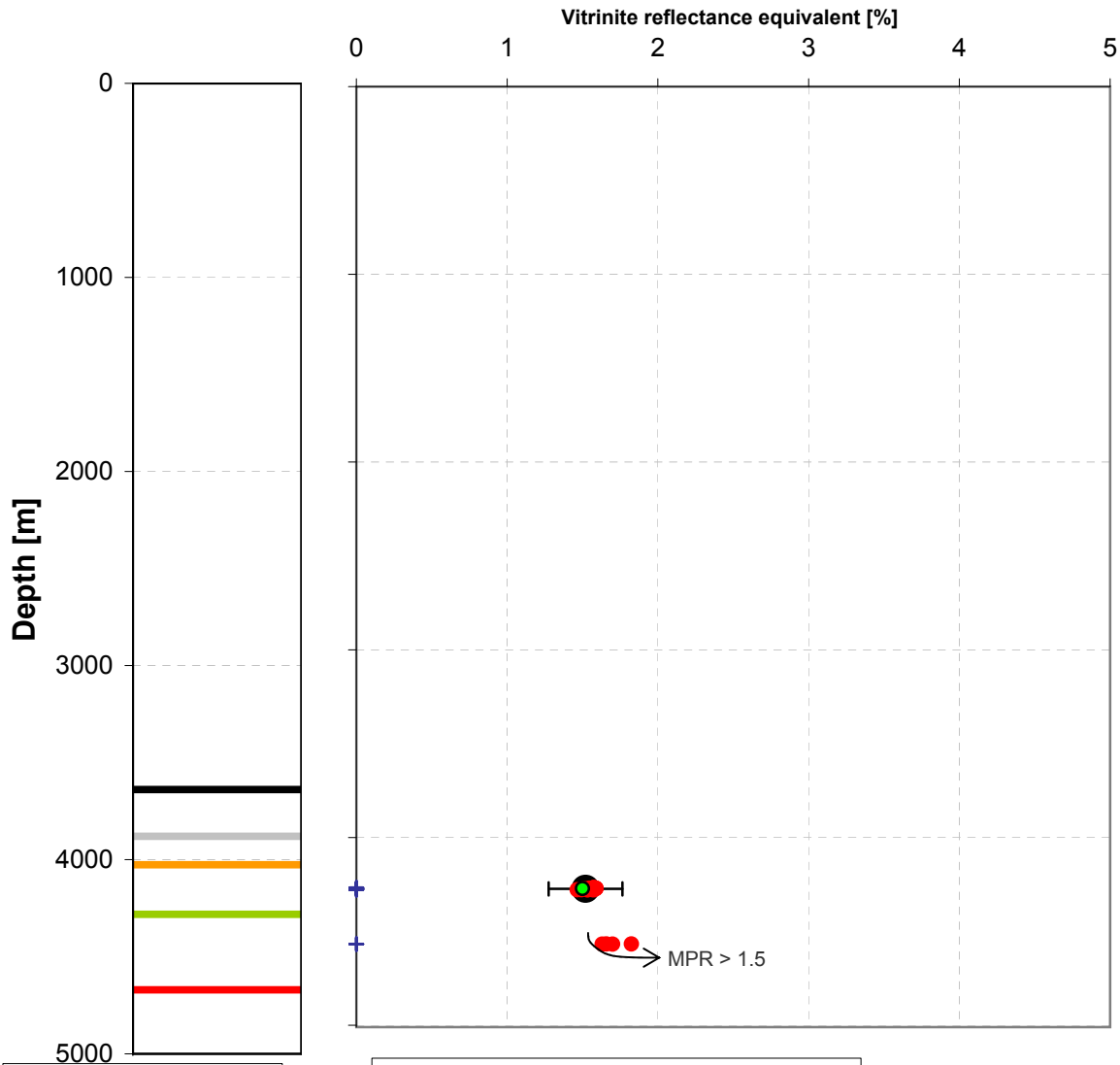




Joint Industry Project Petroplay

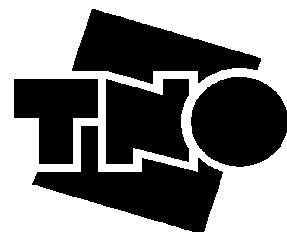
Quality controlled data

44/16-01



- Top Pre-Permian - Top Early WA?-Yeadonian
- Top Namurian B-C - Marsdenian
- Top Namurian B - Kinderscoutian
- Top Namurian A - Chokerian
- Enddepth of well

- A) Vitrinite reflectance
- B) Vitrinite reflectance
- C) Vitrinite reflectance
- A1) Tmax-VR equivalent - highly reliable
- A2) Tmax-VR equivalent - low reliability
- B) Tmax-VR equivalent
- C) Tmax-VR equivalent
- + samples
- MPR

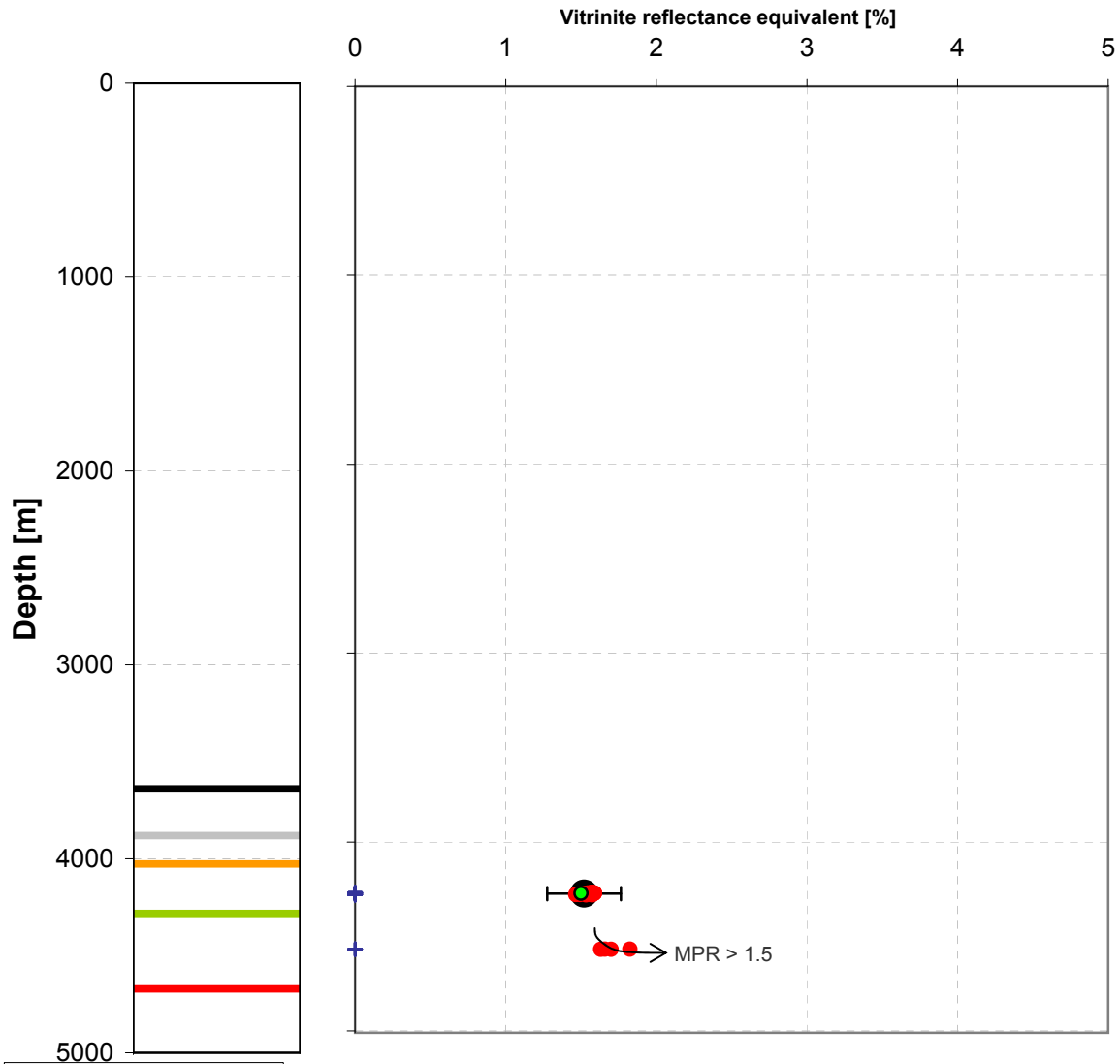




Joint Industry Project Petroplay

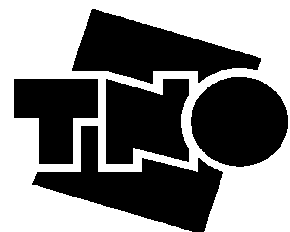
Raw data

44/16-01



- Top Pre-Permian - Top Early WA?-Yeadonian
- Top Namurian B-C - Marsdenian
- Top Namurian B - Kinderscoutian
- Top Namurian A - Chokerian
- Enddepth of well

- A) Vitrinite reflectance
- B) Vitrinite reflectance
- C) Vitrinite reflectance
- A) Tmax-VR equivalent
- B) Tmax-VR equivalent
- C) Tmax-VR equivalent
- + samples
- MPR

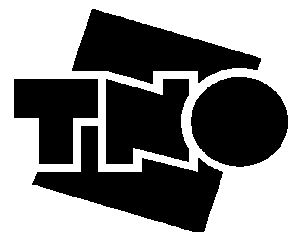
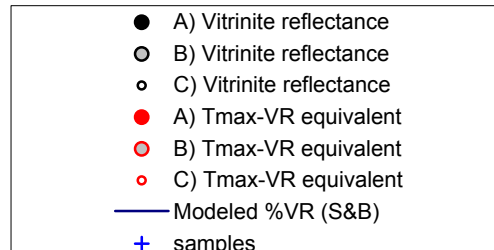
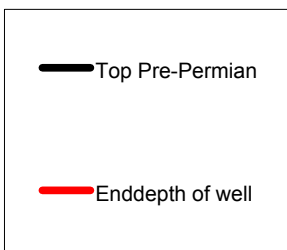
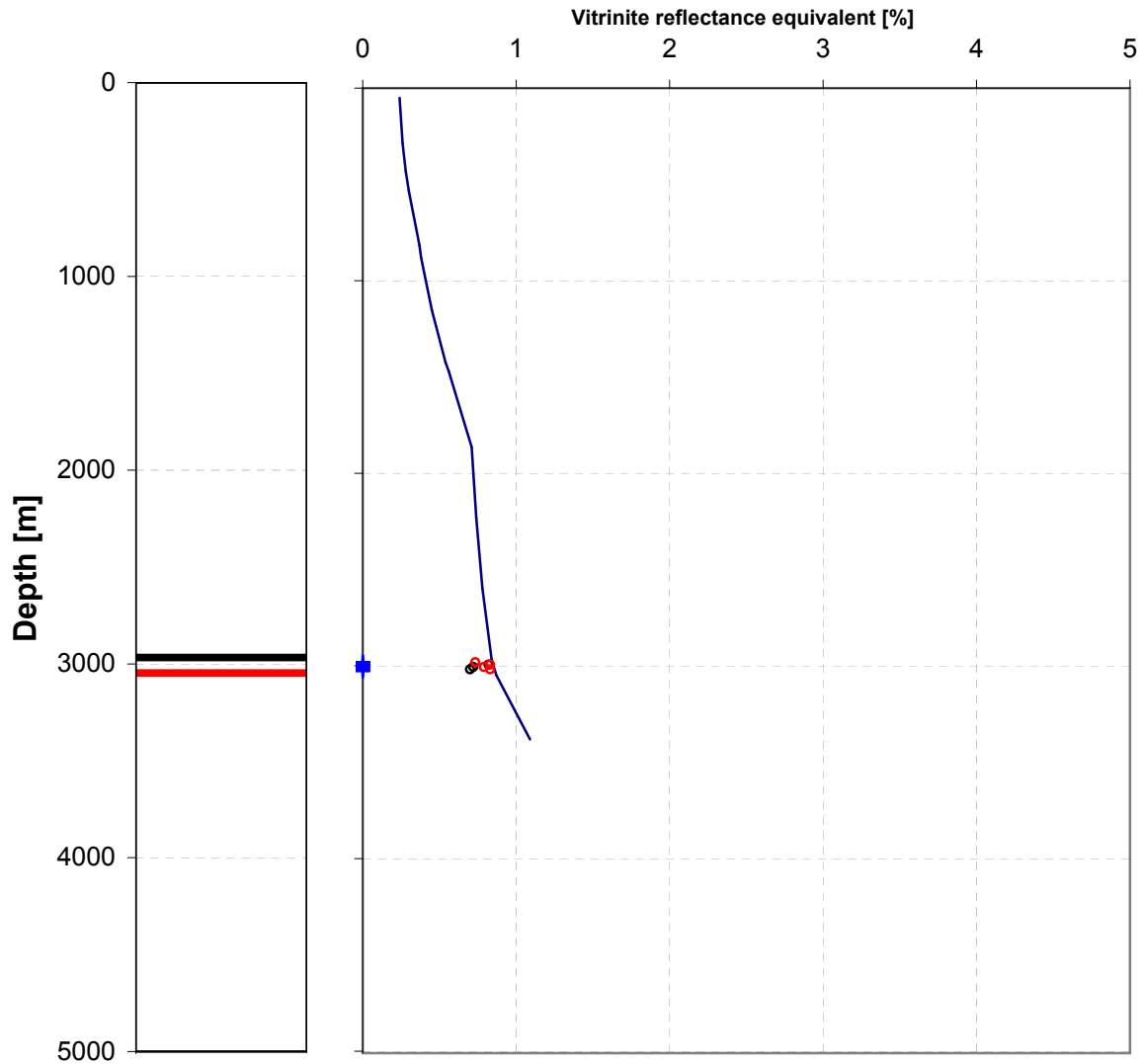




Joint Industry Project Petroplay

Raw data

44/07-01

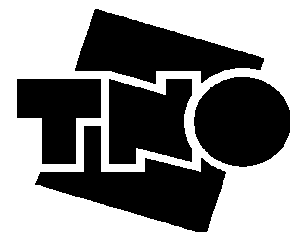
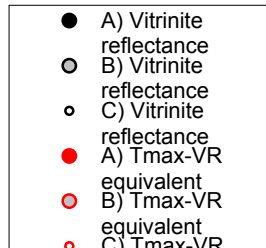
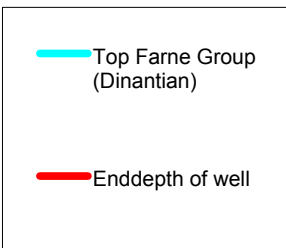
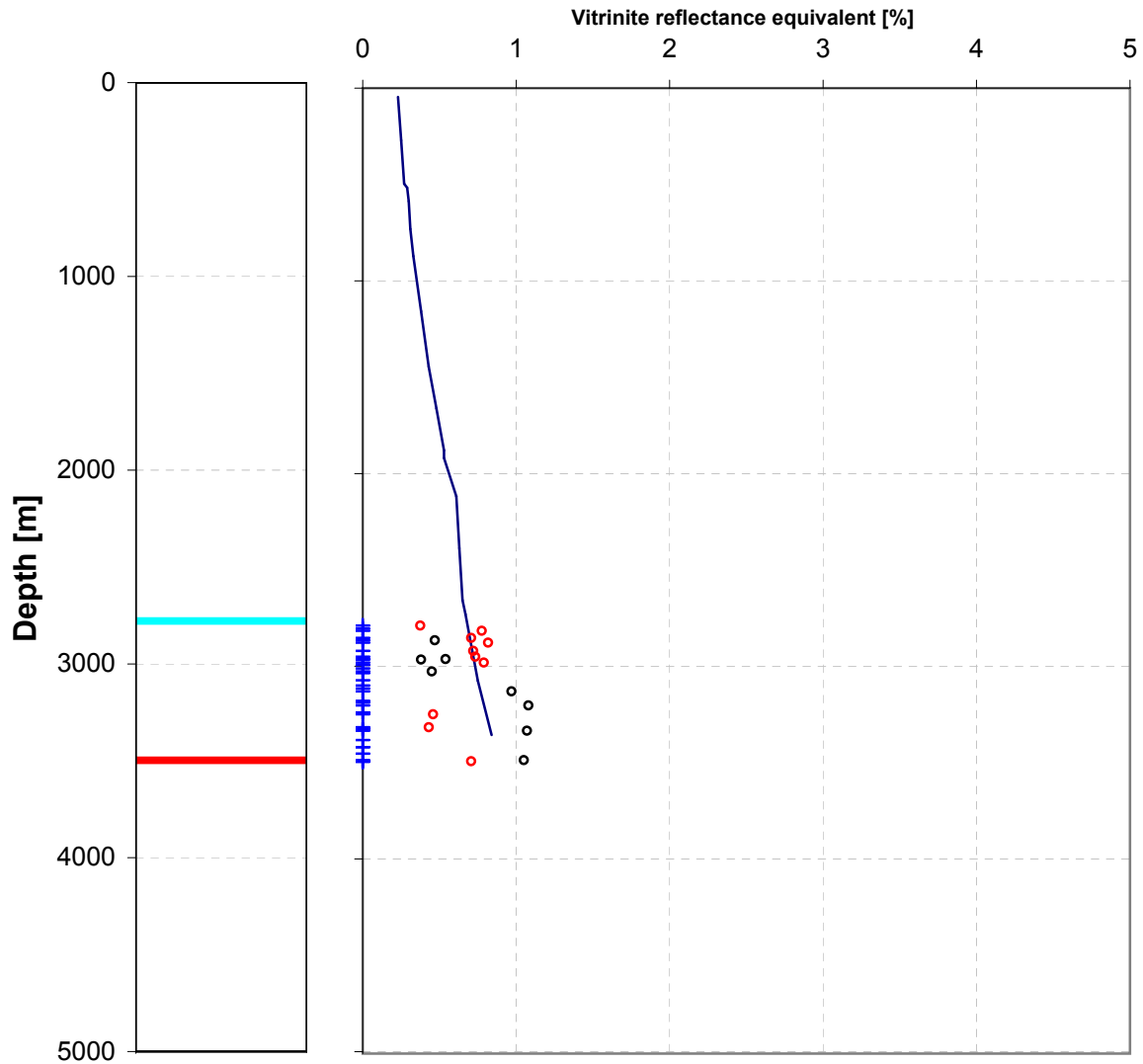




Joint Industry Project Petroplay

Raw data

44/02-01

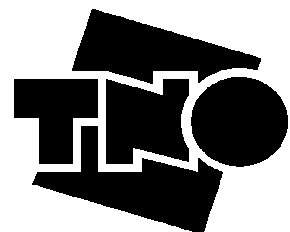
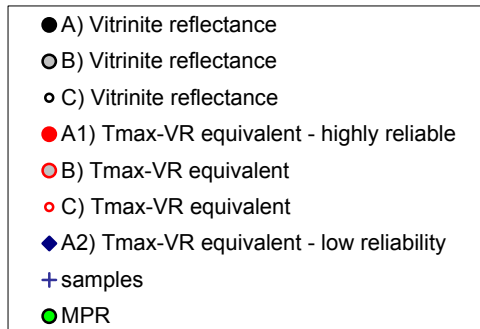
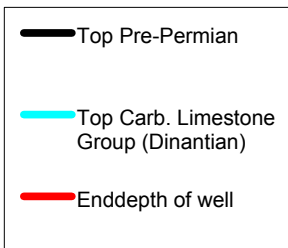
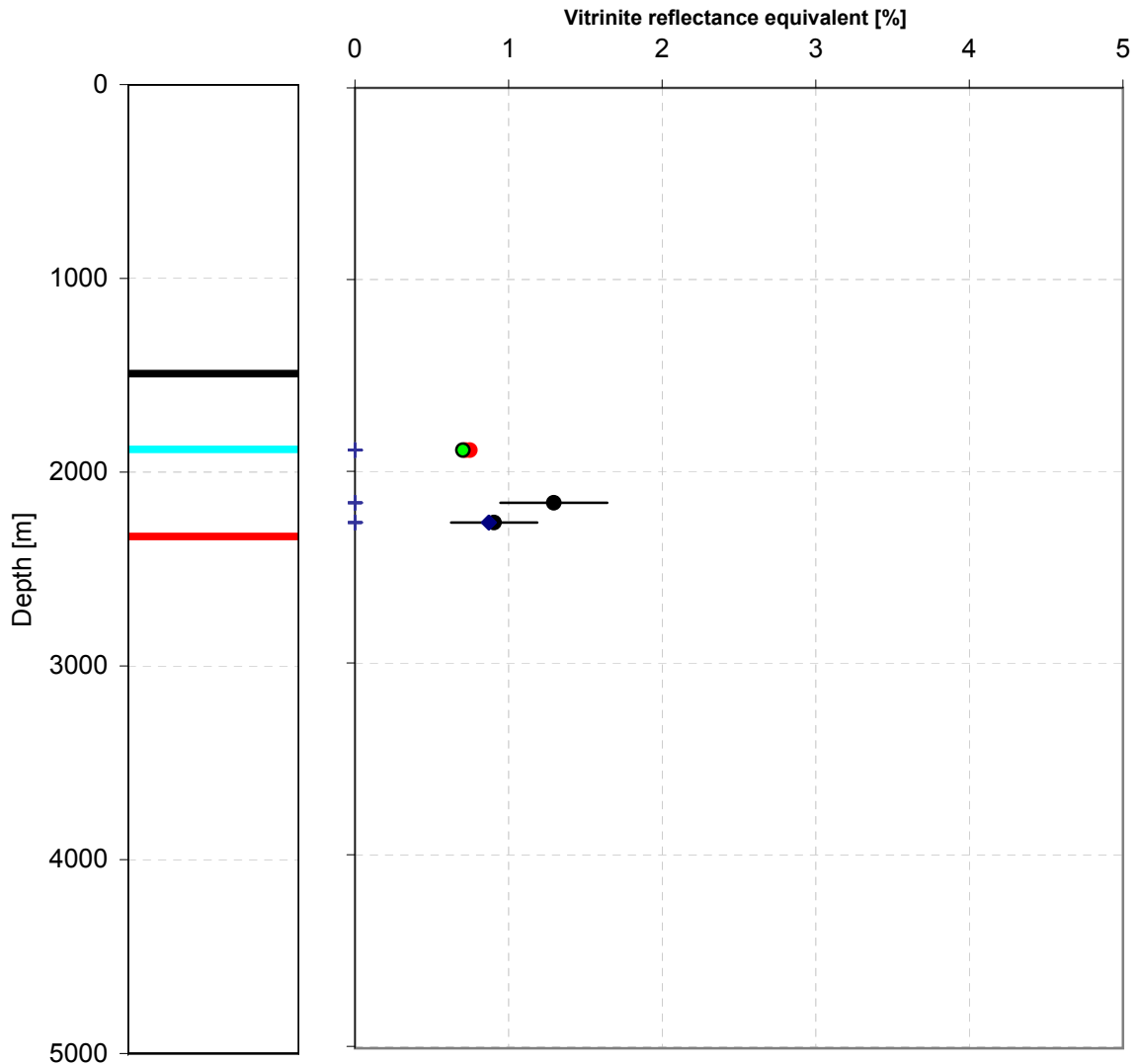




Joint Industry Project Petroplay

Quality controlled data

53/12-02

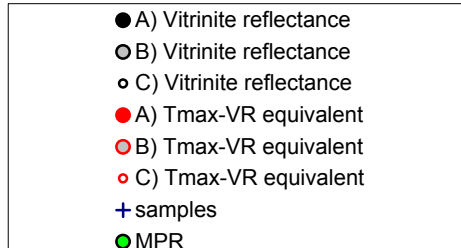
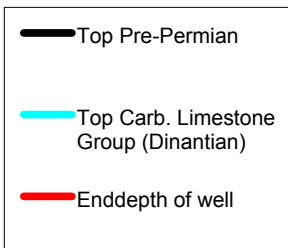
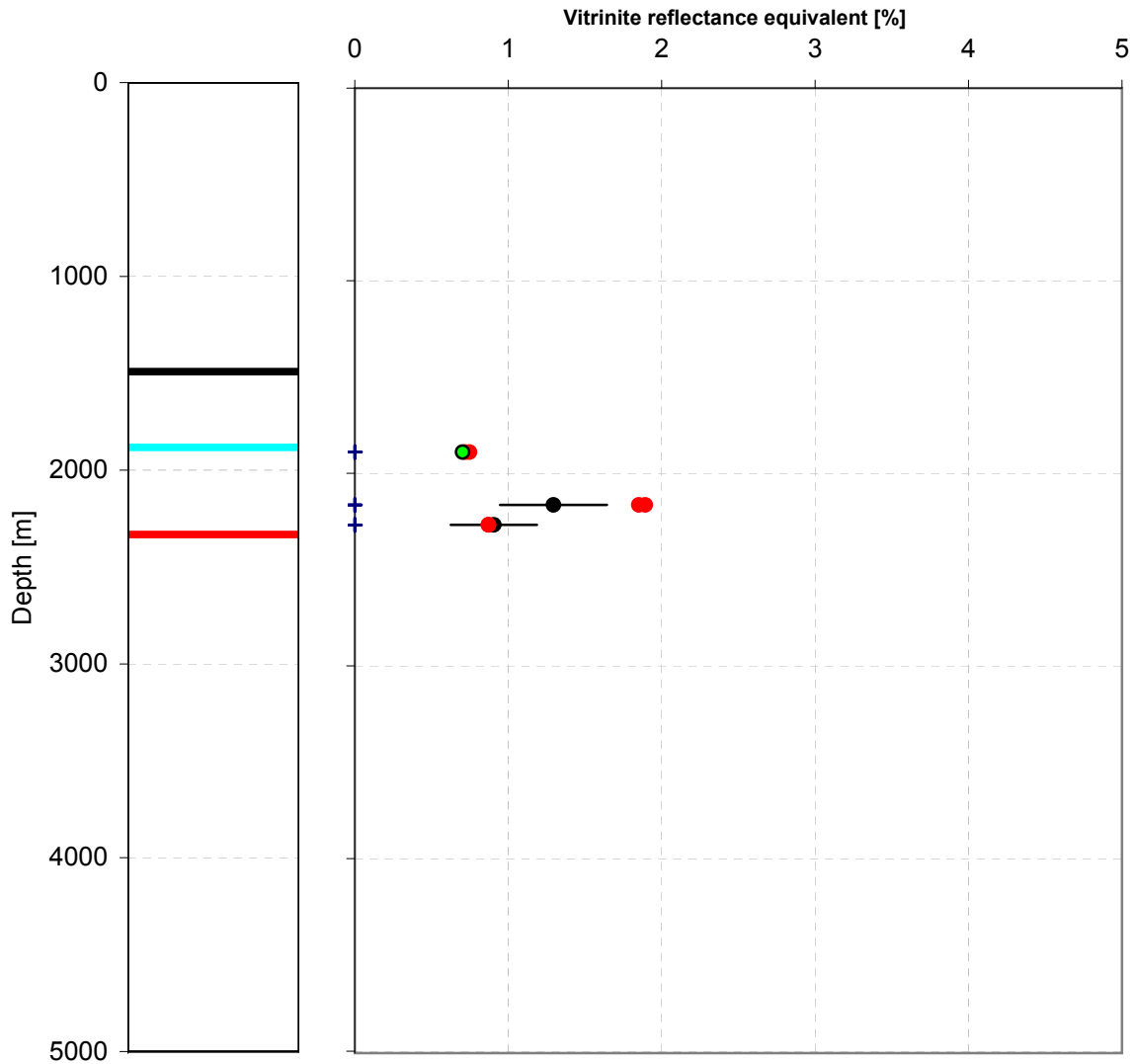




Joint Industry Project Petroplay

Raw data

53/12-02

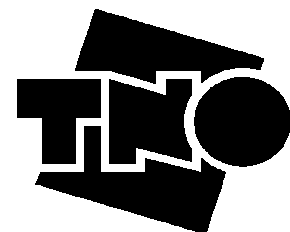
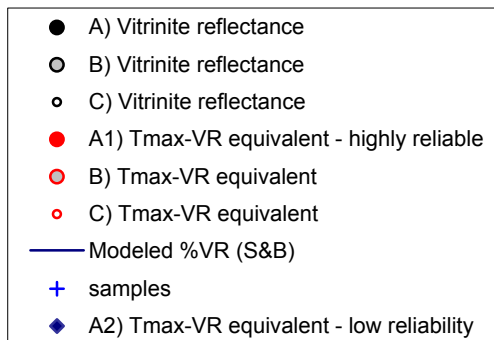
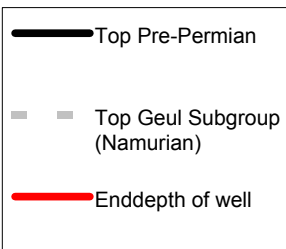
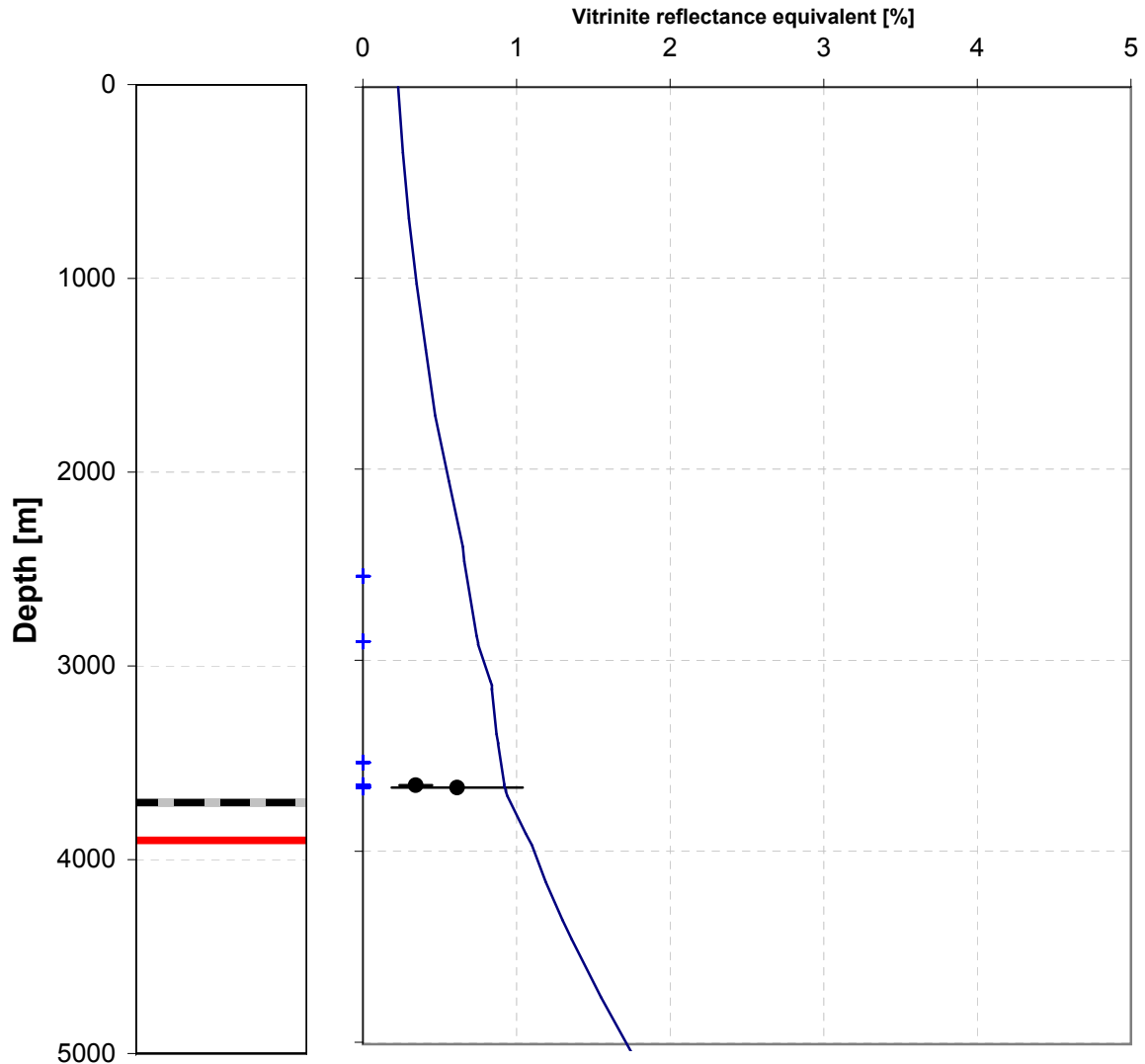




Joint Industry Project Petroplay

Quality controlled data

A11-01

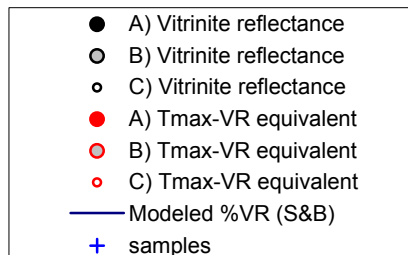
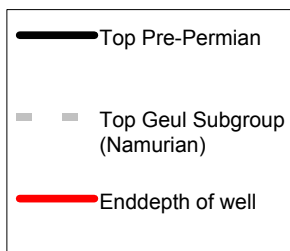
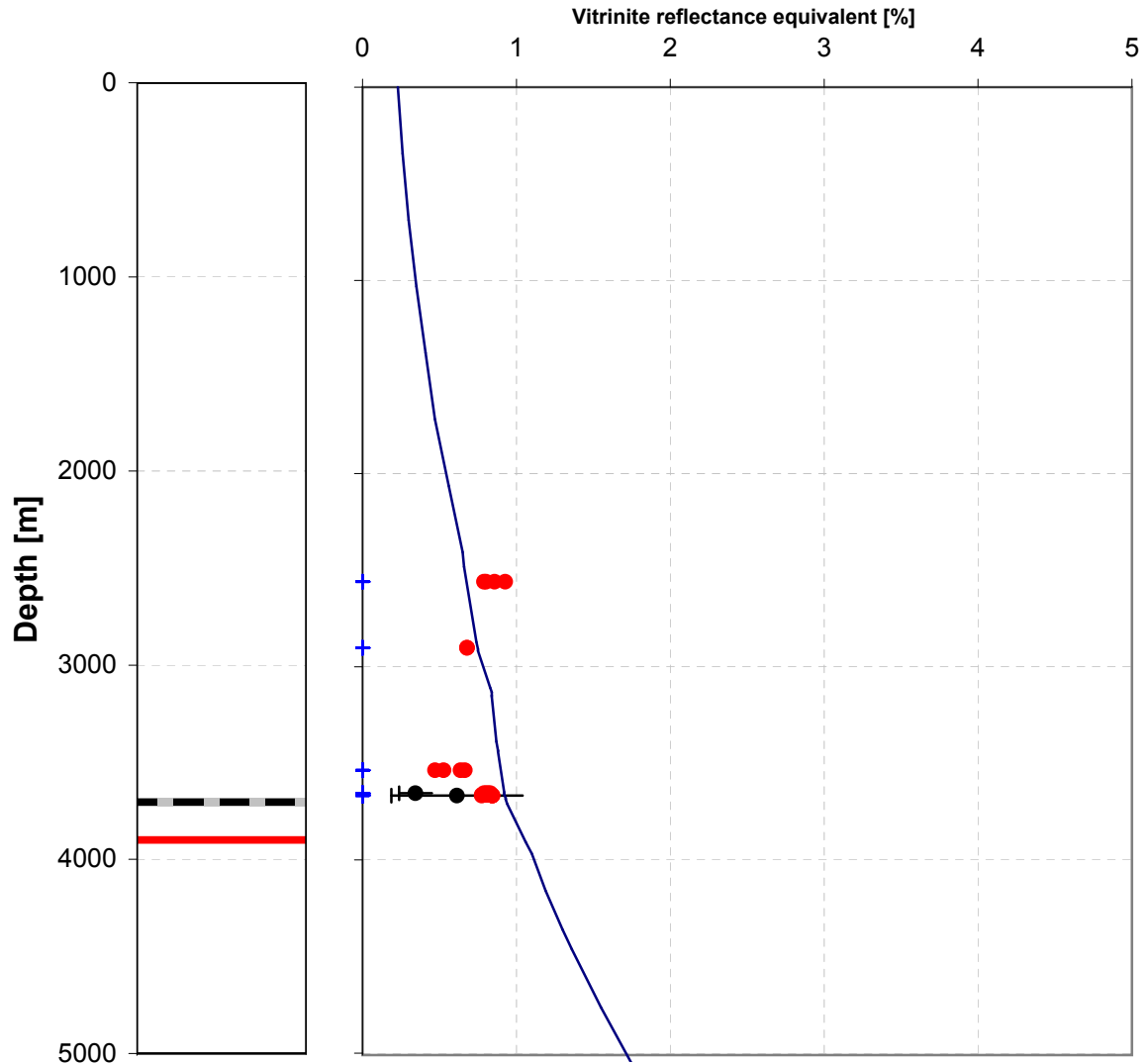




Joint Industry Project Petroplay

Raw data

A11-01

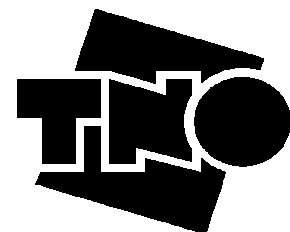
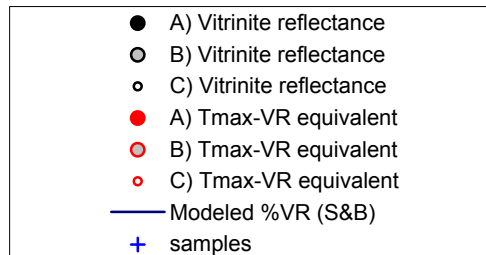
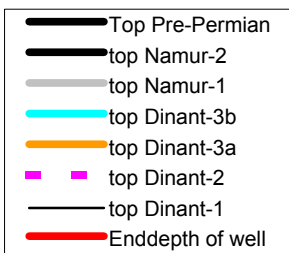
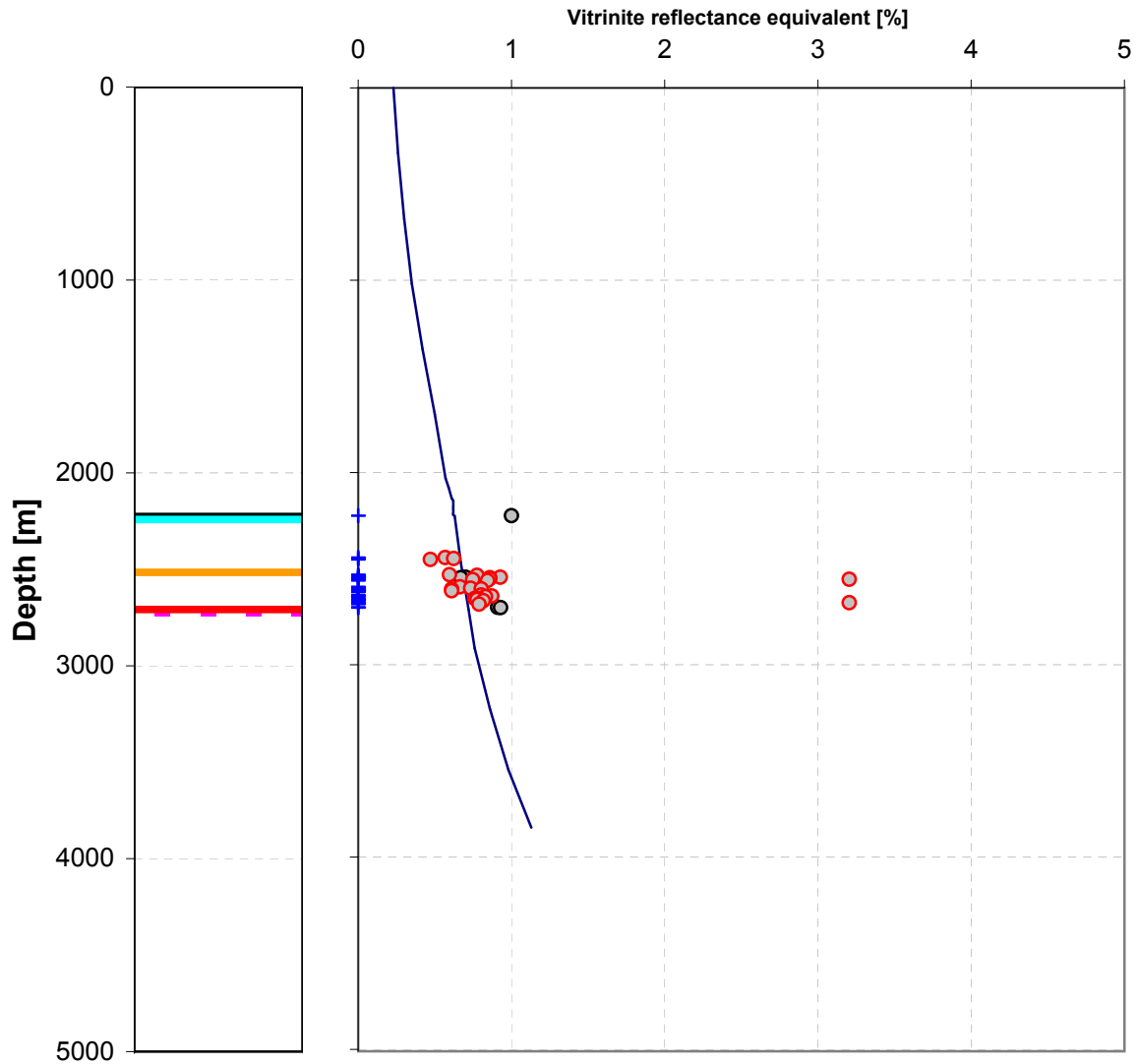




Joint Industry Project Petroplay

Raw data

A16-01

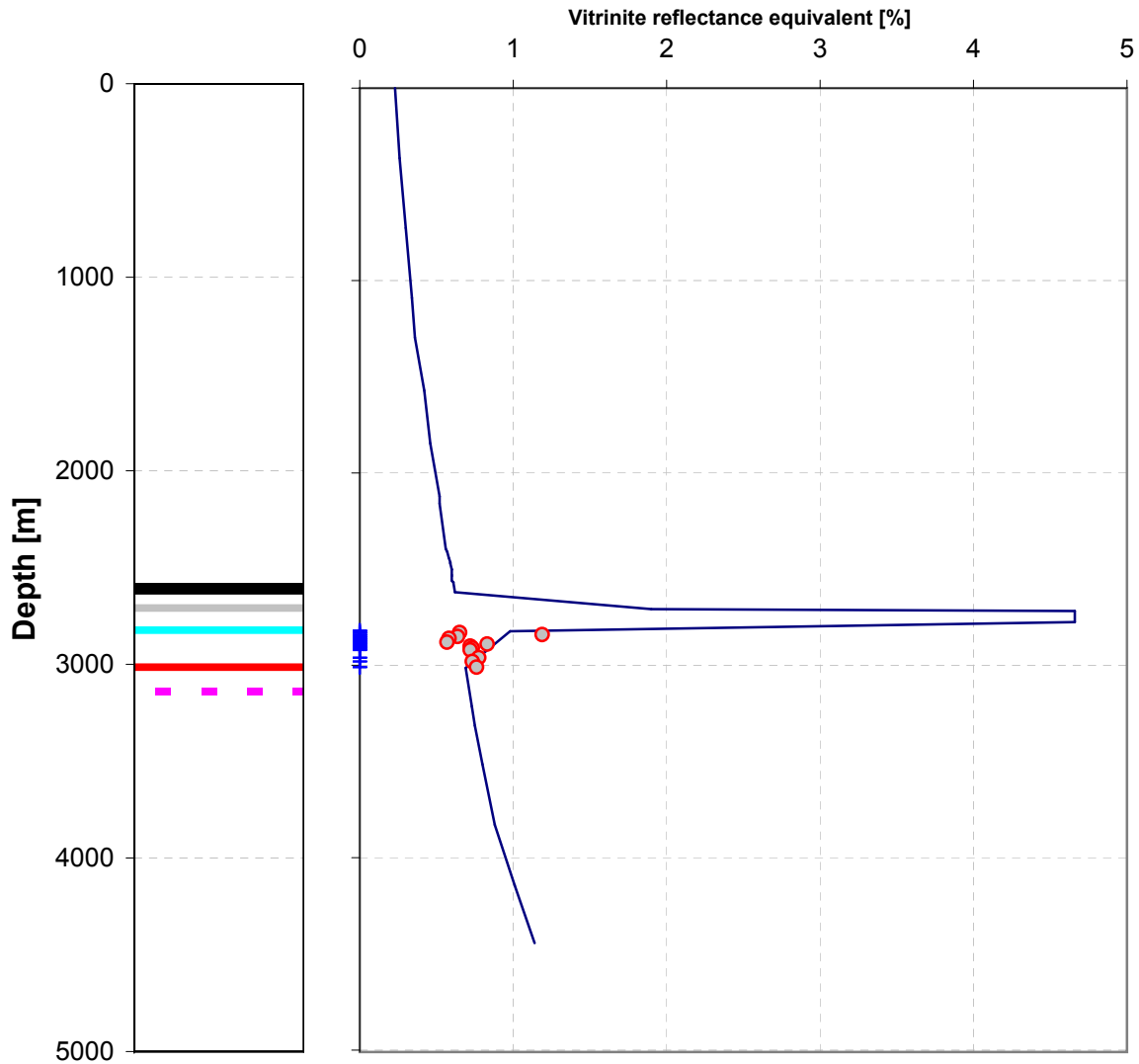




Joint Industry Project Petroplay

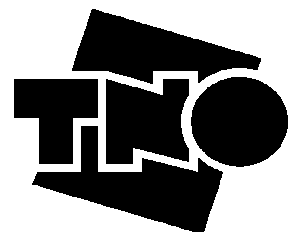
Raw data

A14-01



- Top Pre-Permian
- top Namur-2
- top Namur-1
- top Dinant-3b
- top Dinant-3a
- top Dinant-2
- top Dinant-1
- Enddepth of well

- A) Vitrinite reflectance
- B) Vitrinite reflectance
- C) Vitrinite reflectance
- A) Tmax-VR equivalent
- B) Tmax-VR equivalent
- C) Tmax-VR equivalent
- Modeled %VR (S&B)
- + samples

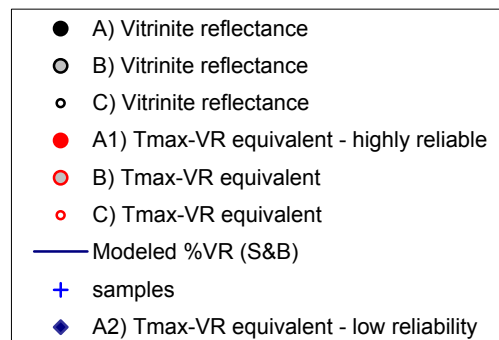
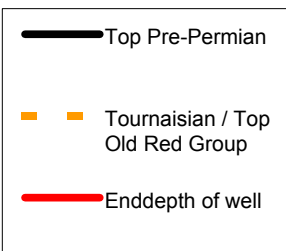
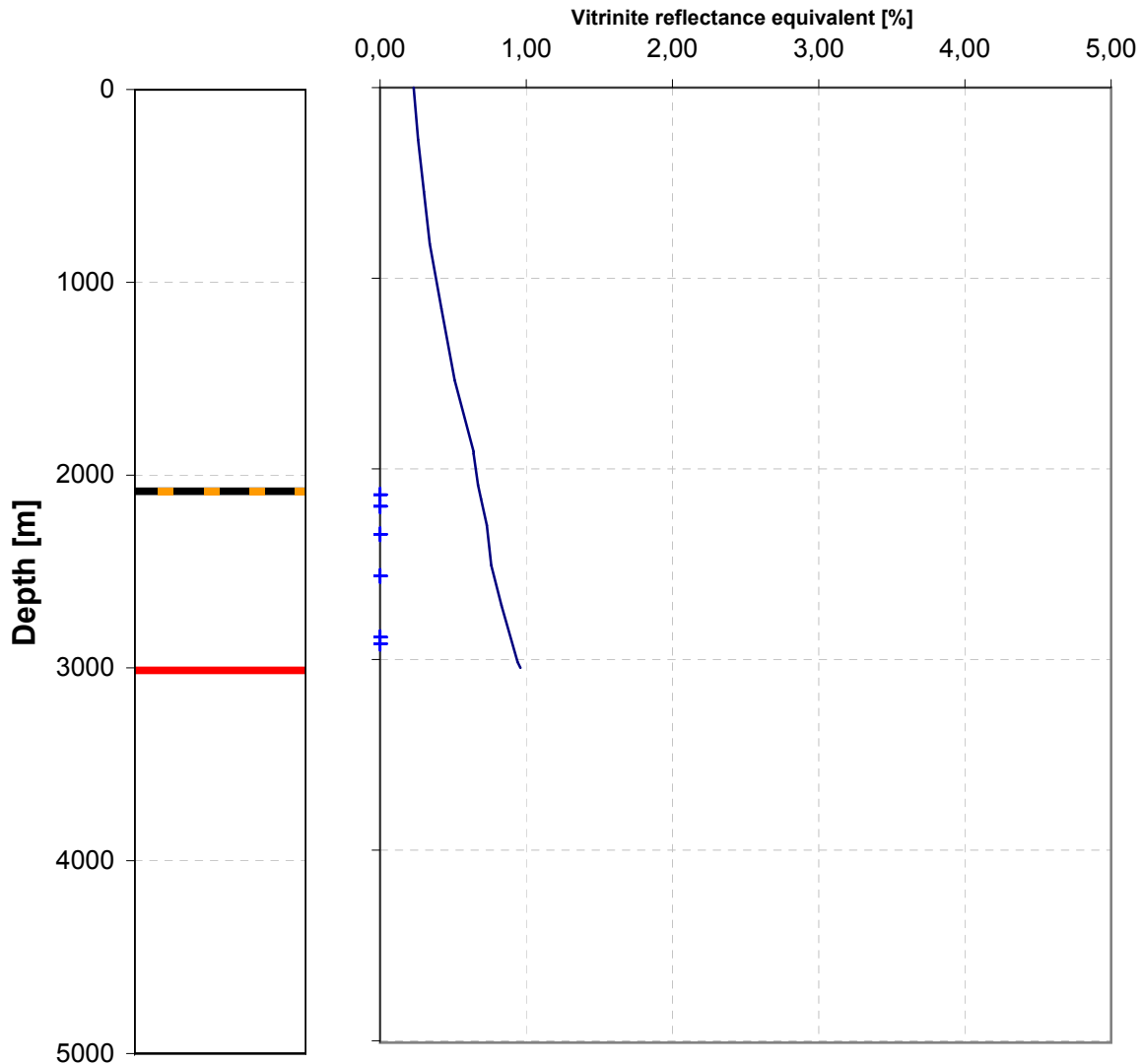




Joint Industry Project Petroplay

Quality controlled data

A17-01

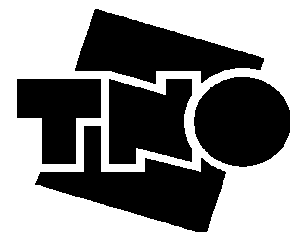
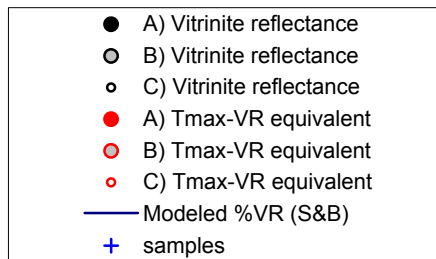
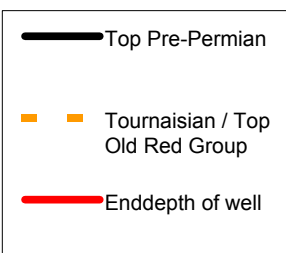
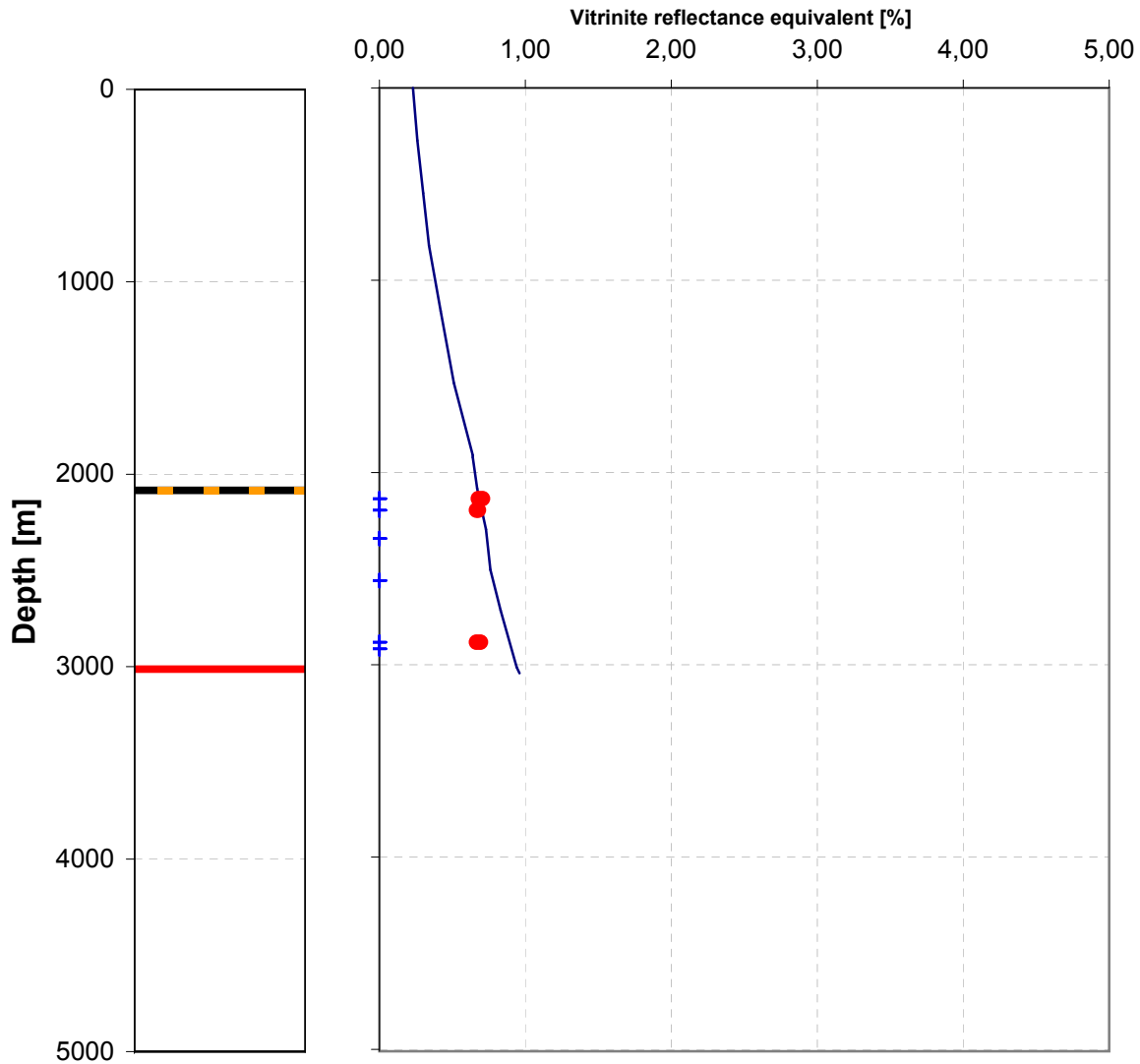




Joint Industry Project Petroplay

Raw data

A17-01

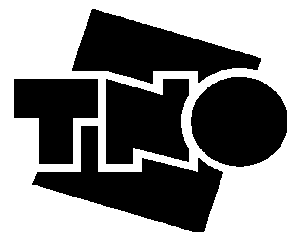
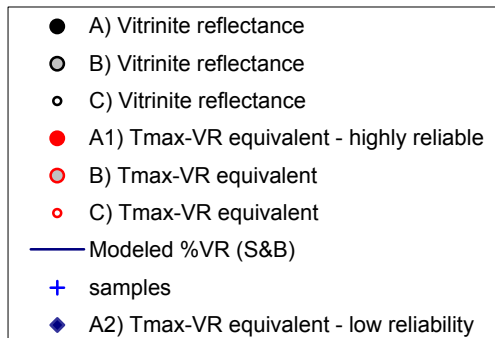
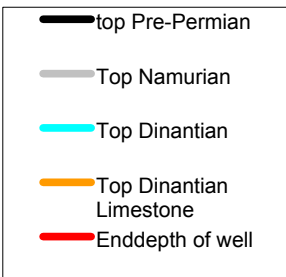
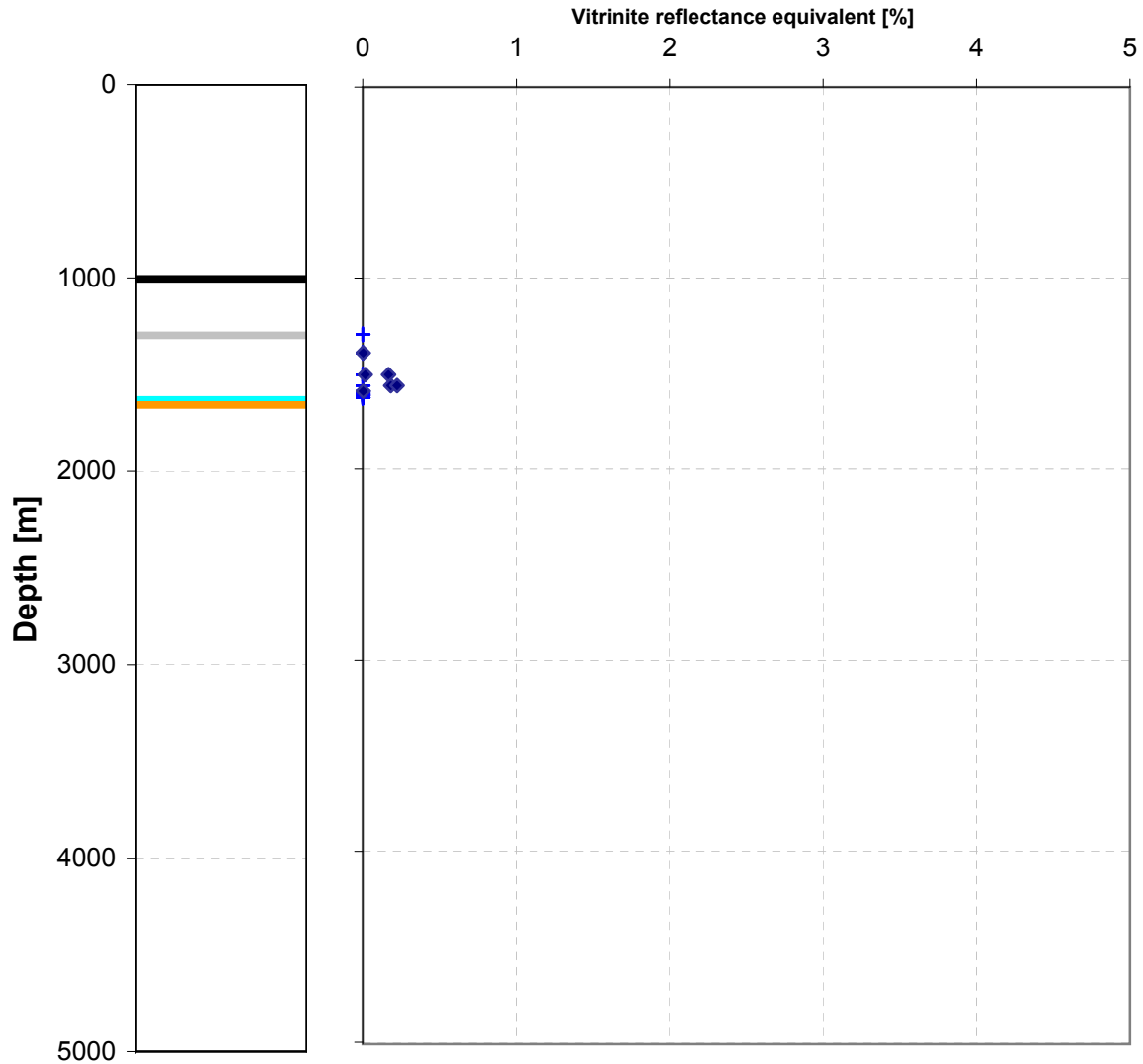




Joint Industry Project Petroplay

Quality controlled data

Beerse-Merksplas

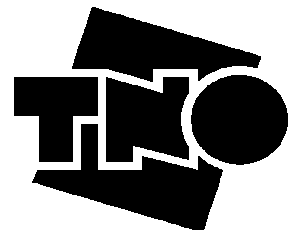
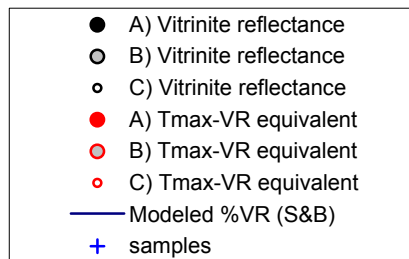
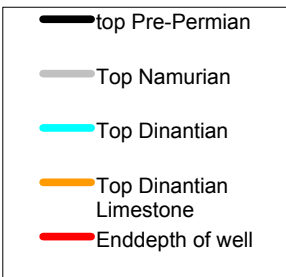
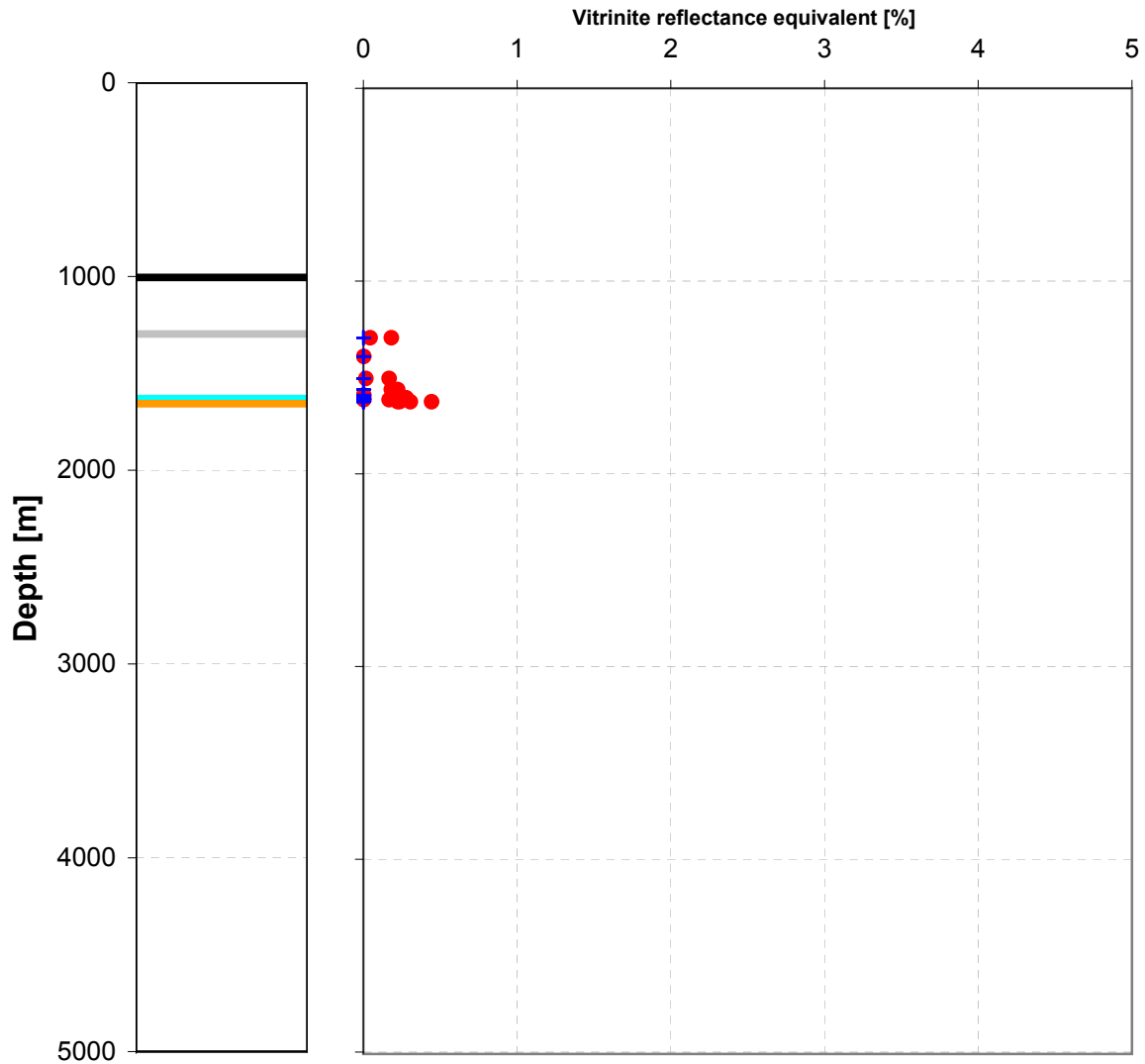




Joint Industry Project Petroplay

Raw data

Beerse-Merksplas

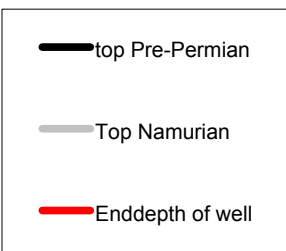
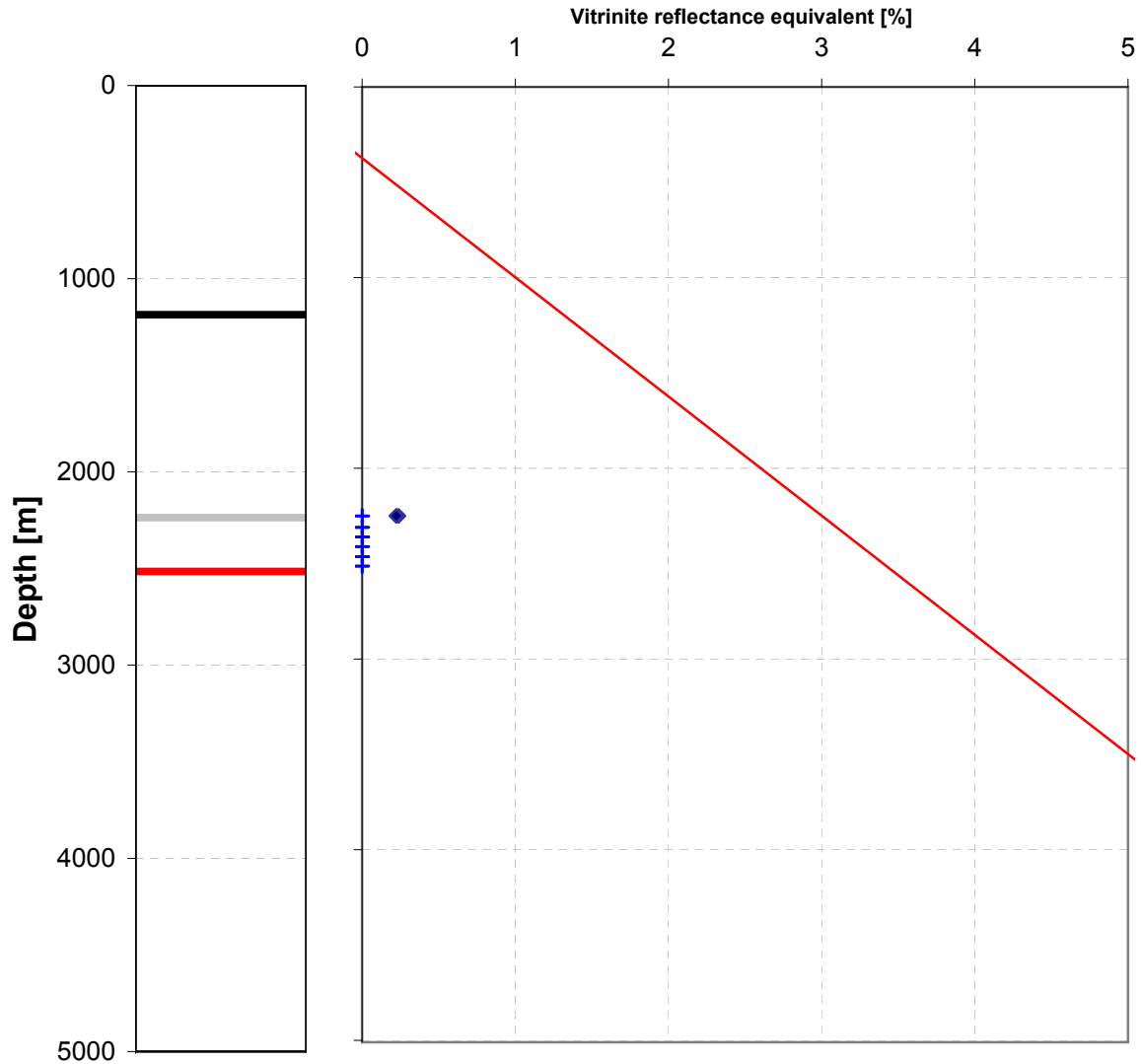




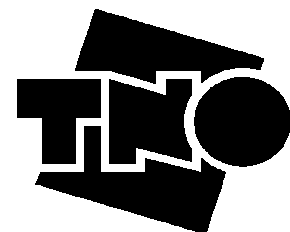
Joint Industry Project Petroplay

Quality controlled data

Meer



- A) Vitrinite reflectance
- B) Vitrinite reflectance
- C) Vitrinite reflectance
- A1) Tmax-VR equivalent - highly reliable
- B) Tmax-VR equivalent
- C) Tmax-VR equivalent
- Modeled %VR (S&B)
- + samples
- ◆ A2) Tmax-VR equivalent - low reliability
- (Vandenberghé et al., 1988)

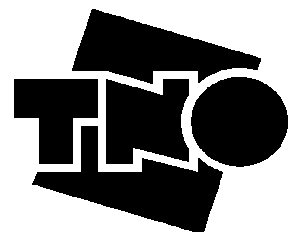
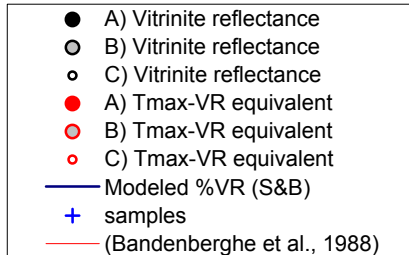
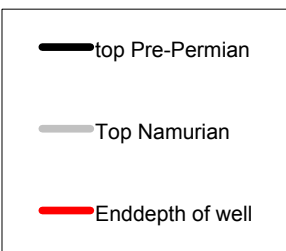
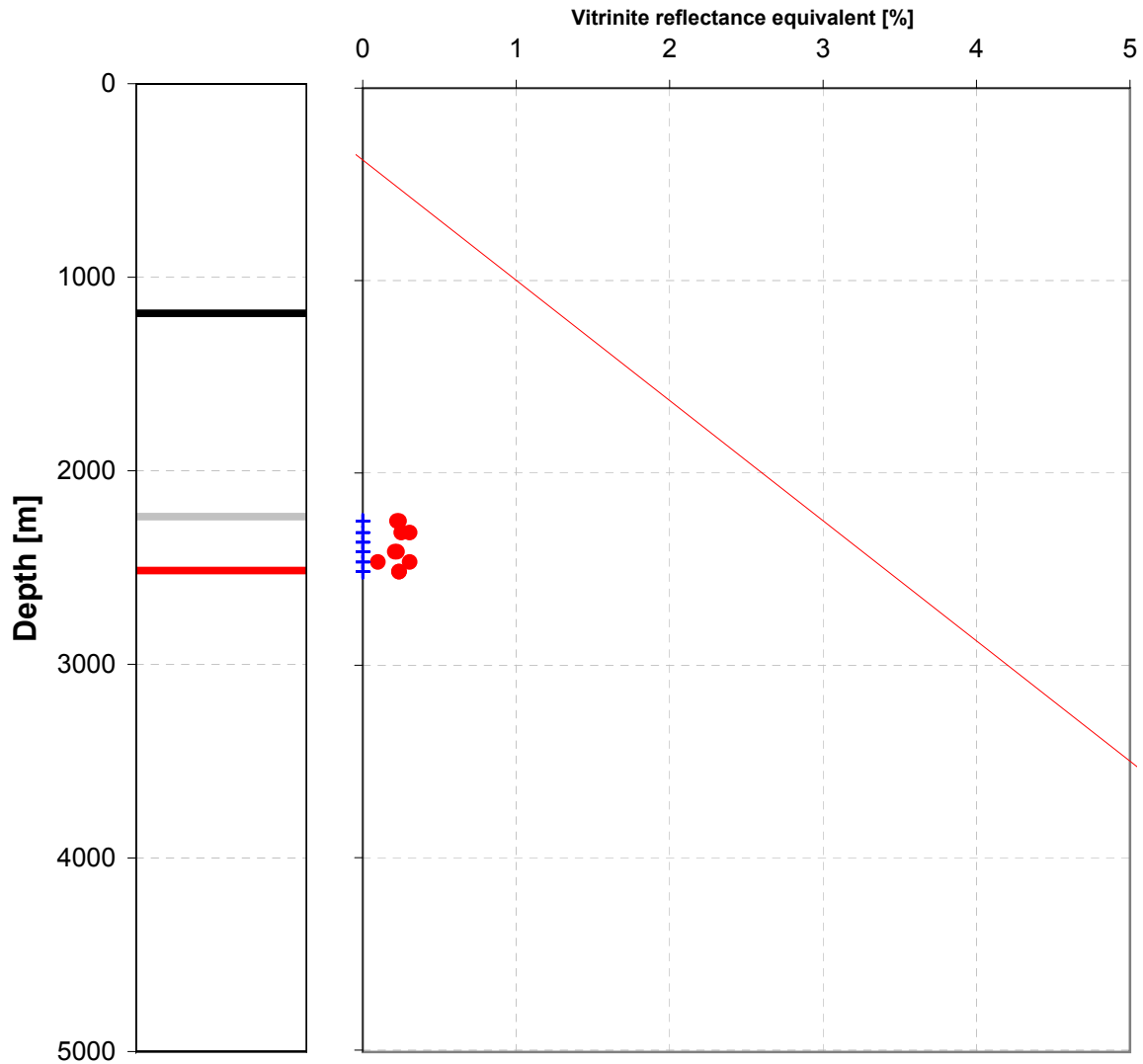




Joint Industry Project Petroplay

Raw data

Meer

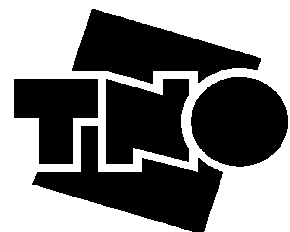
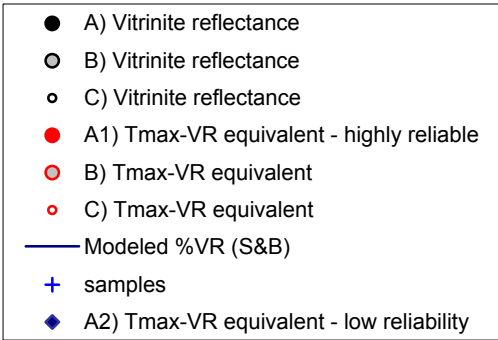
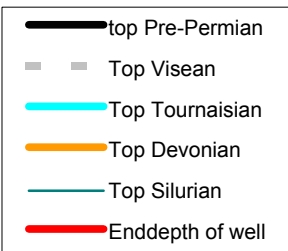
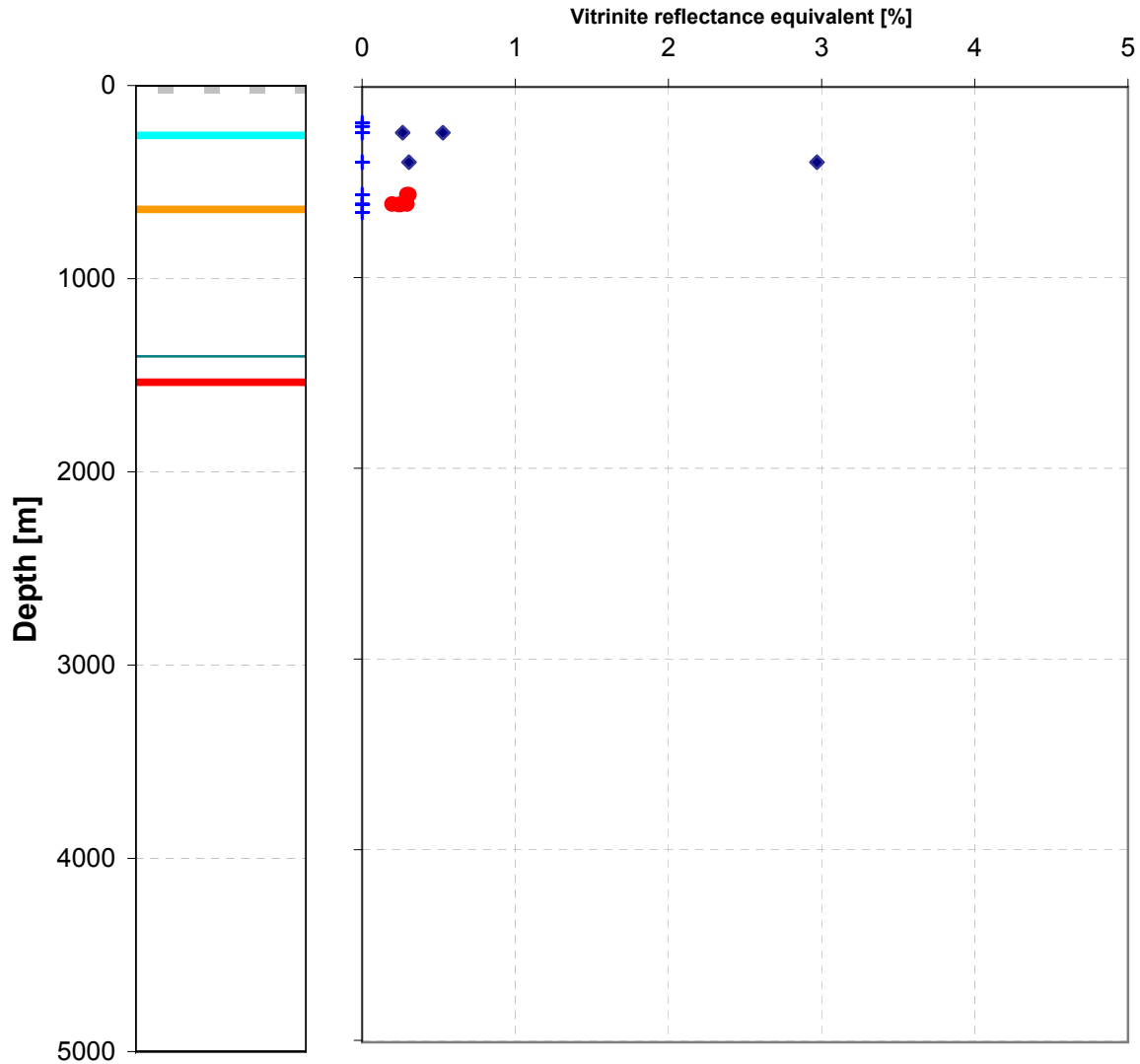




Joint Industry Project Petroplay

Quality controlled data

Leuze

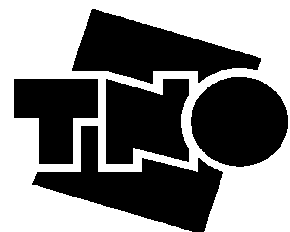
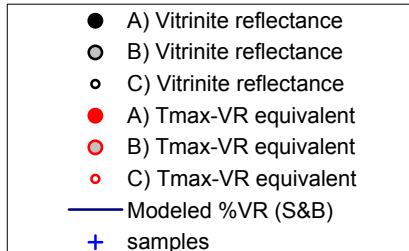
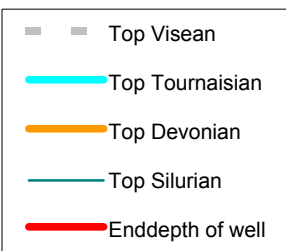
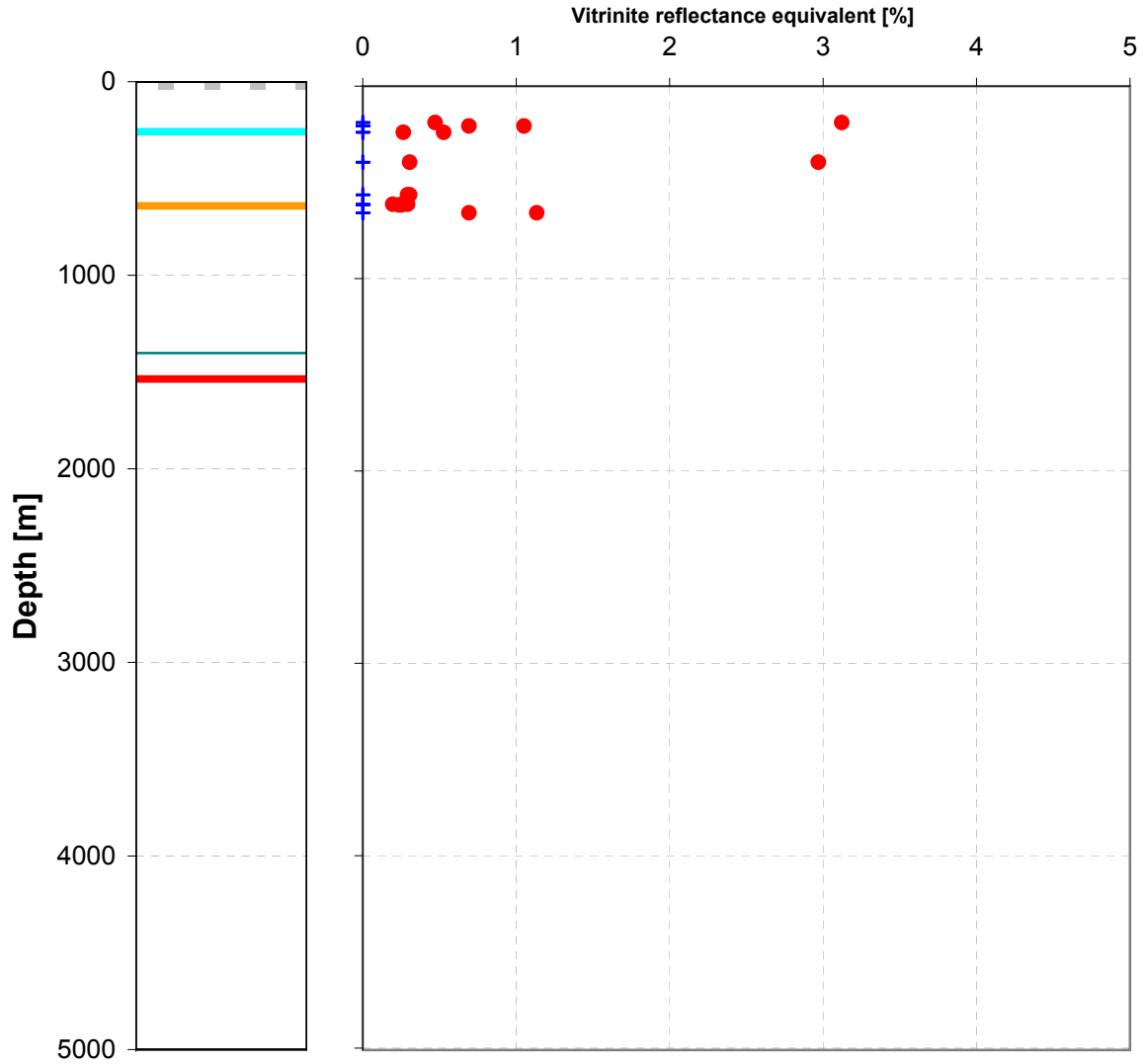




Joint Industry Project Petroplay

Raw data

Leuze

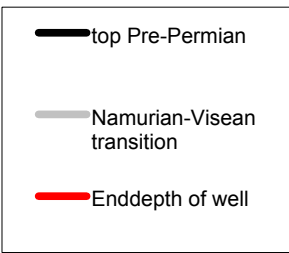
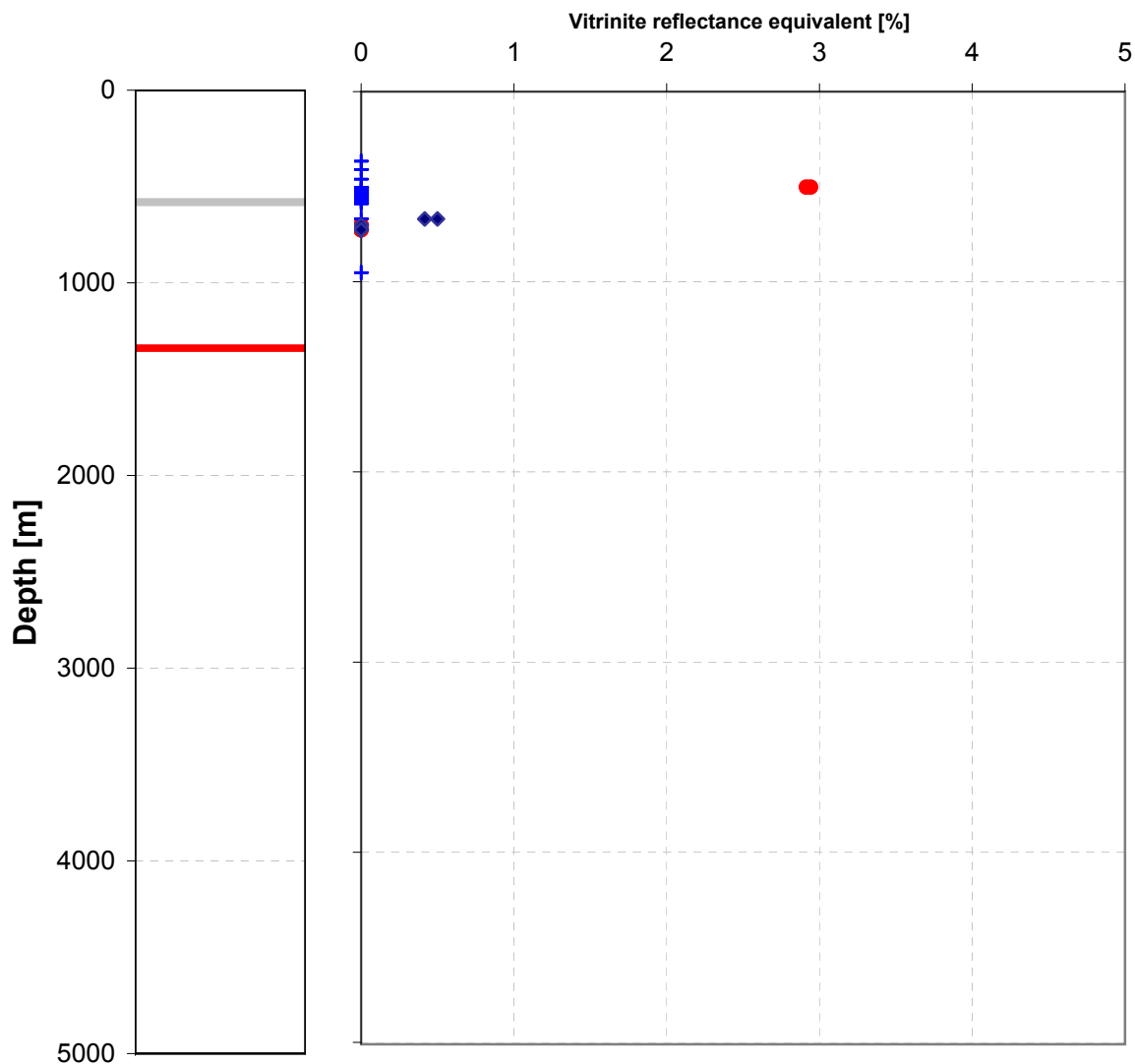




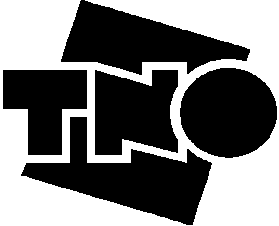
Joint Industry Project Petroplay

Quality controlled data

Halen



- A) Vitrinite reflectance
- B) Vitrinite reflectance
- C) Vitrinite reflectance
- A1) Tmax-VR equivalent - highly reliable
- B) Tmax-VR equivalent
- C) Tmax-VR equivalent
- Modeled %VR (S&B)
- + samples
- ◆ A2) Tmax-VR equivalent - low reliability

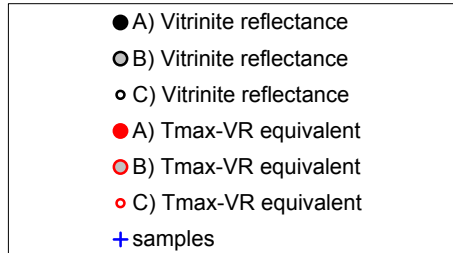
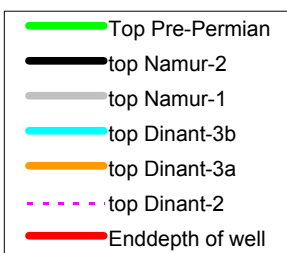
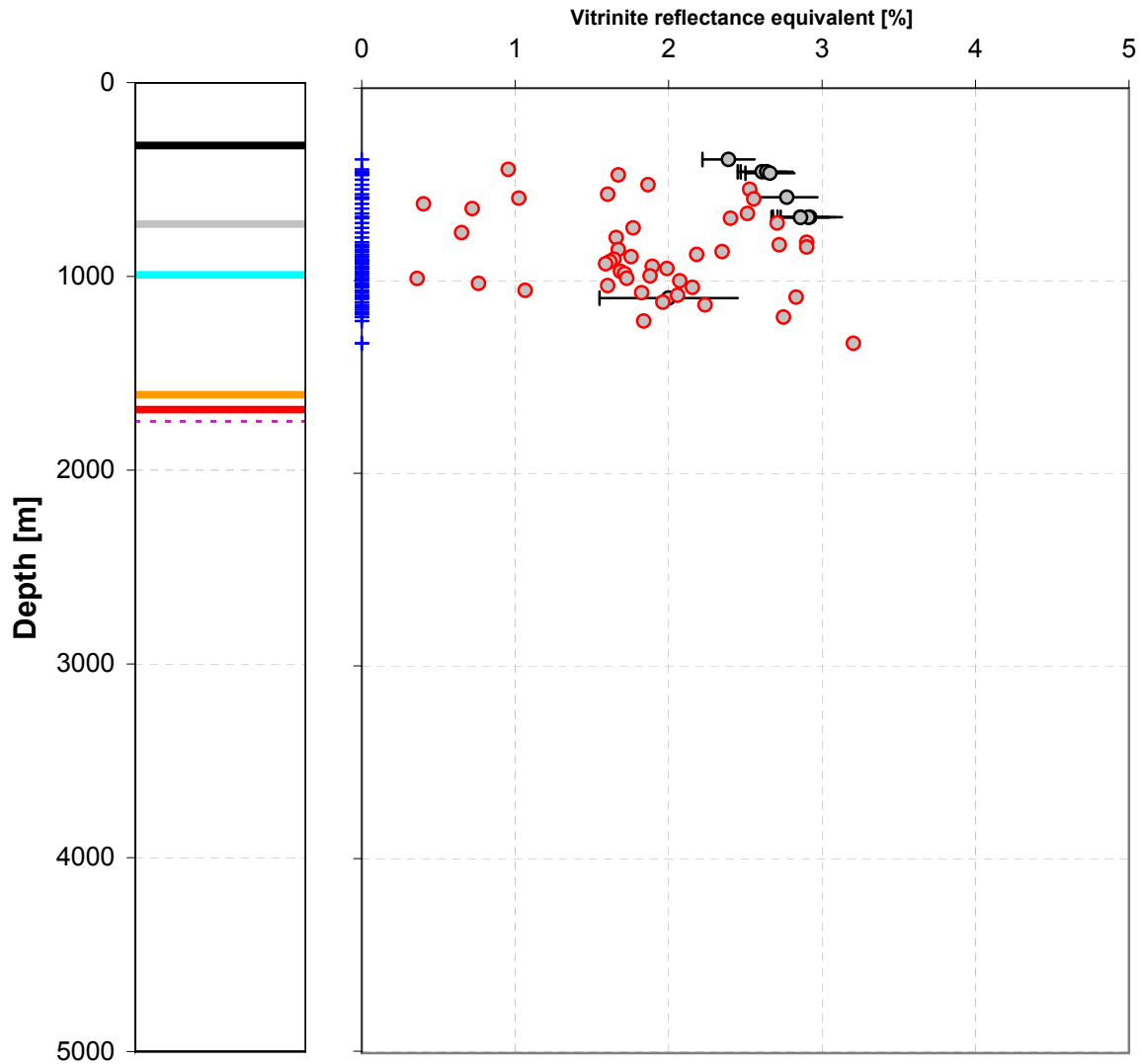




Joint Industry Project Petroplay

Raw data

Geverik-1

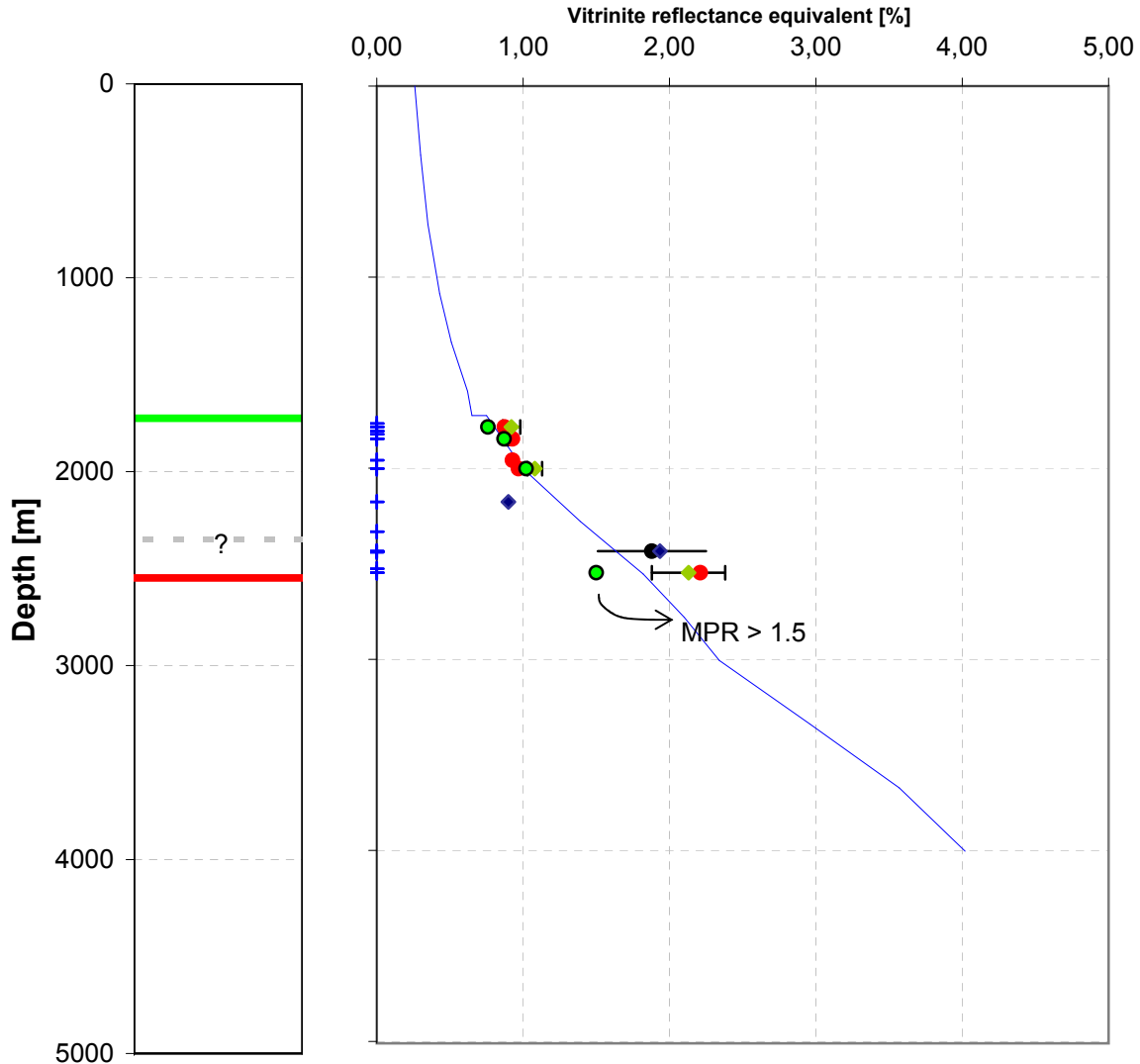




Joint Industry Project Petroplay

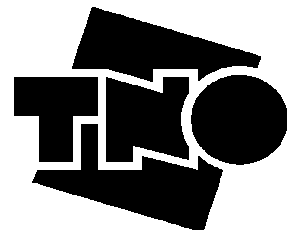
Quality controlled data

Emmeloord-1



- Top Pre-Permian
- top Namur-2
- top Namur-1
- top Dinant-3b
- top Dinant-3a
- top Dinant-2
- top Dinant-1
- Enddepth of well

- A) Vitrinite reflectance
- B) Vitrinite reflectance
- C) Vitrinite reflectance
- A1) Tmax-VR equivalent - highly reliable
- B) Tmax-VR equivalent
- C) Tmax-VR equivalent
- ◆ A) Vitrinite reflectance (max)
- + samples
- ◆ A2) Tmax-VR equivalent - low reliability
- Modeled %VR (S&B)
- MPR

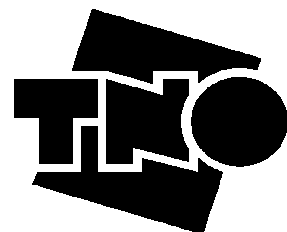
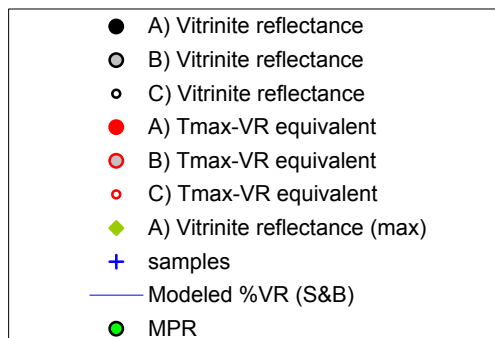
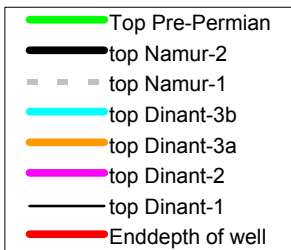
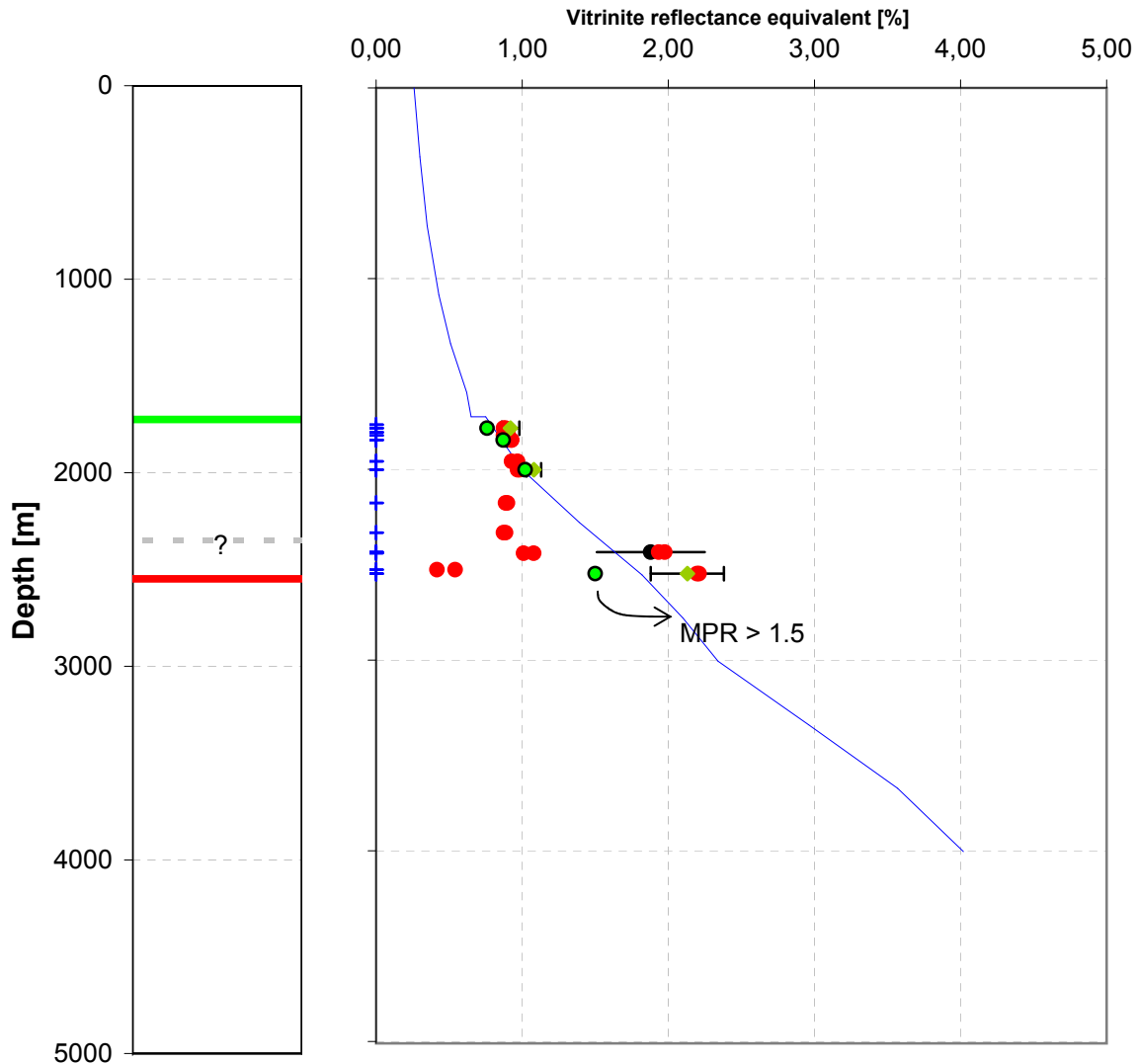




Joint Industry Project Petroplay

Raw data

Emmeloord-1

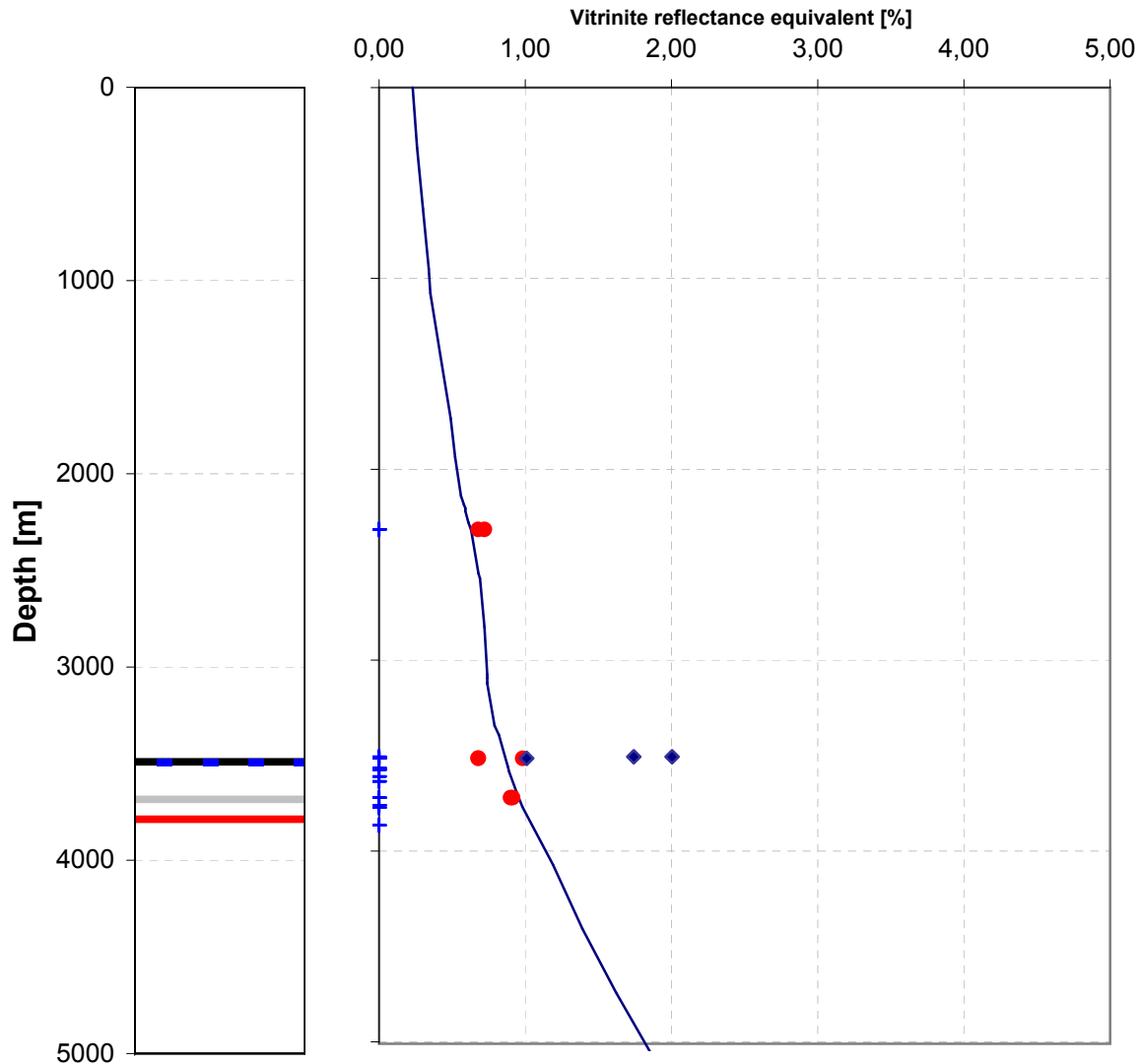




Joint Industry Project Petroplay

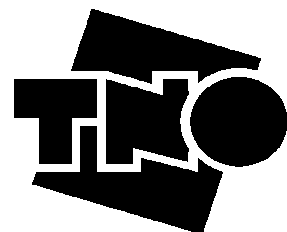
Quality controlled data

E12-03



- Top Pre-Permian
- top Namur-1
- top Namur-2
- top Dinant-3b
- top Dinant-3a
- top Dinant-2
- top Dinant-1
- Enddepth of well

- A) Vitrinite reflectance
- B) Vitrinite reflectance
- C) Vitrinite reflectance
- A1) Tmax-VR equivalent - highly reliable
- B) Tmax-VR equivalent
- C) Tmax-VR equivalent
- Modeled %VR (S&B)
- + samples
- ◆ A2) Tmax-VR equivalent - low reliability

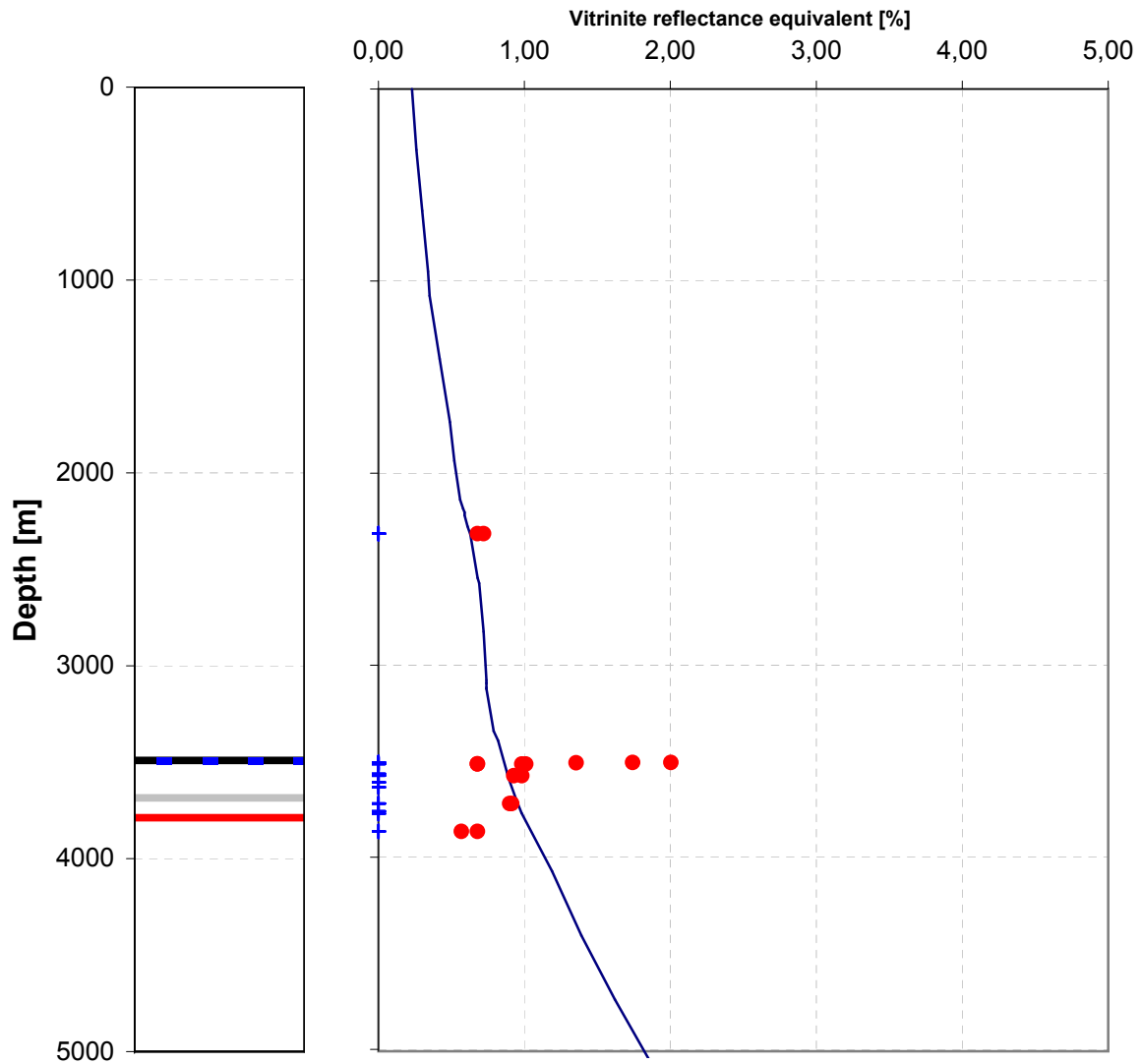




Joint Industry Project Petroplay

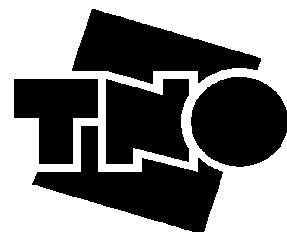
Raw data

E12-03



- Top Pre-Permian
- top Namur-1
- top Dinant-3b
- top Dinant-3a
- top Dinant-2
- top Dinant-1
- Enddepth of well

- A) Vitrinite reflectance
- B) Vitrinite reflectance
- C) Vitrinite reflectance
- A) Tmax-VR equivalent
- B) Tmax-VR equivalent
- C) Tmax-VR equivalent
- Modeled %VR (S&B)
- + samples

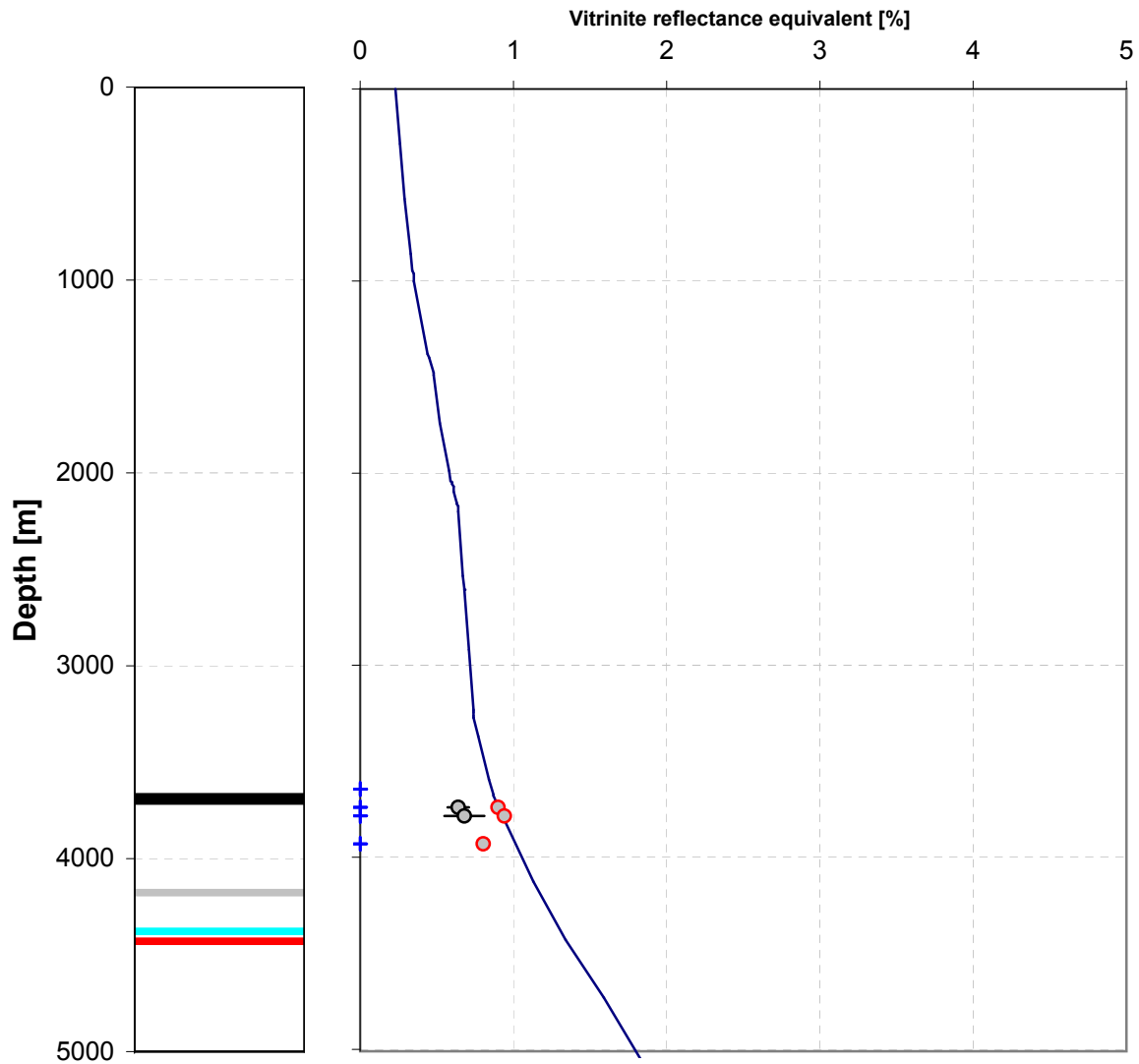




Joint Industry Project Petroplay

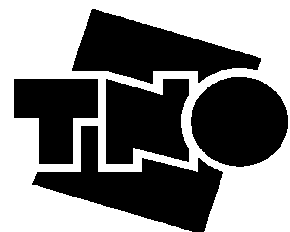
Raw data

E12-02



- Top Pre-Permian
- top Namur-2
- top Namur-1
- top Dinant-3b
- top Dinant-3a
- top Dinant-2
- top Dinant-1
- Enddepth of well

- A) Vitritine reflectance
- B) Vitritine reflectance
- C) Vitritine reflectance
- A) Tmax-VR equivalent
- B) Tmax-VR equivalent
- C) Tmax-VR equivalent
- Modeled %VR (S&B)
- + samples

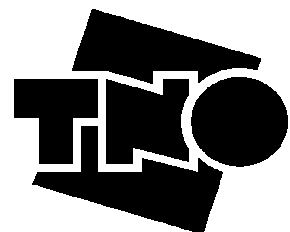
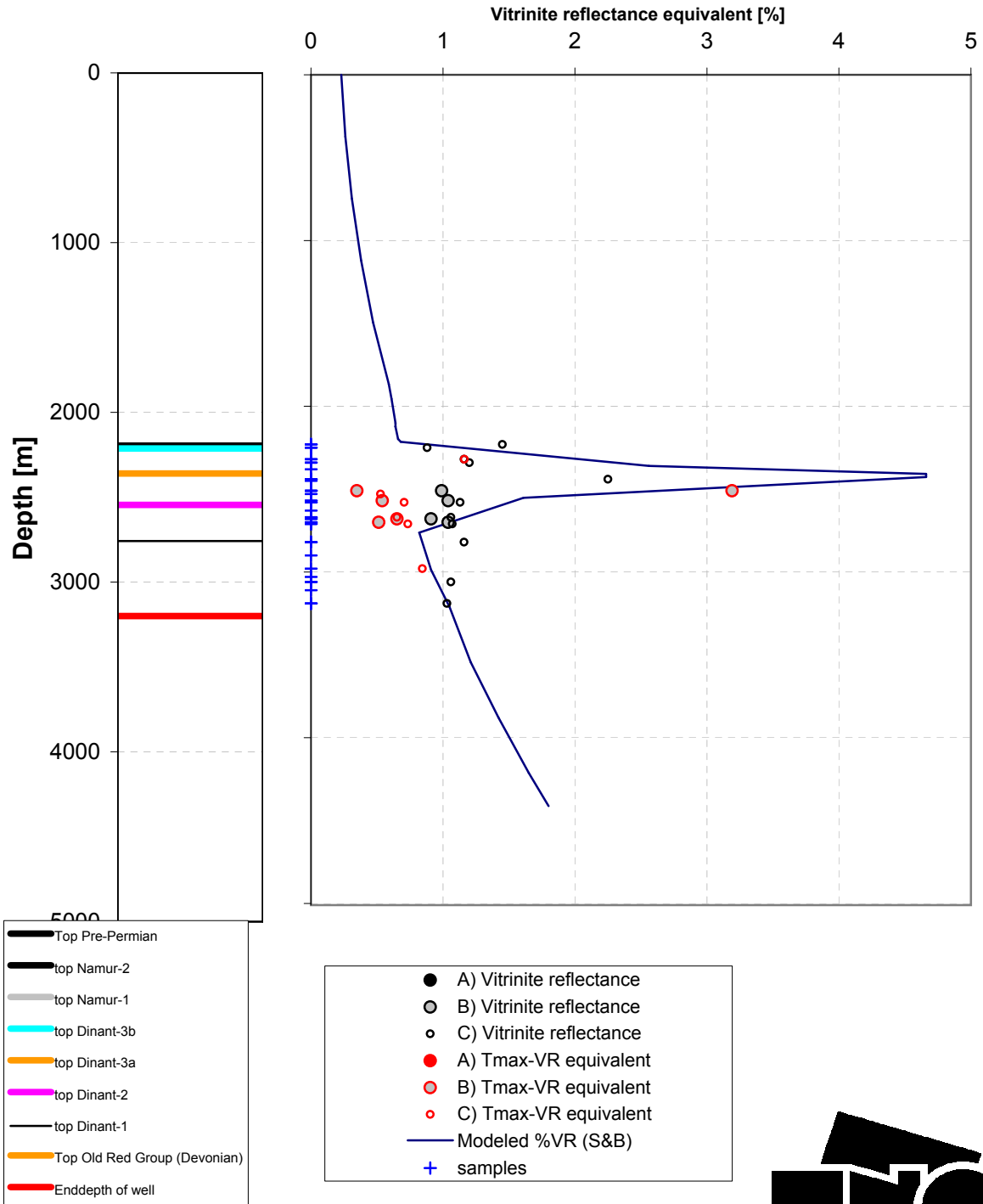




Joint Industry Project Petroplay

Raw data

E06-01

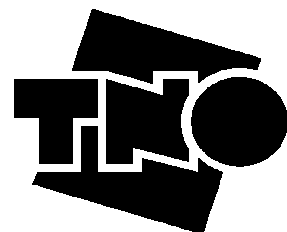
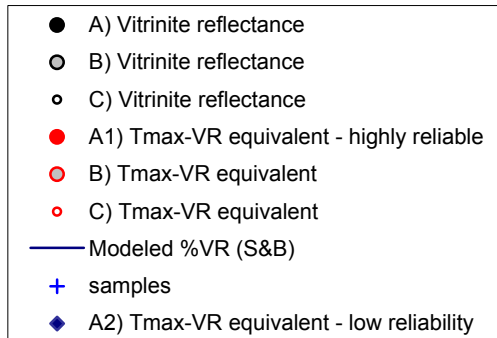
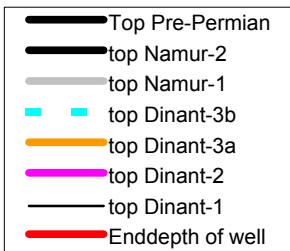
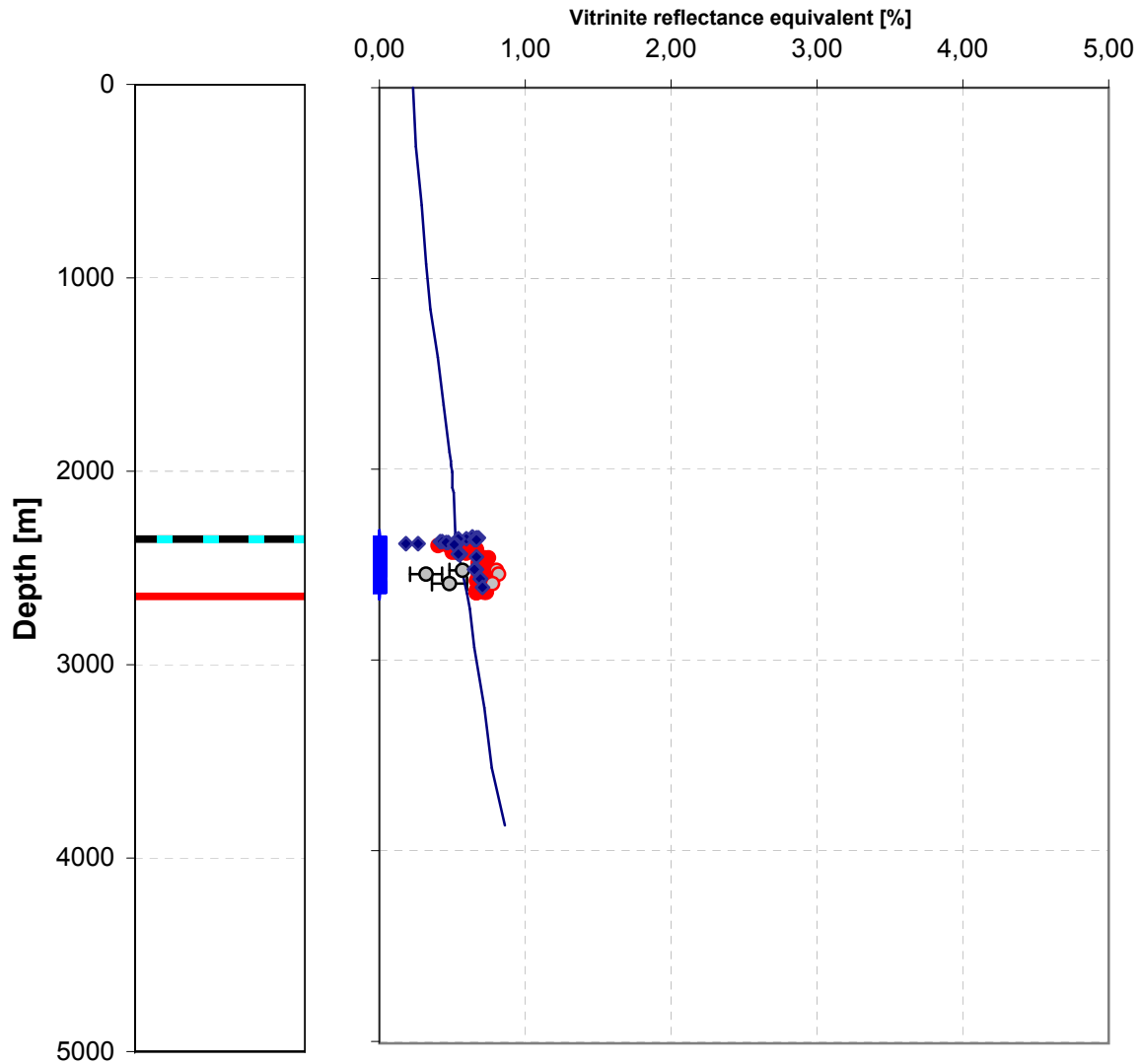




Joint Industry Project Petroplay

Quality controlled data

E02-02

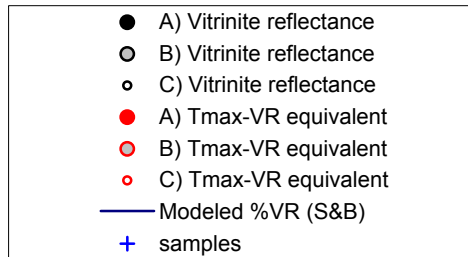
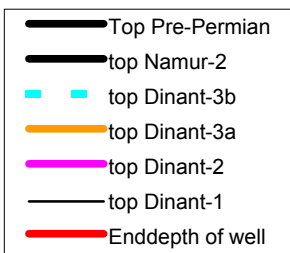
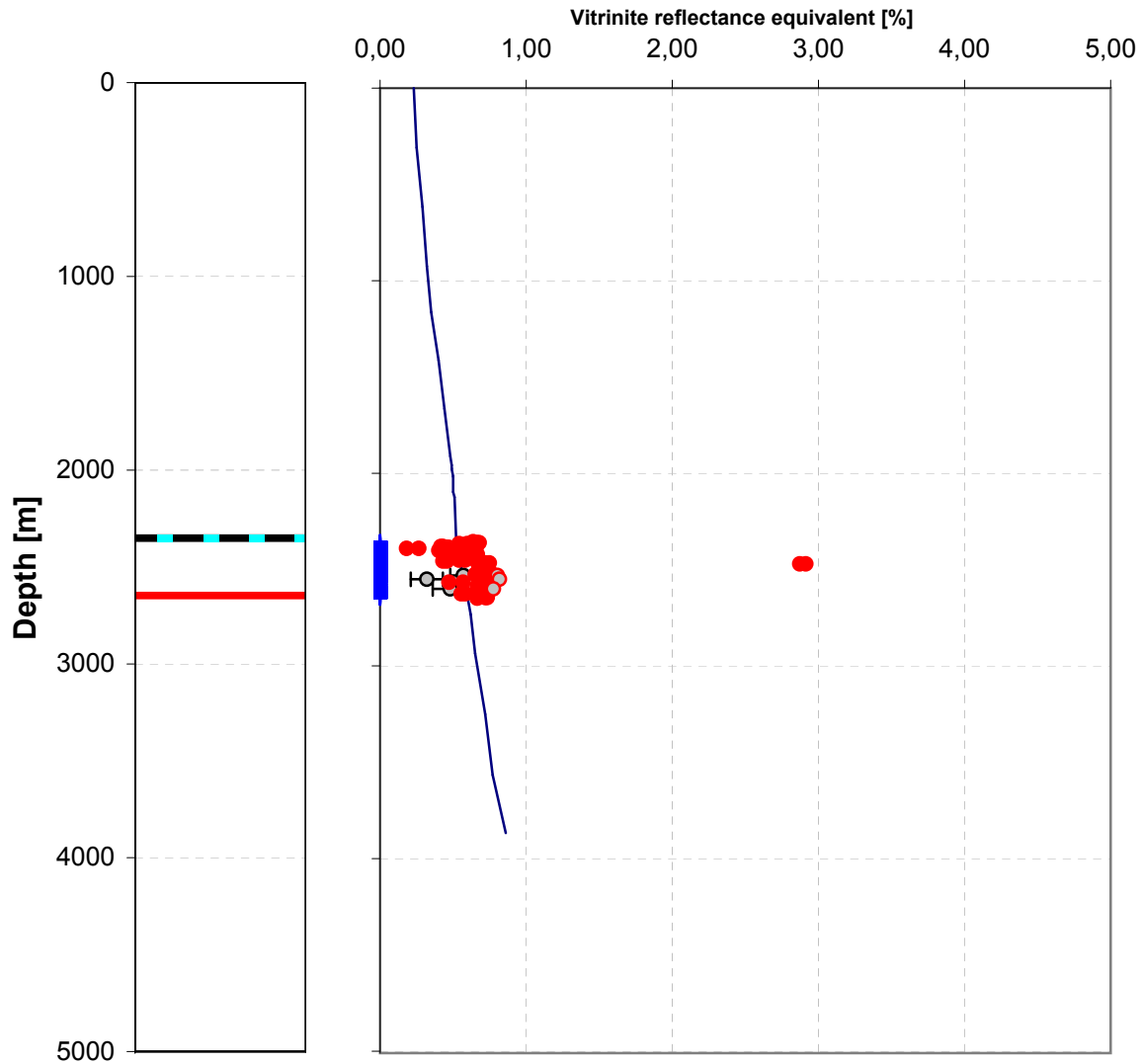




Joint Industry Project Petroplay

Raw data

E02-02

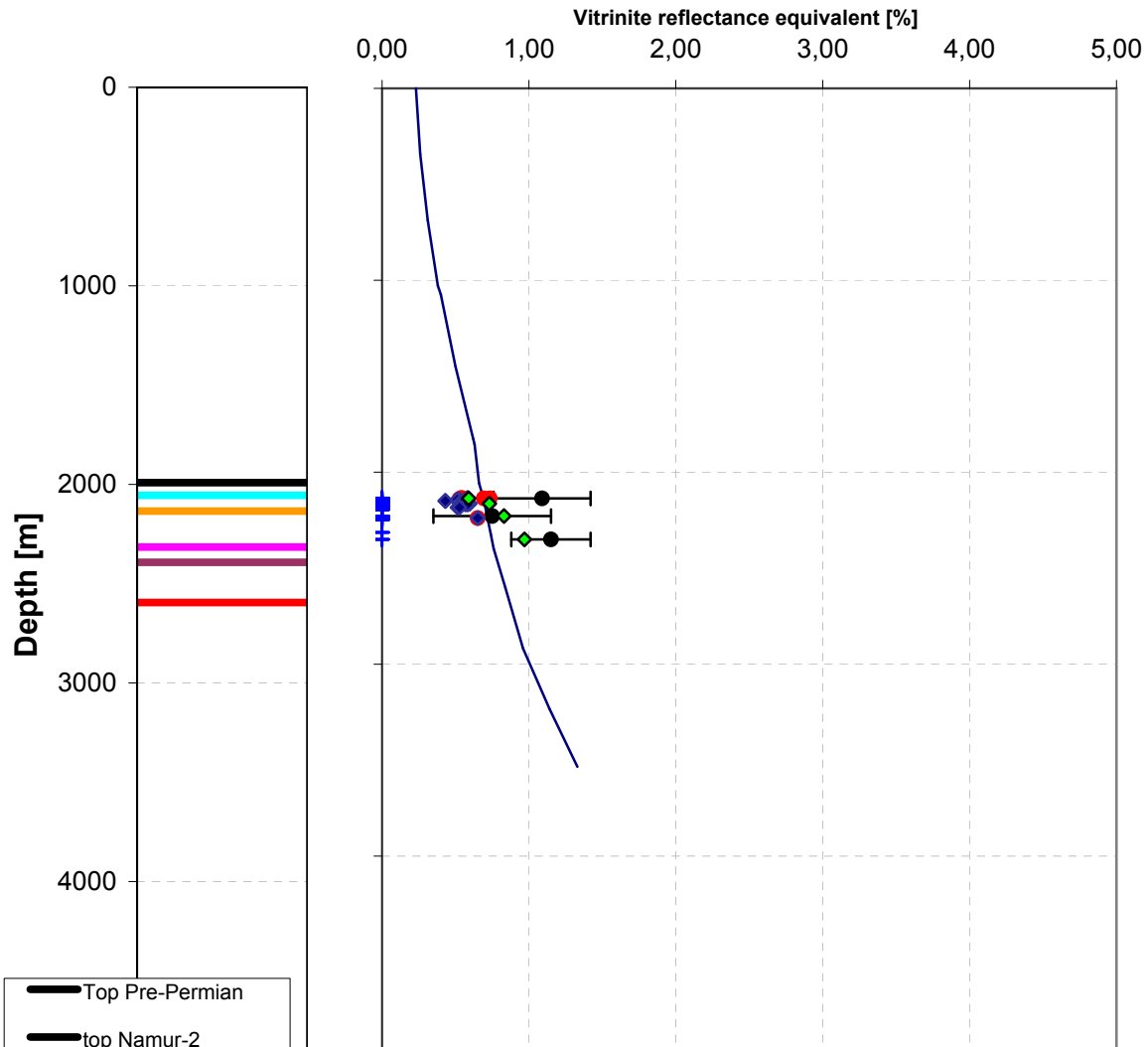




Joint Industry Project Petroplay

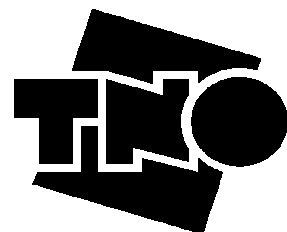
Quality controlled data

E02-01



- Top Pre-Permian
- top Namur-2
- top Namur-1
- top Dinant-3b
- top Dinant-3a
- top Dinant-2
- top Dinant-1
- Top Old Red Group (Devonian)
- Enddepth of well

- A) Vitrinite reflectance
- B) Vitrinite reflectance
- C) Vitrinite reflectance
- A1) Tmax-VR equivalent - highly reliable
- B) Tmax-VR equivalent
- C) Tmax-VR equivalent
- Modeled %VR (S&B)
- + samples
- ◆ A2) Tmax-VR equivalent - low reliability
- ◆ MPR

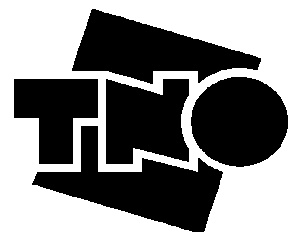
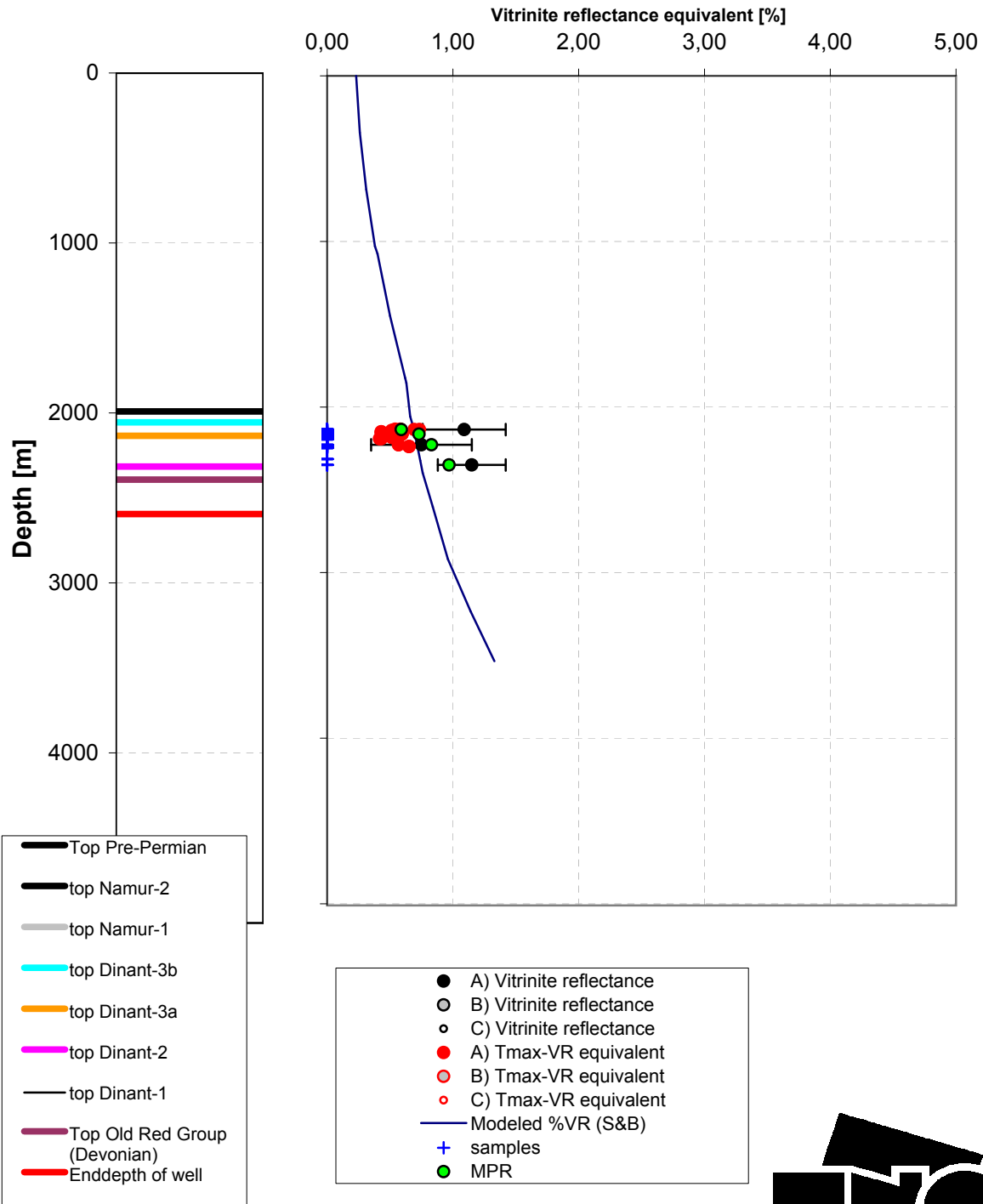




Joint Industry Project Petroplay

Raw data

E02-01

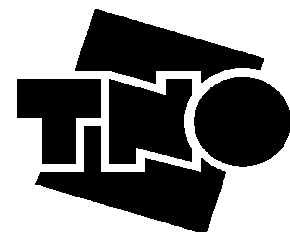
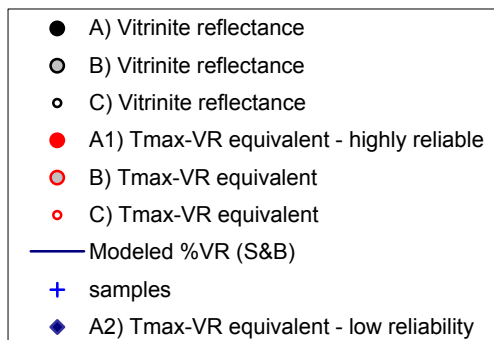
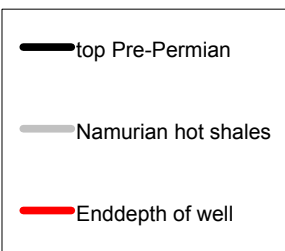
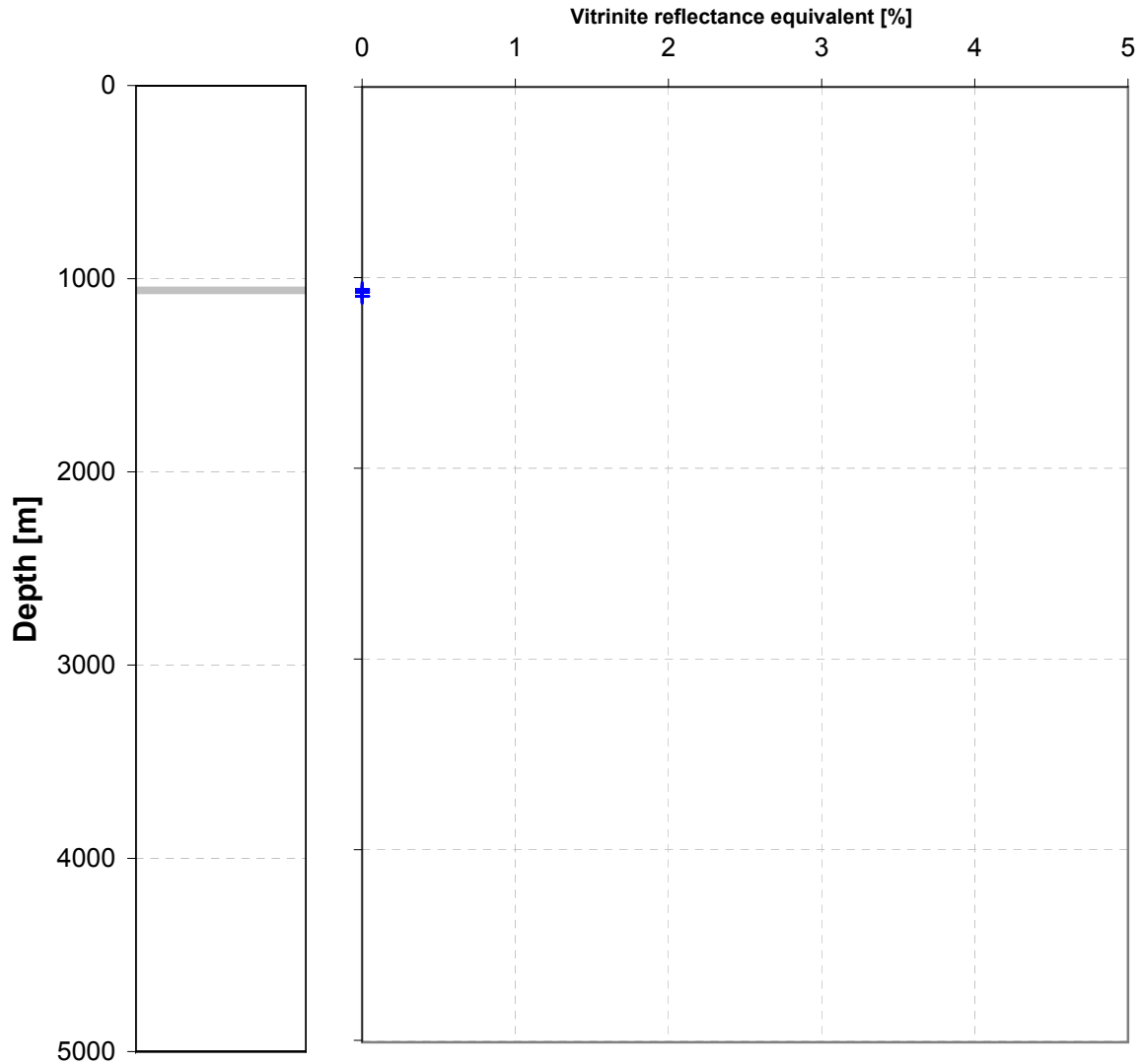




Joint Industry Project Petroplay

Quality controlled data

DZH-01-Heibaart

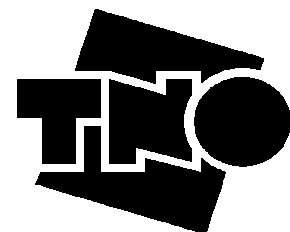
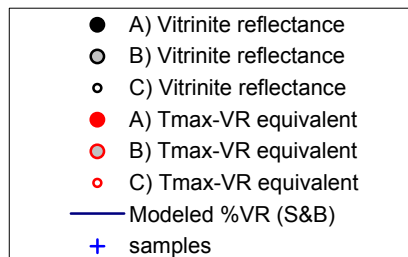
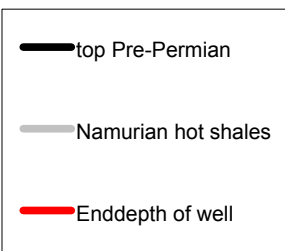
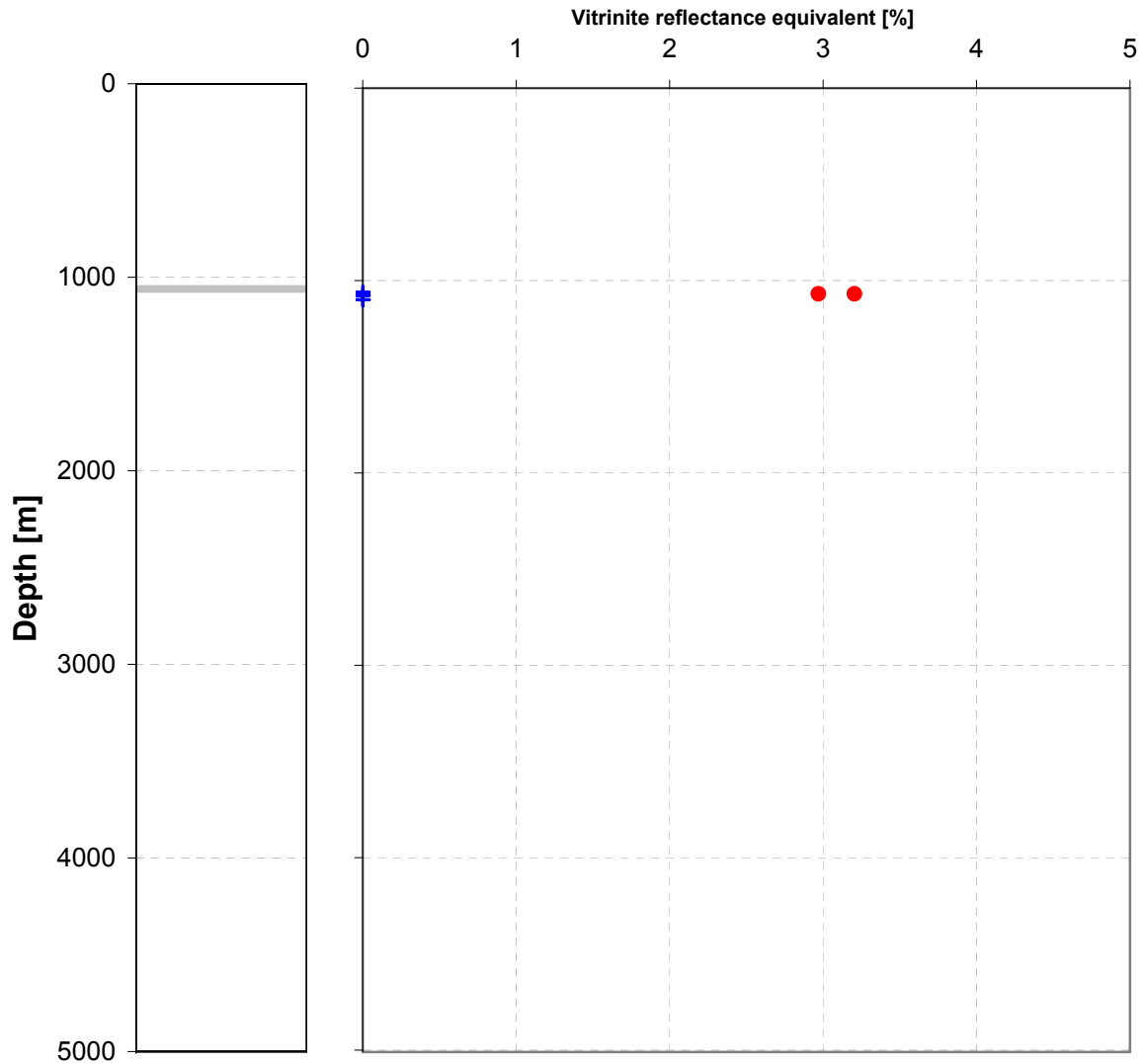




Joint Industry Project Petroplay

Raw data

DZH-01-Heibaart

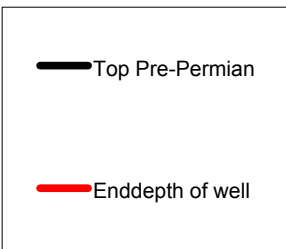
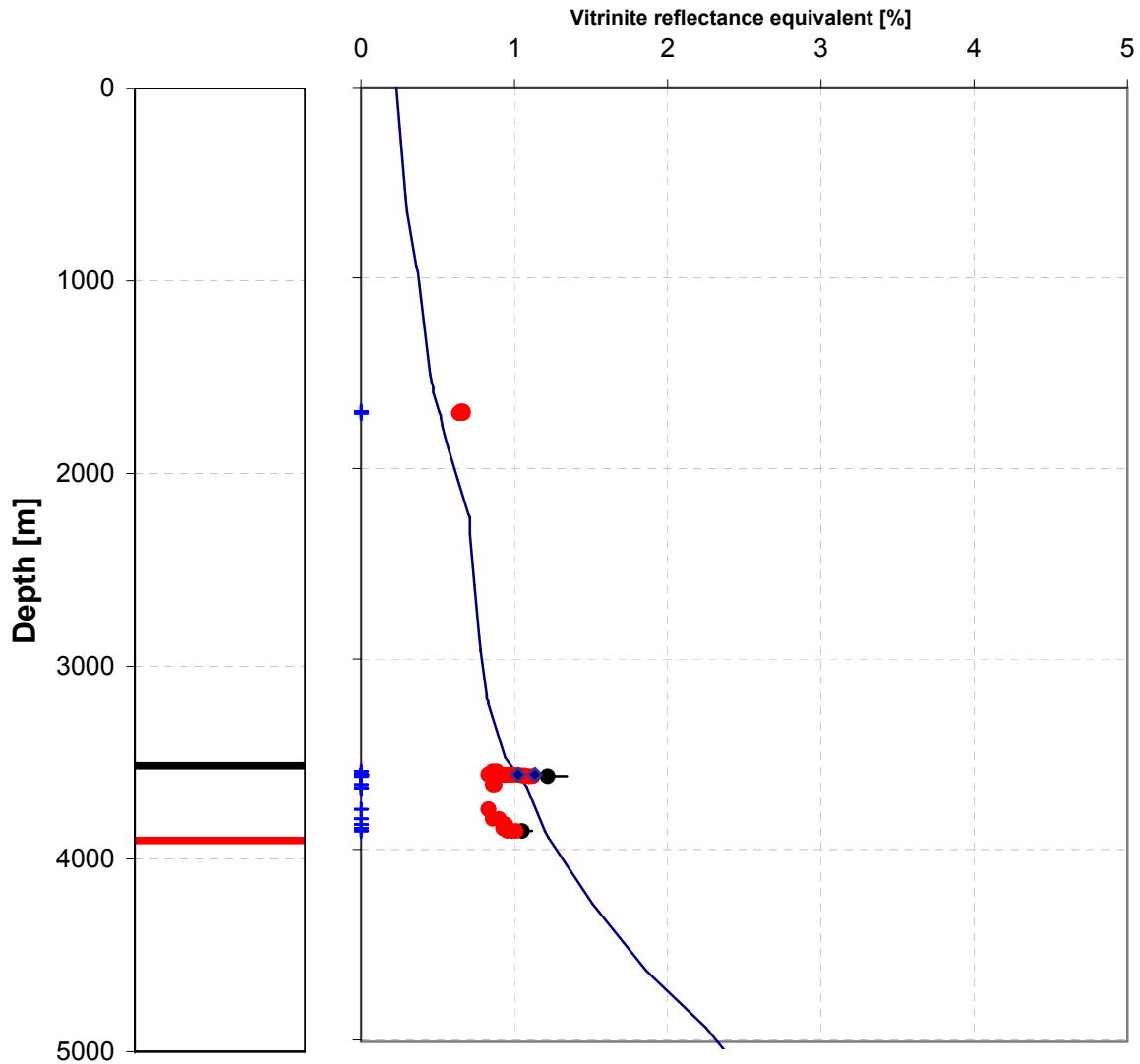




Joint Industry Project Petroplay

Quality controlled data

D15-02



- A) Vitrinite reflectance
- B) Vitrinite reflectance
- C) Vitrinite reflectance
- A1) Tmax-VR equivalent - highly reliable
- B) Tmax-VR equivalent
- C) Tmax-VR equivalent
- Modeled %VR (S&B)
- + samples
- ◆ A2) Tmax-VR equivalent - low reliability

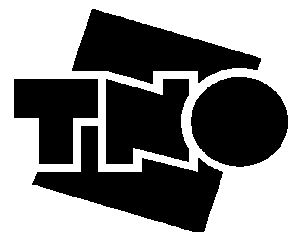
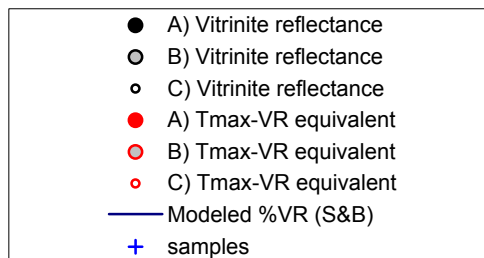
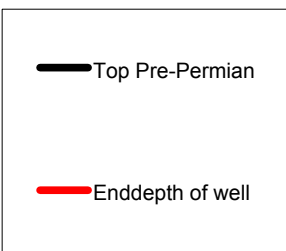
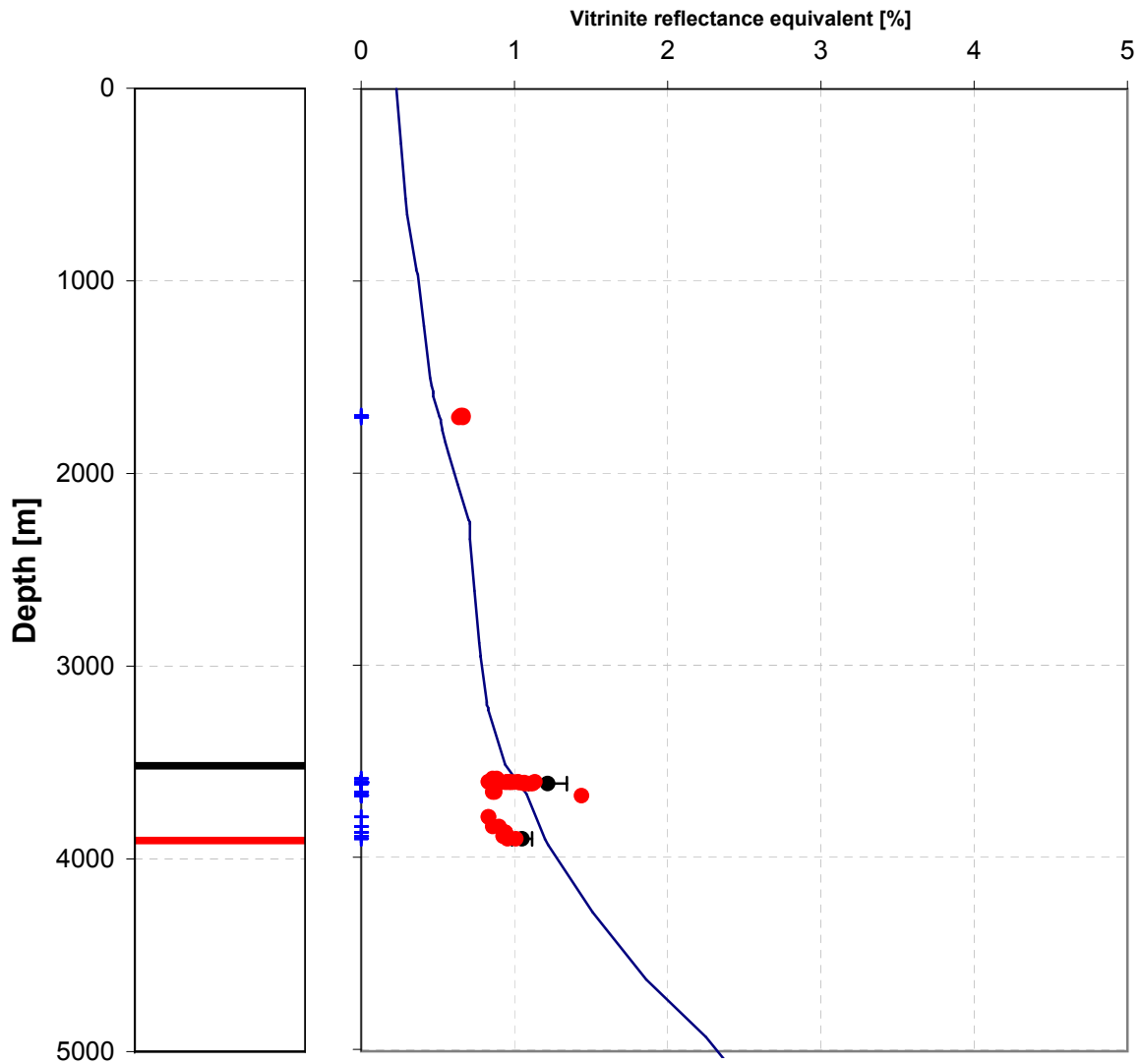




Joint Industry Project Petroplay

Raw data

D15-02

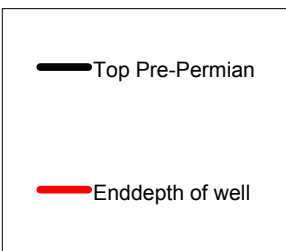
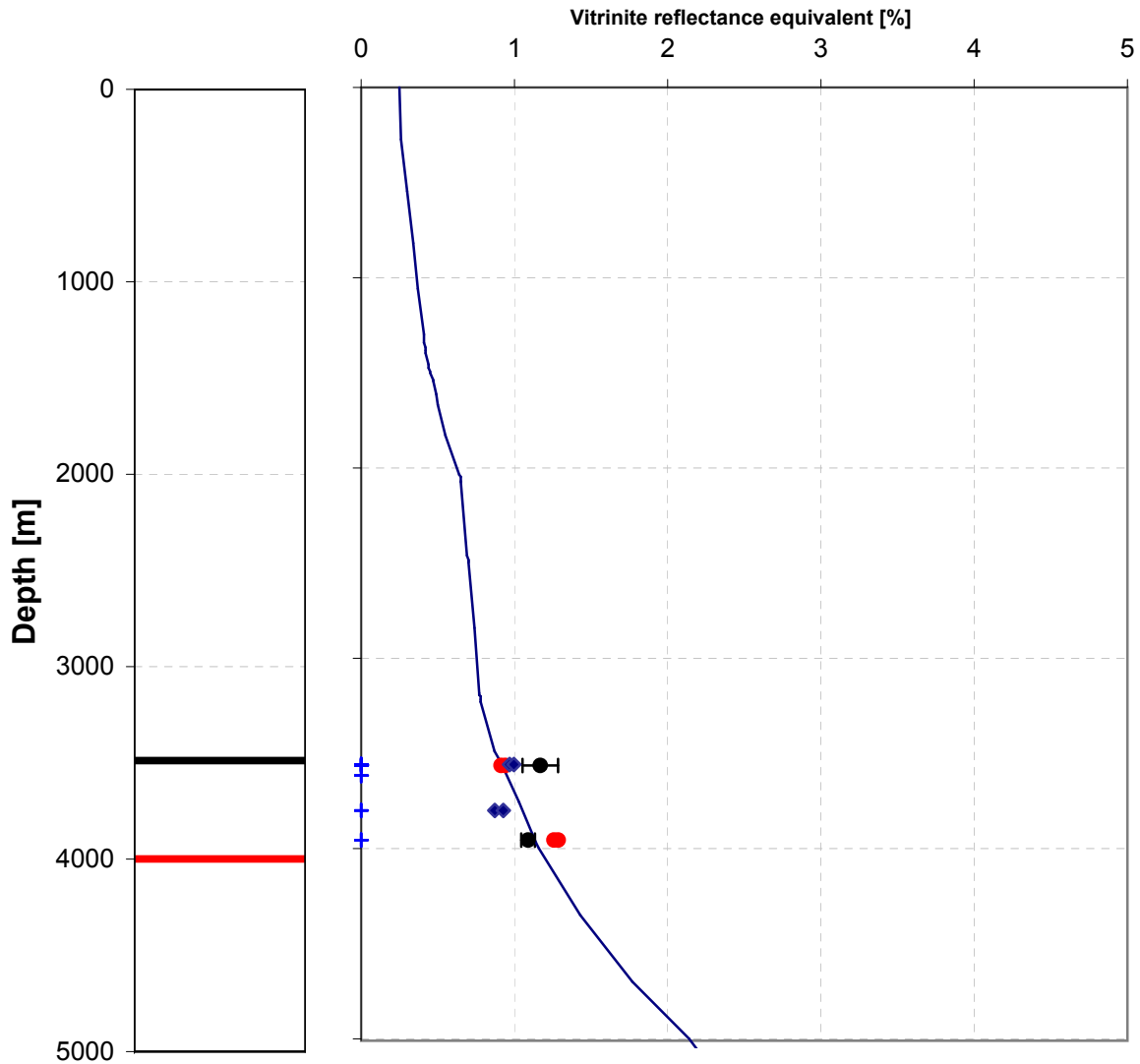




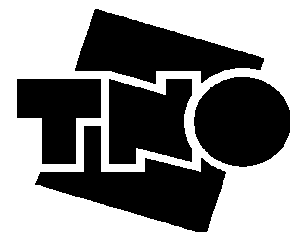
Joint Industry Project Petroplay

Quality controlled data

D12-03



- A) Vitrinite reflectance
- B) Vitrinite reflectance
- C) Vitrinite reflectance
- A1) Tmax-VR equivalent - highly reliable
- B) Tmax-VR equivalent
- C) Tmax-VR equivalent
- Modeled %VR (S&B)
- + samples
- ◆ A2) Tmax-VR equivalent - low reliability

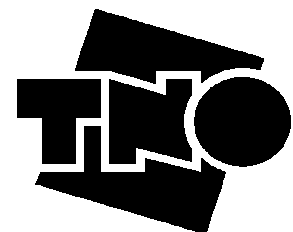
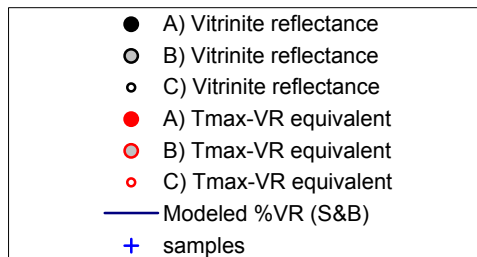
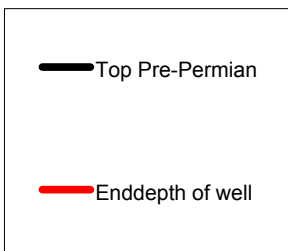
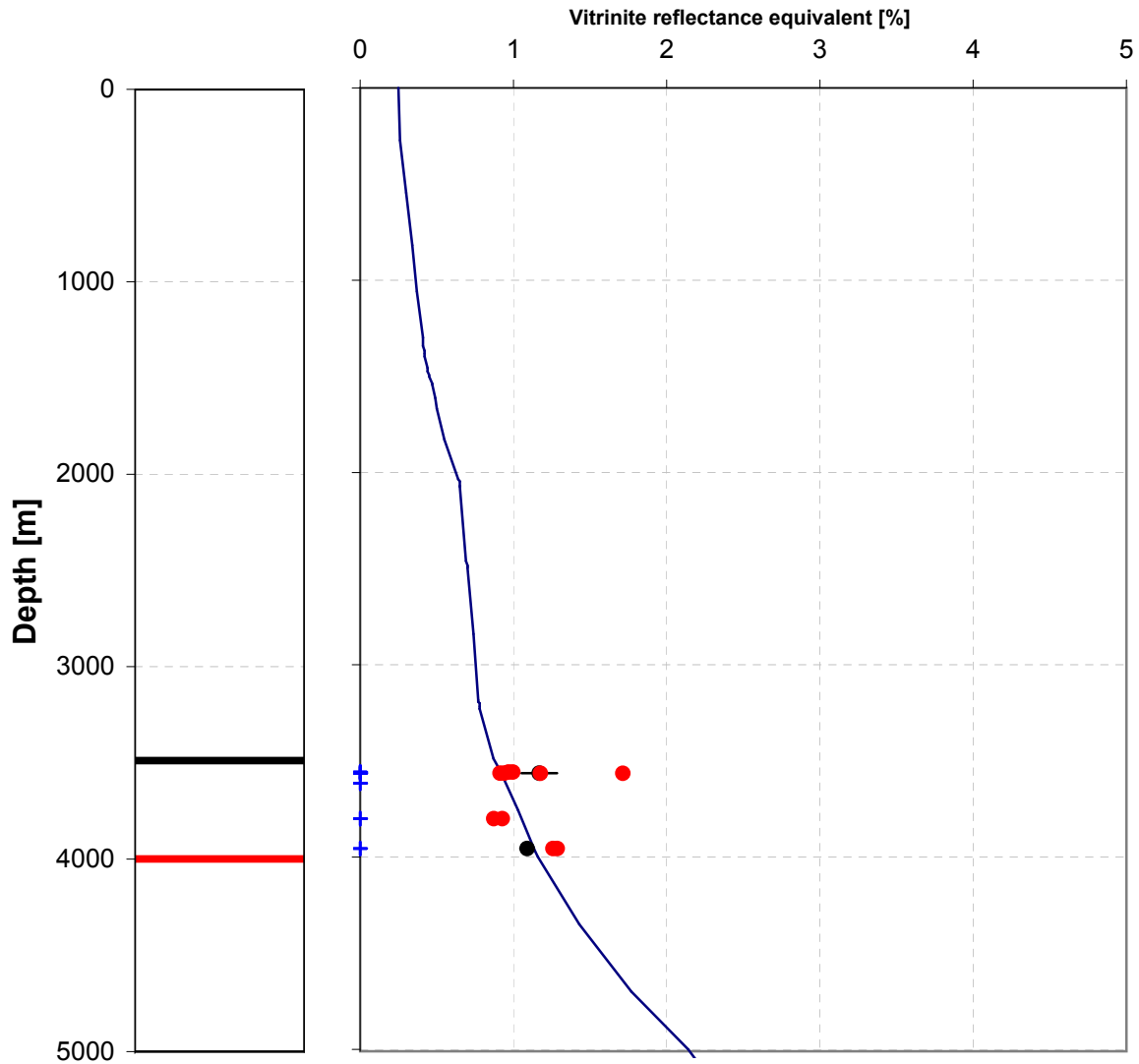




Joint Industry Project Petroplay

Raw data

D12-03

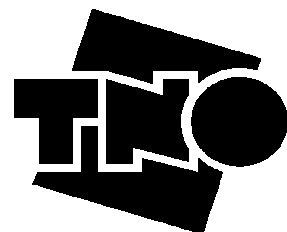
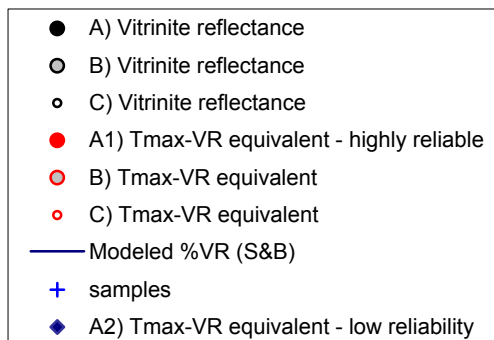
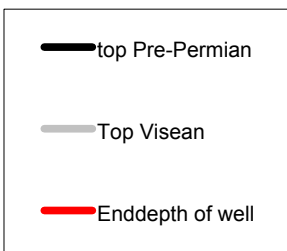
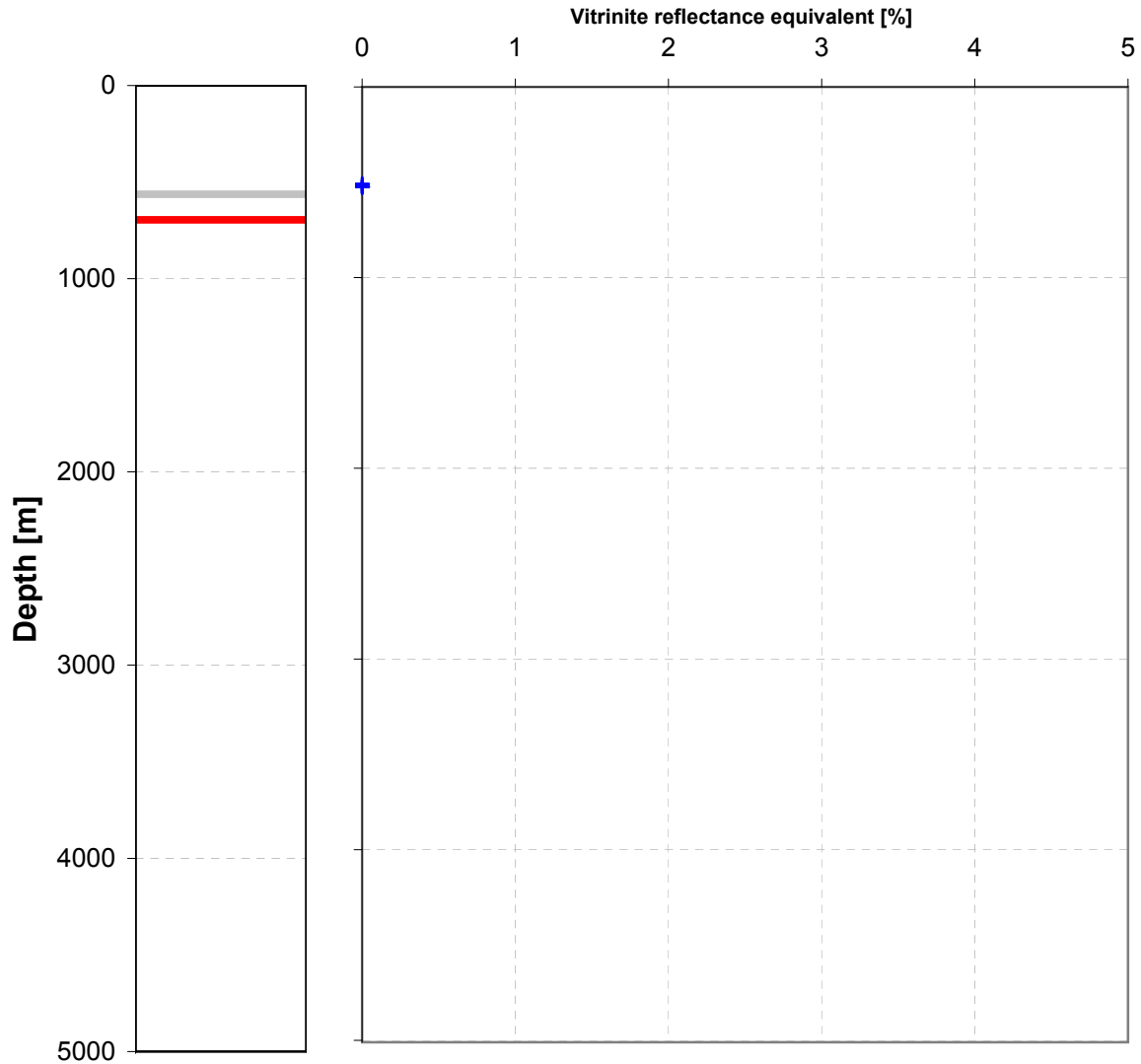




Joint Industry Project Petroplay

Quality controlled data

Booischot

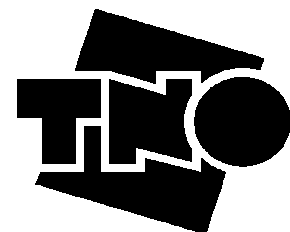
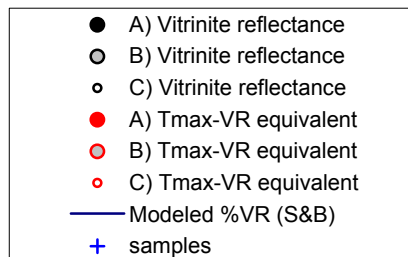
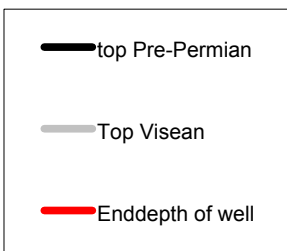
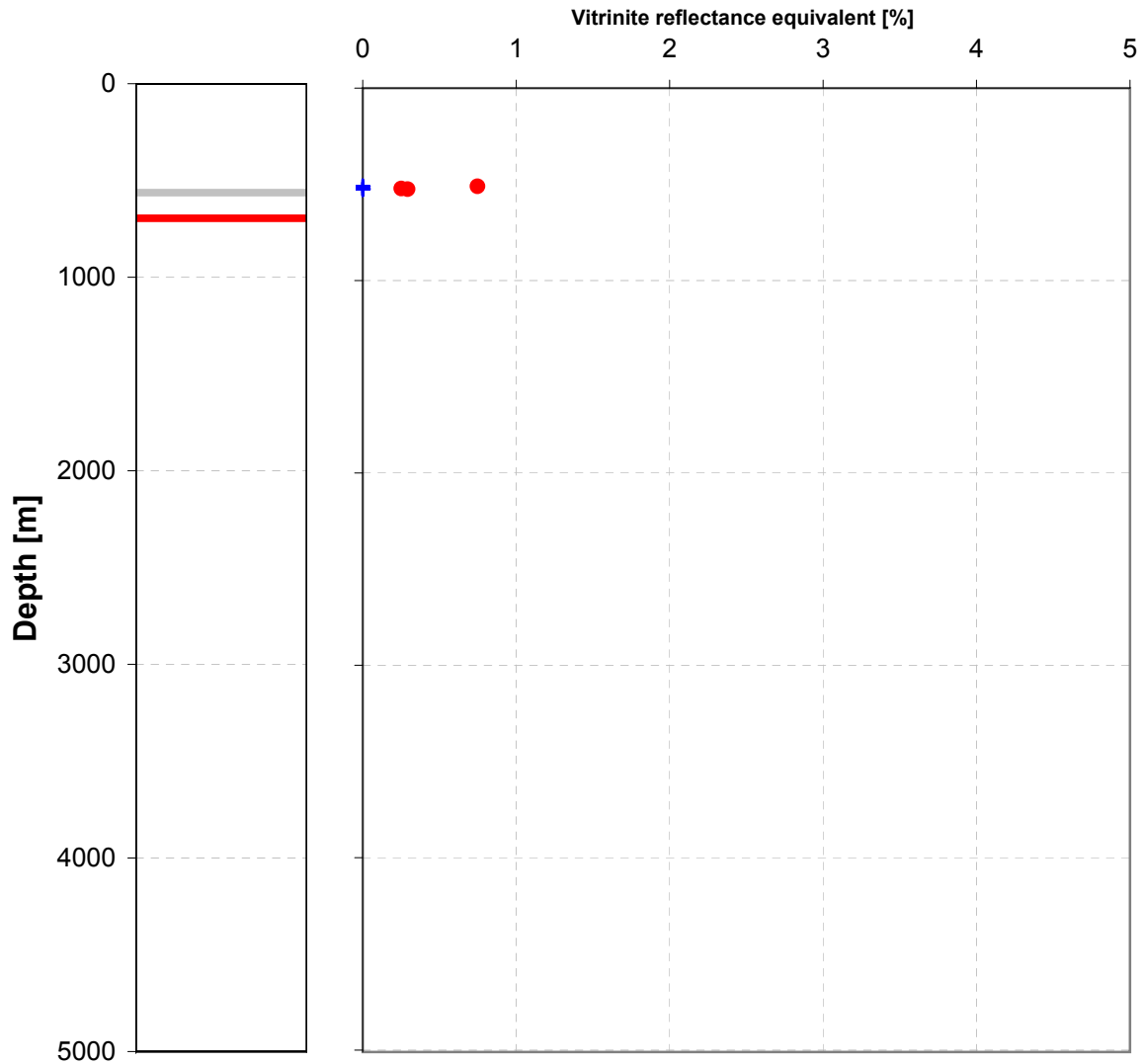




Joint Industry Project Petroplay

Raw data

Booischot

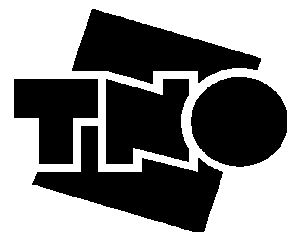
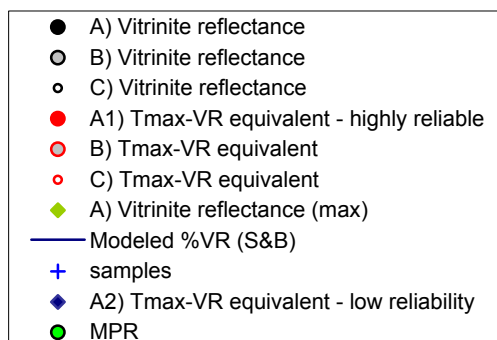
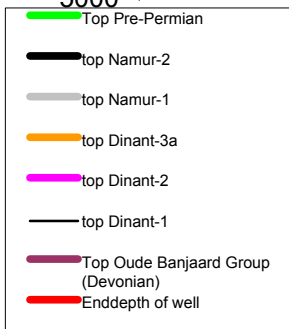
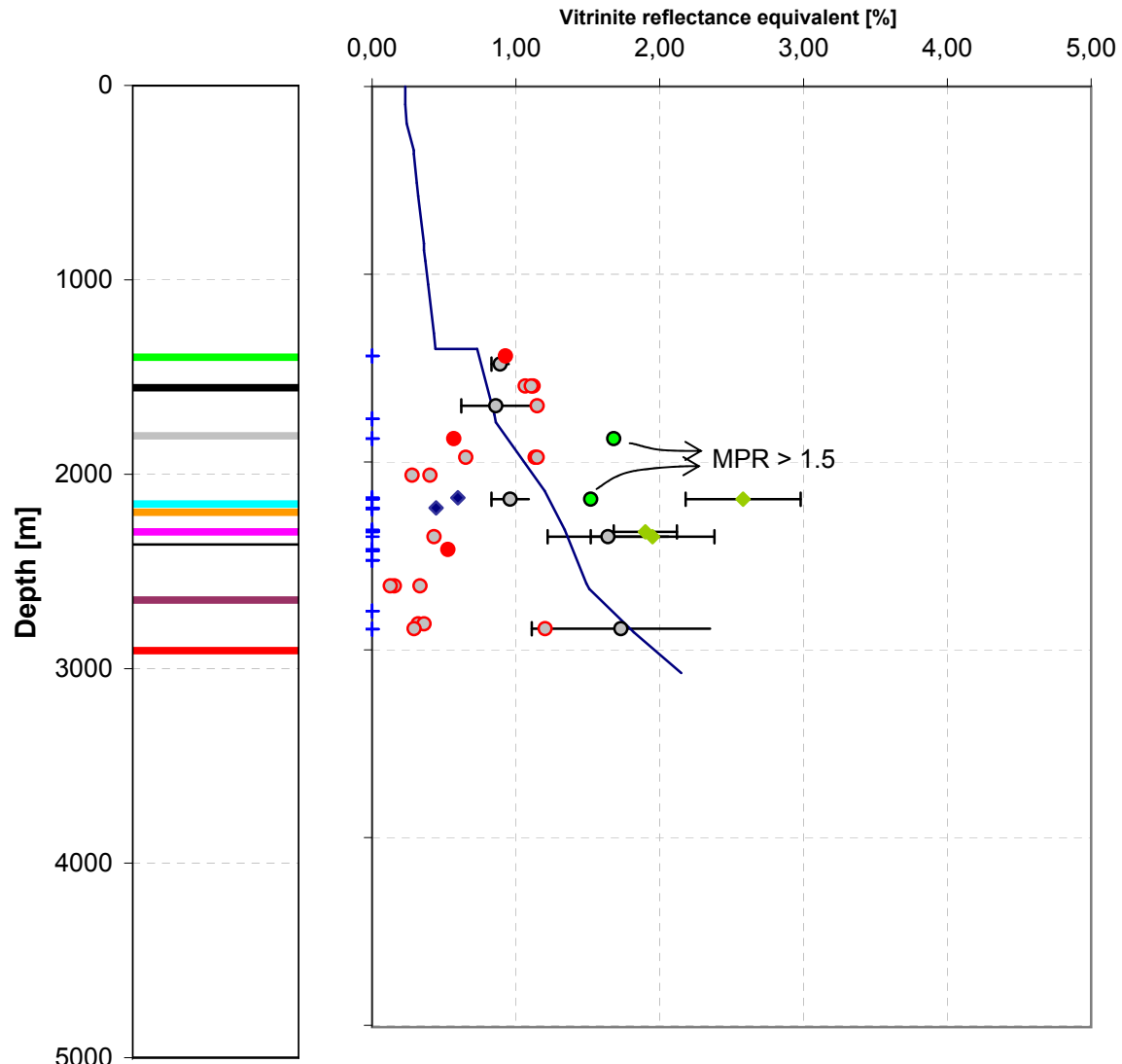




Joint Industry Project Petroplay

Quality controlled data

Brouwershavensgat-1

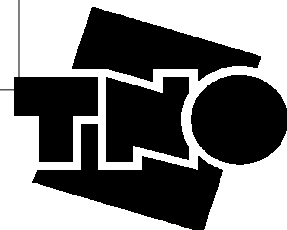
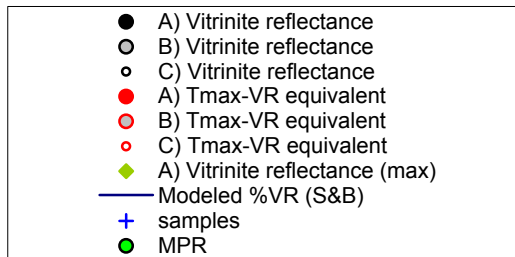
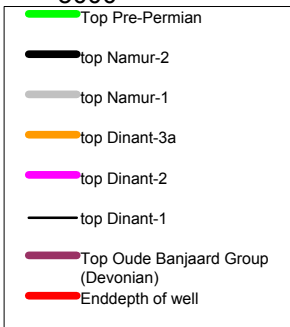
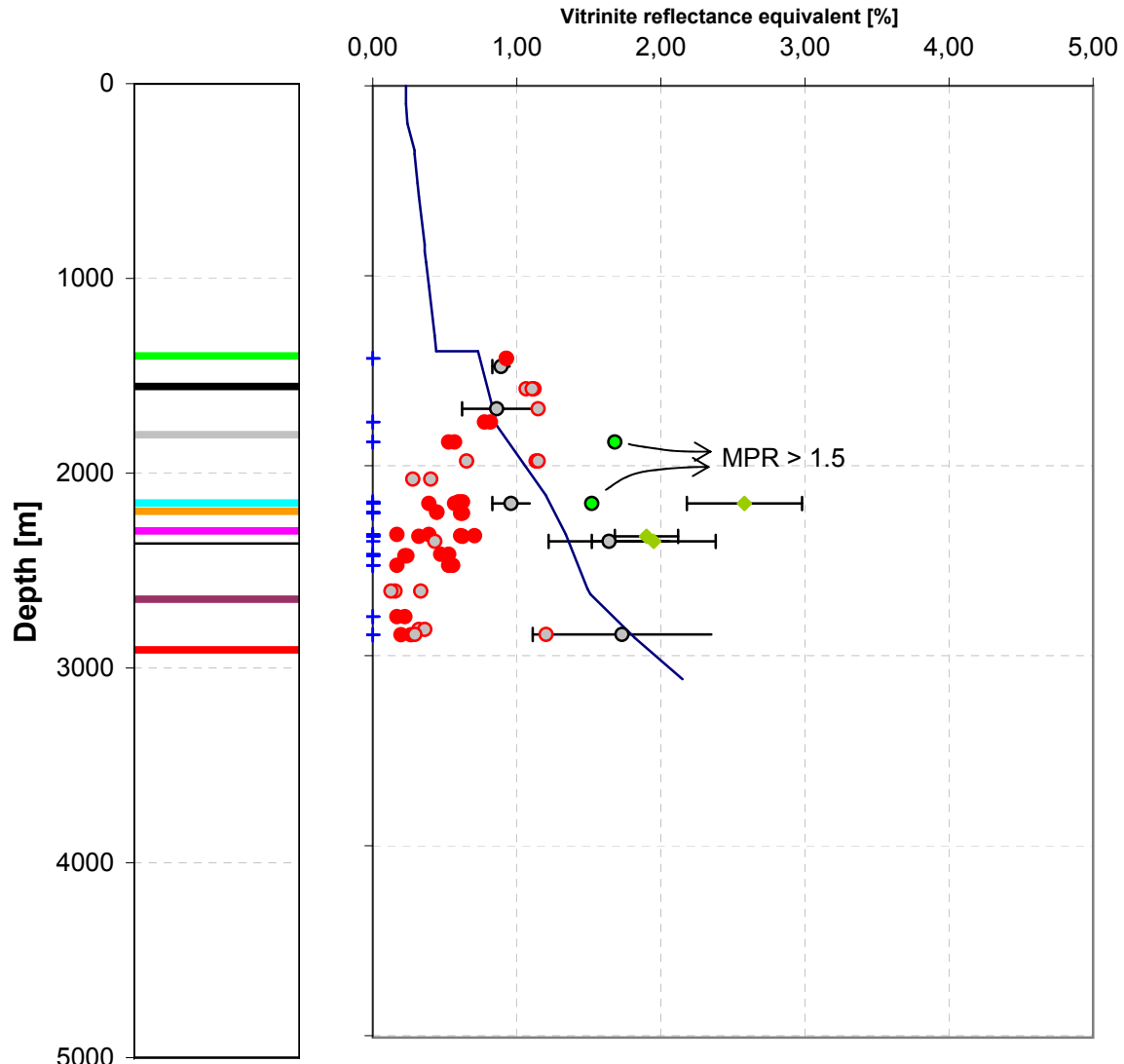




Joint Industry Project Petroplay

Raw data

Brouwershavensgat-1

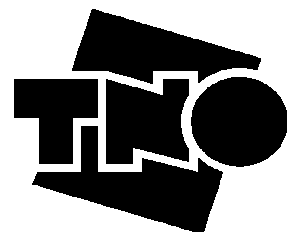
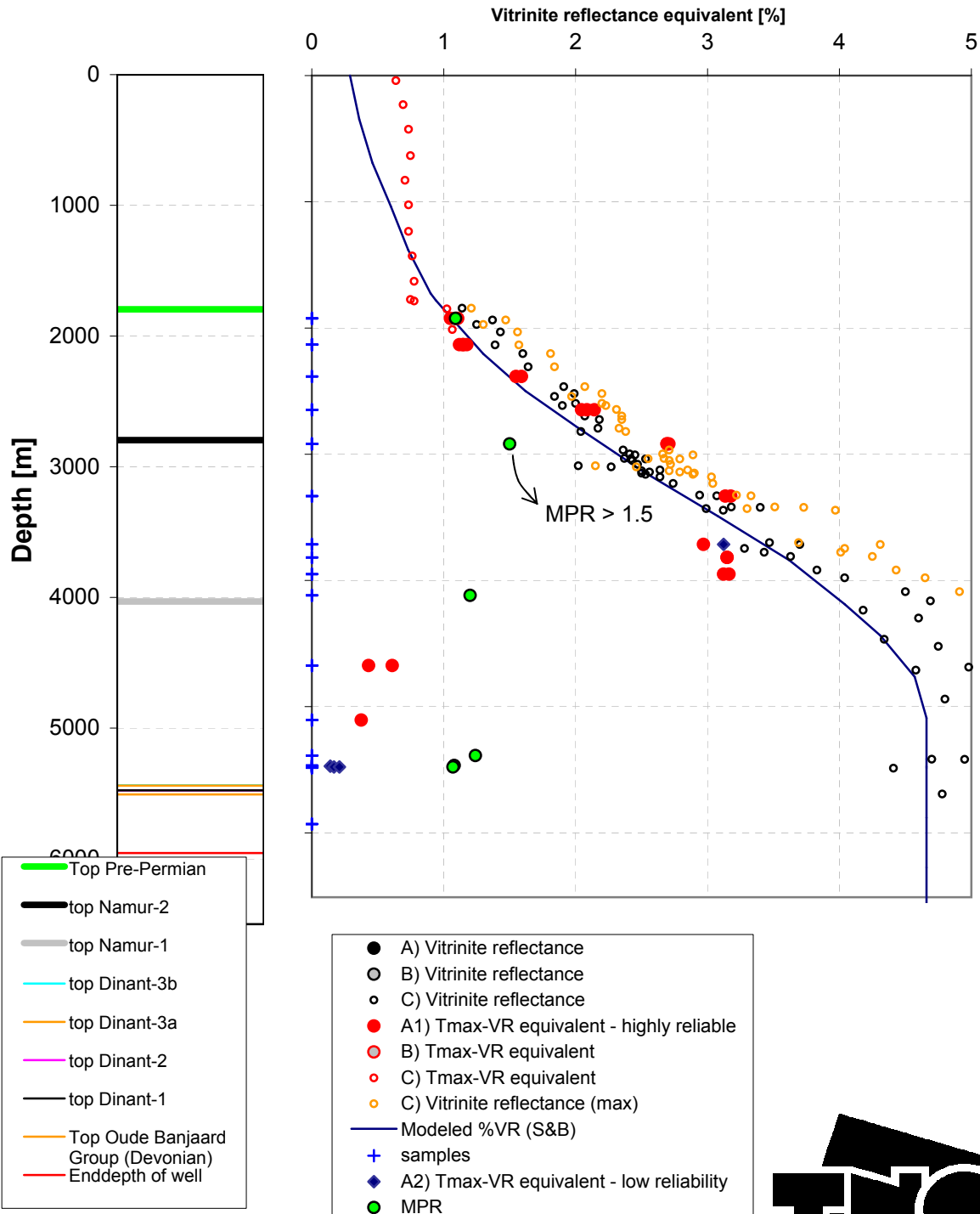




Joint Industry Project Petroplay

Quality controlled data

Münsterland-1

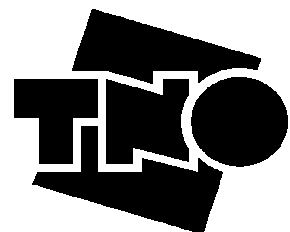
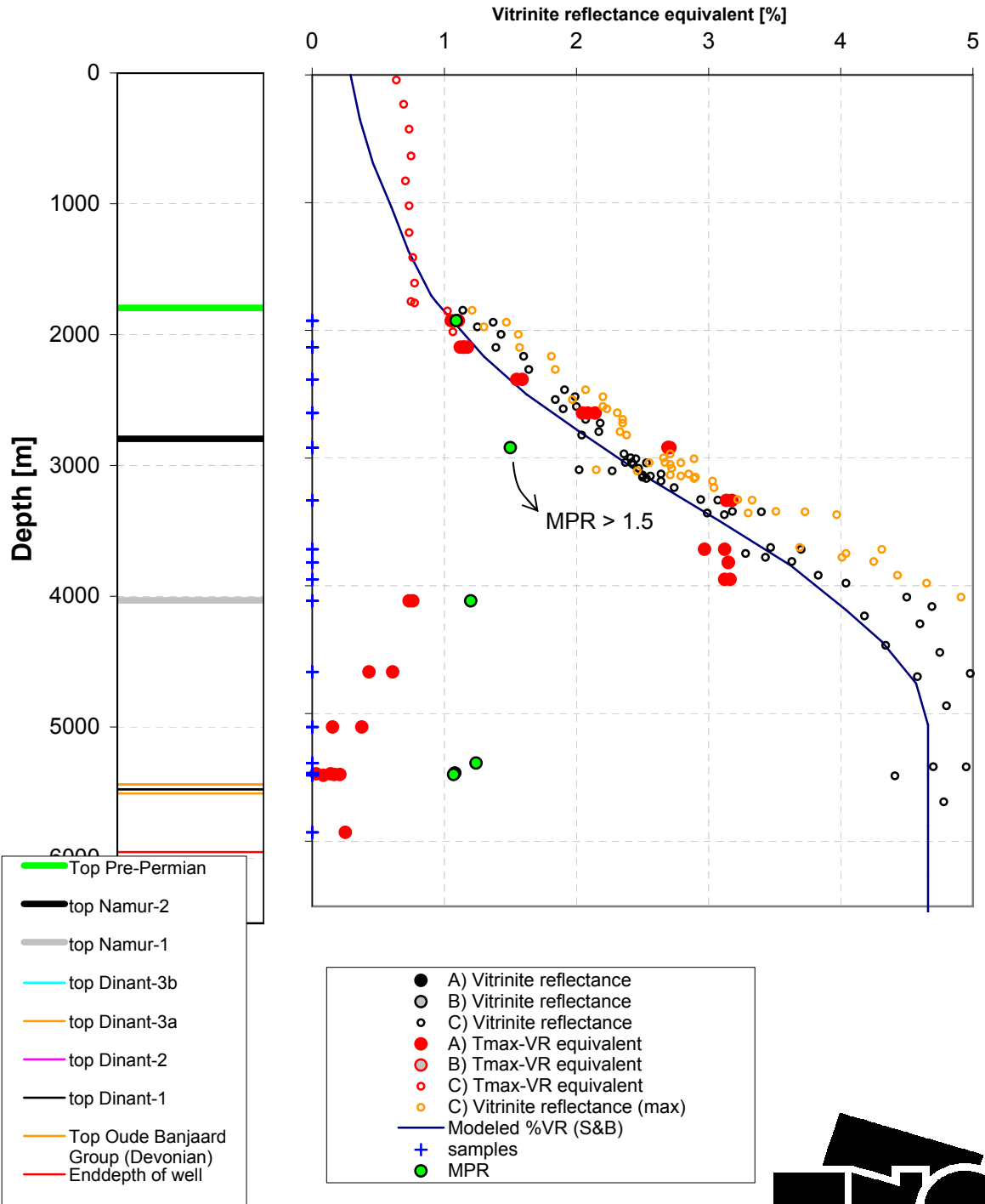




Joint Industry Project Petroplay

Raw data

Münsterland-1

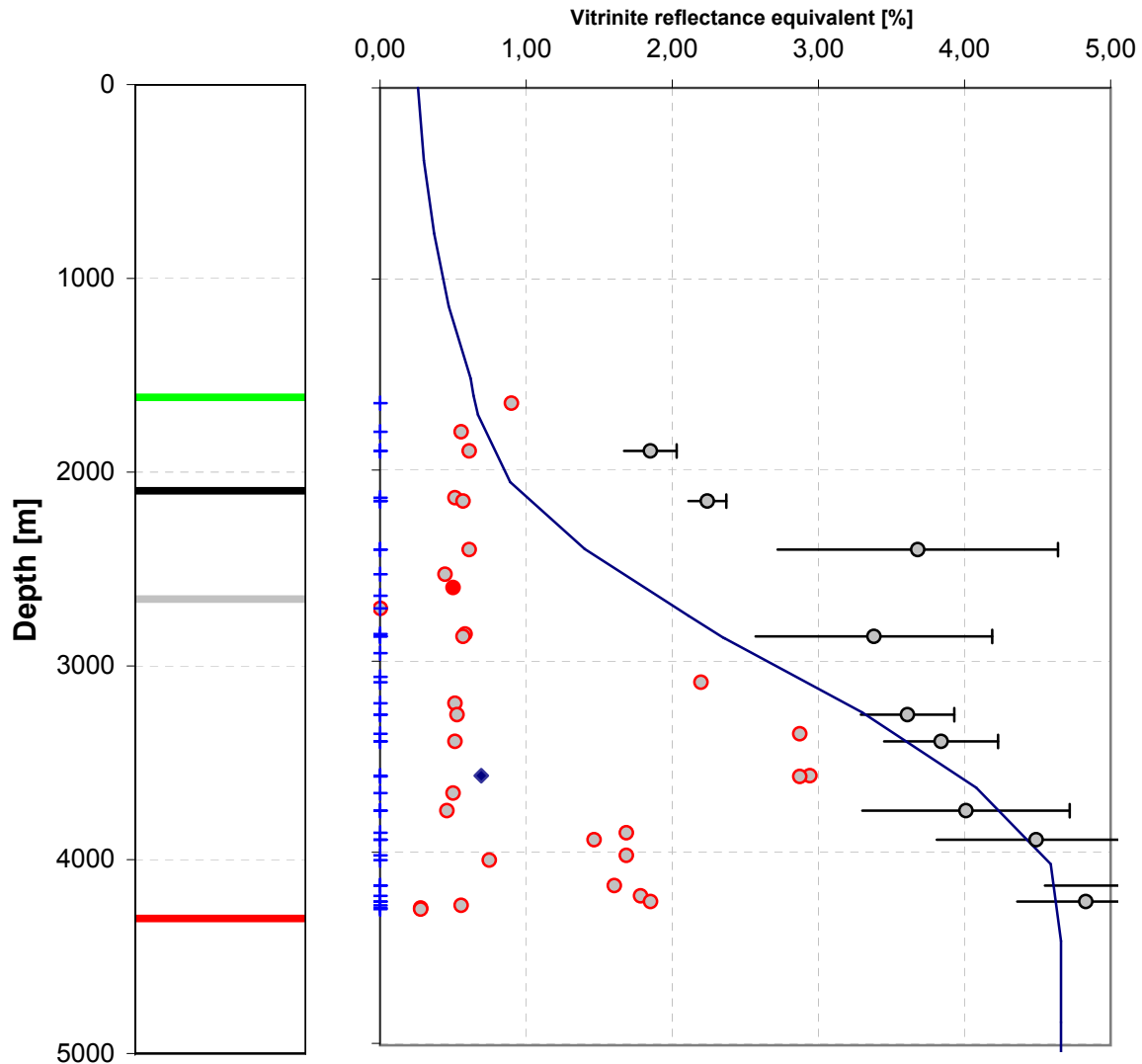




Joint Industry Project Petroplay

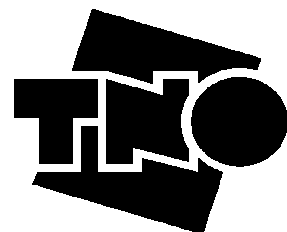
Quality controlled data

Nagele-1



- Top Pre-Permian
- top Namur-2
- top Namur-1
- top Dinant-3b
- top Dinant-3a
- top Dinant-2
- top Dinant-1
- Enddepth of well

- A) Vitrinite reflectance
- B) Vitrinite reflectance
- C) Vitrinite reflectance
- A1) Tmax-VR equivalent - highly reliable
- B) Tmax-VR equivalent
- C) Tmax-VR equivalent
- + samples
- ◆ A2) Tmax-VR equivalent - low reliability
- Modeled %VR (S&B), no intrusions

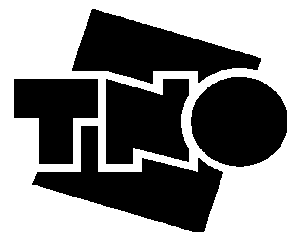
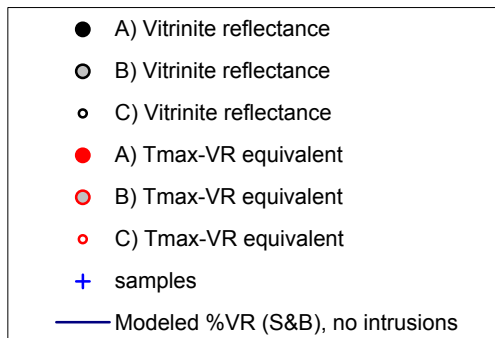
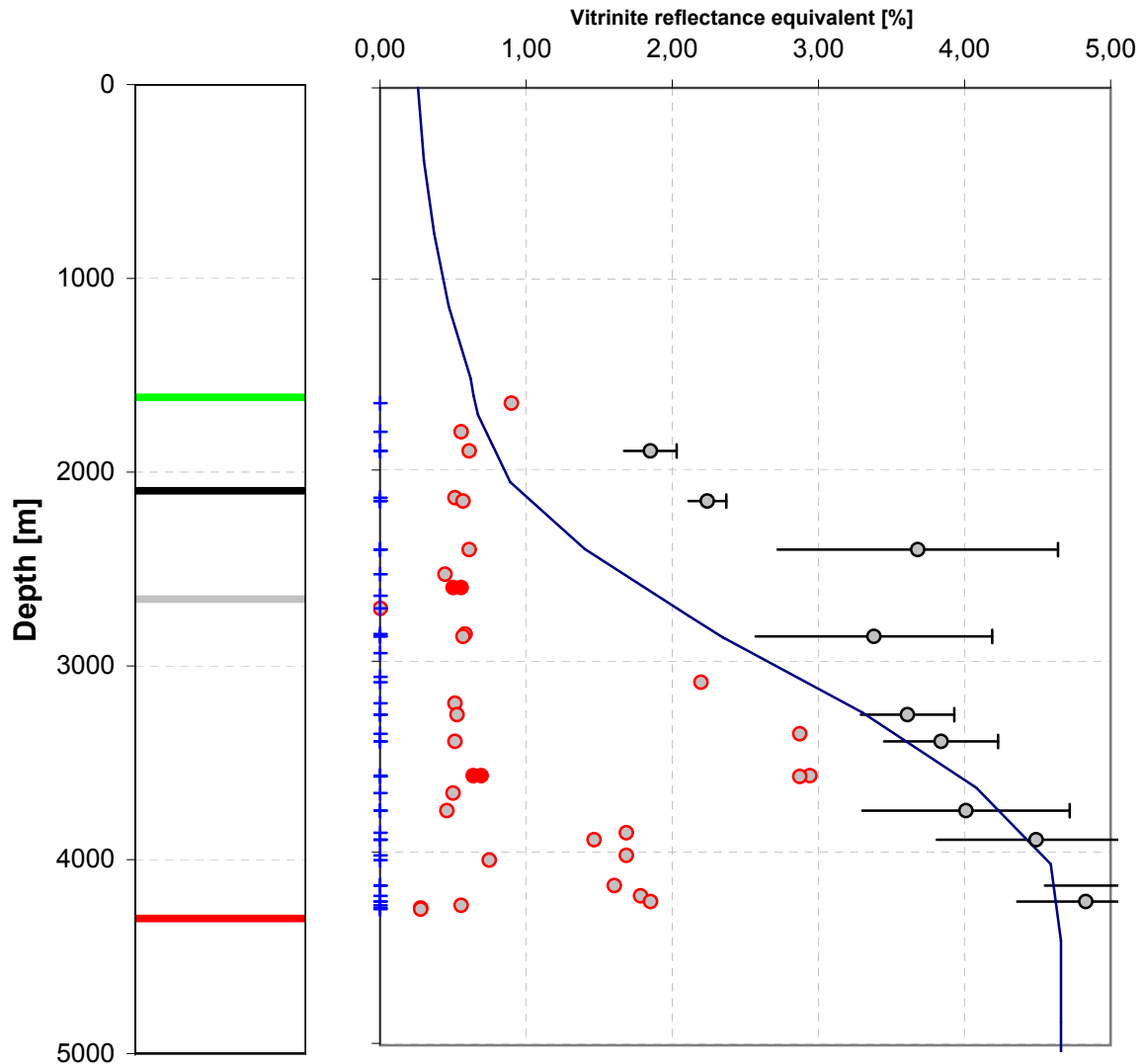




Joint Industry Project Petroplay

Raw data

Nagele-1

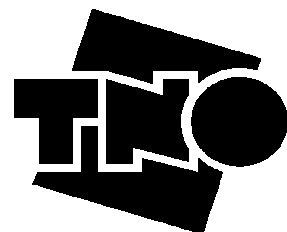
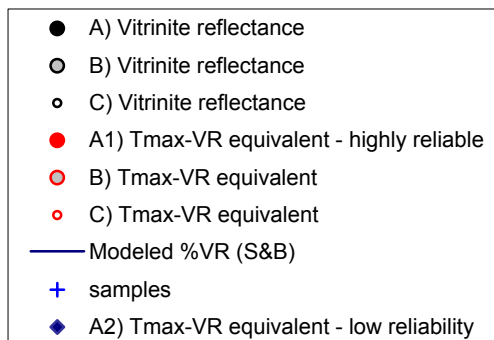
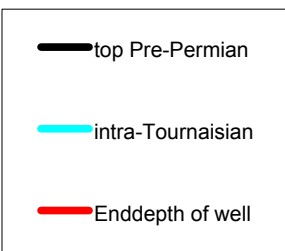
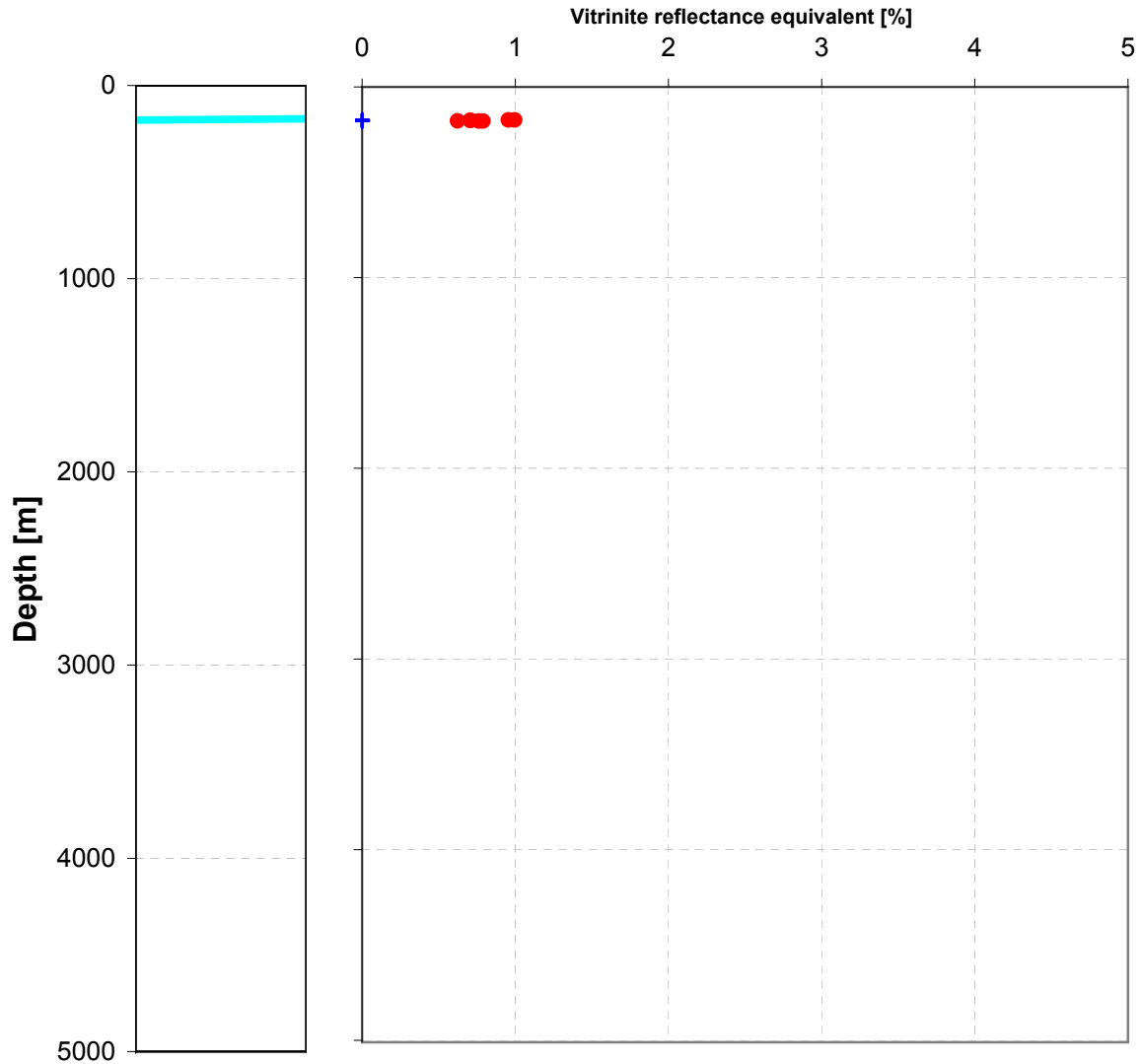




Joint Industry Project Petroplay

Quality controlled data

Wervik

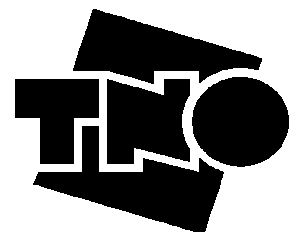
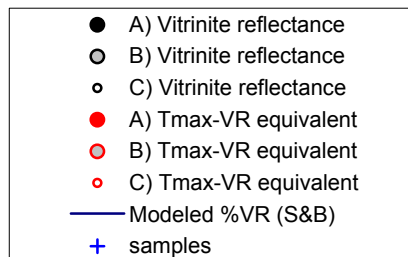
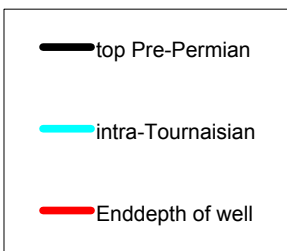
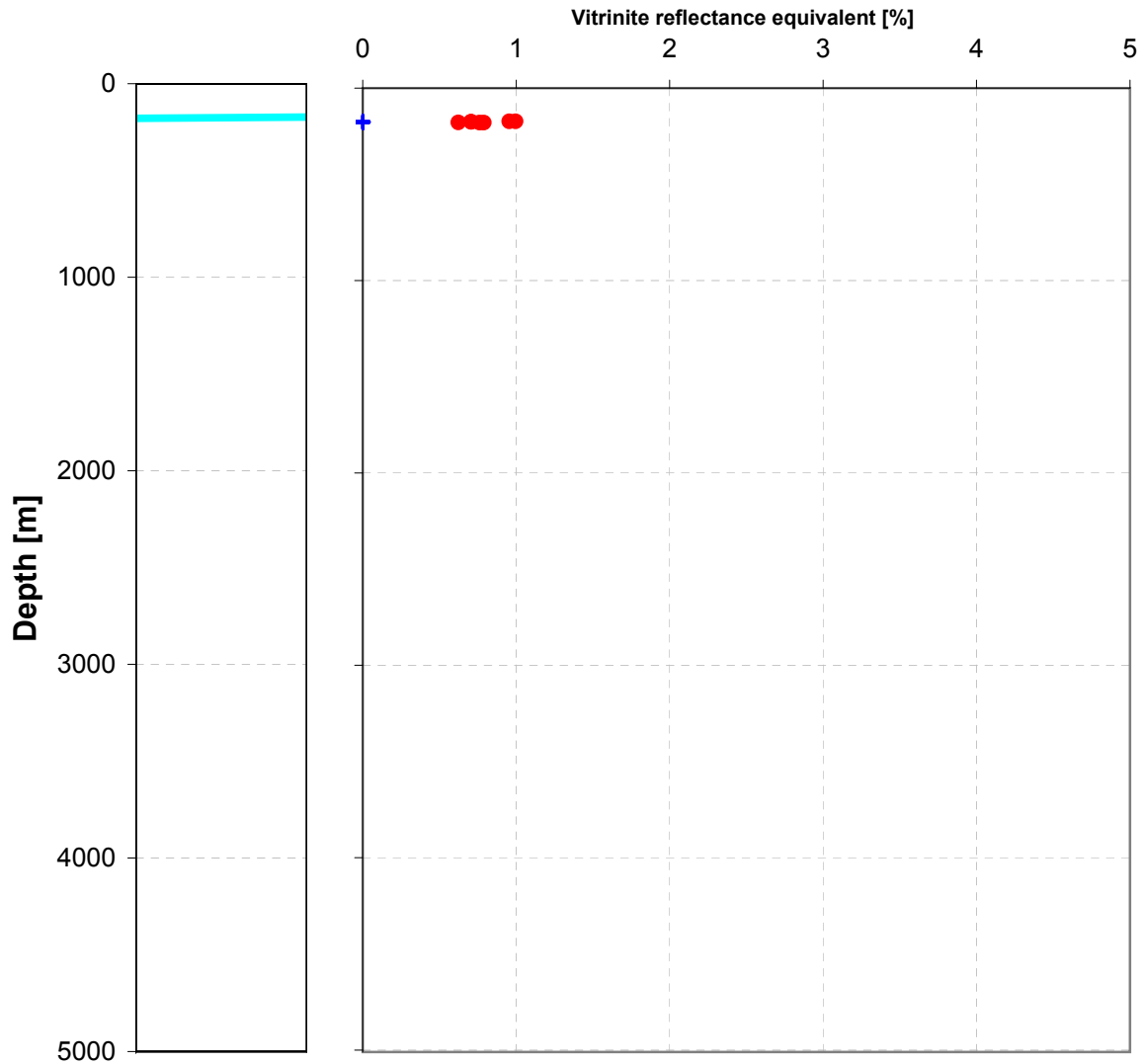




Joint Industry Project Petroplay

Raw data

Wervik

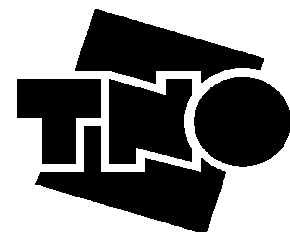
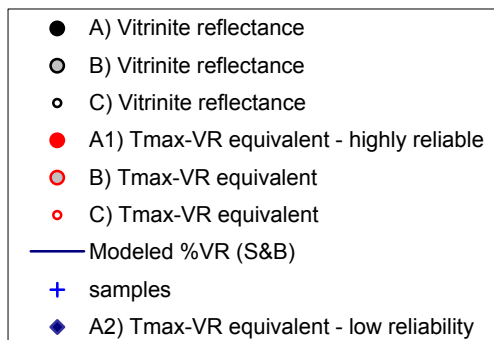
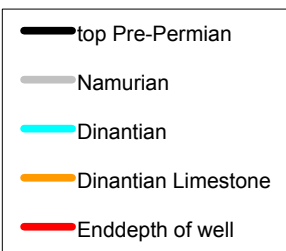
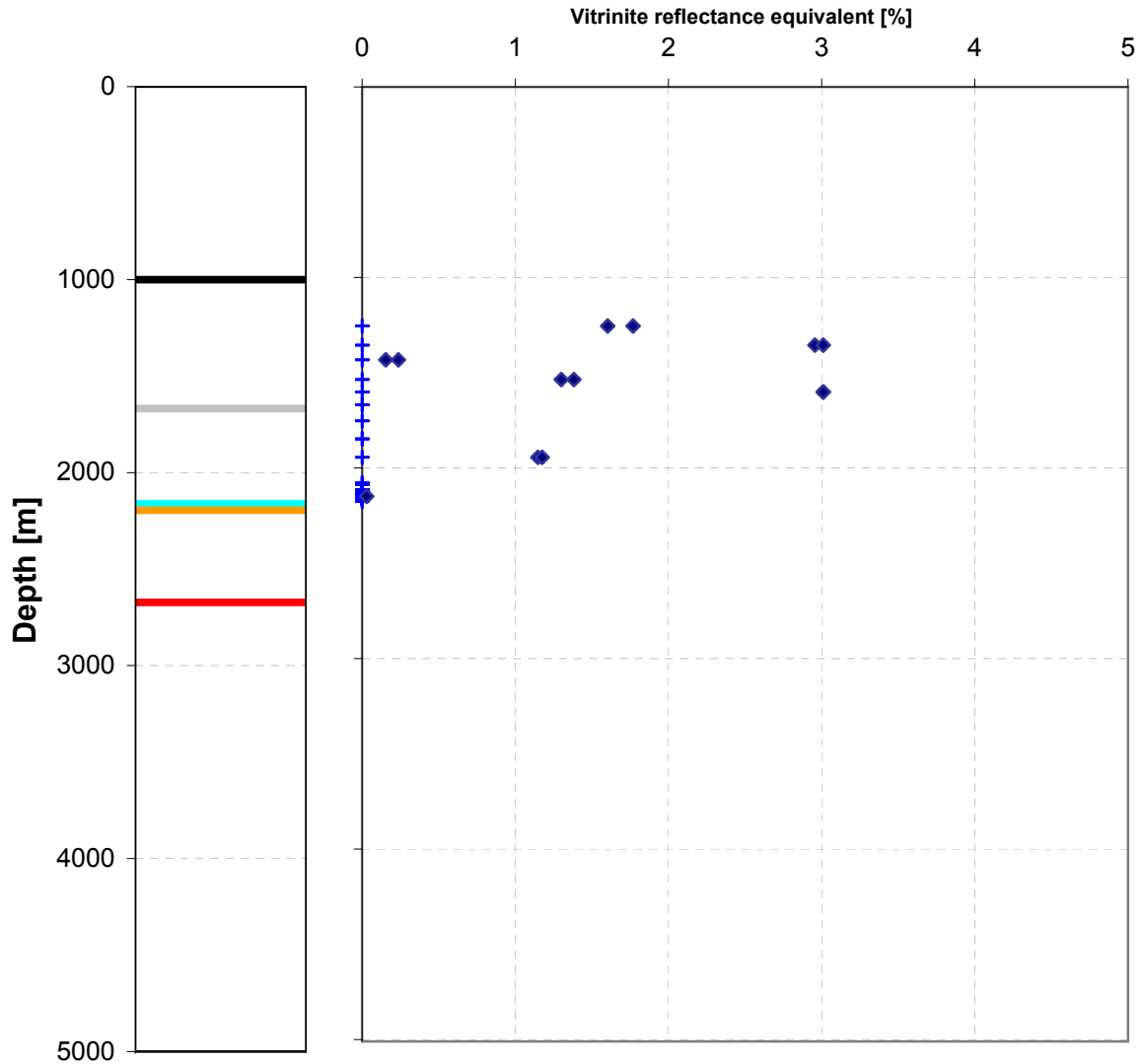




Joint Industry Project Petroplay

Quality controlled data

Turnhout

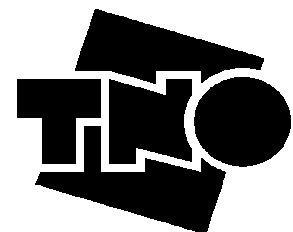
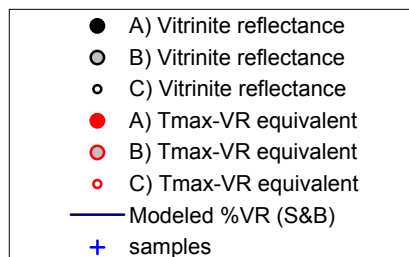
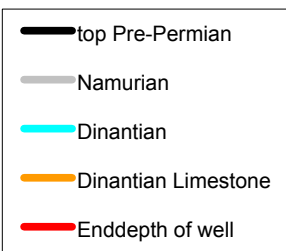
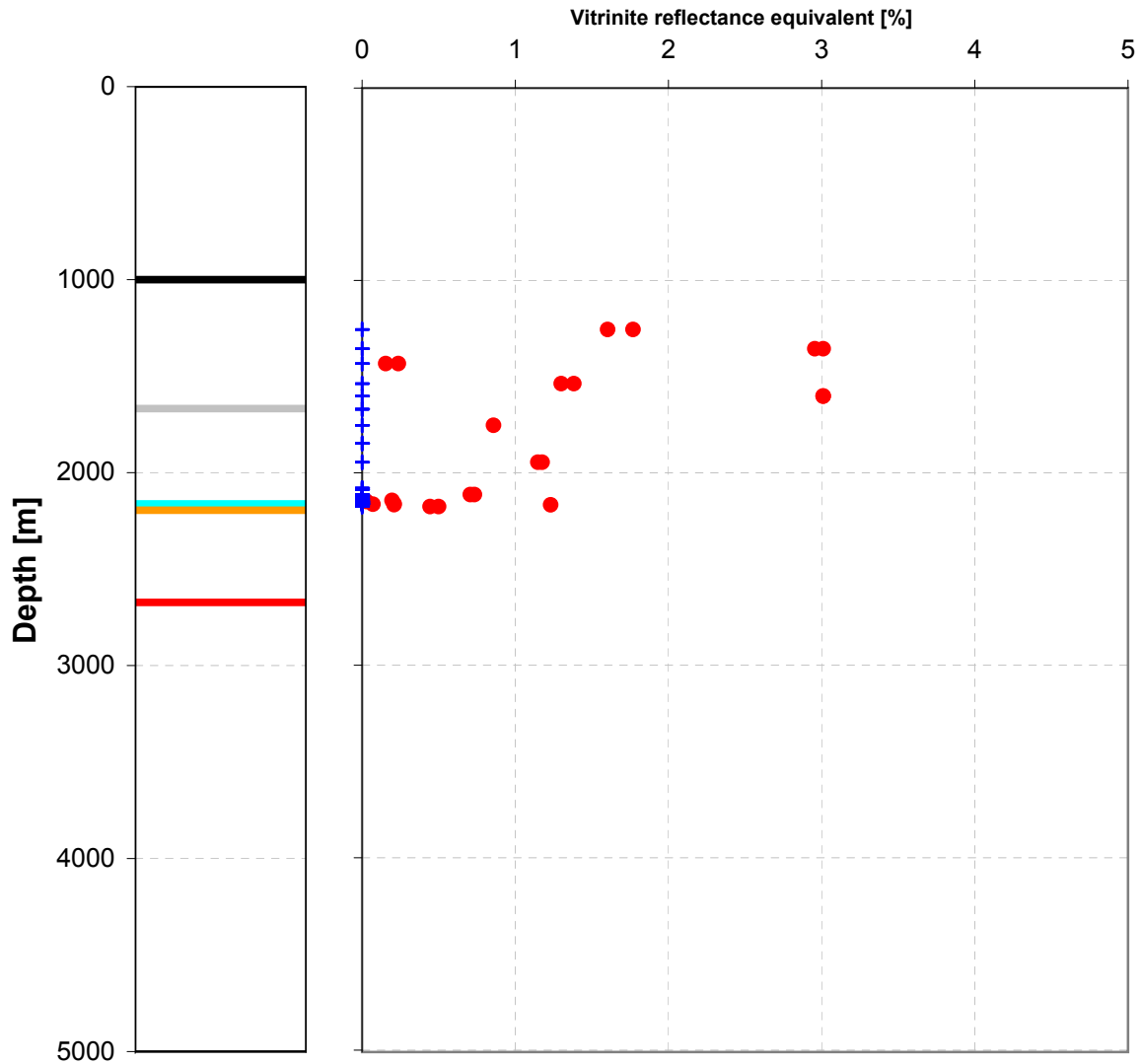




Joint Industry Project Petroplay

Raw data

Turnhout

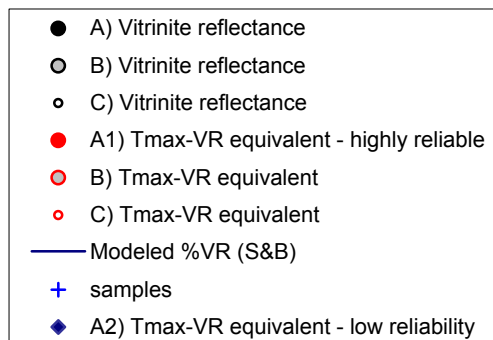
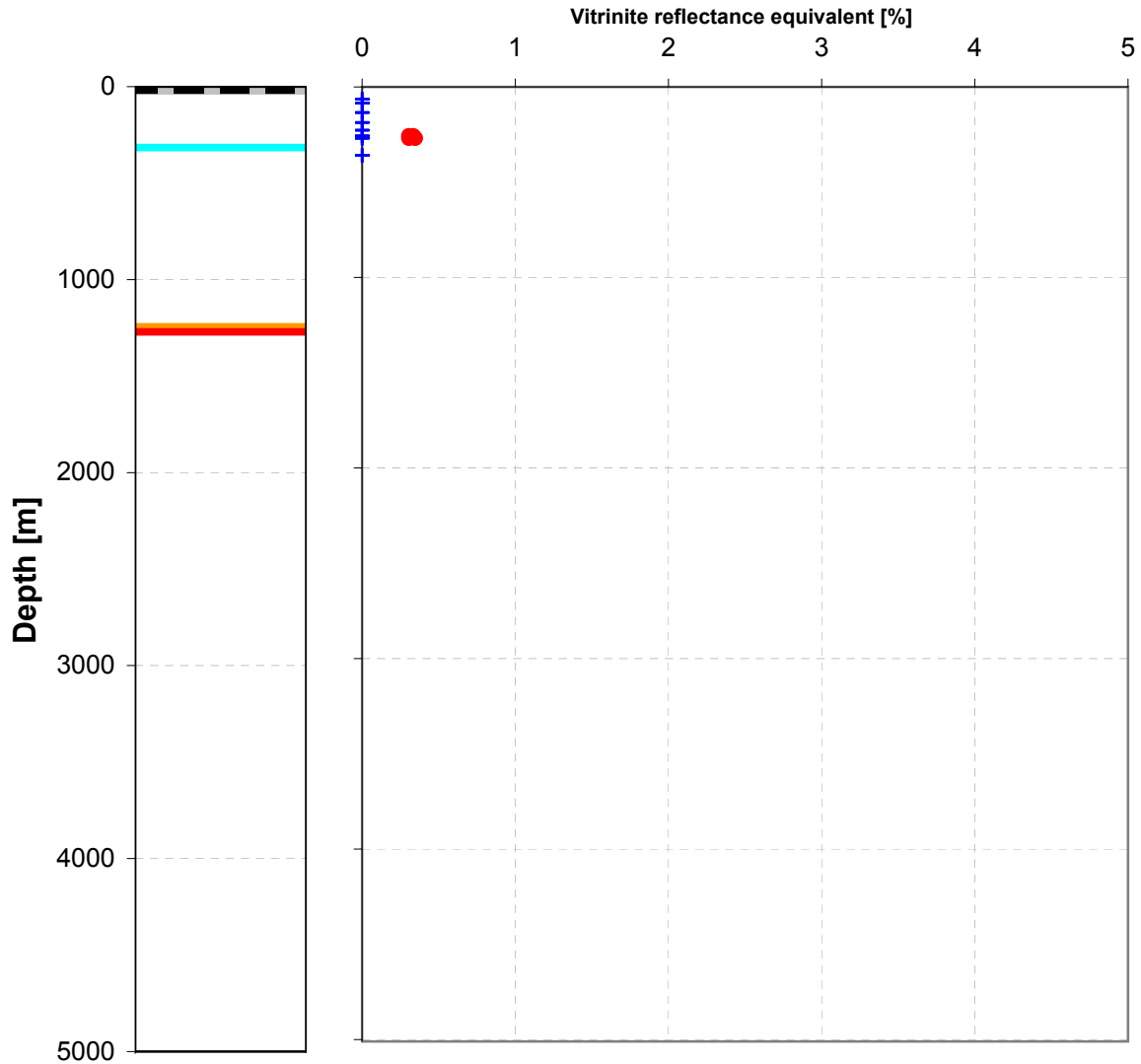




Joint Industry Project Petroplay

Quality controlled data

Tournai

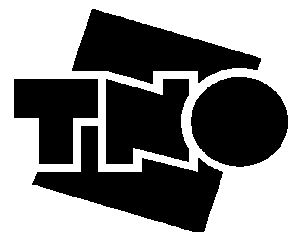
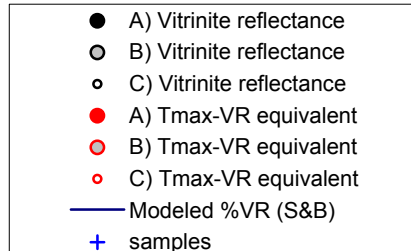
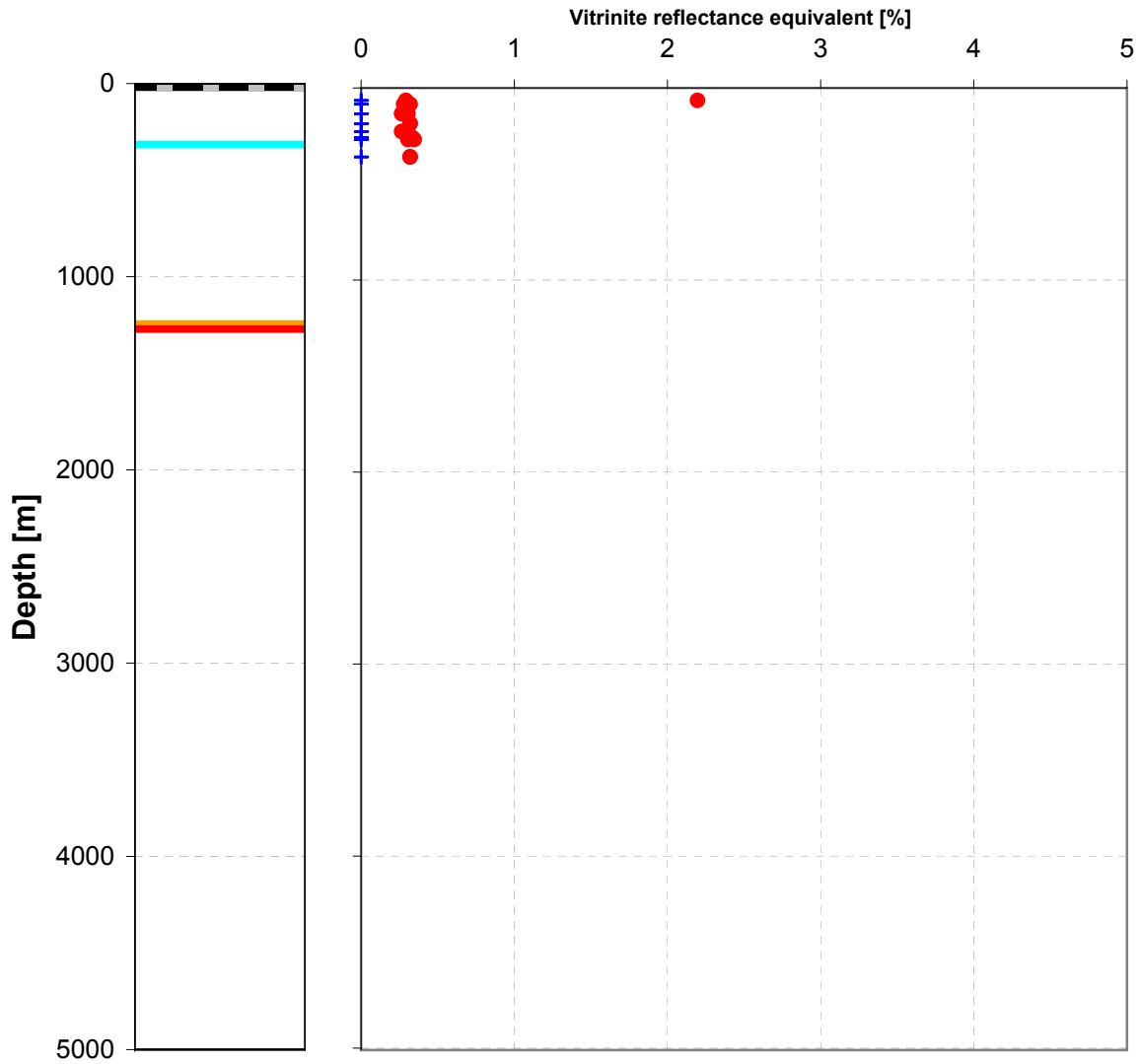




Joint Industry Project Petroplay

Raw data

Tournai

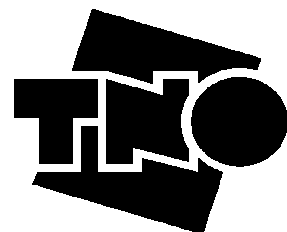
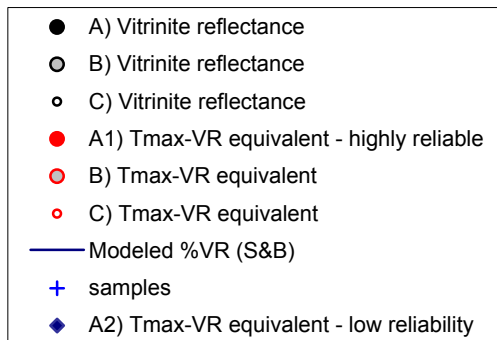
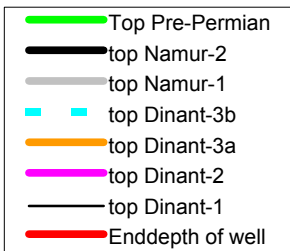
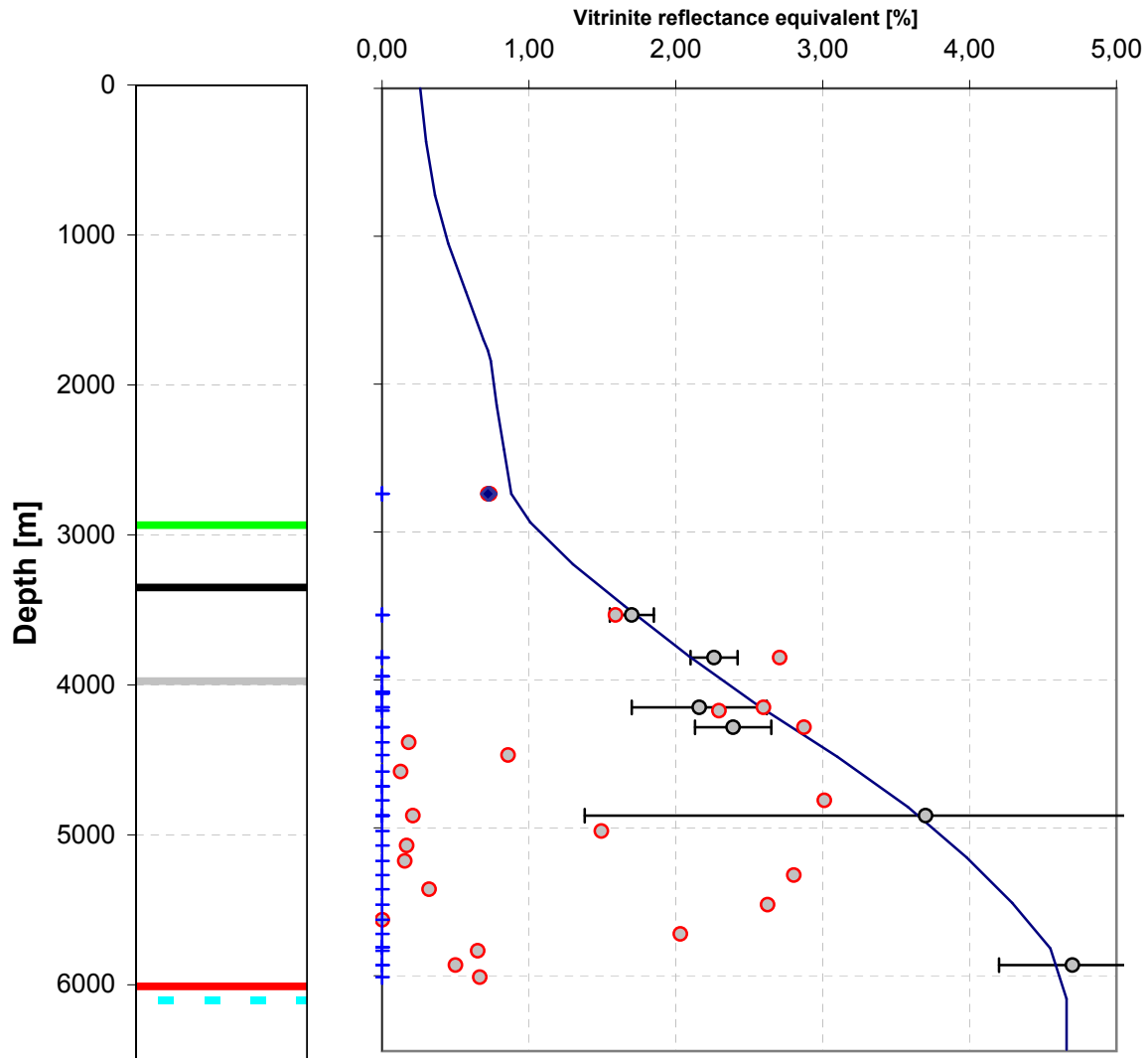




Joint Industry Project Petroplay

Quality controlled data

Tjuchem-02(-S1)

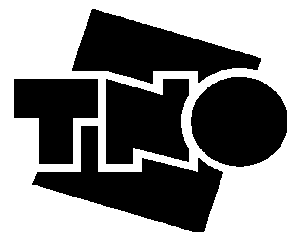
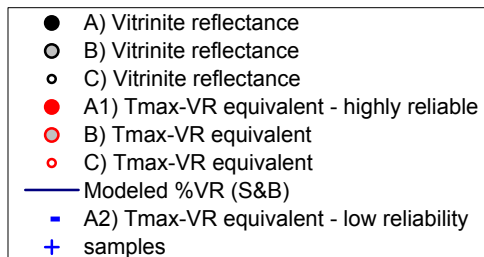
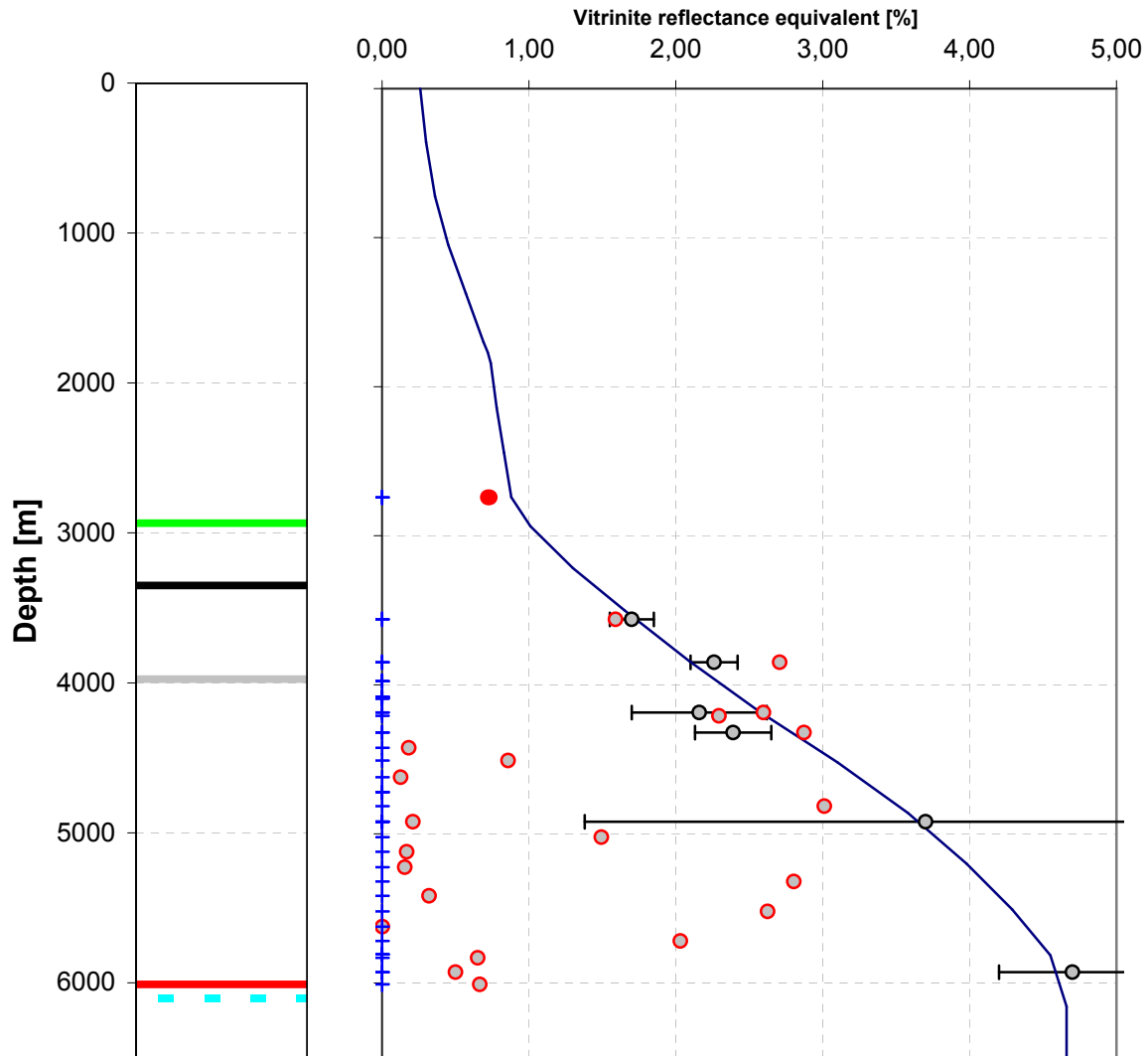




Joint Industry Project Petroplay

Raw data

Tjuchem-02(-S1)

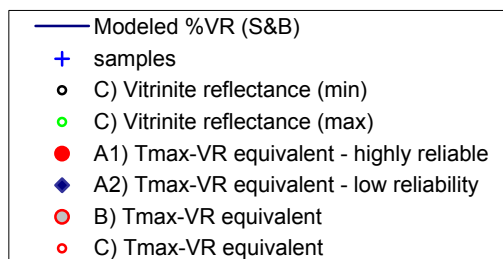
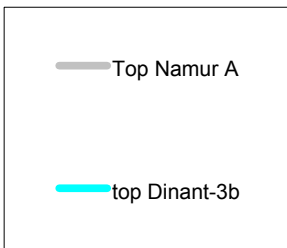
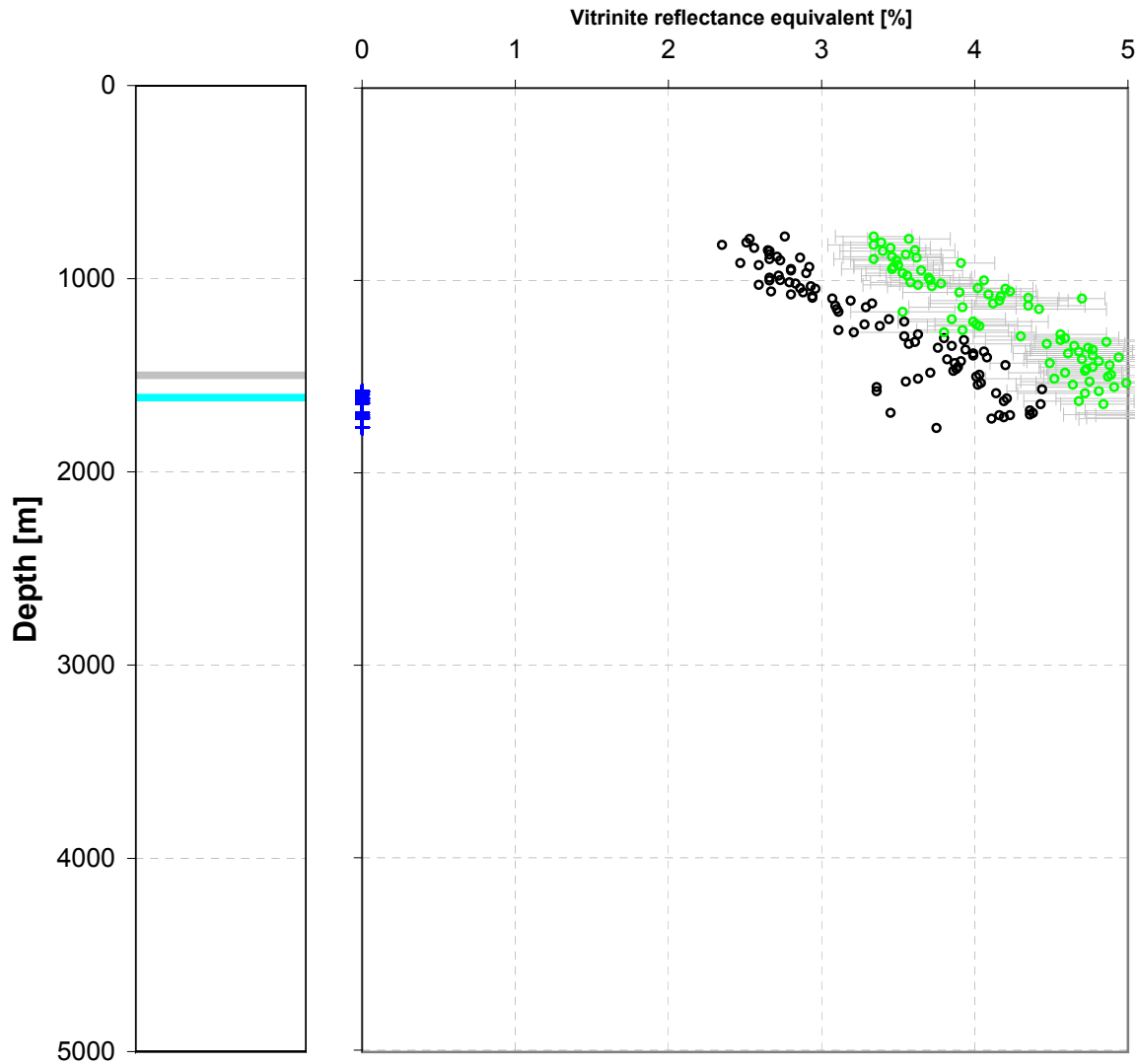




Joint Industry Project Petroplay

Quality controlled data

SWLT-1001

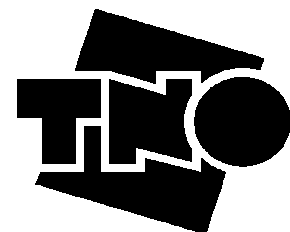
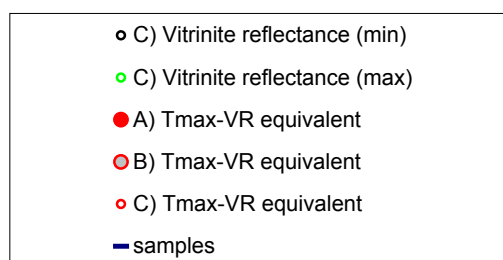
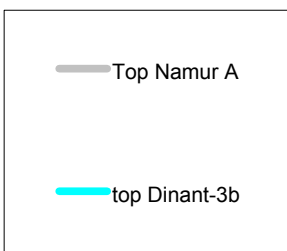
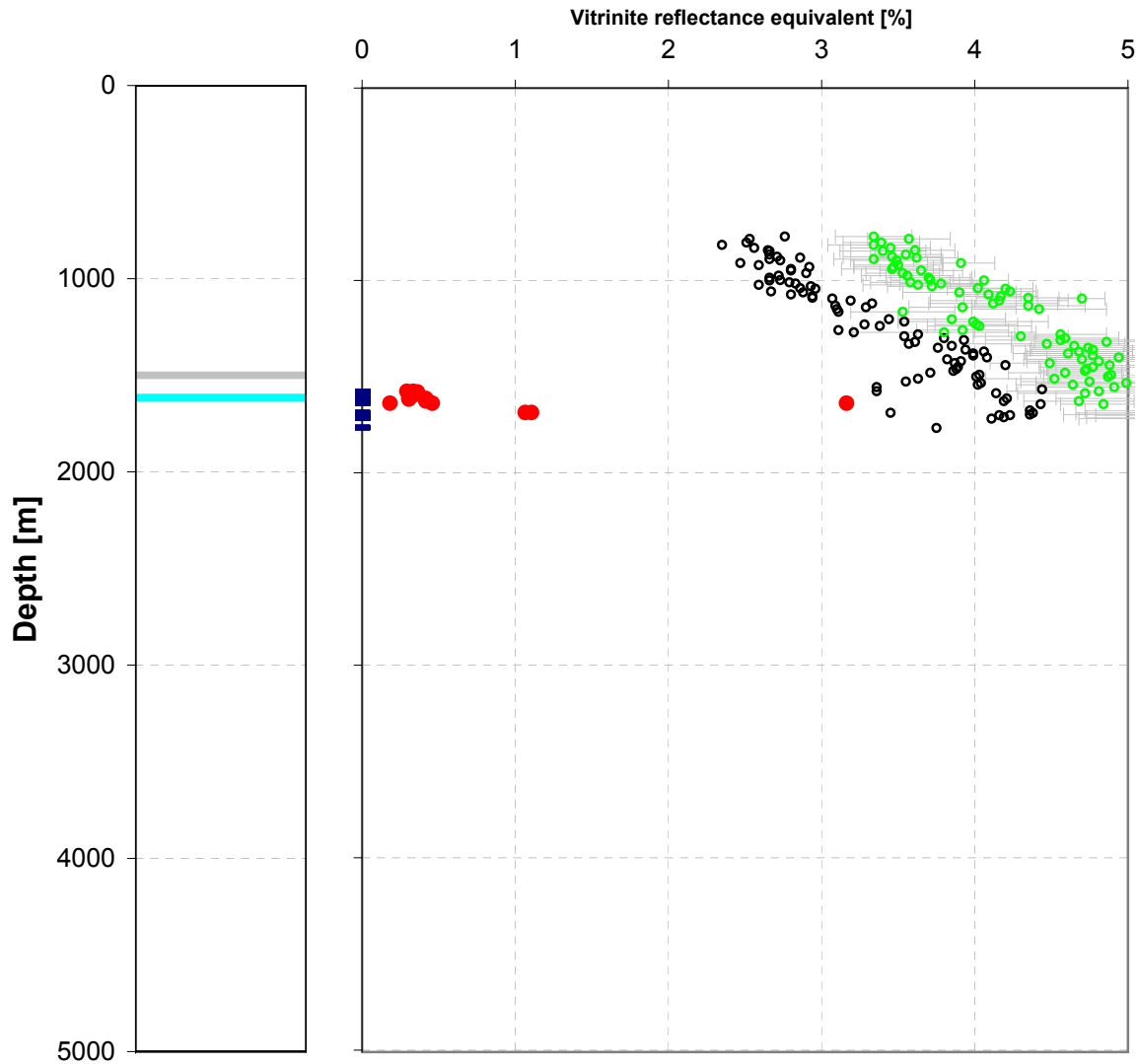




Joint Industry Project Petroplay

Raw data

SWLT-1001

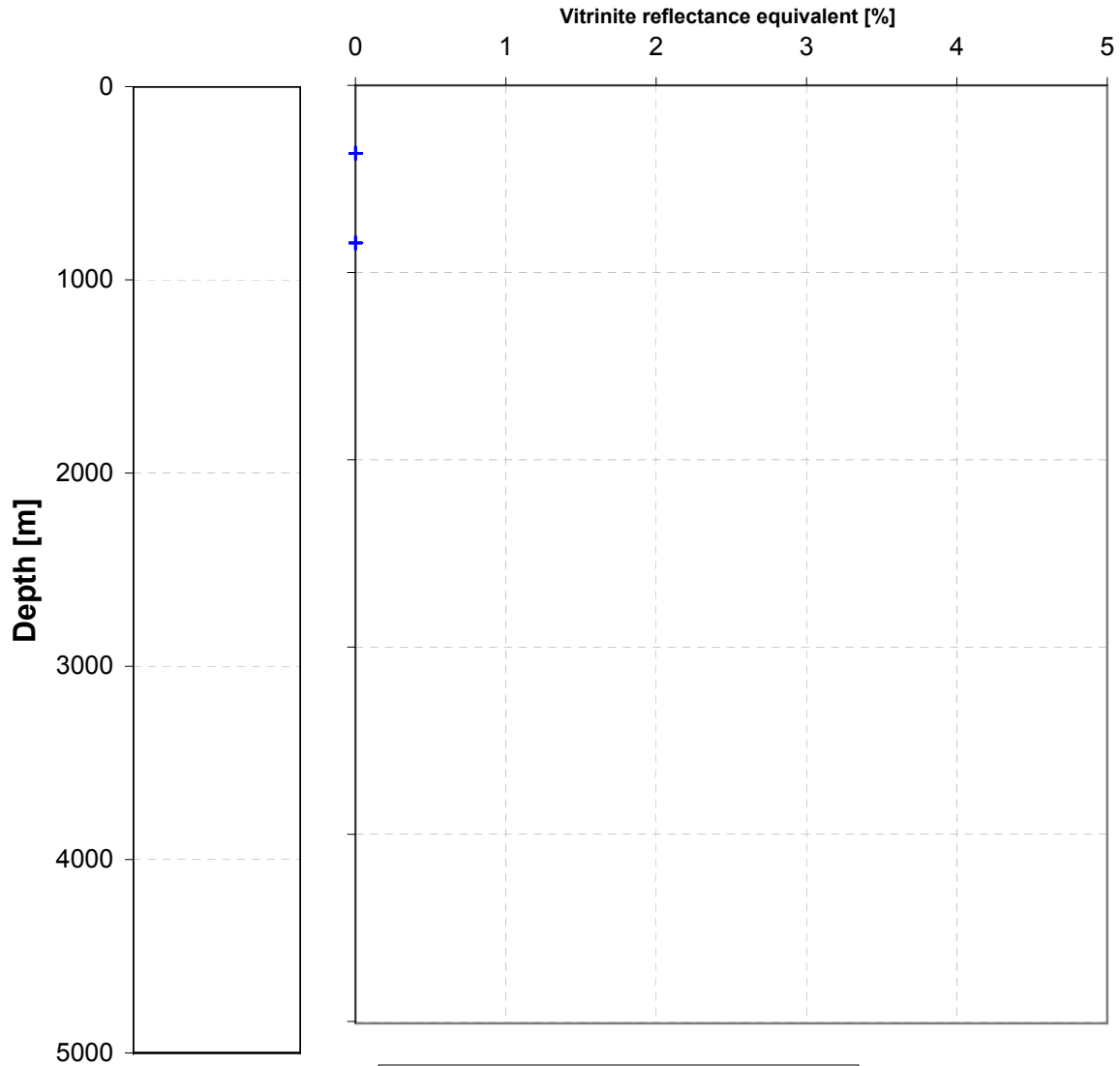




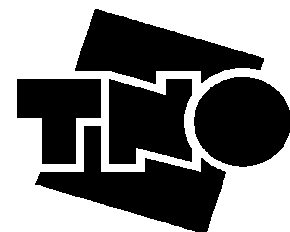
Joint Industry Project Petroplay

Quality controlled data

's Gravenvoeren



- A) Vitrinite reflectance
- B) Vitrinite reflectance
- C) Vitrinite reflectance
- A1) Tmax-VR equivalent - highly reliable
- B) Tmax-VR equivalent
- C) Tmax-VR equivalent
- Modeled %VR (S&B)
- + samples
- ◆ A2) Tmax-VR equivalent - low reliability

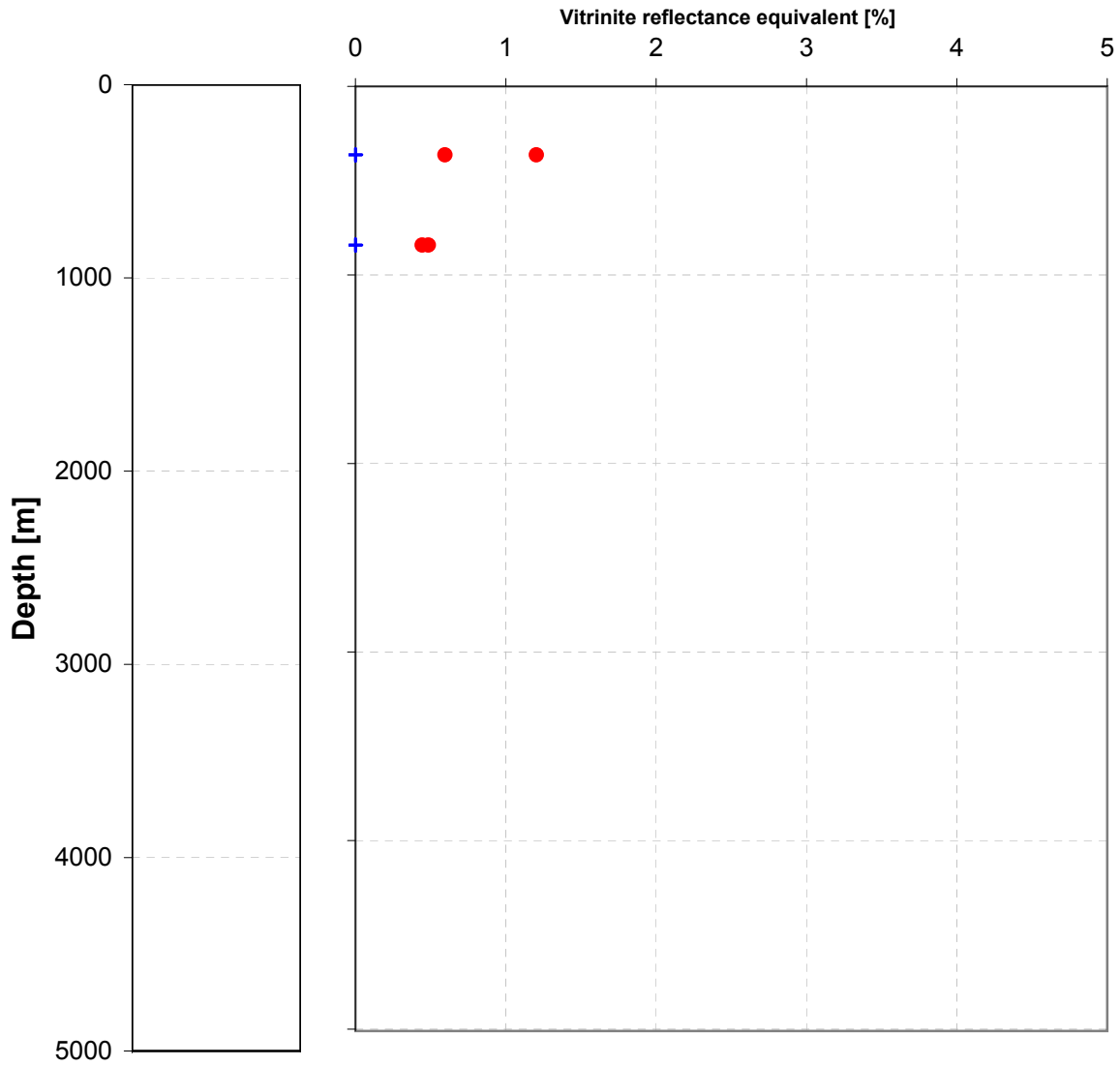




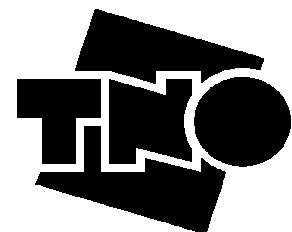
Joint Industry Project Petroplay

Raw data

's Gravenvoeren



- A) Vitrinite reflectance
- B) Vitrinite reflectance
- C) Vitrinite reflectance
- A) Tmax-VR equivalent
- B) Tmax-VR equivalent
- C) Tmax-VR equivalent
- Modeled %VR (S&B)
- + samples

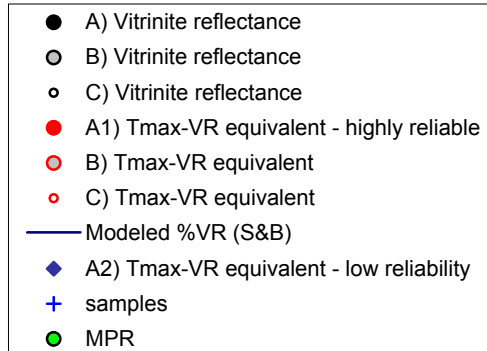
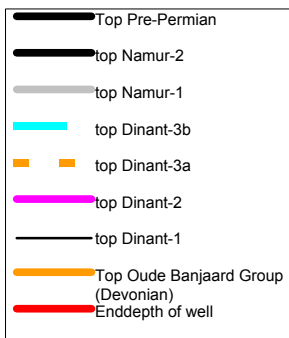
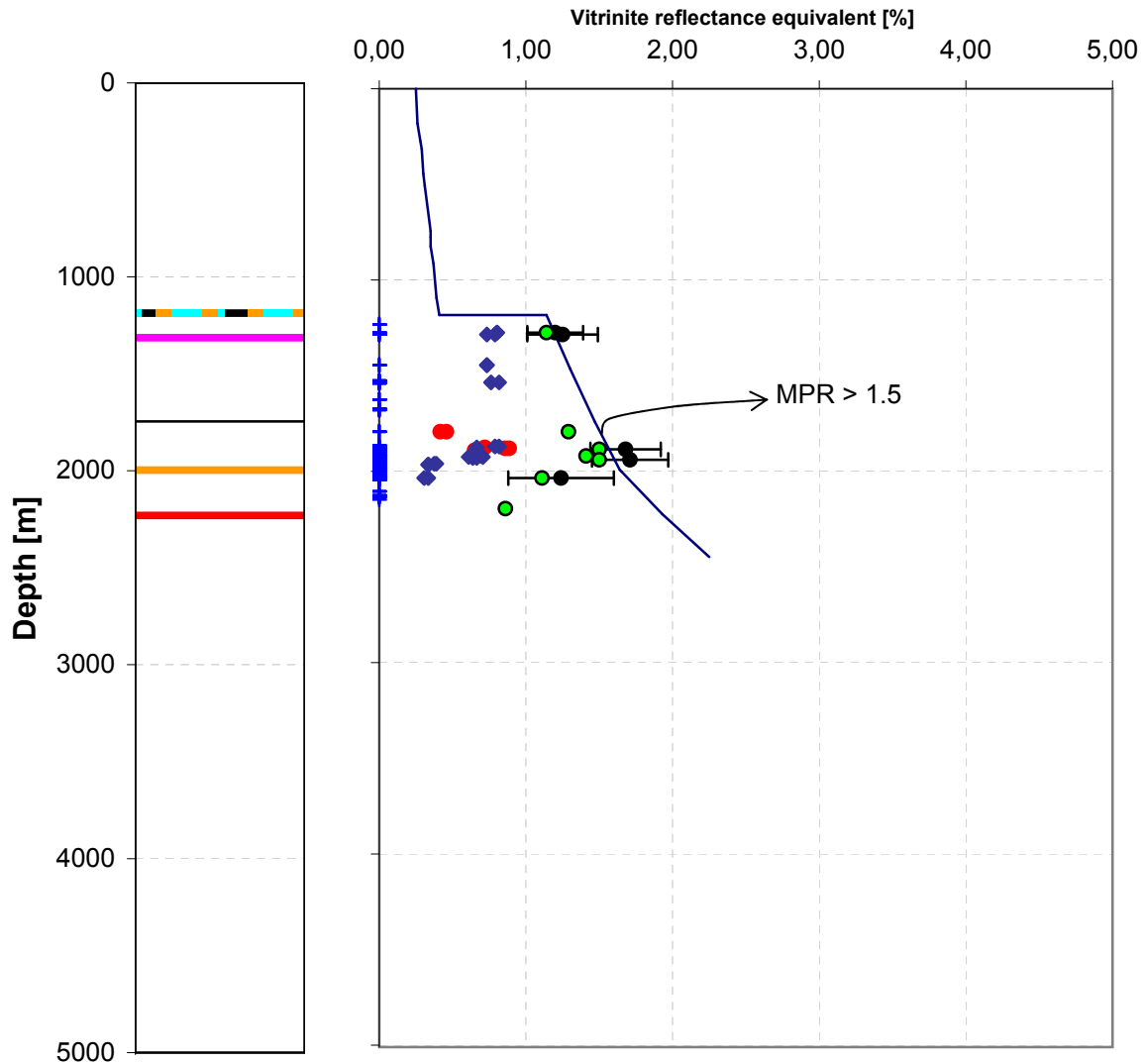




Joint Industry Project Petroplay

Quality controlled data

S05-01

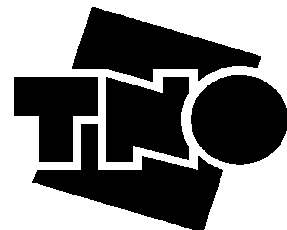
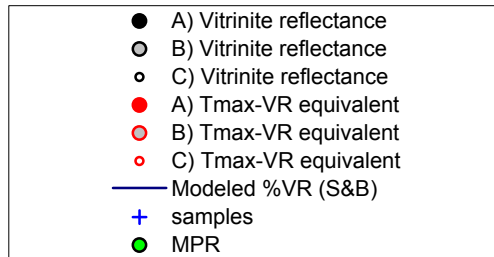
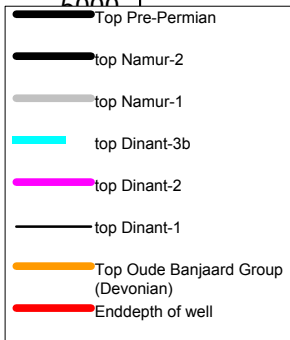
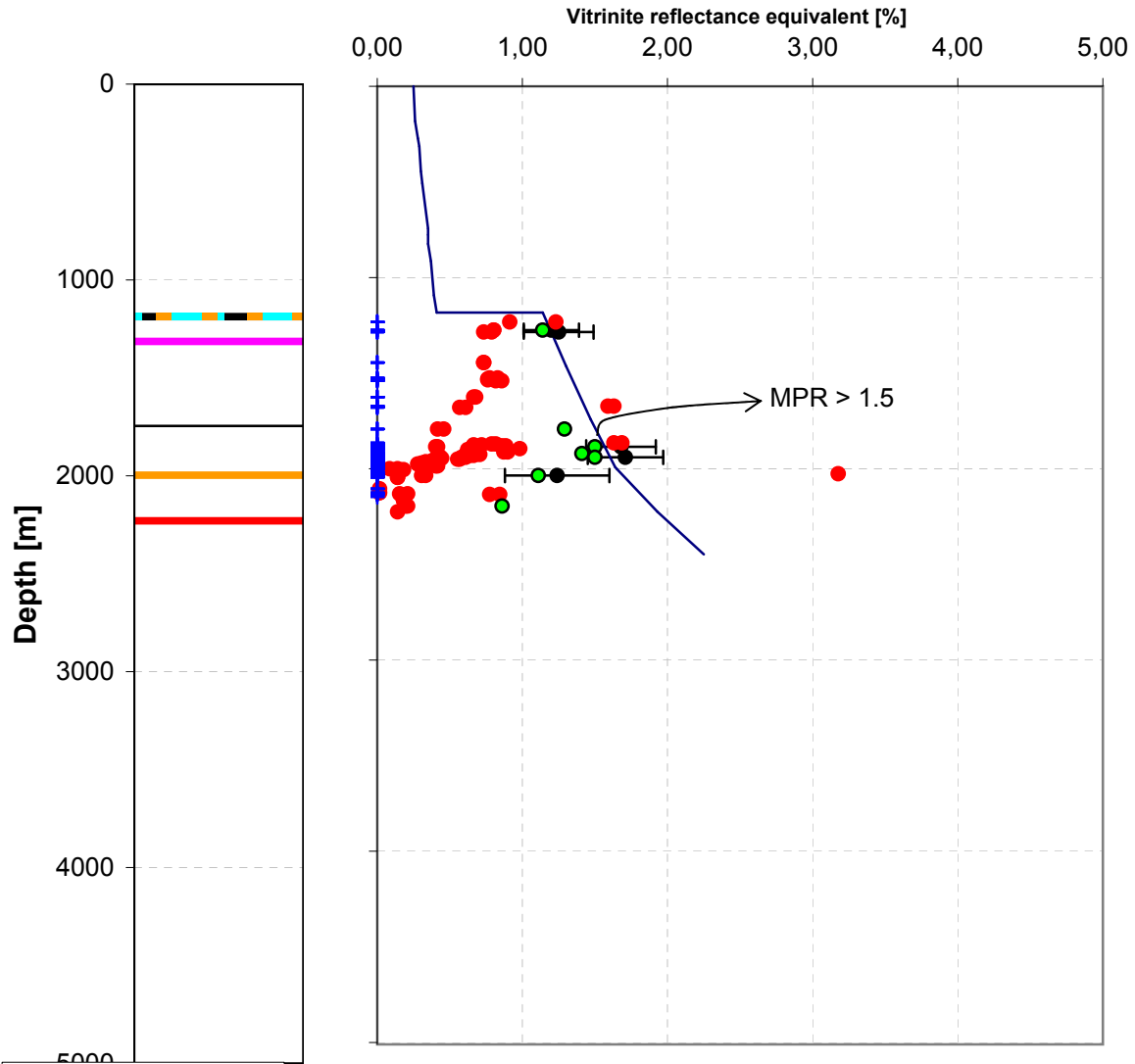




Joint Industry Project Petroplay

Raw data

S05-01

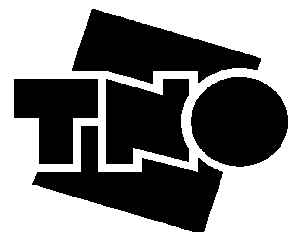
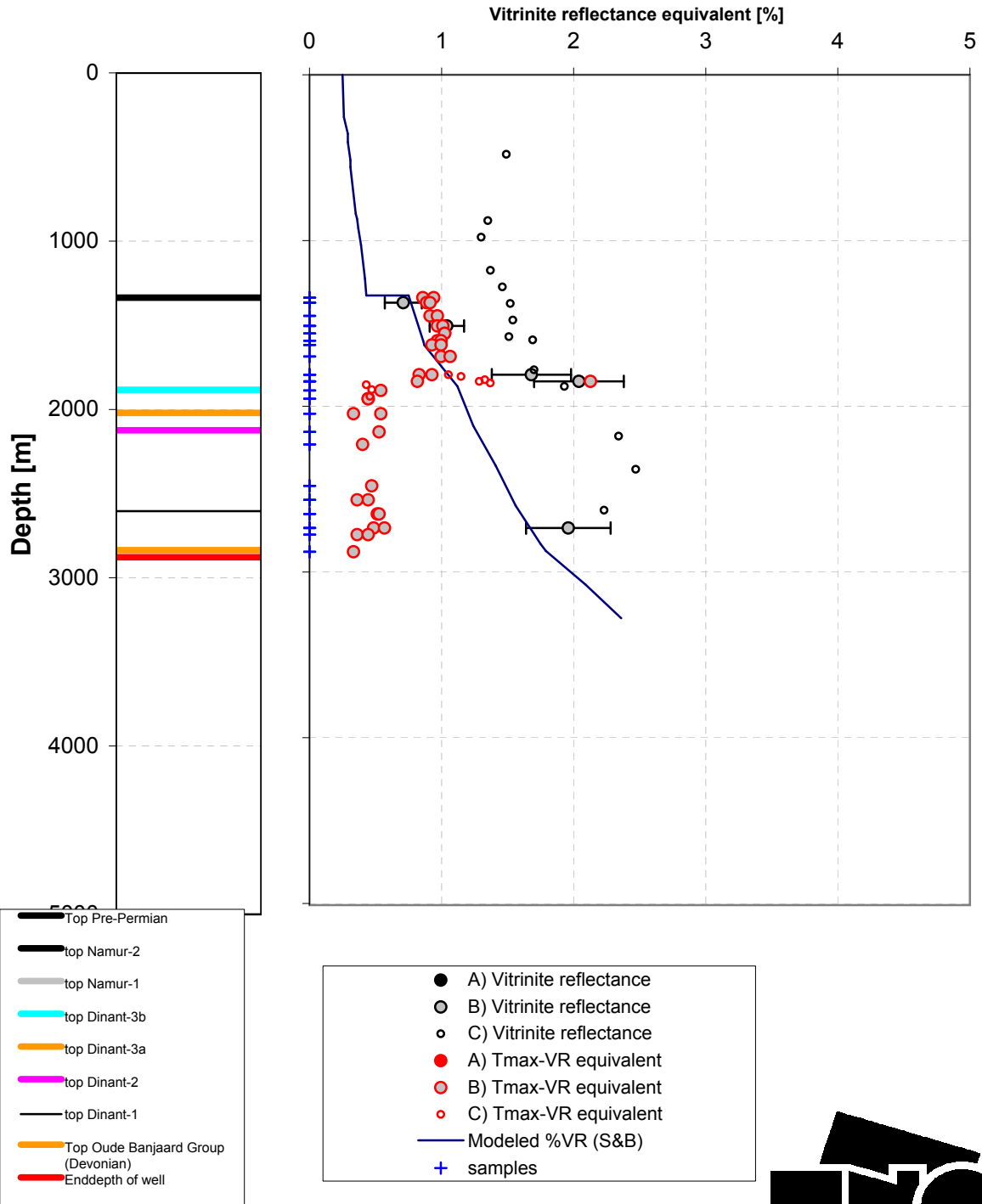




Joint Industry Project Petroplay

Raw data

S02-02

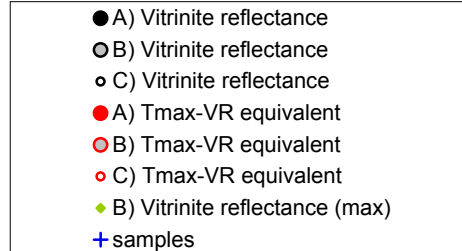
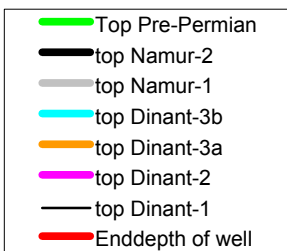
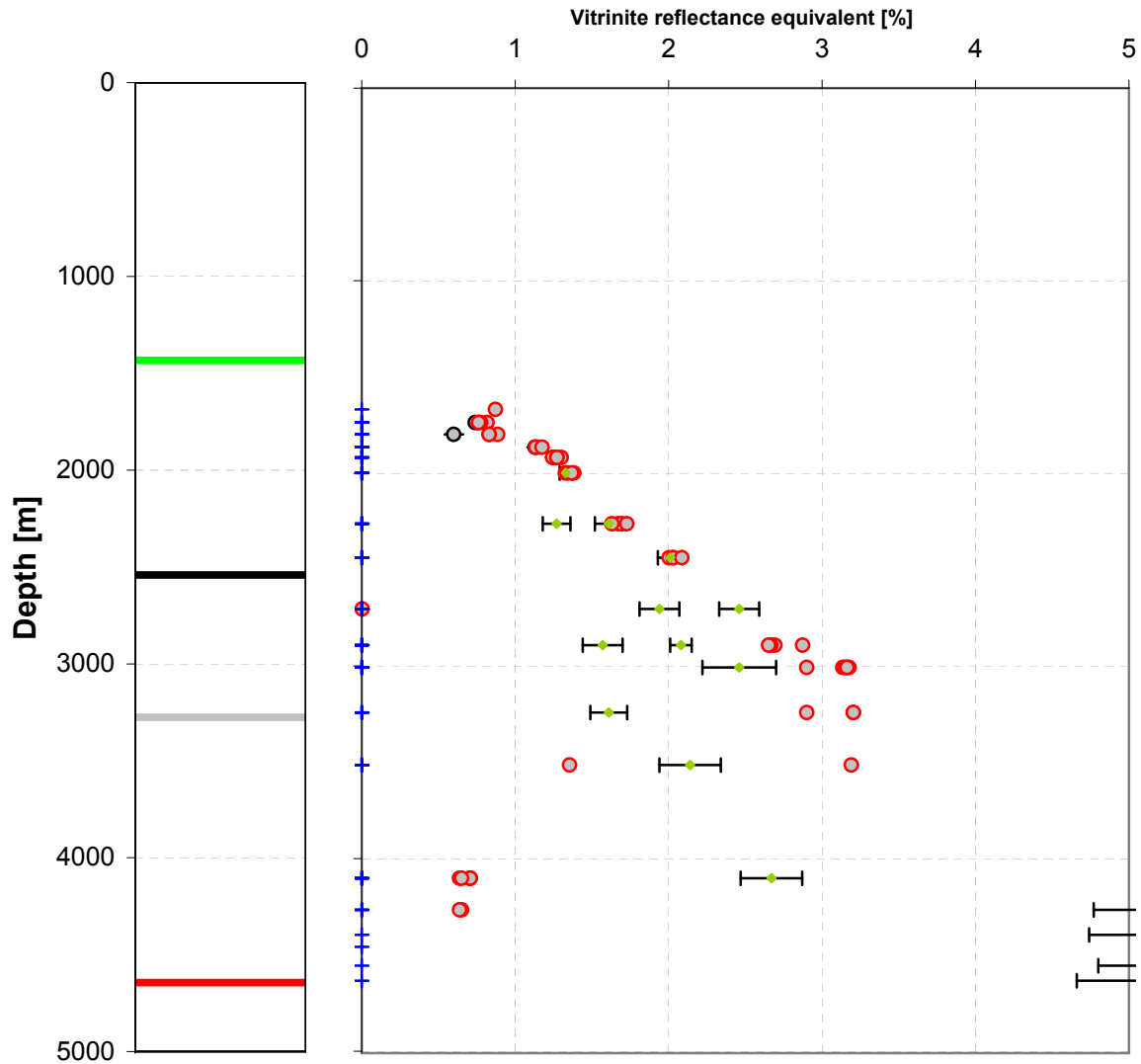




Joint Industry Project Petroplay

Raw data

Rijsbergen-1

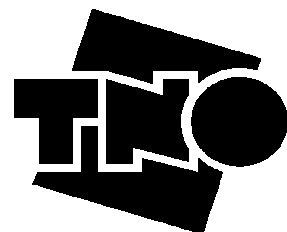
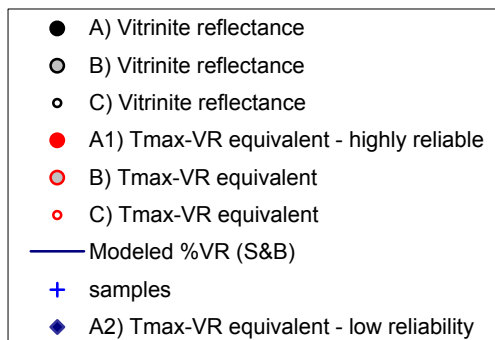
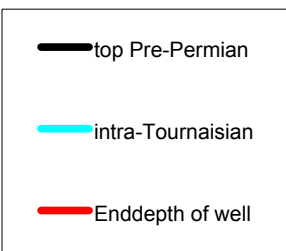
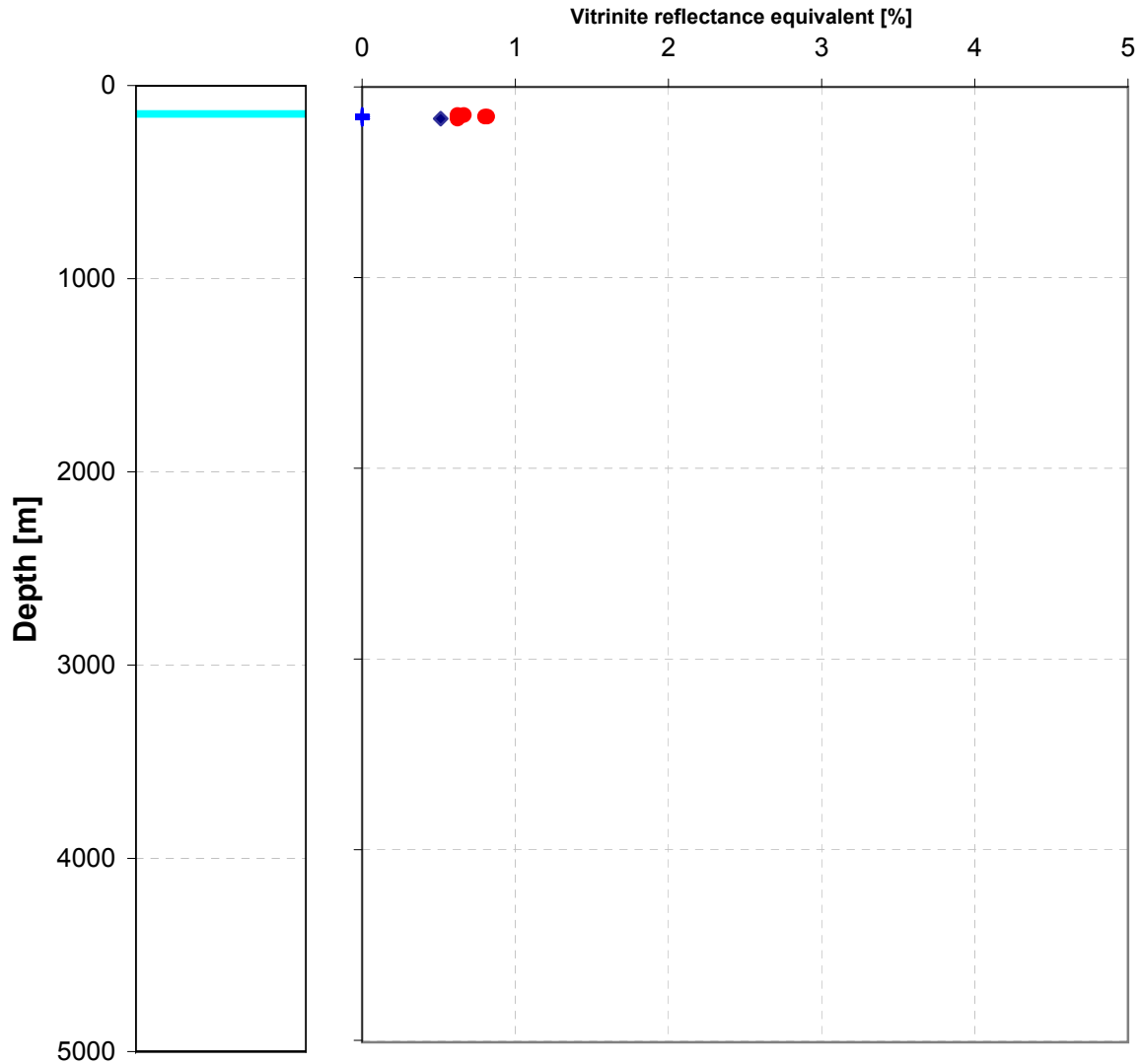




Joint Industry Project Petroplay

Quality controlled data

Rollegem-Tombroek

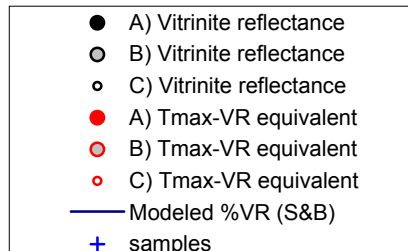
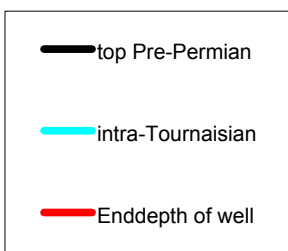
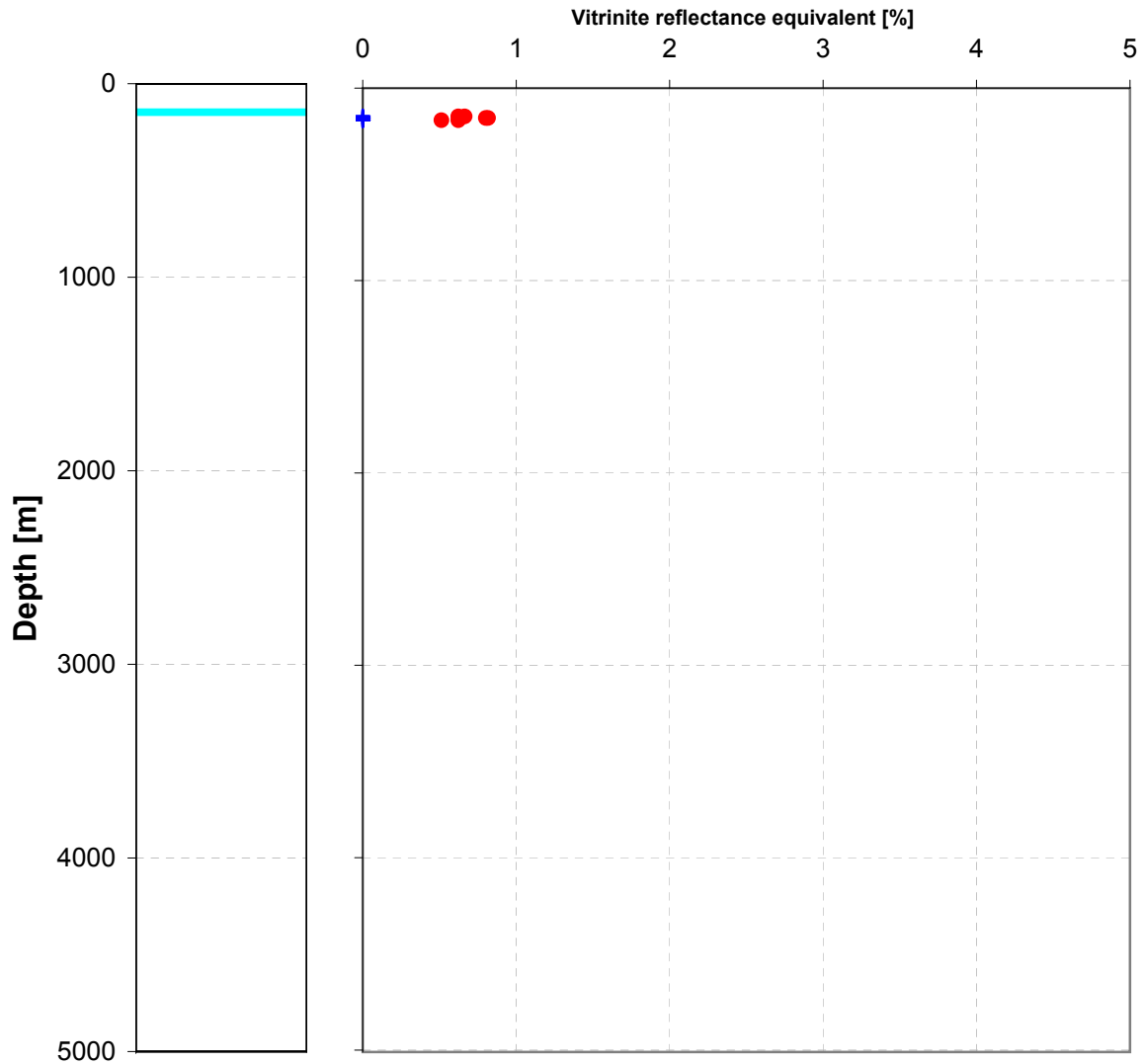




Joint Industry Project Petroplay

Raw data

Rollegem-Tombroek

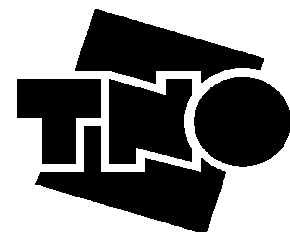
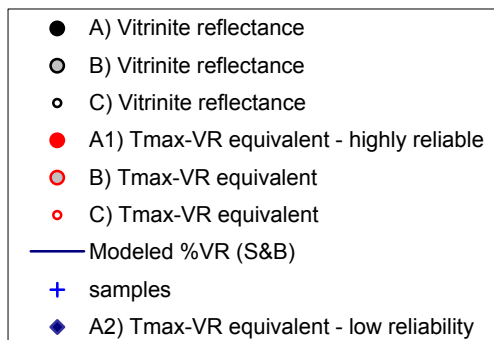
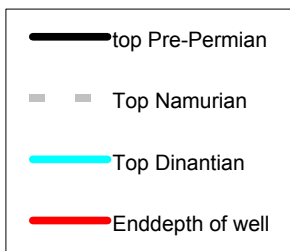
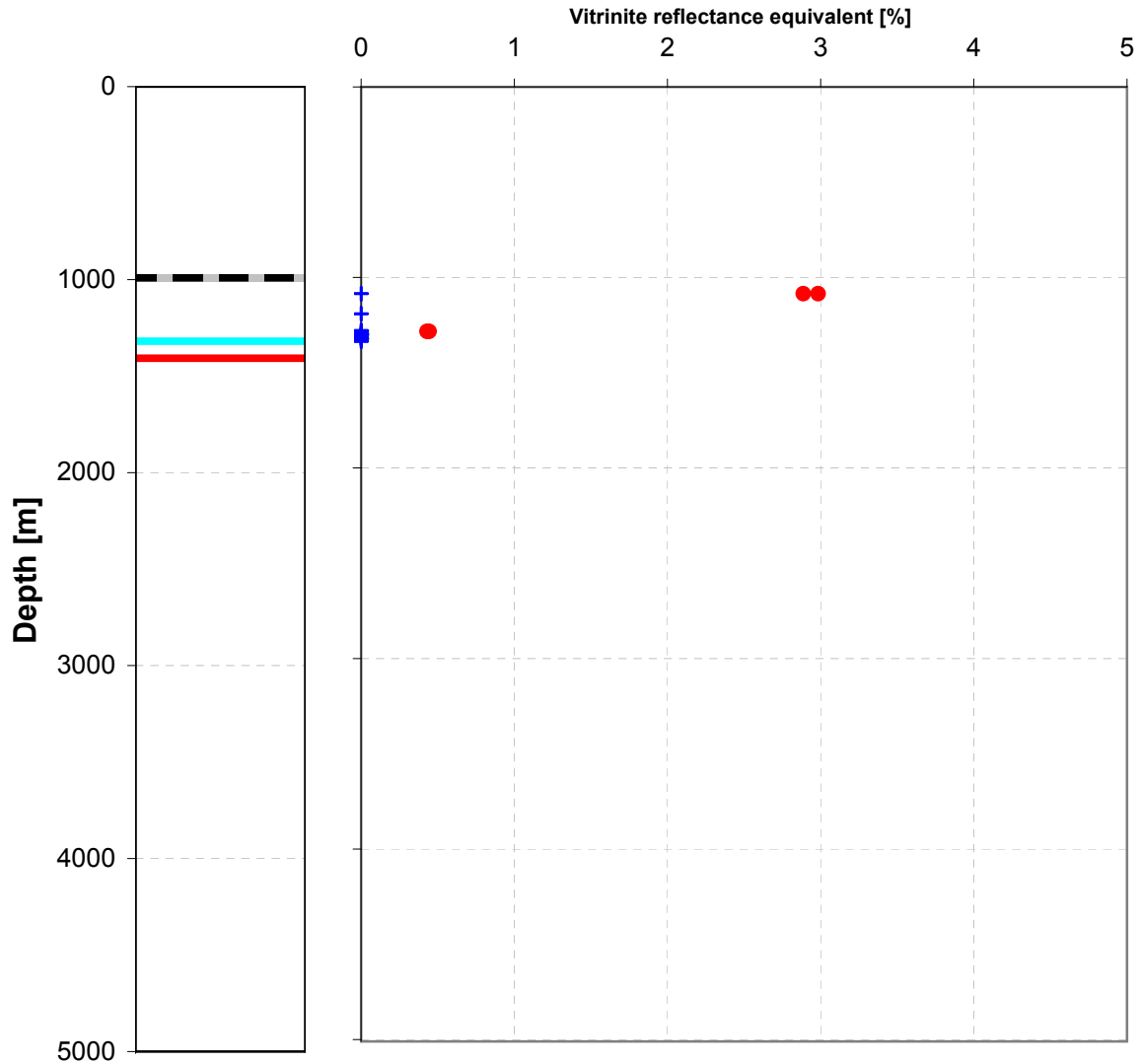




Joint Industry Project Petroplay

Quality controlled data

Rijkevorsel

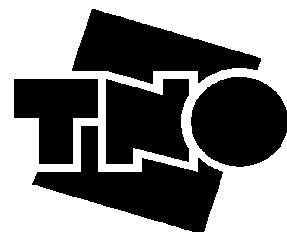
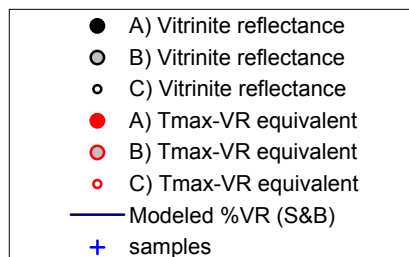
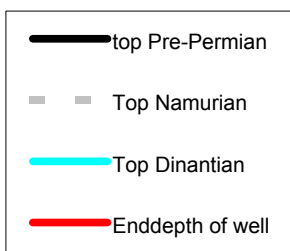
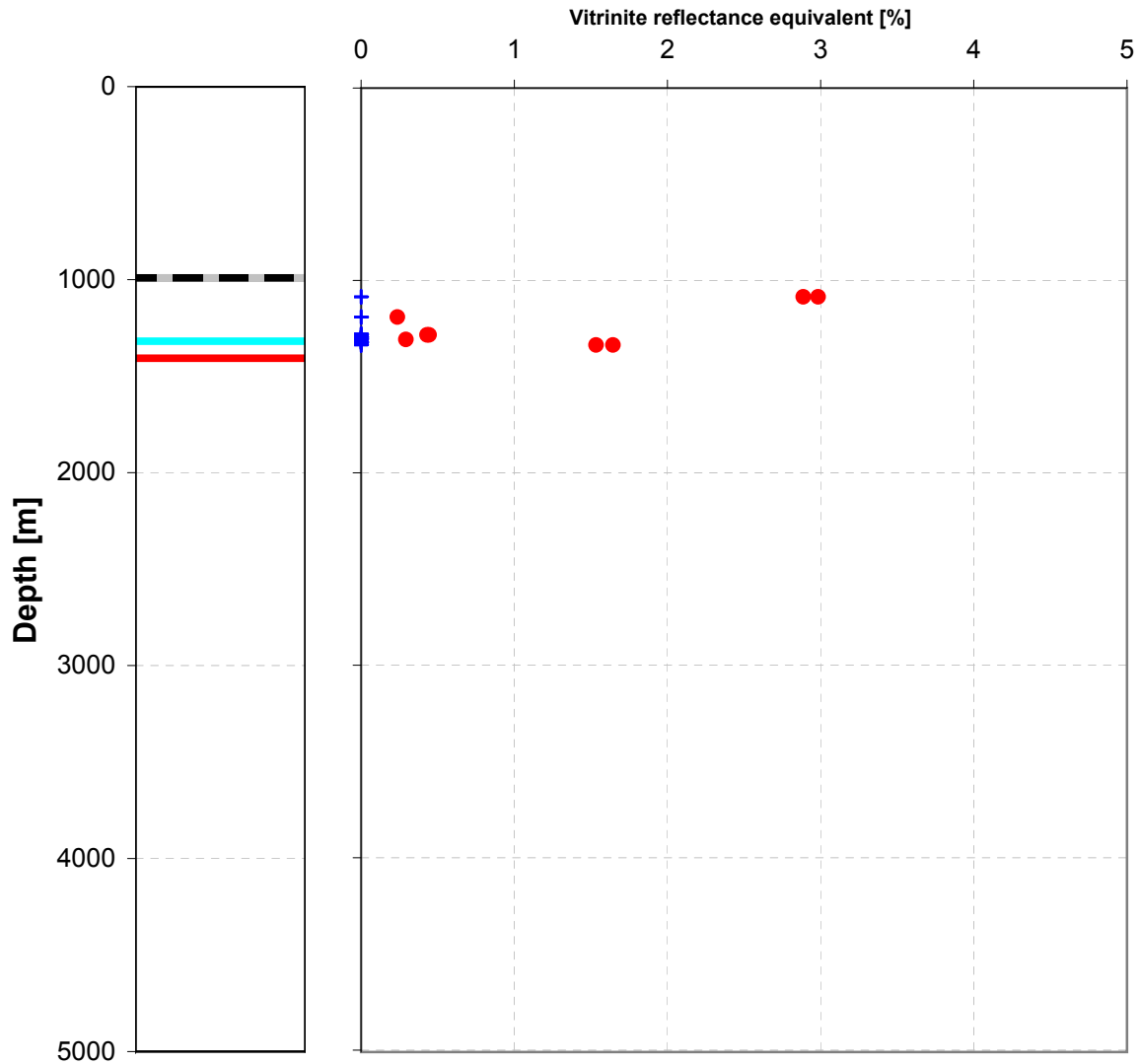




Joint Industry Project Petroplay

Raw data

Rijkevorsel

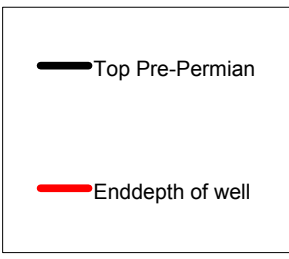
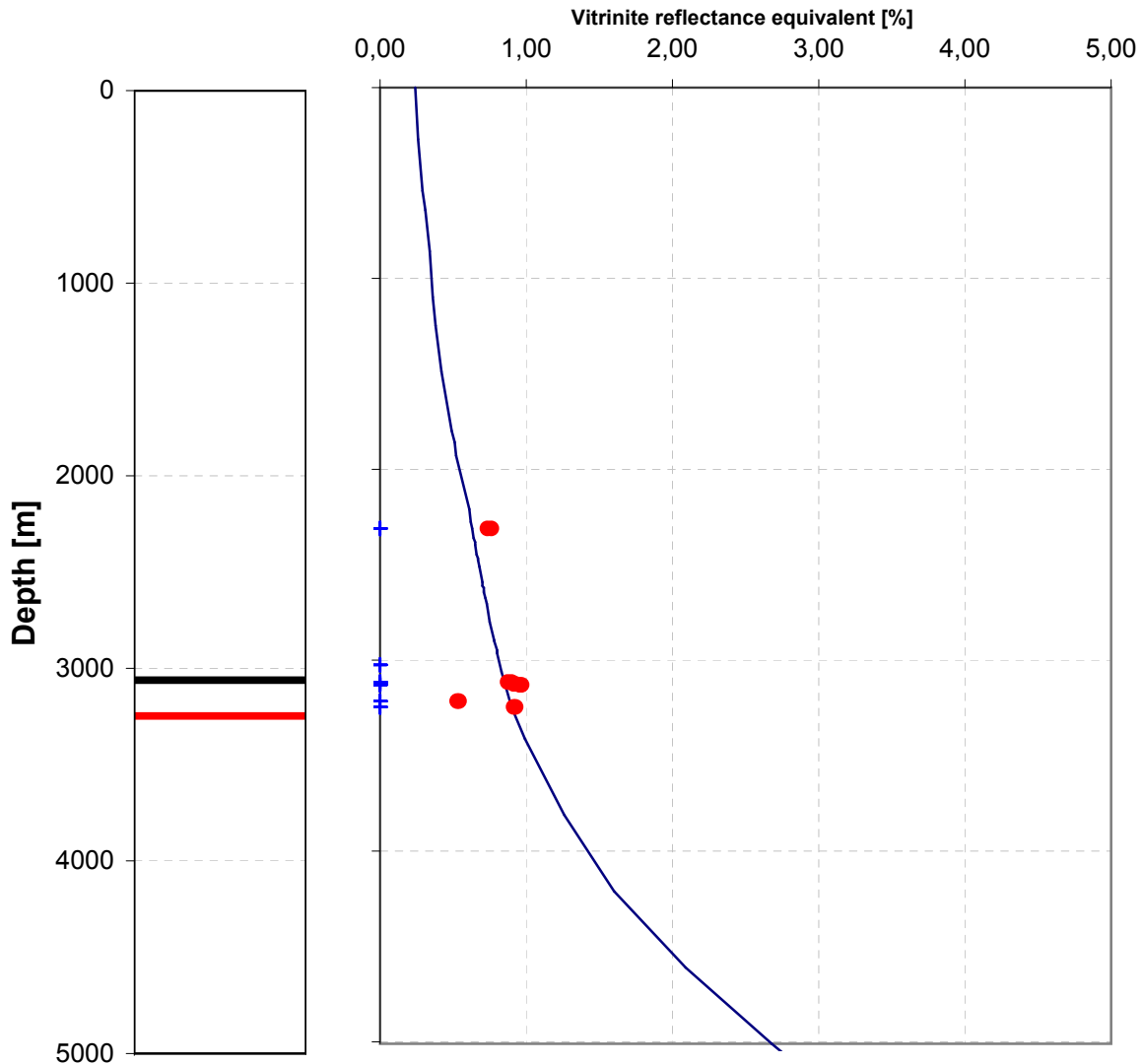




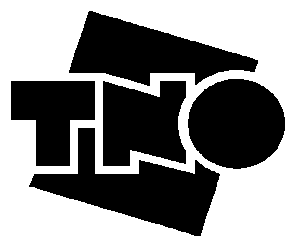
Joint Industry Project Petroplay

Quality controlled data

Q13-03



- A) Vitrinite reflectance
- B) Vitrinite reflectance
- C) Vitrinite reflectance
- A1) Tmax-VR equivalent - highly reliable
- B) Tmax-VR equivalent
- C) Tmax-VR equivalent
- Modeled %VR (S&B)
- + samples
- ◆ A2) Tmax-VR equivalent - low reliability

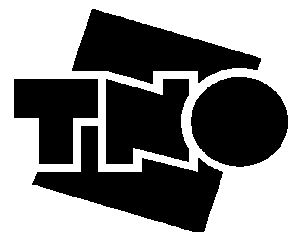
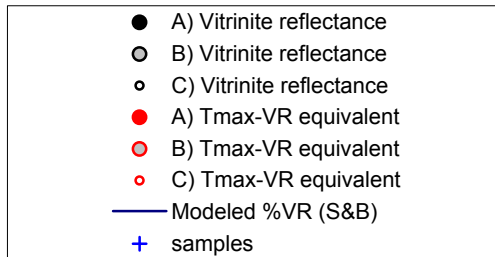
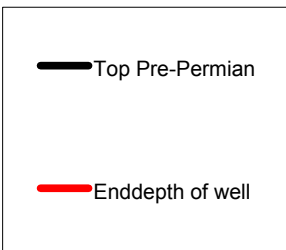
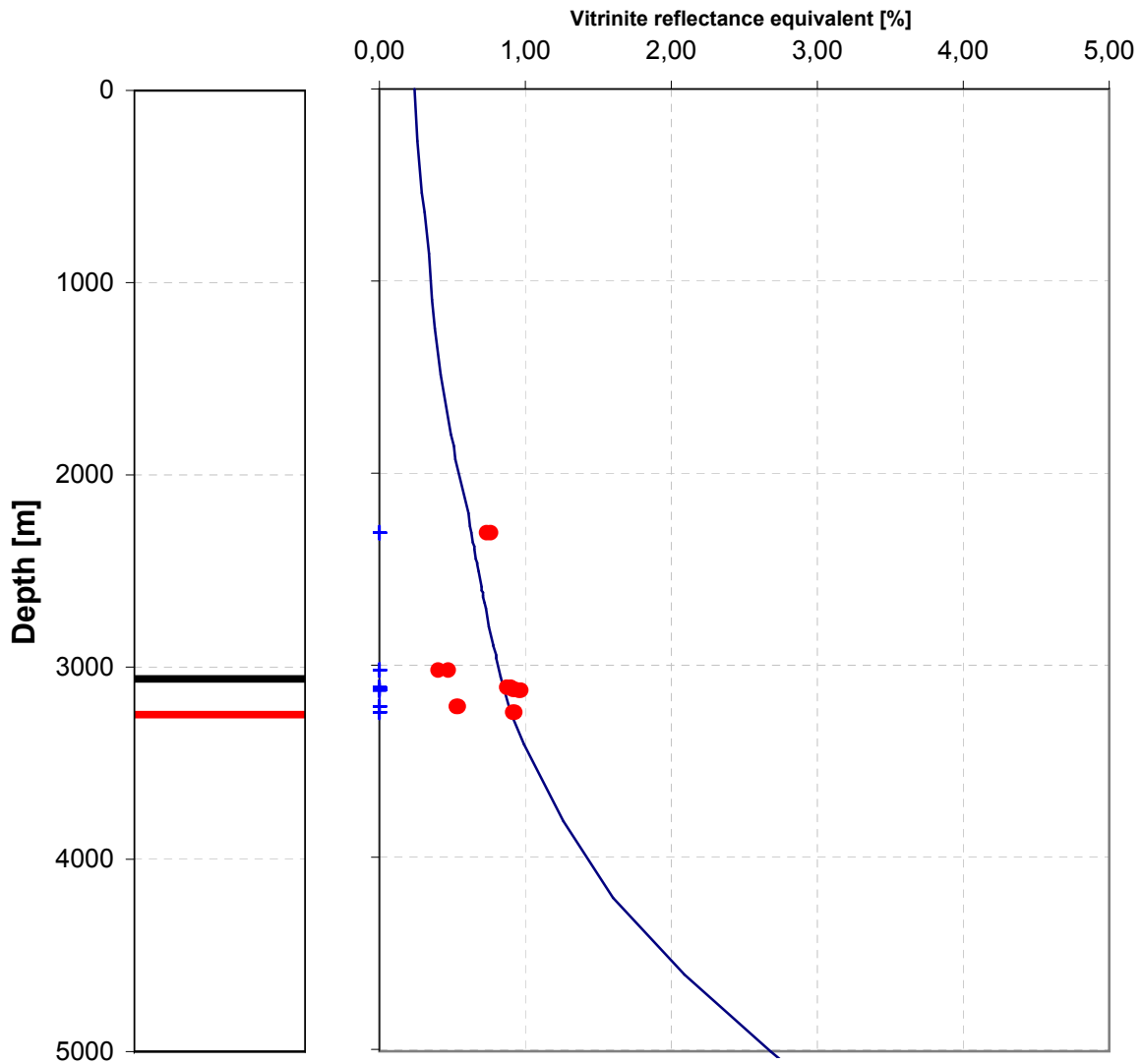




Joint Industry Project Petroplay

Raw data

Q13-03

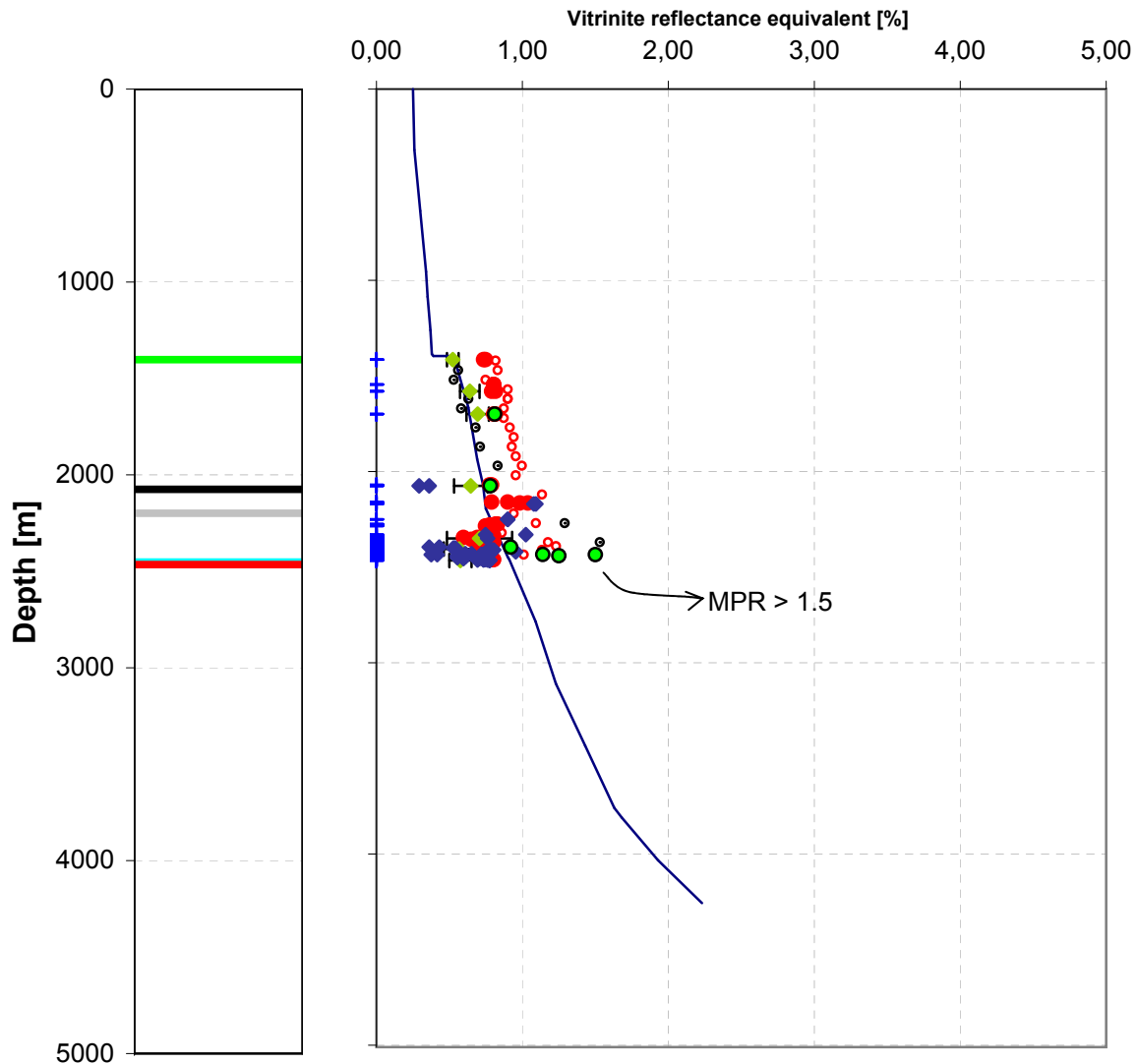




Joint Industry Project Petroplay

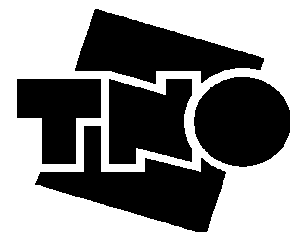
Quality controlled data

P16-01



- Top Pre-Permian
- top Namur-2
- top Namur-1
- top Dinant-3b
- top Dinant-3a
- top Dinant-2
- top Dinant-1
- Enddepth of well

- A) Vitirinite reflectance
- B) Vitirinite reflectance
- C) Vitirinite reflectance
- A1) Tmax-VR equivalent - highly reliable
- B) Tmax-VR equivalent
- C) Tmax-VR equivalent
- ◆ A) Vitirinite reflectance (max)
- Modeled %VR (S&B)
- ◆ A2) Tmax-VR equivalent - low reliability
- + samples
- MPR

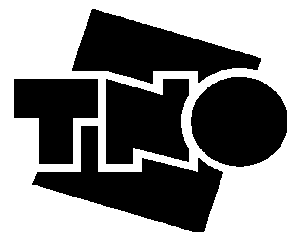
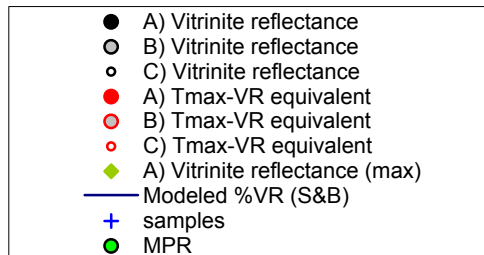
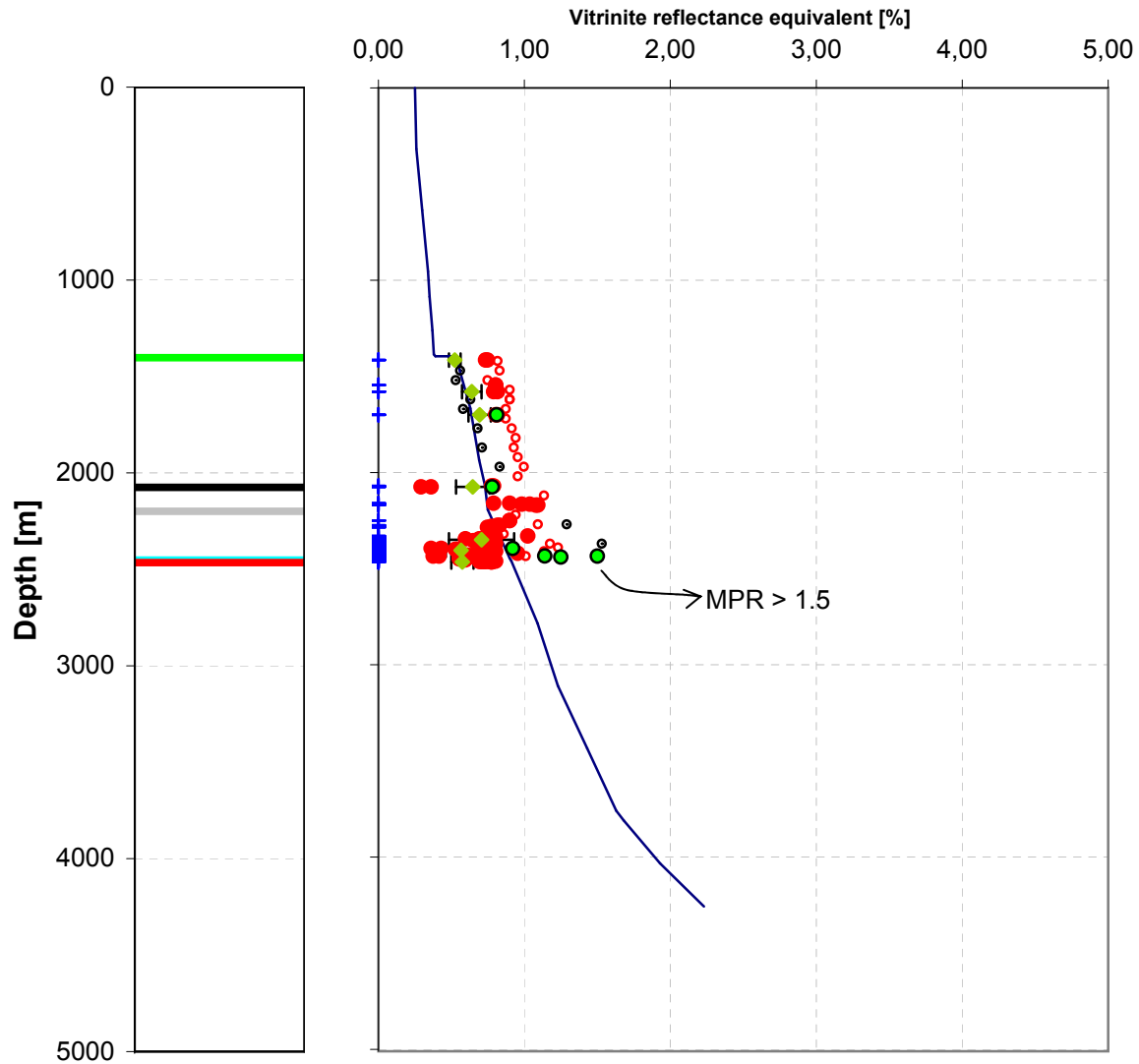




Joint Industry Project Petroplay

Raw data

P16-01

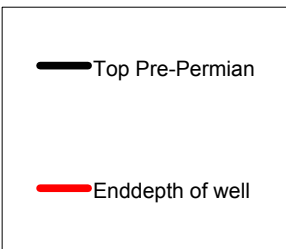
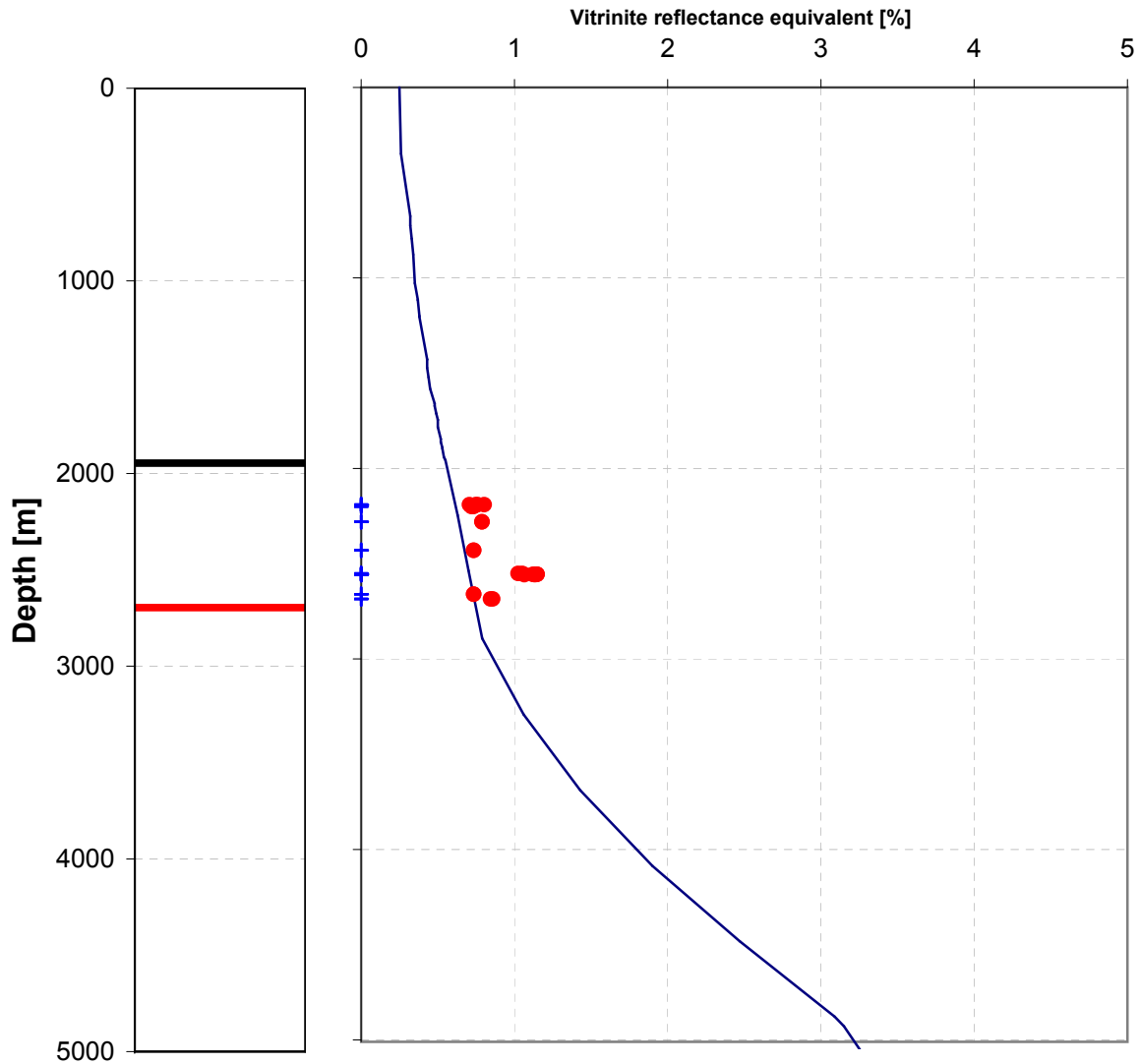




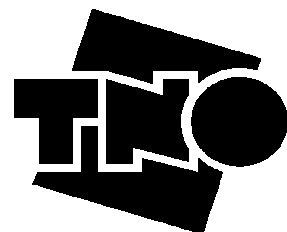
Joint Industry Project Petroplay

Quality controlled data

P10-01



- A) Vitrinite reflectance
- B) Vitrinite reflectance
- C) Vitrinite reflectance
- A1) Tmax-VR equivalent - highly reliable
- B) Tmax-VR equivalent
- C) Tmax-VR equivalent
- Modeled %VR (S&B)
- + samples
- ◆ A2) Tmax-VR equivalent - low reliability

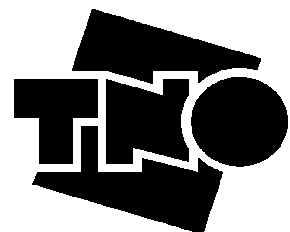
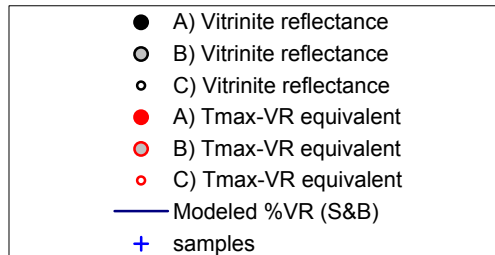
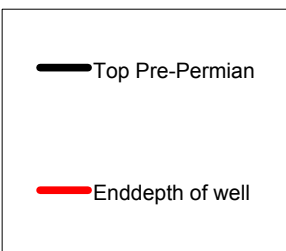
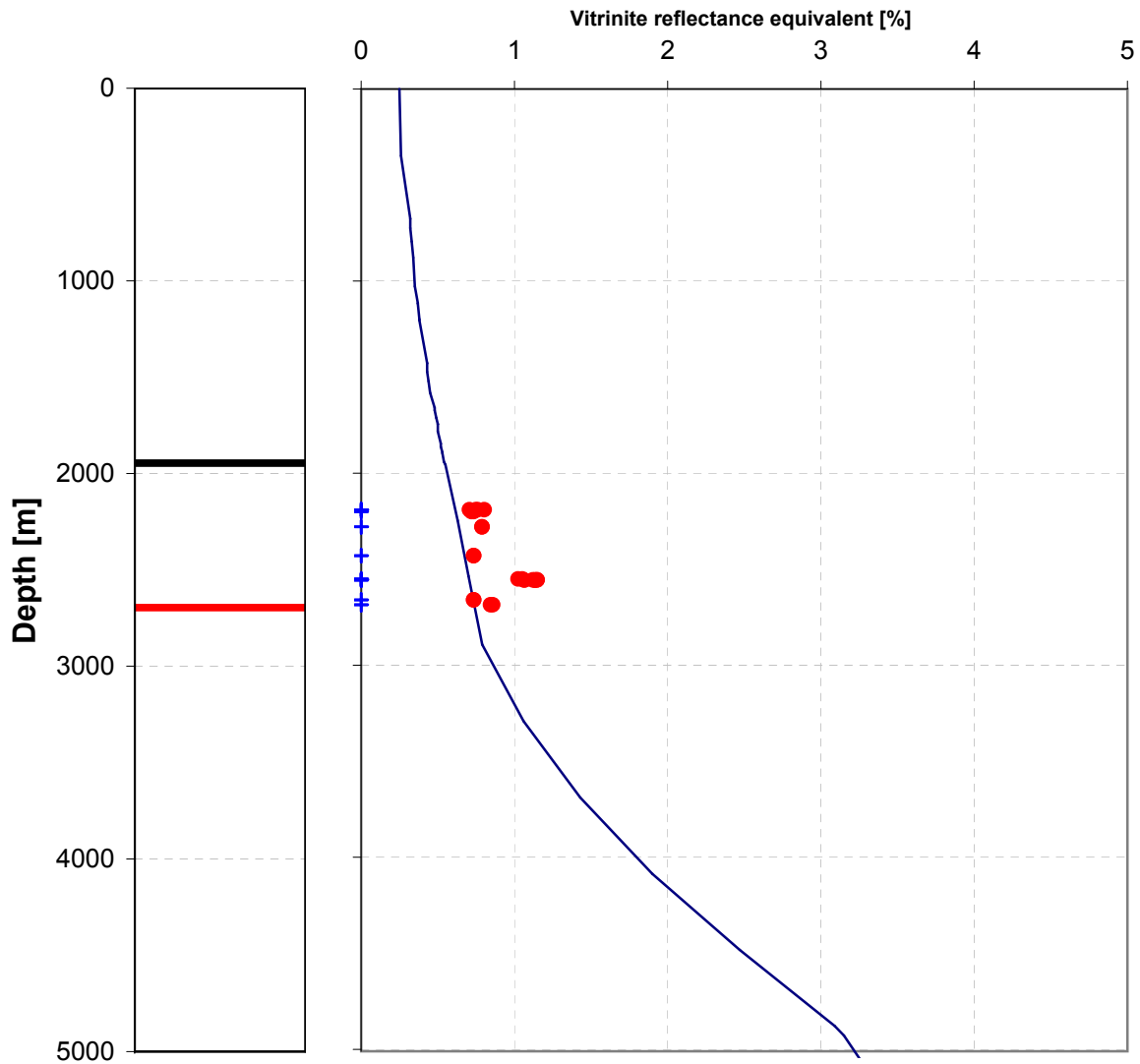




Joint Industry Project Petroplay

Raw data

P10-01

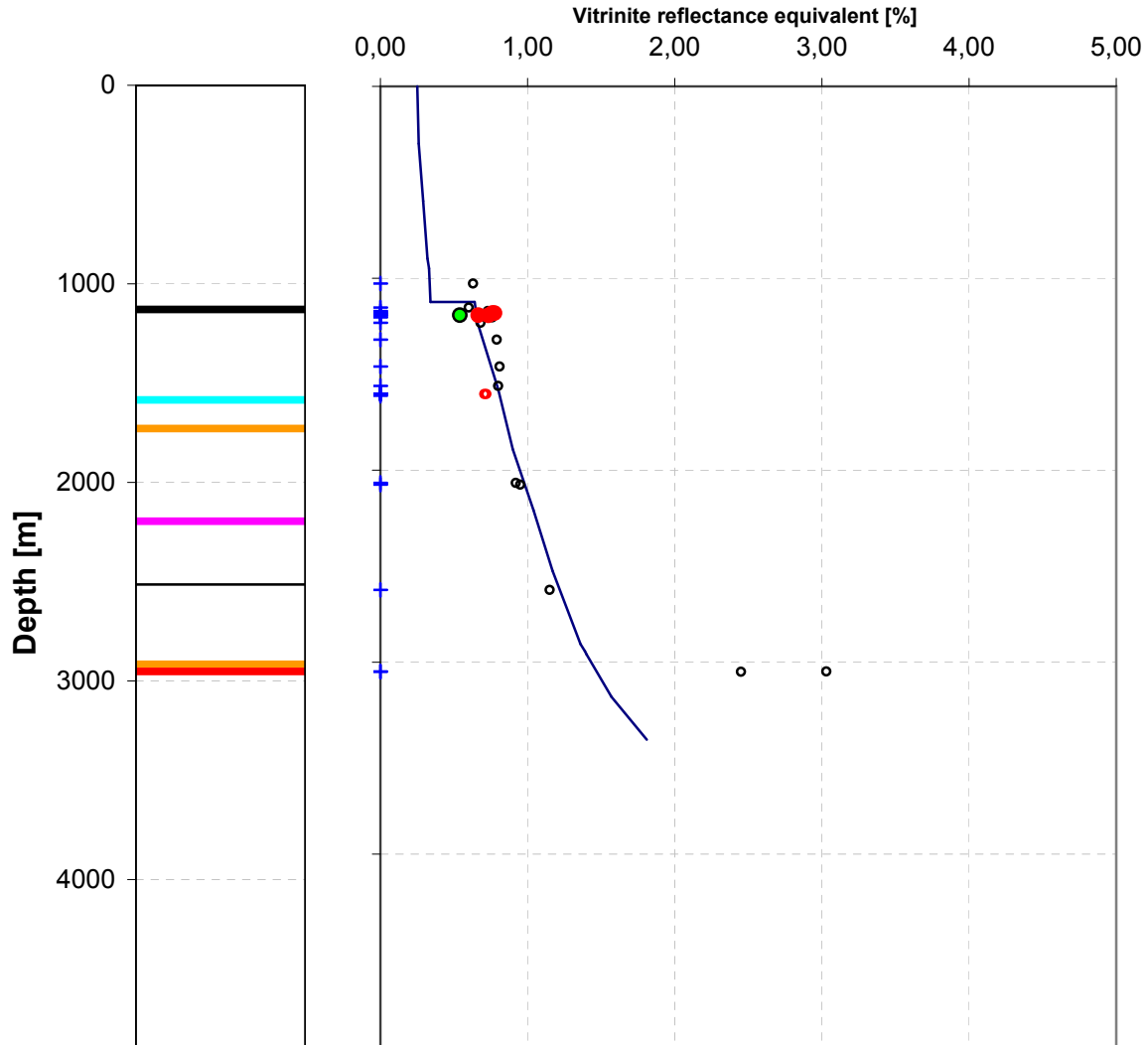




Joint Industry Project Petroplay

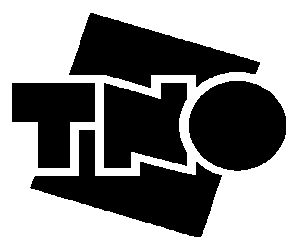
Quality controlled data

O18-01



- Top Pre-Permian
- top Namur-2
- top Namur-1
- top Dinant-3b
- top Dinant-3a
- top Dinant-2
- top Dinant-1
- Top Oude Banjaard Group (Devonian)

- A) Vitritine reflectance
- B) Vitritine reflectance
- C) Vitritine reflectance
- A1) Tmax-VR equivalent - highly reliable
- B) Tmax-VR equivalent
- C) Tmax-VR equivalent
- Modeled %VR (S&B)
- + samples
- ◆ A2) Tmax-VR equivalent - low reliability
- MPR

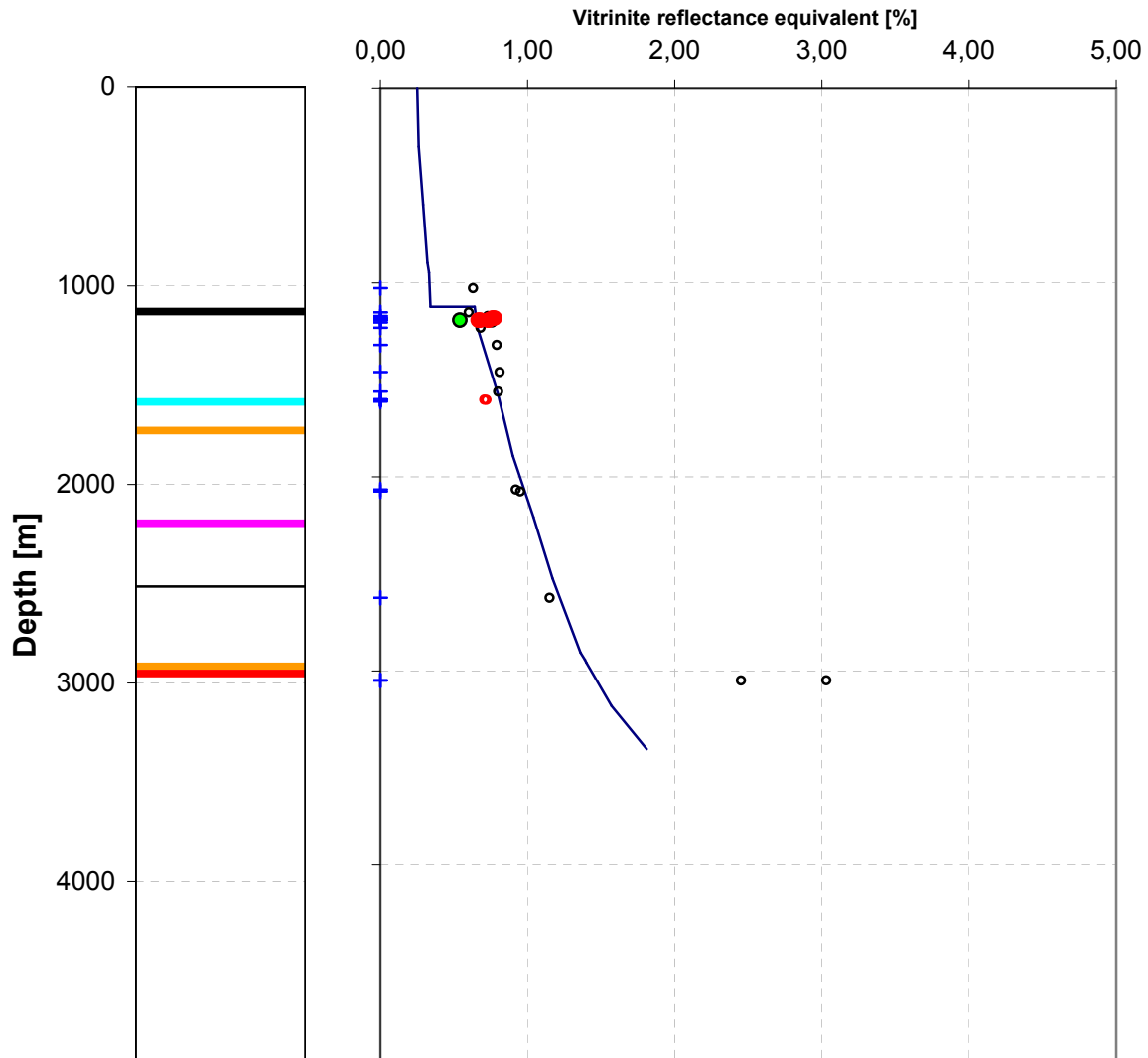




Joint Industry Project Petroplay

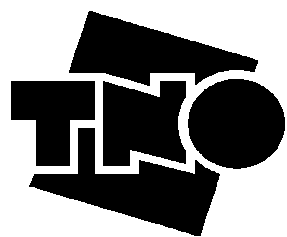
Raw data

O18-01



- Top Pre-Permian
- top Namur-2
- top Namur-1
- top Dinant-3b
- top Dinant-3a
- top Dinant-2
- top Dinant-1
- Top Oude Banjaard Group (Devonian)

- A) Vitrinite reflectance
- B) Vitrinite reflectance
- C) Vitrinite reflectance
- A) Tmax-VR equivalent
- B) Tmax-VR equivalent
- C) Tmax-VR equivalent
- Modeled %VR (S&B)
- + samples
- MPR

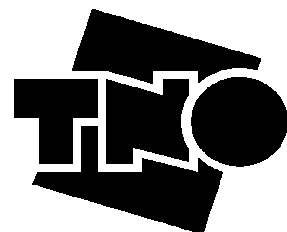
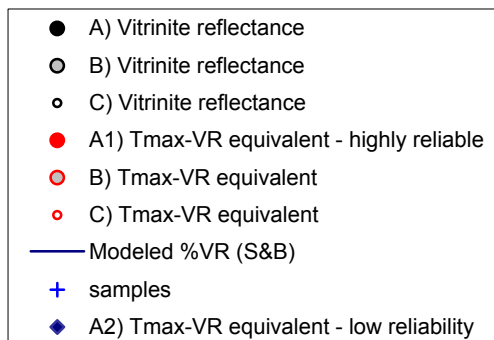
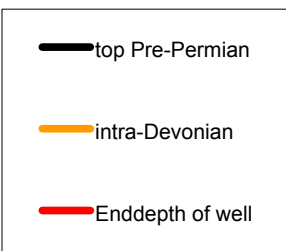
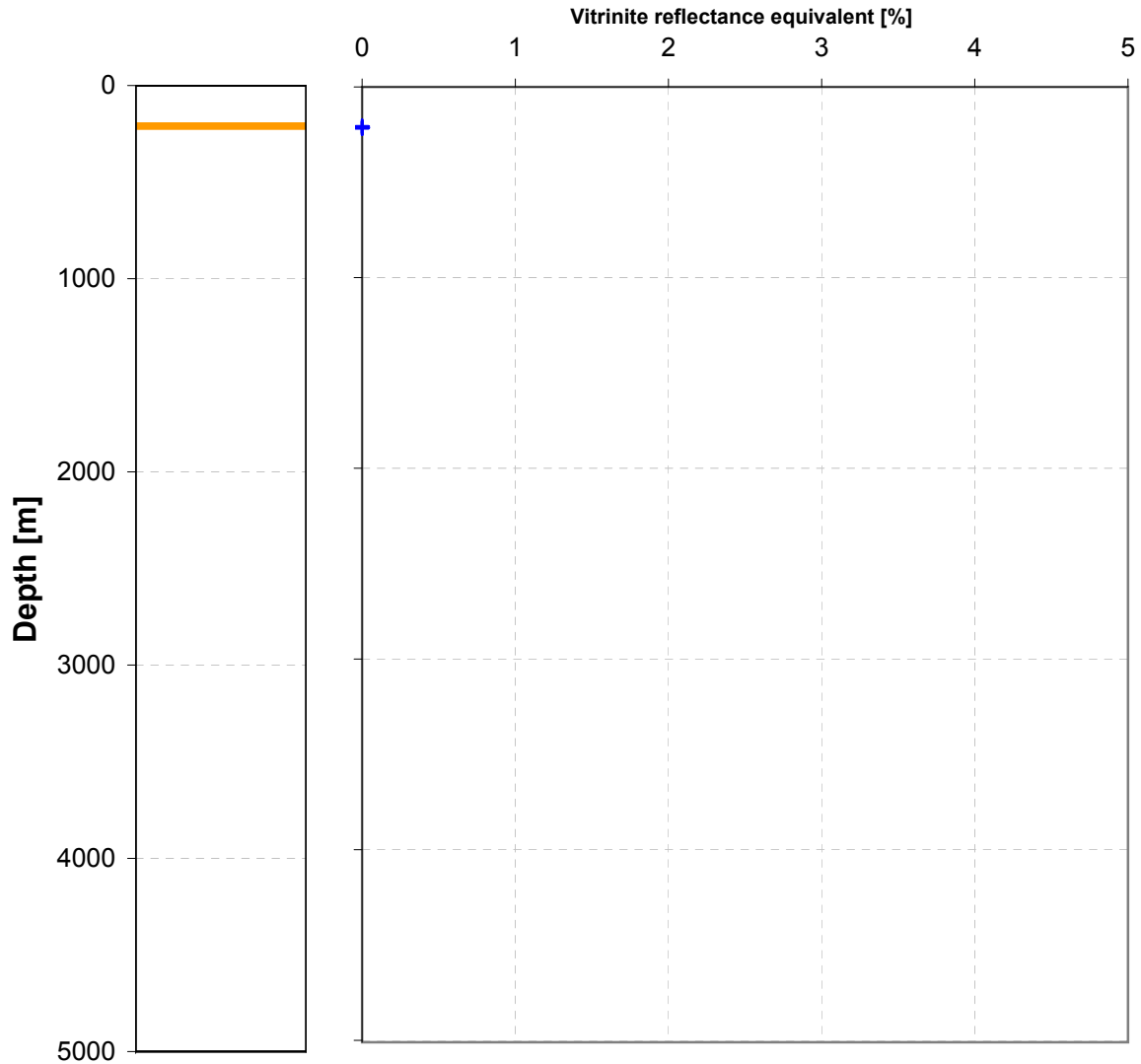




Joint Industry Project Petroplay

Quality controlled data

Nieuwkerke

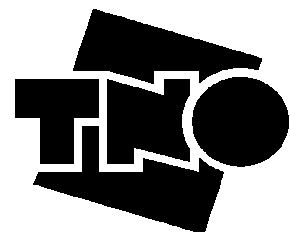
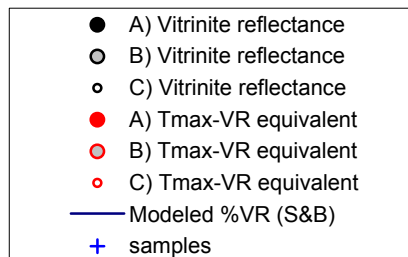
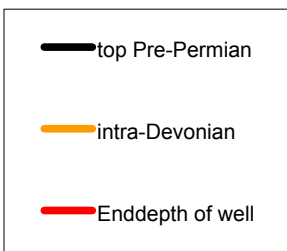
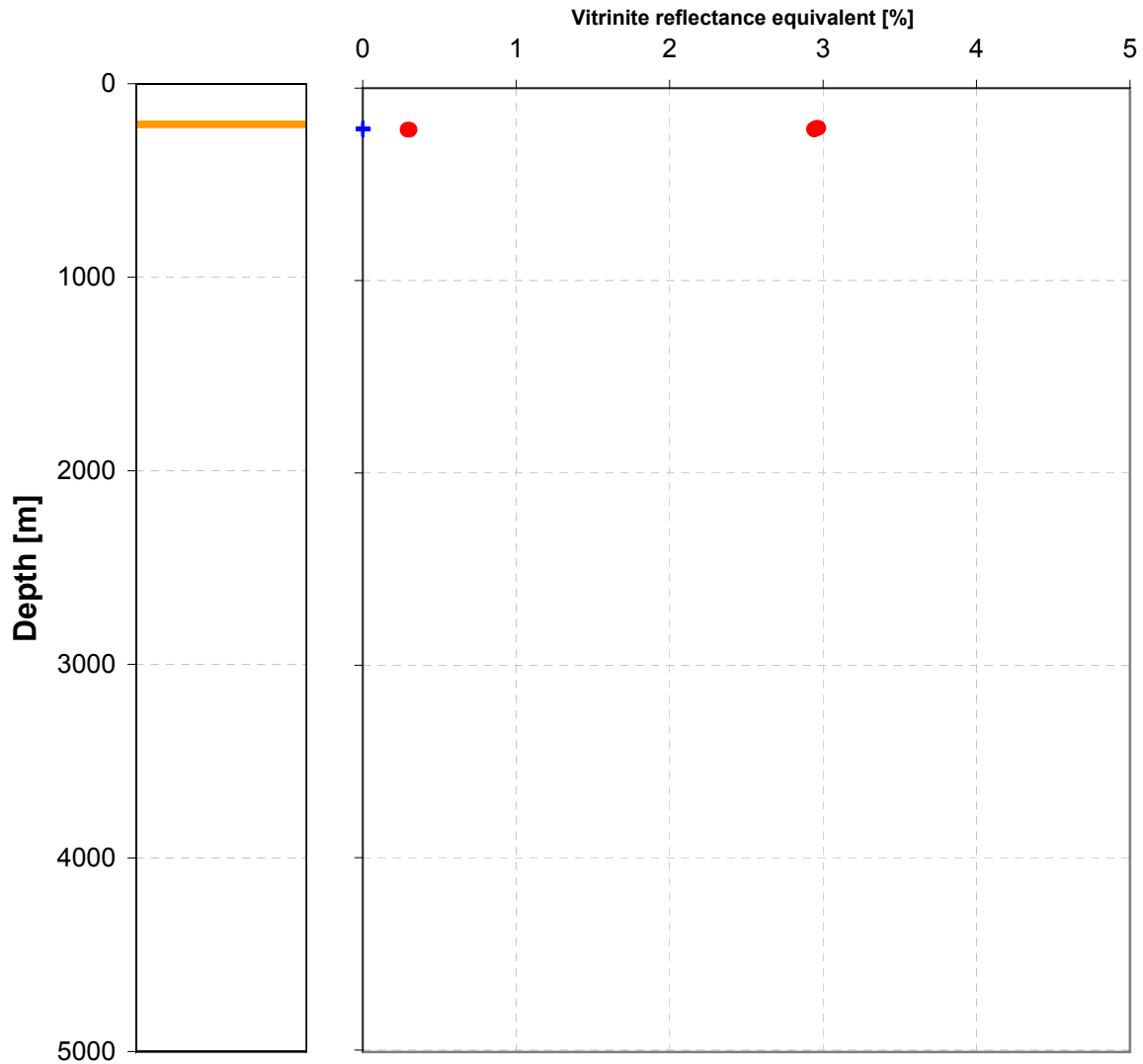




Joint Industry Project Petroplay

Raw data

Nieuwkerke

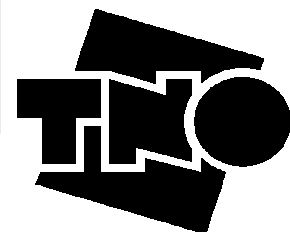
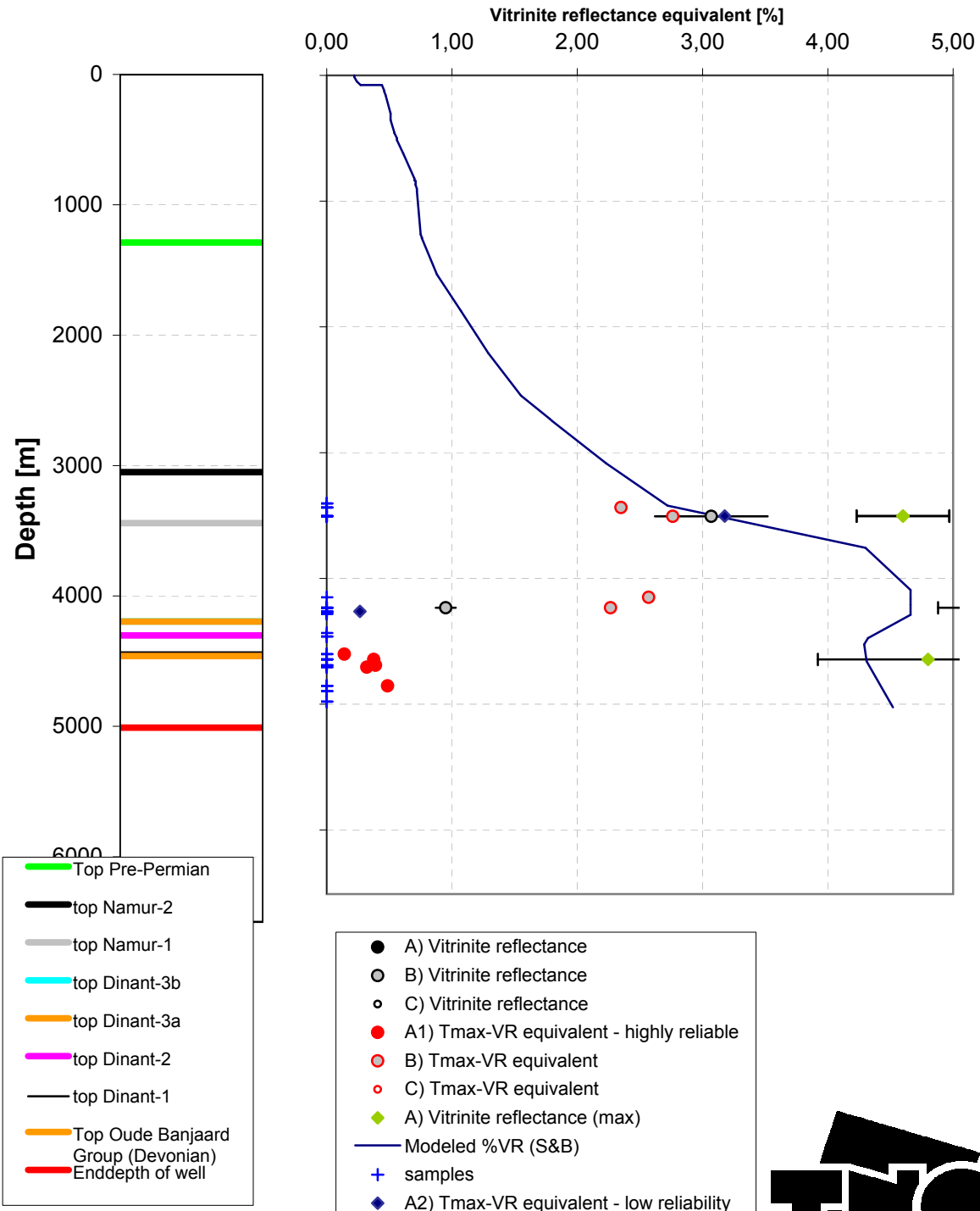




Joint Industry Project Petroplay

Quality controlled data

Winterswijk-1

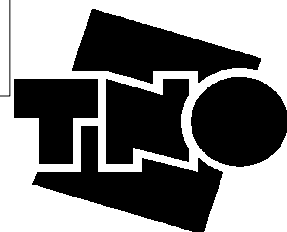
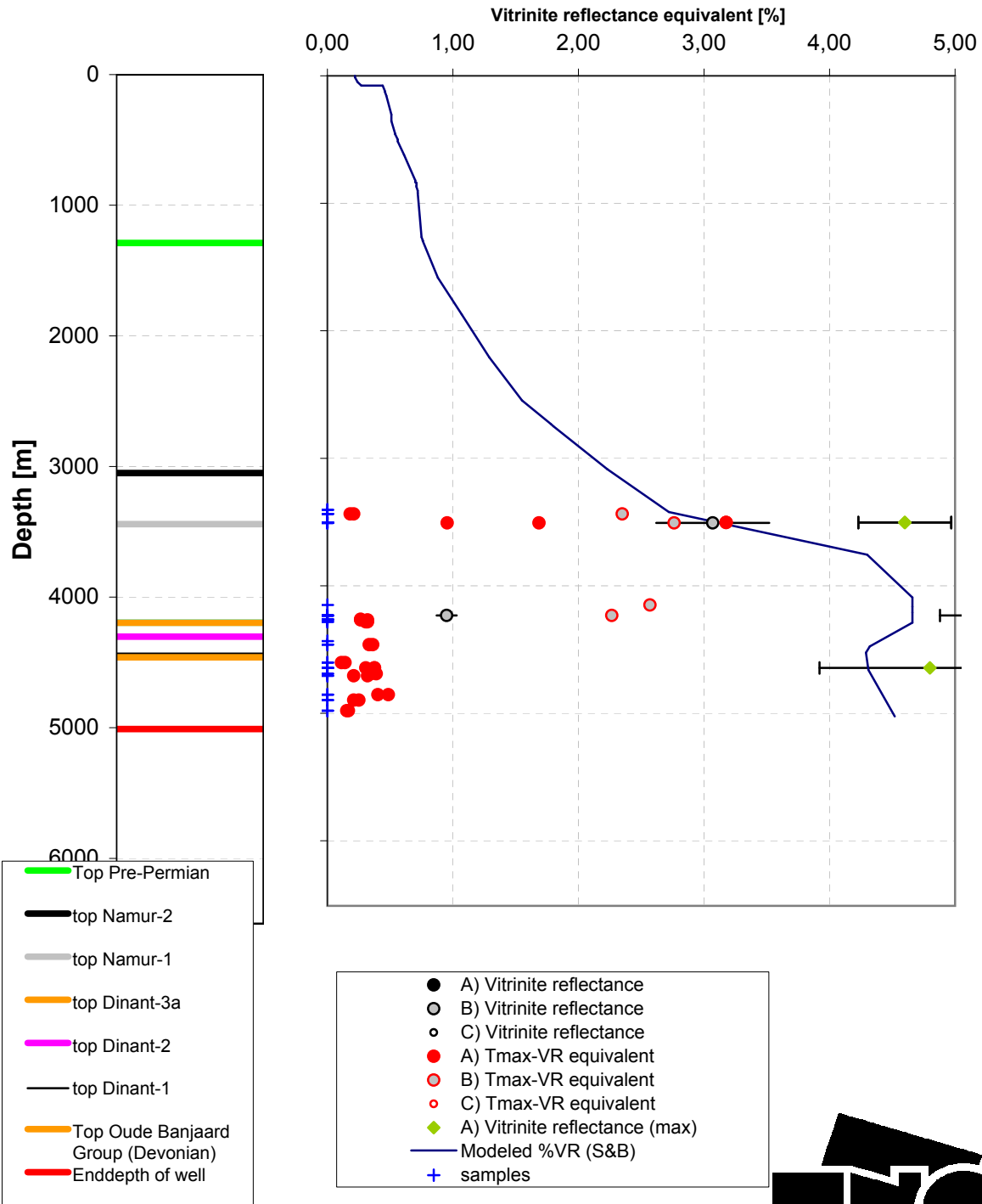




Joint Industry Project Petroplay

Raw data

Winterswijk-1



C Stratigraphic database

C1 - Explanation

Stratigraphic standards

Within the Petroplay project, the stratigraphic information focuses on the age interpretations of the selected wells. The Standard Chronostratigraphy used for the age interpretations has been updated recently. Therefore, an updated Standard Chronostratigraphy is presented in Figure C-1. The information on which the Standard Chronostratigraphy is based is given in this Appendix.

Absolute ages

The use of absolute ages in the Carboniferous is hampered by the absence of one unified scheme. This leads to the existence of multiple age schemes. After discussion with Menning (pers. comm. 2004, 2005), we have decided to follow the absolute ages given in the Gradstein *et al.* (2005). Comparing to the Gradstein *et al.* (2005) ages and the time-scale B ("old ages") of Menning *et al.* (2001), there are three striking differences.

- (1) The Base Permian is placed at 299 Ma, instead of 296 Ma, although this latter date appears too young for NW Europe.
- (2) The base Pennsylvanian (base Bashkirian; mid-Carboniferous boundary) is placed at 318.1 Ma, and the mid-Carboniferous boundary is placed within the Chokerian and not at the base of this stage or the base of the Kinderscoutian.
- (3) The ages of the upper Namurian B and C differ significantly. Menning *et al.* (2001) give Namurian A and B a total age of 3.5 Ma, while Gradstein *et al.* (2005) give a total age of 10.5 Ma.

This results in the following absolute age table.

Standard Stage	Local Stage	Local Substage	Base age	Duration
Sakmarian			294.60	
Asselian	Autunian		299.00	4.40
Gzhelian	Autunian		302.00	3.00
Gzhelian	Stephanian	Stephanian C	303.90	1.90
Kasimovian	Stephanian	Stephanian B	305.00	1.10
Kasimovian	Stephanian	Stephanian A	306.00	1.00
Kasimovian	Stephanian	Cantabrian	306.50	0.50
Moscovian	Stephanian	Cantabrian	307.20	0.70
Moscovian	Westphalian	Westphalian D	309.10	1.90
Moscovian	Westphalian	Westphalian C	311.70	2.60
Bashkirian	Westphalian	Westphalian B	312.50	0.80
Bashkirian	Westphalian	Westphalian A	313.50	1.00
Bashkirian	Namurian	Yeadonian	314.10	0.60
Bashkirian	Namurian	Marsdenian	315.30	1.20
Bashkirian	Namurian	Kinderscoutian	316.30	1.00
Bashkirian	Namurian	Alportian	317.30	1.00
Bashkirian	Namurian	Chokerian	318.10	0.80
Serpukhovian	Namurian	Chokerian	318.50	0.40
Serpukhovian	Namurian	Arnsbergian	323.50	5.00
Serpukhovian	Namurian	Pendleian	326.40	2.90
Visean	Visean	Brigantian	328.80	2.40
Visean	Visean	Asbian	332.60	3.80
Visean	Visean	Holkerian	339.30	6.70
Visean	Visean	Arundian	342.90	3.60
Visean	Visean	Chadian L	345.30	2.40
Visean	Visean	Chadian E	345.80	0.50
Tournaisian	Tournaisian	Ivorean	349.00	3.20
Tournaisian	Tournaisian	Hastarian	359.20	10.20
Famennian	Erian		374.50	15.30
Frasnian	Ulsterian		385.30	10.80
Givetian	Ulsterian		391.80	6.50
Eifelian	Yingtangian		397.50	5.70
Emsian	Ulsterian		407.00	9.50
Praghan	Nagaolingian		411.20	4.20
Lochkovian	Ulsterian		416.00	4.80
Pridoli	Pridoli		418.70	2.70
Ludlow	Ludfordian		421.30	2.60
Ludlow	Gorstian		422.90	1.60
Wenlock	Homerian		426.20	3.30
Wenlock	Sheinwoodian		428.20	2.00
Llandovery	Telychian		436.00	7.80
Llandovery	Aeronian		439.00	3.00
Llandovery	Rhuddanian		443.70	4.70
Hirnantian	Cincinnatian		445.60	1.90

Marine bands

The standard classification of Namurian and Westphalian sediments is based on the occurrence marine bands. Marine bands may be widespread, extend over much of Europe and contain a very specific (marine) fauna (Wagner et al., 1979; Martinsen, 1990, in Martinsen et al., 1995). Therefore, these marine bands are stratigraphically important, and, often, form the boundary between two Carboniferous sub-stages.

A **preliminary** overview of Namurian-Westphalian marine bands of several Carboniferous basins in Western Europe is given in Figure C.2. The diagram lists the marine bands that were found in some British, German and Dutch basins. The most extensive Marine Bands are depicted in the column 'Standard Names'. The stratigraphic positions and the names of the Western European marine bands were all derived from existing literature, given in the Reference List.

Biostratigraphical disciplines

There are two main fossil groups used in the Carboniferous, sporomorphs and Foraminifera. The sporomorphs zonation of Clayton *et al.* (1977) and the foraminifera zonation of Conil *et al.* (1990) are given in Figure C.1.

Other fossil groups, used stratigraphically in the Carboniferous are:

- Conodonts
- Macro-plant remains (Paleobotany)
- Graptolites
- Goniatites
- Rugose corals

However, their use in hydrocarbon industry is limited, and, therefore, they are not included in our overview.

Stratigraphic datums

The age references for the selected wells are primarily based on internal RGD reports. In addition, a number of specific reports are also used in this project. These reports are listed here.

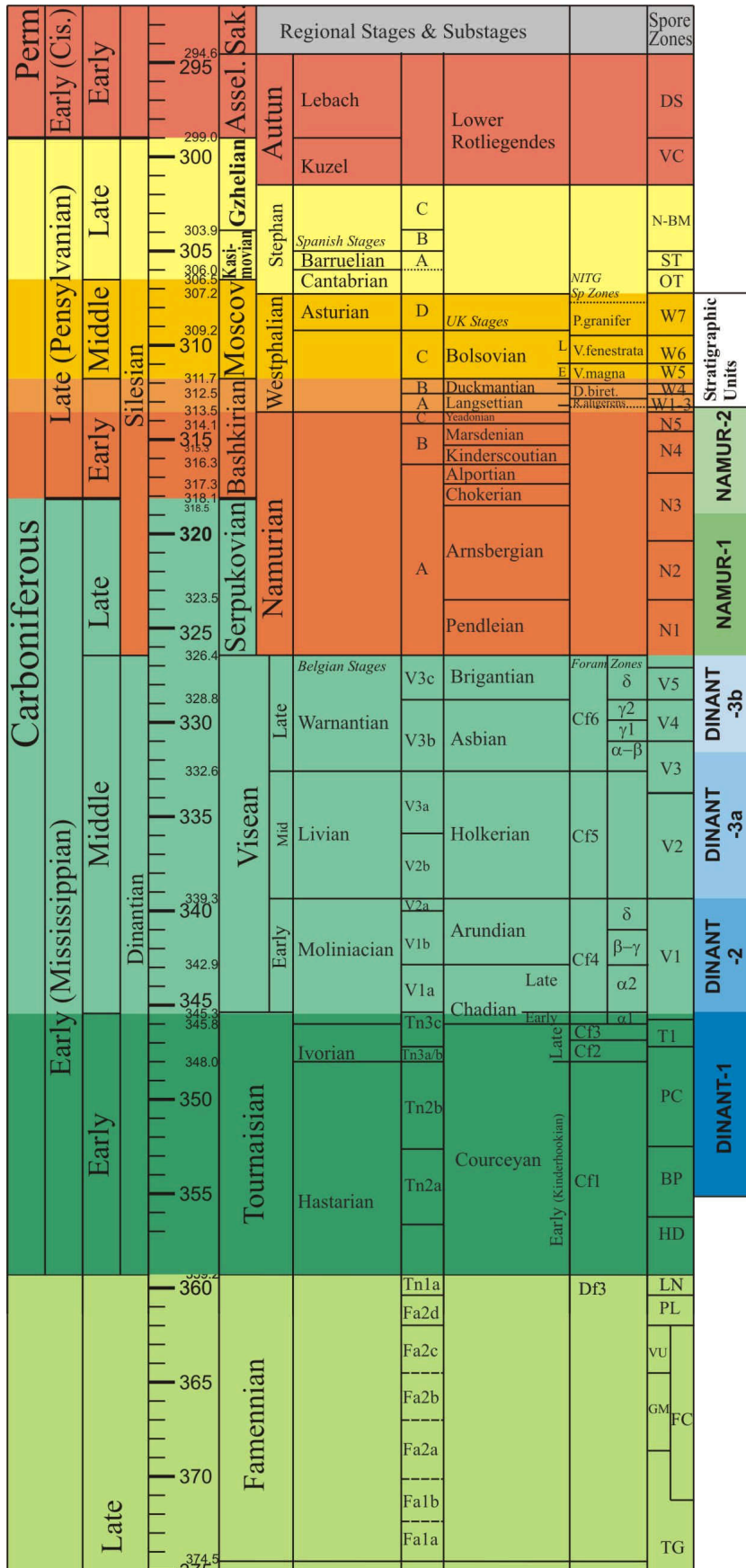
Report no	Date	Source	Well(s)	Remark
lc/21281	March 1992	Simon Robertson	P16-01	Geochemical Evaluation for Wintershall Noordzee B.V.
?	?	CC Ltd	S02-02	NAM Dinantian Project
EO/2391	February 1984	Mobil Producing Netherlands Inc.	S02-02	-
51069 5751	April 1992	Elf Aquitaine C.S.T.J.F.	E12-03	-
-	May 1972	Mobil Producing Netherlands Inc.	A17-01	Final geological well report
-	April 1972	NAM B.V.	E02-01	NAM Biostratigraphy Report
?	?	?	P16-01	P/16-01 Sample Descriptions
-	-	NAM B.V.	E02-02	Biostratigraphic results
		LPP		
?	?	Robertson	E02-01	
5463/003	March 1992	Geochem	A17-01; E02-01	Report to Bow Valley Petroleum (UK) Ltd.
-	August 1990	Halliburton Geo Consultants Ltd.	A16-01	Carboniferous SNS, Phase IV, Vol. III
-	1985	ECL	S02-01	Offshore Netherlands, Biostrat Carboniferous NL
	December 1985	RRI	A16-01, A17-01, E02-01, S02-01	Volume 2, Appendix 2 & 3
		Collinson James Consulting	A16-01, B10-01, E02-01, S02-01, RSB-01	Carb. Dep. Systems SNS, Vol. III
1710	October 1993	Halliburton Geo Consultants Ltd.	A11-01, A12-01, A14-01, A16-01, A17-01, E02-01	Five Countries Study, Vol. 6
4160	July 1991	Geochem	S02-01	Report to Bow Valley Petroleum (UK) Ltd.
9521	October 1995	LPP	A11-01, A14-01, B10-01, E02-01, E02-02, E06-01	Report to NAM B.V.
0004	June 2000	LPP	KTG-01, NAG-01, RSB-01, TJM-02 & ST, WSK-01	Report to NAM B.V.
03-169-C	November 2003	TNO-NITG	KTG-01	internal report
03-170-C	November 2003	TNO-NITG	RSB-01	internal report
Not-included				
Report no	Date	Source	Well	Remark
03-103-C	August 2003	TNO-NITG	confidential	confidential

In addition, additional samples from well E02-01 and UK well 38/3-1 were processed and analysed. The age interpretations from these samples are also included in this study. The age interpretation of 30 wells is provided. These are given in a separate (MS-Excel) document (Appendix C2). The following wells have been interpreted.

No#1	No#2	Name	UWI	Remark	TD	Area
1	1	A11-01	7000		3900.00	2
2	2	A12-01	7001	Carb. n.p.		X
3	3	A12-02	7002	Carb. n.p.		X
4	4	A14-01	7003		3014.00	2
5	5	A15-1	7004	no data	3912.00	2
6	6	A16-01	7005		2708.00	2
7	7	A17-01	7006		3013.00	2
8	8	B10-01	7008	no data	3188.20	X
9	9	E02-01	7021		2595.00	2
10	10	E02-02	8009	no data	2647.00	2
11	11	E06-01	7526		3200.00	2
12	12	E12-02	7960		4428.00	X
13	13	E12-03	8055		3788.00	X
14	14	O18-01	8034		2952.00	1
15	15	P16-01	8070		2465.00	1
16	16	S02-01	7510		1799.50	1
17	17	S02-02	7531		2878.20	1
18	18	S05-01	7511		2230.00	1
19	1	38/3-1	-		3800.00	2
20	2	39/7-1	-		3614.00	2
21	1	BHG-01	1099		2906.80	1
22	2	EMO-01	1295	no data	2547.70	3
23	3	GVK-01	3832		1687.00	3
24	4	KTG-01	1490		1900.00	1
25	5	NAG-01	1646		4303.00	3
26	6	RSB-01	3699		4644.50	1
27	7	TJM-02 & ST	2121		6010.50	3
28	8	WDR-01	2206	no data	1205.00	1
29	9	WSK-01	2224		5009.50	4
30	1	MSTL-01	-			4

Figure C1 (next pages): Silurian - Carboniferous stratigraphy

"Hydrocarbon potential of the Pre-Westphalian in the Netherlands on- and offshore"



"Hydrocarbon potential of the Pre-Westphalian in the Netherlands on- and offshore"

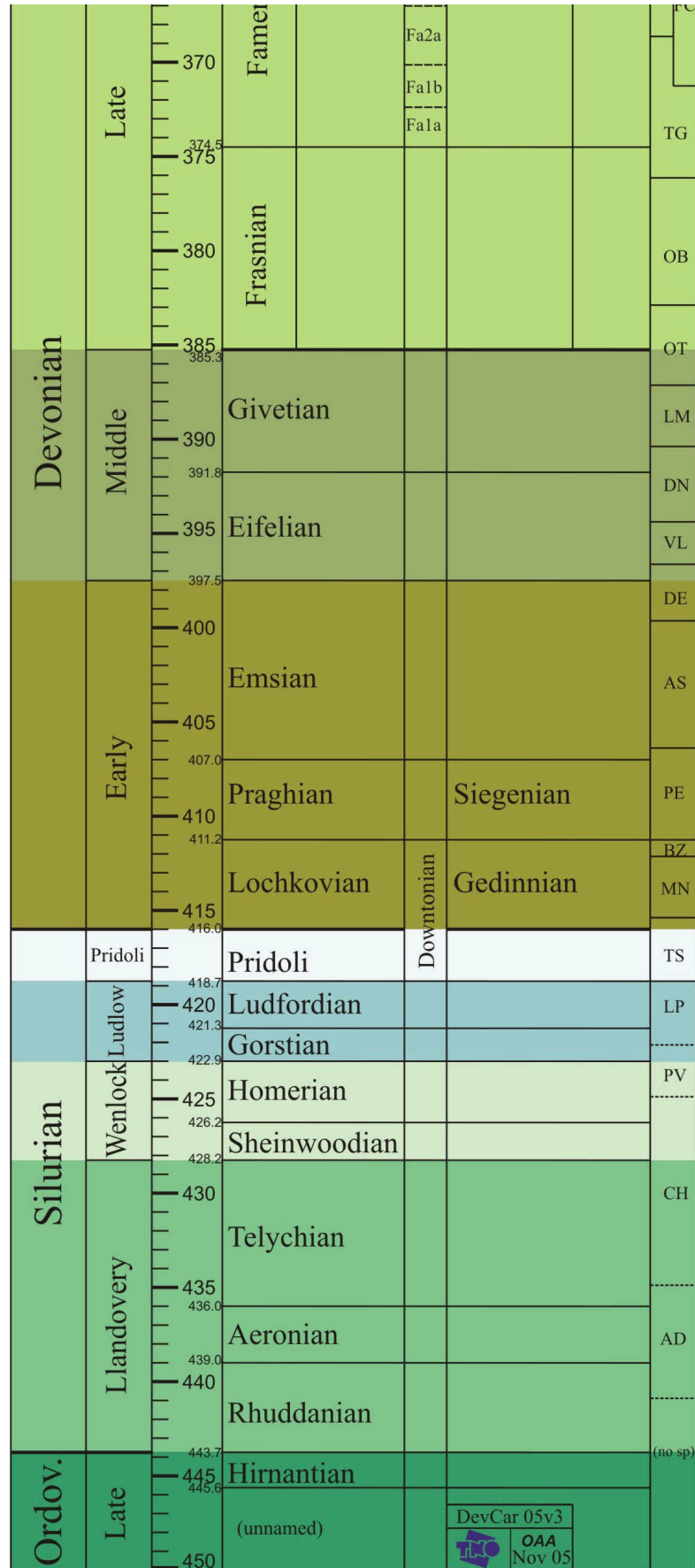


Figure C.2 Summary figure of Namurian-Westphalian Marine Bands (Previous page)

C2 - Biostratigraphic interpretations

The biostratigraphic interpretations are given in a separate (MS-Excel) document. Each worksheet gives an overview per well of the interpretation and used data.

C3 - Stratabugs charts

C3a - Silurian/Devonian

C3b - Dinantian

C3c - Namurian

C4 - Well lithology plots

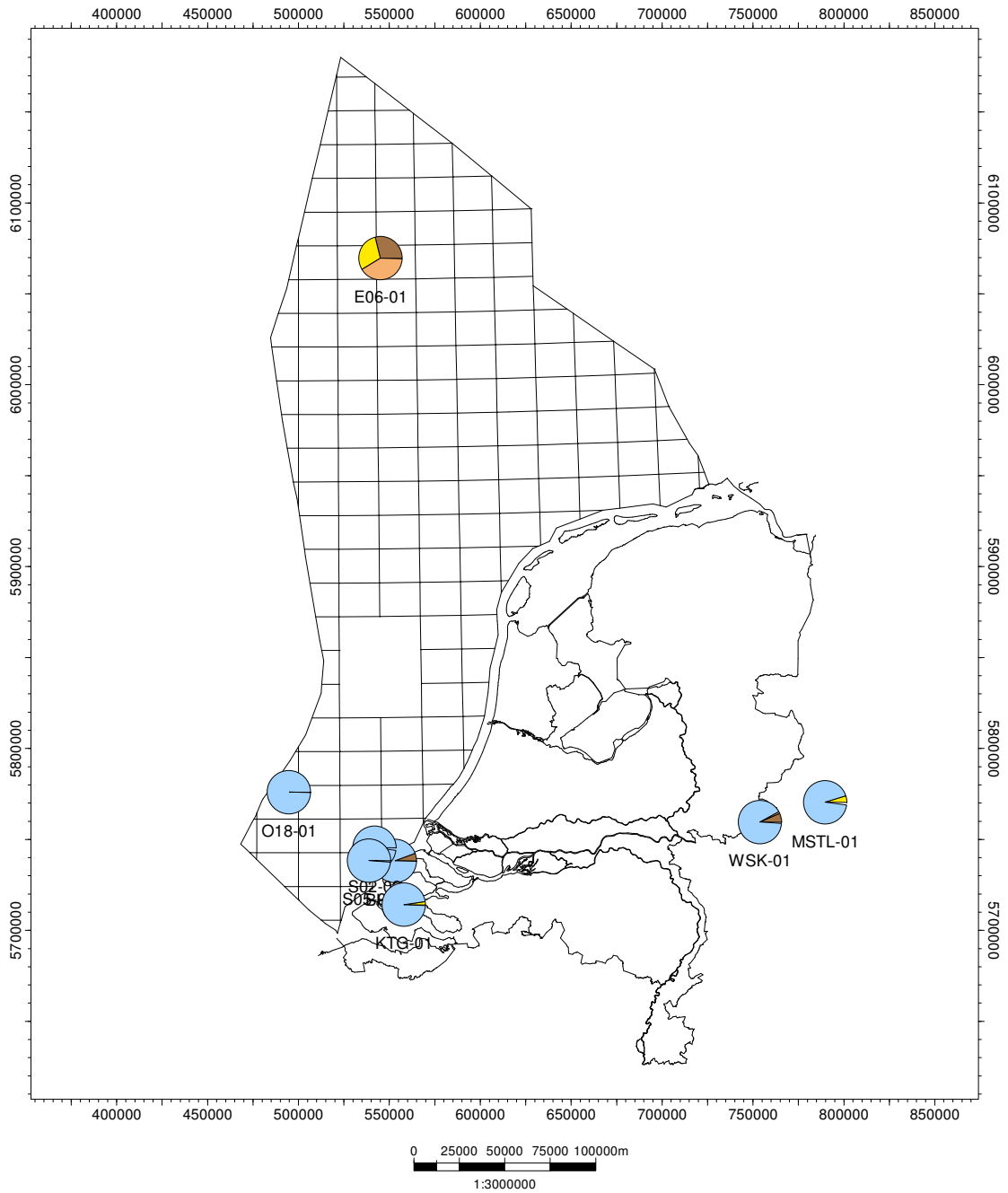


Figure C4-1: Dinant-1



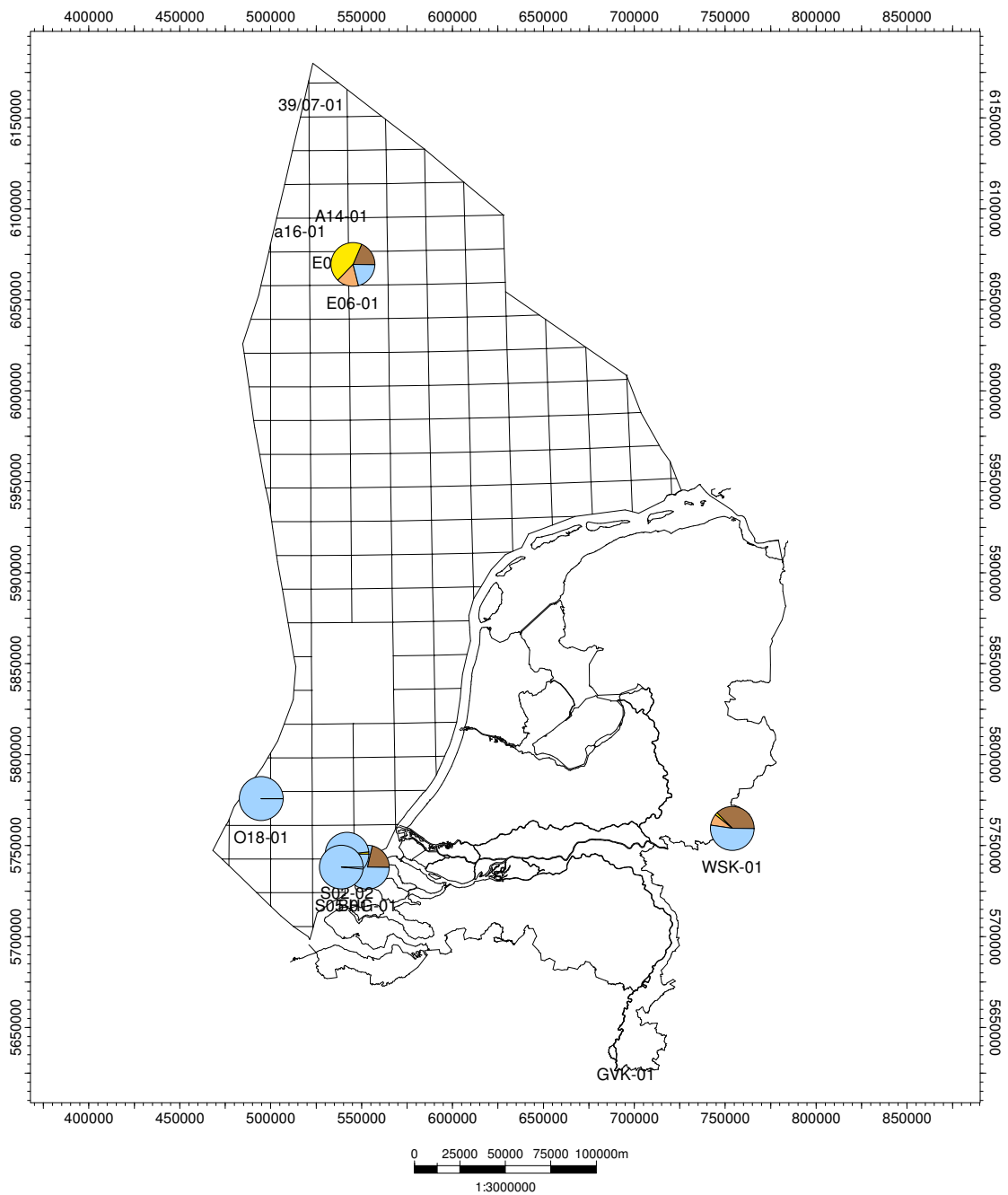
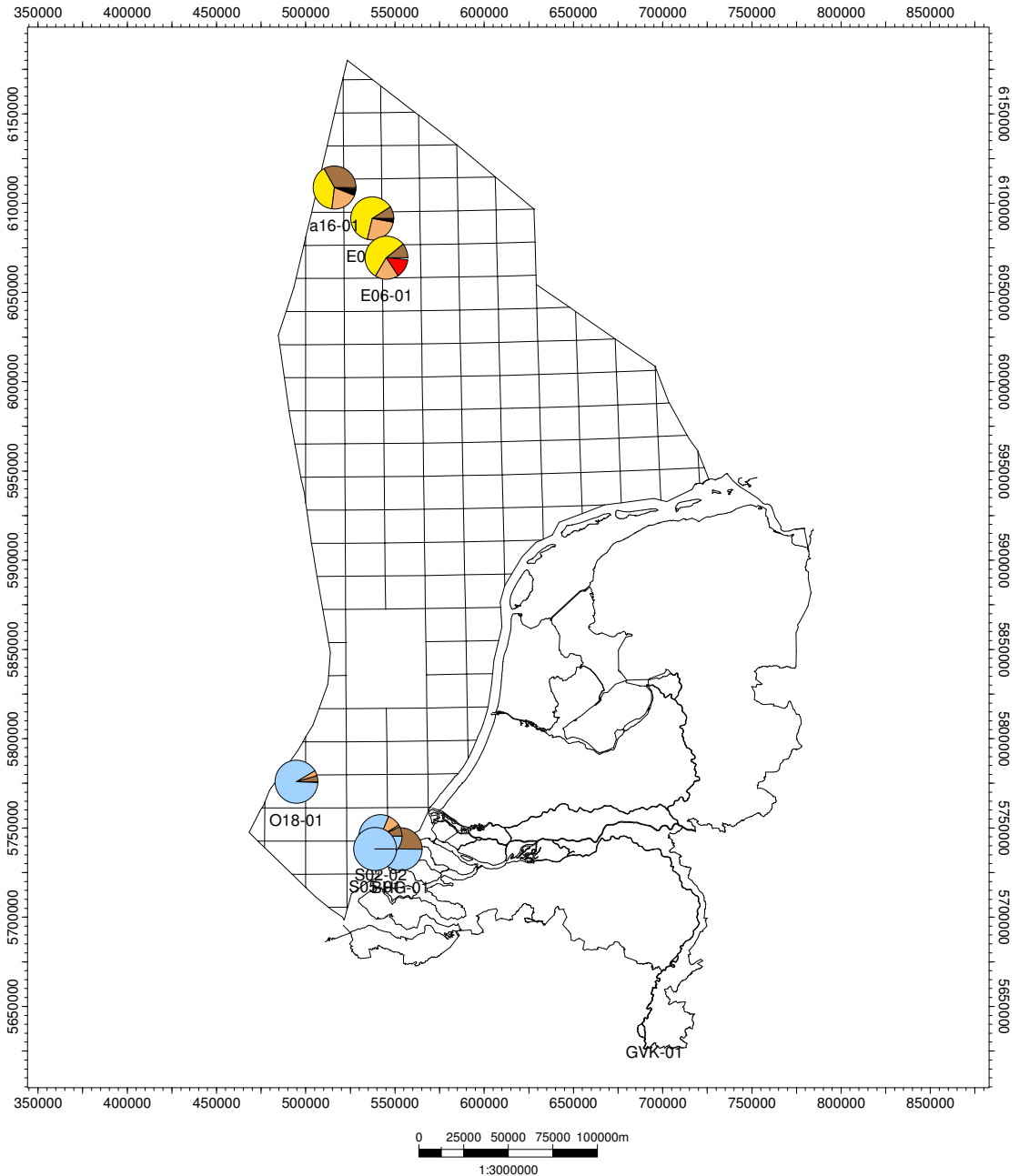


Figure C4-2: Dinant-2

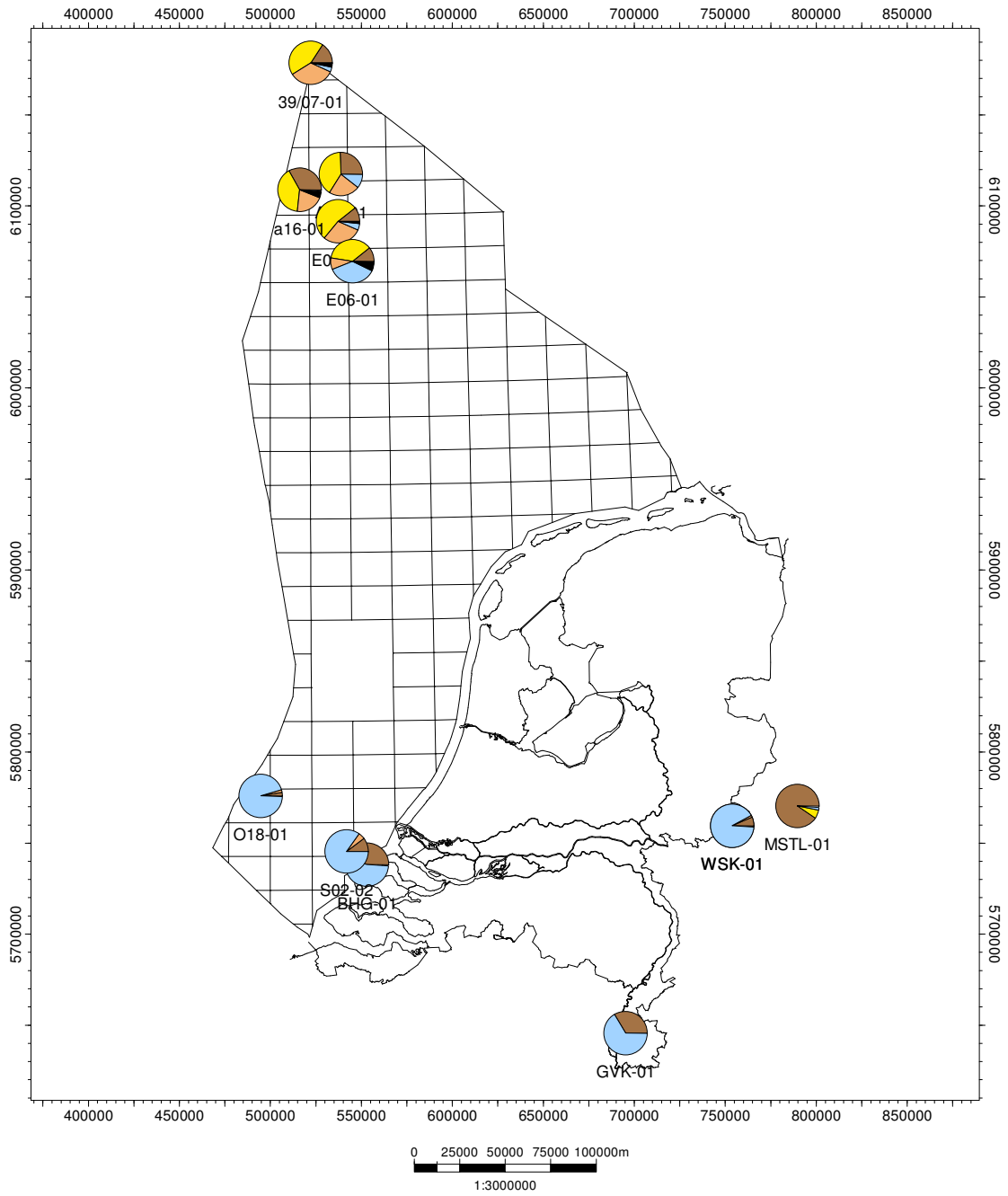




- Well
- Shale
- Sand
- Silt
- Carbonate
- Coal
- Sand with Carb
- Volcanic / Plutonic
- NL borders & rivers
- NL Offshore boundary
- NL Offshore Blocks



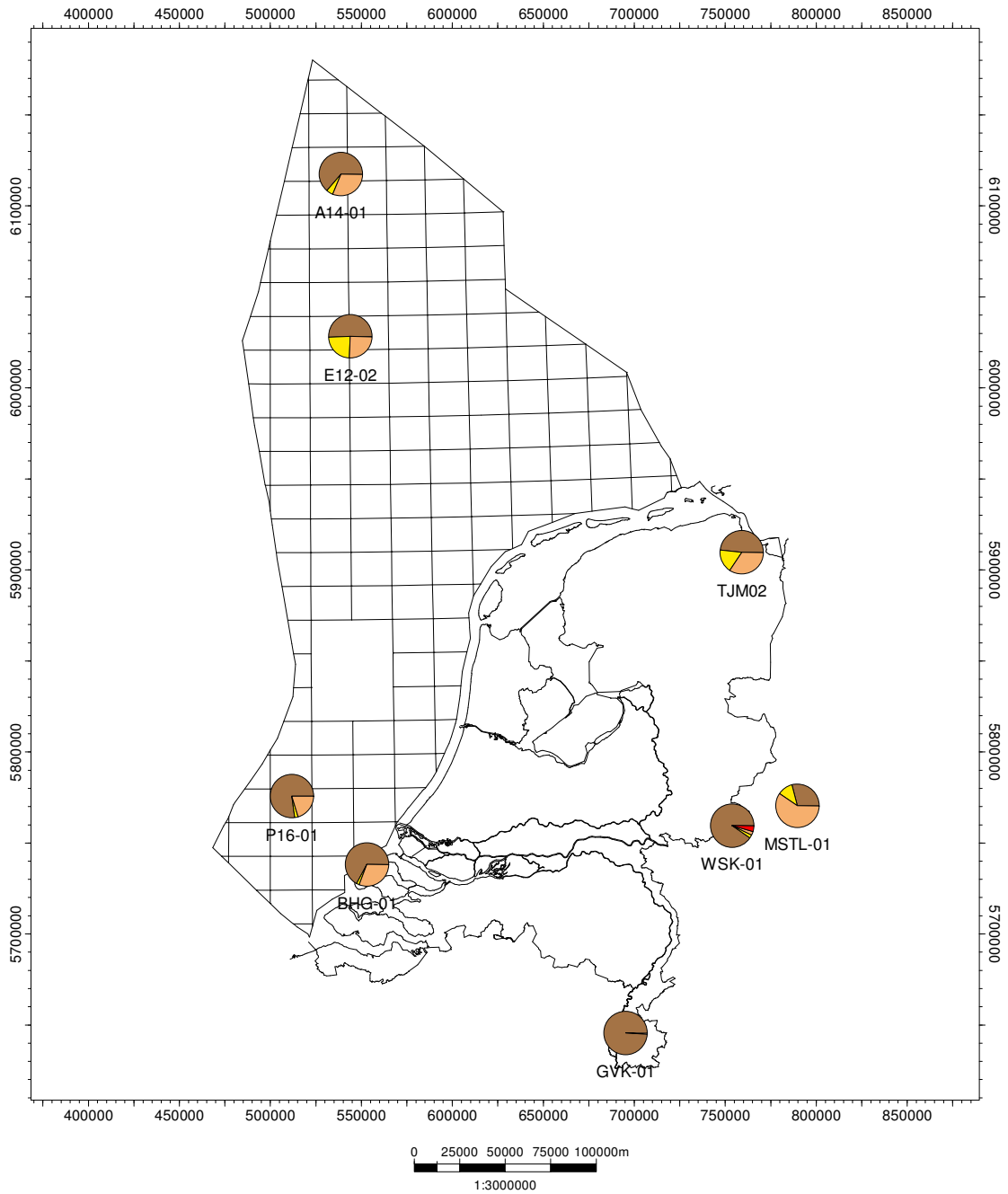
FigureC4-1: Dinant-3a



- | | | |
|-------|---------------------|----------------------|
| Well | Carbonate | NL borders & rivers |
| Shale | Coal | NL Offshore boundary |
| Sand | Sand with Carb | NL Offshore Blocks |
| Silt | Volcanic / Plutonic | |

Figure C4-2: Dinant-3b
















- | | | |
|---|---|--|
|  Well |  Carbonate |  NL borders & rivers |
|  Shale |  Coal |  NL Offshore boundary |
|  Sand |  Sand with Carb |  NL Offshore Blocks |
|  Silt |  Volcanic / Plutonic | |

Figure C4-3: Namur-1



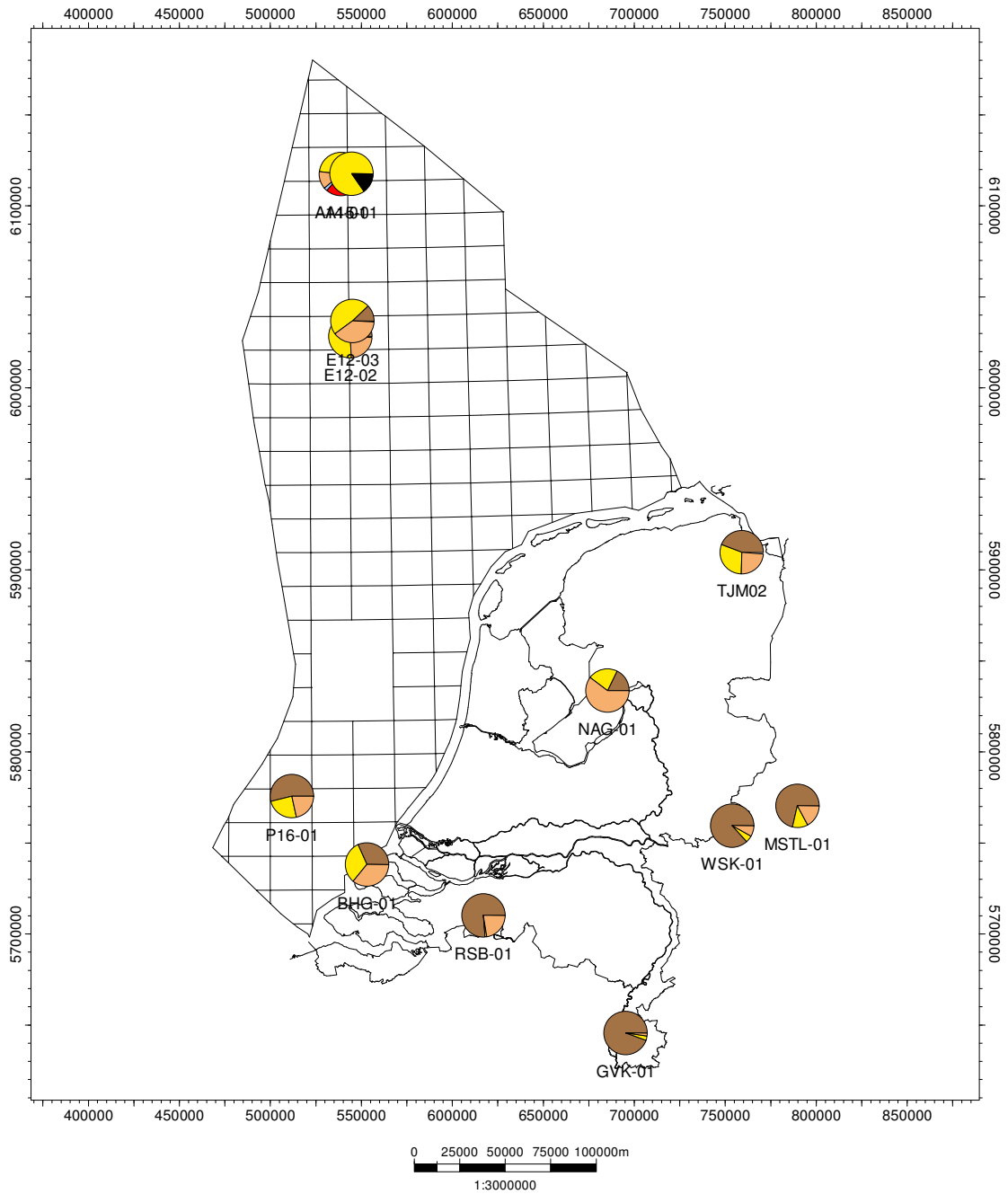


Figure C4-4 Namur-2



D Construction of well correlation panels

Well correlation panels

All biostratigraphic data are combined with log information (gamma ray and sonic logs) and lithostratigraphic data in a Petrel project. Despite the lack of information in certain areas the data integration gave us a new opportunity to subdivide the Early-Carboniferous sediments. The benefit of this new correlation is the consistent definition of units which can be correlated through all areas. This means for instance that the clastic Yoredale Formation is correlated with the Carboniferous Limestone Group. The most important available logs used in the correlation are the sonic and gamma-ray log. Other data which have been used are the lithostratigraphic (DINO database) and chronostratigraphic data. Based on the GR and DT log values for specific depths a simple lithology prediction macro for Petrel has been written.

This macro specifies the following lithologies using the matching rules:

Sand:	$GR < 75 \text{ API}$
Silt:	$75 < GR < 100 \text{ API}$
Shale:	$GR > 100 \text{ API}$ and $DT < 90 \mu\text{s}$
Limestone:	$GR < 75 \text{ API}$ and $DT < 55 \mu\text{s}$
Coal:	$DT > 90 \mu\text{s}$

The combination of lithology colours and the biostratigraphic data provides good insight into the distribution of Early-Carboniferous sediments. Two units have been defined in the Namurian and four units in the Dinantian. For the Devonian no subdivision was made.

Three large (A0-size) well correlation panels are enclosed as:

- Enclosure 1: Devonian well correlation (A1 paper size)
- Enclosure 2: Dinantian well correlation (A0 paper size)
- Enclosure 3: Namurian well correlation (A0 paper size)

E Seismic sections

Appendix E contains displays (A3-size) of 18 seismic lines named E1 – E18. The lines on E1 - E4 were only available as analogue lines and were scanned from paper sections. Of the other lines digital copies were loaded into Petrel. The copies shown here are exports from the Petrel software.

F Hydrocarbon - source rock correlation

One of the main challenges in the Petroplay project was the assessment of potential pre-Westphalian source rocks. A major problem is that actual source rock material is absent or generally has a present-day maturity that is much too high for a proper geochemical analysis.

In this section the solvent extracts of a number of potential pre-Westphalian source rocks are compared with a presumed pre-Westphalian crude oil. This comparison is made on the basis of the GC-MS analysis of the saturate and aromatic fractions by calculating a number of diagnostic biomarker ratios. The crude oil originates from the Welton oil field located in the East Midlands, England.

Results of isotope analyses on a number of source rock extracts will also be used in a first qualitative evaluation. Gas data and isotope data of a set of condensate samples are investigated in order to find possible pre-Westphalian signatures within these data sets.

Welton A5 oil

Within the Netherlands on and offshore area., there are no known oil occurrences with a proven Namurian source. These kind of oil occurrences are found in the eastern onshore part of England. A sample from one of these occurrences was therefore included in this study.

The Welton oilfield in the East Midlands comprises around 60 wells and oil exploration has taken place since the 1950's. The reservoirs consist of Westphalian sandstones. On the basis of biomarker distribution patterns the most likely source rock for the East Midlands oils are the lower Namurian mudstones with type II kerogen from the Edale Gulf. Minor, more localised contributions from organic-rich type II mudstone partings within the Dinantian limestones are also suggested. Bulk and molecular maturity parameters also indicate that these particular formations could have generated hydrocarbons (Ewbank et al., 1993; Ewbank et al., 1995; Cornford, 1998). The published maturity data demonstrate a relative high thermal maturity for the Edale Gulf mudstones (vitrinite reflectance values range from 0.89 to 1.16 %Rr). On the basis of the Methyl Phenanthrene Ratio determined from the GC-MS analysis on this oil sample a vitrinite reflectance equivalent of 0.73 %Rr has been calculated in the current project. Probably, this value reflects the maturity at the time it was generated. The source rock itself may have further matured after expulsion of the petroleum.

Figure F-1 shows the chromatogram (TIC) of the aliphatic fraction of the Welton oil. The chromatogram is dominated by a homologues series of n-alkanes. The lighter n-alkanes in the front-end of the chromatogram seem to be reduced, either due to evaporation or degradation.

The sterane distribution in the samples is derived from the m/z 191 mass chromatogram from the SIM analysis and is given in Figure F-2, whereas the distribution of the terpanes is given in Figure F-3. For each source rock sample a similar analysis was done. From the chromatograms resulting from the SIM analyses, a large number of biomarker ratios have been calculated. By using these ratios direct comparisons can be made between the samples and the crude oil.

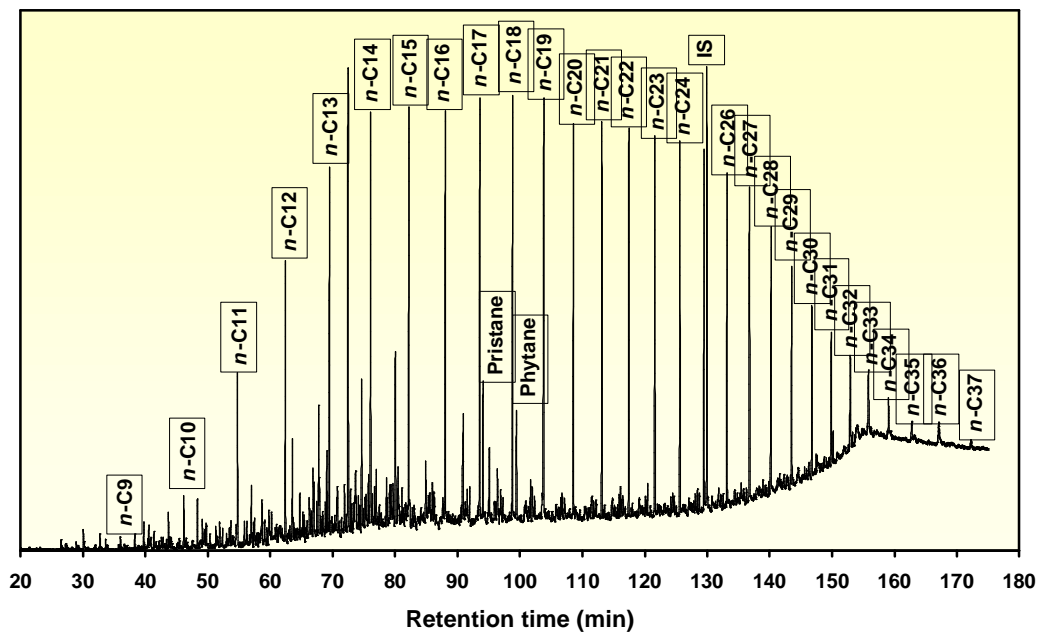


Figure F-1 Chromatogram (TIC) of the aliphatic fraction of the Welton oil

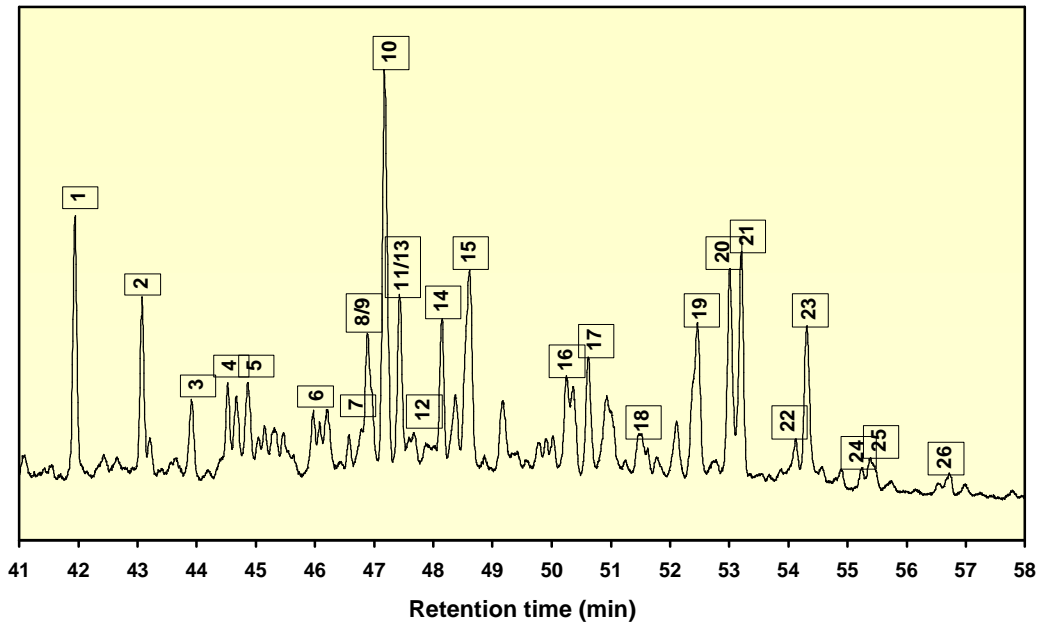


Figure F-2 Chromatogram (m/z 217) showing the distribution of the steranes in the aliphatic fraction of the Welton oil

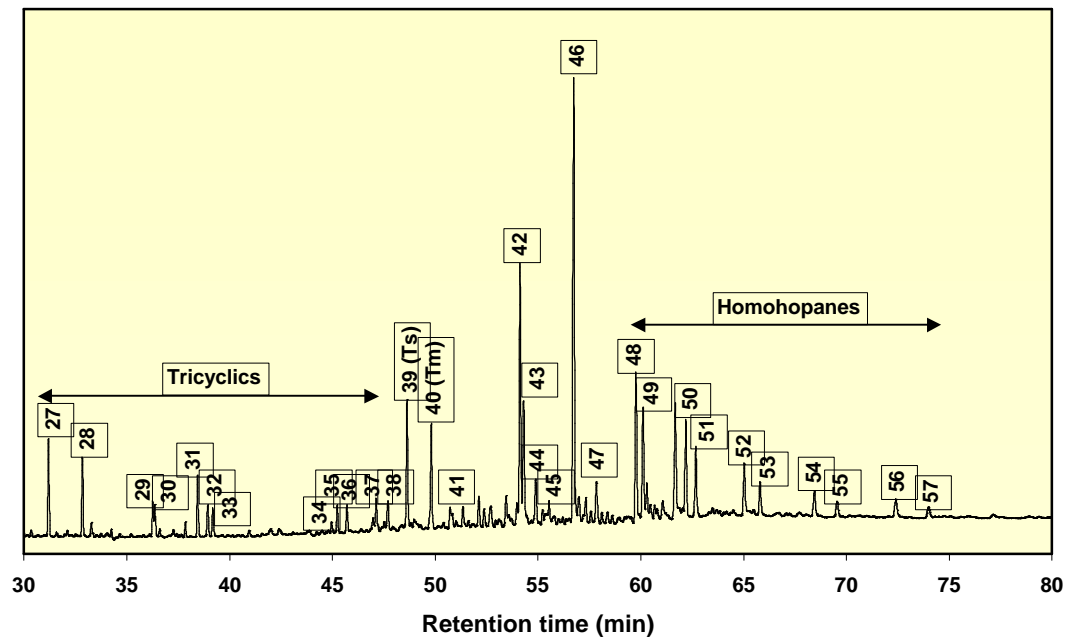


Figure F-3 Chromatogram (m/z 191) showing the distribution of the terpanes (m/z 191) in the aliphatic fraction of the Welton oil

Alkane patterns

In Figure F-4 a comparison is made between the n-alkane distribution pattern of the Welton oil and the source rock extracts. The signals of the n-alkanes are normalised to behenate (internal standard).

The alkane patterns of a large part of the source rock samples are significantly different from the Welton oil, notably in the range of the C₁₁ to C₁₆ alkanes. The Welton oil is a generated, migrated and trapped hydrocarbon. Therefore, the alkane pattern may have undergone several post-genetic alterations (e.g. degradation, water washing, cracking).

If individual stratigraphic units and samples are considered (cf. Chapter 3) the highest resemblance with the Welton oil is noted for the Top Dinantian – Base Namurian source rock extracts. Exception is the sample from well 41/24a-2 (Bowland shale) which has some dominating alkanes in the C₁₁ to C₁₆ range. Figure F-5 shows the alkane patterns of the Top Dinantian - Base Namurian samples (Geverik Member equivalents; lower part of Namurian 1) in which the sample from the Bowland shale of well 41/24a-2 has been removed. The other samples are collected from the Münsterland-1 well and well P16-01.

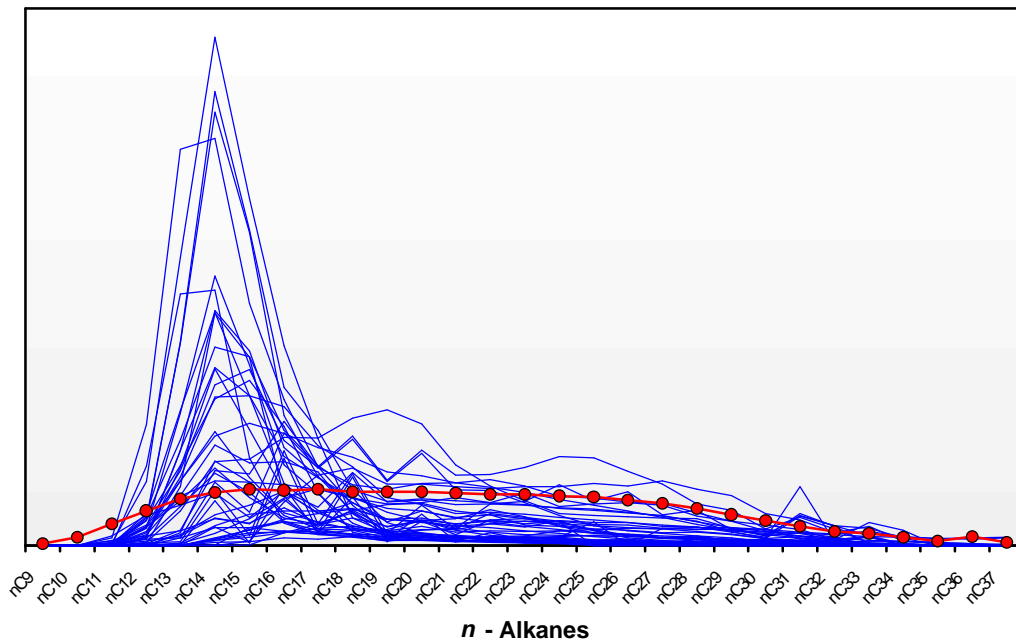


Figure F-4 Comparison between the distribution of the n-alkanes of the Welton oil (red line) and the source rock samples (blue lines)

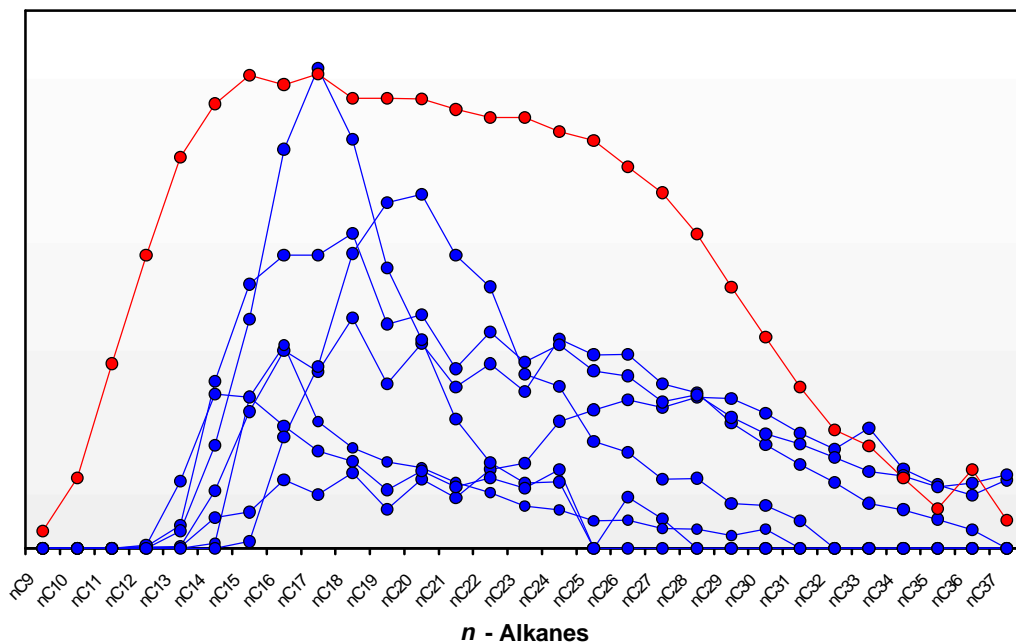


Figure F-5 Comparison between the distribution of the n-alkanes of the Welton oil (red line) and the source rock samples of the Top Dinantian – Base Namurian (blue lines).

Molecular ratios

On the basis of a number of diagnostic ratios, derived from the TIC and SIM chromatograms a comparison has been made between the samples. A total number of 32 ratios have been calculated (see also digital database). In this section some examples

are given to illustrate the applicability of such ratios in the correlation of the Welton oil with some potential source rocks that have been investigated in this project.

The application of the pristane / phytane ratio has been discussed extensively in Chapter 3. Plotting this ratio against the CPI results in a large cluster of samples, including the Welton oil (Figure F-6). Despite the fact that both ratios are also influenced by maturity, they also give information on the organic facies (depositional environment).

Another diagram has been made by plotting the C₂₇ and C₂₉ sterane ratios (see Figure F-7), see also Chapter 3. The samples plotting closest to the Welton oil will have comparable facies or depositional environment. The Welton oil is sourced from the Edale shales, which are time-equivalent with the Top Dinantian – Base Namurian units as defined in this study.

The diagrams demonstrate that indeed the samples from this interval have a similar facies (although there are significant differences between both diagrams). These plots also indicate that other source rock intervals may have an organic matter composition that is comparable to that of the Welton oil. It should be noted, however, that currently no samples from the Edale shale have been analysed, which hampers a good correlation in terms of reproducibility and accuracy. The highest correlation (closest resemblance) with the Welton oil is noted for the Namurian sample of well Emmeloord-1 (see Figure F-6). In Figure F-6 the Emmeloord-1 sample plots somewhat further away from the Welton oil. The closest correlation in the diagram of Figure F-7 is recorded for a sample from the Schouwen Mb. (Dinantian 2) in well S5-01.

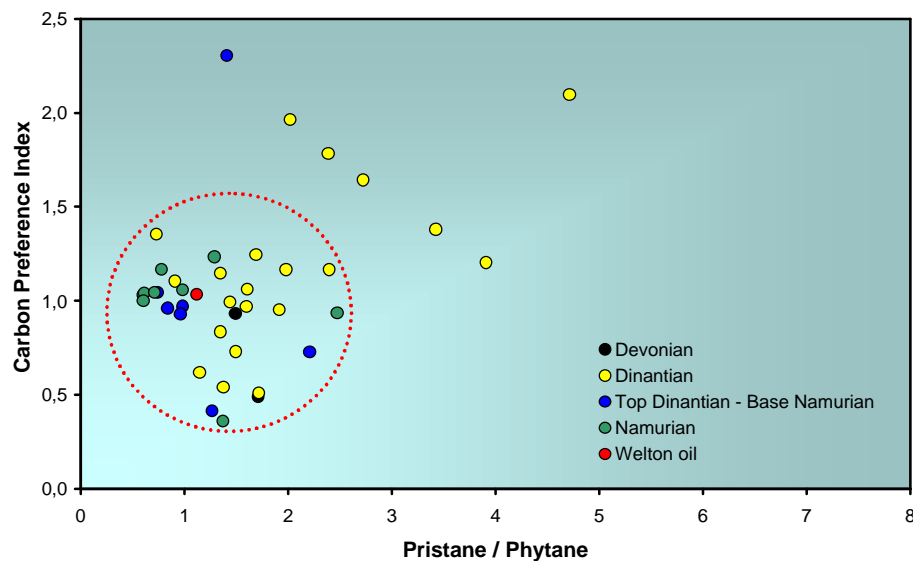


Figure F-6 Diagram showing the comparison between the source rock samples and the Welton oil on the basis of alkane ratios

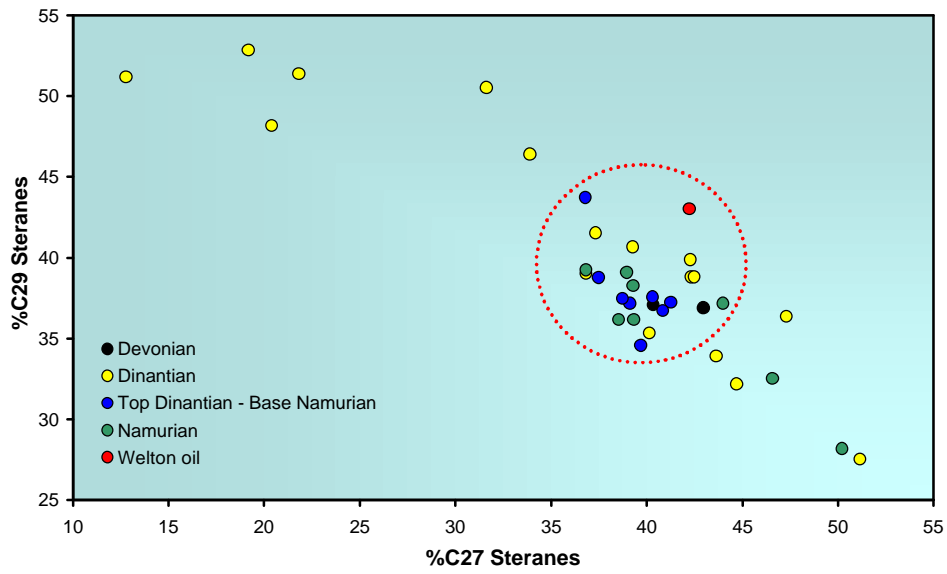


Figure F-7 Diagram showing the comparison between the source rock samples and the Welton oil on the basis of sterane ratios, see also Chapter 3 and the digital database

In Figure F-8 the result of a cluster analysis using the sterane biomarkers that have also been used in the facies triangles of Chapter 3 is given. Based on the clustering procedure, no differentiation can be made of the expected facies similarities. The dendrogram suggests that the Devonian of well S05-01, the Namurian of Münsterland-1 and some Dinantian as encountered in the wells S05-01 and E02-01 all have an organic facies comparable to that of the Welton oil. The Top Dinantian – Base Namurian samples plot some distance away from the Welton oil. In order to include the other variables in a cluster analysis a good differentiation should be made between the (normalised) maturity induced and the source induced variables. Moreover, for a good oil-source rock correlation some additional oil samples from the Welton oil field and possibly other oils should be included. Some further statistical treatment is needed for any statements on the actual oil source rock potential of the pre-Westphalian on the basis of these biomarker correlations.

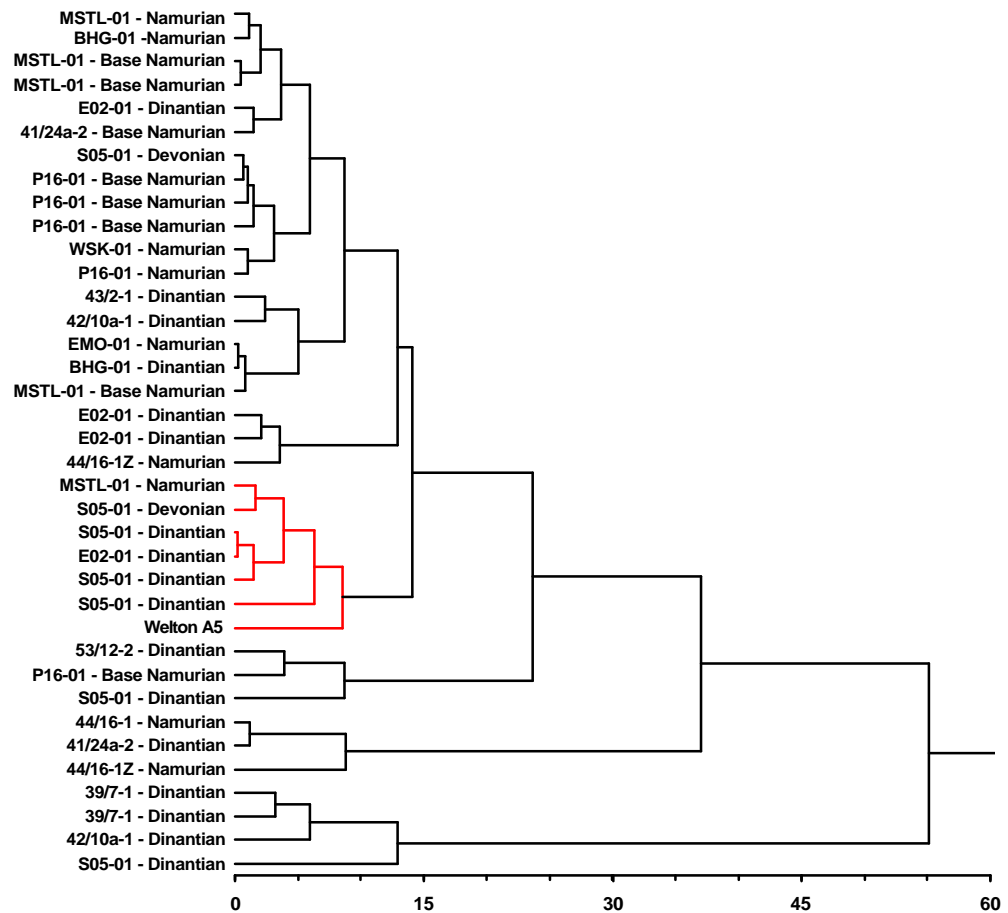


Figure F-8 Dendrogram of the cluster analysis on the C27-, C28 and C29 sterane biomarkers. Samples indicated as Base Namurian represent the Top Dinantian – Base Namurian samples.

Isotope ratios

The results of the carbon and hydrogen isotope analyses are used in the oil-source rock correlation as the isotope signature of the n-alkanes of the Welton oil will still reflect the isotope composition of the source rock from which they were expelled.

The amount of sample material for a number of samples was too low for a GC-IRMS analysis. Even in the samples that are reported the concentration of some alkanes is too low for a reliable isotope signal. New samples preparations will be needed for a thorough GC-IRMS analysis on the full set of samples. An additional clean up during sample preparation will also be needed in order to get a better baseline separation of the n-alkanes. Good baseline separation is needed in order to avoid co-elution of the n-alkanes with other compounds thus influencing the isotope ratio. Therefore, the current results do not have a high reliability.

Figure F-9 shows the pattern of the carbon isotopes for the source rock extracts in comparison with the pattern of the Welton oil. Unfortunately the analysis of only 11 samples provided results that could be used in a further evaluation. The highest similarity with the Welton oil on the basis of this diagram is recorded for the samples from well 41/24a-2 (Bowland and Yoredale), two samples from well E02-01 (Yoredale), the sample from well 39/7-1 (Yoredale), the sample from P16-01 (Base Namurian) and the sample from well Emmeloord-1 (Namurian).

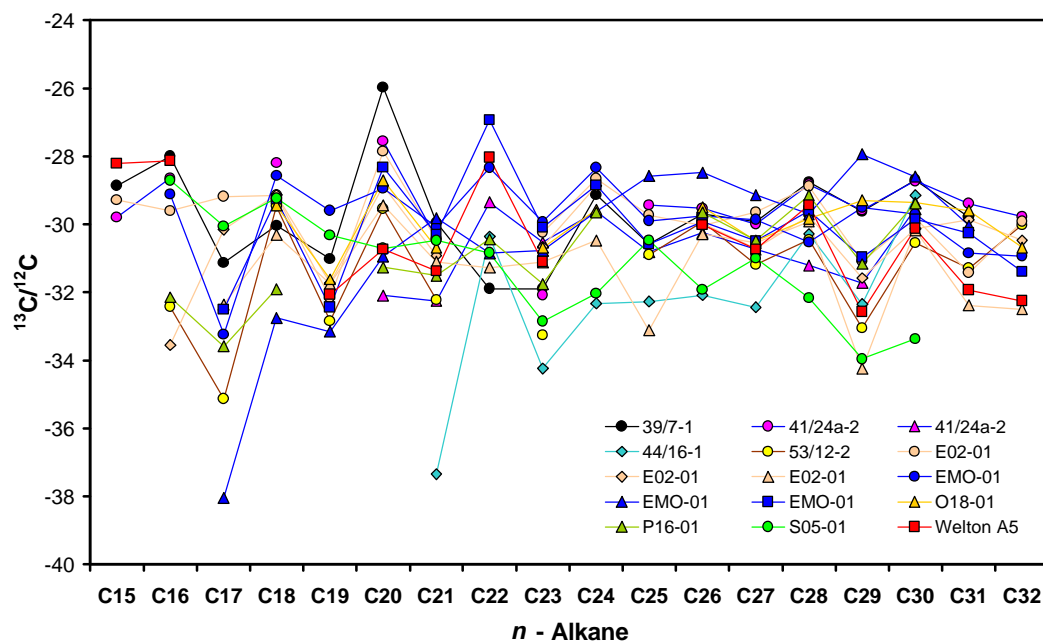


Figure F-9 Carbon isotopes ratios of the n-alkanes of the source rock extracts and the Welton oil

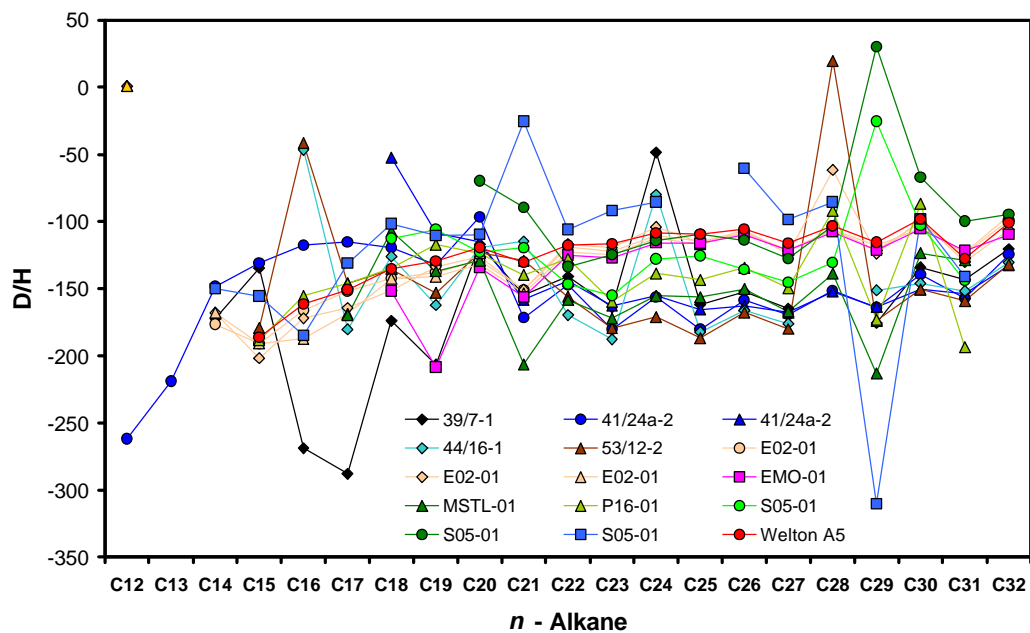


Figure F-10 Hydrogen isotopes ratios of the n-alkanes of the source rock extracts and the Welton oil

For the hydrogen isotope analyses the results of 14 samples could be used (see Figure F-10).

The samples with an almost identical isotope pattern as the Welton oil are the three samples of well E02-01 (Yoredale) and the sample from well Emmeloord-1 (Namurian). Samples with some deviations but still partly comparable with the Welton oil are the two samples from well 41/24a-2 (Bowland and Yoredale), the sample from well P16-01 (Base Namurian) and a sample from well S05-01 (Schouwen Member, Dinantian 2).

It can be concluded that the isotope patterns (carbon and hydrogen) of the Yoredale facies show a relative good correlation with the Welton oil on the basis of the carbon isotope data as well as the hydrogen isotope data. Remarkably, the isotope pattern of the lowermost sample of well Emmeloord-01, which has a (intra) Namurian age, also show a good correlation with the Welton oil.

Gases and condensates

Trapped hydrocarbons (gas, condensate and oil) can be correlated with (potential) source rocks by using a wide range of (mainly) geochemical techniques. The most widely applied techniques use biomarkers and molecular ratios for fingerprinting. Often source rocks can be readily identified on the basis of the molecular and isotopic composition of the trapped hydrocarbons without any information of the source itself. In addition, reservoir filling from more than one source rocks can often be identified with these techniques.

In gas reservoirs the hydrocarbon composition is characterized by lower alkanes (mainly methane) and an absence of biomarkers. Condensate samples generally also lack characteristic biomarkers. In these cases isotope analysis often is the only tool for source rock assessment. Figure F-11 shows the Bernard diagram of the gas data

currently present in the TNO database. Generally gas data are limited to gas compositions for C1-C3 compounds, and carbon isotope data are usually only available for methane. Two distinct processes produce hydrocarbon gas: biogenic and thermogenic degradation of organic matter. Biogenic gas is formed at shallow depths and low temperatures by anaerobic bacterial decomposition of sedimentary organic matter. In contrast, thermogenic gas is formed at deeper depths by thermal cracking of sedimentary organic matter (primary cracking) or by thermal cracking of oil at high temperatures into gas (secondary cracking).

Figure F-11 indicates that most gases have a thermogenic origin generated from coals with a variable degree of coalification (maturation). Methane is a difficult gas molecule to be interpreted isotopically, because of the various possible origins of this compound, including biogenic and thermogenic (Prinzhofer & Huc, 1995). A number of samples deviate from the general maturation trend. A possible cause may be variation in source rock types with a different (isotopic) composition. For a better understanding and interpretation of gas data in terms of source rock differentiations additional analytical data (carbon and hydrogen isotopes of the C2 to C5 compounds) will be needed.

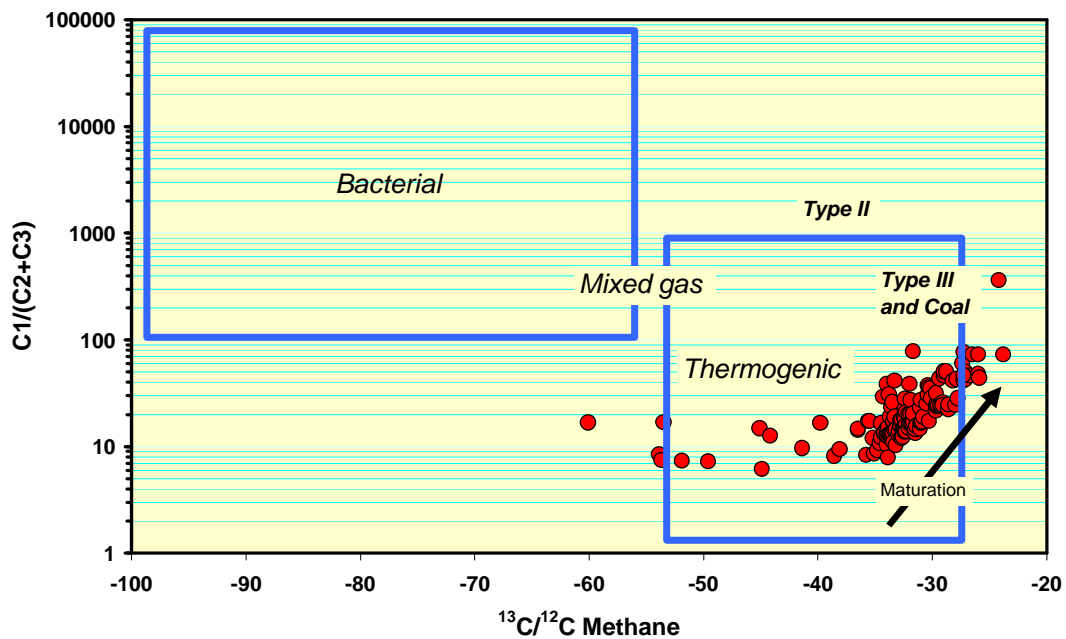


Figure F-11 Bernard diagram of gases from the TNO database

New technological developments, e.g. the development of compound specific isotope measurements, have extended the interpretations and modelling of hydrocarbon data. Both carbon and hydrogen isotope data of higher alkanes are now frequently used for interpretations of the trapped hydrocarbon data in terms of genetic processes, post-genetic processes and source rock assessment. Isotope data of individual components from condensates and crude oils are also an important tool in oil/condensate-source rock correlations. To date, a total number of 31 condensate samples have been analysed with the GC-IRMS system.

Figure F-12 shows the results of carbon isotope measurements on the individual n-alkanes of the selected condensate samples and Figure F-13 shows the results of the hydrogen isotope measurements on the same samples. These results can be used to

differentiate condensates or oil and to correlate source rock extracts to the trapped hydrocarbons. The two figures show that the condensates from the Carboniferous and Rotliegend reservoirs are closely comparable (when the averaged values are considered) and that these reservoirs can be readily differentiated from the Triassic reservoirs. The actual cause for this difference is not yet fully understood, but may be related to differences in source rock.

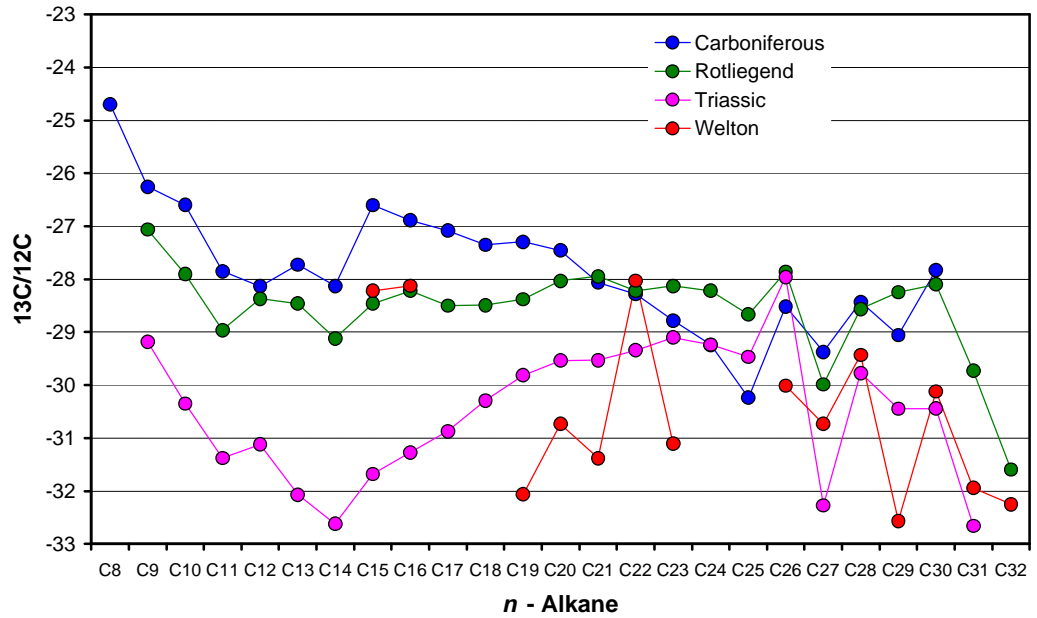


Figure F-12 Averaged carbon isotope values of individual n-alkanes from the condensate samples, differentiated into the three reservoir ages

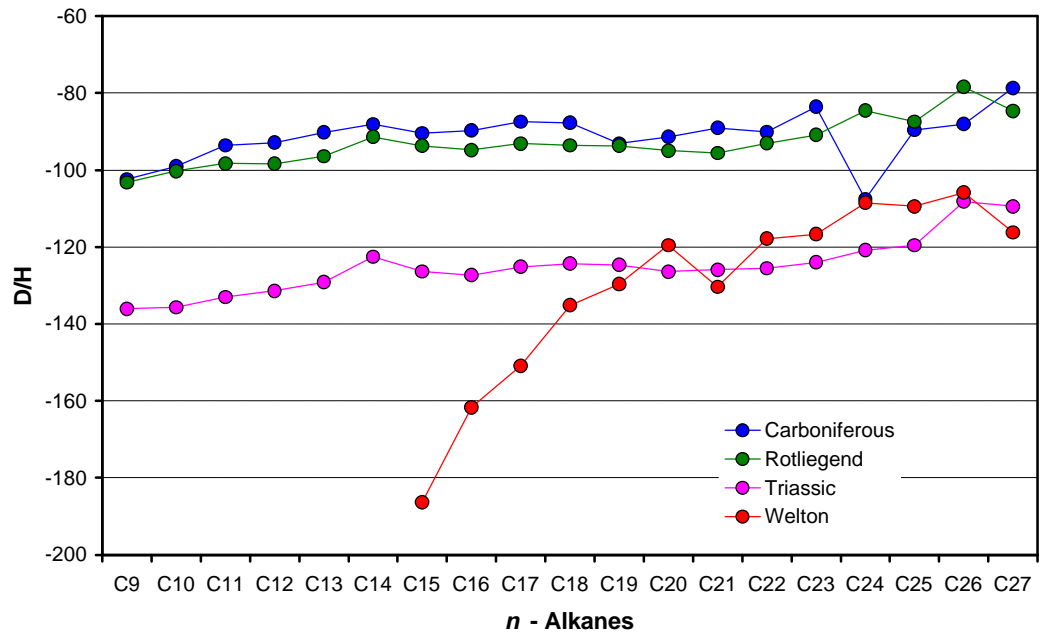


Figure F-13 Averaged hydrogen isotope values of individual n-alkanes from the condensate samples, differentiated into the three reservoir ages

With respect to the carbon isotope values (Figure F-12) there is no good correlation between either of the reservoirs. Yet, the isotope values of the condensates of the Triassic reservoirs show some resemblance with those of the Welton oil in the C₁₉ to C₃₂ range. A better comparison between the condensates and the Welton oil can be made by using the hydrogen isotope data. Figure F-13 shows that in the C₁₉ to C₂₇ range the Welton oil closely resembles condensates (the averaged values) from the Triassic reservoirs. However, major differences are noted for the lower alkanes.

A preliminary conclusion may be that the Welton oil has a different source rock than the condensates from the Carboniferous and Rotliegend reservoirs. The cause of the partial resemblance between the Welton oil and the condensates from the Triassic reservoirs is not fully understood.

Conclusions

Several methods have been applied to correlate hydrocarbons to the analysed source rocks. No straightforward correlation could be established between the Welton oil sample and the source rocks, although the results may indicate that there are potential source rocks present comparable to those suggested for the Welton oil. However, there are too many unknown factors that may have influenced the parameters that are used in this correlation. The impact of, sometimes multistage coalification, (subtle) differences in the type of organic matter, accuracy of some measurements, etc. may be significantly different for each area or even for each individual well. It is therefore recommended to do a more detailed study on some selected wells in combination with a statistical approach that includes all (quality controlled) parameters.

G Input and parameters for the basin modelling

Introduction

The numerical simulation of the evolution of sedimentary basins provides an integrated approach to the understanding of both the petrophysical changes of sedimentary rocks during geological time and of the processes evolving within these rocks and their control by the respective geological conditions. Successful numerical concepts are based on specific types of geological information and control data, the most important parameters being the thermal history and the source rock types, i.e. the respective kinetic parameters that determine the type and amount of generated hydrocarbons. A correlation of the geological events to the thermal history and a calibration by organic temperature and time temperature parameters are therefore essential conditions for a successful numerical simulation of any generation and migration process.

The main goal of the modelling in this study is to evaluate, in a 3D model, the timing of maturity evolution and related generation of hydrocarbons. The three selected areas (Figure G-1) were modelled separately. In this study the state-of-the-art software PetroMod 9.0 from IES has been used.

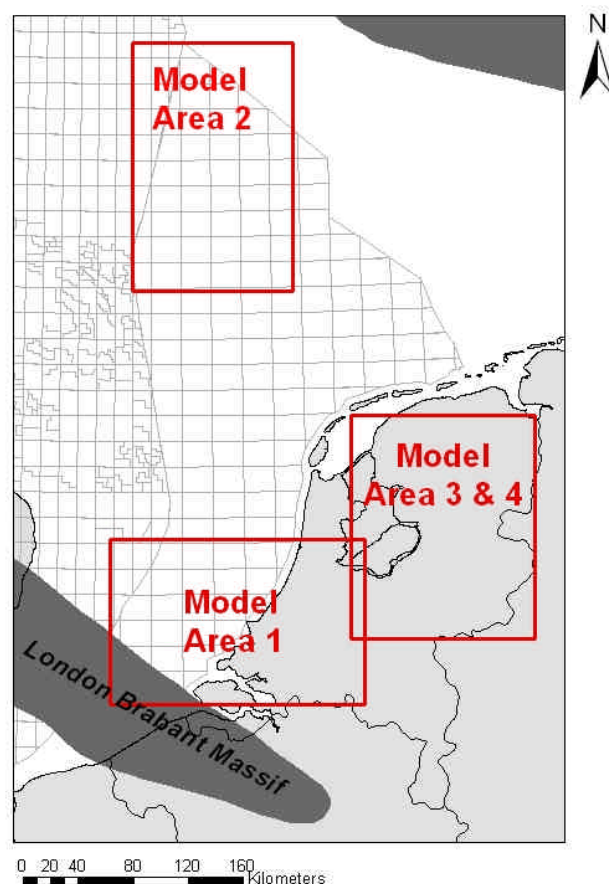


Figure G-1 Outlines of the modelled areas

Prior to the 3D modelling, a 1 D maturity modelling based on stratigraphic well information has been performed. All assigned key wells, which penetrated the pre-

Westphalian, have been modelled for this study. These wells are concentrated on specific locations within the areas, where the pre-Westphalian is generally relatively shallow. In order to cover the entire area, a selection of wells with enddepth in the Upper Carboniferous was also modelled in 1D.

The aim of the 1 D modeling was to get an indication of the burial history of the well, which can be calibrated to available data. From the results of the 1D modeling, erosion maps have been constructed for all areas. For areas 3 and 4 heatflow maps have been constructed as well, since it appeared, that the variation in heatflow in these areas is high. These heatflow maps have been used for the 3D modeling.

Both the 1D and the 3D modelling require numerous input variables. These include many coupled equations that are taken into account, such as equations for fluid phase potential, heat flow, compaction, kinetics, maturity modelling, etc. Besides these equations the model requires also stratigraphical, lithological and thermal information together with material parameters. A selection of parameters with a relatively high impact on the results is given below.

Stratigraphy

Stratigraphy in 1D models

The stratigraphic information has been extracted from previous stratigraphic interpretations, which are stored in the FINDER database of TNO. This stratigraphic well information is very often given at Member level and therefore partly very detailed (Table G-1). The lithostratigraphic interpretation of Van Adrichem Boogaert and Kouwe (1993-1997) has been coupled to chronostratigraphy according to Harland et al. (1990) for Cenozoic, Mesozoic and Upper Paleozoic strata. The stratigraphic framework described in Chapter 2 has been used for the Carboniferous chronostratigraphy. For wells, which did not penetrate the Pre-Westphalian strata, information from the 3D depth grids (see below) model were used for the completion of the Carboniferous stratigraphic section.

Table G-2 summarises the stratigraphic information on Group Level for the 3 different areas. The absolute ages of the stratigraphic units (at Group Level) that were used in the modelling are given. Slight differences of ages between the different areas are due to differences in geological history. In this table also the main erosional phases for the three areas are given. Erosional phases which are only of local importance have been included in the 1D modelling, but are not shown here.

"Hydrocarbon potential of the Pre-Westphalian in the Netherlands on- and offshore"

Table G-1 Example for stratigraphic input in 1D basin modelling, based on stratigraphic interpretations extracted from FINDER.(well A14-01)

Stratigraphic unit	Deposition		Erosion		Stratigraphic unit	Deposition		Erosion	
	Bottom age (ma)	Top age (ma)	Bottom age (ma)	Top age (ma)		Bottom age (ma)	Top age (ma)	Bottom age (ma)	Top age (ma)
NU	22	0			ZEZ2C	255.5	255.1		
NM	38.6	22			ZEZ1W	255.9	255.5		
NL	60.5	42.1			ZEZ1C	256	255.9		
CKEK	65	60.5			ZEZ1K	256.1	256		
CKGR	78	65			RO	268.8	256.1		
Subhercyn CKGR	90.4	85	85	81	Saalian DCHP	305	303	290	288
Subhercyn CKTX	97	90.4	81	78	Saalian DCDG	307	305	288	286
KNGLU	103.5	97			Saalian DCCU	310	307	286	283
Late Kim2 SG	154.7	141	141	140	Saalian DCCK	318.3	310	283	280
Late Kim1 AT	209.5	161	161	158	DCGM	322.8	318.3		
Late Kim1 RN	241	212	158	156	DCGE	331	322.8		
Late Kim1 RBM	243.4	241	156	154.7	XX ????	286.5	286.1		
RBSHM	247.5	243.4			DCGE	331	323		
ZEUC	252	251			CFYD	340	331		
ZEZ4A	252.5	252			CFEB	349.5	340		
ZEZ4R	253	252.5			CFCS	358.3	349.5		
ZEZ3B	254.5	253			ORTP	365	358.3		
ZEZ3G	255	254.5			ORBU	372.5	365		
ZEZ2A	255.1	255			ORPA	379.9	372.5		

Table G-2 Lithostratigraphic units and their absolute depositional ages used as input data for 1D modelling study of area 1, area 2, and area 3.

Stratigraphy	Group Name	Group Symbol	Area 1		Area 2		Area 3/4	
			Bottom age	Top age	Bottom age	Top age	Bottom age	Top age
Neogene	Upper North Sea	NU	24	0	22	0	24	0
	Middle North Sea	NM	38.6	24	38.6	24	38.6	24
	PYRENEAN		38	34			38	34
Paleogene	Lower North Sea	NL	60.5	42.1	65	42.1	60.5	42.1
	LARAMIDIAN		63	60.5			63	60.5
	Chalk	CK	78	65	78	65	78	65
Cretaceous	SUBHERCYNIAN		85	75	85	75	85	75
	Chalk	CK	97	85	97	85	97	85
	Rijnland	KN	140	97	140	97	140.7	97
	LATE KIMMERIAN 2		142	140	141	140	142	140.7
Jurassic	Schieland/Scruff/Nedersaksen	SL/SG/SK			154.7	141		
	LATE KIMMERIAN 2		161	154	161	154.7	161	154
	Altena	AT	209.5	161	209.5	161	209.5	161
Triassic	Upper Germanic Trias	RN	219	209.5	241	212	219	212
	EARLY KIMMERIAN		228	219			228	219
	Upper Germanic Trias	RB	242	228			242	228

	HARDEGSEN		243	242			243	242
	Lower Germanic Trias	RB	256.1	243.4	247.5	241	256.1	243.4
Permian	Zechstein	ZE	256.1	251	256.1	247.5	256.1	247.5
	Upper Rotliegend	RO	268.8	256.1	268.8	256.1	268.8	256.1
	SAALIAN		290	280	290	280	290	280
Carboniferous	Limburg	DCC	315	303	315	303	316.5	303
		DCG	330	315	331	315	326.4	316.5
	Carboniferous Limestone/Farne	CL/CF	345	335	358.3	331	331	326.4
	SUDETIAN		335	330			335	331
	Carboniferous Limestone/Farne	CL/CF	362.5	335			362.5	335
Devonian	Old Red/ Banjaard	OR/OB	377.4	362.5	379.9	358.3	377.4	362.5

Stratigraphy in 3D models

The master input model is based on 28 different horizons (Table G-3). Some of the post-Carboniferous horizons (in bold) were taken from previous mapping programs and some others (in italic) were constructed by splitting layers in order to refine the model and to be able to introduce erosional phases. The horizons represent major lithostratigraphic units, based on . The ages of the stratigraphic units are based on interpretations of the lithostratigraphic units described in Van Adrichem Boogaert and Kouwe (1993-1997). According to the stratigraphic framework of this study, the Epen Formation has been split into two layers (Namur-1 and Namur-2) and the Dinantian layers have been split into 4 layers, Dinantian 1, 2, 3a and 3b. The split ratio has been assigned to 50 % in the Epen Formation, and to 25 % in the Dinantian.

For modelling of different play concepts in area 2, layers Namur-1 and Namur-2 have additionally been split with a split ratio of 33 %.

"Hydrocarbon potential of the Pre-Westphalian in the Netherlands on- and offshore"

Table G-3 Overview of stratigraphic units used in the static 3D model. Layers of post-Westphalian age (in bold) were taken from previous mapping programs; layers in italic were constructed by splitting layers. Carboniferous layers have been interpreted in the scope of the study. Base of Upper North Sea Group- NU (Tertiary); Base of North Sea Supergroup – N (Tertiary), Base of Chalk Group - CK (Upper Cretaceous), Base of Rijnland, Group – KN (Lower Cretaceous), Base of Schieland Group- S (Upper Jurassic), Base of Altena Group - AT (Lower and Middle Jurassic), Base of Lower Germanic Trias Group – RB (Triassic). Base of Zechstein Group – ZE (Permian), Base of Upper Rotliegend Group – RO (Permian), Base of Hunze Subgroup – DC (Upper Carboniferous), Base of Dinkel Subgroup- DC, Base of Maurits Formation –DC, Base of Ruurlo Formation –DC, Base of Baarlo Formation –DC, Base of Epen Formation –DC, Base of Geverik Member - Base Dinantian - CL – (Lower Carboniferous), Base Devonian, Basement

Layer	Age bottom	Age top
NU	23	0
<i>Ntop</i>	34	23
Nbot	65	38
<i>CKtop</i>	78	65
CKbot	96	85
KN	140	96
<i>Stop</i>	141	140
Sbot	154	142
<i>ATtop</i>	198.6	161
ATbotpos	208	198.6
<i>RBtop</i>	218	208
RBbot	250	228
ZE	255	245
RO	258	256
Hunze (DCH)	306	303
Dinkel (DCD)	308	306
Maurits (DCCU)	310	308
Ruurlo (DCCR)	312	310
Baarlo (DCCB)	318	312
<i>EPEN (DCGE)2</i>	321.5	318
EPEN (DCGE)1	325	321.5
GEVERIK MB (DCGEG)	326.4	325
<i>DinantIAN3a</i>	334.55	326.4
<i>DinantIAN3b</i>	342.7	334.55
<i>DinantIAN2</i>	350.85	342.7
Dinantian1	359	350.85
DEVONIAN	416	359
BASEMENT	450	416

Depth of units

Depth of units in 1D modelling

The depth information of the units used in the 1D modeling has been extracted from the interpretations stored in the FINDER database of TNO.

Depth of units in 3D modelling

For the 3D modelling a 3D input model of the subsurface of the Netherlands was developed in PetroMod. The depth grids from the TNO mapping program were used as input for both the onshore and the offshore area. The existing grids of the Netherlands offshore and onshore were merged. These grids of the selected stratigraphic layers are based on seismic interpretation and interpretation of well data. For the construction of the pre-Westphalian grids the results of seismic and (biostratigraphic) well interpretations of this project were used. A constant layer thickness is assumed for the input model if no data is available. The 3 different areas (Figure G-1) have been extracted and were modelled separately (Figures G-2, G-3, G-4).

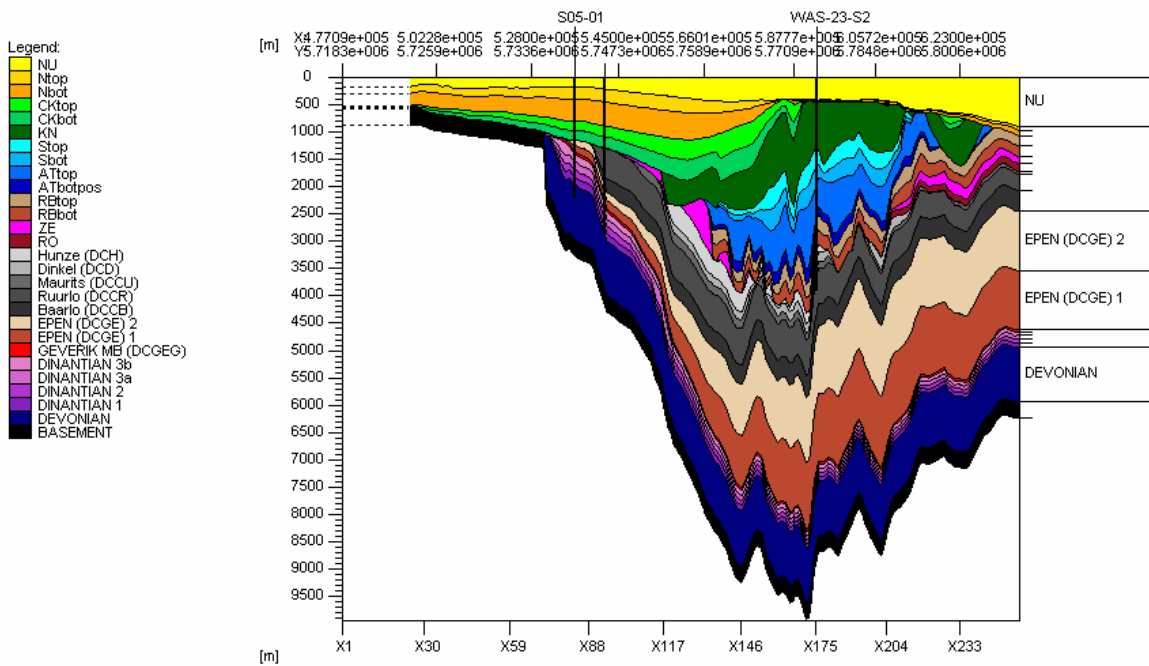


Figure G-2 Example of a profile from the PETROMOD 3D input model showing depth maps and stratigraphic units of Area 1

"Hydrocarbon potential of the Pre-Westphalian in the Netherlands on- and offshore"

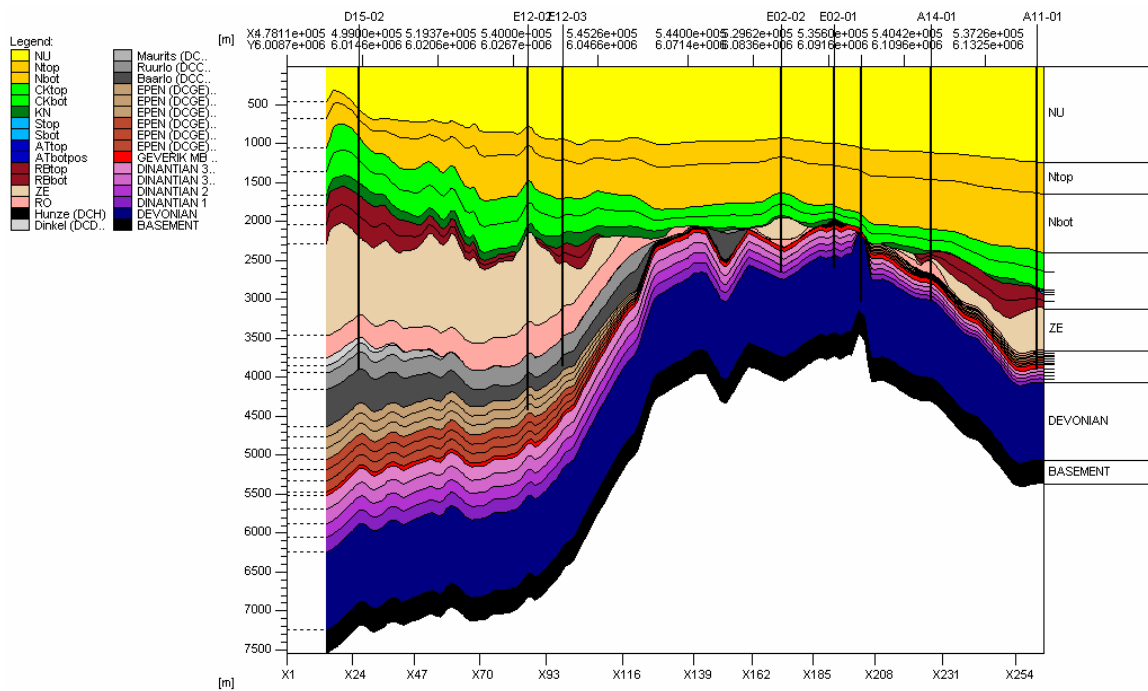


Figure G-3 Example of a profile from the PETROMOD 3D input model showing the depth map and stratigraphic units of Area 2

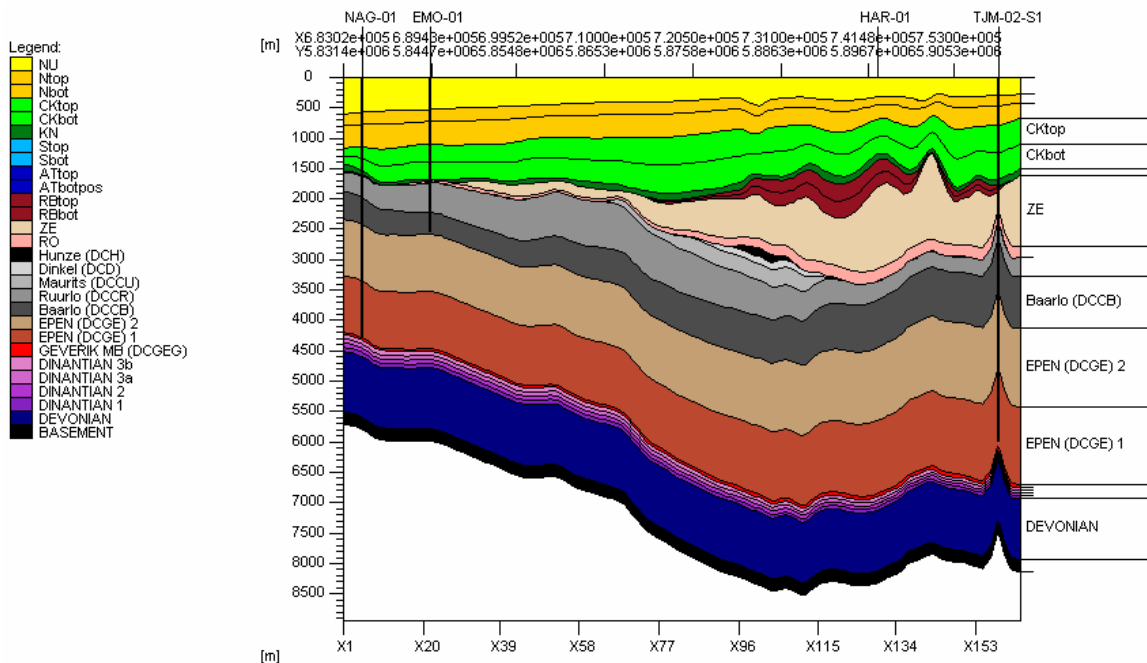


Figure G-4 Example of a profile from the PETROMOD 3D input model showing the depth maps and the stratigraphic units of Area 3&4

Lithology

Lithology in 1D modelling

Lithological information has been derived from the lithological descriptions in Van Adrichem-Boogaert & Kouwe (1993 - 1997) and, if available, from lithological descriptions in well reports. A number of user defined lithologies have been created in Petromod 9.0. For the porosity depth relationship in the 1D models, the IES Compressibility Model has been used. This model gave the best calibration fit with the present day porosity data.

Lithology in 3D modelling

Lithologies, which have been assigned to the stratigraphic units have partly been derived from descriptions of Van Adrichem Boogaert and Kouwe (1993-1997) and partly from facies descriptions of the different units by Ziegler (1990). The lithologies of the pre-Westphalian are variable in the modelling, because they depended on the different play models.

Erosional phases

1 D modelling

A conceptual geological model has been used to estimate the amount of erosion per tectonic phase per stratigraphic unit. Absolute values for the original thicknesses of stratigraphic units in individual wells were estimated using among others literature data, surrounding wells, regional geological information, the structural position of a well (on a structural high or in a basin). The assumed original thicknesses, which can vary per location, are compared with the present thickness in the wells to estimate the amount of erosion in that well. To assign the amount of erosion to a particular erosional phase, the age of the first rock above the erosional event is considered. When two or more erosional phases overlap it is in some cases difficult to assign the relative amount of erosion to the phases. The following erosional phases were taken into account in the 1D modelling and 3 D modelling, with exception of the Sudetian phase which as only be considered in the 1D modelling. The assumed timing of the different erosional phases for the three different areas is given in Table G4. The amount of eroded strata varies strongly in de different areas and is described in detail in Appendix H (erosion maps). Minor differences in the timing of the erosional phase between 1D and 3D modelling can occur. This is partly due to the different kind of stratigraphic input data..

Sudetian phase:

The Sudetian phase is one of the three main NW-European tectonic phases of the Variscan Orogeny. As the deformation front moved progressively north-ward, the Sudetian phase has affected the Carboniferous Limestone group.

Saalian phase:

The Saalian phase is an amalgamation of many unconformities. The Saalian phase resulted from dextral movement between Europe and Africa. This movement caused that the N-S orientated compressional setting changed in a regime with E-W orientated extensional forces at the end of the Carboniferous and the beginning of the Permian. This lead to the formation of a pattern of NW-SE and E-W orientated dextral wrench

faults. A number of horst and Graben structures resulted from this faulting, of which the Eems deep is an example. Extensive volcanism in Germany was also caused by the wrench faulting, and in the Eems Deep the Emmen Vulcanite Formation (Lower Rotliegendes Group) was deposited (Geological Atlas of the subsurface of the Netherlands – onshore, 2004).

In the modelling the term Saalian phase has been used for the uplift and erosion which took place at the end of the Carboniferous. The Saalian phase particularly resulted in extensive erosion on the highs, such as the Gronningen High, Friesland Platform, the London Brabant Massif and the Achterhoek High, because these structural elements experienced uplift during this time.

Early Kimmerian Phase:

The Early Kimmerian Phase is rifting phase related to the opening of the North Atlantic Ocean and the Tethys Ocean. Particularly in south Netherlands, units are tilted and uplifted as a result of the uplift of the London Brabant Massif (TNO – NITG, 2003; TNO – NITG, 2004).

Late Kimmerian I Phase:

During the Late Kimmerian I Phase the Atlantic rifting accelerated, the accentuation of the existing relief, is (together with the rifting during the Mid-Kimmerian and Late Kimmerian II Phases) a possible cause for the absence of Altena Group deposits on the highs, and on the edges of the basins. The Late Kimmerian I phase took place from Middle to Late Jurassic and caused erosion down to at least the Middle Triassic sediments (Upper Germanic Trias Group), sometimes even the Lower Permian (Upper Rotliegend Group) was removed in the northern part of the NL offshore.

Late Kimmerian II Phase:

Part of a rift event, the Late Kimmerian II Phase accentuates the existing relief, the Dalfsen High, Friesland High and Maasbomme. Erosion on these highs was deep, sometimes up to the Limburg Group. In the northern offshore area the Late Jurassic/Earliest Cretaceous sediments (Scruff Group) were not deposited or removed completely or almost completely (A11-01).

Subhercynian Phase:

As a result of the closure of the Tethys Ocean and the opening of the North Atlantic Ocean, the geodynamic setting changed from a (mainly) extensional to a compressional setting. This resulted in a reactivation and inversion of Mesozoic fault structures in several phases. The former basins became highs, and this resulted in extensive erosion on these newly formed highs. Uplift varied in the basins, from 1000m the edges of the basins, to in excess of 2000m in the basin centers. Also on the highs, some erosion occurred before they became the basins, but this generally does not exceed 200m .

Laramide Phase:

The Laramide phase also is an inversion event, but occurred at the end of the Chalk group deposition. The effects of this phase are not as large in the basins as the Subhercynian phase, but particularly affected the basins and highs in the North of the Netherlands. The northward movement of Africa relative to Europe is the main cause of the tectonic event.

Pyrenean Phase:

As the name suggests, is the Pyrenean phase related to the Alpine deformation between Spain and France. Part of the West Netherlands Basin became a high, the Kijkduin High, during this phase, which leads to several hundreds meters of erosion on this structural element (Van den Belt and David, 2002).

3D modelling

Only the major erosional phases (Saalian, Early Kimmerian, Late Kimmerian 1 and 2, Subhercynian, Laramidian, and Pyrenean) have been included in the 3D modelling (see also appendix H). The erosional phases were introduced in the model as erosional thickness grids, i.e. grids that represent the thickness of the eroded amounts. These grids are based on the results of the 1D modelling, by gridding the estimated erosion thicknesses of the calibrated 1D models. The structural elements were taken into account in the gridding procedure. The attributed ages of the onset and end of the erosional phases was based on the presence and absence of stratigraphical units, which differed between the areas (Table G-4). Also, this evaluation showed that the impact of the erosional phases was different in the modeled areas. Therefore, not all erosional phases are included in the different areas (Table G-4).

In Area 1 seven erosional phases have been included in the 3D modelling, assuming that those events had a more or less significant influence on the basin development of the area. These are the Sudetian, Saalian, Early Kimmerian, Late Kimmerian 1, Late Kimmerian 2, Subhercynian, Laramidian and Pyrenean phases.

In Area 2 four major tectonic phases which had an essential effect on geological framework of the area have been distinguished and included. These are the Saalian, Late Kimmerian 1, Late Kimmerian 2 and the Subhercynian phases.

Table G-4 Assumed timing of major erosional events for the 3 areas in the 3D model

Stratigraphic unit	AREA 1		Erosional phases	AREA 2		Erosional phases	AREA 3/4		
	Erosion from	To		Erosion from	to		Erosion from	to	
Nbot	38	34	Pyrenean N	38	34		38	34	Pyrenean N
Cktop	63	60.5	Laramidian CK			Laramidian CK	63	60.5	Laramidian CK
CKbot	85	80	Subhercynian CK	85	80	Subhercynian CK	85	82	Subhercynian CK
KN	80	78	Subhercynian KN	80	78	Subhercynian KN	82	80	Subhercynian KN
Sbot	142	141	Late Kimmerian 2 S	142	141	Late Kimmerian 2 S	142	141	Late Kimmerian 2 S
ATtop	161	159.6	Late Kimmerian 1 AT	161	160	Late Kimmerian 1 AT	161	159.6	Late Kimmerian 1 AT
ATbotpos	159.6	154	Late Kimmerian 1 ATAL						
Rbtop				160	159	Late Kimmerian 1 R	160	159	Late Kimmerian 1 R
RBbot									
RBbot	228	224	Early Kimmerian R						
ZE	0	0		159	156	Late Kimmerian 1 ZE	159	156	Late Kimmerian 1 ZE
RO	0	0		156	154	Late Kimmerian 1 RO	156	154	Late Kimmerian 1 RO
Hunze (DCH)	290	288	Saalien (Hunze)	290	288	Saalien (Hunze)	290	288	Saalien (Hunze)
Dinkel (DCD)	288	286	Saalien (Dinkel)	288	286	Saalien (Dinkel)	288	286	Saalien (Dinkel)
Maurits (DCCU)	286	284	Saalien (Maurits)	286	284	Saalien (Maurits)	286	284	Saalien (Maurits)
Ruurlo (DCCR)	284	282	Saalien (Ruurlo)	284	282	Saalien (Ruurlo)	284	282	Saalien (Ruurlo)
Baarlo (DCCB)	282	280	Saalien (Baarlo)	282	280	Saalien (Baarlo)	282	280	Saalien (Baarlo)
CL	335	330	Sudetian	335	330	Sudetian	335	330	Sudetian

Heat flow

Heat flow can be determined from the thermal conductivity of the heated material and from the measured temperature gradient across the interval of interest. Heat flow measurements are often complicated and need to be estimated. A prerequisite for any heat flow or thermal gradient determination is the definition of an upper boundary temperature at the sediment surface or sediment/water interface as an annual mean value. Problems associated with the heat flow concept are mainly concerned with quantifying and calibration paleo-heatflow values, especially if insufficient calibration data is available.

The simulation program offers an accurate method of determining present day heat flow. This method requires that the thermal properties of the lithologies are taken into account and results in a more accurate thermal conductivity determination. A match of measured and calculated present day temperature will therefore lead to a more accurate present-day heat flow value. In addition, temperature disequilibrium e.g. caused by recent rapid sedimentation is also considered.

Measured regional heat flow values range from lows of 29-42 mW/m² in Precambrian shield areas, ocean trenches, and in areas of older stable and/or compressional tectonic units, to circa 85 mW/m² in areas such as ocean ridges, and occasionally even 125 mW/m² in active rift systems (e.g. the Red Sea) or geothermal active areas. A mean value for the heat flow at the earth surface from 2000 measurements amounts to 63 mW/m² (Kertz, 1969). Kappelmeyer and Haenel (1974) report values of 60 mW/m² for all continents and 61 mW/m² for all oceans and seas. In this study, the applied present-day heat-flow is similar to the average values, circa 60 – 70 mW/m².

Heat flow in 1D modelling

To calculate the temperature development in the 1D well, the boundary conditions of the base and of the top need to be defined. The boundary condition on the base of the well is defined by the basal heat flow, whereas at the top the Sediment Water Interface Temperature (SWIT) needs to be considered.

The basal heat flow is the amount of heat which is supplied to the base of the crust by the underlying mantle. The basal heat flow is mainly controlled by the geographic location, magmatic intrusions and the tectonic setting. In general, tectonic settings where the crustal thickness is reduced (extensional or rift settings), the basal heat flow will increase, in settings where the crust thickens (compressional settings) the basal heat flow will be lower, though there is a large spread in the values (Allen and Allen, 1990). Changes in the tectonic setting will generally lead to changes in the basal heat flow.

Thermal information about present-day temperatures and heatflow has been extracted from internally used temperature and heatflow maps. Special attention was paid to a better insight in regional heatflow patterns. For the calibration of the models maturity data (vitrinite reflectance data (VR) and RockEval Tmax) were used.

Van Balen et al. (2000) present a basal heat flow curve based on forward modeling in well LIR-45, in the West Netherlands Basin (WNB) The curve shows peaks at 222Ma, 145Ma and 90Ma, which correspond to the Early Kimmerian, the Late Kimmerian 2 and the Subhercynian phase respectively, and the small dimple at 120Ma correlates to

the Austrian phase. In order to synchronise the 1D modeling, this HF pattern was applied to all three areas.

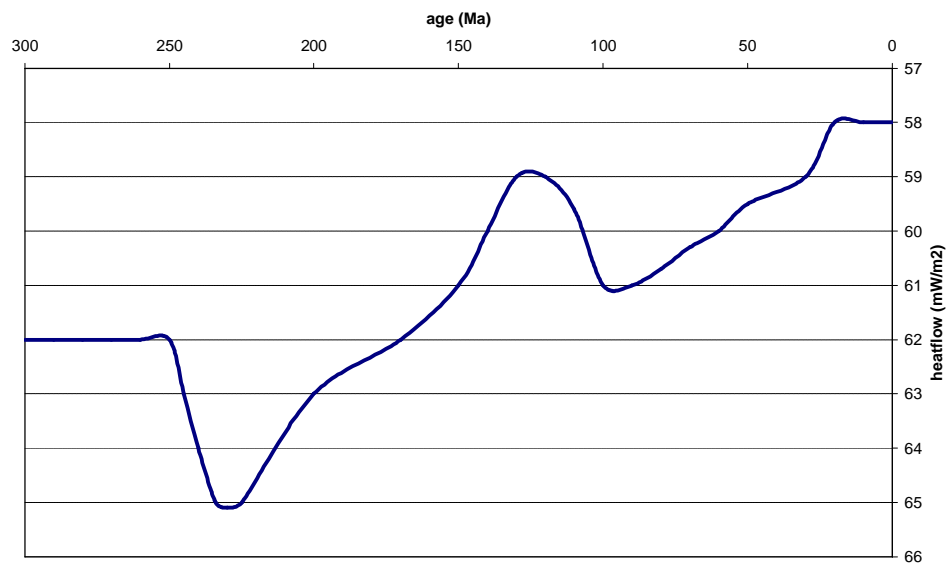


Figure G-5 Heatflow pattern developed by van Balen *et al.* (2000) for the West Netherlands Basin (after van Balen *et al.* 2000)

Preliminary results of the 1D study of Area 3&4 revealed that in order to fit the calibration data great variations had to be modelled in the heat flow distribution. The heatflow pattern described by van Balen *et al.* (2000) (Fig. G-5) has been shifted in order to get an acceptable fit with calibration data (within geological constraints). Furthermore, a heatflow trend described for the Lower Saxony Basin by Kus *et al.* (2005) has been tested. In general, the values proposed by Kus *et al.* (2005) are higher than the values used in this study.

Heat flow in 3D modelling

A constant heat flow of 60 mW/m² through time has been assumed for areas 1 and 2. For Area 3&4 vitrinite reflectance data could not be fitted with a constant heatflow of 60mW/m². Therefore, (paleo) heatflow maps with regional variation were produced on the base of the 1Dmodelling results (Appendix H). In Area 3&4, these maps were used .as input.

Paleo Water Depth (PWD)

PWD in 1D modelling

In all 1D models the PWD is set at 0 m.

PWD in 3D modelling

Boundary conditions for paleowaterdepths (PWD) of the different stratigraphic units have been defined according to current knowledge (Figure G-6).

Sediment Water Interface Temperature

The upper boundary condition to calculate the temperature development is set by the Sediment-Water Interface Temperature (SWIT), which is a function of the surface temperature and the water depth. Both in the 1D and 3D modelling the SWIT has been calculated using an integrated PETROMOD tool, based on research performed by Wygrala (1989). PETROMOD uses a global surface temperature curve generator, based on Wygrala (1989). By defining a continent and latitude a surface temperature from present to 360Ma is defined. Values for ages larger than 360Ma are defined by extrapolating the values for 360Ma. To calculate the SWIT, the water depth needs also to be defined. For continental deposits, such as the Rotliegendes and Zechstein, the water depth is 0m. For marine deposits only two paleo water depths were found. Van der Molen (2004) states that the water depth during the deposition of the Chalk group is variable, but can be averaged at roughly 175m. The Nedersachsen Group is deposited at a water depth of roughly 100m (TNO-NITG, 2003). For all other marine deposits, the water depth is set at 0m.

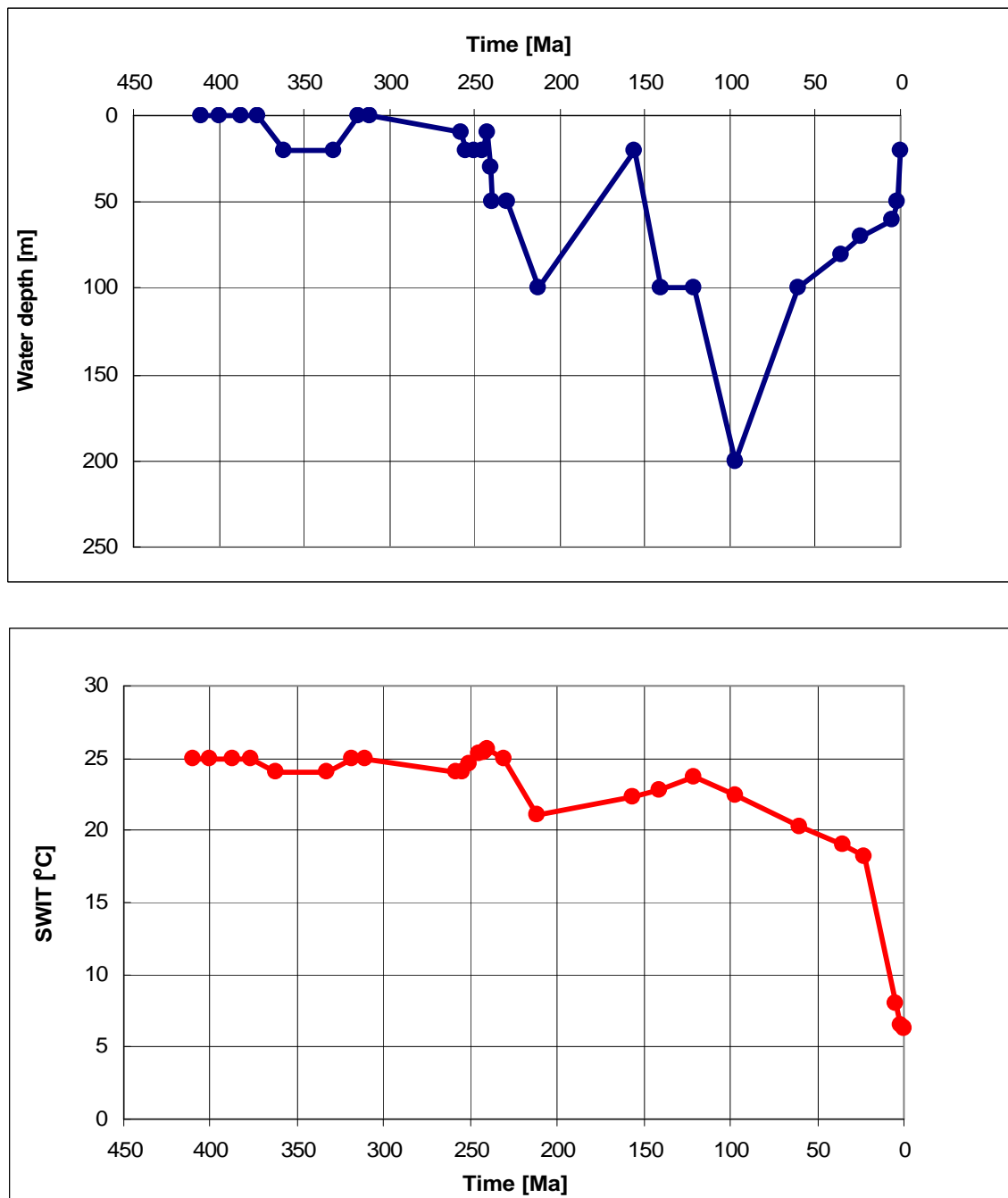


Figure G-6 Overview of paleowaterdepth (PWD) and Sediment-Water-Interface-Temperatures (SWIT) through time

Salt movement

Salt movement in the Zechstein deposits was only considered in the 1D modeling. Salt movement can lead to a significant change in the thickness of the stratigraphic units. PETROMOD allows for this halokinetics by defining an initial thickness of the unit and a thickness change over time. A clear relation between the presence of deformation phases in the geological history and salt movement does occur and the intensity of salt movement is related to the amount of tectonic activity. It is possible

to model an amount or acceleration of salt movement for every tectonic phase, but due to the lack of data and for the sake of simplicity, a simple linear model for the change of thickness of salt layers was employed. This implies that the thickness changes in time are constant.

Intrusives, extrusives and metamorphic layers

Intrusives, extrusives and metamorphic layers have been observed in the stratigraphic record of several modelled wells. Intrusion modelling was only included in the 1D modelling.

According to Sissingh (2004) three significant groups of ages with magmatic events can be distinguished. These are a mid-Carboniferous to Permian one, a Late(st) Triassic one and a Late Jurassic to early Early Cretaceous one.

Source rock characteristics and kinetic model in 3D modelling

Source rock modelling was only performed in the 3D modelling in order to get a good regional overview of the generation and expulsion of hydrocarbons in the selected areas.

In its most widely used form, petroleum generation is modelled by a first-order reaction kinetics where the rate constant obeys the empirical Arrhenius equation (Tissot & Welte, 1984). The latter states that the rate of a reaction increases linearly with time but exponentially with temperature and is conveniently represented by a frequency factor and energy of activation.

The genetic potential of a source rock represents the amount of hydrocarbons that kerogen is able to generate, if it is subjected to an adequate temperature during a sufficient interval of time. This potential depends on the nature and abundance (type) of kerogen, i.e. on its original chemical composition. A quantitative evaluation of the genetic potential can be made on the basis of a standard pyrolysis technique (Espitalie et al., 1988, Burnham 1989). This evaluation for the analysed rock samples is described in Chapter 3.

Within our modelling, a selection was made of the Type of organic matter in the source rock. As explained in Chapter 3, in general three different types of kerogen can be distinguished (Tissot & Welte, 1984):

- Type I Kerogen is mainly derived from algal lipids or from organic matter enriched in lipids by microbial activity. The H/C ratio is high, as well as the potential for oil and gas generation.
- Type II kerogen is usually related to marine organic matter deposited in a reducing environment. The H/C ratio and the oil and gas potential are lower than observed for kerogen type, but still important.
- Type III kerogen is mostly derived from terrestrial higher plants, the H/C ratio is low and the oil potential is only moderate, but at higher temperature abundant gas can be generated. Coal can be characterized as kerogen Type III.

The amount and type of hydrocarbons that are generated from the different types of kerogen are dependent on the kinetic scheme that is chosen within the modelling. Most

of them are based on empirical investigations (Tissot & Espitalie, 1975; Tissot et al., 1988; Burnham, 1989; Quigley et al. 1987; Behar et al., 1997; Ungerer, 1990; Vandenbroucke et al., 1999; Pepper&Corvi, 1995; Espitalie et al., 1988). Some of these schemes predict direct gas generation, while others predict gas generation via an oil phase. The selection of the kinetic scheme is crucial in this respect. Every kinetic scheme is described by a set of reactions that depend on activation energies, frequency factors, and initial amounts of the materials or corresponding distributions of these values. It is assumed that kerogen and oil as the initial products in these reactions can consist of different components.

The transformation ratio is the ratio of the hydrocarbons (oil and gas) actually formed by the kerogen to the genetic potential, i.e. to the total amount of hydrocarbons that the kerogen is capable to generate. The ratio measures the extent to which the genetic potential has been effectively realized.

Although there is consensus within the geochemical and petroleum geological community that coal can source gas and condensate, there are opposite viewpoints on whether coal can (e.g. Hunt, 1991) or cannot (e.g. Katz et al. 1990) be a source for liquid hydrocarbons. The proponents for coal not being a source for reservoirable oil argue that although coals can have a high potential to generate significant hydrocarbons any liquids generated would effectively be retained within the coal matrix because of the micro porosity present in coal (van Krevelen, 1993). Investigations of Forbes *et al.*, 1991 however showed that early expulsion will favor oil while retention and thermal destruction will favor gas and condensate. In this study, the kinetic scheme of Burnham (1989) is selected, where the reaction 'kerogen to gas' is the most dominant reaction. The generated hydrocarbons in the Burnham approach consists of 2 components, i.e. dry gas and medium oil. The Burnham approach starts to generate gas together with minor amounts of oil from a type III kerogen at relatively low temperatures of 100 °C.

The total amount of hydrocarbons generated depends on the amount of hydrogen in the kerogen, which is a limiting factor. Empirical observations (Powell, 1988) suggest that in order for a source rock to be effective as oil source, 10-20 % of its organic matter must equate with type I organic matter about 20 -30 % type II organic matter. This implies that the Hydrogen Indices (HI) in Rock Eval analyses have to be above 200 - 300 mg/gTOC before any oil expulsion potential is implied (Noble et al., 1991). The assumed HI for the source rocks in this study result from the source rock evaluation of the analysed rock samples (see Chapter 3).

Migration in 3D modelling

No specific input is required to model the migration of generated hydrocarbons. The dominant transport mechanism of the different phases in petroleum migration strongly depends on the physical and chemical properties of the kind of petroleum and the type of carrier rock. The properties of the petroleum and the rock result from the lithological input and the kinetic scheme. In most carrier reservoir rock systems, separate phase hydrocarbon migration is the most important transport process. Generally the petroleum mixture which was expelled during the peak phase of expulsion exists in liquid form. Thereby a significant amount of lower molecular hydrocarbons can be dissolved in this liquid phase. The gaseous petroleum phase is generated at much greater depths. Migration is assumed to take place through the rock, fault transport was not considered in this study.

Reservoirs in 3D modelling

Potential reservoirs are determined by the different play concepts and described elsewhere in this report. Reservoir properties, especially compaction relations, were adjusted for the different scenarios.

Calibration in 1D modelling

For the calibration of the wells in all areas vitrinite reflectance (VR) and RockEval data (RE) are used. This data is compared to the calculated Vitrinite Reflectance curve, based on the kinetic model by Sweeney and Burnham (1990). According to the relationship between Rock-Eval data and Vitrinite reflectance data which has been developed in the scope of this study, the RockEval data was recalculated into VR (%R) data according to a linear relationship and has also been used for calibration purposes.

In Area 2 present day temperature data of wells A11-01, A14-01, D12-03, D15-02, E02-02, E12-02 and E12-03 have been included to calibrate the burial history. This was necessary in order to determine the present-day heat flow.

Calibration in 3D modelling

Calibration in 3D was performed by extracting 1D data at well locations, and comparing those to the calibration data as described in 1.14.1.

Area specific input*Area 1*

Area 1 covers the south-western part of the Dutch on and offshore. Main structural elements in this area are the London Brabant Massif and the West Netherlands Basin. 16 wells have been included in the 1 D modelling study in area 1, of which 6 wells reached pre-Westphalian strata Table G-5 lists the wells and the deepest penetrated stratigraphic unit.. Figure G-7 gives an overview of the modelled wells in Area 1.

Table G-5 Overview of the 16 modelled wells in area 1; wells that penetrated pre-Westphalian strata are marked in yellow

Well	depth (m)	deepest penetrated stratigraphic unit	code
BHG-01	2906.8	BOLLEN CLAYST.	OBGC
EVD-01	3096	MAURITS FM	DCCU
GAG-01	3460	STRIJEN FM	DCHS
HVS-01	3841	RUURLO FM	DCCR
O18-01	3051.4	SILUUR	OS
OTL-01	2526.5	HELLEVOETSLUIS	DCDH
OVE-01	1800	CAUMER SUBGR	DCC
P10-01	2696	BOLLEN CLAYST.	OBGC
P16-01	2465	ZEELAND FM	CLZL
PRW-01	3365	STRIJEN FM	DCHS
Q13-03	3247	LIMBURG GR	DC
RSB-01	4644.5	EPEN FM	DCGE
S02-02	2878.2	BOLLEN CLAYST.	OBGC
S05-01	2230	BOLLEN CLAYST.	OBGC
SPL-01	2232	BAARLO FM	DCCB
WAS-23-S2	3915	LIMBURG GR	DC
WOB-01	2751	BAARLO FM	DCCB

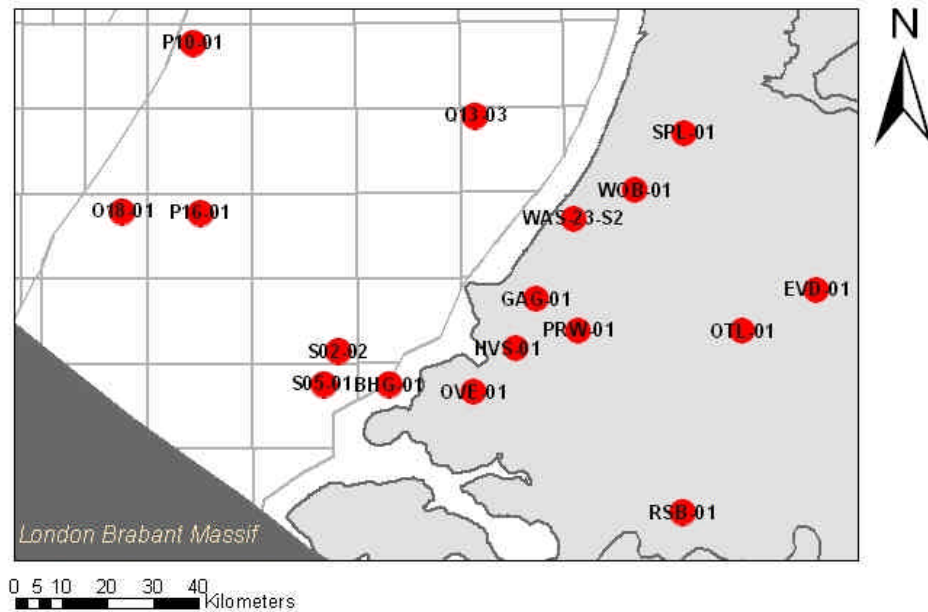


Figure G-7: Overview of modelled wells in Area 1

Source rock and kinetic model:

For the modelling of hydrocarbon generation the Geverik Member was defined as major source rock. Based on the high present day TOC values (up to 10 %), a original TOC content of 20 % has been assumed. The kerogen-oil-gas kinetic of Tissot et al. 1988_T2 and Burnham 1989_T2 was applied for the estimation of the timing of generation and the type and amount of generated hydrocarbon of kerogen type II organic matter (Hydrogen Index (HI) = 500 mg/g TOC).

Area 2

Area 2 covers the A-, D- and E-blocks of the Dutch offshore. The main structural elements in this area are the Elbow Spit High in the north and part of the Southern Permian Basin in the south.

Ten wells in Area 2 have been selected for the 1D modelling study (Table G-6); 9 penetrated pre-Westphalian strata. The wells from the A-block, as well as E02-01, E02-02 and E06-01 are located on the elevated structural element called the Elbow Spit High, which is an elongated extension of the Mid North Sea High. The other four wells (D12-02, D15-03, E12-02, E12-03) are situated in the southern part of area 2 and have been part of the Southern Permian basin. Figure G-8 gives an overview of the modelled wells.

Table G-6 List of wells in Area 2 modelled in 1D

	Well	depth (m)	deepest penetrated stratigraphic unit	Code
1	A11-01	3900	GEUL SG	DCG
2	A14-01	3014	YOREDALE FM	CFYD
3	A16-01	2708	FARNE GROUP	CF
4	D12-03	3999	CLEAVERBANK FM	DCCKM
5	D15-02	3905	MAURITS FM	DCCU
6	E02-01	2595	TAYPORT FM	ORTP
7	E02-02	2647	ELLEBOOG FM	CFEB
8	E06-01	3200	TAYPORT FM	ORTP
9	E12-02	4428	GEUL SG	DCGM
10	E12-03	3788	GEUL SG	DCGM

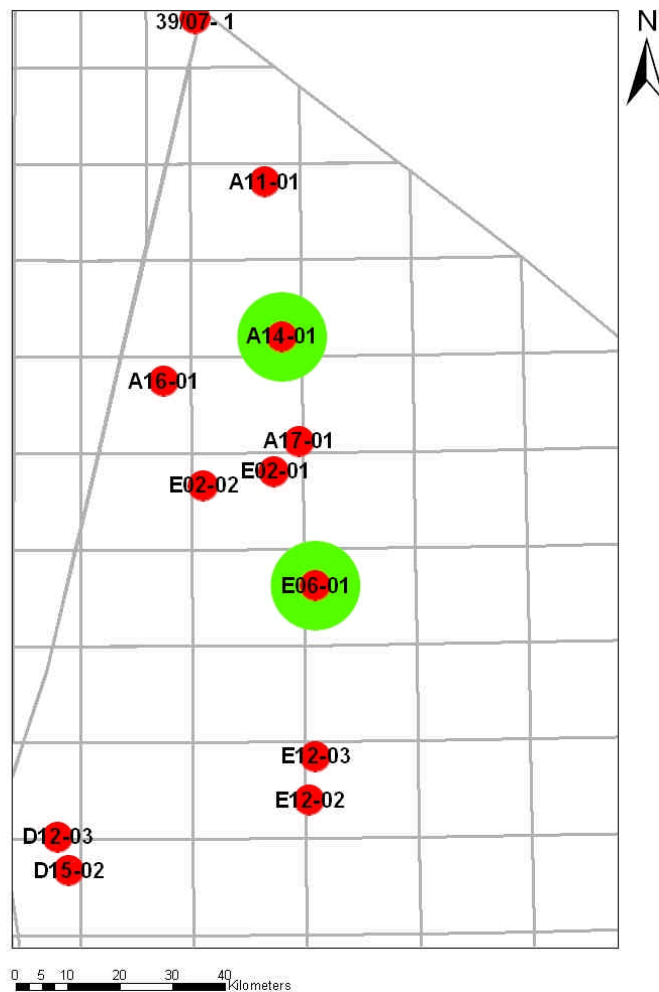


Figure G-8 Overview of modelled wells in area 2. Wells with known and modelled intrusions are indicated in green

Source rocks and kinetic model

In area 2 two source rocks have been defined, i.e. the Bowland and Edale shales as lower ('near-base') Namurian source rocks and the Yoredale Formation as a Dinantian source rock. The 'near-base' Namurian source rocks have the same characteristics as the Geverik Member. For the estimation of the timing of hydrocarbon generation and the amount of hydrocarbon generation, the kerogen-oil-gas kinetic of Tissot et al. 1988_T3 and Burnham 1989_T3 was applied for the Yoredale Formation. An initial Hydrogen Index of 250 mg/gTOC is assumed for the organic matter of the Yoredale formation. TOC values have been estimated from TOC measurements (Tab.). The TOC content of the more shaly facies is 2.5 %, the TOC content of the more sandy facies is 1%.

Intrusions

Intrusions are present in wells A14-01 and E06-01. Because they may lead to an increase of the maturity due to an additional heat impuls, these intrusions were modelled.

Area 3&4

Area 3&4 comprise the eastern onshore area of the Netherlands. Area 3 is the northern part, area 4 the southern part. (Fig. G-9). The most important structural elements in Area 3 are the Central Netherlands Basin, Friesland Platform, Lower Saxony Basin and Groningen High. Main structural elements in Area 4 are the Central Netherlands Basin and the Maasbommel High.

44 wells have been modelled in Area 3&4, of which 5 reached pre-Westphalian strata. Those are the wells Nagele-1, Emmeloord-1 and Tjuchem-2-S1 for area 3 and Winterswijk-1 and MSTL-01 (Münsterland 1, Germany) for area 4. For the establishment of erosion maps and regional heatflow maps a series of wells have been modelled which did not reach pre-Westphalian strata. Table G-7 list the wells and the deepest penetrated stratigraphic unit. Figure G-8 gives an overview of the modelled wells in Area 3&4.

Table G-7 Overview of the 44 modelled wells in area 3and 4; wells that penetrated pre-Westphalian stata are marked in yellow 9 (to be completed)

Well	depth (m)	deepest penetrated stratigraphic unit	code
AKM-02	2487	LIMBURG	DC
BHM-01	3502	LIMBURG	DC
CLD-01	3135	DINKEL	DCDT
COV-10	3241	LIMBURG	DC
DAL-07	4020	HUNZE	DCHL
DWL-02	3797	LIMBURG	DC
EMO-01	2547.7	LIMBURG	DC
EMM-07	4364	HUNZE	DCHL
GLH-01	4498	BAARLO	DCCB
GRL-01	4652	HUNZE	DCHL
HAR-01	3489	LIMBURG	DC
HAW-01	3348	LIMBURG	DC
HGL-01	2900	LIMBURG	DC
HRL-01	3022	COPPERSHALE	ZEZ1K
KLH-01	2609	DINKEL	DCDT
NAG-01	4302	EPEN	DCGE
NOR-01	3330	DINKEL	DCDT
NSL-01	2322	RUURLO	DCCR
RAW-01	3046	DINKEL	DCDT
ROT-01-S1	2805	LIMBURG	DC
SLO-01	2709.4	ROTLIEGEND	ROSLU
TBR-01	2890	ROTLIEGEND	ROSL
TJM-02-S1	5815	GEVERIK	DCGE
VLV-01	4191	HUNZE	DCHL
WDV-01	3186	MAURITS	DCCU
ZBR-01	2780	LIMBURG	DC
ZEW-01	2000	RUURLO	DCCR
APN-01	1553	MAURITS	DCCU
COR-01	1284.26	RUURLO	DCCR
DEW-05	2190	HUNZE	DCDT

DRO-01	3504	LIMBURG	LIMBURG
GEL-01	1017	RUURLO	DCCR
HGV-01	1500	RUURLO	DCCR
HKS-01	1008	HUNZE	DCDT
HLD-01	1493	LIMBURG	DCCP
JPE-01	1493	LIMBURG	DCCP
LUT-06	3206	HUNZE	DCDT
MSTL-01		Devonian	
PLG-01	1134	RUURLO	DCCR
RAT-01	1380	RUURLO	DCCR
RLO-01	1503.2	RUURLO	DCCR
TUB-08	3206	MAURITS	DCCU
WSK-01	5009.5	OLD RED	OR
ZED-01	1964.5	RUURLO	DCCR

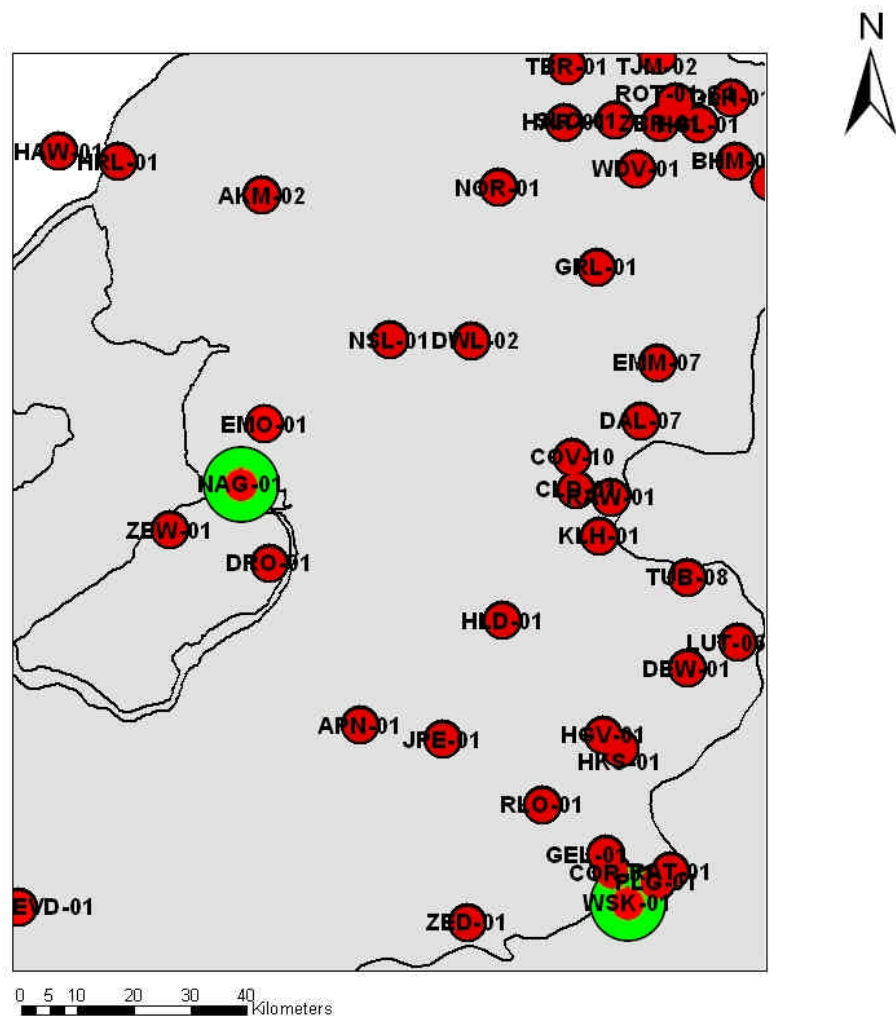


Figure G-9 Overview of Area 3&4 and overview of modelled wells in this area. Wells with known and modelled intrusions are indicated in green

Salt movement

There are two Zechstein units (ZEZ3H and ZEZ2H) which show thickness changes due to salt movement in the study area. Both layers are assumed to consist completely of halite. The original thickness of these layers is set to 100m, based on wells unaffected by salt movement. The moment of initiation of salt movement is set on the Late Kimmerian I tectonic phase (161 Ma). For the model, this means that between the moment of deposition and 161Ma, the thickness of units ZEZ3H and ZEZ2H is 100m, and between 161Ma and the present the thickness change linearly to the present thickness.

Kinetic model

For the modelling of hydrocarbon generation the Geverik Member was defined as major source rock. Based on the high present day TOC values (up to 10 %), a original TOC content of 20 % has been assumed. The kerogen-oil-gas kinetic of Burnham 1989_T2 was applied for the estimation of the timing of generation and the type and amount of generated hydrocarbon of kerogen type II organic matter (Hydrogen Index (HI) = 500 mg/g TOC).

Intrusions

Well Winterswijk-1 shows an olivine-dolorite intrusion in the Limburg group, at a depth of 4078m. According to Sissingh (2004), the age of this intrusion is 218 Ma (late Triassic). This intrusion influenced the maturation of the coal layers of the Limburg group to some extent, which can be seen in Appendix B.

H Results and discussion of the 1-D maturity modelling

H1 Burial history

Area 1

The relation between Variscan subsidence and uplift and Cenozoic subsidence is crucial for the evaluation of the contribution of of pre-Westphalian source rocks to the petroleum system.

In the vicinity of the London Brabant Massif and further to the north, the Variscan unconformity is modelled as the major uplift phase in this area. Sediments have been eroded in different phases, however the total amount of eroded Lower and Upper Carboniferous strata varies between 1650m in well Brouwershavense Gat-1 and 2070 m in S05-01. The wells in the vicinity of the London Brabant Massif reached thus their deepest burial during the Carboniferous (Figure H-1). Well P16-01, however has just recently reached a depth, which starts to exceed the deepest burial during the Carboniferous.

To the east of the London Brabant Massif a zone occurs where 1D modelling identifies wells which reached their deepest burial sub-recent. The wells are situated at the margin of the London Brabant Massif. The base of the Namurian in well P10-01 and well Q13-03 is postulated around 4000 m, in well HVS-01 the base Namurian is postulated at about 5000 m and in two other 2 wells (PRW-01 and GAG-01) the base of the Namurian is postulated at about 6000 m (Figure H-2).

Further towards the northeast wells reached the maximum burial during the Jurassic or Cretaceous (Figure H-3 and H-4).

On the London Brabant Massif the highest maturity was already achieved at the end of Carboniferous. Further to the east however a zone does exist where highest maturity is reached a present day. Towards the east and the north the maturity is rapidly increasing. Calculated vitrinite reflectance amounts to 1.7 – 2.5 %Rr for base Namurian in wells P10-01, Q13-03 and HVS-01. Wells PRW-01 and GAG-01, which are situated towards the centre of the West Netherlands Basin show calculated VR values of about 3.8 % Rr. These high calculated VR result from a high thickness of the Epen Formation, which is assumed for the wells further to the east. In the West Netherlands Basin, the highest maturity has been reached during the Mesozoic.

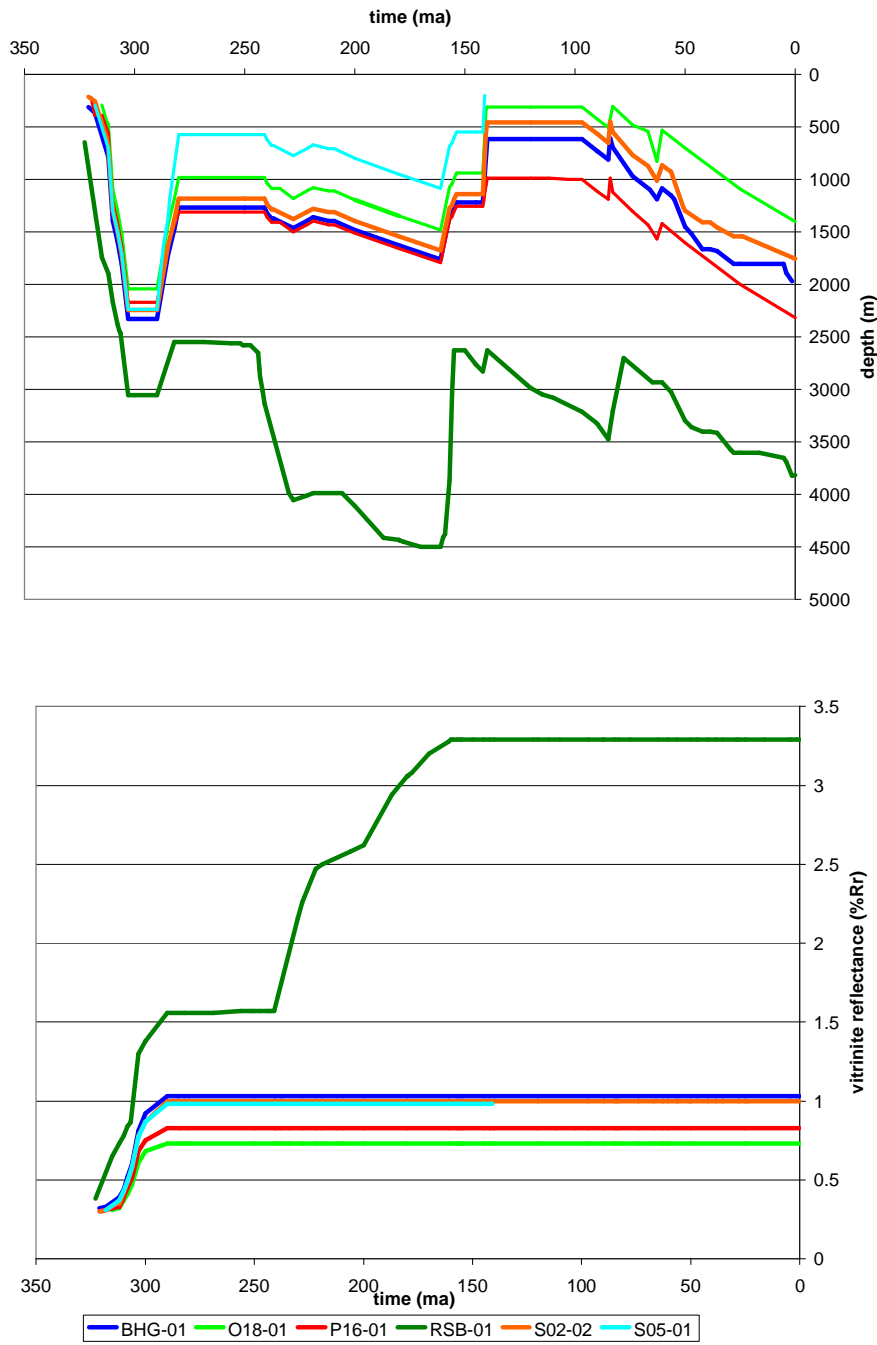


Figure H-1 a) Burial history diagrams of the wells BHG-01, O18-01, P16-01, RSB-01, S02-02 and S05-01

b) vitrinite reflectance vs time for wells BHG-01, O18-01, P16-01, RSB-01, S02-02 and S05-01

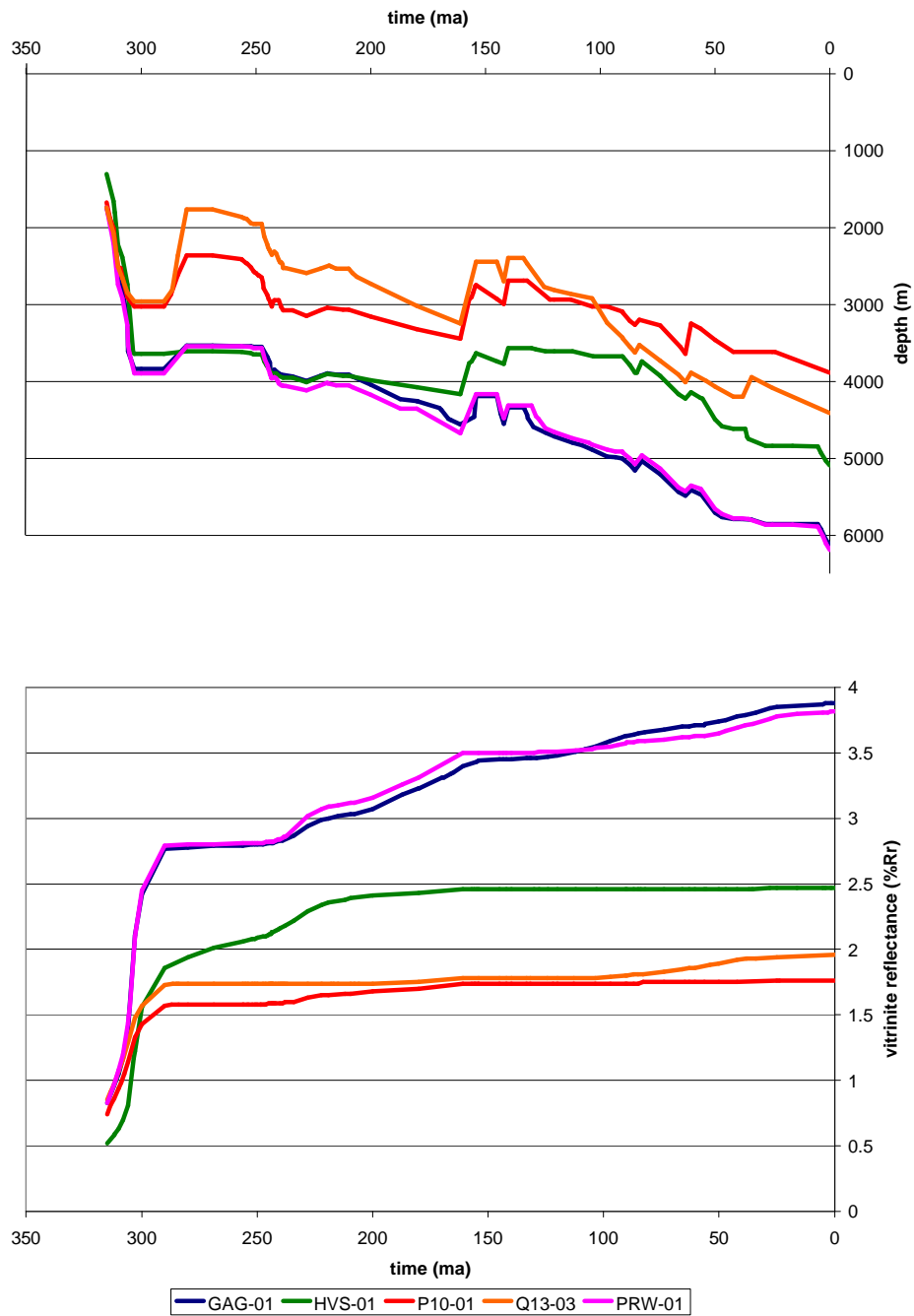


Figure H-2 a) burial history of wells GAG-01, HVS-01, PRW-01, P10-01 and Q13-03, which reached their deepest burial sub recent

b) virinite reflectance vs time plot of wells GAG-01, HVS-01, PRW-01, P10-01 and Q13-03; the wells show an sub recent increase in VR.

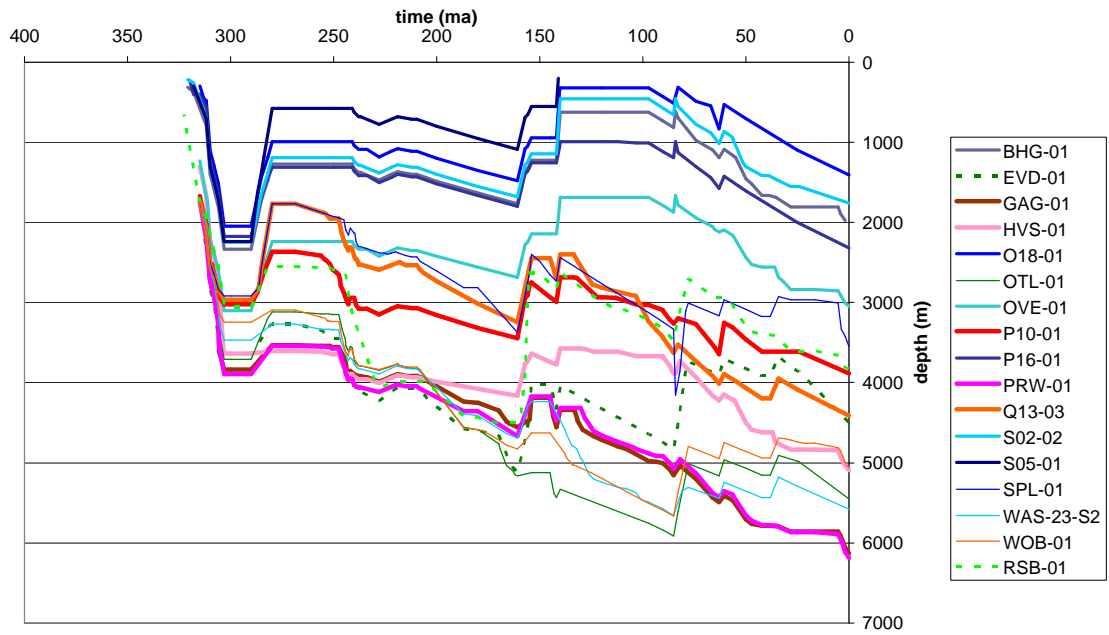


Figure H-3 Graphs for layer DCGE of all modelled wells in area 1. Blue lines (bold): wells reached deepest burial during Carboniferous. Red lines (bold) wells reached deepest burial sub recent, Green lines (bold and dashed) wells reached deepest burial during Jurassic. Thin lines of various colours: wells reached deepest burial during Cretaceous

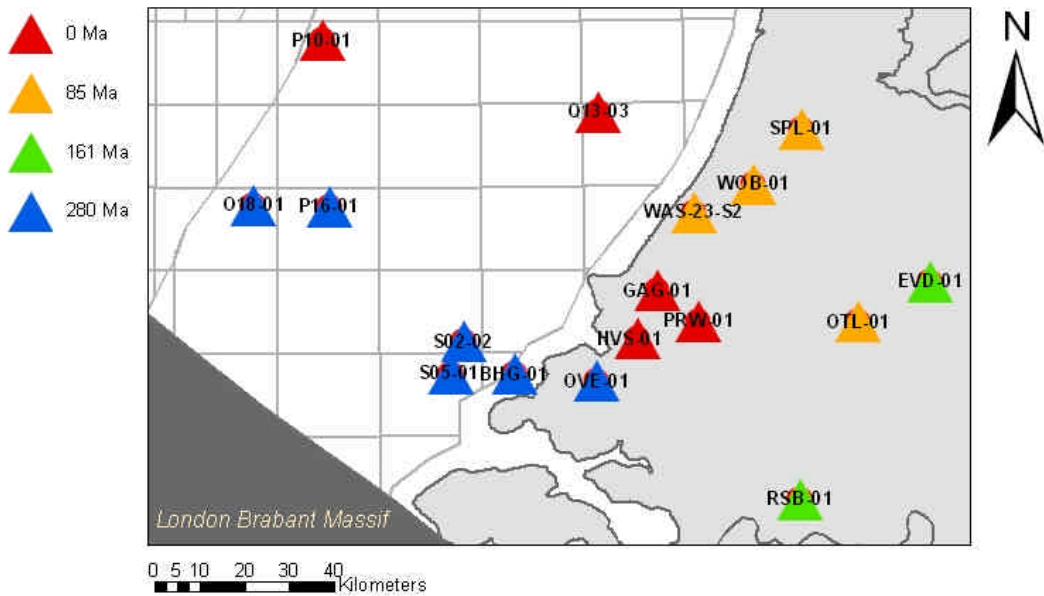


Figure H-4 Overview of the time period of maximum burial for the wells in area 1 as achieved from 1 D modelling

Area 2

Modelling study of selected wells from the A-, D- and E-blocks of the Dutch offshore revealed that the investigated wells have very similar burial histories, despite their position on different structural elements. Both the wells on the Elbow Spit High (A11-01, A14-01, A16-01, A17-01, E02-01, E02-02, E06-01) and in the adjacent structural low (D12-03, D15-02, E12-02, E12-03) are characterised by three important burial episodes (Figure H-5). These took place in the Upper Carboniferous, the Late Permian-Middle Jurassic and in the period since the latest Cretaceous until present-day. The continuous burial since the latest Cretaceous exceeded former burial and therefore determines the present day maturity of the source rocks. At present time it is subsided at the greatest depths (Figure H-6). The second most important burial event took place Late Permian to the Middle Jurassic.

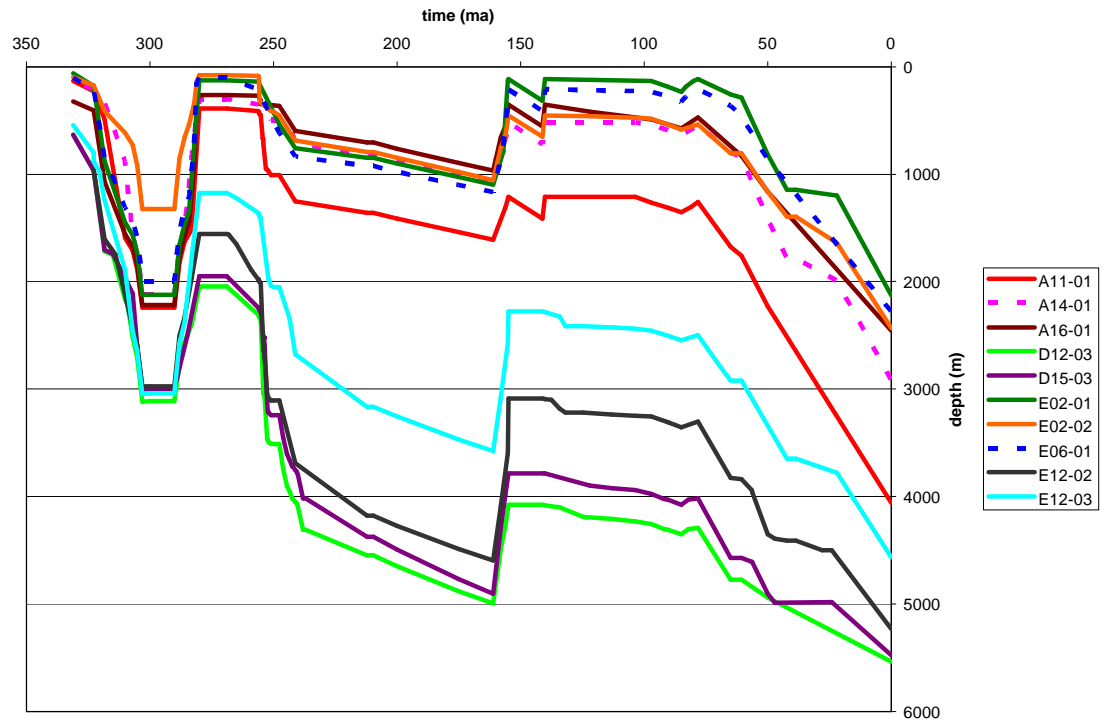


Figure H-5 Graph showing burial history of the Yoredale Formation (CFYD) of the Farnes Group (CF) for all modelled wells in area 2. The Wells situated on the Elbow Spit High show a high amount of erosion at the end of the carboniferous, the wells situated in the ‘Southern Permian Basin’ showing high amounts of sedimentation and erosion during the Mesozoic. Nevertheless, the wells reach their deepest burial at present

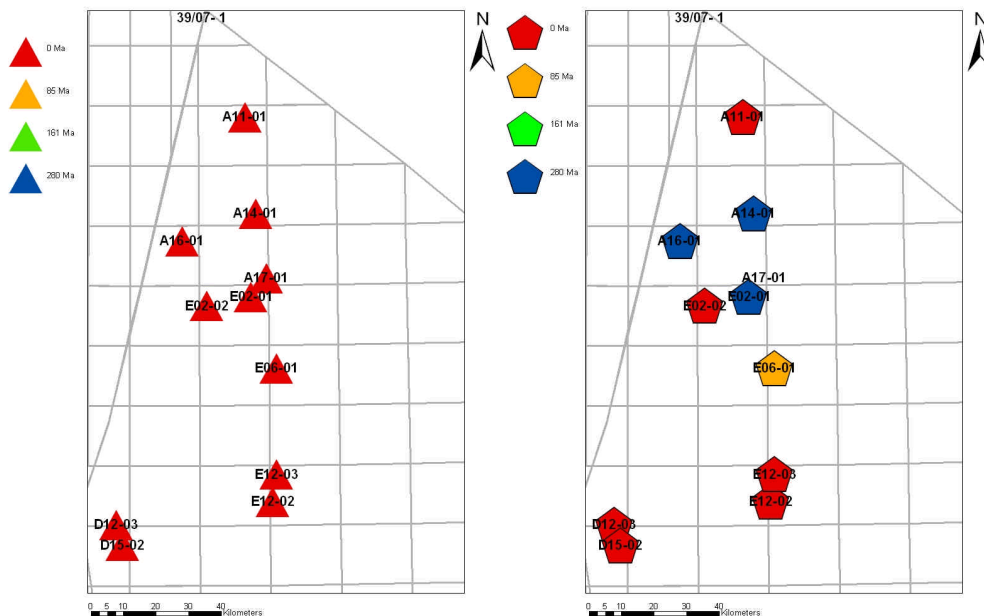


Figure H-6 Overview of the time period of maximum burial (left) and latest increase in maturity (right) for the wells in areas 2 as achieved from 1D modelling.

The effect of the burial history on the maturity does vary between the structural elements. In the centre of the Elbow Spit High the maturation reached its maximum already during Carboniferous, while towards the eastern and southern margins maturity is reaching its maximum at present day (Figure H-6). Here, the maturity is increasing since about 50 Ma, beginning at the Upper Cretaceous. This is due to a high sediment load, especially during the Tertiary.

The intrusions in wells A14-01 and E06-01 were included in the modelling. Intrusions give an additional heat pulse to the sediments, which may lead to an increase of the maturity. Only in well E06-01 higher values have been observed due to this intrusion (Figure H-7). The intrusion is dated to be of Jurassic age. The intrusion in well A14-01 has not been dated, but is modelled as being of Carboniferous age. The impact of the intrusion on the vitrinite reflectance of the Farne Group in well A14-01 is only minor.

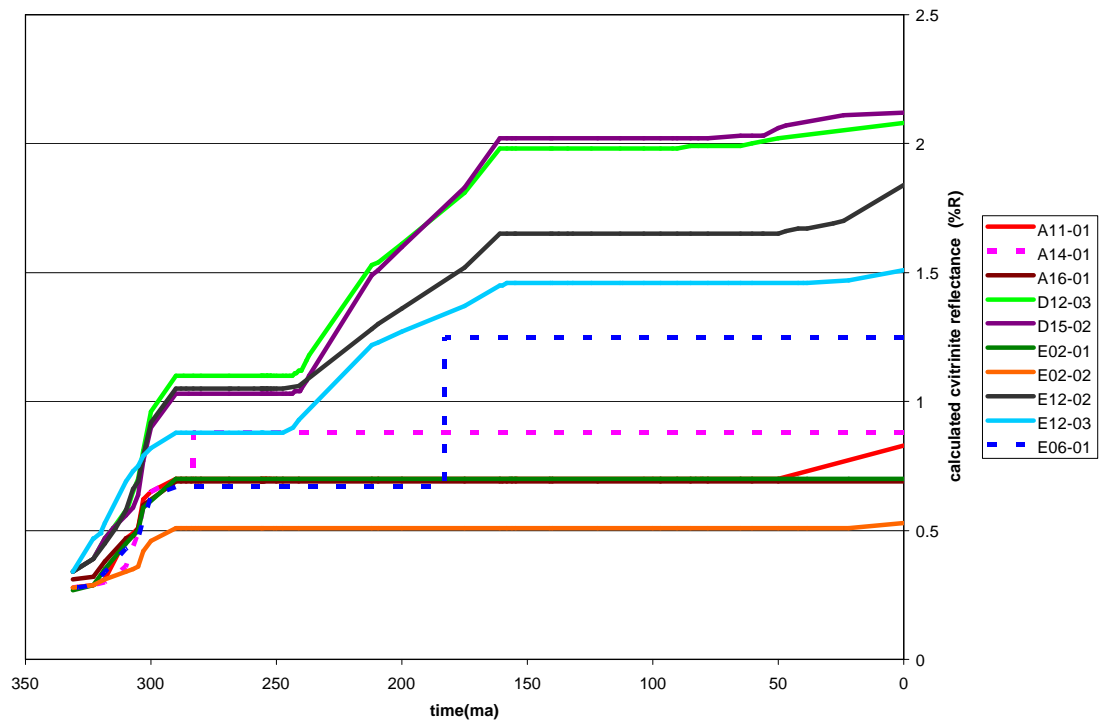


Figure H-7 vitrinite reflectance vs time plot of wells in area 2
 4 wells – D12-03, D15-02, E12-02 & E12-03 - located in the southern part of area 2 (Southern Permian Basin) show a continues increase in vitrinite reflectance during the past 50 million years, as well as 2 wells - A11-01 & E02-02 - the Northern part which are located at the margin of the Elbow Spit High. Wells A14-01, A16-01, E02-01 and E06-01 do not show any increase in vitrinite reflectance since the end of the . The strong increase in VR in wells A 14-01 and E06-01 is due to additional heating in relation to an intrusion. The intrusion in wel E06-01 is dated to be of Jurassic origin, the intrusion in well A14-01 has not be dated, but is modelled as Carboniferous age.

Area 3&4

The variation in burial history of different parts of Area 3&4 is very large (Figure H-8). 1D Modelling of the selected set of wells identified several regions in the area with comparable geological history. These regions correspond to the major structural elements in Area 3&4.

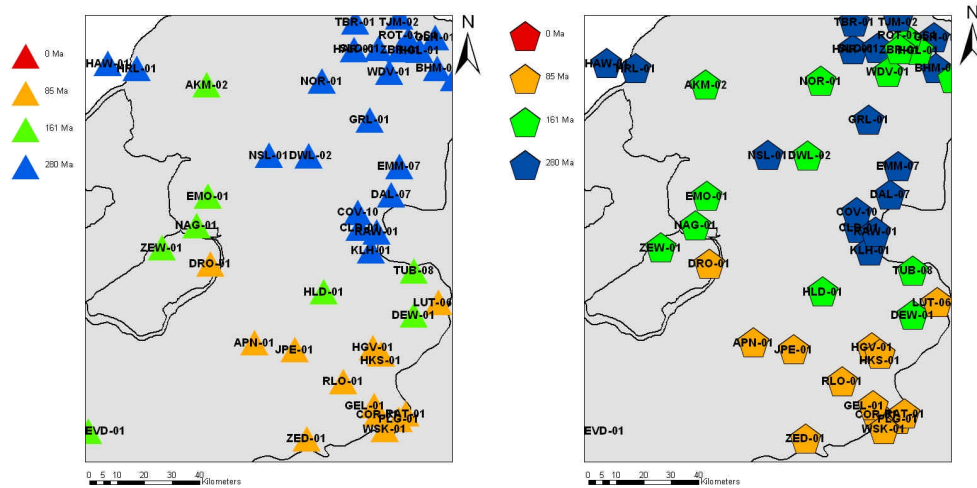


Figure H-8 Overview of the time period of maximum burial (left) and latest increase in maturity (right) for the wells in areas 3 and 4 as achieved from 1 D modelling. In the south of the area, deepest burial and latest increase in vitrinite reflectance occurred prior to the Subhercynian uplift. Area 3&4 are diagonally subdivided by a northwest-southeast trending zone which show deepest burial and latest increase in vitrinite reflectance already prior to the Late Kimmerian 1 phase.

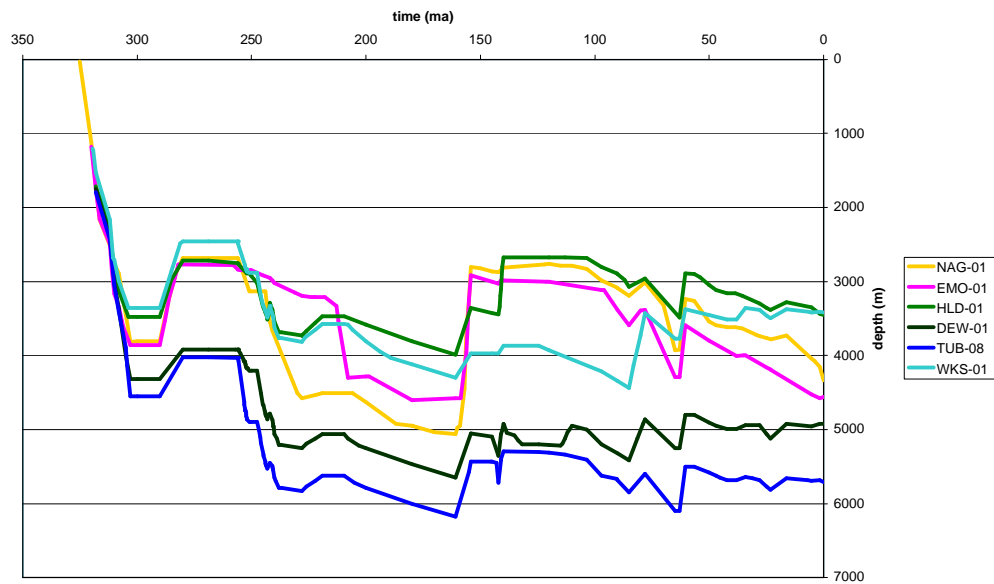
In order to present the results systematically and synoptically, the following division is maintained:

- Wells that reached deepest burial and latest increase in vitrinite reflectance during the Jurassic
- Wells that reached deepest burial and latest increase in vitrinite reflectance during the Cretaceous
- Wells that reached deepest burial at present-day, but latest increase in vitrinite reflectance during the Jurassic
- Wells that reached deepest burial and latest increase in vitrinite reflectance at present-day

Wells that reached deepest burial and latest increase of vitrinite reflectance during Jurassic or earlier

In the center of the area a northwest-southeast trending seem to occur with wells that reached their deepest burial and latest increase in vitrinite reflectance already in the Jurassic. The highest maturity in well Nagele-1 was already reached during the Jurassic at its deepest burial. The measured vitrinite reflectance can only be fitted with the assumption of a relatively high heat flow through time as well as a high heat flow during the Carboniferous (see below). Well Emmeloord-1 also shows relatively high vitrinite reflectance values at the top of the Carboniferous. The measured vitrinite reflectance values can only be fitted with the assumption of a relatively high (Carboniferous) heatflow (see below). There seems to be a relation with elevated heatflow, which could be attributed to a margin feature.

Well Winterswijk-1 reached its highest maturity already at the end of Triassic, in relation with the additional heat impulse of the intrusion.



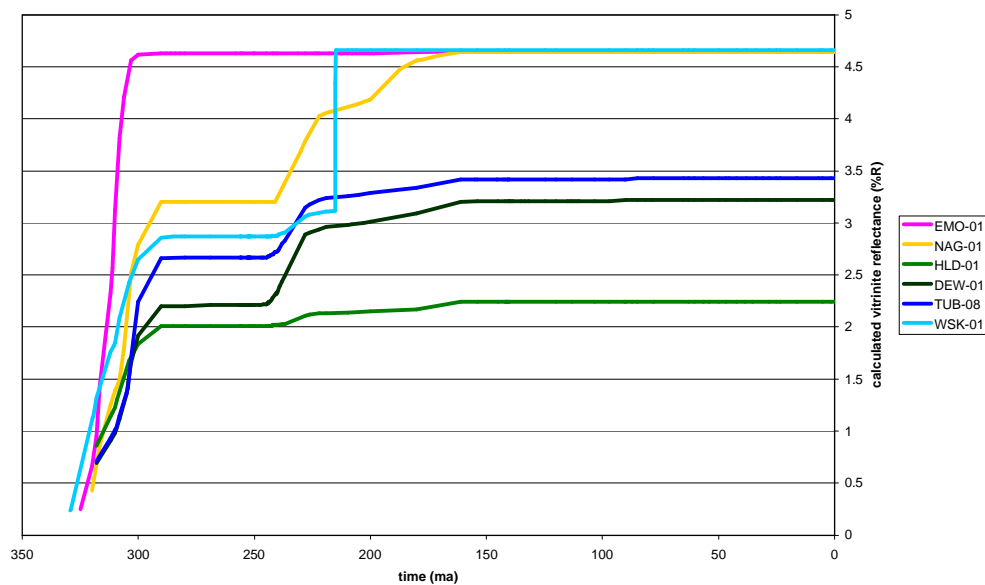


Figure H-9 Burial history diagrams (top) and calculated vitrinite reflectance vs. time (bottom) of a selection of wells in Area 3&4.

Wells that reached deepest burial and latest increase in vitrinite reflectance during the Cretaceous

Most of the wells that reached deepest burial and most important coalification phase during the Cretaceous are situated in the Central Netherlands Basin. Maximum burial was experienced shortly before the initiation of the Subhercynian phase (85Ma).

East of the area, well Münsterland-1 also reached deepest burial and latest increase in vitrinite reflectance during the Cretaceous. The maturity of the samples of the well have extensively be studied. Maturity was reached prior to the Subhercynian inversion, although others suggest a pre-Cretaceous maturation (Littke *et al.*, 2000). Latter is based on a coalification jump between Cretaceous and directly underlying Carboniferous strata.

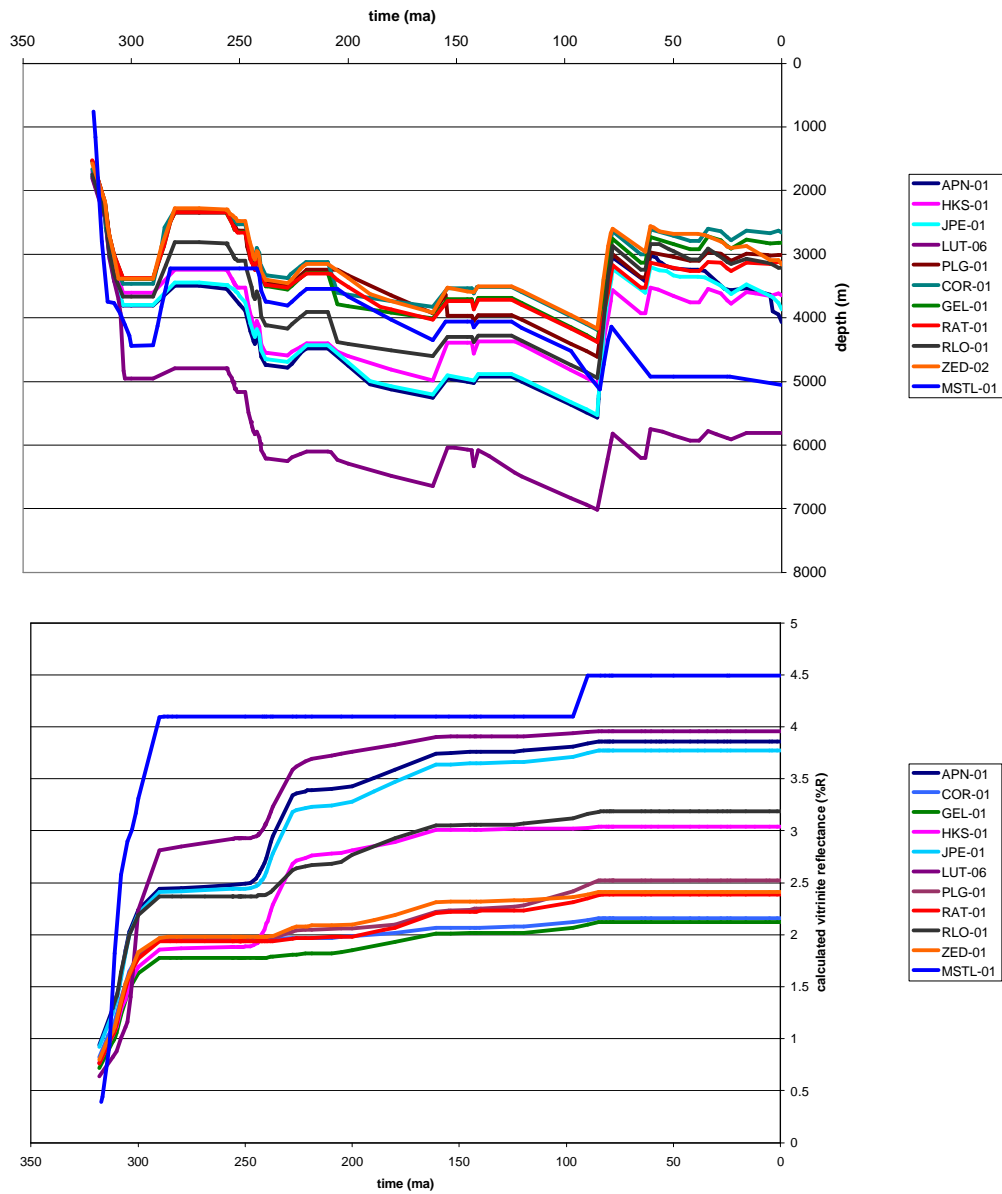


Figure H-10 Burial history diagrams (top) and calculated vitrinite reflectance vs. time (bottom) of a selection of wells in Area 3&4.

Wells that reached deepest burial at present-day, but latest increase in vitrinite reflectance during the Jurassic

The burial diagrams of the wells located mostly in the northern part of the area indicate that the present burial depth is the maximum burial depth. The burial of these wells is characterised by a very continues subsidence with only minor effects of inversion and erosion. During most of the geological history, this area has been either platform or

structural high. It is therefore assumed that Cenozoic tilting and subsidence resulted in the present maximum burial depth. Nevertheless, an increase in vitrinite reflectance can not be observed from the Jurassic onwards. This is probably due to the fact, that a heatflow trend through time has been applied with higher heatflow values during the Jurassic (in order to model Jura rifting). Present day temperatures and heatflows are too low to initiate a further increase in vitrinite reflectance (see below). Possibly this effect is also related to salt tectonic in this area.

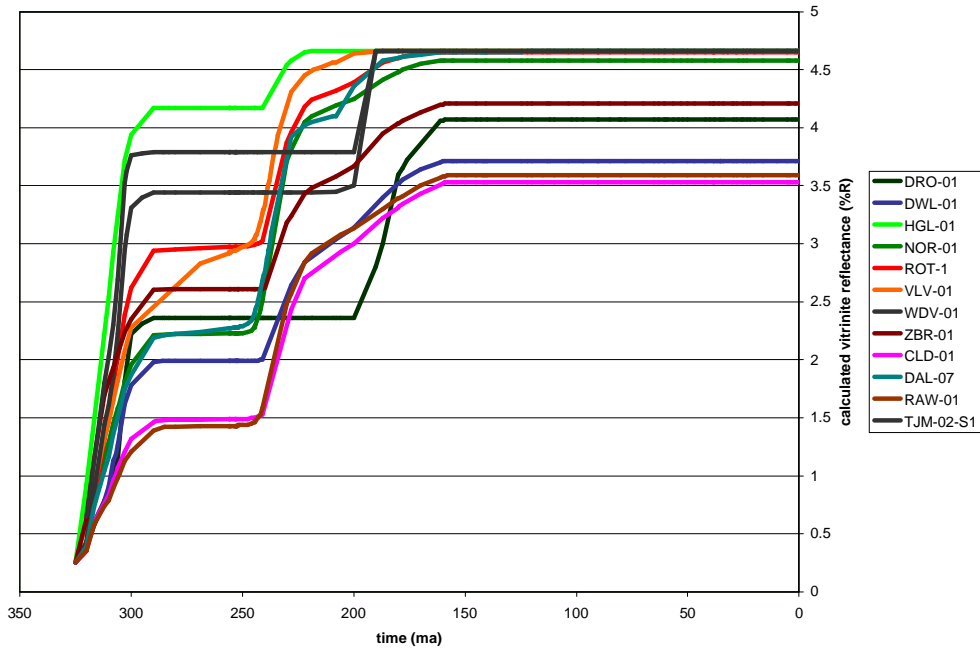
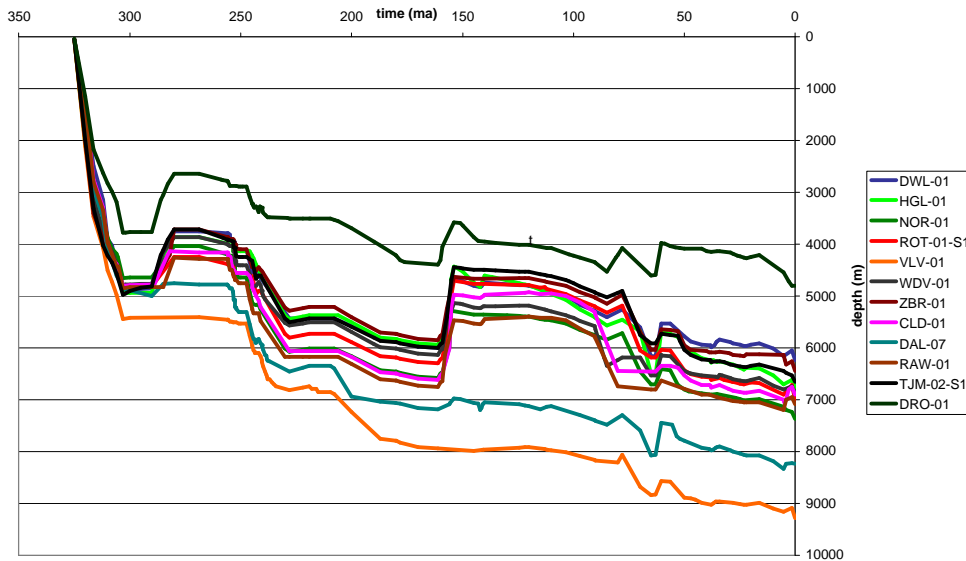
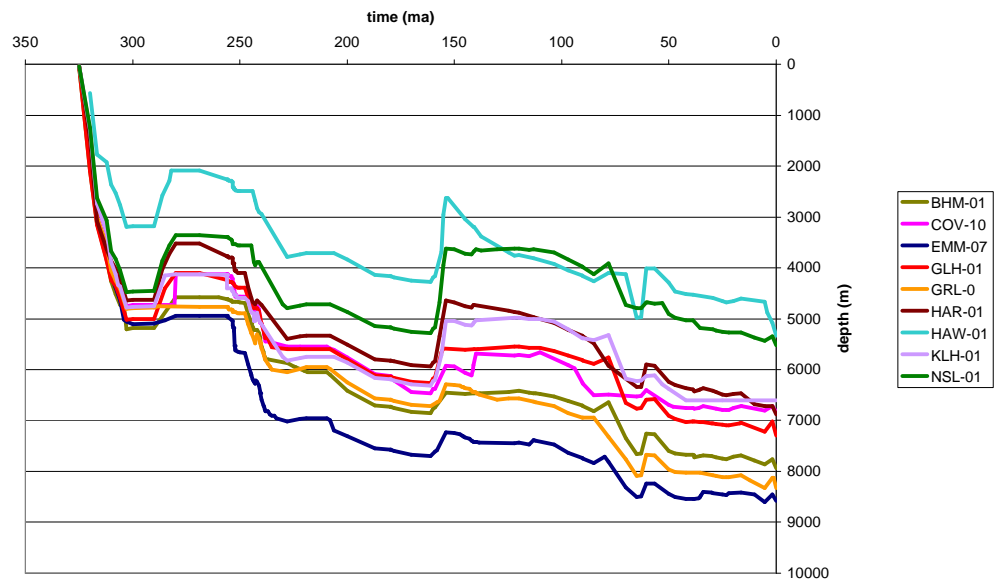


Figure H-11 Burial history diagrams (top) and calculated vitrinite reflectance vs. time (bottom) of a selection of wells in Area 3&4.

Wells that reached deepest burial and latest increase in vitrinite reflectance at present-day

Figure H-12 shows the burial history graphs of the wells which reach their deepest burial at present and where the vitrinite reflectance started to increase again during the past 50 Ma. The wells show a considerable sedimentation during Zechstein and Triassic and a moderate sedimentation during Jurassic times. Uplift occurred during the Late Kimmerian I phase. Further subsidence can be observed during Early Cretaceous, followed by an uplift during the Laramidan tectonic phase. This phase was followed by a continuous subsidence until present day – interrupted by minor tectonic phases. The onset of this subsidence phase resulted in the increase in vitrinite reflectance, which is still increasing to date.



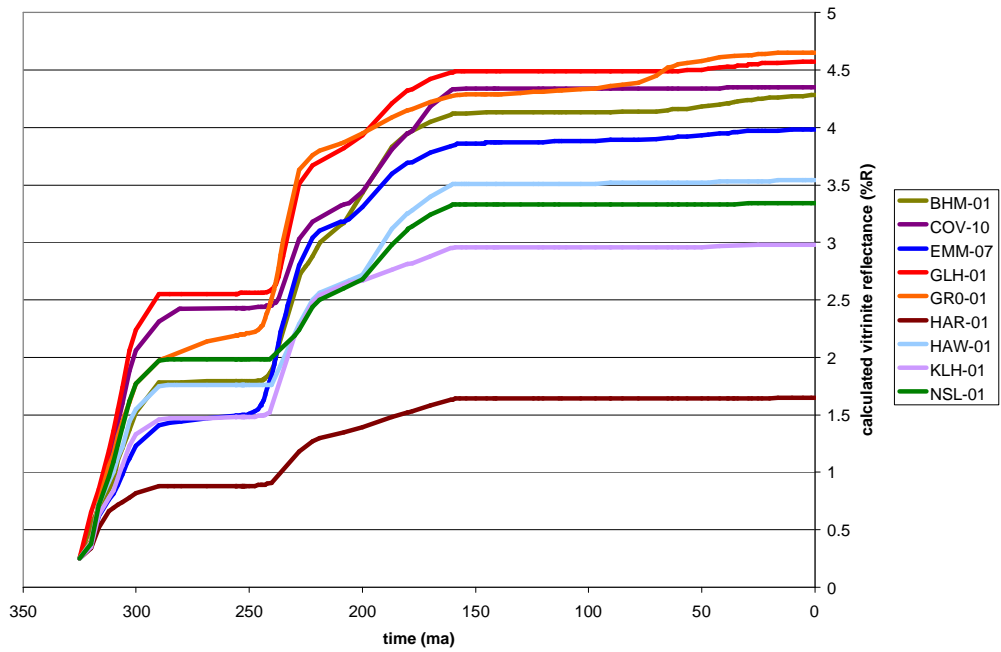


Figure H-12 Burial history diagrams (top) and calculated vitrinite reflectance vs. time (bottom) of a selection of wells in Area 3&4.

H2 Maps of erosion events

Area 1

Erosion maps have been contoured for the most prominent erosional phases in area 1, which are:

- Saalian, erosion of Carboniferous sediments (Figure H-13)
- Early Kimmerian, erosion of Triassic sediments (Figure H-14)
- Late Kimmerian 1, erosion of Altena sediments (Figure H-15)
- Late Kimmerian 2, erosion of Schieland sediments (Figure H-16)
- Subhercynian, erosion of Rijnland sediments (Figure H-17)
- Subhercynian, erosion of Chalk sediments (Figure H-18)
- Laramidian, erosion of Chalk sediments (Figure H-19)
- Pyrenean, , erosion of Noordzee sediments (Figure H-20)

Area 2

Erosional maps have been contoured for the most prominent erosional phases in area 2. Erosion grids were created based on the results of the 1D modelling. In the gridding procedure the gridding was constrained by the bounding faults of the structural elements in Area 2. Table H-1 gives an overview of the estimated amounts of deposition and erosion for the two major tectonic elements in area 2.

Table H-1 *Estimated thickness values of the eroded sediments during the Saalian and Late Kimmerian 1 phase*

Wells	Group symbol	Final estimation of thickness [m]
A11-01, A14-01, A16-01, A17-01, E02-01, E02-02, E06-01 – “high” area	AT	300
	RN	100
	RB	200 (150 when partly eroded)
	DC	1800
D12-03, D15-02, E12-02, E12-03 – “low” area	AT	500-600
	RN	400-500
	RB	500 (300 when partly eroded)
	DC	1000

Maps of the following erosional phases were made:

- Saalian, erosion of Carboniferous sediments (Figure H-21)
- Late Kimmerian 1, erosion of Trias sediments (Figure H-22)
- Late Kimmerian 1, erosion of Altena sediments (Figure H-23)
- Late Kimmerian 2, erosion of Schieland sediments (Figure H-24)
- Subhercynian, erosion of Chalk sediments (Figure H-25)

Area 3&4

One of the main results of the modelling in this area was the quantification of the effect of the heat flow. It was concluded that the heat flow history was dominant over the effects of erosion. In order to fit the model to the calibration data, it was chosen to fix the assumed amounts of erosion to the values that were based on the geological conceptual model. Erosion grids were created based on the input of the 1D modelling.

Erosion maps have been contoured for the most prominent erosional phases in area 3, which are:

- Saalian, erosion of Carboniferous sediments (Figure H-26)
- Late Kimmerian 1, erosion of Triassic sediments (Figure H-27)
- Late Kimmerian 1, erosion of Altena sediments (Figure H-28)
- Late Kimmerian 2, erosion of Schieland sediments (Figure H-29)
- Subhercynian, erosion of Rijnland sediments (Figure H-30)
- Subhercynian, erosion of Chalk sediments (Figure H-31)
- Laramidian, erosion of Chalk sediments (Figure H-32)
- Pyrenean, erosion of Noordzee sediments (Figure H-33)

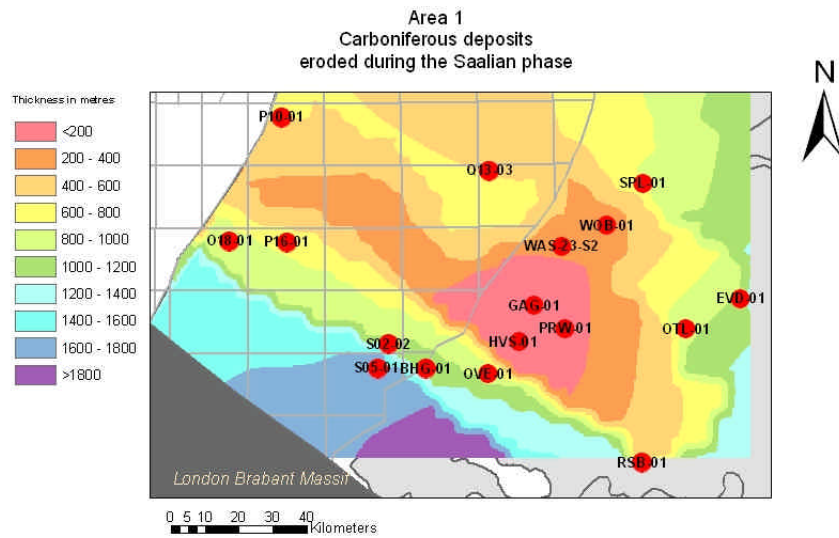


Figure H-13 Map of the eroded thickness of sediments by the Saalian erosion in Area 1. The Saalian erosion had the greatest impact on the London Brabant Massif. The map shows the total erosion of Hunze, Dinkel, Maurits, Ruurlo and Baarlo Formation. The erosion amount of these Formations on the London Brabant Massif is about 2000 m and decreases towards the northeast. In the West Netherlands Basin the estimated amount of erosion is with about 200 m low. In some wells the Saalian phase even eroded the Epen Formation and part of the Zeeland Group (e.g. in well S05-01). Due to the lack of data (only few wells penetrated these formations) no maps have been constructed for those Formations.

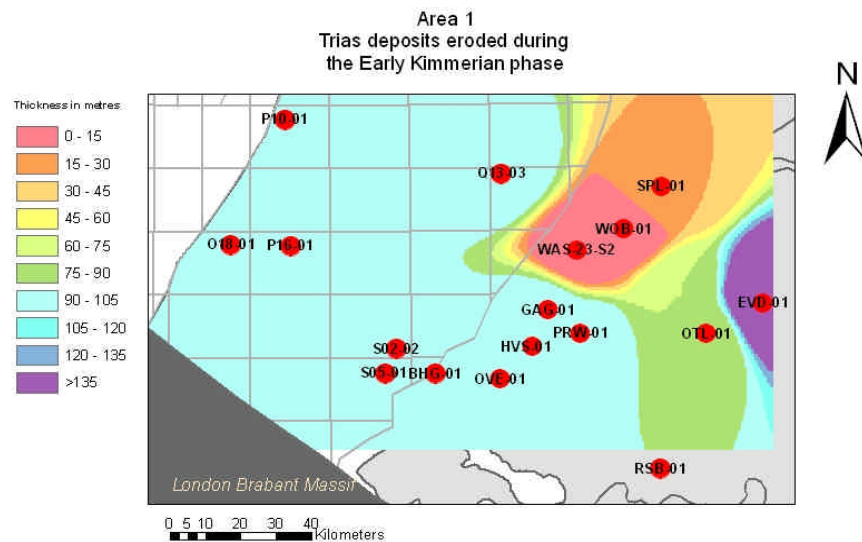


Figure H-14 Map of the eroded thickness of sediments by the Early Kimmerian erosion in Area 1. The early Kimmerian phase was of minor influence and eroded about 250 m in the western part of the area.

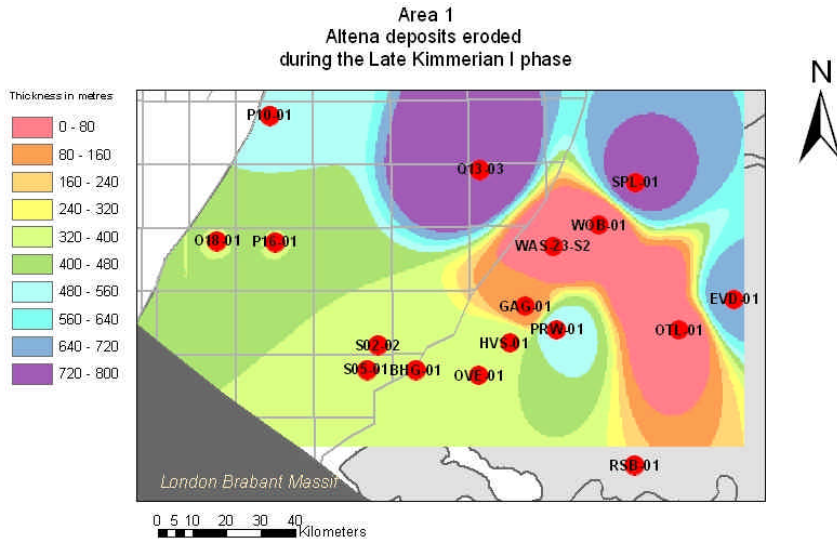


Figure H-15 Map of the eroded thickness of sediments by the Late Kimmerian 1 erosion in Area 1. The Late Kimmerian 1 phase had great impact in area 1 and eroded up to 850 m in the northern part of the area.

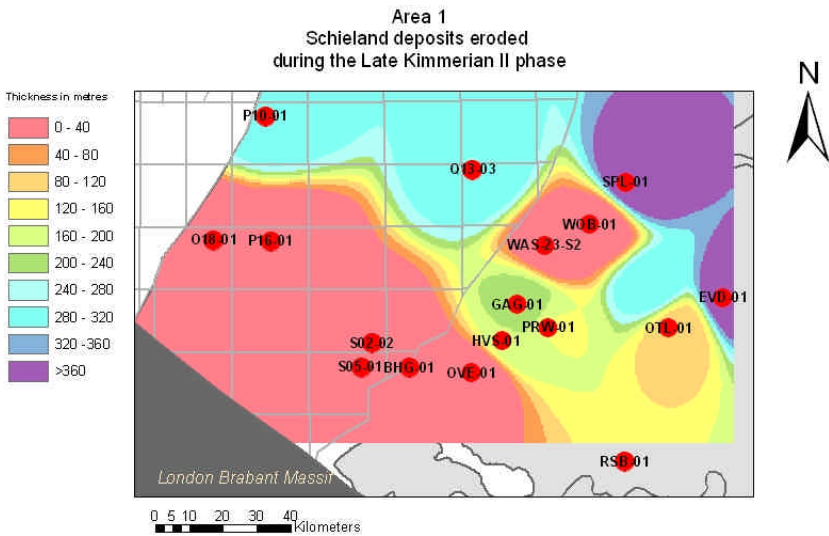


Figure H-16 Map of the eroded thickness of sediments by the Late Kimmerian 2 erosion in Area 1. The Late Kimmerian 2 phase eroded the lower part of the Schieland Group to an extent of about 300 m of sediments in the northern part of the area.

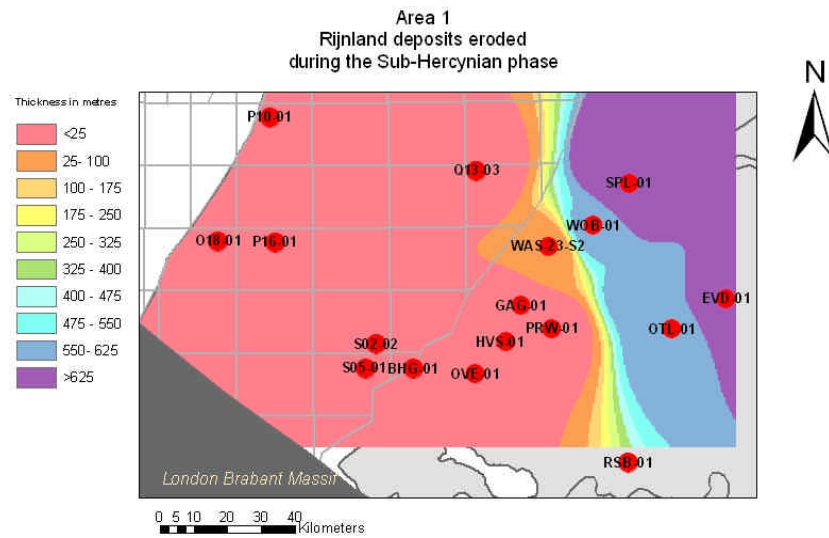


Figure H-17 Map of the eroded thickness of sediments by the Subhercynian erosion in Area 1. In the eastern part of area 1 the Subhercynian phase eroded up to 800 m of amounts of the Rijnland Group.

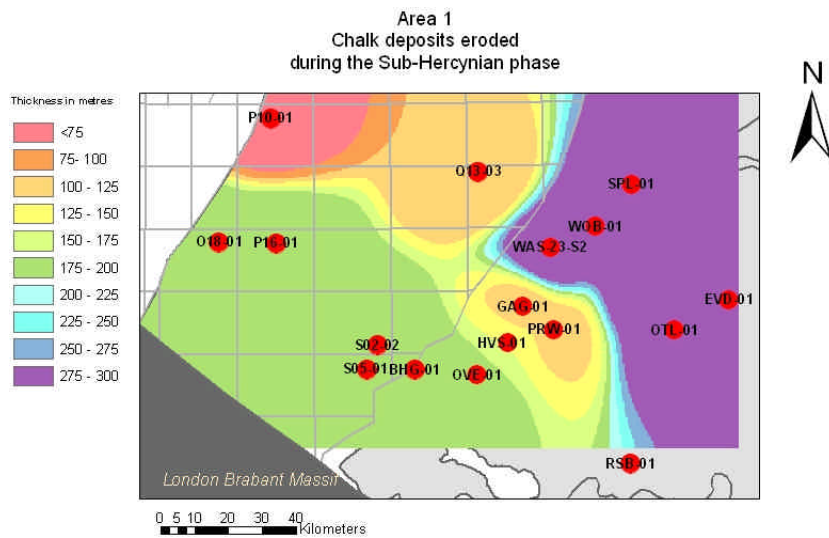


Figure H-18 Map of the eroded thickness of sediments by the Subhercynian erosion in Area 1. The Subhercynian phase eroded the lower part of the Chalk group. The impact of this erosional phase was greatest in the eastern and south-western part of the area where between 200 – 300 m of Chalk have been eroded.

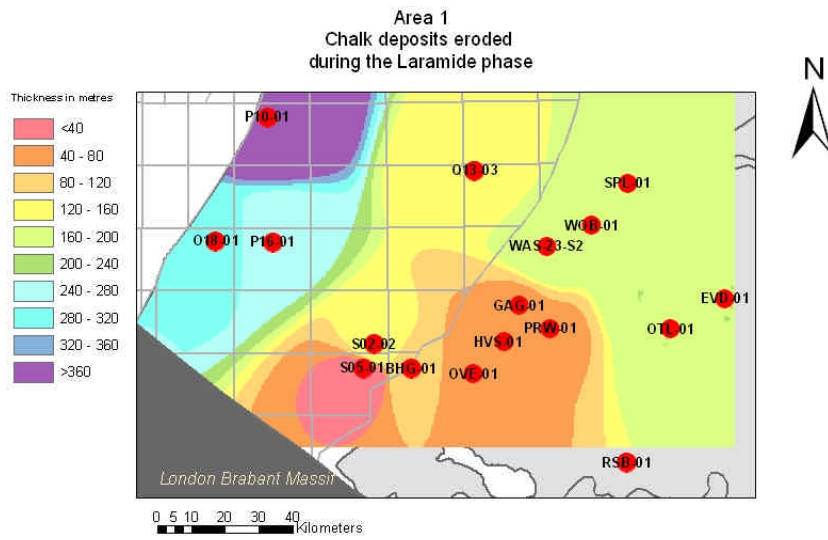


Figure H-19 Map of the eroded thickness of sediments by the Laramidian erosion in Area 1. Laramidian phase eroded the upper part of the Chalk Group in this area and was most active in the north-western part of area 1. Here about 450 m of sediments were eroded. Erosion decreases towards the southeast.

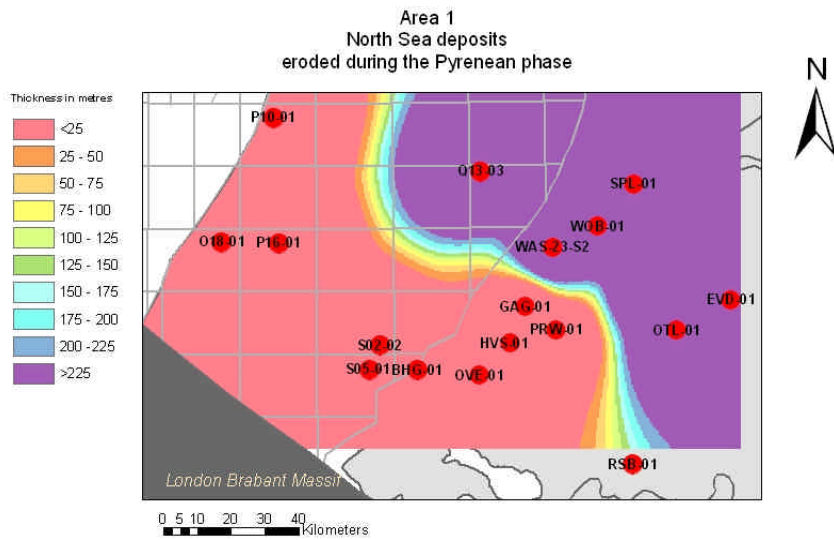
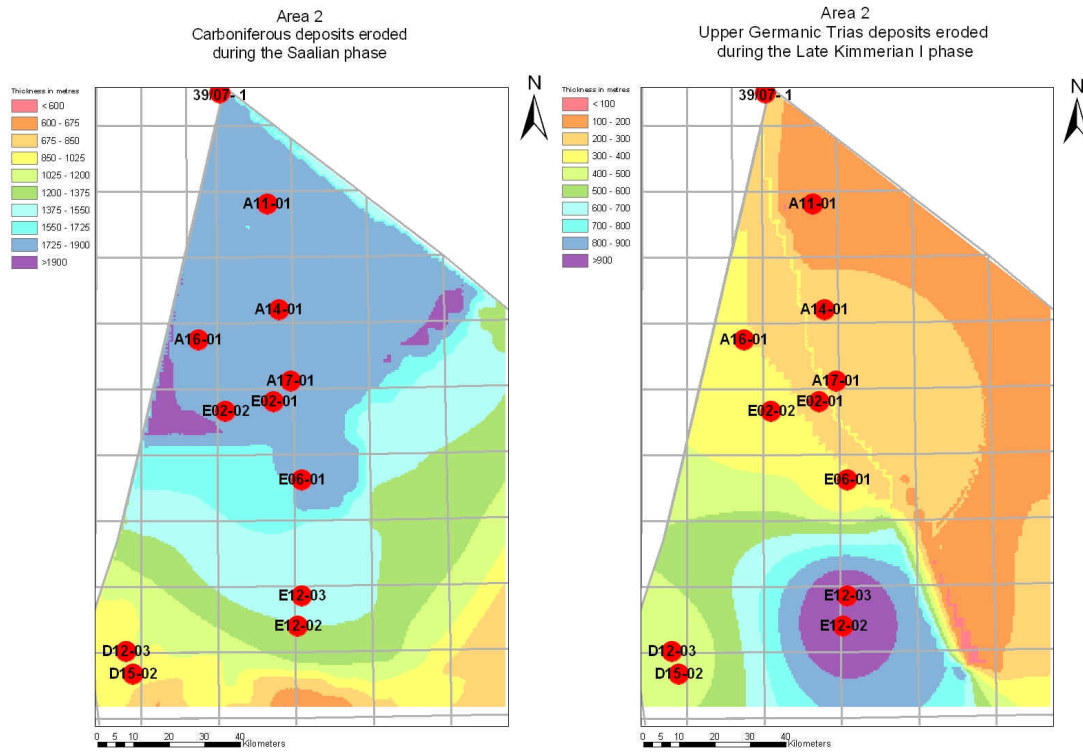


Figure H-20 Map of the eroded thickness of sediments by the Pyrenean erosion in Area 1. The Pyrenean erosion in area 1 was active in the north-eastern part, where about 250 m of sediments have been eroded.



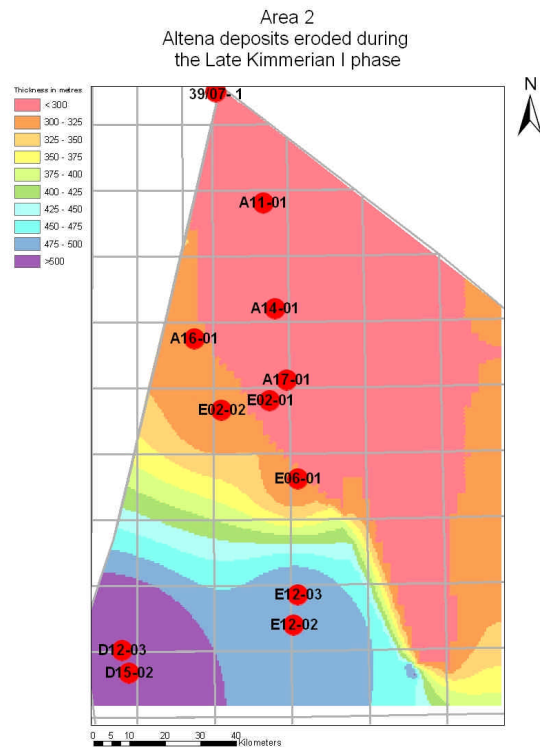


Figure H-21 Map of the eroded thickness of sediments by the Saalian erosion in Area 2. The Saalian phase was on of the major tectonic phase in the area and eroded up to 1850 m of the Limburg Group (Hunze t/m Baarlo) in the northern part of the area. Towards the south, the amount of erosion decreases. In wells E12-02 and E12-03, ca. 1400 m have been eroded and in well D15-03 and 13-02 about 1000 m.

Figure H-22 Map of the eroded thickness of sediments by the Late Kimmerian 1 erosion in Area 2. The Late Kimmerian 1 phase was of importance in area 2 and eroded 500 m Jurassic (AT) in the southern part of area 2.

Figure H-23 Map of the eroded thickness of sediments by the Late Kimmerian 1 erosion in Area 2. The Late Kimmerian 1 phase was of importance in area 2 and eroded 500 m Triassic in the southern part of area 2.

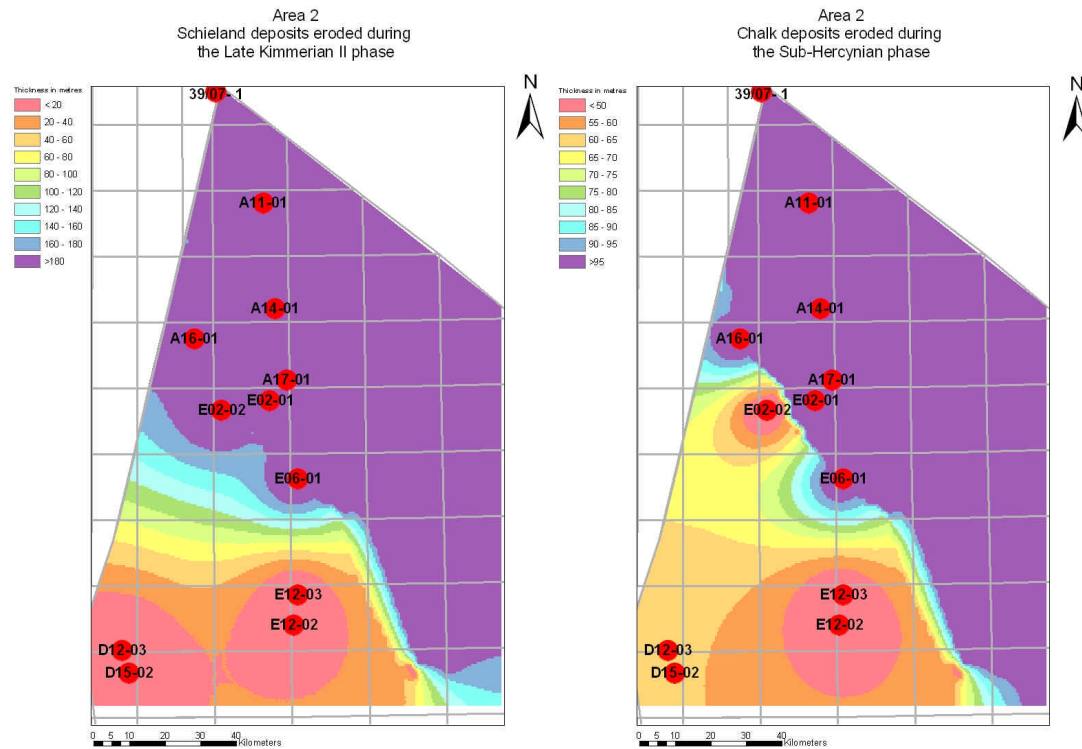


Figure H-24 Map of the eroded thickness of sediments by the Late Kimmerian 2 erosion in Area 2. The lower part of the Schieland group was eroded by the Late Kimmerian 2 phase which eroded about 200 m of sediments in the northern part of the area.

Figure H-25 Map of the eroded thickness of sediments by the Subhercynian erosion in Area 2. The Subhercynian phase was only of minor influence in area 2. In the north eastern part about 100 m of Chalk have been eroded. In the southern part, only ca. 50 m have been removed by the Subhercynian event.

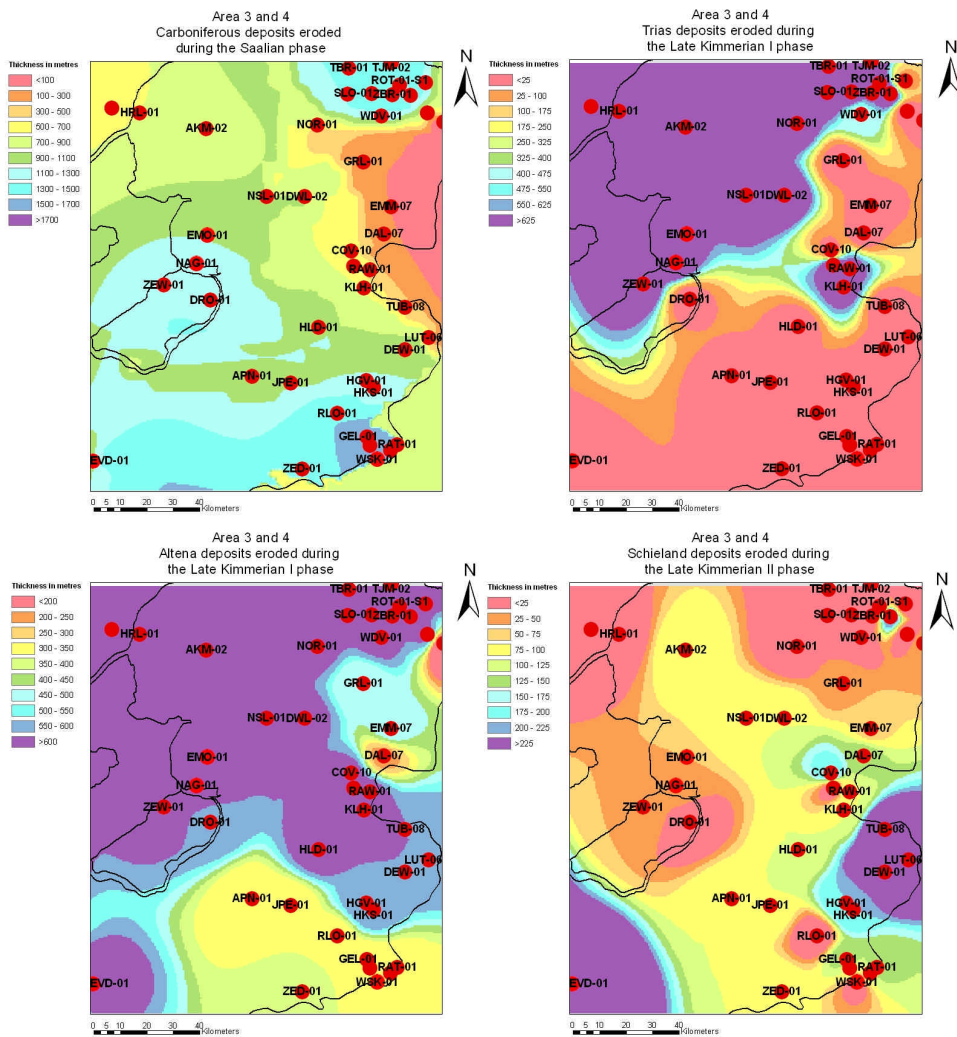


Figure H-26 Map of the eroded thickness of sediments by the major Saalian erosion in Area 3&4. Up to 1600 m of the Limburg Group (Hunze to Baarlo) were eroded. The highest uplift occurred in the north around well TJM-02-S1 and in the south around well DRO-1. Towards the east and west the amount of erosion decreased to about 600 – 700 m. The greatest uplift in the south eastern part was 1600 m.

Figure H-27 Map of the eroded thickness of sediments by the important Late Kimmerian 1 erosion in Area 3&4. Up to 750 m of Triassic were eroded in the north, and in the south only small amounts of Triassic has been eroded.

Figure H-28 Map of the eroded thickness of sediments by the important Late Kimmerian 1 erosion in Area 3&4. Up to 600 m of Jurassic (AT) was eroded in the north, and about 300 m in the south.

Figure H-29 Map of the eroded thickness of sediments by the Late Kimmerian 2 erosion in Area 3. The Late Kimmerian 2 phase was only of minor importance in Area 3&4 and eroded about 100 m of Upper Jurassic sediments.

"Hydrocarbon potential of the Pre-Westphalian in the Netherlands on- and offshore"

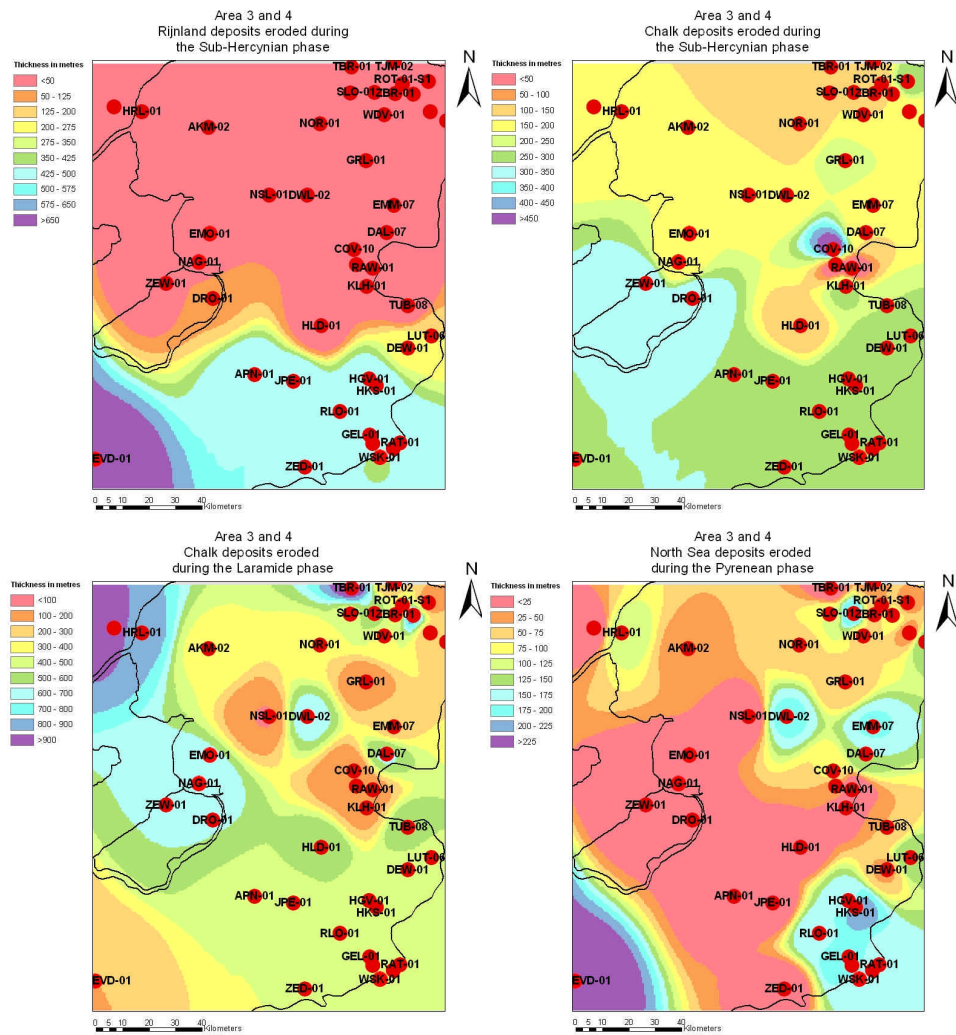


Figure H-30 Map of the eroded thickness of sediments by the important Subhercynian erosion in Area 3&4. The uplift induced by this tectonic event was about 800 – 900 m and about 600 m of Lower Cretaceous was removed as well as about 300 m of Chalk. In area 3 the Subhercynian phase eroded between 100 an 200 m of Chalk

Figure H-31 Map of the eroded thickness of sediments by the important Subhercynian erosion in Area 3&4. About 300 m of Chalk in the north and about 100 to 200 m of Chalk in the south were removed.

Figure H-32 Map of the eroded thickness of sediments by the Laramidian erosion in Area 3&4. The Laramidian phase eroded about 450 m of Chalk in the southern part. The influence of the Laramidian phase is low in the central part, but at the margins (around wells Nagele-1 in the south and wel TJM-02-S1 in the north the Laramidian uplift caused the erosion of about 600 to 1000 m of Chalk.

Figure H-33 Map of the eroded thickness of sediments by the Pyrenean erosion in Area 3&4.

H3 Heat flow maps

The assumed heat flow as described in the input (after Van Balen *et al.*, 2000) gave satisfying calibration results for Areas 1 and 2. This model assumes a slightly higher heatflow at the beginning of Jurassic, due to the occurring of rifting. In Area 3&4, it appeared that heat flows were required that varied both in time and per location.

Area 3&4

It was assumed that the geological model, including the amounts of erosion, was valid in Area 3&4. This implied that, in order to get a fit with the calibration data, the heatflow values had to be changed compared to the assumptions in Areas 1 and 2. Especially in the area 3 around wells Nagele-1 and Emmeloord-1 a high Carboniferous heatflow had to be assumed.

Based on the results of the 1D modelling, heat flow maps were constructed for different time periods, i.e. 250, 222, 90, and 0 Ma (Figures H-34 to H-37). These maps served as input to the 3 D model of Area 3&4.

"Hydrocarbon potential of the Pre-Westphalian in the Netherlands on- and offshore"

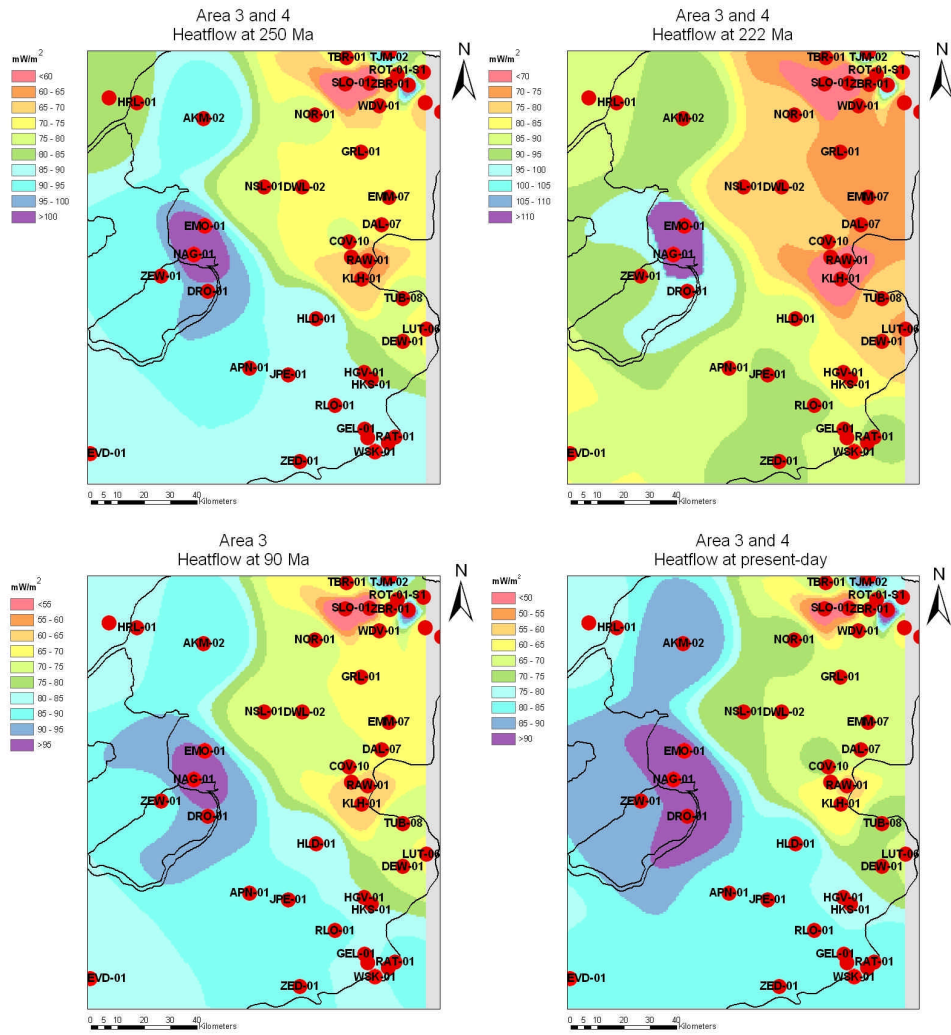


Figure H-34 Map of the heat flow values in Area 3 at 250 Ma.

Figure H-35 Map of the heat flow values in Area 3 at 222 Ma.

Figure H-36 Map of the heat flow values in Area 3 at 90 Ma.

Figure H-37 Map of the heat flow values in Area 3 at present-day.

I Results of the 3-D basin modelling

II Area 1

Burial history reconstruction

The burial history reconstruction is described in Chapter 4.

Maturation

The calculated vitrinite reflectance of the organic matter of the Geverik Member increases from 0.5 %R on the London Brabant Massif to almost 5 % in the centre of the West Netherlands Basin. The calculated vitrinite reflectance increases rapidly at the margin of the London Brabant Massive (Figures I-1 and I-2).

Timing of Hydrocarbon generation

Most of the hydrocarbons have been generated at the end of the Carboniferous (see Figure 4.6, Chapter 4). Nevertheless, generation and expulsion took also place during the Tertiary. According to the vitrinite reflectance data the transformation ratio of the Geverik Member varies between 0 % on the London Brabant Massif to 100 % in the West Netherlands Basin as can be seen in the maps of Appendix J. The small intermediate zone can be observed, where the transformation ratio varies between 30 and 80 % (Figure I-3). A recent increase in the last 65 Ma can be observed in a small region of Area 1 in the vicinity of the boundary fault. It seems that in the northern part of the area a major increase occurs between 60.5 and 23 Ma from 39 to 53 %. Between 23 Ma and present only a minor increase in the transformation ratio to 60 % can be observed. In the southern part of the region around well Brouwershavense Gat-1 the increase in the transformation ratio between 65 and 23 Ma is less prominent (from 25 to 36 %), whereas the transformation ratio increases to 50 % in the recent 23 Ma.

This indicates that there is a small zone in Area 1 where recent transformation of organic matter to hydrocarbons has taken place.

An overview of the transformation ratio through the geological time is given in Figure I-4.

Depending on the chosen type of kinetics, the area with a range in transformation ratio between 30 and 80 changes slightly as can be seen in Fig. I-5. The blue isolines show the area according to the kinetics of Burnham 1989, the green isolines show the area according to the kinetic of Tissot et al. 1988, the yellow area shows the area according to the multi-kinetic approach of Espitalie et al. 1988. Obviously, the Tissot and the Espitalie multicomponent kinetics start to generate at higher temperatures, therefore the area of transformation is moved to the east toward the West Netherland Basin. As can be seen by the scale in the figure, the spatial variation of hydrocarbon generation in relation to the chosen kinetics varies between 10 km in the southern part and 40 km in the northern part.

Migration and Accumulation

N.B: Due to the grid size of individual cell and the general scope of the study, it has to be noted that the description of accumulations are only *indicative* for possible pathways and formed reservoirs. In order to get more reliable descriptions, the grid needs to be refined.

Expulsion of hydrocarbons already started during Carboniferous in the eastern part of the basin, as can be seen in Fig. I-6. During Zechstein, the kitchen moves towards the north and start to fill reservoirs from there as well, and until present day, the kitchen moves further towards the Northeast. While temperature is rising, the early generated hydrocarbons are cracked, migrate further upwards and get possible lost during erosional phases.

At present day, accumulations are concentrated at a small line along the London Brabant Massif (Fig. I-7). It seems that most of the early generated accumulations have disappeared, also traces can possibly be found in existing reservoirs.

Hydrocarbons generated at a later stage could have been trapped in pre-Westphalian reservoirs. However, the grid size of the current model does not allow to trace smaller accumulations which have possibly generated during the Tertiary.

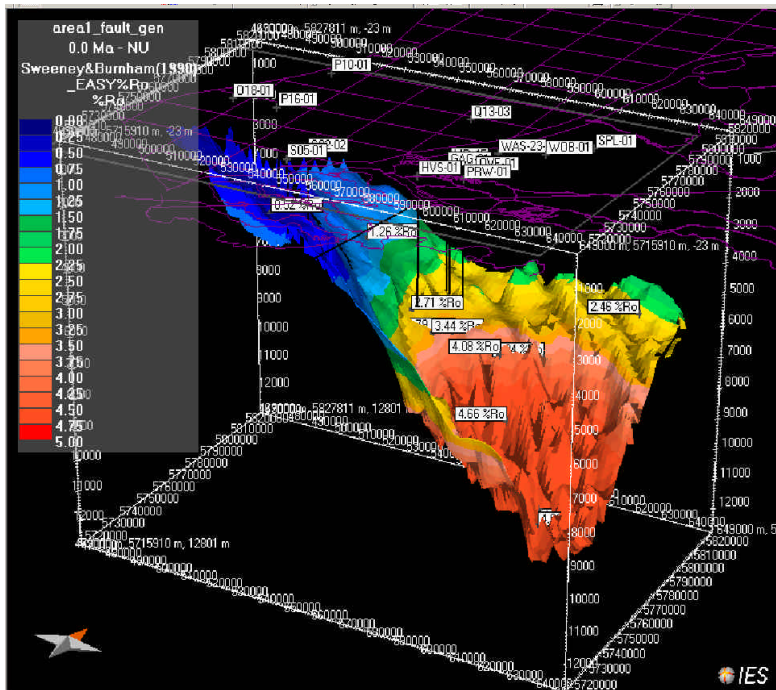


Figure I-1 3D view of the calculated vitrinite reflectance of the Geveik Member (after Sweeney & Burnham, 1990)

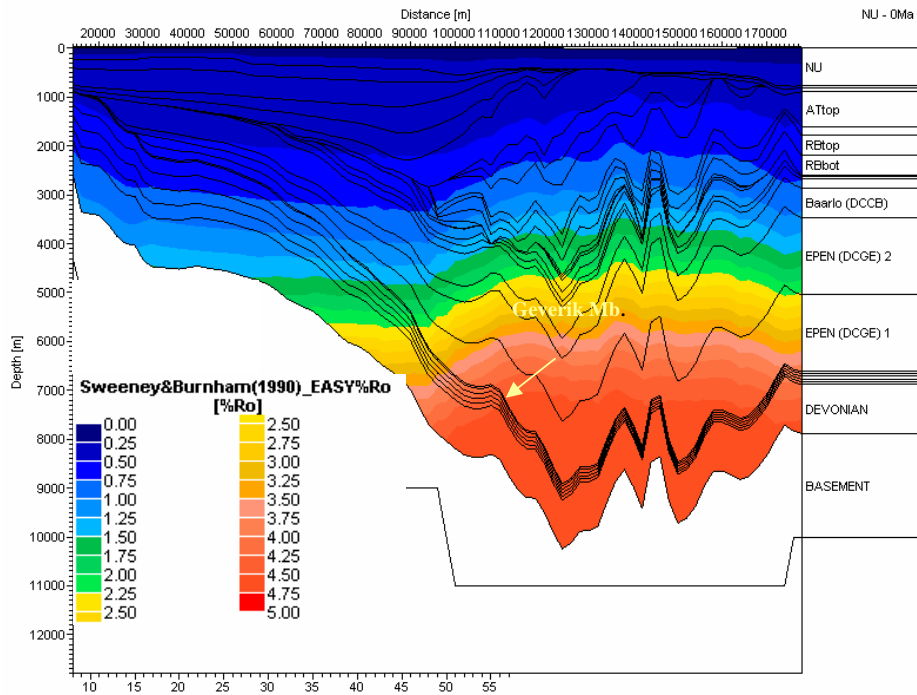


Figure I-2 Profile A-A' of calculated vitrinite reflectance after Sweeney & Burnham, 1990 at present day.

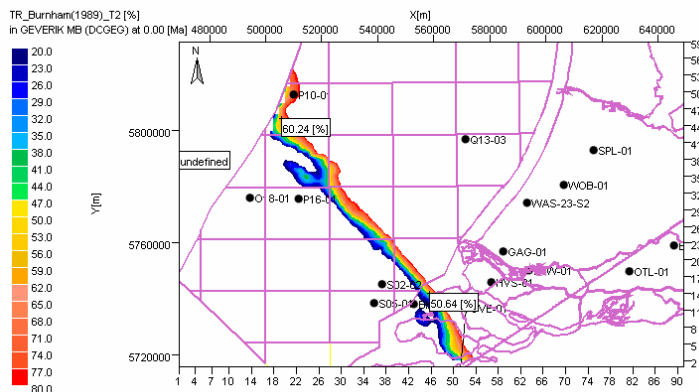
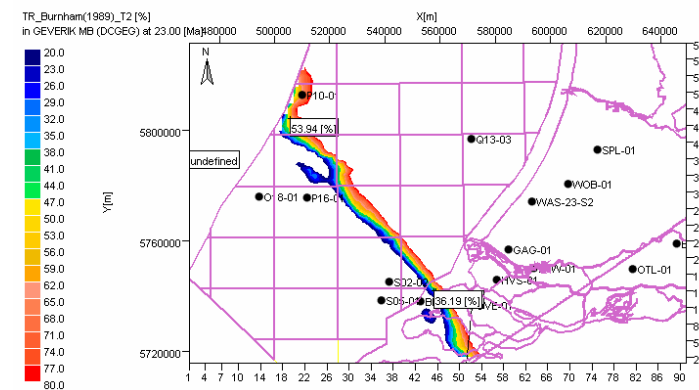
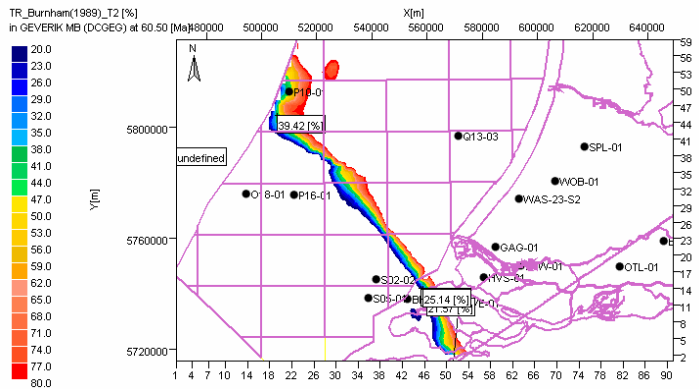


Figure I-3 Transformation ratio of the Geverik Member at 60.5, 23 and present – only values between 20 and 80 % are shown (Burnham 1989_T2 kinetics). (The transformation ratio measures the extent to which the genetic potential of the source rock has been effectively realized)

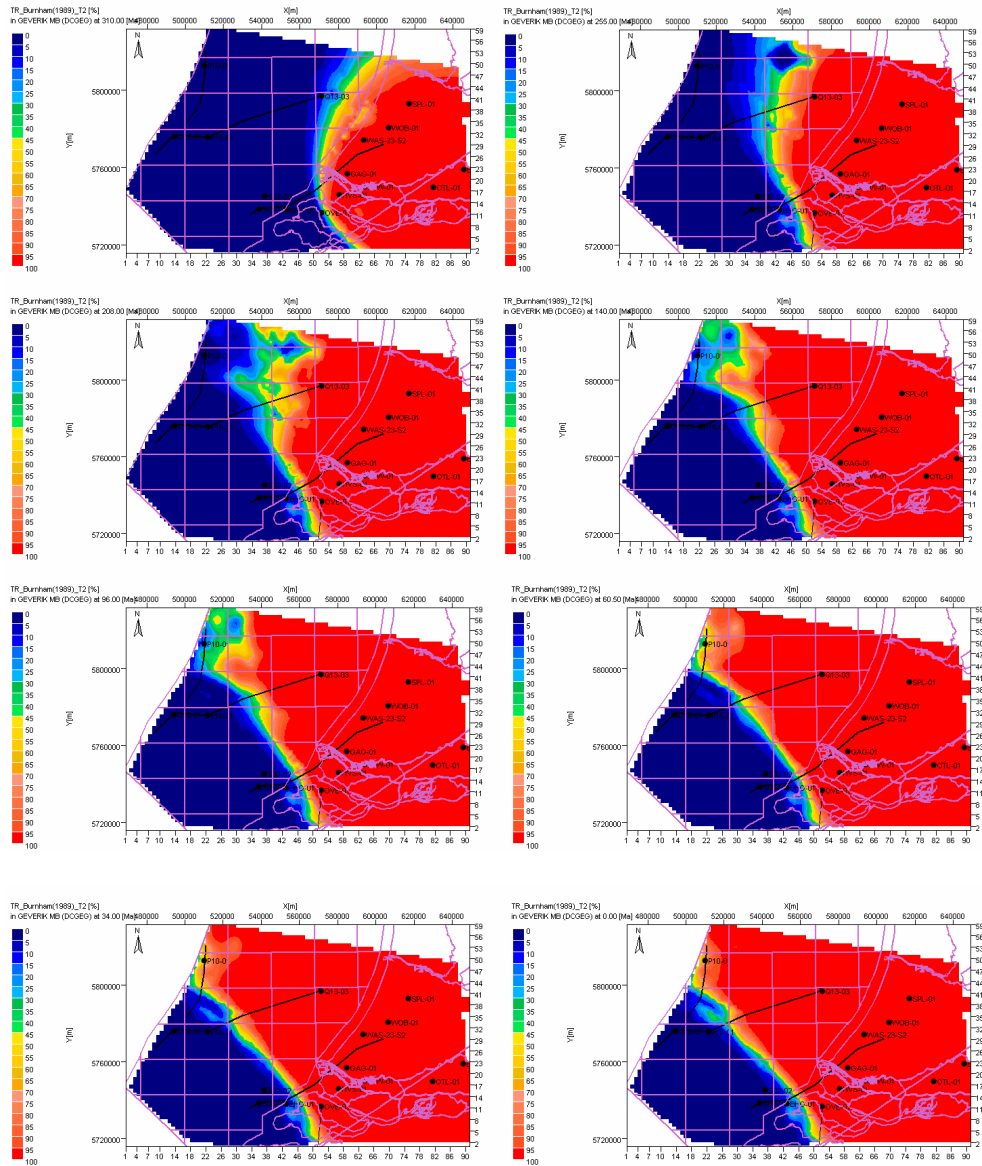


Figure I-4 a – h Transformation ratio through time

- a) 310 Ma
- c) 208 Ma
- e) 96 Ma
- g) 34 Ma

- b) 255 Ma
- d) 140 Ma
- f) 60.5 Ma
- h) 0 Ma

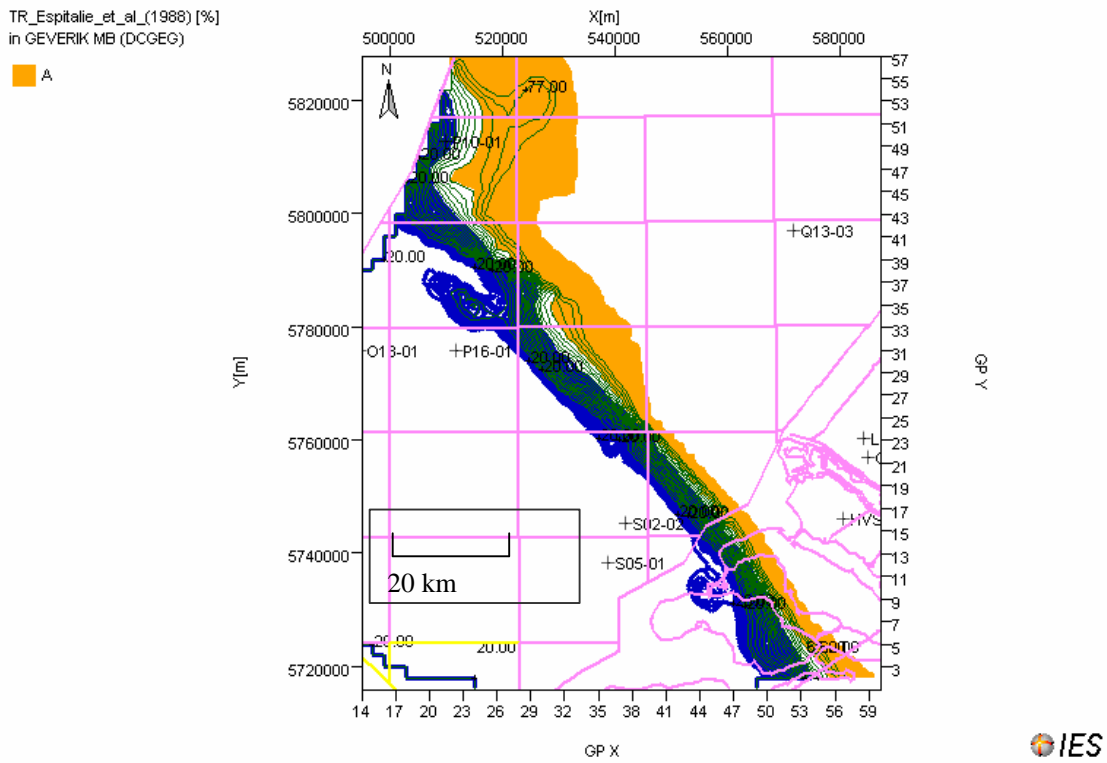


Figure I-5 Differences in transformation ratio using different kinetic models. Green lines: Tissot et al. _T2, 1988, blue lines; Burnham_T2, 1989, yellow area: Espitalie et al. 1988. The lines and different coloured area show a range in transformation ratio between 20 and 80 %)

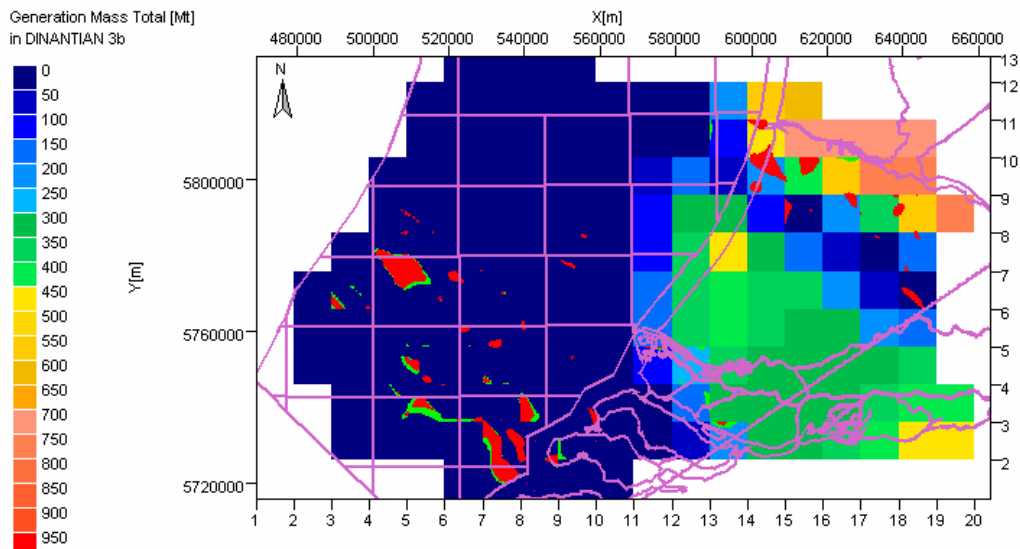


Figure I-6 Total hydrocarbon generation (liquid in green, vapour in red) at 312 Ma, showing the area of early generation in the southeastern part of Area 1. The filling of the reservoirs started from the southeastern corner

The differences in the transformation ratio between the different kinetics can also be observed for Area 2. Tissot et al._T2, 1988 and Espitalie et al. 1988 show a greater area where the transformation ratio reaches values between 30 and 80 % (Fig. I-9).

Exemplified for the Dinantian source rock (Yoredale Formation) the deepest Dinantian layer has been selected to illustrate the timing of hydrocarbon generation according to the kinetics of Burnham_T3, 1989. The increase in the transformation ratio during the past 65 My is obvious from the maps in Appendix J. At 65 Ma bp the transformation ratio for most of the area varied between 3 and 20% in the vicinity of the Elbow Spit High, except for the south-easternmost part of the area towards the Central Graben, where the transformation ratio already reached values around 70%. At 23 Ma the transformation ratio had increased to 75 % at the southeastern margin of the area. At present time, the transformation ratio between 50 and 80 % for the southern and eastern part of the area around the Elbow Spit High. At the southern margin the transformation ratio reaches values up to 97 %.

It can be concluded that a major phase of hydrocarbon generation occurred between 65 Ma and present day.

Migration and Accumulation

N.B: Traps of the size below the applied grid size have not been detected in the model. That might explain the the fact, that no accumulation has been modeled in around E12-03, although one does exist. Nevertheless, the description show that preservation of hydrocarbons in the area around the Elbow Spit High is likely due to the late generation in this area. The high N₂ content in the E12 accumulations is still subject of investigation and not yet clear.

Different play concepts have been developed for area 2. Two main source rocks have been defined, the Dinantian Yoredale Formation and the base Namurian Bowland Formation. Hydrocarbons, generated from these source source can be trapped in two occurring source rocks, the Dinantian 3b and the Namurian 2 deposits.

The source rock facies of the Dinantian is only developed at the margins of area 2. Hydrocarbon generation from the Dinantian source rock starts at about as early as Carboniferous in this area, but amounts are small. At about 208 Ma bp generation takes place in the south-western and eastern parts of the area and major accumulations have been formed in the A en E blocks. Smaller accumulations occur in the B, D and F blocks (Fig. I-10)

At 96 Ma bp bigger accumulation started to form at the eastern margin of the Elbow Spit High towards the Step Graben in the B and F blocks. At present more smaller accumulations seem to form in the southern and eastern part of the Elbow Spit High.

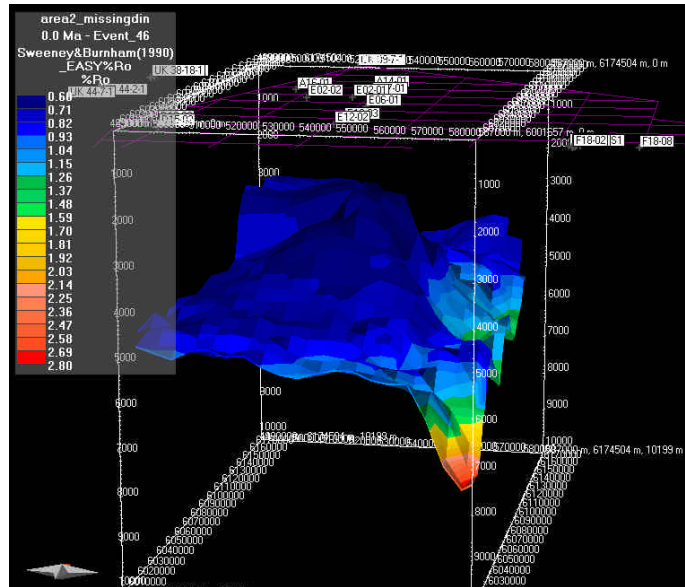


Figure I-8 3D view of calculated vitrinite reflectance values at present day (after Sweeney & Burnham 1990)

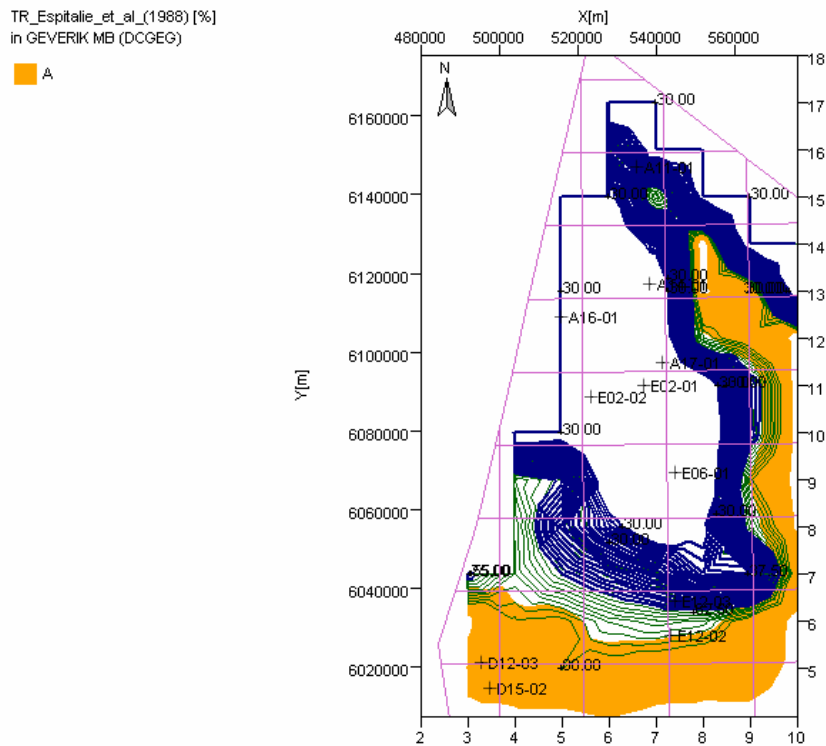


Figure I-9 Differences in transformation ratio using different kinetic models. The lines and different coloured areas show a range in transformation ratio between 20 and 80 %. Green lines: Tissot et al., 1988, blue lines: Burnham, 1989, yellow area: Espitalie et al., 1988

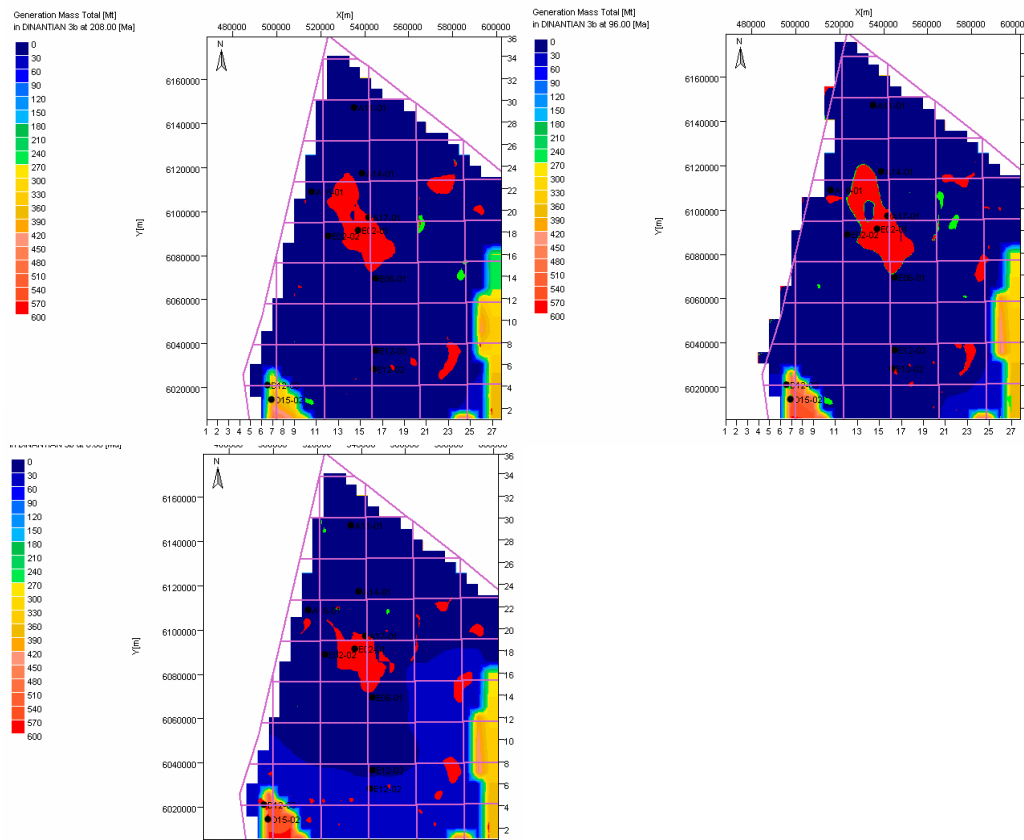


Fig. I-10 Dinantian 3b source and reservoir: Hydrocarbons generation from the Dinantian 3b source rock at 218 Ma, 92 Ma and present-day. Hydrocarbons are trapped in the reservoir facies of this layer. Colour of accumulations gives indications about the physical conditions of the hydrocarbons; red: vapour, green: liquid.

I3 Area 3&4

Burial history reconstruction

The burial history reconstruction is described in Chapter 6. The present day depth of the base Namurian source rock varies in areas 3 and 4 between 4000 m in the western part and 9000 m in the eastern part (Figure I-11).

Maturation

The present day calculated vitrinite reflectance of the organic matter of the base Namurian source rock is in general high and ranges in the the greatest part of areas 3 and 4 between 3 and 5% R_r (I-12). A high maturation has already been achieved at the end of the Carboniferous with values ranging from 2 to 4 %R (Appendix J). The high reflectance values are due to the high heatflows which obviously occurred in Area 3&4 during the geological history and is more than in areas 1 and 2 not only a function of burial depth (Appendix H). Due to the early phase of high maturation, the transformation of the organic matter already took place during the early Carboniferous and all organic matter was transformed to hydrocarbons at the end of Carboniferous. More information about the timing of hydrocarbon generation in Area 3&4 is given in Chapter 6. It should be noted at this stage, that in well Emmeloord-1 a potential Upper Namurian source rock has been identified (Appendix F), which probably also generated hydrocarbons at the second main phase of burial during the Jurassic.

Migration and accumulation

N.B.: Due to the grid size of individual cell and the general scope of the study, it has to be noted that the description of accumulations are only *indicative* for possible pathways and formed reservoirs. In order to get more reliable descriptions, the grid needs to be refined.

The major phase of hydrocarbon generation occurred in the Carboniferous and the prospectivity of Area 3&4 strongly depends on the preservation potential of the reservoir.

The accumulation history of this area is presented for a play concept of area 3, which has been supported by the seismic investigation of the area. The seismic data indicated the occurrence of a Dinantian reef-like structure in the vicinity of well Emmeloord-1. This structure has been implemented in a hypothetical model as can be seen in Fig. I-13 and I-14.

Generation occurred already early in Carboniferous and lead to the occurrence of many liquid and vapour accumulations in the area (Fig. I-15). But already at the end of the Carboniferous the all liquid accumulations had been transformed to vapour accumulations and the size and amount decreased (I-16). At 250 Ma bp almost all hydrocarbons accumulations had disappeared. It is interesting to note, that despite the early generation of hydrocarbons and the very likely major losses through time, a small vapour accumulation still exists in the model until present day close to well Emmeloord-1 (Fig. I-17).

Although the early generation of hydrocarbons in this area does not favour their accumulation, contributions to reservoirs from pre-Westphalian sources can not be excluded.

"Hydrocarbon potential of the Pre-Westphalian in the Netherlands on- and offshore"

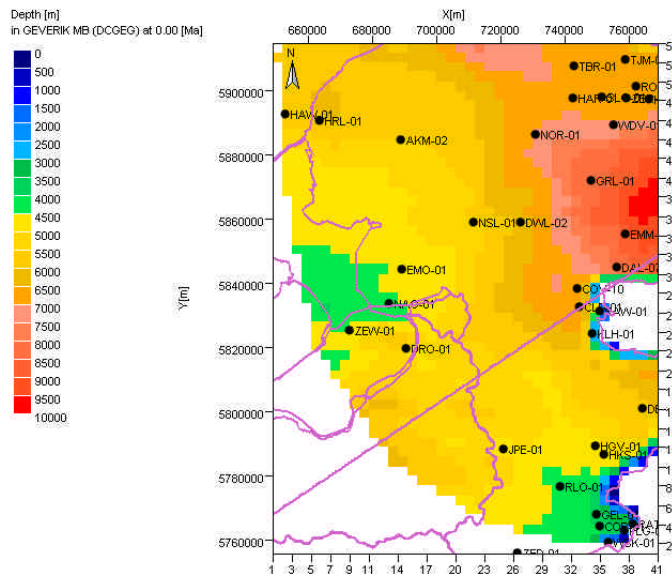


Figure I-11 Depth (m) of the base Namurian source rock of Area 3&4

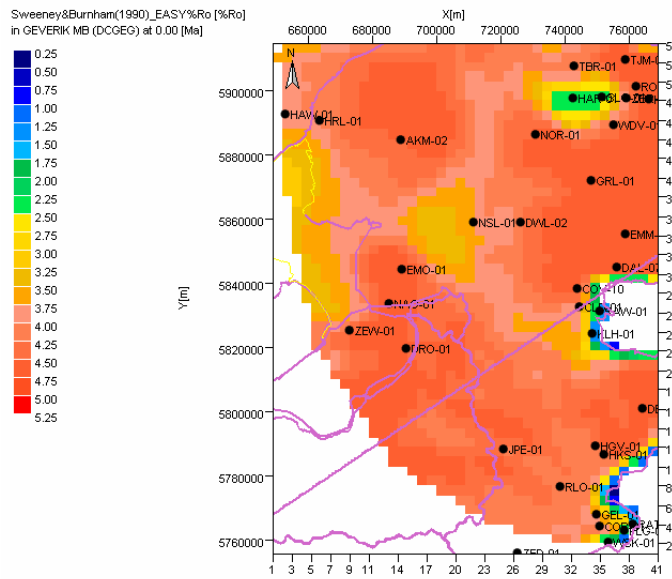


Figure I-12 Map of calculated vitrinite reflectance of Area 3&4 after Sweeney & Burnham, 1990 at present day.

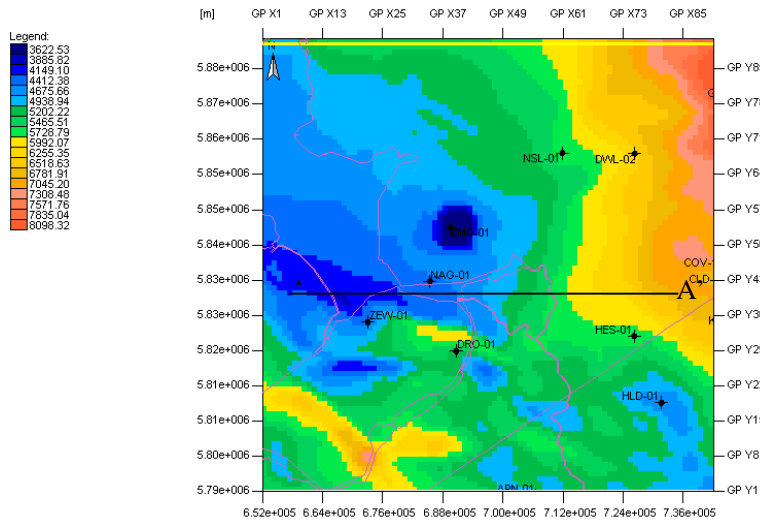


Figure I-13 Depth of the base Namurian source rock around a hypothetical Dinantian reef-like structure

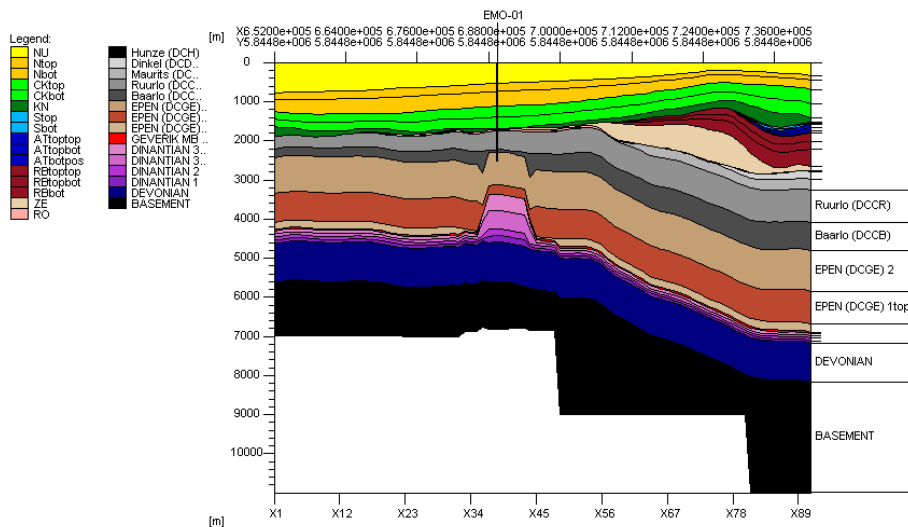


Figure I-14 Profile along line A – A' across well EMO-01 of a hypothetical model assuming a reef like structure in the Dinantion below well EMO-01

"Hydrocarbon potential of the Pre-Westphalian in the Netherlands on- and offshore"

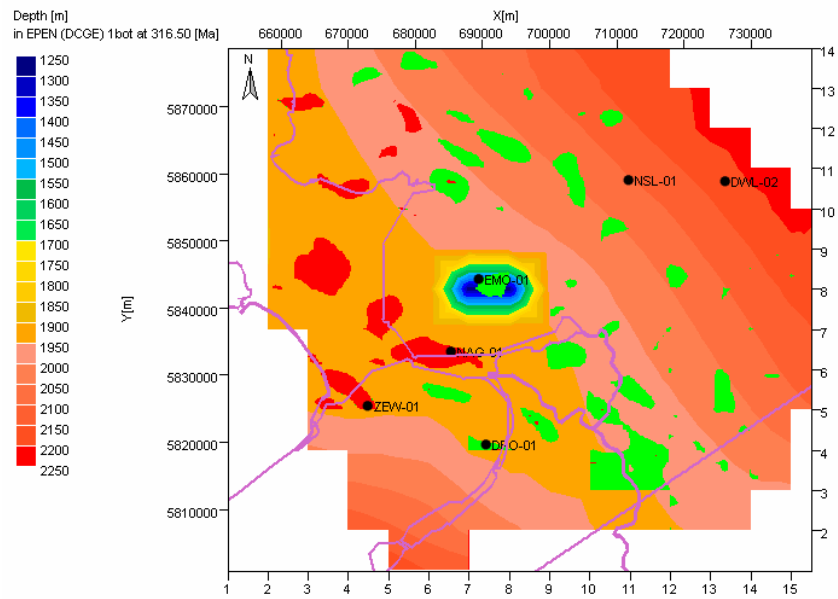


Figure I-15 Hydrocarbon accumulations from a base Namurian source rock at 316.5 Ma (colour of accumulations gives indications about the physical conditions of the hydrocarbons; red: vapour, green: liquid)

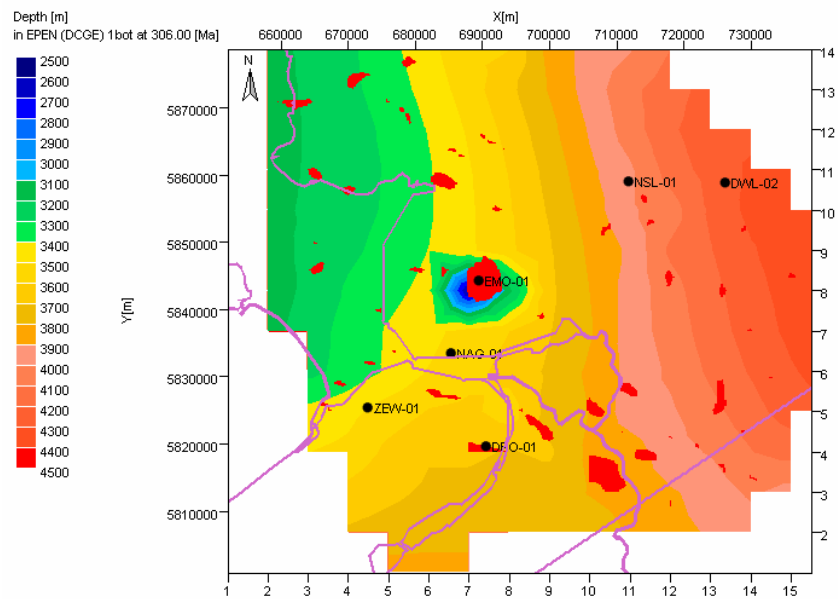


Figure I-16 Hydrocarbon accumulations from a base Namurian source rock at 306 Ma (colour of accumulations gives indications about the physical conditions of the hydrocarbons; red: vapour, green: liquid)

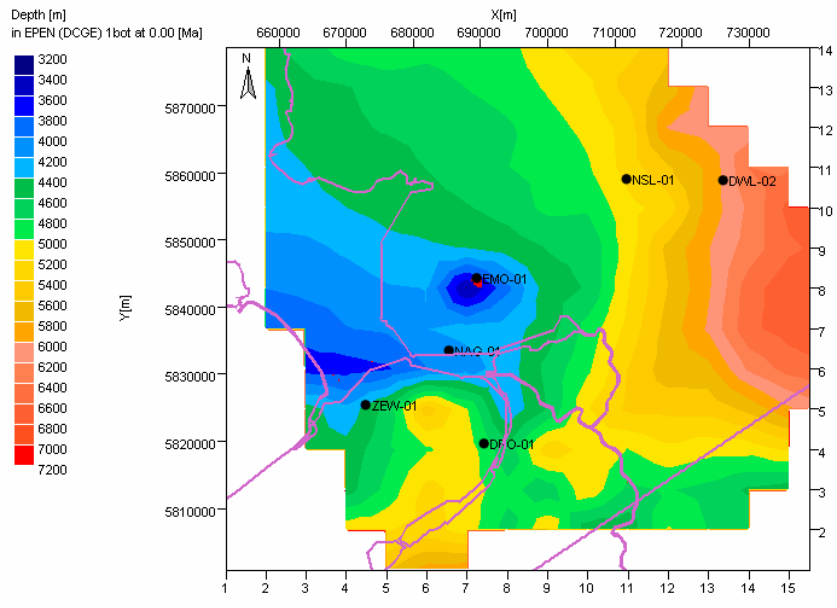


Figure I-17 Hydrocarbon accumulations from a base Namurian source rock at present day (colour of accumulations gives indications about the physical conditions of the hydrocarbons; red: vapour)

J Maturity maps

The 3D basin modelling resulted in maps of the maturity and the transformation ratio (% of the total amount of hydrocarbons that can maximally be generated from a source rock) at different stages in geological history.

A selection was made of these maps; the following maps are included

Area 1

Maturity maps

- Base Namurian, 306 Ma
- Base Namurian, 60.5 Ma
- Base Namurian, present-day

Transformation ratio

- Base Namurian, 96 Ma
- Base Namurian, 60.5 Ma
- Base Namurian, 34 Ma
- Base Namurian, present-day

Area 2

Maturity maps

- Top Dinantian, 306 Ma
- Top Dinantian, 154 Ma
- Top Dinantian, present-day
- Base Namurian, 306 Ma
- Base Namurian, 154 Ma
- Base Namurian, 34 Ma
- Base Namurian, 23 Ma
- Base Namurian, present-day

Transformation ratio

- Base Namurian, 60.5 Ma
- Base Namurian, 34 Ma
- Base Namurian, 23 Ma
- Base Namurian, present-day

Area 3 and 4

Maturity maps

- Base Namurian, 306 Ma
- Base Namurian, present-day

Appendix J Maturity maps

The 3D basin modelling resulted in maps of the maturity and the transformation ratio (% of the total amount of hydrocarbons that can maximally be generated from a source rock) at different stages in geological history.

A selection was made of these maps; the following maps are included

Area 1

Maturity maps

Base Namurian, 306 Ma

Base Namurian, 60.5 Ma

Base Namurian, present-day

Transformation ratio

Base Namurian, 96 Ma

Base Namurian, 60.5 Ma

Base Namurian, 34 Ma

Base Namurian, present-day

Area 2

Maturity maps

Top Dinantian, 306 Ma

Top Dinantian, 154 Ma

Top Dinantian, present-day

Base Namurian, 306 Ma

Base Namurian, 154 Ma

Base Namurian, 34 Ma

Base Namurian, 23 Ma

Base Namurian, present-day

Transformation ratio

Base Namurian, 60.5 Ma

Base Namurian, 34 Ma

Base Namurian, 23 Ma

Base Namurian, present-day

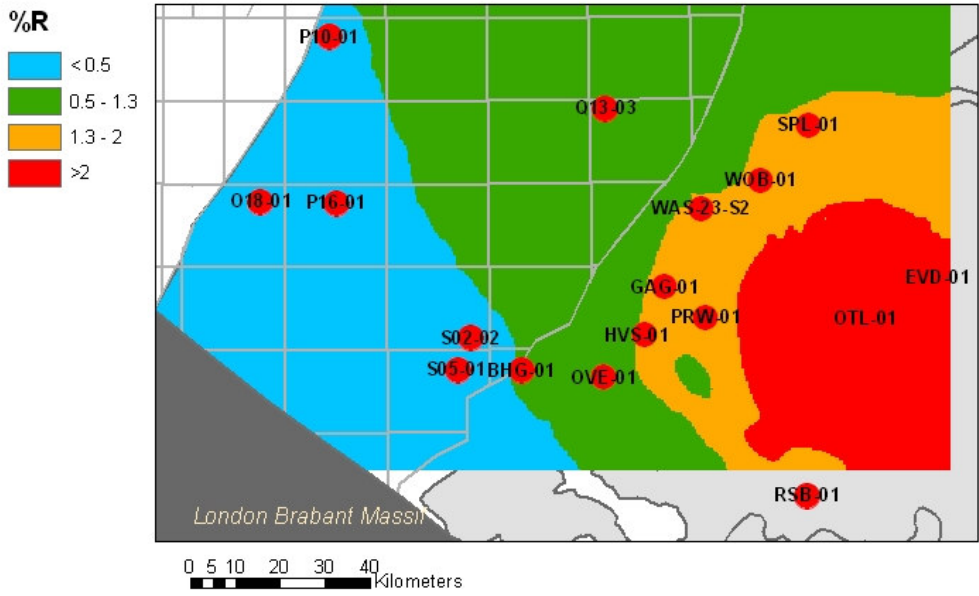
Area 3 and 4

Maturity maps

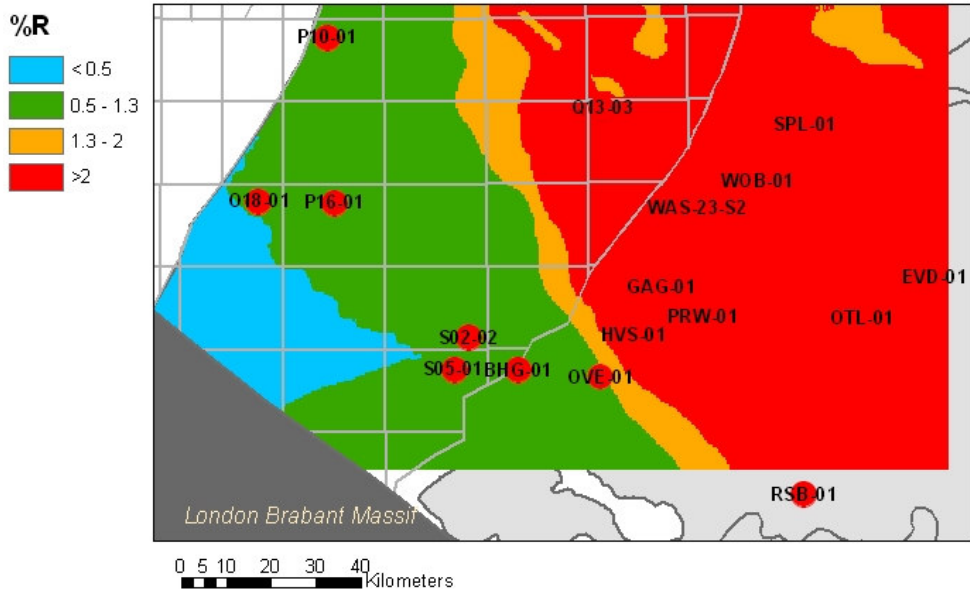
Base Namurian, 306 Ma

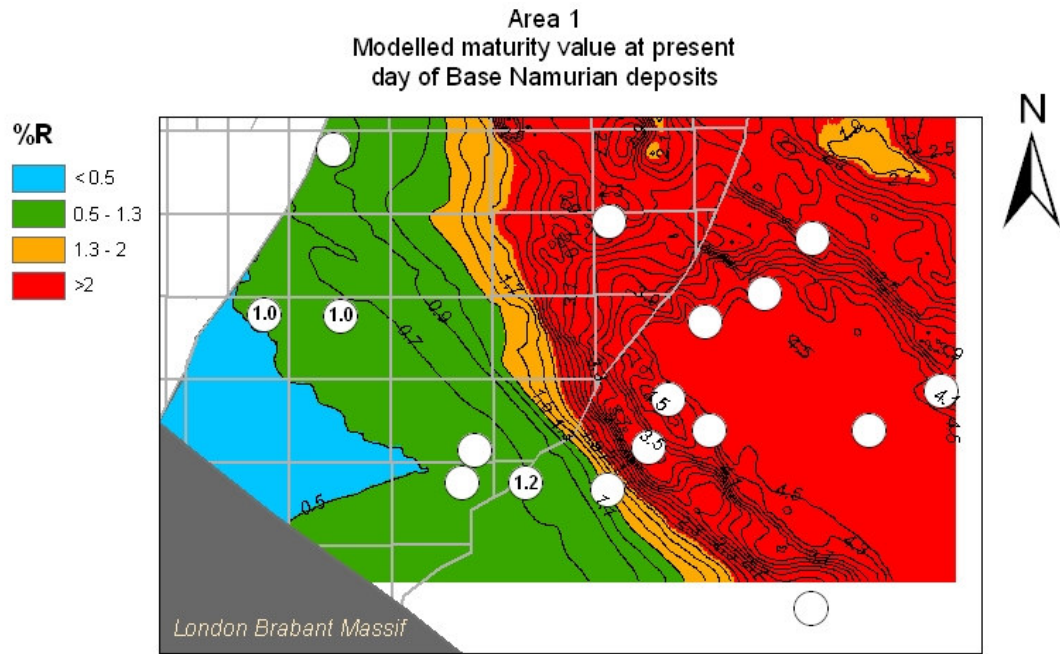
Base Namurian, present-day

Area 1
Modelled maturity at 306 Ma
of Base Namurian deposits



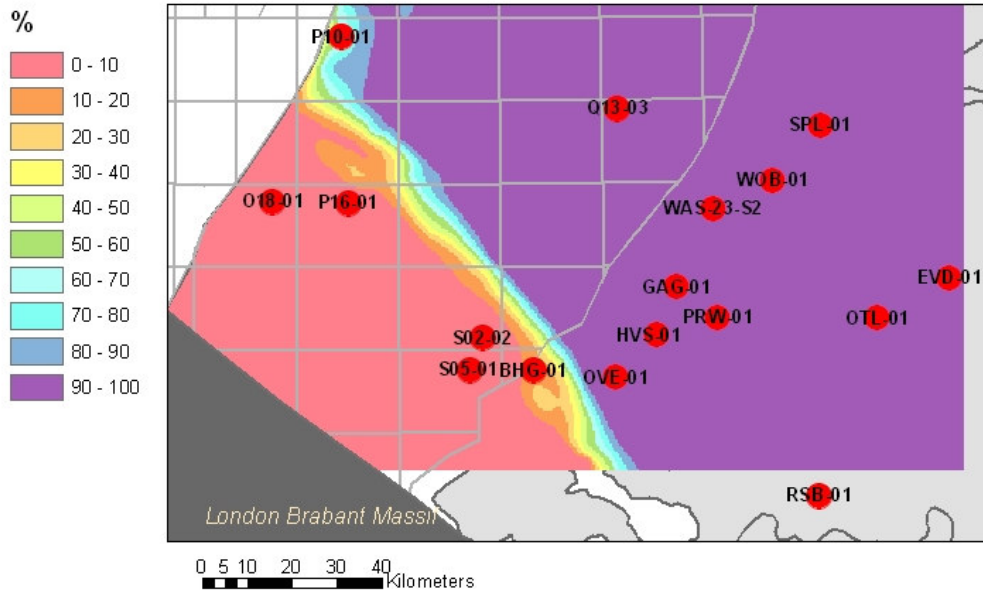
Area 1
Modelled maturity at 60.5 Ma
of Base Namurian deposits



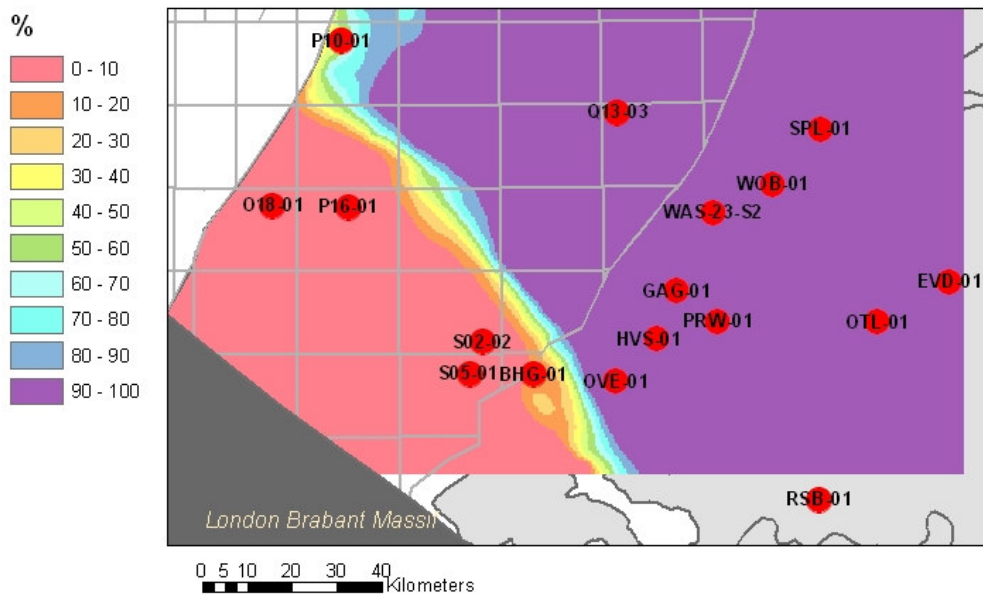


Values in white circles represent measured values, as identified in Appendix B.

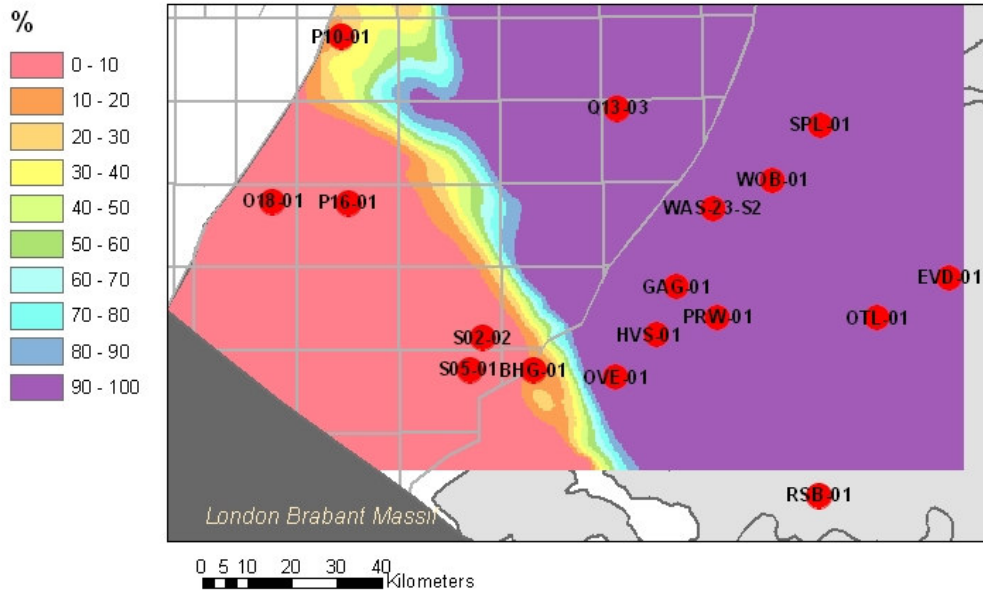
Area 1
Transformation ratio at 96 Ma
of Base Namurian deposits



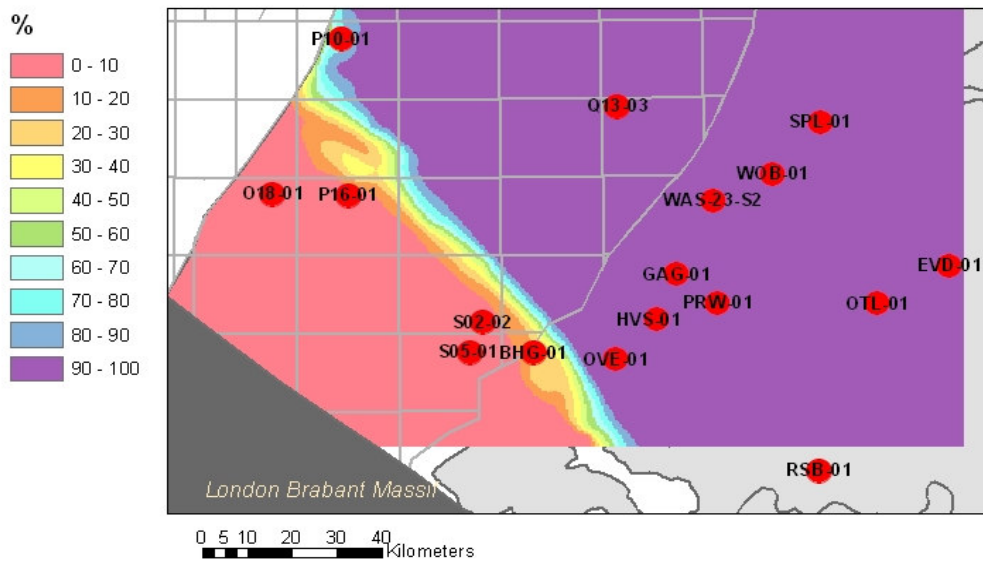
Area 1
Transformation ratio at 60.5 Ma
of Base Namurian deposits



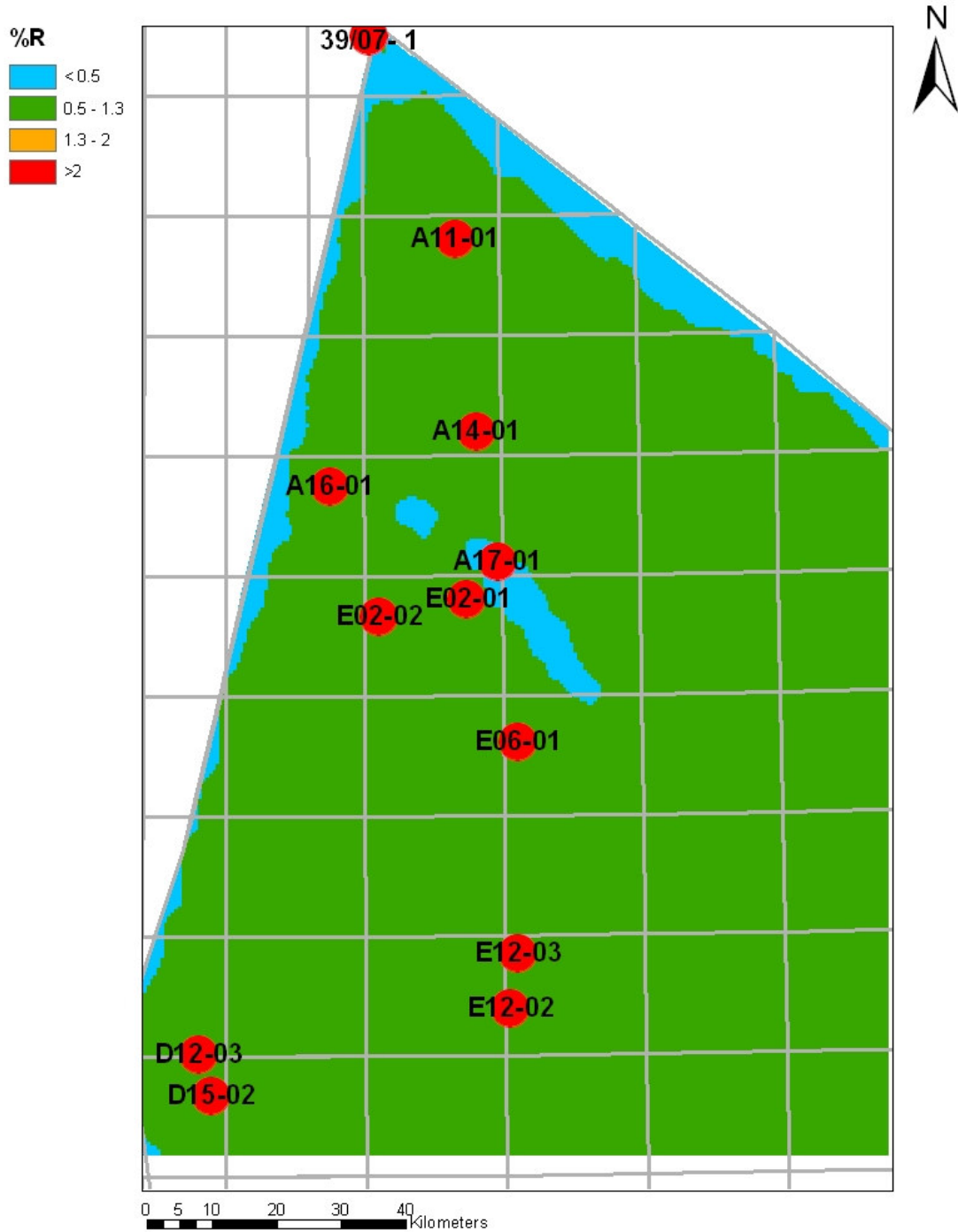
Area 1
Transformation ratio at 34 Ma
of Base Namurian deposits



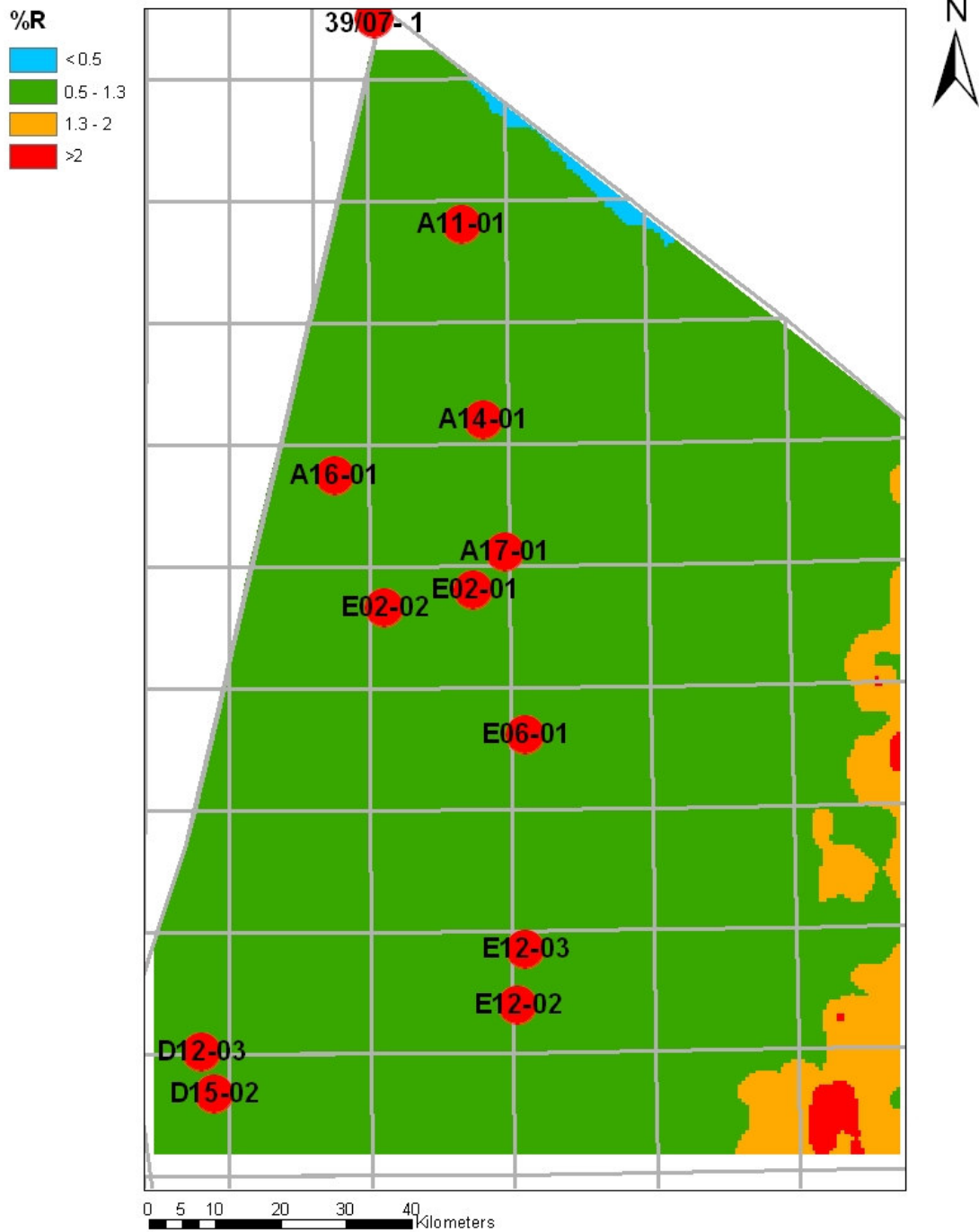
Area 1
Transformation ratio at present day
of Base Namurian deposits



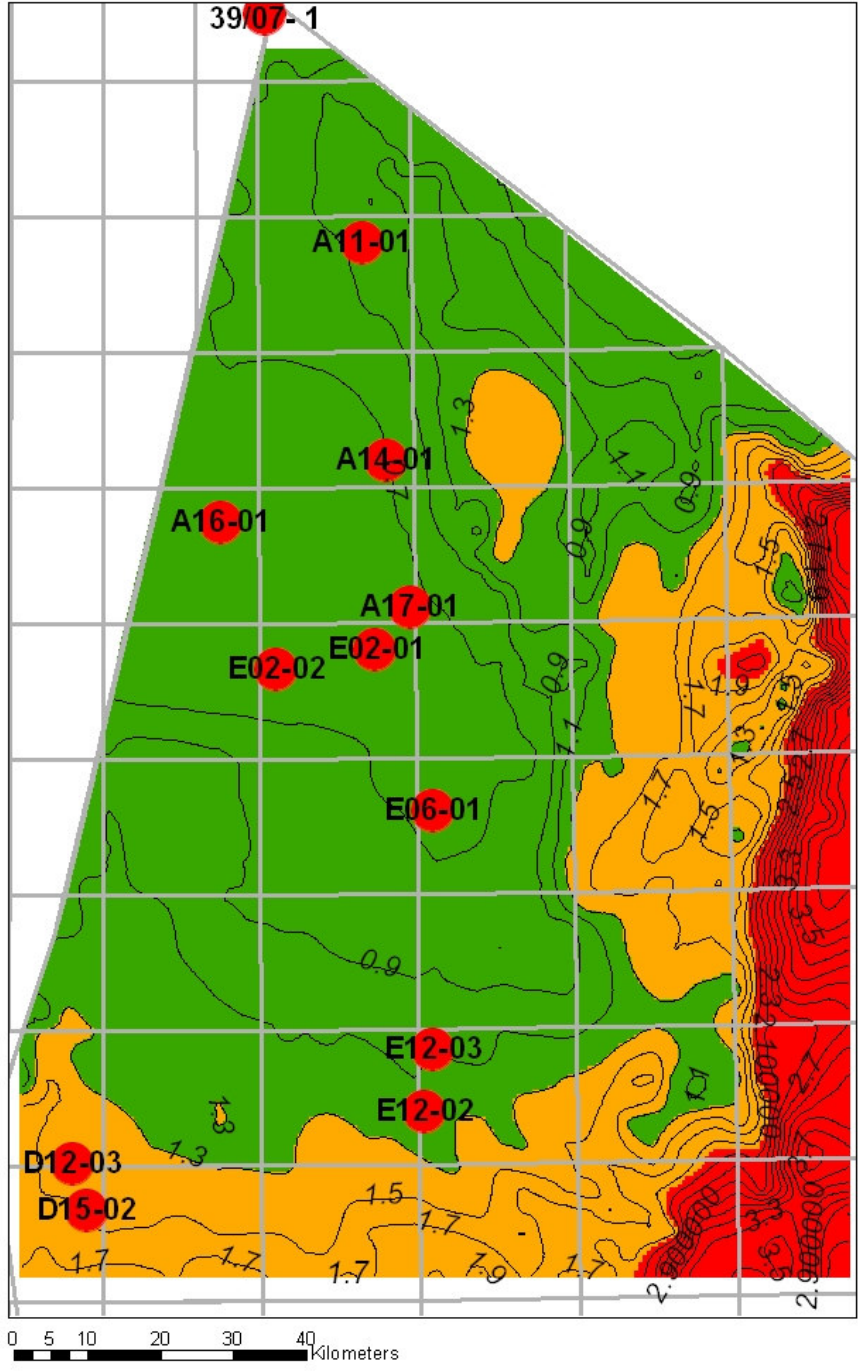
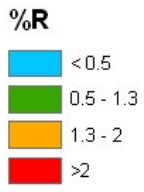
Area 2
Modelled maturity at 306 Ma
of Top Dinantian 1 deposits



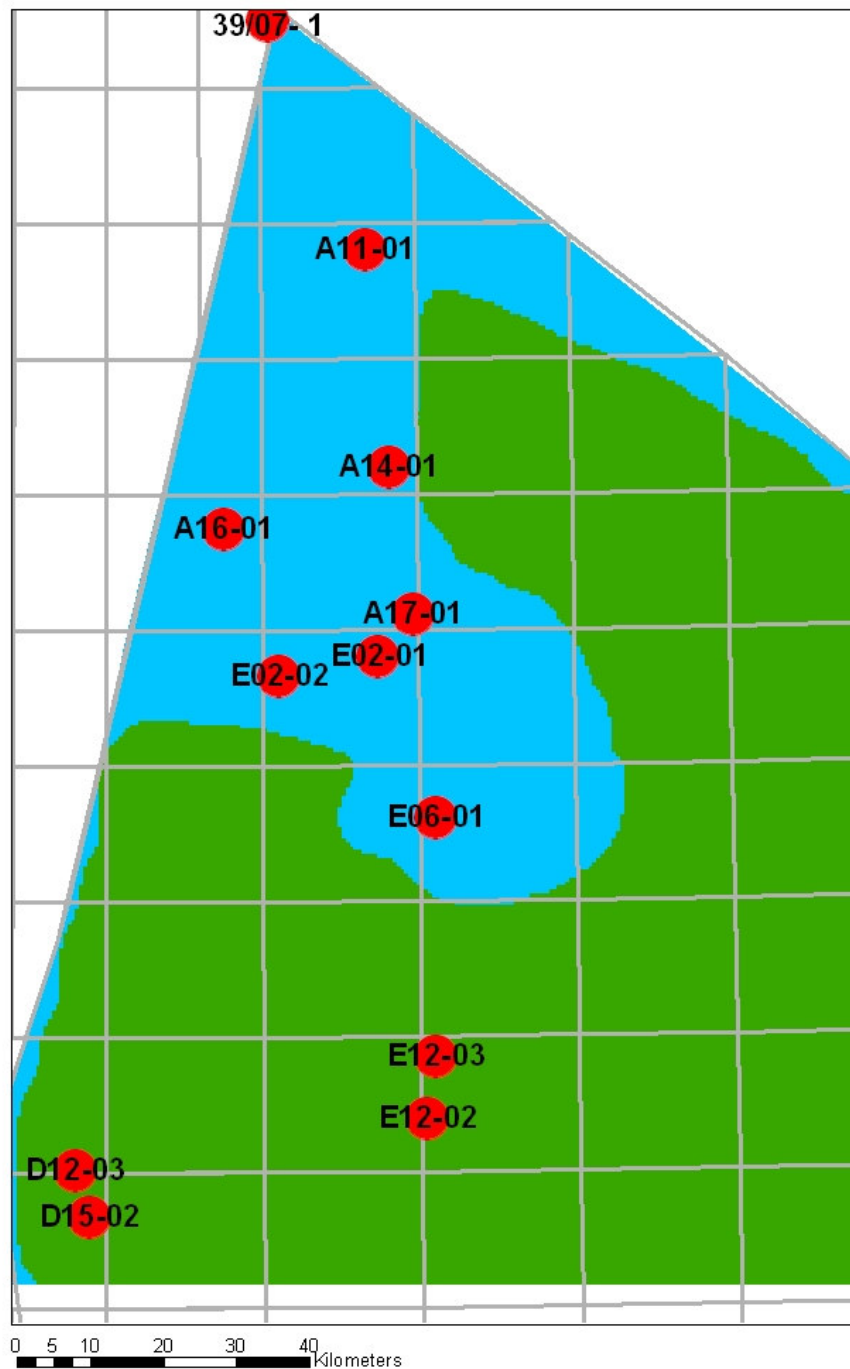
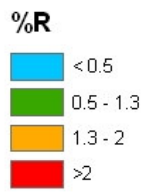
Area 2
Modelled maturity at 154 Ma
of Top Dinantian 1 deposits



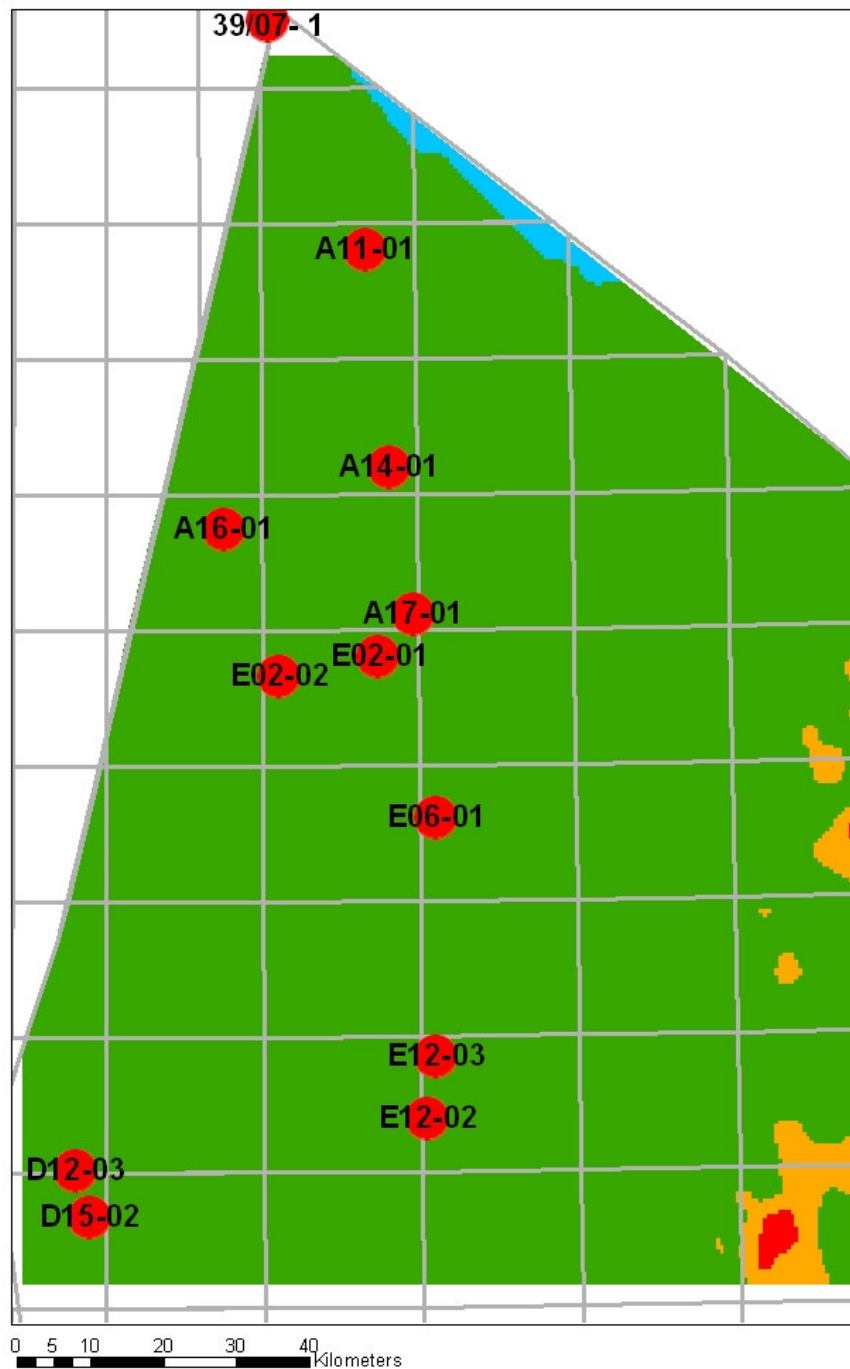
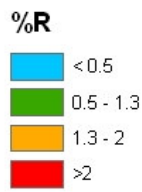
Area 2
Modelled maturity at present day
of Top Dinantian 1 deposits



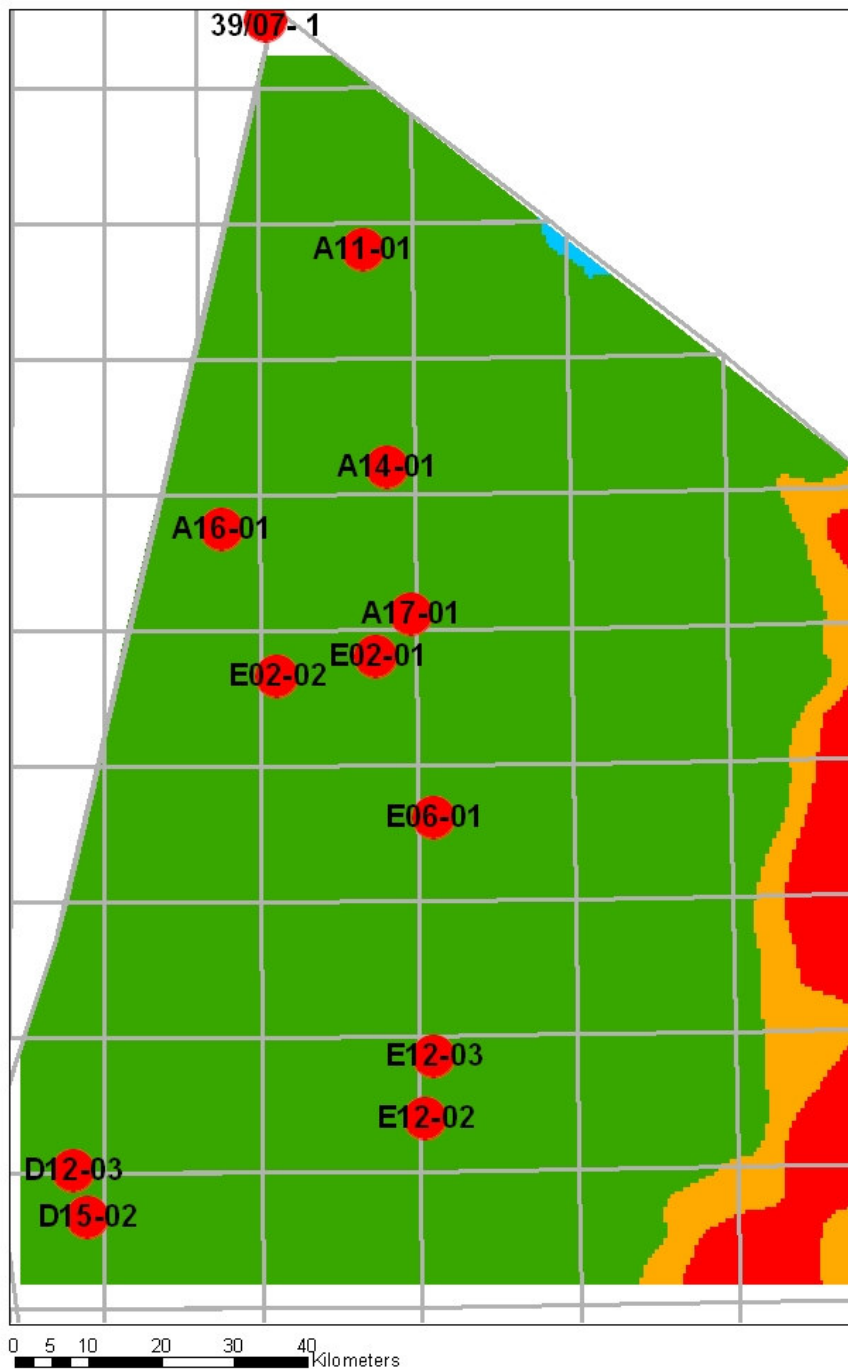
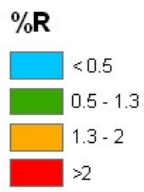
Area 2
Modelled maturity at 306 Ma
of Base Namurian deposits



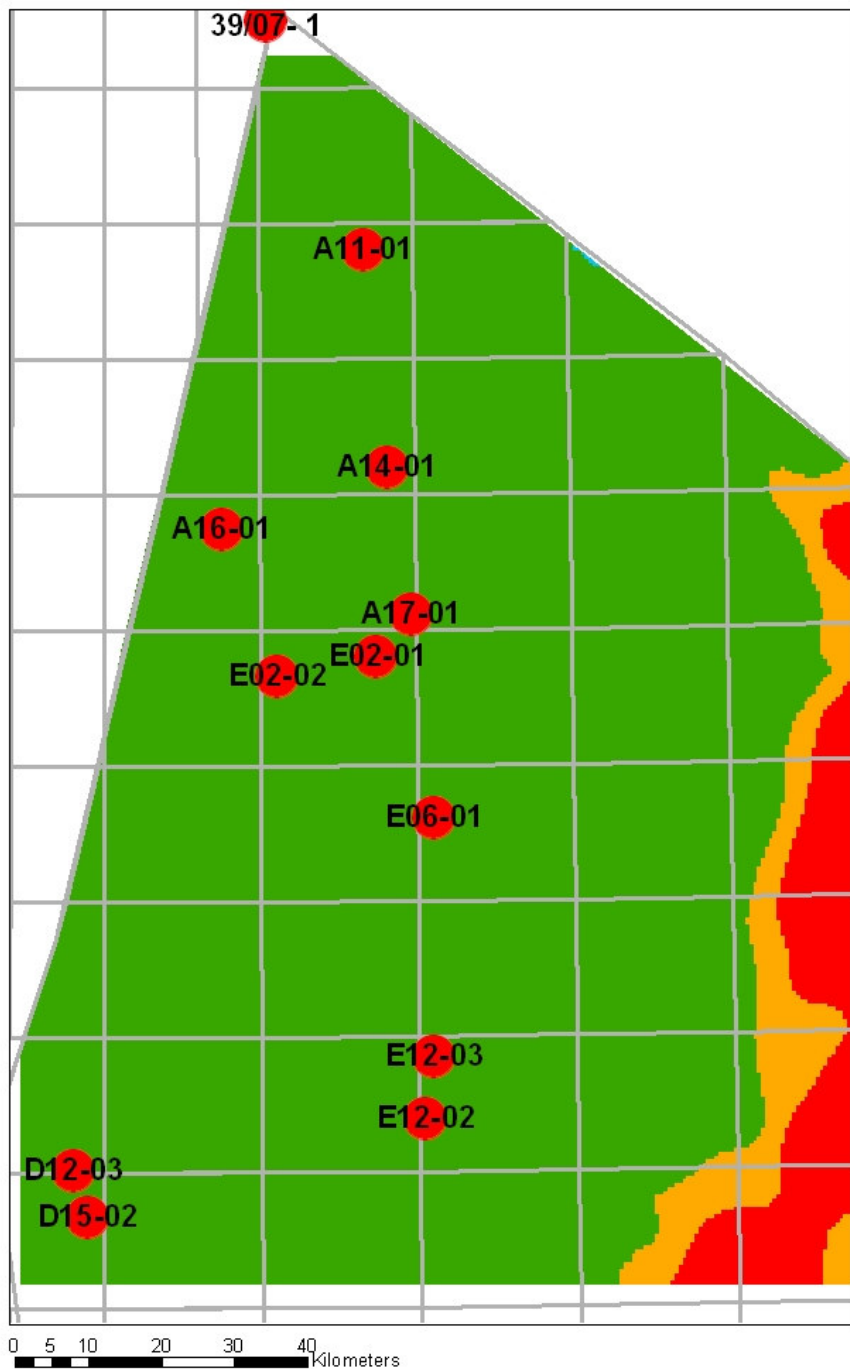
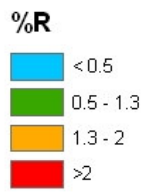
Area 2
Modelled maturity at 154 Ma
of Base Namurian deposits



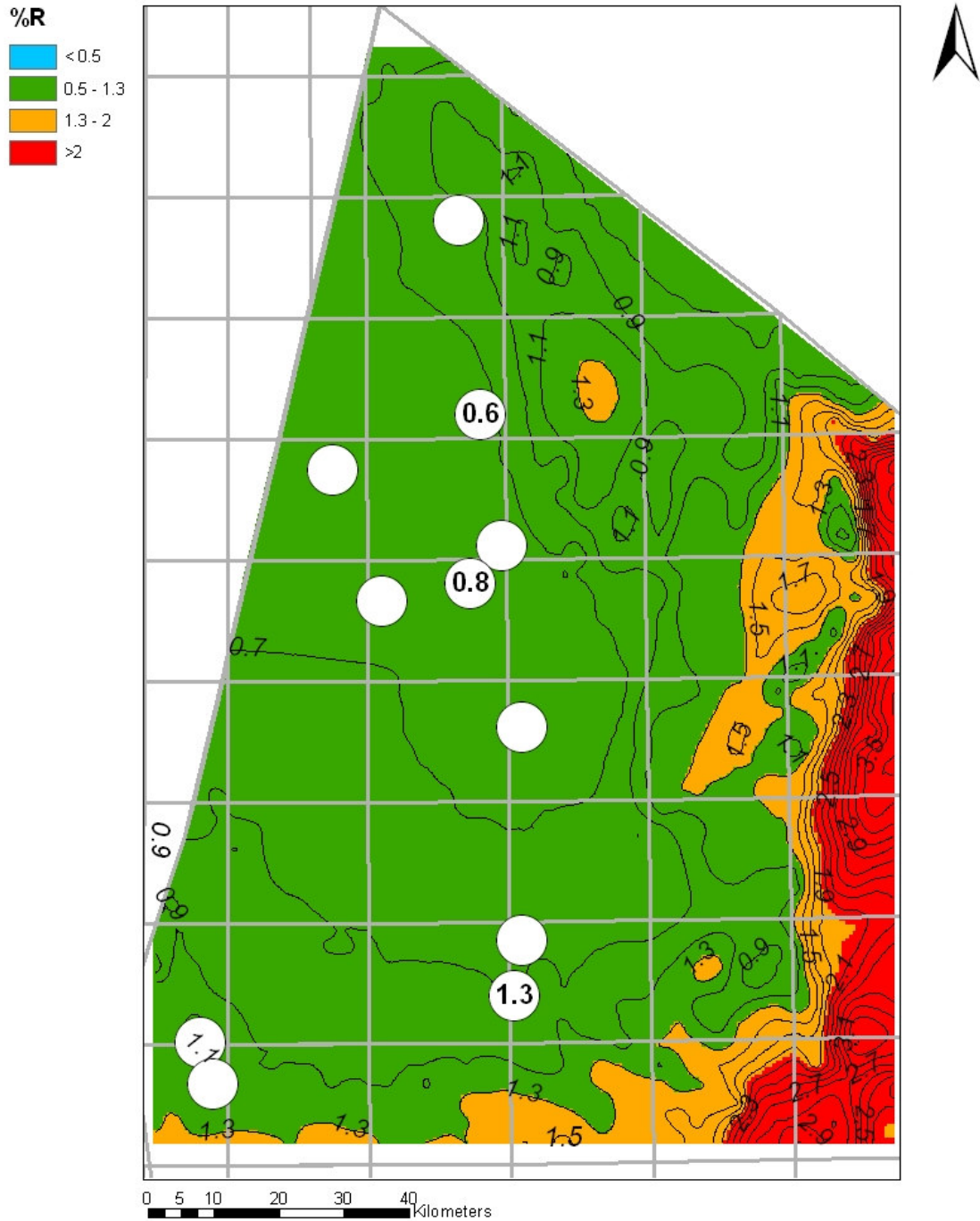
Area 2
Modelled maturity at 34 Ma
of Base Namurian deposits



Area 2
Modelled maturity at 23 Ma
of Base Namurian deposits

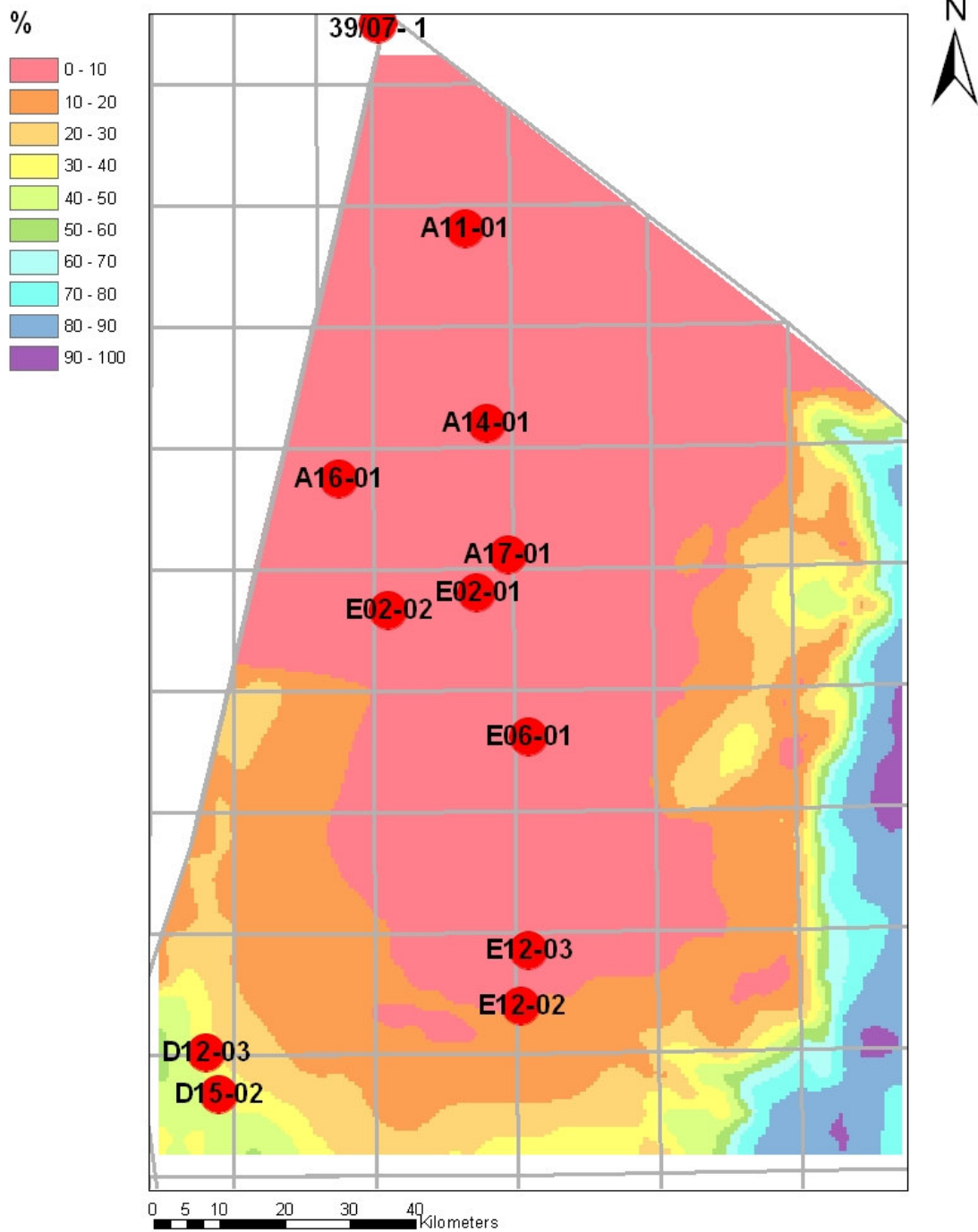


Area 2
Modelled maturity at present day
of Base Namurian deposits

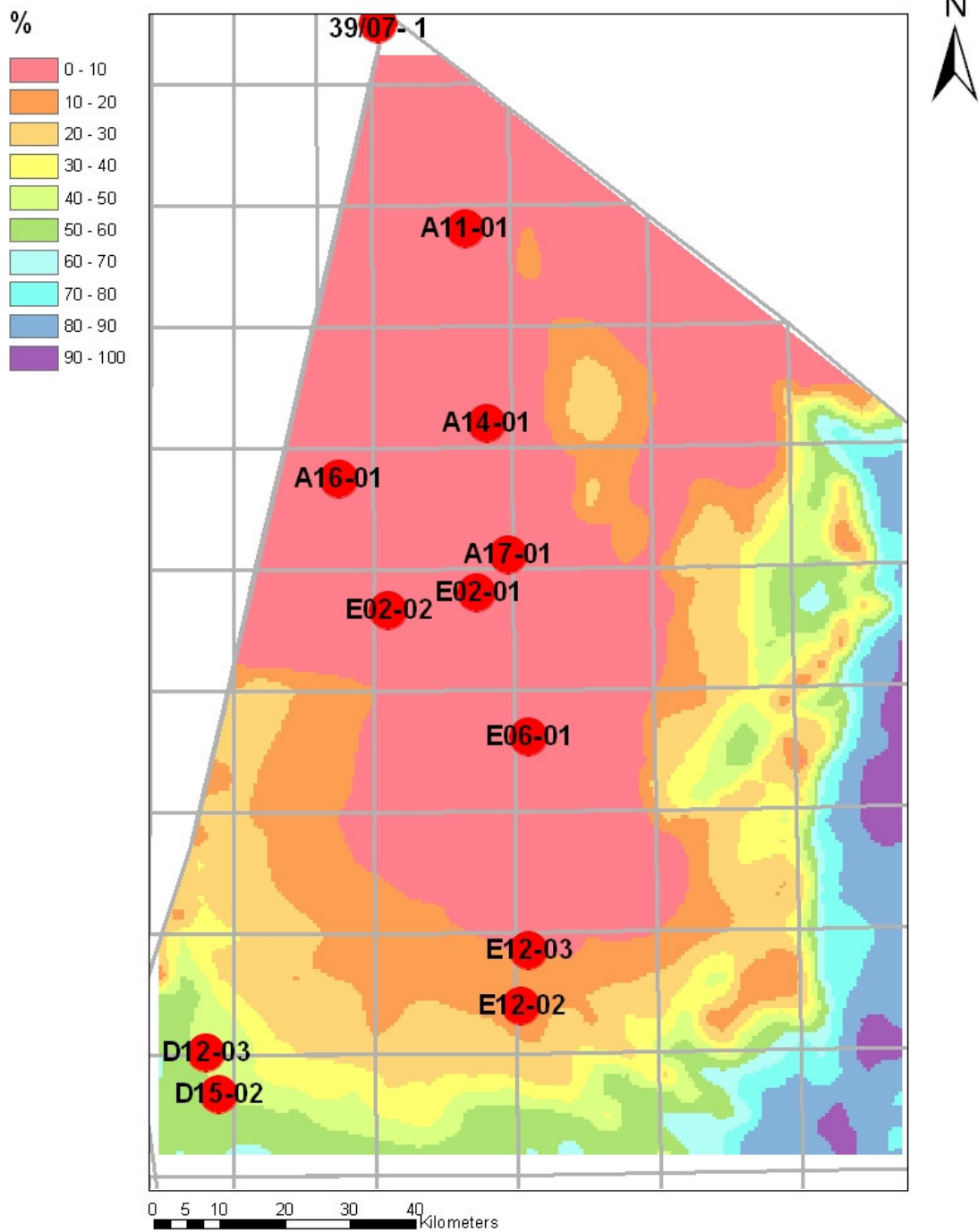


Values in white circles represent measured values, as identified in Appendix B.

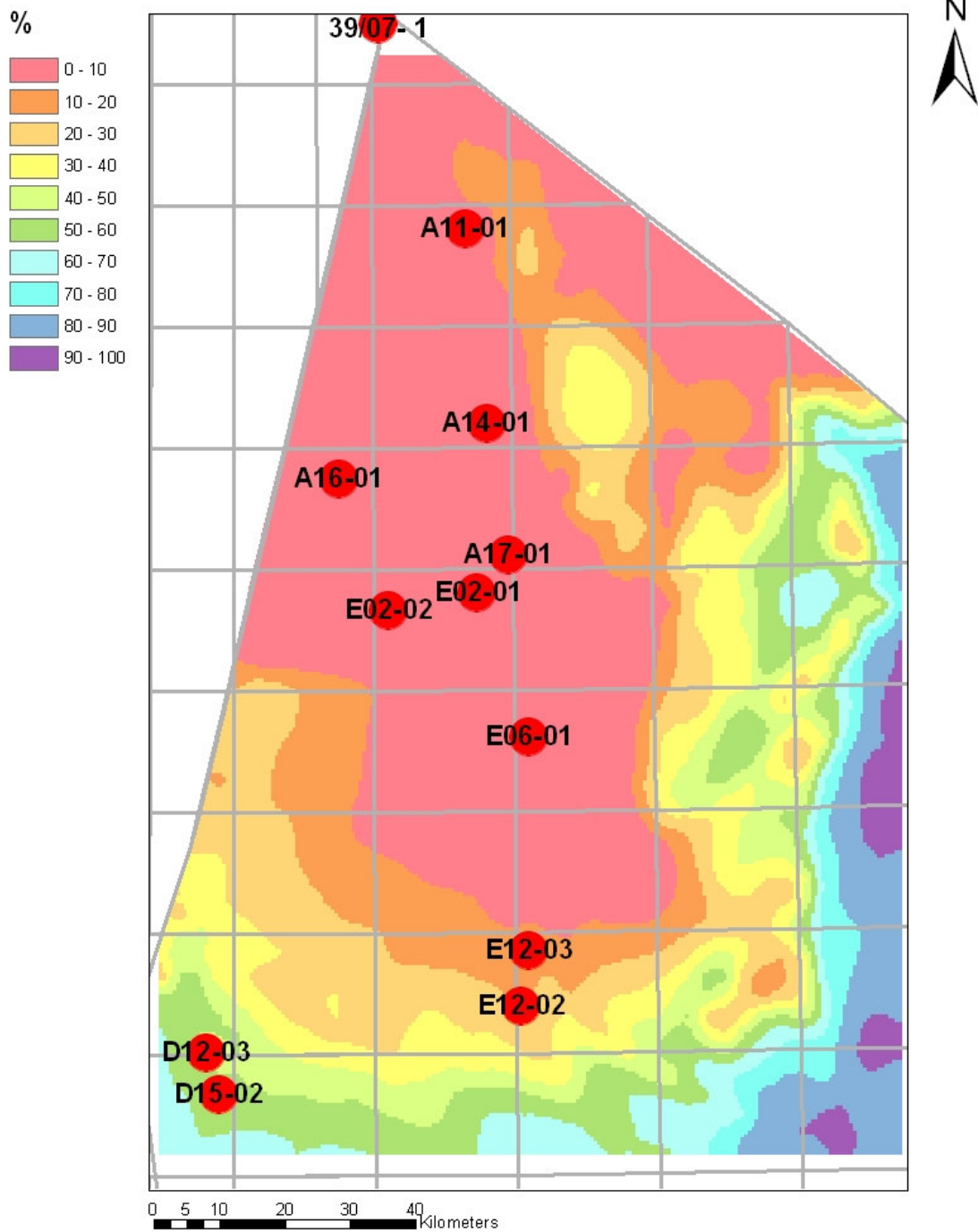
Area 2
Transformation ratio at 60.5 Ma
of Base Namurian deposits



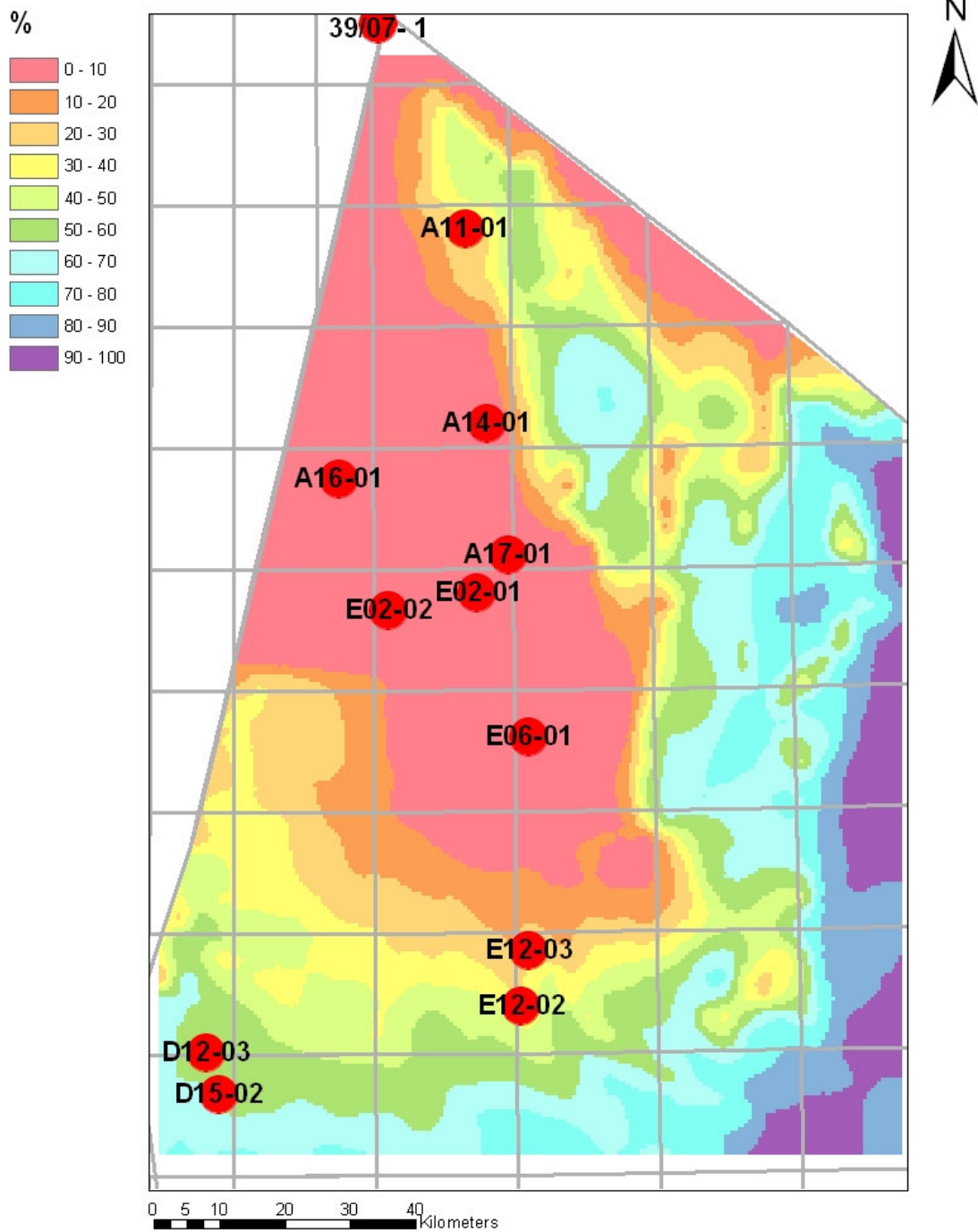
Area 2
Transformation ratio at 34 Ma
of Base Namurian deposits



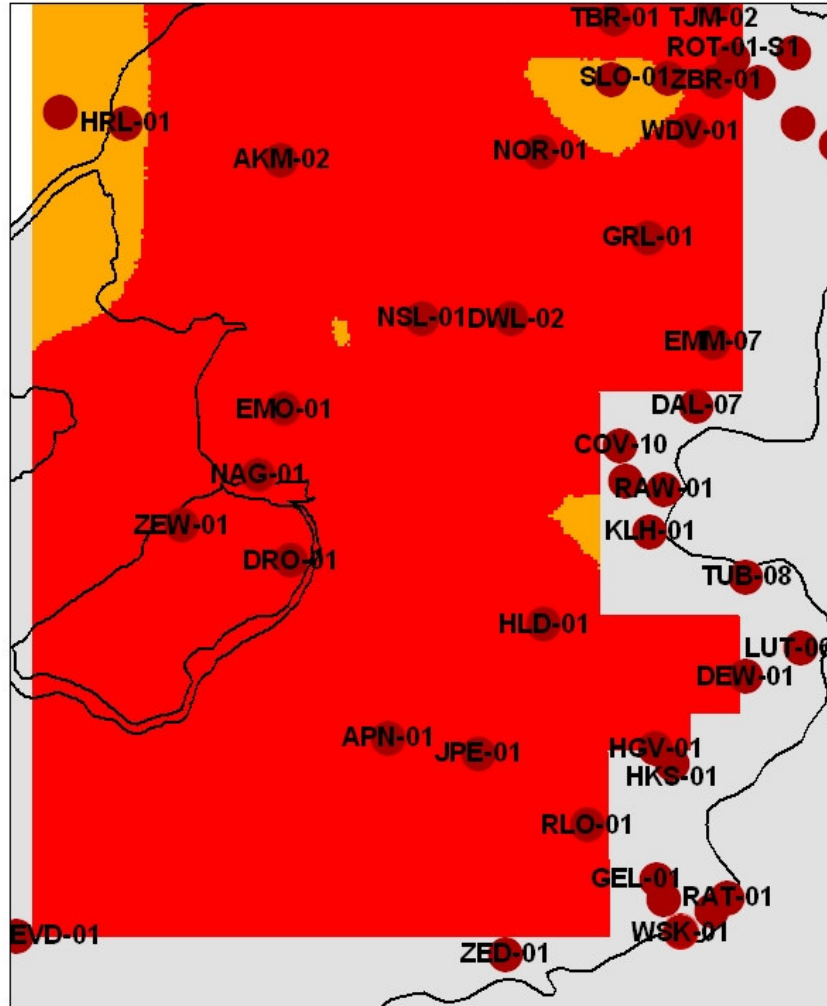
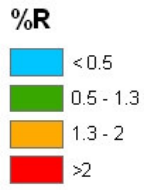
Area 2
Transformation ratio at 23 Ma
of Base Namurian deposits



Area 2
Transformation ratio at present day
of Base Namurian deposits

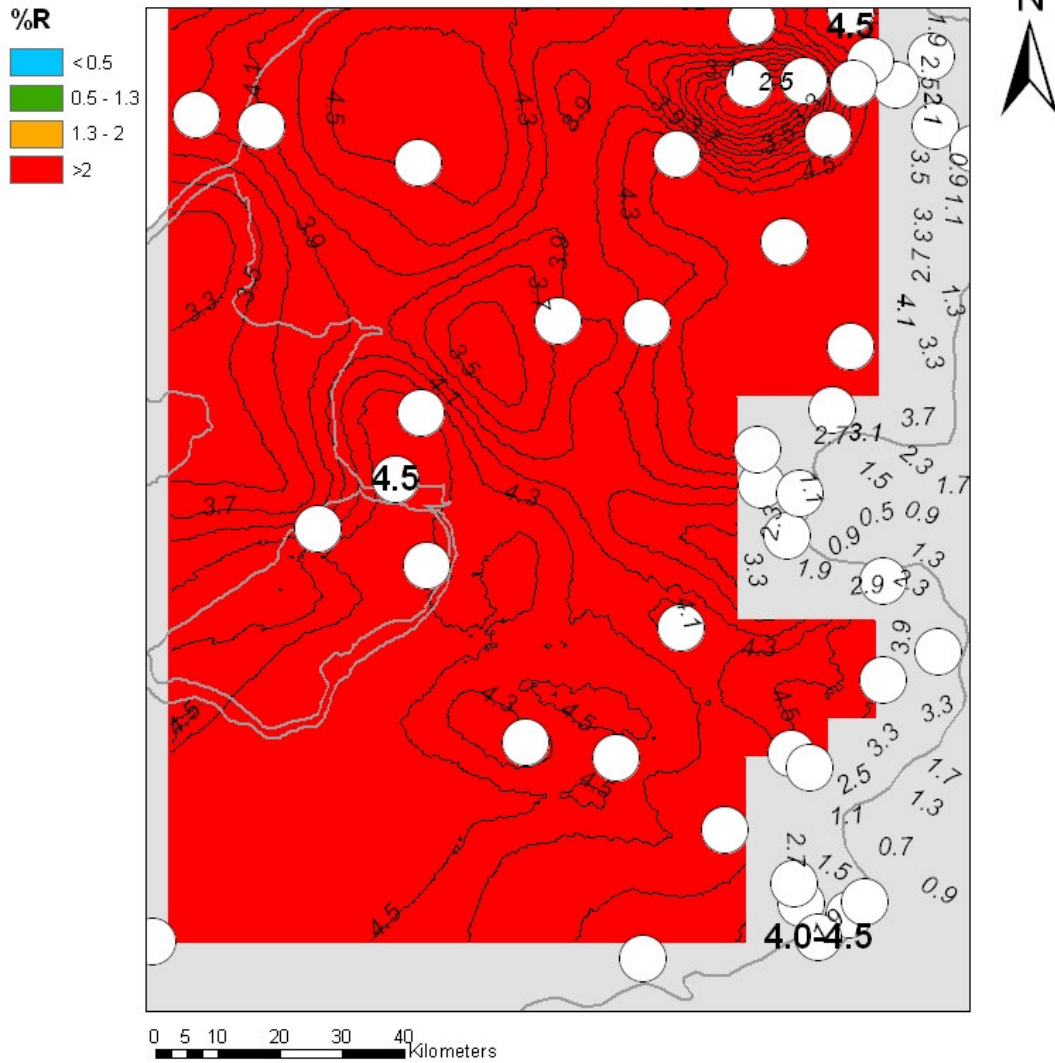


Area 3 and 4
Modelled maturity at 306 Ma
of Base Namurian deposits



0 5 10 20 30 40 Kilometers

Area 3 and 4
 Modelled maturity at present day
 of Base Namurian deposits



Values in white circles represent measured values, as identified in Appendix B.

K Gravity modelling of the Netherlands on- and offshore

Introduction

In continuation of the forward gravity modelling of the onshore Dutch subsurface (Dortland, 2003) a similar study has been carried out for the complete Dutch territory, onshore and offshore together. The gravity effect of eight individual layers down to and including the Rotliegend has been calculated with respect to a reference density. The summed gravity effect of the layers has been subtracted from the observed gravity field to obtain a residual gravity field. This residual represents the gravity field that can be considered to be due to density variations in the pre-Permian rocks. Gravity highs indicate the presence of high-density (with respect to the reference density) material, whereas gravity lows will indicate the presence of relatively low-density material.

The residual can give an indication of potential Dinantian basement blocks. The Dinantian 'block and basin' principle (illustrated in Figure K1) gives rise to possible local deposits of marine source rocks in the basins and local development of reservoirs in the blocks (Dortland, 2003). However, it should be kept in mind that the presence of *low*-density crustal intrusions will have a negative effect on the gravity field, and can therefore (partly) counteract the positive gravity effect of the relatively *high*-density Dinantian blocks.

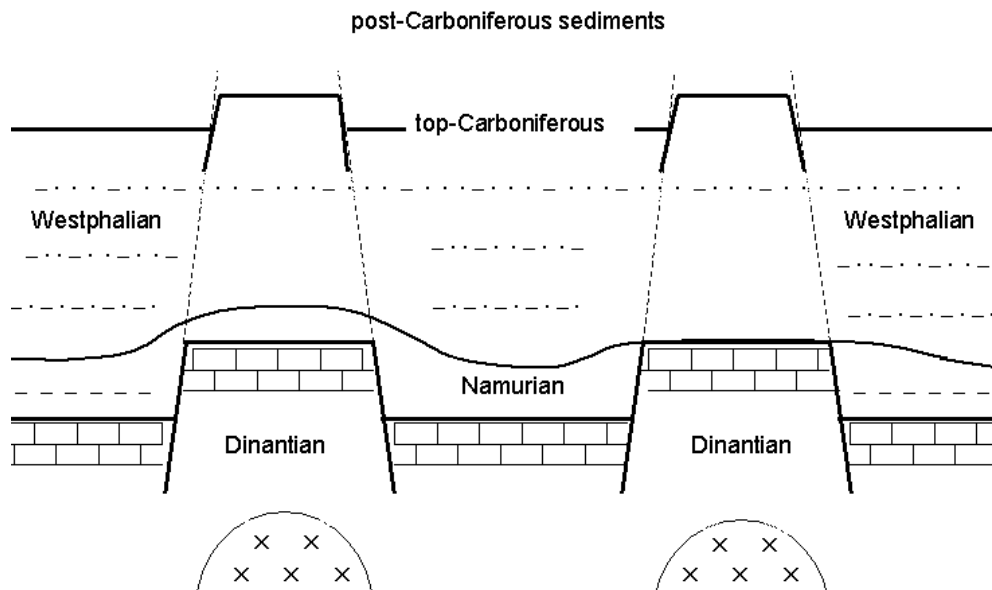


Figure K-1 A simplified model of the Dinantian block and basin principle. During the Sudetian tectonic phase faulting is accompanied by uplift of the Dinantian blocks. These Dinantian blocks are assumed to be related to the presence of deeper intrusions (Collinson et al. 1993; Besly, 1998). The Sudetian tectonic phase is followed by sedimentation of Namurian and Westphalian sediments, resulting in a thick sedimentary sequence in the basins and a thinner sequence on top of the Dinantian highs. In later tectonic phases the faults of the Sudetian and older tectonic phases are reactivated, resulting in a similar faulting pattern in the Upper Carboniferous.

Method

The geological model of the Dutch territory

Table K3 gives an overview of the chronostratigraphy and lithostratigraphy as defined in the Dutch onshore and offshore territory. Figure K2 shows a depth map of the top-pre-Perm, together with an overview of the main Mesozoic structural elements. As the water column can have a significant effect on the gravity field, especially in channels where the ocean bottom reaches depths up to 70 meter, an extra layer is added on top of the model. This layer is based on the bathymetry map of the offshore Dutch territory.

Table K3: Overview of the chronostratigraphy and lithostratigraphy as defined in the Dutch territory.

Layer	Chronostratigraphy	Lithostratigraphy
1	Quaternary, Tertiary	North Sea Super Group
2	Late Cretaceous	Chalk Group
3	Early Cretaceous	Rijnland Group
4	Late Jurassic	Schieland Group
5	Early + Middle Jurassic	Altena Group
6	Triassic	Upper and Lower Trias Group
7	Late Permian	Zechstein Group
8	Early Permian	Upper and Lower Rotliegend Groups

A regional velocity model

In 2001 a regional velocity distribution for the onshore Dutch territory was determined from the acoustic data from over 600 wells located in the Netherlands (Doornenbal, 2001). For each layer a linear velocity equation was formulated taking into account regional differences due to, for example, inverted areas such as the West Netherlands Basin, the Vlieland Basin and the Lower Saxony Basin. The linear velocity equation is formulated as:

$$v(z) = v_0 + k \cdot z \quad (1)$$

with v_0 the velocity at depth $z=0$ and k the gradient. Recently, this regional velocity distribution has been extended to the offshore territory. The resulting values of v_0 and k we used in this study are summarized in Table K4. These are average values for the whole of the onshore and offshore area, thus not specifically taking into account inverted areas. Taking the average can result in an underestimation of densities in inverted areas, and an overestimation of densities in non-inverted areas.

"Hydrocarbon potential of the Pre-Westphalian in the Netherlands on- and offshore"

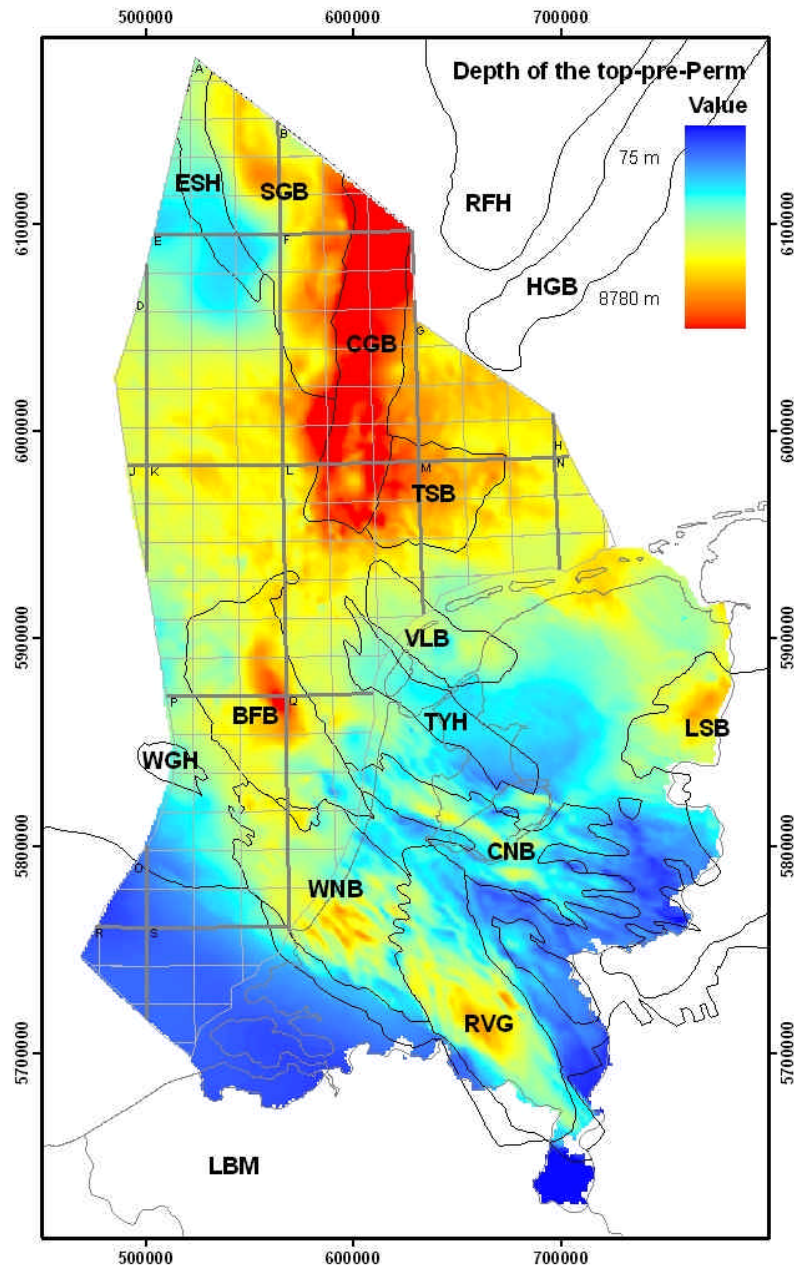


Figure K2 A depth map of the top-pre-Perm, together with an overview of the main Mesozoic structural elements of the Netherlands. Abbreviations: BFB= Broad Fourteens Basin, CGB= Central Graben, CNB= Central Netherlands Basin, HGB= Horn Graben, LBM= London-Brabant Massif, LSB= Lower Saxony Basin, MBH= Maasbommel High, RFH= Ringkobing-Fyn High, RVG= Roer Valley Graben, SGB= Step Graben, TSB= Terschelling Basin, TYH= Texel IJsselmeer High, VLB= Vlieland Basin, WGH= Winterton-Gulf High, WNB= West Netherlands Basin.

Table K4: Overview of the v0 and k values used in this study.

Layer		v0	k
1	North Sea Super Gp	0.35	1747
2	Chalk Gp	1.03	2098
3	Rijnland Gp	0.69	1738
4	Schieland Gp	0.54	2161
5	Altena Gp	0.46	2171
6	U+L Trias Gp	0.45	2908
7	Zechstein Gp	-	-
8	U+L Rotliegend Gp	0.37	2973

The density model

We developed a density model based on the regional velocity model of the Dutch on- and offshore territory, using Gardner's relationship to convert the seismic velocities to densities for all layers except the Zechstein Group and the water layer. Gardner *et al.* (1974) conducted a series of empirical studies and determined the following relationship between velocity and density:

$$\mathbf{r} = aV^{1/4} \quad (2)$$

where ρ is in g/cm^3 , a is 0.31 when V is in m/s and is 0.23 when V is in ft/s. For the water layer a constant density of 1.024 g/cm^3 was used. In line with Dortland (2003), we generalized the density distribution for the Zechstein Group as follows:

$$\mathbf{r}_{\text{zechstein}} = \mathbf{r}_{\text{anhydrite}} \quad \text{for } D_{\text{zechstein}} \leq 250\text{m}. \quad (3)$$

$$\mathbf{r}_{\text{zechstein}} = \frac{250}{D_{\text{zechstein}}} * \mathbf{r}_{\text{anhydrite}} + \frac{D_{\text{zechstein}} - 250}{D_{\text{zechstein}}} * \mathbf{r}_{\text{rocksalt}} \quad \text{for } D_{\text{zechstein}} > 250\text{m}. \quad (4)$$

With $\rho_{\text{anhydrite}} = 2.91 \text{ g/cm}^3$, $\rho_{\text{rocksalt}} = 2.20 \text{ g/cm}^3$ and $D_{\text{zechstein}}$ the thickness of the Zechstein layer at the specific longitude-latitude location.

For the onshore Dortland (2003) compared the density model with well log densities. The results showed that Gardner's relationship tends to underestimate the log densities for all layers, except the top layer (North Sea Super Group), with a deviation of 4% or less.

Gravimetric backstripping

Gravimetric backstripping removes the gravity effect of known structures (sedimentary layers, g_{sed}) from the observed Bouguer gravity (g_{obs}). We used this technique to obtain a residual gravity field (g_{res}) for the pre-Permian sediments:

$$g_{\text{res}} = g_{\text{obs}} - g_{\text{sed}} \quad (5)$$

The observed Bouguer gravity is shown in Figure K3. It is a compilation map of datasets mainly collected by Shell, the British Geological Survey (BGS) and the Delft University of Technology (TUD) in the Netherlands. In section 0 the map is further discussed. For the offshore, the Bouguer anomaly is taken equal to the free-air anomaly. A drawback of this equalization is the fact that the Bouguer anomaly is now dependent on variations in sea bottom depth. To account for this effect, the extra water layer was added to the model.

To calculate the gravity effect of each layer a 3D forward gravity modelling method was used, developed by Starostenko and Legostaeva (1998). To reduce calculation times to acceptable proportions all available grids were re-gridded to a 5000-meter spacing, resulting in a grid of 65×113 grid cells.

The gravity effect was calculated at sea level and with respect to a reference density of 2.67 g/cm³. This value is, at least for the onshore Dutch territory, a good approximation for the mean density of the Upper Carboniferous (pers. comm., Dr. W. Bredewout). In this way, after backstripping, the residual gravity field shows anomalies caused by material between the top of the Carboniferous and the Moho with a density deviating from this reference density, or anomalies caused by variations in depth of the Moho.

Results

Figure K4 shows the gravity effect of the individual layers. Summation of the gravity effect of all layers results in a map that displays the gravity effect of the post-Carboniferous sedimentary sequence (Figure K5). As one can expect, this map shows small gravity effects in the south and east where the post-Carboniferous sedimentary sequence is relatively thin or even absent (southern Limburg). Whereas in the northern part of the Dutch territory, along the Central Graben, the gravity effect is very large due to the thick (> 8km) post-Carboniferous sedimentary sequence.

The residual gravity field (Figure K6) is obtained by subtracting the gravity effect of the post-Carboniferous sedimentary sequence from the observed Bouguer gravity anomaly map. The residual shows a dominant gravity high along the Central Graben and less pronounced gravity highs located at the Broad Fourteens Basin and West Netherlands Basin. Gravity highs indicate the presence of material with a density higher than the reference density ($\rho_{ref} = 2.67 \text{ g/cm}^3$).

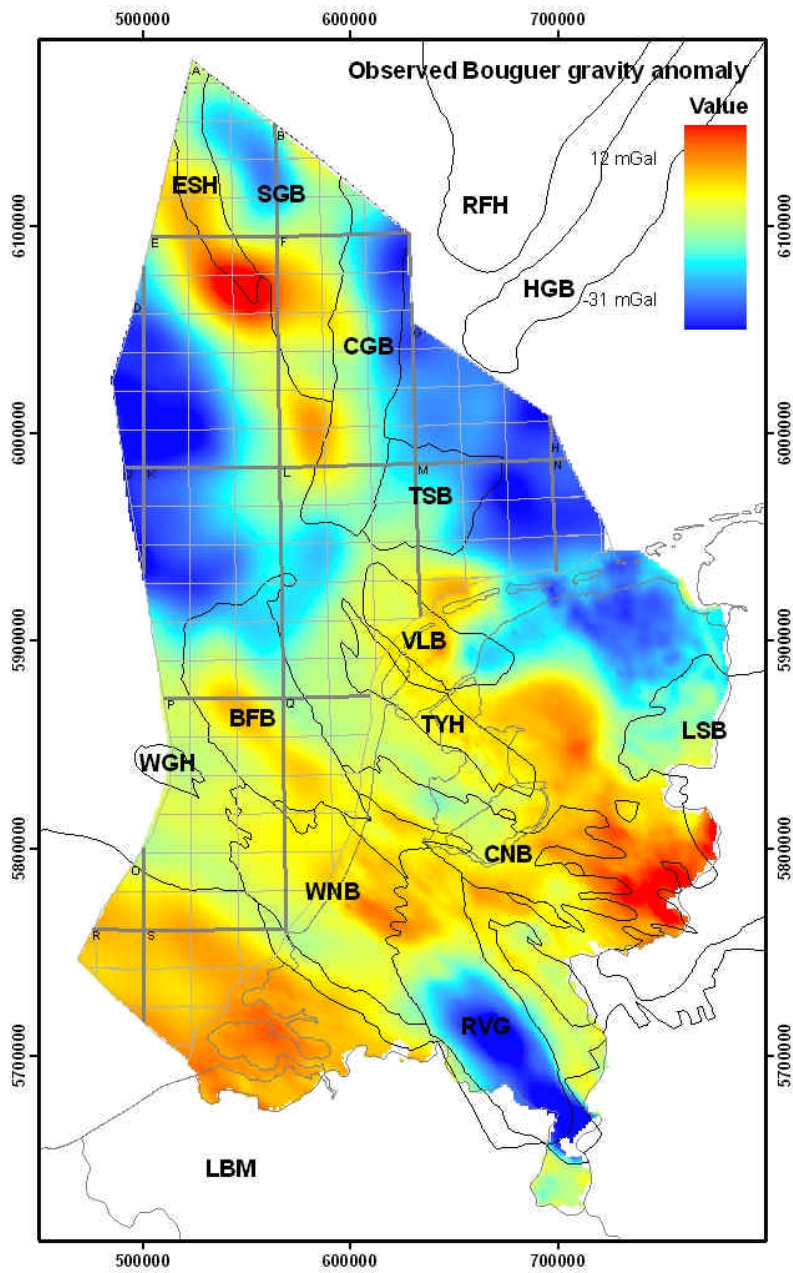


Figure K3 The observed Bouguer gravity anomaly map.

"Hydrocarbon potential of the Pre-Westphalian in the Netherlands on- and offshore"

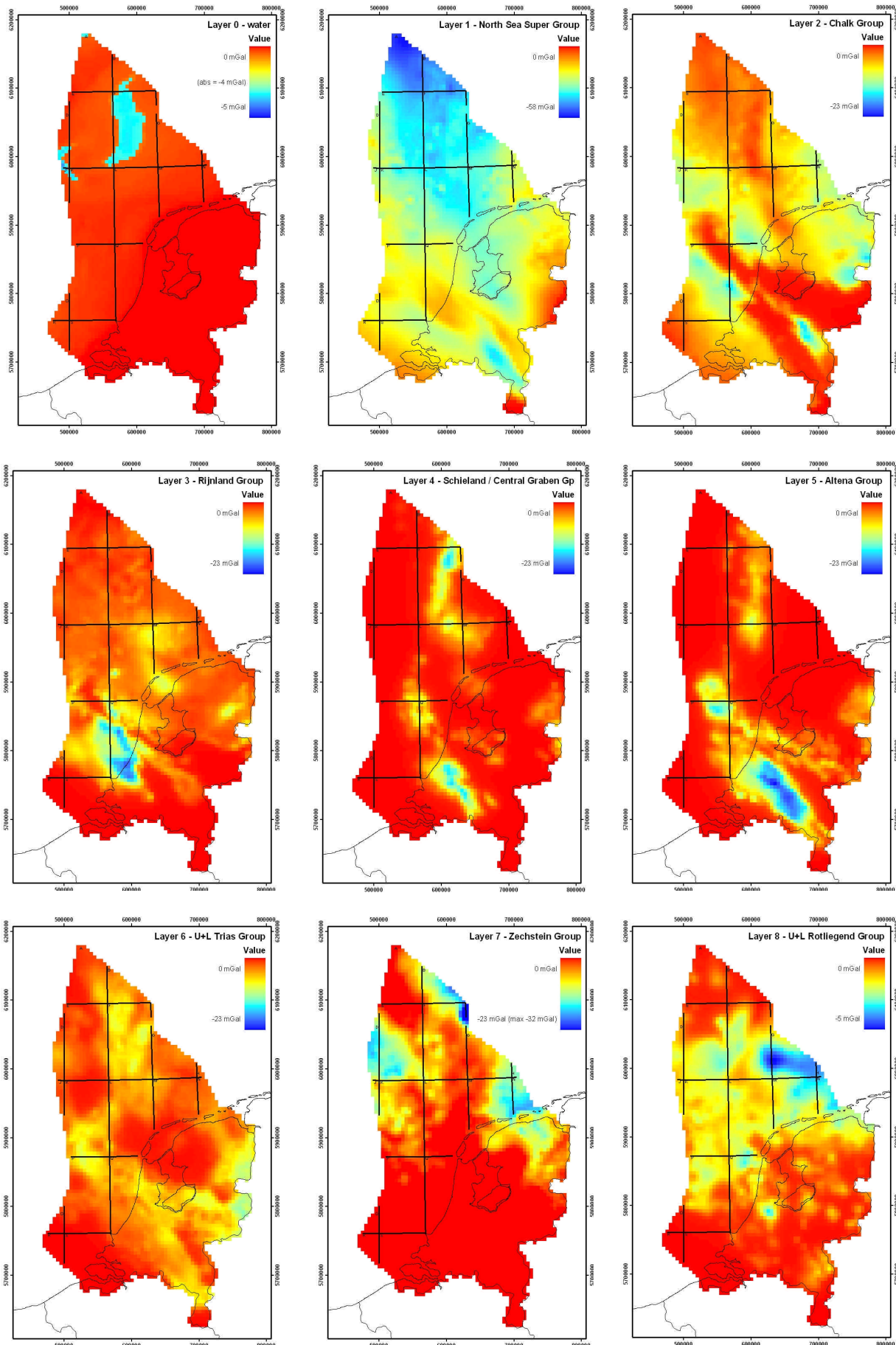


Figure K4 The gravity effect of the individual layers (mind the different legends of layers 0, 1 and 8)

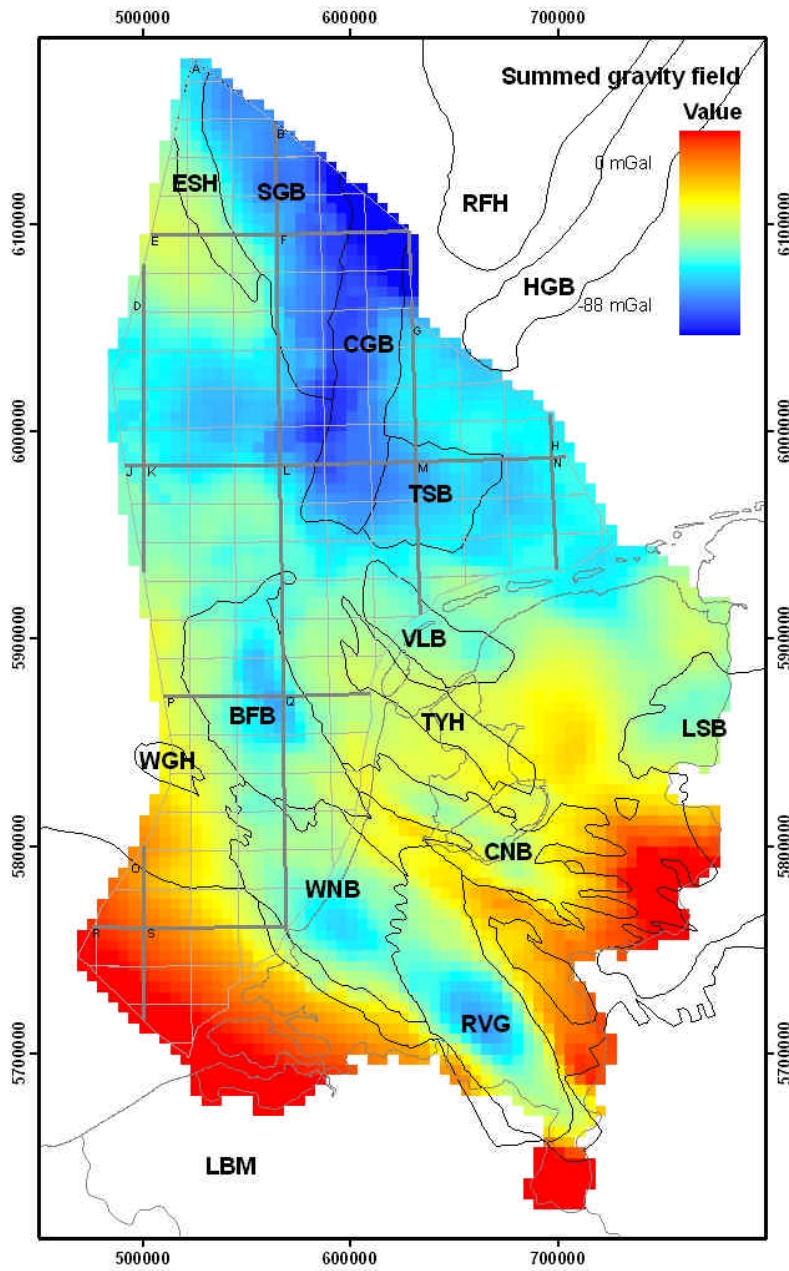


Figure K5 The summed gravity effect of the post-Carboniferous sedimentary layers plus water layer.

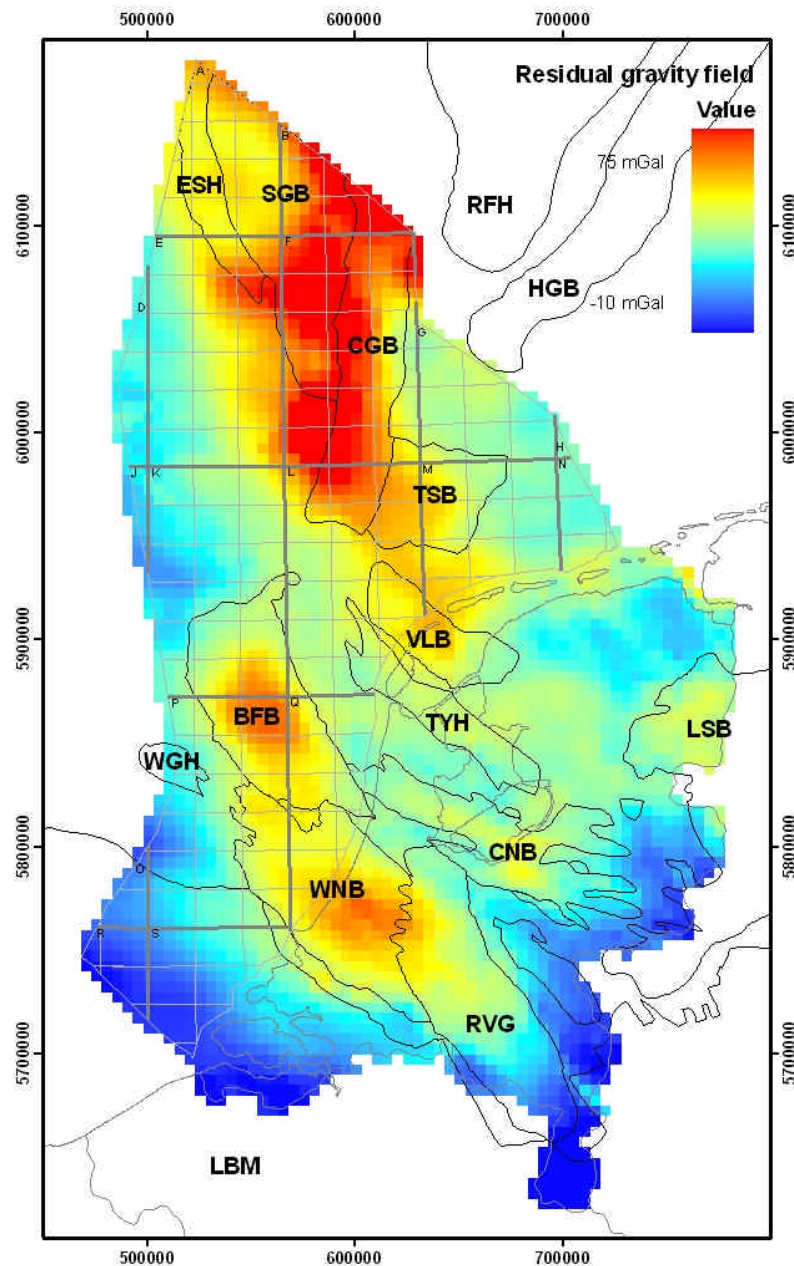


Figure K6 The residual gravity field after subtracting the summed gravity effect from the observed Bouguer gravity field.

Discussion

The observed Bouguer gravity anomaly map

Before any remarks can be made about the residual gravity field, the observed Bouguer anomaly map (Figure K3) needs some explanation. In this map the stable basement high of the London-Brabant Massif is characterized by a WNW-ESE trending gravity high. In the east of the Netherlands and southern Limburg the gravity highs are caused by the relatively shallow presence of Carboniferous and older sediments. The Roer Valley Graben shows a negative Bouguer anomaly, due to the thick succession of relatively uncompacted Tertiary and Quaternary sediments. In the north, the gravity lows are mainly caused by the presence of a relative thick Zechstein layer with salt diapirs. The

gravity high in the north of the Dutch territory partly overlies the Central Graben (CGB), Step Graben (SGB) and Elbow Spit High (ESH). The highest value in the observed Bouguer field (12 mGal) is found here at the south-eastern end of the ESH. The gravity high above the ESH can be explained by the shallow presence (<1800 m below sea level) of Carboniferous and older sediments (Figure K2). To the contrary, the extension of this gravity high above the SGB is unexpected when one considers the thick post-Carboniferous sedimentary sequence. The gravity high in the southwest corner of the F-block is even more contradictory due to the very thick post-Carboniferous sedimentary sequence (up to 8 km). The high gravity anomaly band along the graben could be related to crustal thinning beneath the graben.

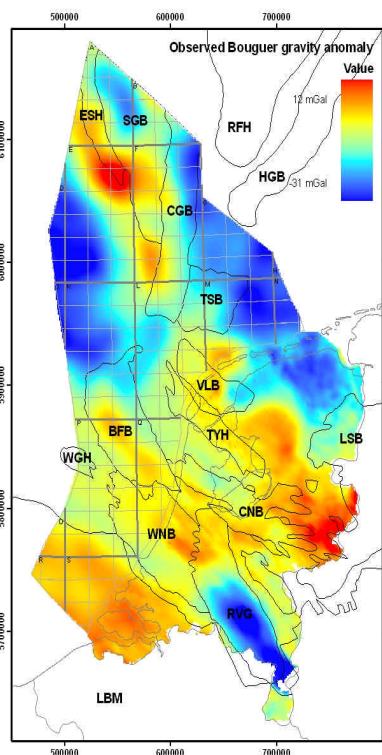


Figure K3 repeated

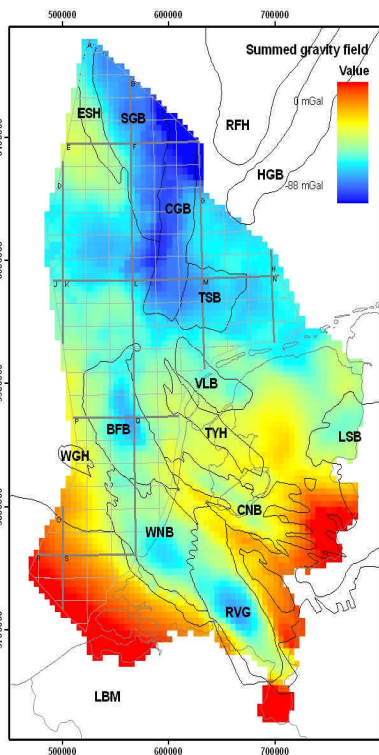


Figure K5 repeated

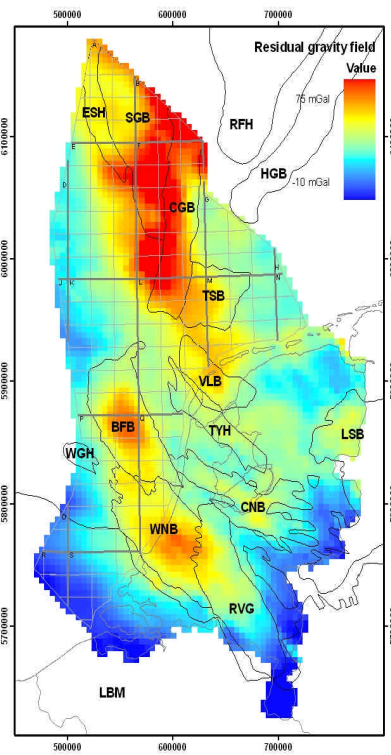


Figure K6 repeated

The summed gravity field and residual gravity field

As can be expected, the summed gravity field is closely related to the thickness of the post-Carboniferous sedimentary sequence. The biggest contribution is seen in the Roer Valley Graben (RVG), West Netherlands Basin (WNB), Broad Fourteens Basin (BFB) and Central and Step Grabens (CGB and SGB). Subtracting the summed gravity field from the observed field results in gravity highs at the WNB, BFB and along the CGB and SGB. Along the RVG the observed major negative Bouguer gravity anomaly has been compensated by the gravity effect of the post-Carboniferous sedimentary sequence. As mentioned by Dortland (2003), this indicates that the observed negative anomaly of the RVG is mainly a supra-crustal feature caused by the thick sedimentary succession of relatively uncompacted sediments (thick North Sea Super Group). This suggests a clear difference in structural development between the RVG and CGB.

Central Graben and Step Graben

During the Early Triassic the tensional stress regime induced by crustal extension and lithospheric thinning can be regarded as the first onset of rifting along the CGB. According to Ziegler (1982) this extension continued until the end of the Early Cretaceous. The main rifting period was during the Late Jurassic, resulting in the thick sections that accumulated in this period. During the Late Cretaceous and Paleocene inversion took place, possibly related to the Alpine orogeny (Ziegler, 1987), leading to thin or even absent Early and Late Cretaceous sediments. After the inversion episode(s), relative quiet regional subsidence took place, resulting in a thick Tertiary and Quaternary sequence.

The thick Triassic, Jurassic and Tertiary and Quaternary sequences thus formed, contribute greatly to the summed gravity effect of the post-Carboniferous sedimentary sequence along the SGB and CGB (Figure K5). However, as mentioned in the previous section, the observed Bouguer anomaly (Figure K3) shows a primarily positive gravity anomaly along the CGB and SGB, indicating the presence of relatively dense material. The residual gravity field (Figure K6) shows an even more pronounced gravity high along the CGB and SGB, due to subtraction of the large negative gravity effect of the thick Triassic, Jurassic and Tertiary and Quaternary sequences. Errors in our density model, or errors in our velocity model due to average v_0 and k values (section 0) leading to errors in our density model, can never add up to such a big gravity effect that the residual gravity high along the CGB disappears. This favors the model of crustal thinning beneath the graben, though not exactly beneath the graben, but more to the west, partly beneath the CGB and partly beneath the SGB. Deep seismic reflection profiles in the BIRPS Atlas show a considerable shallowing of the Moho, associated with crustal thinning during Triassic-Jurassic rifting, beneath the northern part of the CGB outside the Dutch territory (Klemperer and Hobbs, 1991). Velocity models show basement thinning beneath the graben by a factor of two (Klemperer and Hobbs, 1991).

West Netherlands Basin

The possible explanations for the residual gravity high in the West Netherlands Basin as outlined in the onshore gravity study of Dortland (2003) still apply. One explanation is the presence of high-density crustal intrusions. Dirkzwager (2002) proposes the origin of Cretaceous magmatic rocks to be attributed to rifting activity and subsequent thermal subsidence of the WNB during the Late Jurassic-Early Cretaceous. Dortland shows that the gravity effect of a high density crustal intrusion (40 km in diameter, 5 km high, base at 11 km) can have a considerable effect on the gravity field and a wavelength similar to the wavelength of the WNB residual gravity high. A map of the magnetic anomaly in the Dutch territory could be of help in locating the presence of magmatic intrusions. Furthermore, a shallowing Moho could be an explanation of the residual gravity high. This is in agreement with the Late Cretaceous uplift and subsequent erosion of the WNB (van Balen et al., 2000). In general, Moho uplift and a reflective lower crust are thought to be associated with a high(-er) heat flow when compared to adjacent areas (Meissner et al., 1994). The WNB is marked by the occurrence of a high heat flow (Dirkzwager, 2002) and a reflective lower crust (Duin *et al.*, 1995). However, the interpretation of deep seismic reflection data along the coast of the Netherlands does not give an indication of a shallowing Moho beneath the WNB (Duin et al., 1995). Finally, Dortland (2003) shows that Gardner's relation tends to underestimate well log densities. Higher densities in the WNB (closer to $\rho_{ref} = 2.67 \text{ g/cm}^3$) would give a less negative effect in the summed gravity field, and thus a less pronounced gravity high in the residual gravity field. However, adding 5% to the density model does not completely remove the residual gravity high. Therefore, the presence of a Dinantian

block beneath the WNB is not unlikely. Whether or not this block is accompanied by a deep crustal intrusion is not determinable from the residual gravity field obtained in this study.

Broad Fourteens Basin

Together with the WNB, RVG and CGB, the Broad Fourteens Basin also experienced uplift during the Late Cretaceous. However, for the BFB and RVG this uplift was greater than for the WNB, resulting in erosion of Jurassic sediments as well. Despite the difference in structural history the observed Bouguer gravity field and calculated residual gravity field show comparable anomalies for the WNB and BFB. As for the WNB, a shallowing Moho could be an explanation for the residual and observed gravity high, though this has not (yet) been observed in deep seismic reflection data.

The difference in residual gravity above the CGB and WNB/BFB can be explained by the difference in depth of the Moho. According to the BIRPS Atlas [Klemperer and Hobbs, 1991] the Triassic-Jurassic rifting phase in the graben has had considerable impact on the depth of the Moho. This effect is probably significantly larger than the effect of Moho shallowing associated with inversion in the WNB, BFB and RVG during the Late Cretaceous.

Conclusions

In this study a residual gravity field was obtained by subtracting the gravity effect of the post-Carboniferous sedimentary sequence from the observed Bouguer gravity anomaly. The main features to be seen in the residual gravity field are gravity highs at the Central and Step Graben, Broad Fourteens Basin and West Netherlands Basin. The differences in residual gravity between these gravity highs might be explained by a difference in depth of the Moho. Rifting and associated crustal thinning of the Central Graben during the Triassic, Jurassic and Early Cretaceous resulted in considerable shallowing of the Moho beneath the Central Graben. For the WNB and BFB, a (less pronounced) shallowing of the Moho associated with the Late Cretaceous inversion period could be an explanation of the residual gravity highs. However, this effect has not (yet) been observed in deep reflection seismic data.